MNHB

Journal of
Geophysical Research

VOLUME 64 DECEMBER 1959 NUMBER 12

THE SCIENTIFIC PUBLICATION

OF THE AMERICAN GEOPHYSICAL UNION

Journal of Geophysical Research

An International Scientific Publication

This Journal welcomes original scientific contributions on the physics of the earth and its environment.

Manuscripts should be transmitted to J. A. Peoples, Jr., Geology Department, University of Kansas, Lawrence, Kansas. Authors' institutions, if in the United States or Canada, are requested to pay a publication charge of $15 per page, which, if honored, entitles them to 100 free reprints.

Subscriptions to the *Journal of Geophysical Research* and *Transactions, AGU* are included in membership dues.

Non-member subscriptions, *Journal of Geophysical Research*. .$30 for back Volume of 1959, $6 for this issue; $20 for the calendar year 1960.

Non-member subscriptions, *Transactions, AGU*. . . . .$4 per calendar year, $1.25 per copy

Subscriptions, renewals, and orders for back numbers should be addressed to American Geophysical Union, 1515 Massachusetts Ave., Northwest, Washington 5, D. C. Suggestions to authors are available on request.

Beginning with the January 1959 issue (Vol. 64, No. 1) the *Journal of Geophysical Research* is published monthly by the American Geophysical Union, the U. S. National Committee of the International Union of Geodesy and Geophysics organized under the National Academy of Sciences-National Research Council as the U. S. national adhering body. Publication of this journal is supported by the National Science Foundation and the Carnegie Institution of Washington. The new monthly combines the type of scientific material formerly published in the bi-monthly *Transactions, American Geophysical Union*, and the quarterly *Journal of Geophysical Research*. The *Transactions, American Geophysical Union* will continue as a quarterly publication for Union business and items of interest to members of the Union.

Published monthly by the American Geophysical Union from 1407 Sherwood Avenue, Richmond, Virginia.
Second class postage paid at Richmond, Virginia.

PREPUBLICATION OFFER

BY

AMERICAN GEOPHYSICAL UNION

1515 Massachusetts Ave., N.W., Washington 5, D. C., U.S.A.

[Offer void after January 10, 1960 (U. S. and Territories, Canada, and Mexico) and after January 20, 1960 (all others).]

Physics of Precipitation

Geophysical Monograph No. 5 of the American Geophysical Union (Publication No. 746 of the National Academy of Sciences—National Research Council) is based on a conference held in Woods Hole, Massachusetts, June 3-5, 1959, under the chairmanship of Dr. Helmut Weickmann and the honorary chairmanship of Prof. Tor Bergeron. It will make an illustrated book of about 425-450 pages in the two-column format of the previous Geophysical Monographs, size 7 by 10 inches, and will be ready for distribution in February 1960. It will be cloth bound and will contain some 45 papers by some 50 well-known authorities with relating discussions on the following themes:

Morphology of Precipitation Clouds and Cloud Systems
Morphology of Precipitation and Precipitation Particles
Fundamental Precipitation Processes
Hail Formation
Artificial Precipitation Control

The authors included are as follows: Tor Bergeron, J. Namias, J. Malkus, C. Ronne, T. Fujita, C. E. Anderson, J. Smagorinsky, B. Ackerman, P. M. Austin, W. Hitschfeld, C. J. Grunow, U. Nakaya, K. Higuchi, C. Magono, R. Wexler, A. Goetz, O. Preining, W. A. Mordy, M. Neiburger, C. W. Chien, P. Squires, S. Twomey, C. Rooth, B. J. Mason, H. W. Georgii, D. B. Kline, S. J. Birstein, J. P. Lodge, R. Saenger, R. List, R. M. Cunningham, C. W. Newton, W. B. Beckwith, H. Dessens, R. J. Donaldson, Jr., A. C. Chmela, C. R. Shackford, G. E. Stout, R. H. Blackmer, R. E. Wilk, R. E. Hallgren, C. L. Hosler, R. H. Douglas, O. Essenwanger, F. E. Volz, B. Vonnegut, C. Moore, H. T. Orville, C. J. Todd, L. J. Battan, A. R. Kassander, W. E. Howell, and R. G. Semonin.

The book (list price, $12.50) is offered at prepublication prices (valid until January 10, 1960, for U. S. and Territories, Canada, and Mexico, and until January 20, 1960, for all others) as follows:

	To Members	To Non-Members[a]
Payment with order, postage paid	$9.00	$ 9.50
Payment on delivery, plus postage	$9.75	$10.25

[a] Note that subscribers to publications of the American Geophysical Union are not members.

STANDING ORDERS: For those having standing orders for the Geophysical Monograph Series, the order will be entered at the $10.25 rate, net, plus postage, unless advance payment (noting payment is for a standing order) is received. For those having standing orders for publications of the National Academy of Sciences—National Research Council, the order will be entered at the list price less the usual per cent.

PREVIOUS GEOPHYSICAL MONOGRAPHS: Geophysical Monograph No. 1 (Antarctica in the International Geophysical Year, price $6.00), Geophysical Monograph No. 2 (Geophysics and the IGY, price $8.00), Geophysical Monograph No. 3 (Atmospheric Chemistry of Chlorine and Sulfur Compounds, price $5.50), and Geophysical Monograph No. 4 (Contemporary Geodesy, price $5.50) are still available.

Purchase Order

TO AMERICAN GEOPHYSICAL UNION
1515 Massachusetts Avenue, N. W., Washington 5, D. C., U.S.A.

Please enter (my) (our) order for ______________________ copy/copies of Geophysical Monograph No. 5.

☐ Enclosed is $____________ for this order at $ ____________
($9.00 per copy—price to members only)
($9.50 per copy—price to non-members, including subscribers to AGU publications)

☐ Upon receipt of the invoice, (I) (we) will remit $____________ (plus postage) promptly at
$ 9.75 per copy—price to members, plus postage)
($10.25 per copy—price to non-members, plus postage)
(List price, $12.50)

______________________ ______________________
Typed Name Address

______________________ ______________________
Signature

[Offer void after January 10, 1960 (U. S. and Territories, Canada, and Mexico) and after January 20, 1960 (all others).]

Journal of

GEOPHYSICAL RESEARCH

VOLUME 64 DECEMBER, 1959 No. 12

INTERNATIONAL SYMPOSIUM ON FLUID MECHANICS IN THE IONOSPHERE

A Review of the International Symposium on Fluid Mechanics in the Ionosphere

R. BOLGIANO, JR., *Organizing Secretary*

Cornell University, Ithaca, New York

For many years after the discovery of the Kennelly-Heaviside layer, the ionosphere was assumed to be essentially uniform horizontally. Later the variation from daytime to night-time hemispheres was taken into account, and in this way it was possible to explain a large body of radio phenomena. As a consequence more complex models of ionospheric structure received little attention at that time. By the middle 1930's, however, evidence was beginning to accumulate indicating that the ionosphere is highly irregular in both time and space. Recognition of this condition helped radio physicists and engineers to explain, at least qualitatively, many 'abnormal' propagation events. A full understanding, sufficient to permit quantitative predictions, could not be achieved without far greater knowledge of the nonuniform nature of the ionosphere. Thus, the study of the structure of irregularities became an important field of ionospheric physics.

By means of ionospheric sounders, multiple-station analyses, interferometric techniques, and high-frequency and VHF radars, a wealth of factual data about ionospheric inhomogeneities was collected during the 1940's and early 1950's. They were found in all sizes, from thousands of kilometers down to a few meters, in a variety of shapes, and in general were thought to be moving with velocities that ranged from near zero to hundreds of meters per second. Parallel with the gathering of data, there developed many explanations as to how and why these irregularities are produced and what happens to them subsequently. Some of the principal causes were determined to be variabilities in ionization rate, high-energy particles, meteors, and the mixing of gradients by air currents. Recombination, diffusion, and convection by winds were believed to account for much of their later development. The important role that fluid motions in the atmosphere play in these processes was recognized by nearly all investigators and certainly needed no emphasis. The detailed nature of this role, on the other hand, was a matter of considerable controversy.

Appreciation of the part played by winds and air currents in forming and re-forming many of the inhomogeneities in the ionosphere led many workers to anticipate a whole range of irregularity sizes. Nonetheless, lack of knowledge of the actual fluid mechanics involved resulted in the usual assumption of Gaussian shapes (and spectra). The Gaussian assumption, however, did not predict the phenomenon of VHF ionospheric scatter transmission. Finally, the suggestion was made that, despite stability arguments to the contrary, the ionosphere might indeed be turbulent. The resulting predictions were susceptible of experimental verification; tests were conducted, and the findings were positive.

This, however, did not bring matters to a

close, by any means. Numerous interpretations of the various data evolved. Some of the meteor observations appeared to be explained at least as well, if not better, without the introduction of turbulence. Several different theories of turbulent mixing were developed, which yielded conflicting predictions. Moreover, the empirically deduced frequency scaling law (corresponding to the form of the spectrum) was not in close agreement with turbulence theory. Then there was the fundamental question whether or not turbulence could exist in the highly stable density gradient characteristic of the ionosphere.

The situation was such at the time of the Twelfth General Assembly of URSI in 1957 that it was considered a joint study by a group of ionospheric physicists and fluid dynamicists would prove worth while, not only in shedding light on the ionospheric problem but also perhaps in increasing the interest of fluid mechanics theorists in an important portion of the earth's fluid envelope. Here occurred the genesis of this symposium. Early in 1958 the International Council of Scientific Unions, under the presidency of Dr. L. V. Berkner, asked Professor Booker to organize such a meeting to be held approximately one year before the next General Assembly in 1960. The Symposium was to be sponsored by the International Scientific Radio Union in collaboration with the International Union of Theoretical and Applied Mechanics and the International Union of Geodesy and Geophysics.

Professor Booker was soon joined by Dr. Batchelor as IUTAM representative, and together they laid the groundwork. An organizing committee was constituted, consisting of H. G. Booker, *chairman*, G. K. Batchelor, S. Chapman, W. E. Gordon, D. F. Martyn, R. W. Stewart, and R. Bolgiano, Jr., *organizing secretary*. Financial support was sought and received from UNESCO, from the U. S. National Science Foundation, and from the Office of Naval Research of the U. S. Navy Department.

Early in the organizational process the broad objectives of the meeting were set out. It was to serve, first of all, to bring to bear on both the field of ionospheric physics and the field of fluid mechanics the full force of current knowledge in the other field. This necessarily would involve much exchange of information, since few ionospherists were intimately familiar with fluid mechanics, to say nothing of turbulence, and vice versa. It was hoped that, out of such an exchange and mutual consideration of the revelant facts and theories in both fields, a new physical theory would develop that would be able to account for a major portion of the many, varied ionospheric data, yet be consistent with the accepted and tested notions of fluid mechanics. A further aim was to heighten the interests of some fluid mechanists in the ionosphere as a domain in which there are challenging fluid problems to be solved. Last, but certainly not least important, was the objective of familiarizing many of the ionospheric physicists with fluid dynamics and turbulence theory.

It was decided that, to ensure a reasonable chance of success for the primary objective, the symposium would have to take the form of a small, informal, 'workshop' type of meeting. Participation would be by invitation only and would be limited to approximately thirty members of each field. In this way free discussion of raw ideas would be encouraged and a significant step forward might be taken. Because of the wide divergence of the two disciplines, three days were set aside for more or less tutorial exchange. Another two days were thought essential for constructive discussions of the problems and of new ideas, and a final day would be needed for summing-up. The schedule was arranged with a weekend in the middle so that participants would have an opportunity to consolidate their thoughts.

The morning half of each of the first three days was turned over to the ionospherists, who presented their experimental and theorized knowledge of the 70- to 500-km altitude interval to the members in fluid mechanics. The afternoons were similarly spent with the fluid dynamicists conveying to the ionospheric people information on nonuniform fluid motions (including turbulence) as they are known to exist, or may exist, in the atmosphere. There were two invited papers only each morning and afternoon, thus leaving some time for questioning by the participants and for an occasional additional item of factual information. Preprints of the invited papers were distributed a day or more in advance of their presentation so that participants could familiarize themselves with the material.

These days were certainly successful. All the papers served excellently the tutorial purpose for which they were intended, and a number of them contained sufficient new or not fully appreciated ideas to be inspiring as well. In particular, mention should be made of Sheppard's discussion relating to possible driving mechanisms for large-scale motions in the intensely stable ionosphere. His suggestion of the possible role of slantwise convection elicited as much interest from the other fluid dynamicists as from the ionospherists. Millman's and Greenhow's reports of highly anisotropic large-scale structure at meteoric levels (6 km in the vertical, 150 km in the horizontal) were especially illuminating. Long's description of internal standing waves in a stratified fluid and of the jet-type motions characteristic of such flows was very helpful. It was immediately observed that such motions may account for much of the large-scale structure in the ionosphere. Dungey's mechanism of electron convergence, due to the earth's magnetic field, was considered to be of considerable importance as a possible basis for explaining some phenomena and for discounting existing explanations of other phenomena. Oboukhov's discussion of the scattering of sound waves in the troposphere, though not directly applicable to the problems at hand, was very interesting in that it provided new data in support of the turbulence theories. Martyn's suggestion of instability of electron density deviations in an upward-moving F region precipitated much valuable discussion. If a single criticism were to be leveled at the outcome of the first three days, it would be that, both mornings and afternoons, there were not as many probing questions by members of the opposite field as might have been desirable.

Monday was largely given over to the communciation of additional, current information. Several new and interesting notions were set forth. Hines' elucidation of the role of gravity relative to flow in the stably stratified ionosphere was a valuable adjunct to Long's previous analysis. In particular, Hines' consideration of vertically propagating waves leads to the interesting possibility of phenomena for which the amplitude increases with altitude. Of similar importance was Greenhow's redetermination of the rate of viscous dissipation of turbulent kinetic energy on the basis of the diffusion of visual meteor trains. The new value of 7×10^{-3} watt/kg is more than an order of magnitude less than the value previously calculated from the observed large-scale motions.

Tuesday morning was devoted primarily to a series of short expository talks on the structure of and the role of turbulence in the ionosphere. These were especially illuminating to many of the ionospheric physicists. The afternoon was largely spent in further consideration of the effects of the earth's magnetic field.

With no hope of formulating a generally acceptable theory to describe the observed ionospheric phenomena in terms of established fluid dynamics, Wednesday was given over, for the most part, to a panel discussion in an attempt to secure a number of individual opinions as to what progress had been made and where the problems stood at that time. This proved to be very successful and highly worth while; consequently this final panel discussion has been reproduced in the *Transactions* in somewhat greater detail than the rest of the sessions.

The principal conclusions of the symposium can be stated as follows:

1. Turbulence is a common occurrence in the ionosphere, at least to an altitude of 100 km. This has been established from evidence of the diffusion of long-duration visible meteor trains, which proceeds at a rate several orders of magnitude higher than that attributable to molecular diffusion alone.

2. The viscous dissipation rate, ϵ, is appreciably smaller than some previous estimates had placed it. Even this new estimate may be somewhat high, since the large visual meteors very likely produce turbulent wakes of their own.

3. The large-scale anisotropic motions are not adequately described by theory customarily applied to laboratory turbulence. The bulk of the energy probably resides in motions more properly classed as semicoherent winds: (random) gravitational waves, thermal winds, convective columns, i.e. motions having 'lifetimes' long compared with their characteristic periods. The intensity of fully developed turbulence may be no more than 1 per cent of the total energy.

4. Predictions (even in order of magnitude) of the structure and intensity of small-scale atmospheric turbulence, from observations of the

large-scale motions alone, should be made with caution. The relation is sensitive to several factors, in particular to the degree of stability of the atmosphere.

5. The earth's magnetic field has negligible direct effect on turbulence but may affect it indirectly via the dynamo action.

6. Several possible driving mechanisms for the large-scale motions exist. However they suggest that turbulence should be highly local in time and space, and this is quite contrary to the evidence from ionospheric scatter transmission and radio meteor echo data.

7. Hydromagnetic effects probably account for a number of ionospheric phenomena.

Much work remains to be done on nonuniform flows in a stable atmosphere, on the interaction of gravity waves with one another and with turbulence, and on the electron density deviations induced by such complex fields of motion.

Although significant progress was made during the symposium, it is possible, in retrospect, to recognize some aspects of it that may justifiably be criticized. Perhaps the most serious criticism that might be made is that the over-all problem of fluid mechanics in the ionosphere was approached from a position somewhat too firmly entrenched in preconceived notions. As a result a disproportionate amount of attention may have been directed toward turbulence, as the mechanism, and toward meteor data, as the source of information. It is possible that even greater progress would have resulted had more emphasis been placed on the study of organized motions (waves), and had other radio sounding techniques, such as direct backscatter experiments, been relied upon more heavily for the factual data. On the other hand, some of the principal conclusions reached in the meeting might never have materialized under those circumstances.

Fifty-six individuals from five continents participated in the symposium. Their names and affiliations are listed at the end of this paper.

In closing this brief account it should be noted that the success of this undertaking can in large measure be credited to Professor Booker and Dr. Batchelor, for having the foresight to perceive the true value of such a meeting as well as the determination and persistence to bring it to reality. The inestimable assistance of members of the research staffs in the Schools of Aeronautical and Electrical Engineering at Cornell, especially of those individuals responsible for the recording and reproduction of the daily discussion record, must also be acknowledged. Without their willing and able efforts, both in the taking of notes and in the rapid reduction of that material to a coherent account, the present proceedings would be seriously deficient.

Participants

G. K. Batchelor, Cavendish Laboratory, Cambridge University

D. R. Bates, Department of Applied Mathematics, Queen's University of Belfast

W. Becker, Institut für Ionosphären-Physik, Max-Planck Institut für Aeronomie

K. Bibl, Ionosphären-Institut, Breisach/Rhein

R. Bolgiano, School of Electrical Engineering, Cornell University

H. G. Booker, School of Electrical Engineering, Cornell University

S. A. Bowhill, Ionosphere Research Laboratory, Pennsylvania State University

K. Bowles, National Bureau of Standards, Boulder

S. Chapman, Geophysical Institute, College, Alaska

S. Corrsin, Mechanical Engineering Department, The Johns Hopkins University

J. P. Dougherty, Cavendish Laboratory, Cambridge University

J. W. Dungey, Department of Mathematics, King's College, Newcastle-on-Tyne

J. A. Fejer, Defence Research Telecommunications Establishment, Ottawa

H. Feshbach, Massachusetts Institute of Technology

F. N. Frenkiel, David Taylor Model Basin, Washington

C. Gartlein, Physics Department, Cornell University

F. Gifford, Weather Bureau Office, Oak Ridge

T. Gold, Scripps Institution of Oceanography, La Jolla

S. Goldstein, Division of Engineering and Applied Physics, Harvard University

G. S. Golitsyn, Institute of the Physics of the Atmosphere, Moscow

J. S. Greenhow, Jodrell Bank Experimental Station, University of Manchester

F. R. Hama, Institute for Fluid Dynamics and Applied Mathematics, University of Maryland

M. Hasegawa, Rector of Fukui University, Japan

H. Hasimoto, Department of Aeronautics, Kyoto University

C. O. Hines, Defence Research Telecommunications Establishment, Ottawa

I. D. Howells, Cavendish Laboratory, Cambridge University

. R. Koster, Department of Physics, University College of Ghana

. S. G. Kovasznay, Department of Aeronautics, The Johns Hopkins University

I. Krook, Harvard College Observatory, Harvard University

. C. Lin, AVCO-Everett Research Laboratory

. R. Long, Civil Engineering Department, The Johns Hopkins University

I. S. Longuet-Higgins, National Institute of Oceanography, Wormley

. A. Manning, Radio Propagation Laboratory, Stanford University

. Manring, Geophysics Corporation of America

. F. Martyn, Upper-Atmosphere Research Laboratories, C.S.I.R.O., Australia

. Maxwell, Radio Astronomy Station, Harvard College Observatory

. M. Millman, Radio and Electrical Engineering Division, National Research Council, Canada

. S. Monin, Institute of the Physics of the Atmosphere, Moscow

I. V. Morkovin, The Martin Company, Baltimore

. I. H. Nicholl, Department of Mechanical Engineering, Laval University

. Nichols, School of Electrical Engineering, Cornell University

I. Nicolet, General Secretary, C.S.A.G.I.

A. M. Oboukhov, Institute of the Physics of the Atmosphere, Moscow

H. A. Panofsky, Department of Meteorology, Pennsylvania State University

O. M. Phillips, Mechanical Engineering Department, The Johns Hopkins University

J. A. Ratcliffe, Cavendish Laboratory, Cambridge University

N. Rott, School of Aeronautical Engineering, Cornell University

P. G. Saffman, Cavendish Laboratory, Cambridge University

W. R. Sears, School of Aeronautical Engineering, Cornell University

P. A. Sheppard, Department of Meteorology, Imperial College, London

R. W. Stewart, Department of Physics, University of British Columbia

F. M. H. Villars, Lincoln Laboratory, Massachusetts Institute of Technology

A. H. Waynick, Ionosphere Research Laboratory, Pennsylvania State University

A. D. Wheelon, Space Technology Laboratories, Inc.

R. W. H. Wright, Department of Physics, University College of Ghana

C. S. Yih, Engineering Mechanics, University of Michigan

Transactions of the International Symposium on Fluid Mechanics in the Ionosphere

Morning Session

Thursday, July 9, 1959

Chairman: H. G. Booker

Chairman: Gentlemen, it is a pleasure to welcome you here this morning at the start of this symposium on the fluid mechanics of the ionosphere. I have arranged no formal welcoming address, nor do I intend to give one myself, since I believe you are well aware of the purpose in our meeting at this time and of the workshop nature which it is hoped this conference will assume. The first three days are to be spent half in orienting the fluid mechanics people to the character and problems of the ionosphere and half in familiarizing the ionospheric physicists with the pertinent fluid mechanics theory. After the weekend the discussion will be aimed toward the elucidation of some of the current problems in the field.

This morning's session is to be devoted to the presentation of background information about what the atmosphere is like at ionospheric levels and, in particular, about what the ionization situation there is. The first paper, on the constitution of the upper atmosphere, is to be given by M. Nicolet.

Constitution of the Atmosphere at Ionospheric Levels

Marcel Nicolet

A physical picture of the upper atmosphere cannot be obtained without determining whether the vertical distribution depends on mixing or diffusion or on a chemical or photochemical equilibrium. It was shown how dissociation and recombination of molecular and atomic oxygen and nitrogen are distributed with altitude. The structure of the atmosphere deduced from density measurements was related to the variation of the mean molecular mass as influenced by diffusion effects. In addition, the manner in which the heat budget is affected by conduction was considered. [See paper under same title, this symposium.]

Chairman: I think we can handle the discus sion in the following way. We will have im mediately any specific questions you would lik to put to Dr. Nicolet. Then we will have M Ratcliffe's paper in the same manner. Genera discussion and any relevant short communica tions that some of you may wish to make ca follow toward the end of the morning. Shall w now have specific questions on Dr. Nicolet paper?

Lin: Dr. Nicolet, in connection with your re mark that the temperature of the upper atmos phere on the light side of the earth appears t be the same as on the dark side, could this no be due to a very small recombination rate c particles? If the high solar flux is used in th dissociation of more and more of the mole cules, and if recombination is inhibited, the tem perature on the light side of the earth might no increase.

Nicolet: It seems difficult to believe tha enough of the solar energy can be so stored a to keep the temperature on the light side fron increasing.

Martyn: I have been left with the impressio that the densities on the two sides of the eart differ by a factor of 10. Is that correct?

Nicolet: The satellite data indicate constan density on the two sides of the earth; the rock data give quite different results.

Dungey: Have you considered the Van Alle radiation as a source of heat?

Nicolet: I believe it could play a minor rol at best, and that only in polar regions of th earth.

Chairman: If there are no further specifi questions, let us proceed with Mr. Ratcliffe paper.

Ionization and Drifts in the Ionosphere

J. A. Ratcliffe

Knowledge of the vertical distribution, and of horizontal irregularities and movements, of electrons in the ionosphere was summarized. The mechanisms by which electrons can be moved, either by fluid motions of the neutral air in which the electrons are imbedded or by electric fields arising from charges elsewhere in the ionosphere, were discussed. A statistical description of a randomly moving distribution function, which is commonly used by ionospheric physicists, was explained. [See paper under same title, this symposium.]

Chairman: Mr. Ratcliffe has certainly plunged us squarely into the midst of our problems with his discussion of drifts in the ionosphere. Are there any specific questions?

Sheppard: Is there much change over the globe in the direction and magnitude of the mean drift to which you referred?

Ratcliffe: The curve I showed on the slide was in fact for Manchester. Variation of the mean drift velocity over the globe has not been studied extensively; much more attention has been paid to the semidiurnal component.

Rott: Is it correct to apply the results of your analysis both to the electric fields and to the wind forces? The wind force depends upon velocity differences and is caused by collisions. Since collisions already have been taken into account for the termination of the path, it seems they have been taken into account twice in two different ways.

Ratcliffe: The results I have given are for velocity differences.

Martyn: I am much interested in Mr. Ratcliffe's remarks about sensitive measurements of traveling disturbances in the E layer. Did he mean to imply that traveling disturbances in the E and F layers are related? I have not found a single case in which a traveling disturbance travels with the same vector velocity in both layers.

Ratcliffe: No, I have no knowledge at all as to how the E- and F-layer traveling disturbances are related. I simply wanted to make the point that such disturbances occur at least as frequently in the E layer as in the F layer.

Goldstein: Would it not be fruitful to investigate the effect of the inhomogeneity of the atmosphere on space charge?

Ratcliffe: That is certainly an important problem, to which considerable attention has been paid. I believe Mr. Martyn undoubtedly will say something about it.

Becker: I am firmly convinced that, in contradiction to Mr. Ratcliffe's statement, the electron density in the trough between the E and the F layers may, at times, fall below the E-layer maximum by far more than 20 per cent. [See correction at end of session.]

Ratcliffe: I believe rather strongly that the 20 per cent limit on the depth of the trough can be substantiated if proper account is taken of both the ordinary and extraordinary rays.

Chapman: Would not diffusion fill the gap relatively rapidly?

Ratcliffe: Yes. I believe diffusion would fill the gap to 10 per cent in about 20 minutes.

Lin: Could the magnetic field be moved by irregularities of sufficient size?

Ratcliffe: The irregularities about which I have been speaking are quite weak. Moreover, their effect on the magnetic field has been included in any case.

Chapman: A change of phase of 7°/km of the solar semidiurnal wind variation has been mentioned. This would amount to the considerable change of 90° in only 13 km. Is it likely that such a large rate of change will be maintained over an extended height interval? The change with height of the lunar atmospheric tides is indicated by lunar daily magnetic variations, and the rapid change of phase may explain some of the differences in the behavior of the solar and lunar daily magnetic variations.

Ratcliffe: This matter of change of phase is certainly important.

Hines: Rocket results support Mr. Ratcliffe's contention that the trough between the E and F layers is quite shallow.

Martyn: What Mr. Hines has said is certainly true. Moreover, I should like to point out that, in connection with the gap, the important point to note is that if the trough is very shallow the Hall conductivity there will exert a shunting effect on the whole region below. One may again find oneself without adequate conductivity in the ionosphere. If the trough is deep, there is no problem in this respect.

Batchelor: I should like to ask Mr. Ratcliffe whether turbulent diffusion was taken into ac-

count in his diffusion calculations and, if not, whether there was any good reason for neglecting it?

Ratcliffe: Turbulent diffusion was neglected, although there seems to have been no reason at all for doing so.

Frenkiel: Relatively small motions up and down can support a rather deep trough.

Becker: Vertical motions certainly exist in the ionosphere.

Bibl: Yes, I have much evidence of vertical motions.

Ratcliffe: I believe Mr. Martyn is going to discuss the matter of vertical motions in his talk.

[*Correction by Mr. Becker:* Mr. Becker re quests that the following correction be made t the notes: He agrees that there is practicall no trough around noon, but maintains that trough develops to a remarkable depth towar sunset. The ionization in this trough could b down by much more than 20 per cent from it *E*-layer maximum; in fact, the ionization coul be down by as much as 80 per cent just befor sunset. He believes that the times of rocket as cents should be checked—the ascents may hav taken place around noon. Mr. Becker also be lieves that the rocket results may not provid a sufficient sample to establish the point.]

Afternoon Session

Thursday, July 9, 1959

Chairman: G. K. Batchelor

Chairman: I think I should say, by way of explanation, that the terms of reference given to the speakers who will represent the fluid mechanics side of our subject in these introductory sessions were necessarily a little vague. The ionosphere speakers have the relatively clear-cut task of describing what is known about the ionosphere. The fluid mechanics people, on the other hand, have to describe the portion of their field that is relevant to the ionosphere; and at this stage we are not absolutely clear which parts of fluid mechanics are going to be relevant. We will start, however, with the preconceived notion that turbulence is bound to be the most important single topic, so that the objective of the six fluid mechanics speakers is to give a short course on turbulence —turbulence, of course, in a broad sense, allowing for the effects of the earth's magnetic field, the density gradient, and several other factors as well.

Our first speaker is Professor Stewart, from the University of British Columbia. He is going to give the opening talk on fluid mechanics, which is intended to be a descriptive survey of where and under what conditions turbulence occurs.

The Natural Occurrence of Turbulence

R. W. Stewart

In order to make the scientific meaning c the word *turbulence* clear, it was proposed tha a fluid be called turbulent if each componen of the vorticity is distributed irregularly an aperiodically in time and space, if the flow characterized by a transfer of energy from larg to smaller scales of motion, and if the mea separation of neighboring fluid particles tends t increase with time. It was noted that the que tion of whether or not a flow is turbulent is nc simply a matter of Reynolds number, since th stability of the flow is a criterion of at lea equal importance.

The results of experimental work in recer years by Anderson, Frenkiel and Katz, Kellog Liller and Whipple, and Malkus were consic ered. From these results it seems reasonable t infer that, with the exception of strong inve sion layers, the atmosphere may be assumed t be turbulent everywhere, although the intensit of the turbulence varies widely in both tim and space. The general structure of the turbu lence was deduced on the basis of the Kolm goroff similarity theory of locally isotropic tu bulence, and it was pointed out that in th framework the most important parameter in tl turbulent field is the energy dissipation ϵ. [S paper under same title, this symposium.]

Chairman: I do not think we should emba

on questions and comments now. Let us proceed immediately with the second prepared paper before breaking off for tea. We can then return to the questioning with renewed spirit.

The second paper is to be given by Professor Sheppard, of the Department of Meteorology at Imperial College, London. We thought it would be helpful to have a professional meteorologist tell us about the dynamics of the upper atmosphere.

Dynamics of the Upper Atmosphere

P. A. Sheppard

The mean temperature and motional structure of the stratosphere, mesosphere, and lower ionosphere were described, and the thermodynamics of those regions was considered briefly. Possible disturbances on the mean motion were discussed. It was concluded that vertical convection is a very unlikely cause of such disturbances; that slantwise convection undoubtedly will release potential energy, thus supporting such disturbances; and that small-scale turbulence, though not likely generally, will probably be produced locally (in time and space) in the vicinity of jets in the large-scale baroclinic disturbances. [See paper under same title, this symposium.]

Bowhill: Could Dr. Sheppard please explain what the Rayleigh number is?

Sheppard: The Rayleigh number is a dimensionless number that indicates the readiness with which heat will be transferred through a fluid layer by convective motions as opposed to thermal conductivity. It is

$$Ra = -(gh^3 \, \Delta\theta/\theta)/\kappa\nu$$

where g is the gravitational constant, h the vertical depth of the fluid layer, $\Delta\theta$ the change in potential temperature (or potential density) across the layer, θ the mean temperature (or mean density), κ the thermal diffusivity, and ν the kinematic viscosity. It is applicable to a fluid without shear.

I spoke of the dry adiabatic lapse rate (potential temperature independent of height) as the critical value for convection in the atmosphere. This is not strictly accurate. If the layer is very shallow, many times the dry adiabatic lapse rate is required to generate convection in the fluid ($Ra > 800$ approximately). As h increases, however, the Rayleigh number becomes very large. The Rayleigh instability is not generally important in regard to convection over relatively deep layers.

Kovasznay: I think we owe it to our ionosphere friends to start a debate on the definition of turbulence. How do we distinguish turbulence from space filled with randomly moving shocks?

Stewart: My original definition was intended for an incompressible fluid. Compressibility effects could be included as they are in the definition of turbulence used by astrophysicists. But compressibility effects of this sort are not very important for this conference. The stretching of the vortex lines is particularly important in the definition of turbulence.

Kovasznay: We have to reach one of two kinds of definitions. We can define turbulence mathematically or conceptually. When we go to the laboratory or the atmosphere, how do we decide whether the flow was or was not turbulent?

Stewart: It is important to separate turbulence from other random velocity fluctuations, especially wave motions. Three things are required: (1) stretching of the vortex lines, (2) diffusive character, (3) randomness of the three components of vorticity.

Booker: We know that hydromagnetic forces in the ionosphere add to the difficulty of understanding fluctuations there. In the stratosphere, however, where this added complication is absent, how do we explain the observed spreading of smoke puffs in a region thought to be stable? I believe we should begin by understanding the Richardson number.

Batchelor: Professor Sheppard in his talk brought out a very important point when he spoke of the generation of large-scale disturbances by slantwise convection. This is a means of producing a shear which might then result in small-scale turbulence even in the presence of a vertical density gradient that is stabilizing. I think we should ask him to clarify the essential physical mechanisms involved.

Sheppard: Consider a region of fluid with a horizontal temperature gradient and a stable lapse rate. Lines of constant potential temperature are drawn. A fluid particle moving slantwise at an angle between the horizontal and the lines of constant potential temperature will gain energy from the atmosphere. The disturb-

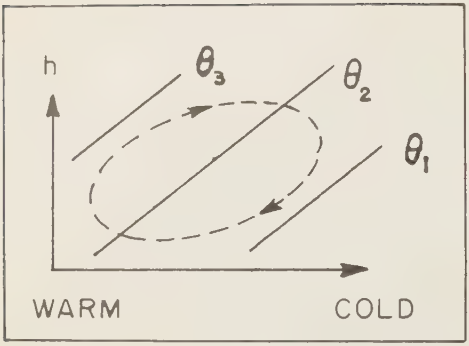

FIG. 1—The mechanism of slantwise convection.

ance can thus grow and its motion can increase, producing overturning of the fluid in a slantwise direction. The existence of boundaries complicates the problem. In the upper atmosphere we do not know how much the different layers will interact. It is difficult to say what the depth of these disturbances will be. Their size is probably determined by the second derivative of velocity, $\partial^2 V/\partial z^2$. In the mesosphere these disturbances would probably exist in multiples, one atop the other and out of phase, giving rise to a highly complicated wind shear pattern, consistent with such observations as are being made on the winds in the mesosphere.

Batchelor: With regard to the Richardson number, it is sufficient for this purpose to think of it purely in dimensional terms. It describes the relative importance of buoyancy forces to inertial forces. Think of a fluid particle that migrates vertically a distance l through a mean shear flow with an accompanying mean density gradient $\partial\rho/\partial z$. The buoyancy force acting on it is of the order $\delta\rho g$, where $\delta\rho = l\ \partial\rho/\partial z$. The work done against this force is $\delta\rho g l$. The difference in mean velocity at the two positions is δu. The kinetic energy released by the migration is thus of the order $\rho(\delta u)^2$. If the work done against buoyancy forces is much larger than the kinetic energy released, the motion will extinguish itself; and if the work done against buoyancy forces is much less than the kinetic energy released, the buoyancy forces will have only a small effect on the motion. The ratio of the two energies may be put in the form of the Richardson number as usually quoted,

$$\frac{(1/\rho)(\partial\rho/\partial z)g}{(\partial u/\partial z)^2}$$

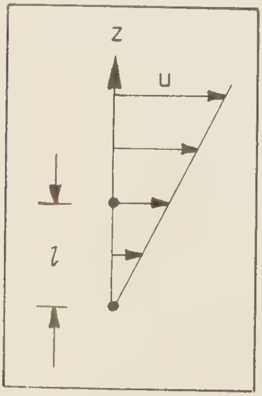

FIG. 2—Flow model for consideration of Richardson's number.

Sheppard: Horizontal gradients in velocity exist in the upper atmosphere and may create turbulence in addition to that created by slantwise convection. Whether or not this is a sufficiently energetic source of turbulence will have to be worked out.

Stewart: I should like to add that in the case of vertical motion in a stably stratified atmosphere a fluid particle may move upward, losing kinetic energy and gaining some potential energy, then fall back, regaining the kinetic energy. If the transport mechanism of heat is sufficiently different from the transport mechanism of momentum, the Richardson number could be much larger than unity, yet turbulence could exist.

Ratcliffe: My comments go back to the original, more general discussion. As ionospheric people we observe small-scale randomly varying structure in the ionosphere. We ask you as fluid dynamicists, first, given large-scale smoothly varying forces in a plasma-free fluid, what mechanisms will give small-scale randomly varying disturbances whether you call it turbulence or not? Second, if we cannot explain observations in the ionosphere by these mechanisms, would it help to consider a plasma imbedded in this fluid?

Batchelor: It is important to know whether

the kind of motion that has been reported to us is turbulent. It is important because turbulence is an extremely efficient mechanism for generating a small-scale motion out of a large-scale one.

Oboukhov: I disagree with the idea that turbulence is any process in nature that is not understood. It is important to distinguish between turbulence (random velocity fluctuations) and stochastic noise (random distribution of acoustical waves) in a compressible medium.

Martyn: First, I want to say in connection with doubts affecting Mr. Sheppard's presentation that we should probably all agree that meteor winds do give the correct air velocities up to 90 or 100 km.

Second, we have been considering the explanation of observed random velocity fluctuations. There are also random changes in electron density, sometimes as high as 50 per cent. Could the fluid dynamicists tell us what is the order of magnitude change in density accompanying the velocity fluctuations in turbulence?

Batchelor: The density variations caused directly by the turbulent motions are negligible. If large density variations exist, I should expect them to have been caused by some other mechanism, say differential heating.

Hines: The distortions of meteor trails that have been observed can be explained fairly well by wave motions. This will be discussed in more detail later. However, to answer Dr. Martyn, these wave motions are accompanied by strong density variations and could be the source of the observed density changes. This leads to the question of whether random waves with strong coupling (as these have) are the same as turbulence. By your earlier comment, Professor Batchelor, did you mean the coupling of waves does not lead to transfer of energy from large-scale to small-scale motions?

Batchelor: My comment referred to uncoupled waves. When the waves are coupled there would be generation of small-scale motion, a condition close to turbulence.

Morkovin: Can we fluid mechanicists agree that turbulence does not provide the energy to create observable density fluctuations directly? Some other source such as heating, light absorption, or gravity first produces density or temperature gradients which are then transformed into density or temperature fluctuations by the kinematics rather than the dynamics of turbulence.

Frenkiel: Mr. Morkovin, you meant the density and not the density of electrons, is that correct? A nonturbulent region in the ionosphere having a regular variation of air density, but an irregular distribution of electrons, could readily exist.

Morkovin: I did not mean fluctuations in electron density. I should like to add that random fluctuations in ordinary density can also be brought about by different wave mechanisms such as the random sound waves mentioned by Professor Oboukhov. Such waves usually have coupled density and pressure fluctuations, whereas, in turbulence, pressure fluctuations are of a lower order of magnitude. Waves can of course be random when driven by random sources. We saw an example of such randomness this morning in Dr. Nicolet's slide showing density fluctuations driven by random solar activity.

Ratcliffe: I should like to take up one point mentioned by Dr. Martyn, the question of the reality of the winds as exhibited by meteors. Meteor observations lead to the semidiurnal rotating wind. Reflected wave measurements, at greater heights, also lead to observations of the semidiurnal rotating wind. Putting these results together you find a smooth curve that gives the phase of the semidiurnal rotation from 85 to 110 km. There is some doubt whether the irregularities move with the wind above about 90 to 100 km.

Manning: I should like to point out the reason why we believe that meteorgrams *do* represent wind velocities. If the ionization in the meteor trail did not move with the air, it would be because of the force imposed by the earth's magnetic field. Since the magnetic field is inclined at a large angle to the horizontal, it would induce a vertical as well as a horizontal velocity. We have shown that the vertical mean drift velocity is no more than 1.5 m/sec as compared with horizontal mean drift velocities of 50 to 70 m/sec.

Chairman: May I say in conclusion that we have made some progress in noting possible mechanisms of generating turbulence in the presence of vertical stabilizing density gradi-

ents. The argument that turbulence would be suppressed in view of the large value of the Richardson number is evidently too simple, since it takes account only of the vertical density gradient averaged over the horizontal plane. At least two mechanisms for generation of turbulence have been pointed out: (1) shearing motion in the horizontal plane produced by the thermal wind; (2) shear, with no particular preference of direction, associated with the large-scale disturbances produced by what Professor Sheppard called slantwise convection.

Morning Session

Friday, July 10, 1959

Chairman: D. F. Martyn

Chairman: Gentlemen, I think most of us got the impression yesterday that the discussion (the theoretical discussion) might have got a little bit ahead of the fact. And so this morning Dr. Millman will present to us some facts which, I think the ionospherists are agreed, do show rather clearly the actual movements of the air up to heights of approximately 100 km, plus or minus a few kilometers. So, without further ado I will ask Dr. Millman to deliver his paper, describing these observed movements.

Visual and Photographic Observations of Meteors and Noctilucent Clouds

P. M. Millman

The primary parameters that determine the altitude of a visual meteor—meteor velocity, brightness, and angle of the path to the vertical—were discussed. It was noted that persistent meteor trails show a similar height distribution to meteors and reveal differential wind motions of various types, as well as giving evidence of rapid expansion of the train during the first few minutes after the fall of a meteor. A vertical spacing of about 6 km between major wind currents was reported as typical. It was pointed out that noctilucent clouds exhibit velocities comparable with those of meteor trails and often reveal a pattern of roughly parallel lines with a spacing of 9 km. [See paper under same title, this symposium.]

Chairman: Well, gentleman, I think it would be worth while spending perhaps 10 minutes (before we have an intermission) on specific questions on Dr. Millman's paper, and then I've no doubt that the fluid mechanists will want to ask questions about the wind shears, and so forth. But, before I ask the meeting for questions of that nature, one thing does occur to me, and it is puzzling to a nonexpert in these matters: What is the orientation of those photographs (shown by Dr. Millman)? It is hard to tell what is horizontal and what is vertical. And I should like to ask Dr. Millman if he could say anything about the relative magnitude of the horizontal and vertical velocities?

Millman: I must apologize. That is one of the things I certainly meant to cover and didn't. The meteor train velocities are essentially horizontal. There are some vertical motions, on special occasions. If I were to give a ratio, I'd say the motions are 90 per cent horizontal and 10 per cent vertical, this being the same whether averaged by frequency of occurrence or in absolute amount. Thanks, Mr. Chairman, for bringing that up.

Chairman: Well, in the few minutes that we have for discussion, I am sure you will want to direct your attention to specific questions tending to elucidate what Dr. Millman has said.

Krook: I wish Dr. Millman would give us some figures of the material density and energy density (as compared with the local background) introduced by these meteor trains.

Millman: The energy introduced by meteors corresponds to that of solid particles the weight of which varies from a fraction of a gram to several grams. For the very big, low trains, the weight is as much as a hundred pounds. Those that form in the upper regions are of lower weights. A zero-magnitude meteor traveling at 40 km/sec corresponds to a mass of about 1 gram, and this gives a kinetic energy of just under 10^{13} ergs. If the low densities determined

Harvard are correct, such an object corre-sponds to about a 3-cm-diameter meteor. How-ever, many of these trains are produced by aeroidal matter which is denser, like heavy k and nickel-iron.

I don't want to get on the subject of the number of ions left along the trail, but I could mention that values of electron line density along the trail range from 10^{8}/cm to 10^{16} or $10^{?}$/cm. The dividing line between what in the radio meteor case we call the overdense and underdense conditions is 10^{12}/cm.

Ratcliffe: That is, orders of magnitude larger than the background.

Lin: This is the 'line density.'

Martyn: Do the fluid mechanists understand what is meant by 'overdense trail'?

Millman: Dr. Greenhow will cover that in the next paper.

Oboukhov: What can you say of the density and temperature lapse rates deduced from meteor observations?

Millman: Meteor observations have shown densities that are in agreement with the more recent rocket and satellite data.

Frenkiel: You referred to various types of meteor trains. Are there certain types at specific altitudes at which the diffusion is not very dense? What, for instance, is the diffusive behavior at 90 to 95 km?

Millman: Owing to the extremely heterogeneous nature of the visual material, it is difficult to answer this question. For single observations of a train, no accurate height determinations are possible.

Lin: How much information is there on the spectral content of the trains?

Millman: In the nineteenth century, N. Konkoly and A. Herschel made observations with visual spectrographs. These, unlike the modern photographic determinations of the spectra directly behind a meteor, refer specifically to the long-duration trains. They concluded that the sodium D lines, magnesium green, and several other lines of varying intensity were present.

Panofsky: The pictures you presented will give you the components of wind only in the plane of the sky. What about directions away from the observer? Are the velocities quoted estimated total velocities?

Millman: They are estimated total average velocities. You cannot get the radial component with only one station. This applies also to Liller and Whipple's observations, which were made from one station.

Martyn: Those square-shaped trains you showed, were they horizontally or vertically oriented?

Millman: They were probably reproduced as seen by the observer, but I am not certain.

Phillips: I'd like to remark on the tabulation of the maximum size of the eddies shown on the board. It may be that the observations are associated more with the wake due to the meteor than the ionosphere. The data suggest that the size varies as the cube root of the time, and this is what one would expect (due to the wake).

Millman: That's an interesting concept. I am only trying to report observations, without dealing with the theoretical aspects.

Manning: This interesting remark of Dr. Phillips refers to the large visual meteors which, as a result of the large amount of momentum transfer, may create their own turbulence. The 'radio meteors' are much smaller. The results of Hawkins quoted refer to a very large meteor; perhaps the observed rate of expansion of that trail is a direct result of the meteor's fall.

Ratcliffe: Is there any evidence whether the light emitted by a meteor trail is due to charged or uncharged atoms?

Millman: The light of the meteor itself shows atomic lines of ionized state, as well as nitrogen bands. Immediately behind the meteor, the light shows very low excitation of the neutral atoms Na, Fe, Mg, and Ca. The long-duration train is chiefly (visual data) neutral Na and Mg. The ionized lines cut off sharply behind the head of the meteor. The auroral green line may show for a second or so in the upper part of the meteor path.

Chapman: I have suggested a cause for the long duration of meteor trains (published in the volume *Aurora and Airglow*). The observed luminosity may persist up to durations of an hour by drawing 'dissociation energy' from other atoms. I suggested that sodium and possibly other atoms might catalyze the recombination of atomic oxygen, giving luminosity in much the same fashion as the sodium line in the night airglow is produced.

Chairman: 'Measurements in the 80- to 100-km region from radio echo observations of

meteors.' I've left one word out of the title, just to avoid any controversy.

Measurements of Turbulence in the 80- to 100-Km Region from the Radio Echo Observations of Meteors

J. S. Greenhow and E. L. Neufeld

The use of radio echoes from meteor trains to measure irregular winds at heights of 80 to 100 km was described, and recent results were reported. It was stated that large irregularities with a vertical scale of 6 km, a horizontal scale of the order 150 km, and a time constant of 6×10^3 seconds have been observed; that the rms wind velocity associated with these irregularities is 25 m/sec; that turbulent wind shears of the order of 10 m/sec km have been found, although occasionally shears as high as 100 m/sec km have been noted. Lower limits for the scale and time constant of the smallest eddies were determined on the basis of the universal equilibrium theory of turbulence. [See paper under same title, this symposium.]

Chairman: Gentlemen, I suggest that we direct our questions, first of all, specifically at Dr. Greenhow and then later on continue the discussion of both papers.

Long: You said that the length scale of the order of 150 km was thought to be horizontal?

Greenhow: Yes. The horizontal scale is thought to be 150 km and the vertical scale only 6 km.

Batchelor: I found Dr. Greenhow's discussion of turbulent diffusion very interesting. But I am not clear why he identifies the duration of the trail with the time constant of the smallest eddies. The 'smallest eddies' are those so small that the viscous forces act strongly. The eddies that would be most important in diffusing the trail would be those on a scale comparable with the width of the trail. The question then is: What sort of width would the trail have at a time of about half its lifetime?

Greenhow: Ten meters is a reasonable value for the width of the reflecting column, which we believe is of the same order as the scale of the smallest eddies. The observed echo durations can be used to set limits for the parameters of the smallest eddies. This leads to a scale of a few tens of meters.

Bibl: Did you try a harmonic analysis, for lunar tide effects, involving higher terms?

Greenhow: If we average several days' observations, no components greater than 2 m/sec a left, other than the solar 12- and 24-hour tid components. The magnitude of the 12-hour ha monic is 20 m/sec.

Sheppard: With regard to what Dr. Gree how said this morning, that, at the levels co cerned, 'it was always turbulent,' in a pap several years ago you said something rath different: that it was 'only occasionally turb lent' at these levels. I just want to clarify th point.

Greenhow: Yes. We now believe that the a mosphere is always turbulent between heigh of 80 and 100 km.

Sheppard: Do you find any seasonal var tion in the scale of turbulence?

Greenhow: Over a 3-month period we ha detected no variation.

Sheppard: At what heights are the measu ments, and how are they determined?

Greenhow: The results refer to the heig range 85 to 100 km: A direction-finder meth was used initially. It is accurate but labo ous. We have therefore calibrated rate of dec of echo amplitude against height, and get ±3-km accuracy. Height differences on any o trail in the spaced station experiment are kno much more accurately.

Morkovin: How did you get the estimate density? If I understood correctly, the tr diameter was 4 km after 100 seconds. What important is the relative dispersion betw particles, not the displacement from where be were before. Can you elucidate this point?

Greenhow: This 4 km is the diameter trail would have assuming strong eddy diffus to be present. The experiments I describ showed that the broadening was one or t orders of magnitude less than this, showing th small-scale turbulence with a time constant 0.4 second is not present.

Ratcliffe: I am going to ask a question, which may possibly clarify what you peo are discussing. If I have understood correc Dr. Greenhow imagines that the trail begins being very narrow, straight, and very den Now, if you take the initial linear density electrons of 10^{16}/cm, which he stated is an tense one, then by theory this very inte trail would slowly widen itself by ordinary d fusion....

Martyn: 'ambipolar' [diffusion] . . .

Ratcliffe: . . . ordinary ambipolar diffusion. hen the volume electron density in this trail omes less than that which is critical for the io-wave frequency, am I right in understand- that this is the instant at which Dr. Green-v suggests the trail will begin to give a much akened echo? If it is, then I've just done a ntal calculation (which he hadn't time to do cause people have kept shooting questions at n). I make out that it is then expanded to) meters in radius. So it seems to me that one the figures that people have been asking out is this: if you begin with a linear density 10^{16} electrons per linear centimeter, if this ng spreads by ambipolar diffusion to 100 ters in radius, then it has just ceased to re-ct radio waves. I just did that little calcula-n because it was one somebody asked for and . Greenhow hadn't been given time to do it.

Greenhow: I guessed 10 meters for the radius the overdense column. The formula for trial dius used by Mr. Ratcliffe presumably is $r^2 =$ Dt, where $D \sim 4 \times 10^4$ cm²/sec. However, s is not the radius of the reflecting column, ich is the cylinder inside which the electron nsity exceeds the critical density. The radius this cylinder remains almost constant with ne at about 10 meters until the end of the ho.

Martyn: Ambipolar diffusion, not eddy diffu-n.

Batchelor: To what did the estimate 4 km fer?

Greenhow: This was under the assumption at eddy diffusion was present.

Kovasznay: That would just replace D by other factor?

Greenhow: Yes, by a D that increases with ne as the bigger and bigger eddies become ective.

Chairman: Are we all clear on that now? od. At this time, Dr. Millman would like to esent some additional information arising m his radio observations of meteors.

TE ON SOME OBSERVATIONAL CHARACTERISTICS OF METEOR RADIO ECHOES

P. M. Millman

Range-time records of meteor radio echoes observed at Ottawa were reported. The advantages of this measurement technique in separating the return from various portions of the path were pointed out. It was noted that the trains are rapidly broken up into rough patches that may persist for several minutes. The fading rate for the longer-duration echoes was given as 20 cps. [See paper under same title, this symposium.]

Martyn: The point has been made during previous discussion that possibly the meteor creates its own disturbance in the atmosphere. It would be very helpful if there were some means of disposing of that suggestion, or if we had some discussion of it. One point that does occur to me is that Dr. Millman and Dr. Greenhow have been observing very different kinds of meteors, by and large. Dr. Millman has been concerned with very large meteors, up to several pounds, whereas Dr. Greenhow's are really micrometeorites, the size of pinheads or specks of dust. It does seem to me that the results are not quite the same: Dr. Greenhow's rms velocities are about half those observed for the large meteorites. Very large chunks of matter coming into the atmosphere ought to create a much bigger disturbance than dust particles.

Greenhow: Yes. The radio meteors are all very faint—6, 7, 8 magnitude. Their masses are measured in milligrams. The amount of energy in the wake is negligible.

Batchelor: Is there some estimate of the Reynolds number of the wake of a meteor?

Corrsin: Before the coffee break, we calculated for Dr. Millman's meteors a wake Reynolds number of 200 to 250. This might indicate why there is not much difference between the large and small structure.

Millman: Weights may be several kilograms for meteors producing long-duration visual trains. The largest meteors for which we have radio data are -5 magnitude, weight about 100 grams.

Bates: I wish to call attention to the technique, recently developed, which supplements the meteor technique to some extent. This is the ejection of matter (sodium) from rockets. The results so far indicate that shears below 120 km are similar to those deduced from meteor data; above that level, very small.

Howells: We have seen some evidence against turbulence on a scale smaller than a Fresnel

zone. Would you expect this from the whole trail?

Greenhow: I think the fact that we get only a small number of discrete echoes from the trail suggests that we are dealing with the large scales only.

Howells: Large compared with a Fresnel zone?

Greenhow: A radar equipment cannot see anything smaller than a Fresnel zone: this could be a few meters long when the trail becomes distorted.

Bowles: I'd like to ask whether the discussion perhaps treated several different conditions that we need to consider. Then I'd like to mention something that we have observed similar to Dr. Millman's observations. I believe that Dr. Greenhow's records show the large majority of the things observed, although conditions conducive to small-scale turbulence may nevertheless exist part of the time. I'd like to treat the triangular echo described by Dr. Millman. We have been doing, over an oblique path, measurements of the signal strength for long-duration meteors. We find that in a significant number of cases the decay is more or less exponential, with a half-life of some 20 seconds.

Greenhow: I have purposely kept off the (thorny) subject of echo amplitude decay. Depending upon whether linear, logarithmic, or a combination of both types of scales is used, it is possible to fit decays of almost any variety.

Millman: A paper by Millman and Rao on the triangular (*b*-type echo) is being prepared for the *Canadian Journal of Physics.*

Manning: Dr. Greenhow has presented results on the height structure of the winds at meteoric heights, based upon an experiment in which he compared echoes returned from a single trail at different heights. It may be interesting to compare his results with those we have obtained at Stanford, using several independent experimental approaches [L. A. Manning, Air motions and the fading, diversity, and aspect sensitivity of meteoric echoes, *J. Geophys. Research,* in press]. We have assumed that the trail distortions can be attributed to horizontal winds similar to those photographed by Whipple and Liller, and we describe the wind profile as a Gaussian function with an arbitrary wavenumber spectrum function. Use is made of experimental observations on (1) the loss aspect sensitivity of radio reflections with t passage of time, (2) the gradual rise and subs quent precipitous drop in average fading fr quency versus time, (3) the loss of correlati of fading patterns in spaced receivers with tir and increase in spacing, and (4) the delay aft echo appearance before the echo starts to fac

The results showed that (1) the air motio of the type photographed by Whipple ar Liller contain relatively little velocity in scal less than 1 or 2 km, (2) the rms North-Sou component of velocity is about 50 m/sec, (the rms value of the relative maxima of t wind gradient is about 100 m/sec/km, (4) t horizontal components of wind velocities becor independent when the height differential about 6.4 km, and (5) the time constant rotation of the smaller eddies must be long than for the maximum observed shears of ($\sec^{-1}$ for scales of 1 or 2 km.

From the early Stanford work on winds usi the radio-meteor Doppler techniques [L. Manning, O. G. Villard, Jr., A. M. Peterso *Proc. IRE, 38,* 877–883, 1950; L. A. Mannin A. M. Peterson, O. G. Villard, Jr., *J. Geoph Research, 59,* 47–62, 1954], we found an avera downward vertical drift velocity of 1.5 m/s although the value zero is not excluded by t precision of measurement. The rms vertic velocity was shown to be no more than rough 10 m/sec but is probably considerably le Taken together with our measurements of ho zontal speeds of 70 m/sec or so (confirmed the more extensive measurements of J. S. Gree how, *Phil. Mag., 45,* 471–490, 1954, and of W. Elford and D. S. Robertson, *J. Atmospheric a Terrest. Phys., 4,* 271–284, 1953), these resu show the air motions to be strongly confined the horizontal.

Longuet-Higgins: I should like to refer to t existence of 'double trails.' These are said to hollow cylinders, but turbulent wakes are n generally of this form. Is it possible that t ions and electrons are moving apart in opposi directions?

Greenhow: No. I don't think so.

Martyn: In ambipolar diffusion, they [io and electrons] go with each other.

Booker: I should like to see if I could pe suade Dr. Millman to quote a figure which

ously avoided quoting in his paper. He ribed a distortion of meteor trains as well as read of the train, but he never actually gave umerical value for the diffusion. Are the s of spread involved in the long-duration eors of the same order of magnitude as those molecular diffusion?

illman: The only figure I have is 6 m/sec (for 31 trains) for average spread in radius (12 m/sec for diameter) over the first few minutes after train formation.

Booker: Is there any possibility that it is ordinary molecular diffusion? It's the power of 10 that is wanted.

Martyn: I saw a calculation in Australia . . . off by 10^3.

Afternoon Session

Friday, July 10, 1959

Chairman: R. W. Stewart

hairman: Professor Corrsin, of the Mechani- Engineering Department, The Johns Hop- University, will continue our course in ulence with a discussion of some working ons of turbulence.

utline of Some Topics in Homogeneous Turbulent Flow

Stanley Corrsin

The broad problem of turbulence and its in- insic difficulties, both mathematical and phys- al, were outlined. Correlation and spectral ethods of analysis were noted, the kinematic d dynamic relations for the isotropic case ere set down, and the mechanism of energy ansfer among spectral components was de- ribed qualitatively. Reynolds numbers were scussed, and a detailed comparison was made some characteristic lengths. Various theories turbulent energy transfer were considered riefly and compared. [See paper under same tle, this symposium.]

hairman: I am sure many of you have ques- s you would like to ask Professor Corrsin. I gest, however, that we hold all questions il after the next paper, at which time there be ample opportunity for general discus- and perhaps for several short related con- utions as well.

t this point we turn somewhat aside from strict study of turbulence to consider the cts of a stable density gradient, a condition now know to be characteristic of the iono- ere.

Motion of Fluids with Density Stratification

R. R. Long

The mathematical complications of the theory of fluids with density stratification in a gravitational field were pointed out. It was noted, however, that the problem is tractable by the use of boundary-layer theory in some interesting nontrivial cases. A few of these were discussed, and it was shown that under many circumstances flow of a stratified fluid is characterized by the presence of strong velocity concentrations or jets. This phenomenon, as observed in the laboratory, and in the atmosphere and oceans, was compared with the theory.

Batchelor: From one of Professor Long's formulas it can be seen that the disturbance results in instability when the relative velocity of the two streams exceeds twice the speed of the disturbance in the absence of any relative motion of the two streams. Does he know of a simple physical reason why this speed should be critical?

Long: No.

Bowles: Could Professor Corrsin indicate the relation of radio scattering to the manner in which the turbulence spectrum varies with wave number?

Corrsin: I should like to refer that question to Dr. Batchelor.

Batchelor: The subject will be taken up in detail tomorrow, but I can say now that the general action of turbulence is evident. The

turbulent fluid convects electrons, which are also subject to 'molecular' diffusion. In the range of wave numbers relevant to forward scattering (the inertial subrange) the spectrum of the spatial distribution of electron density is found to have the same dependence on wave number as the distribution of velocity. The cutoff wave numbers are not always the same in the two cases, however.

Hasimoto: In the problem of the motion of a flat plate considered by Professor Long, has a linear approximation been considered?

Long: A Stokes' flow type of solution has been obtained and fair agreement with experiment observed, but some question remains whether the velocities are low enough for the approximation to be valid.

Booker: It would seem important that the method of obtaining correlations be defined. This refers particularly to the presence of the factor 2π in the Fourier analysis. Some data that apparently agree may be in error by as much as a factor of 10.

Corrsin: As far as turbulence is concerned we still stand on the original definition of correlation function as given by Taylor.

Frenkiel: Where should a factor π appear?

Corrsin: It only appears in the definition of the wave number in terms of wavelength. Since a turbulence 'scale' is not a wavelength in any simple sense, we arbitrarily choose to relate characteristic scales and wave numbers without employing the factor 2π.

Goldstein: One should be careful in nonisotropic situations when two completely different scales are present. In particular the method Greenhow described this morning was not clear.

Greenhow: The fall-off in velocity correlation both vertically and horizontally was investigated. In the vertical direction the correlation appeared to fall to zero in about 6 km, whereas the fall in correlation over a similar horizontal separation was barely significant.

Frenkiel: It should be pointed out that zero correlation does not mean the same as *no correlation.*

Bowhill: It seems important to decide where on the autocorrelation function the structure size occurs. For instance, Greenhow chose the point where the autocorrelation function crossed over. If instead a parabola were fitted to the curve a considerably different value for th vertical structure would be obtained.

Corrsin: The only thing that really seem important is that each worker carefully expla how his determination is made.

Kovasznay: It seems decessary to incluc two parameters except in special cases, one fo the integral scale and one for the microscale.

Goldstein: Since the length scale depends o the area under the correlation curve the defin tion used for this seems important, particular with nonisotropic turbulence.

Corrsin: Experimentally the procedure is t measure the correlation function in all direc tions for nonisotropic turbulence.

Frenkiel: It should be pointed out that th correlation curves are not identical when meas ured in different directions, even in isotrop turbulence. The curve for the horizontal com ponents of the velocities at two points along horizontal direction is different from the curv for two points along the vertical direction.

Chairman: It would seem appropriate a this time to have two short communicatior relative to this matter of flow in a stably strat fied atmosphere.

On the Structure of Turbulence in Electrically Neutral, Hydrostatically Stable Layers

H. A. Panofsky

Varied evidence of the quasi-horizontal na ture of eddies in stable layers, at altitudes fro 100 meters to 13 km, was reported. It was sug gested that a whole spectrum of such aniso tropic eddies exists. [See paper under same titl this symposium.]

On the Similarity of Turbulence in the Presence of a Mean Vertical Temperatur Gradient

A. S. Monin

The frequency spectrum of vertical turbu lence components was considered in the case o a vertical temperature gradient. Similarit methods were employed, one to describe th energy and inertia ranges, another (Kolmogo roff) to describe the inertia and dissipatio ranges. It was suggested that, since both theo ries hold in the inertia range, a relation can b determined between the two unknown univers functions involved. It was claimed that predic

ns based on both theories are in good agree-
nt with measurements. [See paper under
ne title, this symposium.]

tchelor: At what height were these meas-
ents carried out?

onin: From 1 to 4 meters above the ground.

ewart: Were these the components of the
ity in the wind direction?

onin: These were vertical velocities.

nofsky: Other measurements seem to dis-
e with the $-5/3$ law. In particular, aircraft
surements, which seem applicable, average
to a slope of -1.9 to -2.0.

ewart: Recent measurements of turbulence
ocean tidal stream at high Reynolds num-
agree with the $-5/3$ law over a range of
e numbers with a factor of 100.

ines: Is a horizontal wind varying rapidly
e vertical direction a horizontal or vertical
r?

eppard: Vertical.

orkovin: Would Professor Corrsin give
e information on laminar and turbulent
es as applied to meteors?

orrsin: The classical problem of an axisym-
ric turbulent wake has been well covered in
essor Goldstein's book. The wake width
s as $\delta \sim x^{1/3}$. The maximum velocity
ement decreases as $\Delta u \sim x^{-2/3}$. These values
obtained from similarity and mass and
entum conservation. The problem of the
t on a small wake by relatively large turbu-
fluctuations has not really been studied.
nazi has presented results for wakes in a
intensity turbulent regime.

orkovin: There seem to be some discrepan-
between measurements on small meteors
those on large meteors. Besides diffusion
s, the immediate appearance of the full
e in the ionograms of larger meteors might
ibly be attributable to differences in laminar
turbulent wakes.

orrsin: It should be pointed out that the
nolds number in a wake decreases with dis-
e behind the generating body so that a
e can go from turbulent to laminar.

Goldstein: The critical Reynolds number for a wake is different from that for other flows.

Corrsin: A reasonable critical value for a wake flow would seem to be about 10. (The Cavendish fluid dynamics group suggests, on the basis of some of their recent experiments, that 100 may be a better value for round wakes.)

Ratcliffe: Would Professor Long clarify the model he discussed and its relation to the problems under study by this group?

Long: The model presented seems like the simplest possible that will allow analysis with perfect fluid theory, therefore making the problem tractable.

Ratcliffe: Since the model requires the introduction of a discontinuity into the fluid, what relation would the solution have to a continuously varying medium?

Long: From the laboratory experiments on continuously varying media agreement has been obtained with the model considered. This agreement encourages extrapolation to atmospheric problems.

Ratcliffe: The laboratory experiments show only motions induced by flows over objects; could this have any relation to the static atmosphere?

Long: Though this is true, the experiments and theory indicate that disturbances of stratified fluids lead, typically, to jetlike motions. Such motions are indeed observed in the troposphere, and there is every reason to believe that they occur in the ionosphere. In fact, they would explain many of the observations presented this morning.

Rott: The typical length of a jet given by you was 10^{10}; was this centimeters?

Long: Yes, for molecular diffusion.

Rott: Could this type of flow occur even though it is several times the circumference of the earth in length?

Long: Observations indicate the typical jet length in the troposphere to be several thousand miles. This is very much less than the length given above.

Morning Session

Saturday, July 11, 1959

Chairman: S. Chapman

Chairman: Since we have a great deal of ground to cover this morning, I suggest we commence immediately with Professor Booker's paper.

Radio Scattering in the Lower Ionosphere

H. G. Booker

Various radio phenomena that may be related to turbulent irregularities in the ionosphere were noted and discussed. It was decided that measurements of scattering from below the E region are most readily interpreted and give maximum information as to motions in the 70- to 100-km interval. A general theory of scattering by (anisotropic) irregularities was developed, showing that the scattering cross section depends on the Fourier spectrum of the dielectric constant deviations evaluated in the associated mirror direction at the scale $\lambda/(4\pi \sin \theta/2)$. In applying these results to the ionosphere, various correlation functions, the corresponding spectra, and the angle and frequency dependence that result were presented for comparison with empirical data. Some recent NBS data were displayed. These indicated a somewhat variable frequency scaling law but always a higher power than the simplest interpretation of turbulence would suggest. [See paper under same title, this symposium.]

Booker: In connection with the talks by Messrs. Millman and Greenhow Friday morning I should like to add the following comments. Mr. Greenhow stated that his radio observations of long-duration, overdense meteor trails indicated that often the trail remained smooth (on a scale of a few meters) for times of the order of 100 seconds, and that this fact was inconsistent with my estimate of the time scale of an irregularity of this size. I should point out that the overdense trail will quickly become surrounded by underdense ionization. Thus the local wavelength of the radiation at the point at which the rough overdense trail is encountered might be very large. This will greatly reduce the scattering effectiveness of the rough trail, and thus the echo will still appear as an approximately specular reflection, even though the trail may actually be quite rough. Of course, the underdense ionization will also produ scattering, but perhaps the sensitivity of Gree how's equipment was not sufficient to dete this.

The explanation of the meteor 'head echoe observed by Millman appears to require t very rapid formation of scattering centers fro overdense trails. Perhaps this scattering com from the underdense ionization. It would see worth while to examine carefully the relati sensitivity of Millman's and Greenhow's equi ment.

Chairman: We are running somewhat behi schedule already. Consequently, I shall not c for questions but shall ask Dr. Martyn to pr ceed at once with his paper. In view of the tim he has kindly agreed to restrict his talk so th we shall be assured of ample opportunity f discussion before the end of the morning.

Large-Scale Movements of Ionization in the Ionosphere

D. F. Martyn

The complex causes of variations in and m tions of ionization were noted, as was the dif culty of differentiating real and virtual motio An instability mechanism for deviations in io zation density on the under side of an upwar moving layer was suggested. It was pointed o that the temporal and spatial morphologi predicted by this mechanism appear to be co sistent with those of the occurrence of sporad E, spread F, and radio-star scintillations. [S paper under same title, this symposium.]

Martyn: Professor Booker made some co ments regarding radio-star scintillation, sprea F, and sporadic E to which I should like to a a few words. These phenomena are most like to occur when the dynamo currents of the ion sphere are flowing to the east (the H co ponent of the geomagnetic field is maximum although there is some doubt about this in t auroral zone.

A slab of ionization density λN, imbedd in a medium of uniform ionization density which also contains a uniform electric field

d a uniform magnetic field H, and which is rmal to the direction $\mathbf{E} \times \mathbf{H}$ will move with velocity

$$V = \frac{E}{H}\left(1 + \frac{\nu_e \nu_i}{\omega_e \omega_i}\right)^{-1}$$

ich can be seen to be independent of λ. If consider a sphere under the same conditions, wever, it will move with a velocity, *relative the background ionization*, given by

$$\frac{E}{H}\left(\frac{\lambda - 1}{\lambda + 2}\right) \quad \text{if} \quad \frac{\nu_e \nu_i}{\omega_e \omega_i} \ll 1$$

The analogous result for a cylinder is given by

$$\frac{E}{H}\left(\frac{\lambda - 1}{\lambda + 1}\right)$$

the Hall conductivity is important this becomes

$$\frac{u(\lambda^2 - 1)}{4\lambda \cos^2 (\alpha - \beta) + (\lambda - 1)^2}$$

ere

u = velocity of background ionization.
$\tan \alpha = \omega_e/\nu_e$.
$\tan \beta = \omega_i/\nu_i$.

ow, however, the irregularity no longer moves a solid body.

Chairman: At this time Mr. Becker, of the ax-Planck Institut, will present some additional evidence of vertical movements.

[Mr. Becker showed some slides illustrating observations of large upward movements of the F region which did not appear to produce any particular change in the structure of the F region as revealed by the contours of constant ionization density.]

Becker: I should like to ask Mr. Martyn if thinks that upward movements of the F region must produce spread F?

Martyn: They are most likely to at night.

Becker: Our observations were made near dnight.

Bowles: I want to report on some observans of equatorial spread F which appeared to in fairly well with Dr. Martyn's ideas. A forrd-scatter experiment along a north-south e, performed in conjunction with ionospheric undings, indicated the presence of small irgularities of the order of a few meters in diamer at heights up to 500 km. The scattering centers, together with a particular type of spread F that exhibits no retardation effects, appeared when the F layer began to rise just after sundown.

Ratcliffe: I should like to warn against overemphasizing the region below 100 km and to add a few comments to Mr. Booker's talk. Problems arise in the upper regions because, for one thing, the diffraction pattern produced on the ground by a reflected radio wave may show smaller-scale sizes than the irregularities in the ionosphere that produced the pattern. It is also very difficult to say at what height, if it is in fact a fairly localized height, a diffraction pattern is imposed on a radio wave that passes through part or all of the ionosphere. In spite of this, however, most ionospherists would probably agree with the following statements:

1. In both the E and the F regions there are sometimes isolated traveling disturbances of the order of 10 to 100 km in extent.

2. Even when there is no traveling disturbance, a wave reflected from the ionosphere always produces a diffraction pattern on the ground which is caused by irregularities of the order of 10 km and larger.

3. There is circumstantial evidence for the existence of real small-scale irregularities (correlation wavelength down to 200 meters) in the E region. In the F region the situation is not too clear.

4. Except at the equator, the irregularities are statistically circularly symmetric in a horizontal plane. At the equator they are elongated considerably along the magnetic field lines in both the E and the F layers.

5. There is evidence that the irregularities are disk-shaped rather than circular. They do not extend far in the vertical direction.

6. Most workers agree that there are F-region irregularities above 250 km.

Kovasznay: What is the relation between the exponent n involved in the power-law radio-scattering formulas discussed in Mr. Booker's paper and the exponent (call it m) involved in the spectral power laws of three-dimensional turbulence.

Batchelor: The scattering cross section is given by

$$\sigma \propto [\overline{(\Delta\epsilon)^2} F(\mathbf{k})]/\lambda^4$$

where

$$k = |\mathbf{k}| = (4\pi/\lambda) \sin(\theta/2)$$

and $F(\mathbf{k})$ is the density of contributions to $\overline{(\Delta\epsilon)^2}$ in wave-number space. In the ionosphere, where the fluctuation $\Delta\epsilon$ in refractive index is caused by a fluctuation ΔN in electron density, we have $\Delta\epsilon \propto \lambda^2 \Delta N$. Then, assuming that the distribution of ΔN is statistically isotropic,

$$\sigma \sim [\overline{(\Delta N)^2} E(k)]/k^2$$

where $E(k)$ is the density of contributions to $\overline{(\Delta\epsilon)^2}$ on the wave-number magnitude axis. Booker has inferred from the experiments that

$$\sigma \sim \overline{(\Delta N)^2} k^{-n}$$

where $4 < n < 6$, which corresponds to $E(k) \propto k^{2-n}$.

For wave numbers in the inertial subrange we should expect

$$E(k) \sim k^{-5/3}$$

This does not agree very well with the value of n observed in the NBS experiments. Perhaps in those experiments k was near the cutoff wave number, where the spectrum falls off more rapidly.

Oboukhov: What was the lifetime of the irregularities responsible for the scattering at the 80- to 90-km level discussed by Professor Booker?

Booker: The lifetime is not known.

Lin: What is the relation between the fluctuations of ionization density and the fluctuations of neutral air density?

Batchelor: There probably are no significant fluctuations of neutral air density.

Bowles: I should like to add a comment on the NBS scatter experiment discussed by Professor Booker. Much of the variation in the power-law exponent is a diurnal effect most probably attributable to meteors. If this were eliminated, n would remain restricted to a range of about 5.5 to 6.

Batchelor: It is unnecessary and unwise to bring the correlation function into the theory of scattering. Since one ends up with the Fourier transform of the correlation function (which is the spectrum function), it is more sensible to try to determine directly the form of the spectrum function from turbulence theory. Guessing at the correlation function is a very poor way of determining the spectrum function at the large wave numbers relevant in the scatter experiments, because the tail of the spectrum is very sensitive to variations in the form of the correlation near the origin.

Booker: I agree with this, but many ionospherists find it conceptually easier to think in terms of the correlation function.

Frenkiel: Some general restrictive conditions can be placed on the correlation functions. These, together with equivalent conditions on a one-dimensional spectrum function, are:

(1) $f(k) \geq 0$	(1) $-1 \leq R(h) \leq +1$
(2) $\lim_{k\to\infty} f(k) = 0$	(2) $\int_0^\infty R(h)\, dh = L > 0$
(3) $\lim_{k\to 0} f(k) = \frac{2L}{\pi}$	(3) $\lim_{h\to\infty} R(h) = 0$
(4) $\int_0^\infty f(k)\, dk = 1$	(4) $\lim_{h\to 0} R(h) = 1$

where $f(k)$ is the one-dimensional spectrum function, L is the scale of the turbulence, and $R(h)$ is the correlation function. In addition,

$$\frac{d^2R(0)}{dh^2} \leq 0$$

although it is possible to use functions to represent correlations which do not verify this latter inequality if appropriate precautions are taken (assuming that near $h = 0$ these functions are considered approximate).

Corrsin: In turbulent flow, different quantities do not always behave in the same way. For instance, in certain wind-tunnel experiments the temperature fluctuations may have a completely different structure from that of the velocity fluctuations.

Booker: I hope we shall hear more on this subject in the future.

Wright: Some of our observational data support Dr. Martyn. The data indicate an f^{-8} frequency dependence law for scattering from sporadic-E ionization. The ellipticity of the ir-

egularities appears to decrease during magnetic isturbances.

Booker: An NBS sporadic-E experiment gave n f^{-18} frequency dependence. Although the frequencies were different in the two cases, $4\pi L/\lambda)\sin(\theta/2)$ was about the same.

Bibl: The study of vertical movements in the ' region can yield information of importance to ne fluid mechanists. I will discuss this informaon and show moving pictures in a later session.

Batchelor: Professor Booker, can you say hat was the width of the columns of auroral nization responsible for the aspect-sensitive uroral echoes.

Booker: No. I cannot give a figure for the idth of those columns. It is unknown.

Morkovin: There appear to be a number of ypes of ionospheric disturbances that should ot be attributed to turbulence.

Booker: That is certainly true. The 80- to 90-m region is not too different from the lower tmosphere, but even as you get to the E reion important differences arise, such as the effect of the magnetic field. The F region is very different from the lower atmosphere.

Morkovin: In the lower atmosphere, wave phenomena, such as discussed by Mr. Long, could provide disturbances not covered by the usual description of turbulence.

Booker: This subject should certainly be discussed more fully.

Fejer: Dr. Martyn, will your instability mechanism work above the F-region maximum of ionization density?

Martyn: There are two main differences between the regions above and below the maximum: (1) Above the maximum the gradients are much smaller, and thus the perturbation must move much farther to create a given effect than it would have to move below the maximum. This gives the ionization more time to decay. (2) Diffusion will smooth out the irregularity much more rapidly at the high altitudes above the F-region maximum. Thus the instability mechanism will be much more effective at the sharp under side of the F layer.

Afternoon Session

Saturday, July 11, 1959

Chairman: S. Goldstein

Chairman: Well, gentlemen, we have come a ood way since Thursday morning. We have earned much about the nature and structure f the ionosphere and about turbulence and moions in stratified media. I am sure that in this nal session of our 'exchange program' (beore the real 'work' begins on Monday) many f you will have questions you will wish to ask r comments you will want to make. I therefore uggest that we proceed directly with Profesor Oboukhov's paper.

The Scattering of Waves and the Microstructure of Turbulence in the Atmosphere

A. M. Oboukhov

The scattering of electromagnetic waves by inhomogeneities in the ionosphere was described briefly, and the analogy with the scattering of sound waves by temperature deviations was noted. The theory of sound-wave scattering was developed, and its relation to the microstructure of temperature was clearly shown. An experimental investigation of the angular dependence of the scattering of sound waves was reported. Fair agreement was found for scales greater than 5 cm, but at smaller scales the signal intensity dropped too rapidly. This was explained on the grounds that the effects of viscosity and conduction are important at these smaller scales. [See paper under same title, this symposium.]

Chairman: Are there any specific questions you would like to address to Professor Oboukhov before we continue with Mr. Dungey's paper?

Kovasznay: As presented, Mr. Oboukhov's paper treated the scattering of a scalar quantity by a scalar. I should like to point out that the velocity field, a vector, could be important also.

Oboukhov: Although the temperature field is ordinarily the most important factor, it makes no difference in the theory what the cause is. Therefore the effects of the velocity field, water vapor, and everything else are all included in the theory. In the sound-scattering experiments, the turbulence level was not measured by an independent means because of the difficulty of making such measurements.

Fejer: Has the scattering of radio waves in the ionosphere been investigated?

Oboukhov: That is only a proposed project. It should be noted, however, that wavelengths of less than 3 meters should be used.

Magnetohydrodynamics in the Upper Atmosphere

J. W. Dungey

Various appropriate approximations and idealizations were set forth, and the equations of motion of the charged particles were developed. From these, expressions for the electric field were developed, and it was noted that the velocity field of the ionized gas (as distinct from that of the neutral air) may not be divergence-free. The possibility of relatively intense compression of the ionized gas was suggested and analyzed in terms of Fourier components. [See paper, this symposium.]

Kovasznay: Could Mr. Dungey please explain how his paper is related to turbulence? Is this not simply a mechanism for amplification of electron density irregularities?

Dungey: Agreed, but I should like to point out that, given the velocity field, I can by this means determine the electron density spectrum.

Chairman: I understand that Mr. Howells, of Cavendish Laboratory, has some very closely related ideas he would like to communicate. This would seem to be the appropriate time to hear them.

On the Spectrum of Electron Density Produced by Turbulence in the Ionosphere in the Presence of a Magnetic Field

I. D. Howells

The equations of motion of the ionized particles under the influence of both electric and magnetic fields were given, and from them the spectra were developed for altitudes below 140 km. For greater altitudes it was noted that the charged-particle motion is restricted approximately along the magnetic lines of force but that greatly elongated irregularities would still not be produced. It was concluded that turbulence cannot produce such anisotropic irregularities. [See paper under same title, this symposium.]

Hines: Mr. Howells, can you say anything as to the relative speeds of propagation of the very small-scale components in the various directions?

Howells: The Fourier components in wave number space outside the sphere of viscous cutoff will move at about the same rate in all three directions, since the strain rates are the most important factor.

Villars: It should be noted that there are two methods of producing irregularities in the ionization field: (*a*) an effective convective field which is nondivergence-free even in a divergence-free velocity field as outlined by Mr. Howells; and (*b*) the convective action of turbulence on a nonuniform ionization field. I wonder about the relative importance of the two mechanisms.

Howells: I should say that below 80 km the factor $(n_0\Omega_+\Omega_-/\nu_+\nu_-)^2$ is too small for the first mechanism to be important. In the upper E layer, the first mechanism could be important. Notice that the spectrum produced by the two mechanisms will be different.

Martyn: I wonder if Mr. Dungey would care to comment on the source of the initial turbulence above 140 km? Would not the magnetic damping be large?

Dungey: Magnetic damping cannot be large because of the large collision time between the neutral and charged particles at 140 km. Viscosity can damp, however. Also I should point out that turbulence in the E region can produce an irregular electric field and thus an effect in the F region.

Lin: Was the 140-km height obtained on the basis of collisions between positive ions and neutrals?

Howells: Yes.

Ratcliffe: Collisions between charged particles cannot be important below an altitude at least of the order of 200 km.

Chairman: It seems to me that at this point the session should be thrown open to general questions.

Ratcliffe: I wonder if Mr. Dungey could tell

what the order of magnitude of the electron nsity irregularities in the range of 100 to 5 km would be due to magnetic compression sed on the previously given values of velocity d electron density?

Dungey: I think the limiting factor probably uld be electron recombination. I will give a merical value later.

Krook: If I have understood correctly, Mr. ungey has used a scalar pressure for the stress nsor. I wonder how serious this is at 140 km?

Goldstein: If the gas is sufficiently rarefied, is could always become important.

Dungey: I do not think the magnetic field is e important factor in making this approxima-on. If the vorticity is small compared with e collision frequency, the approximation should valid.

Ratcliffe: I recall several cases above the *D* level where the magnetic effects seemed important and the irregularities were elongated along the magnetic field. Could the mechanism described in these papers produce this type of situation?

Howells: No. It would produce isotropic disturbances.

Sheppard: Should we infer from the discussion that magnetic effects in the motion of the neutral air are small, at least up to 140 km?

Dungey: Not quite; however, the ion–neutral particle collision frequency is of the order of 1/hr, and so it will require a large time-scale motion.

Batchelor: The most important magnetic effect will be in increasing the electron density as described earlier.

Morning Session

Monday, July 13, 1959

Chairman: J. A. Ratcliffe

Chairman: As a result of a meeting of the ganizing Committee over the weekend there s been a change in the day's program. First, shall be chairman this morning, replacing Dr. tchelor. Second, a new plan will be followed. veral short papers will be presented on carelly developed ideas which, nonetheless, extend a somewhat more speculative direction. The llowing is an approximate outline:

1. Dr. Benjamin Nichols (Cornell) will present a paper on the subject of elongated irregularities.
2. Dr. R. W. H. Wright (U. College of hana) will speak on the same general topic in e *F* region with particular emphasis on spread at the geomagnetic equator.
3. Following these papers, Mr. Ratcliffe will esent a summary of the known data on the nosphere above 100 km. The region below 0 km will be summarized on Tuesday after a orking party composed of Messrs. Booker, owles, Greenhow, Manning, and Millman has scussed the data available.
4. The rate of diffusion and dispersion of visible meteor trails will be estimated by Dr. Millman.
5. Dr. Nicolet will present a tabulation of the variation of several parameters with height in the ionosphere.
6. Dr. C. O. Hines (D.R.T.E., Canada) will discuss atmospheric waves.

Evidence of Elongated Irregularities in the Ionosphere

B. Nichols

Observations of the backscatter of radio waves from ionospheric irregularities under both auroral and nonauroral conditions were described that indicate the presence of small-scale irregularities, elongated along the earth's magnetic field. It was noted that such anisotropic deviations in electron density have been detected at altitudes from 80 to 300 km and that the most accurate measurements (of auroral ionization at about 100 km) give evidence of scales of tens of meters along the earth's magnetic field and of tens of centimeters normal to the field. [See paper under same title, this symposium.]

Chairman: I suggest that questions be di-

rected first at elucidating particular points of the paper. For example, I should like to know: (*a*) What were the lengths of the auroral irregularities? (*b*) How was the thickness estimated?

Nichols: The length was judged to be ~10 to 20 meters. The thickness was estimated from the highest frequency (~60 cm, Canadian observations) used on aurora, which should have irregularities of thickness less than $\lambda/2$.

Ratcliffe: You mean there is a correlation distance of the order you mention in the aurora?

Nichols: Yes.

Dungey: How much variation in height, direction, and occurrence from night to night is observed on *F*-region irregularities?

Nichols: The heights and directions are deduced by plotting contours; this is not a very sensitive measure, and the aerial beams are quite broad. The *F*-region auroral backscatter phenomenon is of much less common occurrence than the *E*-region auroral backscatter, as would be expected, since it could only be observed from points far from the auroral zone. I don't think I can make a statement on how much it varies.

Millman: On what range of wavelengths is the aspect sensitivity deemed important? I wish to call attention to the results McNamara has been getting in northern Canada looking south toward the auroral zone using 50 Mc/s radar equipment.

Nichols: I tried to restrict myself to the cases where evidence of elongation was clean. It is quite true that as one increases the wavelength, perpendicularity conditions are less stringent. At a radio wavelength of 6 meters the echoes received may be as much as 8° off perpendicular, while at a wavelength of 75 cm 2° to 3° off is about maximum. Most of the data I referred to were obtained at the shorter wavelength.

Greenhow: Some of the E-layer measurements we have made indicate that the scattering polar diagram of the irregularities has a width of about 3° at a wavelength of 8 meters, corresponding to a length of 160 meters.

Ratcliffe: Are these auroral?

Greenhow: Yes, aligned along the earth's magnetic field.

Manning: I should like to add that the 200 Mc/s observations by Heritage mentioned earlier by Dr. Nichols also included some echoes tending to have a very abrupt rise with gradual decay. Some of these have also been correlated with the passage of large meteors although the observed echoes do not show normal meteor behavior.

Hines: Is there evidence from the movements of aurora referred to that these are not due to a moving precipitation of particles, that is, that the observed motions are due to the productio mechanism rather than true drifts?

Nichols: I don't think so.

Batchelor: I should like to point out the remarkably small lateral width observed on auroral backscatter, something of the order of a meter and not much larger than the mean free path of 10 cm. At these heights the molecula diffusivity is about 2×10^5 cm^2/sec, whic would give a radial spread of 9 meters in 1 second if the irregularities were initially of ver small width. This suggests strongly that th observed small width is a feature of the manne of production of the ionized column and is no attributable to the effect of the medium. Is th ionization due to incoming protons? And, if so would the columns produced by the protons b expected to be very narrow?

Bates: There is appreciable evidence tha incoming proton streams are not the main caus of aurora. Rocket experiments, for example, suggest that the major flux at auroral altitude may be due to fast electrons. Incident corpuscle may be in narrow columns.

Ratcliffe: May I suggest that topics on th production of auroras be continued only if the have a direct bearing on the fluid mechanic problem.

Krook: It seems to me that it is necessary t separate the two effects.

Ratcliffe: I should like to ask whether th Doppler shifts of radar echoes from meteo trails correspond to the auroral drift velocitie deduced at the same point.

Bowles: I have observed this to be the cas in my work at College, although the meteo radiants and heights involved necessitate som qualification of the point.

Chapman: The auroral zone is often characterized by strong electrical currents, carried b the motion of electrons. The total current alon the zone can be estimated at various point

ng the zone from the magnetic measurements the ground. If a reasonable cross section for e current and a reasonable electron density e assumed, the speed of the electrons can be lculated. The result agrees in order of magnide with the speeds found by Dr. Nichols with s radar measurements at College, Alaska.

Bowles: As Professor Nichols has pointed t, the observational evidence of nonauroral egularities should not be overlooked. There such observational evidence for equatorial egularities at 500-km heights as well as the anford Research Institute scatter soundings nonauroral periods.

Stewart: What fraction of the total ionizan is involved?

Nichols: The variation is less than 1 per cent.

Geomorphology of Spread F and Characteristics of Equatorial Spread F

R. W. H. Wright

The characteristics of spread F in the magnetic equatorial zone were outlined, and evidence of vertical velocities, retardation and loss of stratification in the later evening, and negative correlation with magnetic activity was presented. It was also noted that radio-star scintillations and rapid fading of long-distance, high-frequency transmissions in equatorial regions show very similar variations and correlation. Spaced receiver measurements were reported that indicate highly elongated, field-aligned irregularities in the equatorial F layer. [See paper under same title, this symposium.]

Morkovin: Would Professor Wright kindly plain what he means by the 'elongation,' and ate how it is defined?

Wright: The scales were deduced from the autocorrelation of the drifting pattern north-south and east-west. The ratio NS/EW was defined as elongation.

Martyn: Dr. Wright has shown us that spread F, sporadic E, and scintillation all tend to decrease at the equator during magnetic storms. Was this for ΔH (magnetic field) increasing or decreasing?

Wright: We used the international K_p indices. The jet currents were reduced at such times.

Chairman: At this time I should like to call on Dr. Millman for his discussion of diffusion of visible meteor trails.

Millman: From the limited amount of material with me here in Ithaca, I have assembled very approximate data on the rate of dispersion of four meteor trails. They include both visual and photographic evidence. Results are summarized in Table 1. The data of the third meteor, studied by Hawkins, are the most reliable. It should be mentioned that Hawkins observed two symmetric peaks of visual intensity at the outer edges of the trail for the first two times given; these were 75 and 150 meters in width respectively.

In each case the diffusion coefficient was obtained from the relation $r_o^2 = 4Dt$ (r_o = radius where intensity falls to the value $1/e$; D = diffusion coefficient; t = time).

Dobrovol'skii has analyzed the diffusion process for three long-duration visual trails observed in Russia. The first trail was observed for a period of 50 minutes, during which time the diffusion process could be described by means of a diffusion coefficient equal to 2.0×10^3 m²/sec. The second trail was observed for a period of

Table 1—*Meteor trail dispersion data*

No.	Date	Height, km	Time, sec	Diameter, m	Diffusion coefficient, m²/sec
1	Nov. 15–16, 1932	100	180	1000	35
2	Nov. 17, 1939	(90)	360	1200	25
3	Aug. 11, 1956	(88)	33	300	42
			240	600	94
			330	1040	790
4	May 20, 1944	(95)	45	1400	
			60	1700	(3000
			75	2200	...
			90	2500	4000)

150 seconds starting probably a few tens of seconds after the fall of the meteor. During this period the square of the diameter increased linearly with time, the diffusion coefficient being 1.4×10^3 m²/sec. The third trail was observed for about 500 seconds starting perhaps 10 or 20 seconds after the fall of the meteor. Again, the square of the diameter of the trail increased linearly with time at a rate corresponding to a diffusion coefficient of 5.4×10^3 m²/sec. Dobrovol'skii concludes, 'The coefficient of diffusion of trails is several orders higher than the coefficient of gasdynetic diffusion' [O. V. Dobrovol'skii, Diffusion of meteor trails, Academy of Science, Tadzhik S. S. R., *Bull. Stalinabad Astron. Observatory, 1,* 15–26, 1952.]

On the other hand, published data of Greenhow and Neufeld [*J. Atmospheric and Terrest. Phys.*, 1955] indicate the following values of the diffusion coefficient for underdense diffusion trails: at 100 km, $D = 13.8$ m²/sec; at 90 km, 2.8 m²/sec; and at 80 km, 0.57 m²/sec. These values are in agreement with a molecular diffusion mechanism.

In summary, apparently the diffusion of the meteor trails of some minutes' duration may be due to a turbulent mechanism. On the other hand, the radio results indicate that the diffusion of small meteor trails may be laminar.

Krook: What are the visual magnitudes of the meteors considered?

Millman: Visual magnitudes were about −3 for the examples given; the equivalent photographic magnitude is about −5.

Saffman: What are the velocities?

Millman: These were probably 60 to 70 km/sec for the first three examples.

Greenhow: Using some of the photographic meteor trails collected by Dr. Millman, I have made a plot of trail radii as a function of time. The results indicate the presence of small-scale turbulence with a time constant of 30 seconds at a height of 90 km, and lead to a value of $\epsilon = 70$ erg g^{-1} sec^{-1} for the turbulence power. [See J. S. Greenhow, Eddy diffusion and its effect on meteor trails, this symposium.]

Phillips: Just what is seen in the visible trail of these meteors?

Millman: Apparently the visible light comes from excited atoms and molecules of both the meteor and the air. The mechanism of excitation is not fully understood.

Krook: What average energy per particle can be induced by the meteor?

Millman: The energy available for the excitation of the electrons may be as high as several hundred electron volts.

Saffman: Just what temperature is required to make the trails visible, and where may this energy come from?

Chapman: As Dr. Millman said, the mechanism of excitation of the light of meteor trails is not well understood. This is especially so for those trails that continue for an hour or more. I discussed these in my fourth report to the Signal Corps under a contract between it and the California Institute of Technology (1951). These reports had only a very limited circulation, but later I gave my explanation of these persistent trails at a conference on airglow and the aurora at Belfast in 1955 [the report appeared in vol. 5 of Special Supplements to the *Journal of Atmospheric and Terrestrial Physics* under the title *The Airglow and the Aurorae*, Pergamon Press, 1957]. Rejecting the faint possibility that the energy of this light could come, over so long an interval, from that introduced by the meteor itself into the atmosphere, I ascribed its source to energy of dissociation already stored in the atmosphere. This was the source I had proposed in 1931 to explain the energy of the normal oxygen emission 5577 Å in the nightglow, and again, in 1939, to explain the emission of the sodium D light—a well-known constituent of the nightglow. In the case of the sodium, I indicated how the sodium atoms, though they continually become oxidized, could be restored to the atomic form by collision with an oxygen atom, leaving molecular oxygen and an excited sodium atom. Thus the sodium atoms continually catalyze the recombination of atomic oxygen, and in the process some of the oxygen dissociation energy is converted into sodium light. I should say that the dissociation potentials involved are not well enough known to make it certain that this process is possible on the basis of energy considerations, but the possible failure, according to the known values, is only 0.1 electron volt, indicating the need for more accurate measurements. In any event, an analogous process, perhaps in

lving hydrogen instead of oxygen, but based the same principle of drawing energy from existing store, would be the alternative. It is own that meteors introduce sodium, magsium, etc., into the atmosphere. I suggest that is sodium, or other element(s) capable of catazing recombination and drawing on the exist- stores of dissociation energy in the atmosere, must be present in unusual (though probly still small) amount in those meteors that ve a long-enduring trail. It will of course dife and become dispersed over a broader trail time passes, but as long as the store of energy which it can draw is not too much depleted, can continue to cause the emission of light. oservations of the spectrum of such long-enring trails have been made and can be used check this theory.

Millman: It is important to distinguish beeen two types of meteors entering the atmosere. The first, the comet type, are sometimes lled dust balls. These have a density of 0.1 to)1 that of water, but there is no record of a met-type meteor falling to the earth's surce. They seem to have a cometary origin and follow the orbits of the comets. The second pe is the asteroidal. These have a specific avity of 3 to 8, and many have reached the rth's surface.

Goldstein: Is there any way to distinguish tween these objects by their trails?

Millman: They can be distinguished by the ectrum and also in general by the original bit.

Sheppard: Before ascribing this behavior to e medium rather than to the meteor we ould ascertain the temperature increase due the passing of the meteor.

Saffman: At a distance behind a large meteor about 1000 meteor diameters the temperature the wake, at a distance from the axis of out 50 meteor diameters, is probably an order magnitude greater than the ambient temperare, and will be somewhat greater along the is.

Stewart: Are there visible cometary meteors?

Millman: Cometary-type meteors exist from ry faint objects to a photographic magnitude about −8.

Manning: A formula to predict the temperare expected in a meteor wake is

$$T\,(^\circ\mathrm{K}) = \frac{\text{Line density of electrons/meter}}{10^{14} \times \text{Fraction of meteor atoms ionized}}$$

and an estimate of the fraction of meteor atoms ionized would be 0.1.

Chairman: Now I should like to ask Dr. Hines to present his paper on waves in the atmosphere.

An Interpretation of Certain Ionospheric Motions in Terms of Atmospheric Waves

C. O. Hines

Internal atmospheric waves, both gravitational and compressional in nature, were proposed and analyzed briefly. It was shown that the accompanying motions may have a close resemblance to measurements of ionospheric movements. The possibility was suggested therefore that many of the observations may have their proper interpretation in terms of these waves. [See paper under same title, this symposium.]

Long: Where might these waves come from?

Hines: A first possible source is that they propagate up from the lower atmosphere; a second possible source is the tides that are known to exist in the ionosphere.

Long: Are these really internal waves due to buoyancy?

Hines: Yes. They are internal waves, and buoyancy dominates at the long periods, although compressibility is still important even then.

Dungey: Could the slantwise convection currents provide a possible source?

Hines: Yes.

Dungey: Why have you only chosen to consider phase propagation upward—which you say means energy propogation downward—when tidal energy is taken to propagate upward?

Hines: This is because on the graph I have only exhibited these modes. Both directions exist in the formulation.

Long: Would you elaborate on your infinitesimal assumption?

Hines: The nonlinear terms were neglected, and the resulting linear equation was solved. Substitution of this solution into the complete equation then showed that the nonlinear terms are 10 per cent of the largest linear terms for a value of u_x between 30 and 40 m/sec.

Oboukhov: Could the waves generated by mountains act as a source?

Hines: This is one possible source; at moderate altitudes the exponential growth seems to dominate the viscous damping.

Martyn: Are boundary conditions or temperature fluctuations considered?

Hines: Neither were considered at this stage of analysis, but they are obviously pertinent to any further development.

Chairman: S. C. Lin, AVCO-Everett Research Laboratory, would like to present another possible cause of irregularities in the ionosphere.

Lin: The effect of a steady radiation flux on the initially stably stratified atmosphere may result in a Taylor-type instability [G. I. Taylor, *Proc. Roy. Soc., A, 132,* 499, 1931]. The basic cause is the selective heating of the various absorption layers, which upsets the initial stability of the atmosphere, causing bubbles of the rarefied air to rise.

Take for example photodissociation of O_2 in the lower E region. In a crude estimate, one may assume the dissociation profile (i.e., degree of dissociation of O_2 versus altitude) to be a step function, even though available experimental data are not sufficient to indicate the actual sharpness of such a profile. [See, for example, Byram, Chubb, and Friedman, *Phys. Rev., 98,* 1594, 1955; Miller, *J. Geophys. Research, 62,* 351, 1957.] Then consider Lyman-α radiation from the sun with an energy flux of 3.4 ergs/cm^2 sec and an absorption coefficient of 10^{-20} cm^2, as given in Dr. Nicolet's paper (Table 3). The depth of the region in which most of the absorption would take place is a few kilometers (with maximum absorption around 75 km). The heat capacity per square centimeter column of this absorption layer is approximately 2.4×10^5 ergs/°K, so that the rate of density change at constant pressure is roughly

$$\frac{\partial \ln \rho}{\partial t} = -\frac{\partial \ln T}{\partial t} \approx -3 \times 10^{-8} \quad \text{per sec}$$

(The characteristic nonradiative atomic recombination time at the altitude considered is of the order of days, so that only about half of the Lyman-α energy will be available for local heating of the gas). Thus, in about 3 hours after sunrise, density change of the order of 3×10^{-4} should be observed. This amount would seem sufficient to produce vertically rising disturbances with velocities of the order of 10 m/sec in the E region. This source of atmospheric disturbance may partly account for the diurnal variation of the scattering activity in the vicinity of 80 to 90 km reported by Professor Booker [See section 4 of the paper by H. G. Booker 'Radio scattering in the lower ionosphere,' this symposium.] Diffusion could limit this activity but rough estimates indicate that it does not play an important role at the absorption altitude considered.

Sheppard: How might the horizontal discontinuities arise?

Lin: When the whole absorption layer becomes unstable, it breaks up into bubbles.

Batchelor: It should be mentioned that there is a certain amount of initial stability that must be overcome before any instability can arise.

Lin: Yes. In any quantitative treatment, the amount of initial stability of the atmosphere as well as the finite gradient of the O_2 dissociation profile should be taken into account.

Chairman: Dr. Nicolet, would you care to comment on your table of atmospheric parameters?

Nicolet: In referring to this table it should be noted that there is considerable uncertainty in the temperature gradient above 100 km.

Morkovin: Could we have some information on Coulomb interactions?

Nicolet: At the F_1 layer with a temperature of 500°K and an electron density of 10^4 1/cm^3 (night) to 10^5 1/cm^3 (day) the range in the electron collision frequency with positive ions is from 3×10^9 1/sec to 2×10^{10} 1/sec. For the F_2 layer with a temperature of 1200°K and electron number density of 5×10^5 1/cm^3 to 10[illegible] 1/cm^3, the electron collision frequency range is 2.5×10^{10} 1/sec to 4.5×10^{10} 1/sec.

Ratcliffe: I should like to report one particular observation made by the radio reflection technique which is probably of importance. It is frequently found that, in the E layer, regions in which the electron density is irregular lie above regions in which it is smooth, and that the transition from the one to the other occurs within a distance of 1 or 2 km.

Chairman: I shall now step down from the

TABLE 2—*Atmospheric data*

ight	No. density, cm^{-3}	Temperature, °A	$d\theta/dz$, °A/km	Free path, cm: mol./mol.	Free path, cm: mol./el.	Collision freq., sec^{-1}: mol./mol.	Collision freq., sec^{-1}: mol./el.	Kinematic viscosity, cm^2/sec
20	2×10^{18}	213	1	9×10^{-5}	5×10^{-4}	5×10^{8}	1×10^{10}	2
40	9×10^{16}	263	12	2×10^{-3}	1×10^{-2}	2×10^{7}	8×10^{8}	50
60	8×10^{15}	264	8	2×10^{-2}	0.1	2×10^{6}	8×10^{7}	5×10^{2}
80	6×10^{14}	200	9	0.3	2	1×10^{5}	5×10^{6}	6×10^{3}
00	2×10^{13}	222	10	10	15	4×10^{3}	1×10^{5}	2×10^{5}
20	1×10^{12}	278	12	100	8×10^{2}	3×10^{2}	1×10^{4}	4×10^{6}
40	1×10^{11}	368	14	1.3×10^{3}	7×10^{3}	40	2×10^{3}	4×10^{7}
00	10^{9}	1500		4×10^{5}		0.4		10^{10}

air for a few minutes in order to present e summary I promised you at the beginning this session.

Ratcliffe: First, by definition, the ionosphere divided into three regions. Below 90 km is e D region; from 90 to 150 km is the E re- on, and above 150 km is the F region. Four ints may be made on the region above 100 km.

(i) The ionosphere is irregular with very few ceptions.

(ii) When the irregularities are described by atial Fourier analysis the wavelength is eater than 10 km in the horizontal plane. The regularities are horizontally isotropic except ar the equator, where they are elongated in e north-south direction. The vertical scale is proximately 1 km.

(iii) At night, scintillation phenomena are served in the F region. The irregularities are gned along the magnetic field and when de- ribed by Fourier analysis measure 2 to 3 km ross and 20 to 30 km along the field. Such enomena are sometimes observed in the E gion but probably are not aligned. These may ve Fourier components down to 200 meters d sometimes occur in layers.

(iv) Traveling disturbances are observed at heights above 100 km. They move at 50 to 100 m/sec, and may have lengths from 100 to 2000 km and thicknesses of 10 to 200 km. These increase with magnetic disturbances in moderate latitudes.

Martyn: In the equatorial zone all irregularities from E to F are reduced when an electrojet is produced by magnetic disturbances. The electrojet is an eastward flow of electric current.

Stewart: Is there information on the heights and directions of these traveling disturbances?

Ratcliffe: There is no information on the height; the direction of movement is predominantly east to west. The front slopes forward.

Bibl: Cannot smaller disturbances be present?

Ratcliffe: Forward-scattering star scintillation data do not indicate such disturbances.

Nichols: It is important to remember that the scales observed will depend on the character of the experiment. The forward-scattering experiments will favor the larger eddy sizes, and backscatter experiments give evidence of smaller sizes than those stated by Mr. Ratcliffe.

Martyn: Care should be taken in stating horizontal isotropy even away from the equator.

Ratcliffe: Yes. The auroral and quasi-auroral disturbances should also be included as exceptions.

Afternoon Session

Monday, July 13, 1959

Chairman: P. A. Sheppard

Chairman: This morning we heard some interesting and I suspect highly relevant ideas put forth. Let us continue in the same manner this afternoon. The first speaker will be Mr. Manring, who will describe for us some measurements of ionospheric winds by means of artificial clouds.

Some Wind Determinations in the Upper Atmosphere Using Artificially Generated Sodium Clouds

Edward Manring

Results were given on two experiments in which sodium clouds were emitted from rockets and the effect of high-altitude winds on the clouds was observed. Triangulation photographs were taken with a 200-km baseline. The sodium was sunlit and optically thick. As a result, wind measurements have been made over an altitude interval 77 to 200 km. It was not possible to measure the diffusion rate accurately, and no significant vertical motion was detected. [See Manring and others, *J. Geophys. Research, 64,* 587–591, 1959.]

Sheppard: A similar rocket experiment was performed in Woomera by Dr. Groves, covering the range 75 to 126 km. In this experiment no vertical motions were reported below 107 km, but above this height vertical, perhaps convective, motions were observed.

Manring: In our experiment the vertical motion was definitely less than 10 m/sec.

Chairman: Next we shall hear three related contributions dealing with the hydromagnetic properties of the ionosphere. Tentatively these are to be followed by informal reports, requested by the Organizing Committee of Mr. Long on gravity wave motion, Mr. Monin on the effect of stability on turbulence, and Mr. Stewart on isotropy in turbulence. There will be opportunity for questions and discussion along the way.

On the Influence of the Magnetic Field on the Character of Turbulence

G. S. Golitsyn

The equations of magnetohydrodynamics were employed to determine the influence of the earth's magnetic field on turbulence at ionospheric heights. It was shown that below 200 km the presence of the magnetic field is unimportant as regards turbulence, and that above this altitude, the ratio of turbulence microscale to mean free path being proportional to particle number density to the one-fourth power, the problem of turbulence on a scale of interest probably does not exist. [See paper under same title, this symposium.]

Dougherty: Has the anisotropic nature of the conductivity in the ionosphere been taken into account in Mr. Golitsyn's work?

Golitsyn: No, but if the anisotropy had been included, the theory would have been even stronger.

Magnetohydrodynamics of the Small-Scale Structure of the F Region

J. P. Dougherty

The speaker disagreed with Dr. Martyn's ideas about the behavior of an irregularity of ionization density imbedded in a moving background of constant ionization density, as applied to the ionosphere. He believed that any cylindrical irregularity must extend into the E region, and that this fact would seriously alter Martyn's conclusions. [See paper under same title, this symposium.]

Martyn: I should like to explain that my approach to the problem has been to look at the global morphology of various ionospheric phenomena for a number of years. This study indicates that, at the equator, the equatorial electrojet current, which is confined to a region only a few degrees of latitude wide, is a dominating factor. Spread F (or at least one particular variety of it), radio-star scintillation and sporadic E all appear to occur in proportion to the strength of the electrojet. The effect of putting a small irregularity of ionization density in the ionosphere has then been examined and it has been found to move with a velocity different from that of the background. (It has been experimentally demonstrated at Stanford that these forces do exist in a nonuniform medium.) I agree with the assumptions made by M

ıgherty, except for the assumption that the tral particles move with the plasma. This only occur after an appreciable time delay—ut 20 minutes in the F region.

t seems to me the main point of interest in Dougherty's talk is the suggestion that the trical linkage between the E and the F regions y play an important role in this question. F region acts primarily as a motor that is ıg driven by the dynamo in the E region. s still somewhat puzzling why spread F and io-star scintillation maximize at night. Perɔs at this time there is no serious local pling between the E and F regions, and thus damping mechanism suggested by Mr. ugherty would not be effective. The global ıamo field would still exist in the F region, providing the motive power.

ʟᴇᴄᴛʀᴏᴅʏɴᴀᴍɪᴄ Sᴛᴀʙɪʟɪᴛʏ ᴏғ ᴀ Vᴇʀᴛɪᴄᴀʟʟʏ Dʀɪғᴛɪɴɢ Iᴏɴᴏsᴘʜᴇʀɪᴄ Lᴀʏᴇʀ

J. A. Fejer

In general the speaker supported Martyn's onclusions. He showed how the polarization harges are set up on the surface of the irreguırity, which changes the electric field inside he irregularity and thus causes it to drift with velocity different from that of the backround. [In the course of writing down his omments the author became aware of an error n his conclusion. For his final position on this natter, see paper under same title, this symɔosium.]

Krook: Is anything known about the stability one of these blobs which moves through the ckground medium?

Martyn: That problem is currently under instigation.

Dougherty: I think that the motion of the egularities under discussion is controlled by fields in the lower part of the irregularity ıe E region), whereas Mr. Martyn has conıded that space-charge effects are the most portant. It is my conviction that Mr. Marn's mechanism is faulty. I should also like to ɔort that I have examined the motion of an egularity resulting from various electrical d mechanical forces and have found all these ɔtions to be stable.

Chairman: I shall call now on Professor Long make his report.

Mr. Long presented a short discussion of gravity wave motions, pointing out some of the more important features of these phenomena. He also made some comments regarding Mr. Hines' paper on wave motions in the ionosphere, expressing some doubt as to the existence of vertically traveling waves. This was followed immediately by a short communication from Mr. Yih, of the University of Michigan, on a closely related topic.]

Eғғᴇᴄᴛ ᴏғ Dᴇɴsɪᴛʏ Vᴀʀɪᴀᴛɪᴏɴ ᴏɴ Fʟᴜɪᴅ Fʟᴏᴡ

C. -S. Yih

The speaker pointed out that the inertial and gravitational effects that arise in this type of stably stratified motion can often be taken into account by certain transformations of the dynamical equations which allow one to relate the motion of an analogous motion of a constant density fluid. [See paper under same title, this symposium.]

Batchelor: Could we have a clarification of the difference between the waves discussed by Mr. Long and those discussed by Mr. Hines?

Hines: I do not believe the difference is as great as Mr. Long thinks. In order to appreciate this, one must refer to the dispersion equation which, with compressibility included, is

$$\omega^4 - \omega^2 C^2(K_x^{\ 2} + K_z^{\ 2}) + i\gamma g\omega^2 K_z + (\gamma - 1)g^2 K_x^{\ 2} = 0$$

for an assumed

$$\exp i(\omega t - \mathbf{K}\cdot\mathbf{r})$$

form of the wave. One should note the imaginary term. Assume that the wave is not damped in the x direction (K_x real). Then one of two things must be true. Either (1) K_z is pure imaginary (no vertical phase propagation), or (2) K_z is k_z (arbitrary real factor) $+ i\gamma g/2C^2$). Case 1 is often the proper case in ordinary fluid mechanics (although not for sound waves), presumably because of boundary conditions, and it corresponds to the waves dicussed by Mr. Long. Case 2 gives the possibility of vertical propagation. There appears to be no a priori reason for excluding it in the upper atmosphere. It provides the only generalization for sound waves, and it corresponds to the known tidal waves. It now appears to provide an explanation for many of the observed ionospheric motions.

Oboukhov: Acoustic and gravity waves can

be separated, with some difficulty, by an examination of their frequency spectra. The results of this work will be published in an early issue of *Tellus*.

Sheppard: Theory tells us that long gravity waves often have a very high speed (close to the speed of sound). Waves traveling at such velocities are observed in the atmosphere. Is there an inconsistency between such observations and the work reported?

Long: The sort of wave to which Mr. Sheppard has referred should only occur on the free surface of a homogeneous atmosphere. The waves I have dealt with are internal waves, which travel much more slowly. They differ from those discussed by Mr. Hines only in the assumptions about compressibility. I believe the waves I have considered are more likely to be the energy-containing ones. Actually there is not too much disagreement between Mr. Hines and me. I have excluded from consideration waves whose amplitude increases with distance from the dividing surface, whereas Mr. Hines has specifically included these waves.

Chairman: It is apparent that gravity waves certainly must be looked at more carefully in connection with the ionosphere. Let us see now what Mr. Monin has to report.

Turbulence in Shear Flow with Stability

A. S. Monin

The turbulence energy balance was considered under conditions of mean-flow shear and varying density stratification. On the basis of this analysis it was suggested that in a stable situation the energy is reduced and the maximum of the spectrum shifts to smaller scales, whereas in an unstable one the reverse is true. These conclusions were actually based on empirical evidence, but it was claimed that they are justifiable theoretically since the large eddies are most affected by the Archimedes forces. [See paper under same title, this symposium.]

Batchelor: It occurs to me that the similarity conditions needed for theoretical predictions about the effect of the density gradient probably do not apply near the maxima of the curves.

Monin: I should say that similarity does hold for the big eddies.

Bolgiano: I am concerned about the relationship $\epsilon \sim (\delta U)^2/l$ for the dissipation rate. D you consider this valid in the stable case, eve though some of the energy is lost to the buoy ancy forces?

Monin: Yes.

Gifford: I should like to call to your attentio that there are meteorological observations tha support these spectrum curves.

Bolgiano: It must not be overlooked that a the experiments referred to here were performe near the ground and therefore that these resul may not be applicable at higher levels.

Oboukhov: Note that the shift to the left o the spectrum maximum is limited in the unstab case.

Rott: Was K_T determined theoretically o empirically?

Monin: It can be determined empirically.

Corrsin: The ratio of K_T/K is usually of th order of unity but varies somewhat with th type of turbulence; $K_T/K = O(1.4)$ for un bounded, forced convection flows like jets an wakes, $= O(0.7$ to $1.0)$ for boundary-layer an pipe flows.

Sheppard: Could Mr. Monin tell us somethin about the anisotropy of the large eddies as function of stability?

Monin: The anisotropy is certainly differen in the stable and unstable cases. The Australian have done some experimental work in this fiel They find that the ratio of the scale sizes de pends on the Richardson number. I cannot giv the numerical values, however.

Sheppard: Presumably the eddies become fla in the stable case.

Chairman: Interesting as this discussion i I am sure we all are anxious to hear what M Stewart has to report.

Stewart: A great deal has been made of th concept of isotropic turbulence and of the in ertial subrange, which is a range of eddy size making important contributions neither to th Reynolds stress nor to the viscous dissipatio This, in geophysical situations, is an importan range, and it is the only one for which man important theoretical deductions can be mad Nevertheless, it is important to realize tha most of the energy in a turbulent field is i eddy sizes too large to be isotropic. The con cept of isotropy is useful only when dealin with phenomena associated with turbulence o

les considerably smaller than those contain- most of the energy.

The effect of a static density gradient is cer- nly to tend to make the turbulence aniso- pic. However, a dimensional argument will ow that, on a sufficiently small scale, isotropy possible even in the presence of the density adient. In the inertial subrange the analogue the $k^{-5/3}$ spectrum is the behavior

$$U \sim L^{1/3}$$

ere U is a velocity characteristic of an eddy scale L. Even if the turbulence is anisotropic, e dependence of U on L is unlikely to be arkedly different.

Now a 'blob' of fluid which moves up against density gradient a distance h will lose energy the potential field proportional to h^2. Experi- ental studies in laboratory turbulence have own that an eddy of scale L loses all its en- gy to turbulent effects in moving a distance the order of L. Then while moving a distance it loses energy proportional to $L^{2/3}$ to turbu- nt processes. Because of the density structure, wever, it loses energy proportional to L^2. herefore for small enough L the turbulent echanisms will dominate and the density effects will be negligible. On these small scales the turbulence should be at least nearly isotropic.

Lin: A vortex ring does not lose energy in the way just described.

Stewart: True, but a vortex ring is a highly organized motion which is not included in the definition of turbulence that I prefer to use.

Booker: The last two talks are just the sort of thing that the ionospherists have been hoping to hear at this conference. I hope there will be more of it.

Bowhill: I wonder if Professor Stewart can shed any light on the question of at what scale size the L^2 and $L^{2/3}$ dissipation mechanisms become equal in magnitude?

Stewart: This depends on the density gradient. The Richardson number is the critical parameter. It is this that determines the pertinent coefficients.

Chairman: Well, gentlemen, in conclusion I think we must recognize that saying turbulence is turbulence is a dangerous practice. Laboratory turbulence and geophysical turbulence are not necessarily the same thing. In the troposphere, for example, the turbulent energy does not always transfer down from the large sizes to the small. Sometimes the energy of the turbulent motion goes into the mean motion.

Morning Session

Tuesday, July 14, 1959

Chairman: S. Corrsin

Chairman: The program this morning is mewhat more heterogeneous than previous nes. First Dr. Bowles will present a 'report of greement' of the working party that has been nsidering the region below 100 km, as men- oned by Mr. Ratcliffe yesterday. This is to e followed by some further comments on the ame region by Dr. Bowhill. Professor Booker ill then outline some of his ideas on turbulence the ionosphere and will put a number of spe- ific questions to the fluid mechanists. Dr. atchelor will follow this with two expository alks, the first on turbulent mixing of a passive calar, the second on turbulent diffusion. Next Mr. Saffman will give us some information on the wakes of meteors, and finally, if time permits, Mr. Bolgiano would like to make a few comments on the subject of turbulence in a stably stratified atmosphere. Let us now have Dr. Bowles' report.

Bowles: We agree on three broad points which we hope will be of interest to the fluid mechanics people when expressed in the form of firm numbers. In arriving at these numbers, we have avoided using any methods of the theory of turbulence. The three areas of agreement are:

1. Large-scale irregularities. There is prob-

ably more agreement on this subject than on any other. Several methods used in the determination of the size of large-scale irregularities have led to roughly the same results.

2. Velocities of the irregularities. These results refer to analyses of meteor trails only.

3. Small-scale irregularities.

1. Investigations of meteor trails by radio methods (Greenhow, Manning) and by photographic analysis (Liller and Whipple) lead to a vertical scale of the order of 6 km and to a horizontal scale of the order of 150 km. The 6 km refers to the distance between turning points in the meteor trail. In this connection it may be significant that the Norwegians, working under Dr. Landmark, have reported that there is significant variation of these parameters with season.

2. The results given below refer to the velocities of the large irregularities. For one thing, there is still no agreement on the interpretation of radio data in terms of the velocities of the small eddies; for another, the resolution of the optical systems is limited, so that the velocities of the small eddies cannot be observed by these means. The general statement can be made that vertical motions are roughly one order of magnitude smaller than horizontal motions. In connection with radio-wave reflections from the meteor trails, the important thing to note is that the velocities deduced by this method are those of the large-scale irregularities, although the strength of the echoes may well be determined by the small scales.

The various methods used give results that agree within a factor of 2 or 3. The velocities may also vary by a factor of 2 or 3 with season and latitude. At any one height the results are:

(*a*) Mean drift 25 m/sec.

(*b*) Variable long-term components such as tidal motions 25 m/sec.

(*c*) Irregular components (they range from 10 to 50 m/sec) 25 m/sec.

Note that the combination of (*a*) and (*b*) may lead to a drift from 0 to 50 m/sec.

For the gradients of velocity the results are:

(*a*) Steady shear (this refers to the variation of drift with height) 1–2 m/sec/km

(*b*) Shear of the irregular components of velocity: rough median 10 m/sec/km
upper decile 50 m/sec/km

(*c*) Maximum shear (Liller and Whipple) 25–90 m/sec/km.

(*d*) Differential of velocity (measured between neighboring maxima) 30 m/sec

3. The sizes of the small-scale irregularities are all based on radio measurements, and are deduced from the formula discussed by Professor Booker:

$$l \sim \lambda/[2 \sin (\theta/2)]$$

The results for the vertical scale of the small-scale irregularities are given in Table 3. The horizontal scale of the irregularities is probably of the order of 30 meters, and may or may not be anisotropic.

There is no compelling evidence to suggest that at meteor heights ($\sim$90 km) small-scale

Table 3—*Small-scale ionospheric irregularities*

Method used	Heights >85 km	Heights <85 km	Remarks
Reflection at vertical incidence up to 2.4 Mc/s	$l_v \leqq 60$m	$l_v \leqq 60$m	
NBS measurements at 41 Mc/s	$l_v \gg 4$m	$l_v \leqq 4$m	The $l_v \gg 4$m figure for heights > 85 km is based on the argument that no strong echo is found at this frequency at heights >85 km.
Oblique incidence scattering at 30–108 Mc/s	?	$l_v \leqq 15$m	l_v for heights >85 km is ambiguous since it is difficult to differentiate between echoes from irregularities and meteor trails

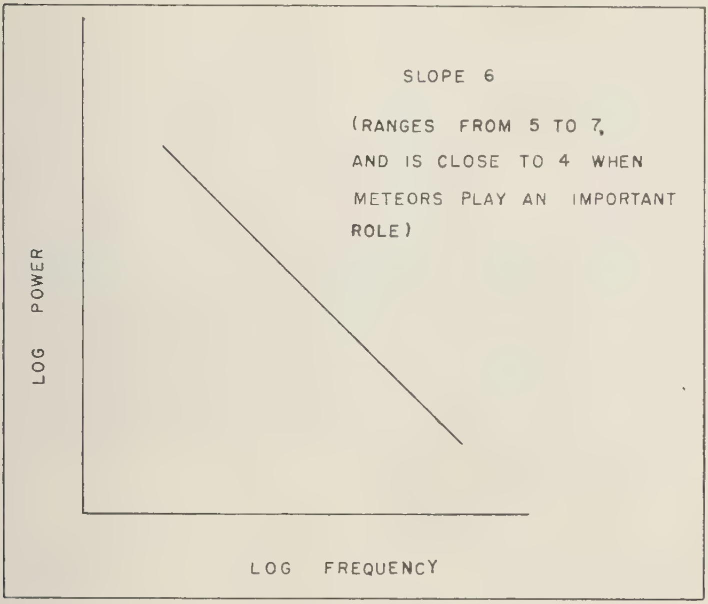

Fig. 3—Frequency scaling law for ionospheric scatter transmission.

regularities of the order of 5 meters exist apart om those connected with the meteor event self.

The graph of Figure 3 has been determined om oblique-incidence scattering of radio waves.

Bowhill: In this same vein I should like to resent the results of a set of radio-wave re- ection measurements referring to the 80- to 00-km range, which have been made at fre- uencies less than 150 kc/s, using both continu- us-wave and pulse methods. These results per- in only to the horizontal structure sizes of rge irregularities of ionization, in particular the part of the spatial spectrum of the ir- gularities that contains most of the mean- uare fluctuation. The size of these large ir- gularities has been taken to be the average stance between the maxima in the curve giv- g echo strength as a function of distance.

Our observations do not show the small scales sponsible for the scattering of VHF radio aves. The effect of those small-scale irregu- rities is to cause the spatial autocorrelation inction of the low-frequency amplitude pattern fall, say, to 0.99 in a very short distance. On e other hand, on records taken at or above 70 kc/s frequency, there is superimposed on the slow variations a much faster variation in both space and time (see Table 4). At frequencies above 100 kc/s the fast variation becomes pre- dominant. That is, in our radio measurements the size of the important large-scale eddies de- creases rather rapidly as the height of reflec- tion increases (small sizes are present in increas- ing amounts).

Two difficulties are associated with the study of irregularities by the method of reflection of radio waves:

Table 4—*Large-scale ionospheric irregularities*

Frequency, kc/sec	Height of reflection, km	Results for L, km		Time period corresponding to L, sec	
		Slow	Fast	Slow	Fast
16	85–90	30	...	400	...
70	~95	10	<2 (slight)	400	100
110		10	<2	400	100
130	95–100	..	<2	...	100

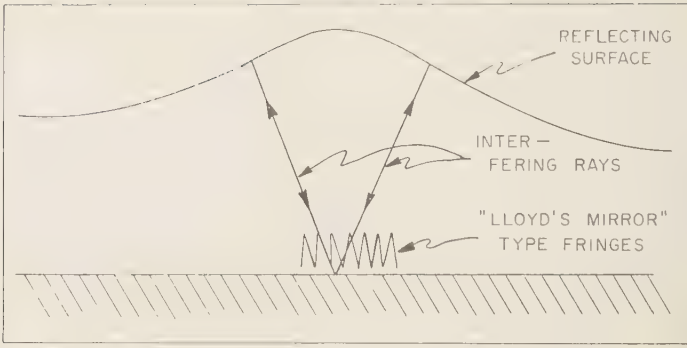

Fig. 4—Diffraction mechanism for large-scale irregularities.

1. For a large-scale irregularity there may be more than one point of reflection. The resulting diffraction pattern will then show sizes smaller than the dimensions of the reflecting irregularities (Fig. 4). At the very low frequencies employed in the experiments described above, however, the deviation in phase from such large irregularities, being less than a radian, was small enough so that this effect could not occur.

2. A more serious difficulty is the fact that the irregularities that give rise to the pattern on the ground can be located anywhere below the level of reflection. The sizes of the large-scale structure of random irregularities need not correspond with the horizontal scale of the drift motions. In fact, 'swirls' about 50 to 100 km in the horizontal motions have been observed at these frequencies [Bowhill, *J. Atmospheric and Terrest. Phys.*, *8*, 142, 1956].

Booker: I should like to substitute the numerical magnitudes that Dr. Bowles has listed into some of the relations of fluid mechanics. This is actually something that the fluid mechanics people should do. By doing it myself I hope to persuade them to make the necessary corrections.

First I should like to draw attention to some numerical facts concerning the hydrodynamic energy densities at the 90-km level. Let us evaluate the energy densities per unit mass and neglect factors of the order of 2. A subscript 1 will be used to denote quantities associated with the energy-containing eddies, and a subscript 2 to denote quantities associated with the smallest eddies. On this basis the translatory kinetic energy per unit mass is of the order of

$$v_1^2 \sim (25 \text{ m/sec})^2 \qquad (1$$

If we interpret the irregular gradients of 1 m/sec/km in terms of rotary motion, we hav an angular velocity of 10^{-2} radian/sec. The as sociated rotational kinetic energy per unit mas is

$$L_1^2(dv_1/dz)^2 \sim (60 \text{ m/sec})^2 \qquad (2$$

Because of the effect of buoyancy we also hav a potential energy per unit mass. In terms o the acceleration g due to gravity, the absolut temperature T and the gradient of potentia temperature $d\theta/dz$, the buoyancy potentia energy per unit mass evaluates to

$$L_1^2(g/T)(d\theta/dz) \sim (40 \ m/\text{sec})^2 \qquad (3$$

From equations 1, 2, and 3 we see that, so fa as order of magnitude is concerned,

$$v_1^2 \sim L_1^2(dV_1/dz)^2 \sim L_1^2(g/T)(d\theta/dz) \qquad (4$$

In other words, we are dealing at the 90-kr level with an irregular motion for which th translatory kinetic energy, the rotary kineti energy, and the buoyancy potential energy ar all of the same order of magnitude. I shoul like to know from the fluid mechanics peopl whether equations 4 is a numerical accident c constitutes a reliable scientific principle. If th latter were true, equations 4 would be very help ful in extrapolating from one height to anothe: since some of the quantities involved in them ar reasonably well known as functions of heigh

The next point that I should like to make is onveniently expressed in terms of kinetic energy per unit volume ρv_1^2. Although the irregur velocities of 25 m/sec occurring at the 90-n level seem high compared with the irregur velocities at tropospheric levels, the same is ot true of energy per unit volume. In dropping om the 90-km level to the tropospheric level e density ρ increases by 10^5. If the energy per it volume were the same in both cases, it ould imply a decrease in v_1 of $10^{-5/2}$. This ould lead to an irregular velocity at troposeric levels of about 0.1 m/sec, which is ughly of the right order of magnitude. In her words, the energy of irregular motion easured per unit volume is approximately the me at the 90-km level as it is at troposeric levels, or:

$$\rho v_1^2 \sim \text{constant} \tag{5}$$

this equation a numerical accident or the atement of some scientific principle?

It should be mentioned that ionospheric peoe have encountered equation 5 before in conction with tidal motion, and the basis for it s been provided by the fluid mechanics peoe. For tidal motion equation 5 is valid from e earth's surface up to the E region, and this the reason tidal velocities are much larger at e E-region level than at ground level.

If equations 4 and 5 are something more than imerical accidents, they would imply a rather idespread applicability of a principle of equirtition of energy to irregular motions in the mosphere. It is important, therefore, that we ould know where equations 4 and 5 stand in e wide spectrum from numerical accident to ientific principle.

The impression created in my mind by equaon 4 is that of 'blobs' of fluid of size L_1 bobng up and down under the buoyancy forces d at the same time executing random walks the horizontal plane. If these blobs of fluid e thought of as spheres 'rolling' on one anher then the first part of equation 4, written the form

$$v_1 \sim L_1(dv_1/dz) \tag{6}$$

ecomes a sort of rolling condition since dv_1/dz the angular velocity of a blob. The approximate numerical validity of equation 6 is based on the fact that a size L_1 of the order of a few kilometers, a velocity v_1 of the order of 30 m/sec, and an angular velocity of the order of 10^{-2} radian/sec fit together in accordance with equation 6.

The above situation would imply an eddy-diffusion process in horizontal planes with an eddy-diffusion coefficient given by v_1L_1. Using a value of v_1 of the order of 30 m/sec and a value of L_1 of the order of a few kilometers we obtain for the coefficient of eddy diffusion at the 90-km level

$$v_1L_1 \sim 10^5 \ m^2/\text{sec} \tag{7}$$

Now the largest figure mentioned by Dr. Millman for the rate of spreading of long-duration visual meteor trails was less than 10^4 m^2/sec. This was based on the analysis by Dobrovol'skii. When some minutes have elapsed after the fall of the meteor, the trail diffuses in accordance with a constant diffusion coefficient large compared with the molecular diffusion coefficient. The fact that the value given by equation 7 is somewhat larger than that indicated by the observations of Dobrovol'skii has to be explained. Possibly Dobrovol'skii's analysis referred to a lower level than 90 km. Let us assume, for the purposes of argument, that the discrepancy between equation 7 and Dobrovol'skii's observations could be cleared up in this way. We would still be faced with the fact that Dr. Greenhow claims that the appropriate value of L_1 in equation 7 is 150 km rather than a few kilometers. If we accept Dr. Greenhow's figure of 150 km for the horizontal scale of large eddies the disagreement between theory and observations is greatly increased.

The problem of explaining the observed rate of diffusion of long-duration visual meteor trails raises a doubt in my mind about the horizontal scale of 150 km that Dr. Greenhow has mentioned. I think he has clearly shown that there is a horizontal scale of the order of 150 km in the atmosphere at the 90-km level. But I am not sure that he has shown that there is no comparable effect at a scale of the order of a few kilometers. Suppose that important irregularities existed in the horizontal direction of the same order of magnitude as those existing in the

vertical direction; would Dr. Greenhow have known this is his experiment? I believe not. It seems to me virtually impossible to reconcile Dr. Greenhow's figure of 150 km with the known facts about the rate of diffusion of long-duration visual meteor trails.

I should now like to turn to the smallest eddies, for which we have the equations

$$v_2 = (\nu\epsilon)^{1/4} \quad L_2 = (\nu^3/\epsilon)^{1/4} \quad t_2 = (\nu/\epsilon)^{1/2} \quad (8)$$

Attempts to derive a figure for the time constant t_2 of the small eddies from radio observations have led to arguments that, in my opinion, are unresolved. On the other hand, Dr. Greenhow yesterday presented an analysis of a visual meteor trail showing that its rate of diffusion over a certain interval of time followed a t^3 law which could be extrapolated back to the molecular diffusion law. In this way he arrived at a value of t_2 of 30 seconds, and this appears to me to be the only definite information that we have about the value of t_2. If we use this value in the third of equations 8, together with the value $\nu = 4$ m²/sec for 90 km, we obtain for the turbulence power per unit mass at the 90-km level

$$\epsilon = 4 \times 10^{-3} \text{ watt/kg} \quad (9)$$

Substitution of this value of ϵ into the other pair of equations 8 gives

$$v_2 = 0.4 \text{ m/sec} \qquad L_2 = 100 \text{ meters} \quad (10)$$

Now it is true that radio scattering experiments at the 90-km level require scales from 20 to 60 meters, and these are somewhat less than the 100 meters appearing in equation 10. There would, however, be no sharp cutoff in the spectrum of turbulence at 100 meters, and equation 10 is not therefore in disagreement with the radio scattering experiments.

So far, the various numerical magnitudes that we have for the 90-km level have fitted together reasonably well. But now we come to a calculation that is alarming. Let us divide the energy per unit mass given by equation 1 by the turbulence power per unit mass given by equation 9. We obtain

$$v_1^2/\epsilon = 625/(4 \times 10^{-3}) \sim 1 \text{ day} \quad (11)$$

This implies that it would take about a day for a large eddy to get rid of its energy by the processes of turbulence and viscosity. Now the time in which a large eddy moves through a distance L_1 at the velocity v_1 is of the order of 100 seconds. Likewise the time during which a large eddy rotates through an angle of the order of a radian is 100 seconds. I was under the impression that these times were supposed to be the same as the time given by equation 11. Why does it turn out that these two times are of a completely different order of magnitude, and what are the implications of this result?

It may be noted that Dr. Greenhow's horizontal scale of 150 km fits in with the time given in equation 11 in the following peculiar way. If we picture the 'blobs' of fluid as executing random walks in horizontal planes, each walk being of 100 seconds' duration, about 1000 random walks will occur during the time given by equation 11. During this time a blob will have been displaced a distance of the order of $(1000)^{1/2}L_1$, and this is of the order of 150 km. Thus, if it really takes about 1 day for a large eddy to acquire and lose its energy, this might fit in with the idea that the driving mechanism is extended over a horizontal distance of the order of 150 km.

I should very much like to have the comments of the fluid mechanics people on the above calculations. It would not be in the least surprising if these comments took the form of making the calculations again in a completely different way. I should like to urge them to make these calculations according to the best ideas that they have. In any event I should like to have specific answers to the specific questions that I have raised.

Corrsin: I do not understand this matter of rotary kinetic energy. In a continuum the translatory kinetic energy is *the* kinetic energy; the rotary phenomena are connected with vorticity or strain rate. I am not certain what you mean by rotary kinetic energy. Do you visualize that it is energy not included in translatory kinetic energy?

Booker: All I have done there is look at the Liller and Whipple data and note that there is not much of a mean gradient—the predominant feature is an irregular gradient. I interpreted this to mean that we are dealing with irregular rotary motion, the energy of which I calculated

elementary ideas. I thought the two were ɔarate and had to be added.

Batchelor: I believe these two kinetic ener-ɛs represent essentially the same quantity, d, therefore, it should be no surprise that the st two terms of expression 1 of Professor ɔoker are of the same order of magnitude.

Long: The fact that the kinetic energy and ə potential energy seem to be of the same ler of magnitude follows from what I said eviously—we assume that we are dealing with avity waves in a steady state.

Hines: In Dr. Booker's consideration of a ıgle eddy sequence it should be noted that the rge-scale eddies must be highly anisotropic, d, consequently, that the time constant of ɛse eddies should not be calculated from the rtical shear alone. Further, if we assume, in ofessor Booker's development, that the sub-ɛipt-1 quantities refer to wave motions of the pe about which I spoke yesterday while the bscript-2 quantities still refer to a turbulence quence, many of his difficulties are eliminated. ıe ratio of horizontal to vertical scales of 18 in good agreement with Dr. Greenhow's re-lts, and the turbulence power would be re-ced, because of the anisotropy, by several or-rs of magnitude from what Professor Booker ɔuld calculate on the basis of the observed rge-scale motions.

Stewart: It seems to me that the proper in-rpretation of the very interesting figure of 1 y calculated by Dr. Booker is that the ve-ɛity v_1 is a measure of the total energy in the stem, not a turbulent velocity at all. The dis-ɔation rate, however, is a true indication of e loss of energy by the system. We find that the energy is replaced in a time of the order 1 day. Since most of the driving mechanisms e probably diurnal, it seems that this all fits gether very well.

Greenhow: A time constant of 1 hour should used for the large eddies, not 100 seconds.

Batchelor: Professor Booker has said that, we put $L = 150$ km into the formula for eddy ffusivity, we arrive at a value much larger an that inferred from observations. It would t make any sense to use a scale of 150 km, cause the scale occurring in the formula for dy diffusivity refers to the scale of the eddies at are internal to the meteor trail. Eddies of the size of 150 km would move the trail bodily without appreciably increasing its width. The maximum scale that can legitimately be put in the formula for eddy diffusivity is the width of the trail.

Chairman: Let us now call on Dr. Batchelor to present his brief account of the effect of turbulent motions on a passive scalar.

Batchelor: In general we want to treat problems where the defining equation is

$$\partial\theta/\partial t + \mathbf{u}\cdot\nabla\theta = \kappa\nabla^2\theta$$

where θ = concentration of the dynamically passive scalar quantity.

$\mathbf{u}$ = a given turbulent velocity field.

κ = diffusivity (due to thermal motion of molecules and electrons) for the quantity θ.

Unless the length scale of the spatial variations of θ is small, molecular diffusion can be neglected and we then have simply

$$D\theta/Dt = 0$$

meaning that surfaces on which θ is uniform move as material surfaces. This is analogous to the law describing changes of the magnetic field $\mathbf{H}$ in a moving, perfectly conducting fluid. The laws describing changes in θ and $\mathbf{H}$ in fluids without molecular or electronic diffusion can also be written (for incompressible flow) as

$$\frac{D}{Dt}(d\mathbf{l}\cdot\nabla\theta) = 0 \qquad \frac{D}{Dt}(\mathbf{H}\cdot d\mathbf{A}) = 0$$

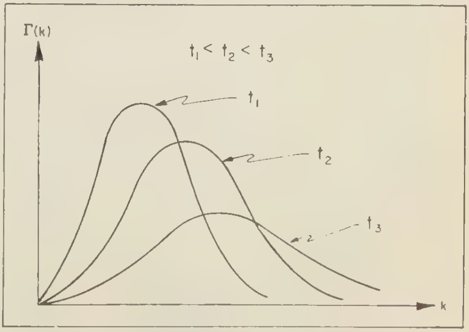

Fig. 5—Decay of fluctuation spectrum.

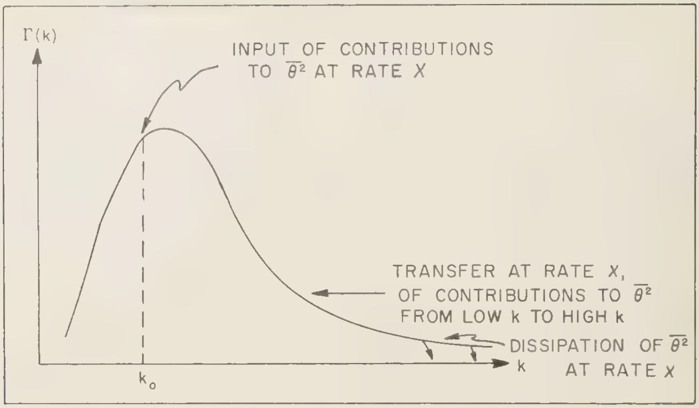

FIG. 6—Steady-state fluctuation spectrum.

where $d\mathbf{l}$ and $d\mathbf{A}$ are material line and surface elements. The solutions of these equations are

$$\nabla\theta \propto d\mathbf{A} \qquad \mathbf{H} \propto d\mathbf{l}$$

Thus, since turbulent motion always tends to increase the separation between material points, and to increase both material line and surface elements, we see that the gradient of θ will tend to increase everywhere. The effect on the wave-number spectrum of $\theta[\Gamma(k)$ say] will therefore be to shift the area under the curve in the direction of larger wave numbers, as in Figure 5, the total area remaining constant when $\kappa = 0$.

If we supply variations of θ steadily on some length scale, and include a small but finite diffusivity κ, we can get a steady state, as shown in Figure 6. From hypotheses similar to those used in the Kolmogoroff theory of turbulence we find that for k large compared with the input wave number k_0 we have

$$\Gamma(k) = f(\kappa, \chi, \epsilon, \mathrm{K}, \nu)$$

If we restrict ourselves to the range of k large compared with the input wave number k_0, but small compared with the wave numbers at which either viscous or conduction effects are appreciable, Γ is a function of the first three variables only. Then, from dimensional arguments, we have

$$\Gamma(k) \propto \chi\epsilon^{-1/3}k^{-5/3}$$

A summary of information that has been obtained recently [*J. Fluid Mech.*, *5*, 1959, 113–139] about the θ spectrum at higher wave numbers where either viscous or conduction effects are important, is given in Figure 7. As the figure shows, the results depend on the ratio of the two diffusivities, ν/κ.

Bowles: How can one estimate the wave number at which the $-5/3$ law ceases to apply?

Batchelor: This reduces to the estimation of ϵ. An empirical relation known to be accurate under most conditions is

$$\epsilon \propto u^3/L$$

where L and u are length and velocities representative of the energy-containing eddies of the turbulence.

Wheelon: Is there any experimental evidence for the $-5/3$ law of a passive scalar other than radio measurements?

Batchelor: I am aware of none at the moment.

Corrsin: Temperature fluctuation fields have been measured in warm air jets and behind electrically heated grids in a wind tunnel. Although the Reynolds numbers all have been too low to justify detailed comparison with a $-5/3$ law, there is evidence that the approach described by Dr. Batchelor is reasonable.

[S. Corrsin and M. S. Uberoi, Spectra and diffusion in a round turbulent jet, *NACA Rept. 1040*, 1951 (originally *NACA Tech. Note* 2124, August 1950).

[A. L. Kistler, V. O'Brien, and S. Corrsin, Preliminary measurements of turbulence and temperature fluctuations behind a heated grid, *NACA*

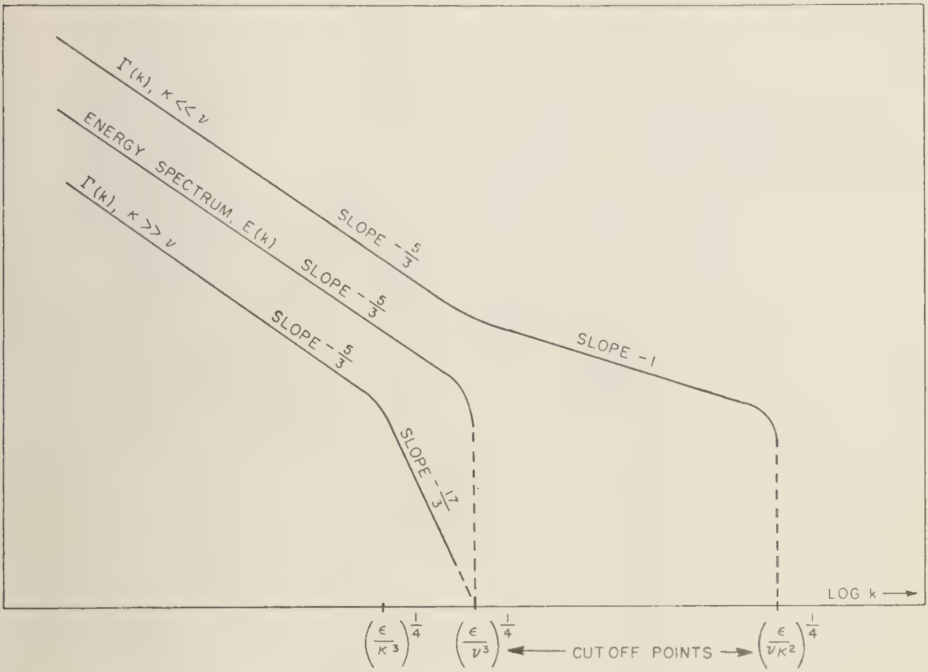

FIG. 7—Turbulent spectra of passive scalar quantities.

esearch Memo 54 D 19, June 1954 (published part as double and triple correlations behind a eated grid, *J. Aeronaut. Sci.*, January 1956).
[R. R. Mills, Jr., A. L. Kistler, V. O'Brien, and Corrsin, Turbulence and temperature fluctua- ons behind a heated grid, *NACA Tech. Note* 288, August 1958.
[R. R. Mills, Jr., and S. Corrsin, Effect of a con- raction on turbulence and temperature fluctua- ons generated by a warm grid, *NASA Memo 5-5- 9W*, May 1959.]

Maxwell: Can we reasonably anticipate that he $-5/3$ law will hold for ionization density in he ionosphere?

Batchelor: This depends wholly on the Reyn- lds number uL/ν of the turbulence; it seems kely that under some conditions in the iono- phere the Reynolds number is large enough for he $-5/3$ law to apply to an appreciable range f wave numbers.

Chairman: Let us hear now about turbulent iffusion.

Batchelor: For a working understanding of urbulent diffusion, we can make use of our knowledge of molecular diffusion, provided that the difference between the time and length scales involved is kept in mind. In molecular diffusion, the length scale is the molecular mean free path, and the time scale is that between col- lisions, both of which are very small compared with the time and length scales involved in turbulent diffusion. In turbulent diffusion the corresponding time scale is that during which a particle's velocity correlation is lost; and the length scale is the distance traveled during that time (relative to axes moving with the mean flow). A good deal of the difficulty in analyzing turbulent diffusion arises from the fact that we wish to consider diffusion over time intervals comparable with the time scale of the turbu- lence. In many cases in which the time and length intervals involved in the diffusion pro- cess are large compared with the time and length scales of the turbulence, we can use the molecular diffusion equation with an eddy dif- fusivity, of the form

$$\text{Eddy diffusivity} \propto lu$$

where l and u are characteristic scales of the turbulent motion (not of an ordered motion such as gravity waves).

We are often interested in the relative motion of particles, as opposed to the motion of one particle relative to a fixed point. If an eddy is large compared with the particle separation, the main effect is to transport the particles with little change in the particle separation. The largest effect will usually come from eddies with a size comparable with the particle separation, since even smaller eddies have smaller energy. An illustration of a problem of relative diffusion is provided by the spreading of a meteor trail.

The trail may be thought of as due to the sudden release of some quantity marking the fluid along a very thin straight line. In the initial stages, molecular diffusion is more important than turbulent diffusion, and the radius of the trail increases according to the relation

$$\overline{r^2} \propto \kappa t$$

When the trail size becomes comparable with that of the smallest eddies, and after a time sufficient for the relative velocity of any two fluid particles on the same cross section of the trail to have lost correlation with its initial value, a purely turbulent diffusion occurs. The spreading is then given by

$$\overline{r^2} \propto \epsilon t^3$$

[See G. K. Batchelor, *Proc. Cambridge Phil. Soc.*, *48*, 345, 1952.] This relation exhibits the accelerating character of relative diffusion, an increase in the trail width bringing into action a larger range of eddy sizes. This kind of growth continues until the trail size reaches that of the energy-containing eddies. After that we can use a relation similar to that for molecular diffusion:

$$\overline{r^2} \propto \mathrm{K}t$$

where K = eddy diffusivity. These three relations for trail radius at different times t after the trail was formed are the ones used by Dr. Greenhow in his analysis of the observations of some visible meteor trails.

Ratcliffe: It is possible to extend this type of analysis to give the shape and rate of change of shape of the trail?

Batchelor: The shape depends upon the large scale eddies which move the trail about bodil without spreading it. The effect of the sma eddies is to make small irregularities on th edge of the trail. These are quickly smoothe out by molecular diffusion, thus effectivel increasing the trail diameter. Which is see first depends on the measuring instrument

Morkovin: Will the density distribution acros the trail be Gaussian?

Batchelor: I believe it will be close to Gaussia although there may be some departures durin the middle period when $\overline{r^2} \propto t^3$.

Corrsin: The temperature wake behind heated wire in a turbulent wind tunnel flo has an almost Gaussian distribution.

Saffman: Large meteors move at Mach num bers greater than 100. Very strong shock wave occur in front of them, and the air passin through this strong shock suffers a substanti increase in entropy and temperature. The wak behind a large meteor consists of a viscous, tu bulent core, fed initially by air that has passe through the boundary layer around the meteo and a larger entropy or temperature wake co taining air that has passed through the stron shock but not through the boundary laye Rough preliminary calculations indicate tha the diameter of the entropy wake will be a order of magnitude greater than the diamete of the meteor. In estimating the Reynolds num ber of the wake, the diameter of the entrop wake rather than the diameter of the bod should be used as a length scale. The tempera ture in the wake will quickly fall, owing t molecular or turbulent diffusion, so that it seem appropriate to use the kinematic viscosity of th ambient air in calculating the Reynolds num ber of the wake at a distance greater tha 1000 body diameters behind the meteor.

Morkovin: When we see sodium trails (seede trails), the wake should be important. On wha was the $20R$ diameter at $1000R$ based?

Saffman: Simply the spreading of strea lines, no diffusion effects.

Krook: Attention should be called to the fac that there will be violent fluctuations in th ablation rate, so that a uniform trail is n necessarily a good approximation. The materi could have an initial velocity on leaving th meteor.

Millman: Small objects give rather uniform ails, but large objects certainly produce irregar trails. However, I should say the breakingf of small particles from the meteor will be ore important than the momentum due to iving.

Turbulent Spectra in a Stably Stratified Atmosphere

R. Bolgiano, Jr.

The role of buoyancy forces in homogeneous turbulent flow in stratified media was discussed, and it was pointed out that the flux of heat, or potential density, when considered from the spectral point of view, represents an abstraction of kinetic energy from the turbulent field over a wide range of scale sizes. It was claimed that this may have the effect of reducing the viscous dissipation rate far below what it would be in a corresponding neutral atmosphere, with the indirect result of markedly increasing the scale size at which the viscous cutoff occurs. The further suggestion was made that, if the stability is sufficiently intense, simple specific forms can be predicted for the energy and fluctuation spectra. [See paper under same title, this symposium.]

Batchelor: I wonder if Mr. Bolgiano's analys applies to a passive scalar quantity.

Bolgiano: The analysis for a passive scalar, ich as electron density or specific humidity, oes through in much the same way; results are similar to those for the potential density deviations.

Sheppard: The basis of Mr. Bolgiano's treatment makes admirable sense to me—the details cannot be adequately discussed following so summarized a presentation. Mr. Bolgiano had provided yet another warning that it must not be assumed that the energy input to the large eddies can be equated to the energy dissipation.

Wheelon: Is the only effect the changing from a $-5/3$ law to a $-7/5$ law?

Bolgiano: No. If there are many stages in the energy cascade, considerable energy may be abstracted by the effects of gravity, and thus the cutoff wave number may be substantially reduced.

Stewart: These arguments seem qualitatively correct, but I do not think a large proportion of the energy will be taken out before the cutoff.

Morkovin: It should be noted that the energy taken out does not necessarily have to be converted into thermal energy locally but can flow away in the form of gravity-wave disturbances of the Hines-Long type. An analogous situation exists in fluid dynamics in the radiation of aerodynamic sound energy from regions of turbulence. It appears that at supersonic speeds this drain of energy can affect the structure of turbulent boundary layers.

Afternoon Session

Tuesday, July 14, 1959

Chairman: M. Krook

Chairman: I understand that Professor Oboukov has some comments he would like to make egarding the last communication this morning. Before proceeding with Professor Gold's paper n the nature of the magnetic restraining forces n the atmosphere, let us hear what Professor Oboukhov has to say.

Oboukhov: To consider the influence of buoyncy on the fine structure of turbulence, I have employed the structure function of a temperaure fluctuation field [see A. M. Oboukhov, *Doklady Akad. Nauk SSSR, 125* (6), 1959]. This structure function is the mean squared temperature difference between the two points of observation. It can be expressed in the form

$$\overline{(\Delta T)^2} = f[r, \epsilon, N, \beta]$$

where r = distance, ϵ = energy dissipation, $N = \kappa\,\overline{(\text{grad } T)^2}$, characterizing the rate of growth of entropy by thermoconductivity, and β — buoyancy. The buoyancy term is given by

$$\beta = g/\bar{T}$$

By dimensional consideration, a specific functional relationship is obtained

$$\overline{(\Delta T)^2} = (Nr^{2/3}/\epsilon^{1/3})f(z/L_*)$$

where z is the height and L_* is the characteristic scale associated with the buoyancy effect,

$$L_* = \epsilon^{5/4}/(N^{3/4}\beta^{3/2})$$

This length scale is related to the length scale proposed by Bolgiano; $L_* \sim k_B^{-1}$. For tropospheric work it is proposed to find the function f by experiments on the different layers near the surface of the ground. Possibly the same might be applied to the ionosphere.

Bolgiano: I am gratified to learn that Professor Oboukhov has obtained results very similar to my own.

Batchelor: Although I am in agreement with the dimensional argument of Professor Oboukhov and the similar results of Dr. Bolgiano, I question the further work of Dr. Bolgiano. It does not seem physically plausible that ϵ, the rate of dissipation of kinetic energy, can be different for different eddy sizes, or that gravity will be a sink for energy in one part of the energy spectrum. If each eddy were independent, then such might be the case; but since the small eddies are part of the large eddies, the large-scale motions will change the vertical position of the smaller-scale motions.

Motions in the Magnetosphere of the Earth

T. Gold

The type of constraint imposed by a strong magnetic field on a conducting fluid is usually considered such that any given set of fluid particles on a line of magnetic force is constrained to remain on this line. This condition is applicable in a system in which all space is occupied by a sufficiently good conductor, but is modified as soon as any insulating surfaces or volumes play a part. In the case of the earth the insulation provided by the lower atmosphere implies a freedom from certain magnetic constraining forces for all the conducting gases above. In particular, a class of motions is not magnetically restrained in which all the gas once on a certain line of force moves later to adjacent lines in a manner that retains it always together on one line at a time. The gas can thus 'interchange' from one line of force to another.

This class of motions must be expected to oc cur, and it would be characterized by symmetr of motion on lines of force. A high-level iono spheric motion in one hemisphere should be ac companied by a symmetrical motion in th other hemisphere at the other base of the sam arched line of force.

Possible influences causing such motions wer discussed, as was the magnetohydrostatic condi tion of the outer gas. A condition for stabilit against convection was found. It was suggeste that these motions, through the associated elec tric fields, control the migration of fluxes of fas particles, such as the Van Allen and auror streams. [See T. Gold, Motions in the magnet osphere of the earth, *J. Geophys. Research, 6* 1219–1224, 1959.]

Dungey: It would seem that ionospheric con trol may be more important than Dr. Gold in dicates. Experimental correlation has been ob tained between the electron densities in the layer and the outer atmosphere.

Gold: Though I agree that motion may b induced from below, it will not be possible fo a magnetic interchange to take place, owing t motion of the E and F layers when insufficien energy is available there to overcome the sta bility of the large outer regions.

Dungey: It would seem logical to present her a short summary of some work of mine relatin to the E and F layers. If a gravitational insta bility occurs in the F region (electron densit increasing upward) this region acts as a dynam driving a current. The current follows the line of force into the E layer, which acts as a re sistance. The result is electromagnetic damping If the resistance can be estimated, the velocitie of motion can be determined. Recent informa tion on the scales of the irregularities indicat that this may be an important mechanism i equatorial spread F.

Hines: The 40° discontinuity in Van Alle radiation has been explained by the great 40 anomalies over Africa.

Gold: I do not accept this explanation of th Van Allen slot. An anomaly removes only pa ticles with very low mirror points, and ther are indications that many other particles ar also removed. Also there are other anomalie over the earth's surface, and measurements the Van Allen radiation do not indicate thes as might be expected if the anomaly mechanis were valid.

Bibl: There are observations of *F*-layer oscil-ations that would seem to support Dr. Gold's heory.

Batchelor: Would it be possible to investi-ate the stability of some simple hydrostatic quilibrium to disturbances of the kind postu-ated in Dr. Gold's theory?

Gold: This would make the problem consid-rably more difficult because it would require hat the molecular velocity distribution be as-umed. This was not necessary in my presenta-ion.

Martyn: Could Professor Gold elaborate on he relation of his theory to the classical ex-planation of the driving mechanism and mor-hologies of the diurnal variations of the mag-etic field and the associated electrojet?

Gold: I do not disagree with the relation be-ween surface observations and what is deduced s occurring at the *E* level. I suggest, however, hat all this may be associated with a wider ange of phenomena reaching to much greater eights.

Chairman: Dr. Manning will now present a omewhat different theory of the radio meteor rail decay process.

ᴀɪʀ Mᴏᴛɪᴏɴs ᴀɴᴅ ᴛʜᴇ Fᴀᴅɪɴɢ, Dɪᴠᴇʀsɪᴛʏ, ᴀɴᴅ Aspect Sensitivity of Meteoric Echoes

L. A. Manning

A theory of the radio meteor trail decay process based on an interpretation in terms of the distortion of such ionization by a wind profile (assumed Gaussian and with no vertical component of velocity) was stated. The model of the reflection process presented was a statistical one: that is, the results were deduced on the basis of an 'average trail' representative of the ensemble of distorted trails. The probability of finding a 'glint' or distortion on the average trail as a function of trail length was calculated, after which the result was applied to estimates of the fading pattern expected, the time variation of aspect sensitivity, and the gradient of wind profile producing such behavior. A vertical scale of 6.4 km, horizontal drifts of 50 m/sec, and a gradient of wind profile of 96 m/sec/km were representative values in good agreement with observations. [See L. A. Manning, *J. Geophys. Research, 64,* 1415–1425, 1959.]

Chairman: Next Dr. Wheelon will tell us omething of how the scattering theories are ised in their application to the ionosphere. This will be followed by Dr. Bibl's communication on movements in the upper ionosphere.

Relation of Turbulence Theory to Ionospheric Scatter Propagation Experiments

A. D. Wheelon

Two turbulent mixing theories were outlined, and the consequent radio propagation predictions were noted and compared with experimental results. The first theory, that attributable to Oboukhov, Corrsin, Batchelor, Silverman, and Bolgiano, leads to a dependence of received signal strength on radio wavelength (when corrected for antenna aperture area) of the form $\lambda^{11/3}$. The second, that developed by Villars and Weisskopf, Wheelon, and Gallet, shows a λ^5 dependence. It was pointed out that recent experimental work appears to favor a λ^6 form and does not give evidence of a viscosity or conduction cutoff. The role of the mean gradient of electron density in the scatter theories was discussed and related to $N(h)$ profiles measured at Penn State, which show a very sharp gradient near the 70-km level. The persistent background signal at higher levels at night was described as probably being the result of faster recombination at the lower levels. The effects of sudden ionospheric disturbances were explained in terms of increased absorption as opposed to increased scattering due to more intense gradients of electron density. [See paper under same title, this symposium.]

Phillips: It does not seem to me that we ought to abandon Oboukhov's arguments simply because there is confusion over lack of agreement with predictions, which are themselves subject to much interpretation. Would someone rather state what is wrong with the physical mechanism and its interpretation?

Batchelor: People familiar with turbulence theory would certainly have a specific objection to the argument used by Dr. Wheelon in arriving at a formula for the spectrum of electron density fluctuations. That argument supposes that the mean gradient of electron density is the only parameter entering into the expression for the spectrum. Current turbulence theory can advance good reasons for supposing that the length scale of the energy-containing turbulent eddies is also a relevant parameter, in the manner of the first theory described by Dr. Wheelon.

Movements and Traveling Disturbances in the Higher Ionosphere

K. Bibl

A number of ionograms were shown depicting rapid changes in the large-scale structure of the ionosphere. It was suggested that many of these changes could be interpreted in terms of vertical movements of the gaseous matter (both ionized and neutral). A time-lapse moving-picture presentation of the ionograms provided an interesting display of the real (or virtual) motions from which some information as to effective velocities could be inferred. A value of the order of 100 m/sec was reported. [See paper under same title, this symposium.]

Morning Session

Wednesday, July 15, 1959

Chairman: H. G. Booker

Chairman: Mr. Bibl has kindly consented to show us another of his interesting moving-picture ionogram films.

[Mr. Bibl pointed out many traveling irregularities in electron density on the ionograms. These always travel downward and are observed primarily in daytime. The motion of the whole layer of ionization was demonstrated, as well as the rapid change in electron-density profile at sunrise.]

Panel Discussion

Chairman: It is impossible on the last day of a conference such as this to get any agreed statement of progress that has been made. It is possible to get individual opinions, however. The ten members of the panel (Stewart, Greenhow, Corrsin, Millman, Sheppard, Bowles, Dungey, Martyn, Monin, Batchelor) will be asked to give their opinions on what they have learned that is new, where the subject of fluid mechanics of the ionosphere stands at this moment, and what research they would propose for the future.

Stewart: I have completed the calculation requested earlier on the altitude above which I would expect turbulent motions to cease. The data are so scanty that the calculation is necessarily very rough. It is a question of the turbulent shear and the stability in the atmosphere. The importance of these effects as compared with inertia is described by the Reynolds number, VL/ν, and the stability parameter $g\ d(\ln\ \theta)/dz$. The stability parameter is nearly constant in the upper atmosphere and equal to about $4 \cdot 10^{-4}$ sec^{-2}. The characteristic length scale to be used in the Reynolds number depends on the characteristic velocity that is used and on the stability. I shall take

$$L \simeq \frac{V}{\sqrt{g[d(\ln\theta)/dz]}} \simeq 50\ Vm$$

where L is a measure of the vertical distance a 'blob' of fluid of speed V may penetrate; L could be larger (by a factor of perhaps 4) because the horizontal scale is generally larger than the vertical scale. The velocity to be used is not 25 m/sec, which describes the large-scale motion from which the turbulence originates, but about one-tenth of that value, which is a good guess for the velocity characteristic of the largest turbulent eddies. This gives a value for the Reynolds number of the turbulence of unity at an altitude of about 120 km. It decreases rapidly with increase in height. Thus the atmosphere will not usually be turbulent above 120 km.

To summarize, we have learned that classical fluid mechanics has little application in the F region. Phenomena there will have to be explained by the ionosphere people and the magnetohydrodynamicists. I believe that below 140 km the large irregularities not already explained by horizontal winds can be described in terms of the internal waves discussed by Mr. Hines and Mr. Long. Below 120 km turbulence will be superimposed on these waves. Mr. Greenhow's estimate of 4×10^{-3} watt/kg for the rate of energy dissipation by turbulence is reasonable. The fact that the total energy in the Hines

ıves has to be replaced once per day is good, ıce 1 day is the period of the most probable urce of these waves. Several mechanisms that ight explain irregularities not connected with ıves have been suggested, e.g. slantwise conction by Mr. Sheppard and local unstable yers such as the oxygen absorption layer by r. Lin.

In the future, observations like those by Mr. reenhow should be continued, with cooperaɔn between stations in order to determine corlations over larger horizontal dimensions, and ereby prove or disprove the internal wave echanism. Experiments using tracers (such : the Kellogg smoke-puff experiments) to easure turbulent mixing should be done at gher altitudes.

Dungey: Although turbulence may not exist ɔove 120 km, it must be recognized that shear ɔws are still prevalent.

Greenhow: We have measured irregularities the lower E region that are strongly anisoopic (6 km vertically by 150 km horizontally). ssociated with these large-scale irregularities e find rms velocities of about 25 m sec^{-1}. We rely if ever see a case when the atmosphere this level is not turbulent with wind speeds this order. I originally thought that these presented large-scale turbulent motions. Now seems more likely that we are dealing with ore regular (wave) motions. It is therefore ıngerous to ascribe an energy dissipation rate $\epsilon = V^2/t \simeq 10^3$ erg sec^{-1} g^{-1} to the large-scale ırbulent motion in this region, although this gure may be used to give lower limits for the me constant and scale of possible small-scale ırbulence.

I was also concerned about Professor Booker's timate of $t_2 \sim 0.4$ second for the time conant of the small-scale turbulence with a scale $\sim$ 1 meter, as these figures are incompatible ith the behavior of long-duration meteor :hoes. I think the explanation is that the largeale eddies from which Professor Booker inrred these values are very anisotropic, and in ıy case are probably not true turbulence, so ıat theories of homogeneous turbulence cannot e applied. It is likely that the above values of and t_2 should be increased to about 20 meters nd 30 seconds, respectively.

The best estimate of the small-scale turbulence comes from eddy-diffusion arguments, using photographic records of long-duration meteor trails. It is found that the turbulent energy dissipation rate required to explain the diffusion of the trails is about 70 erg sec^{-1} g^{-1}. Thus about one-tenth of the energy of the large-scale irregularities goes into the production of small-scale turbulence.

Corrsin: I have learned of the confidence placed by ionosphere people on their interpretations of radio-wave probe measurements. They are based on scattering theory in a statistically homogeneous medium, but have been applied to measurements in a statistically inhomogeneous medium. The simple scattering theory is applicable only if the volume in the scattering fluid has dimensions large compared with the largest irregularities in the motion, and if the smallest irregularities are large compared with the radio wavelength. Theoretical work on scattering by large, diffuse irregularities with small irregularities on the boundaries or 'imbedded' should be done to determine the validity of the interpretations of the measurements.

Is it possible to use polarized radio waves to study the anisotropy of the scattering medium? If so, has it been used?

A better method is needed to distinguish between actual fluid motions and virtual motions of plasma which may result from particle precipitation sweeping over the atmosphere or from ionization and recombination reactions. Rocket methods should prove very useful, especially dual and multiple tracer experiments to give relative dispersion data.

Booker: Ionosphere people have looked into the use of polarized radio waves. If the scattering medium is underdense, the theoretical interpretation of the radio-wave measurements is not difficult, but no new information on the anisotropy is gained. If overdense ionization is involved, new information could be obtained, but unfortunately this is just the situation that is difficult to interpret theoretically.

Millman: I suggest that the fluid mechanics people attack the problem of the relative importance of the turbulent wake and of the shock wave generated by the motion of the meteor itself. Also, the difference in expected behavior between a dust-particle meteor and a

larger meteor with a gas cap should be determined.

My general impression that the observational data on meteors collected from all parts of the world is very consistent has been strengthened at this conference. There are still difficulties in interpreting the data. Professor Manning has proposed a glint theory which explains many observational results, but cannot fully explain some features observed at Ottawa. These require further study. We know that there is not yet a good explanation of the head echo.

I hope soon to collect and analyze quantitatively more data on the diffusion of long-duration meteor trails. I also will look into the delays in radio echoes on the long-duration meteors. In determining details of the meteor echoes a selectivity effect should be pointed out. Details in the meteor echoes are difficult to sort out near the minimum range point because, on a range-time presentation, the echoing points merge. The details are readily observed, however, if the meteor echo is far removed from the minimum range point.

Corrsin: Considerable work on the effects of the wake at low density and high speed is already in the literature. It could be extrapolated to meteors. Considerable knowledge of the properties of the atmosphere as well as of meteors could be gained from artificial meteor observations.

Greenhow: Irregularities along the trail of a meteor giving rise to a head echo may not be due to turbulence, but to irregularities in the initial ionization.

Millman: The latter effect is important for large meteors, but for the small radio meteors, the curve of light intensity versus distance along the trail is usually very smooth.

Sheppard: Mr. Stewart apparently has faith that the larger irregularities in meteor trails and sodium trails are due to gravity waves and that the smaller irregularities are due to turbulence. He may well be right, but can we find some critical experiments on the basis of wave theory to determine just what we have?

My next point refers to Mr. Booker's suggestion (in the discussion, Tuesday morning) that the energy density of turbulence may be independent of height. This is certainly not true in the troposphere and lower stratosphere. Here the large-scale turbulence increases with height to the tropopause, and then decreases, whereas the small-scale turbulence (as measured, for example, on an aircraft accelerometer) decreases with height to the upper troposphere and then appears to become more constant. The pattern of convection is partly responsible for the decrease with height of small-scale turbulence, and, as I have previously indicated, convection is unlikely to be present in the mesosphere and higher levels; but the variation in lapse rate with height aloft is likely to affect the intensity there also. The behavior of turbulence in the troposphere and lower stratosphere provides another reason, over and above those brought out in the symposium by Mr. Greenhow, Mr. Monin, and Mr. Bolgiano, for not inferring the properties of small-scale turbulence from observations only on the large-scale turbulence.

I am not clear about the possible association of and interaction between the disturbances that I have called slantwise convection and the gravity waves of Long and Hines. Slantwise convection can hardly fail to occur in a statically stable medium with a horizontal temperature gradient, but the small-scale turbulence to which it may be expected to give rise would be sporadic and local, whereas my impression from this symposium is that small-scale disturbances are the rule in the upper mesosphere and lower thermosphere. Hence I see the need for a form of disturbance (gravity wave?) in addition to those deriving from slantwise convection. As suggested by Mr. Stewart, a three-station study of the large-scale disturbances isolated by Mr. Greenhow's technique would therefore be very valuable.

Bowles: Speaking as a person concerned primarily with radio-wave propagation, I see two motivations for our studies of the ionosphere.

1. Engineering. Looking to the practical application of radio-wave communication, we should like to know how the curve of scattering amplitude versus frequency should be extrapolated to higher frequences. Here we try to understand the mechanism of radio-wave propagation and scattering in the ionosphere, utilizing all the knowledge we can muster from related fields, including fluid dynamics, in the hope of making improved engineering predictions.

2. Physics. Radio-wave propagation in the ɪnosphere is merely one aspect of the interac-ɪon of waves with a medium having a continu-ɪus variation of refractive index. Thus, radio ɪeasurements may be made of the ionosphere ɪat illuminate the structure of the refractive ɪdex distribution and other closely allied phy-ical phenomena as well.

We have learned at this conference that nowledge in the field of turbulence is not so reat that the fluid mechanics people can im-ɪediately explain all ionospheric irregularities. lso, we have seen that interpretation of the ɪeteor data is, at times (e.g., in overdense ases), very difficult. We must consider, there-ore, other possible causes and explanations, nd I should emphasize that other weak-irregu-arity phenomena, occurring from the lower D egion on outward, certainly must be given qual weight with the meteor-echo techniques.

Dungey: Mr. Ratcliffe thought it might be ɔossible that a horizontal velocity shear (due, ay, to a Hines wave, but requiring a time con-tant greater than 30 minutes) could create a heet of sporadic E. For a shear of 30 m/sec/ cm in the E layer I get

$$\Delta n_e/n_e \sim (\nu_p/\Omega_p)(\partial V_x/\partial z)t$$

$$\simeq (1/40)\cdot(30/1000)\cdot 1800 \simeq 1$$

Hence, this effect may be important.

In my opinion, the future of hydromagnetics n the ionosphere is excellent.

Martyn: The discussion of hydromagnetics during this conference has been restricted some-what because it is new and often complicated. Mr. Booker has mentioned radio-star scintilla-ions, sporadic E, and spread F as all having ɪo good explanation. We have established that hese phenomena are connected with the elec-rojet to the east. It is remarkable that, as Mr. Wright has so definitely shown us, equatorial scintillations are reduced during a magnetic storm, when the general tendency of magnetic disturbances is to make things complex. It seems significant that the electrojet also is re-duced during a magnetic storm. Sporadic E too ɪas been tied to lunar and solar variations in the electrojet. We should concentrate our atten-ion further on observations that will demon-strate this association more definitely.

The mechanism by which this association exists is another matter and requires further theoretical work. For example, in apparently stable layers in the ionosphere irregularities in charge density may be unstable in the presence of an electric field. This problem must be ana-lyzed for various configurations to determine the degree of instability.

There is one other point, a small point, but one in which there appears to be some lack of unanimity. That is the question of the degree to which the ionosphere binds the magnetic field. For the movement of F-region ionization, the relaxation time is given roughly by $\tau = \rho/\sigma H^2$. If the ion density is used in this formula, $\tau = 0.1$ second. Thus the ionization is rigidly tied to the magnetic field, as far as mechanical forces are concerned. If the air density is used, however, $\tau = 20$ minutes, which gives the time necessary to set the atmosphere in motion by the 'motor' action of electric currents. This point has caused some confusion in the course of this conference. It has arisen again and again, and I think we must be very careful about it.

Monin: The ionospheric specialists have made considerable progress in measurements in the ionosphere. The fluid mechanics specialists have made less progress. Fundamental questions have been asked which cannot be answered definitely.

1. What is the origin of turbulence in the ionosphere? (*a*) Sources of turbulence. We have taken only the first steps in understanding the sources. Mr. Sheppard's slantwise convec-tion, wave motion, and radiation are sugges-tions. (*b*) Interaction with the magnetic field. In the troposphere the relative vorticity of motions is small compared with the vorticity of the earth's rotation. Is this true in the iono-sphere, or can the magnetic field produce large vorticity?

2. What is the mechanism for decay of small-scale turbulence in the ionosphere? It may be different from the decay mechanism in the troposphere because the ratio of the mean free path to the Kolmogoroff microscale is different. It may be that we shall have to develop a sta-tistical mechanics theory of ionospheric turbu-lence, rather than a hydrodynamics theory. Smoke-puff diffusion experiments in the ionos-phere would be very useful.

3. What is the influence of stability? Experiments in the lowest layers have been done. The results from different countries concur, but we do not yet have the final answers. The theory should finally be applicable to the ionosphere.

4. What are the nature and structure of the charge density fluctuations in the ionosphere? The ionosphere specialists should develop a full theory to describe their observations, taking into account ionization, recombination, and all such pertinent phenomena.

Batchelor: Four points new to me have emerged from this conference. They may seem evident, but then I find that most research consists mainly in realizing the obvious and that it is a slow and laborious process.

1. We have found several mechanisms by which motion can be generated in the upper atmosphere. Two suggestions by Professor Sheppard stand out, thermal winds and slantwise convection, both arising from the occurrence of variations in the vertical temperature gradient over a horizontal plane. The resulting shearing motion will surely develop turbulence. Despite the existence of a vertical density gradient which is stabilizing when averaged over a horizontal plane, mechanisms for the generation of turbulence can exist.

2. The Hines-Long waves will be a typical phenomenon in the stratified atmosphere, particularly with the jet-type structure that Professor Long pointed out. It is important to distinguish between fluctuations due to gravity waves and those due to turbulence, because their properties are quite different, and ways of making the distinction readily must be investigated. We may be able to determine which we have by measuring the persistence of the velocity of a particle or of the fluid at a point; if it lasts appreciably longer or shorter than $t = L/U$ (where L and U are length and velocity scales of the observed motion), the motion is unlikely to be true turbulence.

3. The observations of the increase of width of meteor trails with time have given valuable information. Many more like those analyzed by Mr. Greenhow would be welcome. Rockets and aircraft can also be used to lay ionization trails in the ionosphere, but they are expensive, and difficult to organize; meteors are free.

Whatever the method for marking the air, my point is that observations of the growth c puffs or line trails by turbulent diffusion is powerful method of investigating the smal scale features of the turbulence.

4. After some misconceived doubts, I no believe that Mr. Bolgiano's contention tha buoyancy forces extract kinetic energy at di ferent length scales of the turbulent motion correct. I see that it is possible to write the vert cal heat flux as an integral over wave-numbe space, and that the integrand can be interprete as a measure of the rate at which kinetic e ergy on a certain length scale is being co verted into potential energy. It seems, ther fore, as he contends, that the rate of transf of energy to eddies of size smaller than l, sa may diminish with l and may not be given b the usual formula u^3/L. I am not yet clear abo the further ideas and assumptions involved i Mr. Bolgiano's 'buoyancy range' of wave num bers, but this is an important and interestin suggestion and should be given serious consic eration.

Booker: From the proceedings at this syn posium it will, I think, be clear to the flu mechanics participants that ionospherists ha been studying irregularities in the ionosphe for quite a long time. The study was, I believ initiated by Ratcliffe and Pawsey in Cambrid some 25 years ago. Only in relatively rece years, however, has there been serious ta among the ionospherists suggesting that turb lence might be a factor in these phenomena.

Recent discussion of turbulence in the low ionosphere dates from the discovery about 8 years ago of the phenomenon of VHF scatt transmission. At that time normal ionospher thinking would not have predicted the ph nomenon of scatter transmission. Although ion spherists were familiar with the existence irregularities of electron density in the ion sphere it was then customary to assume th the spectrum of these irregularities was Gau sian. On a Gaussian spectrum one would n predict the existence of scatter transmission ov any significant range of frequencies. It ha pened, however, that, at about the same tim a similar phenomenon of scatter transmission the troposphere was being investigated, and course it was quite reasonable to explain trop spheric scatter transmission in terms of turb

ıce. It thus came to be recognized that, if rbulence did exist in the lower ionosphere, ere should be a phenomenon of VHF iono-ıeric scatter transmission. In consequence ıospheric scatter transmission was looked for perimentally and was found to exist. The suc-ss of this experiment led ionospherists to look to other phenomena that might be explicable terms of ionospheric turbulence.

One of the most interesting phenomena indi-ting a mixing process in the lower ionosphere the diffusion of long-duration visible meteor ails. It has not always been realized by iono-herists that the width of these trails indi-tes a rate of diffusion several powers of 10 eater than would be expected on the basis molecular diffusion. The observed width of ıg-duration visible meteor trails therefore con-tutes direct evidence of a mixing process akin turbulence. One of the most important things at we can now do is to persuade Dr. Millman analyze in considerable detail his accumula-n of records of long-duration visible meteor ails. If Dr. Batchelor's theory of diffusion is rrect, it should be possible from Dr. Mill-an's data to derive as a function of height) the eddy-diffusion coefficient ultimately de-loped, (*b*) the time constant of the large ed-es, (*c*) the time constant of the small eddies, d (*d*) the turbulence power per unit mass.

I shall await with considerable interest the sults of Dr. Millman's analysis of the observa-ons in the light of Dr. Batchelor's theory.

Chairman: I wish to thank the members of e panel for their very valuable contributions re this morning. After a brief recess, there ll be an opportunity to hear further sum-arizing comments from individuals on the or.

Manning: I have been pleased with the pic-re of motions in the atmosphere below the layer that has been formed at this conference. we interpret the predominant motions as avity waves, and assume that turbulence with locities no more than 5 or 10 per cent of e wave velocity is driven by the shears, a tisfactory agreement is obtained with the eteor data as I know them.

Extensive radio meteor studies of winds have en made at three places in the world: at anford University in California, then at Adelaide by Elford and Robertson, and, as Greenhow has told us, at Jodrell Bank. The Australian results, unlike ours or Greenhow's, do not show the presence of motions of the Hines type. We should therefore consider the geographical distribution of these motions when seeking their mode of excitation.

I agree with Dr. Millman that the glint theory, though necessary, is not necessarily sufficient as an explanation of all meteor behavior. Although it appears to account for the bulk of the observations for small meteors, several of the effects noted with very large meteors may be related to other causes, such as ionization by light from the particle, flaring, turbulent wakes, and perhaps stratification of the sort responsible for sporadic-E ionization at discrete heights.

Oboukhov: The observations by Richardson in 1926 and by Goden in 1936, and recent progress in measurement of turbulent structure in the troposphere, have convinced most people that turbulence is real in the atmosphere. We should now look into the following questions:

1. How does the turbulent energy spectrum vary with height?

2. What is the mechanism of transfer of turbulent energy as a function of height?

3. How do internal waves (gravity waves and sound waves) transfer energy to turbulence, and vice versa?

Hines: I should like first to reintroduce the importance of compressibility in atmospheric gravity waves, because the properties of the internal waves are appreciably influenced by it. [*Note added in proof:* The dispersion equation quoted previously for a compressible atmosphere,

$$\omega^4 - \omega^2 C^2(K_x^2 + K_z^2) + i\gamma g\omega^2 K_z + (\gamma - 1)g^2 K_x^2 = 0$$

may be contrasted with that for an incompressible medium whose density happens to vary as $\exp(\gamma \mathbf{g}\cdot\mathbf{r}/C^2)$, namely

$$-\omega^2 C^2(K_x^2 + K_z^2) + i\gamma g\omega^2 K_z + \gamma g^2 K_x^2 = 0$$

where $\mathbf{g}$ lies in the $-z$ direction. Two differences are apparent, one at the beginning and the other in the last term. The former is important at periods shorter than several minutes, and the

latter at periods greater than a minute, in the actual atmosphere. Other changes occur in the wave formalism, in the relations between U_x, U_z, $(\rho - \rho_0)/\rho_0$, and $(p - p_0)/p_0$.]

Next, I should like to divert some of the attention that has been given the large-scale meteor structures (6 km vertically by something above 100 km horizontally, 100 minutes, as quoted by Greenhow) to the smaller-scale structures ($\sim$1 km vertically). The large ones are apparently dominant, and they are consistent with the wave interpretation, but I should like to know more about the other structures that are present in order to test the wave hypothesis further. An advantage of a wave theory is that it can be so quickly disproved if it is wrong, since it ascribes very definite relations between ω, K_x, K_z, U_x, U_z, $(\rho - \rho_0)/\rho_0$, and $(p - p_0)/p_0$. Given any two of the first three quantities, the third can be deduced, as can the ratios between the others. It would seem to be the job of the ionospherists to provide the pertinent observational data and so permit the test to be made.

The fluid dynamicists should be able to help on absolute magnitudes and energy sources. If wave interaction and energy cascade are important, they may be able to deduce the expected spectrum. This could be tested observationally, and it could be determined whether the known atmospheric tides could provide the requisite energy input. If they cannot, other sources must be examined.

Finally, I should suggest that the two sequences of waves available with the choice $K_z = k_z + ig/2C^2$ [namely the almost-isotropic sequence that exists for $\omega > \gamma g/2C$ (sound waves) and the highly anisotropic sequence that exists for $\omega^2 < (\gamma - 1)g^2/C^2$ (gravity waves)] may give some clues to the fluid mechanists in their approach to gravitational turbulence theory for a compressible fluid, perhaps specifically in further work on the two-sequence buoyant turbulence outlined by Mr. Bolgiano.

Morkovin: At this conference we have seen mechanisms of two types which could lead to turbulence: primary instabilities (Martyn, Sheppard, Lin, etc.) $\rightarrow$ breakdown $\rightarrow$ turbulence; or geophysical motions (Sheppard, Long, Hines, Tides, etc.) $\rightarrow$ secondary instabilities $\rightarrow$ turbulence. In most of these cases, the appearance of turbulence is likely to be spotty i time, space, amplitude, and spectrum, and fa different from that created by a single regula grid in a uniform flow.

The available semiempirical theories, on th other hand, treat only turbulent motions tha are sufficiently aged, homogenized, 'isotropized quasi-stationary, and associated with a singl large scale. The question remains unanswere whether the statistical sampling along the pat of the beam in a given forward-scattering ex periment with a given wavelength correspond to the theoretical model. Now that we hav seen that there are other causes of electron density spottiness besides turbulence (diffusin meteor trails, wave-like motions) it does no appear surprising that the theoretical spectr and spectra inferred from experiments (assum ing the presence of isotropic homogeneous tu bulence alone) should disagree. Nor is it su prising that the working subcommittee on th 80- to 100-km range reached 'no agreement a to the interpretation of radio data in terms o the velocities of small eddies,' as reported b Dr. Bowles yesterday.

The one phenomenon that can furnish cor trolled information on the intrinsically turbu lent features is the diffusion of tracers, prefe ably multiple tracers. Also, it does not appea out of the question in the near future to see experimental conditions for scattering whe the medium would be much more steady and i properties more measurable, as in ionic win tunnels and arc-jet tunnels.

Rott: There has been considerable intere recently in hypersonic flows past blunt bodie The meteor people have not made good us of this. Theories have been worked out fo large and for small values of the Knudse number, λ/D, and efforts have been made t close the gap at $\lambda/D \simeq 1$. Although much o the work applies to the flow near the bod it is possible and would not be difficult to giv a good description of the wake. A short bibli graphy of recent work is appended.

BETHE, H. A., AND M. C. ADAMS, A theory for th ablation of glassy materials, *J. Aeronaut. Spa Sci., 26*, 321, 1959.

HAYES, W. D., AND R. F. PROBSTEIN, *Hyperson Flow Theory*, Academic Press, 1959.

LEES, L., Laminar heat transfer over blunt-nose bodies at hypersonic flight speeds, *Jet Propu*

on, 26, 259–274, 1956. A survey article on vis-
ous flow near the body.
s, L., AND T. KUBOTA, Inviscid hypersonic flow
ver blunt-nosed slender bodies, *J. Aeronaut.
ci., 24,* 192, 1957.
, S. C., Cylindrical shock waves produced by
stantaneous energy release, *J. Appl. Phys., 25,*
, 1954.
DYKE, M. D., The supersonic blunt body
problem—review and extensions, *J. Aeronaut. Space Sci., 25,* 485, 1958.

Chairman: In bringing the meeting to a close, I should like, on behalf of the Organizing Committee, to thank the many participants whose contributions have made this symposium a success.

Constitution of the Atmosphere at Ionospheric Levels

Marcel Nicolet

C.S.A.G.I., Uccle, Belgium

Abstract—A physical picture of the upper atmosphere cannot be obtained without determining whether vertical distribution depends on mixing or diffusion or on a chemical or photochemical equilibrium. It is necessary to determine how dissociation and recombination of molecular and atomic oxygen and nitrogen are distributed with height. The structure of the atmosphere deduced from density measurements is related to the variation of the mean molecular mass depending on diffusion effects. In addition, it is necessary to know how the heat budget is affected by conduction.

Introduction—Kinetic theory is the basis of the determination of the principal parameters of the neutral atmosphere in which the ionospheric phenomena occur.

A simple treatment of the problem of the atmospheric constitution is possible if the hydrostatics is studied in an atmosphere in which the temperature distribution is known. Since such a parameter is not yet known, however, it is necessary to examine in some detail the behavior of the pressure or density at great heights in order to be able to develop ideas underlying the behavior of the atmosphere.

The hydrostatics of the terrestrial atmosphere—On the assumption that the gas is a continuous medium, and letting p be the pressure, ρ the density, and g the acceleration due to gravity, the equation of hydrostatic equilibrium is

$$dp/dr = -g\rho \qquad (1)$$

where r is the radius of the sphere including the atmosphere and the earth.

If no account is taken of the effect of the mass of the atmosphere compared with the mass of the earth, the variation of g due to the atmosphere itself can be ignored, and, therefore, the variation of the gravitational attraction with increasing height can be expressed by

$$g_a a^2 = gr^2 \qquad (2)$$

in which the subscript a denotes the value of the quantities at a given distance a from the earth's center.

Further, let m_i be the mass of a molecule the gas; the density is

$$\rho_i = n_i m_i \qquad (3$$

where n_i denotes the number density (or t concentration).

Formula 3 can be applied to several kinds molecules when the internal molecular stru ture is ignored; we have then

$$m = \Sigma n_i m_i / \Sigma n_i \qquad (4$$

$$m \equiv \rho/n \qquad ($$

so that the ratio, m, of the density to the nun ber density is the mean molecular mass of t gas.

Since the terrestrial gas is almost a perfe gas, the pressure p is given by

$$p = nkT \qquad (6$$

in which T is the temperature and k the Bolt mann constant (gas constant for one molecule Using (6) and (2), the equation of hydrostat equilibrium (1) becomes

$$\frac{dp}{p} = \frac{dn}{n} + \frac{dT}{T} = -\frac{g_a m a^2}{kT}\frac{dr}{r^2} \qquad (7$$

which is the general relation between pressur density, and temperature.

This formulation corresponds to an atmo phere in which the density is appreciable a in which the potential is only due to the field force of the earth's attraction and is pra tically unaffected by the potential of centrifug force due to the axial rotation.

s a preliminary, let us consider an iso-
mal atmosphere, $T = T_a$, in which $m =$
tant. Integration of (7) gives

$$\frac{p}{p_a} = \frac{\rho}{\rho_a} = \frac{n}{n_a} = e^{-[a/(a+z)][z/H_a]} \tag{8}$$

$_a$ is the scale height

$$H_a \equiv kT/mg_a \tag{9}$$

$$z = r - a \tag{10}$$

ne height above a. Thus, it is clear that
ula 8 cannot be used for too large values

terrelation between pressure, density, and perature—When the atmosphere remains ectly mixed (*homosphere*), its mean molecu- mass m is given by molecular nitrogen 1 per cent in volume), molecular ogygen 0 per cent), and argon (0.9 per cent). Thus,

$$= 48.08 \times 10^{-24}\text{g} \qquad = 28.973 \quad \text{physical units} \tag{11}$$

ith perfect mixing the constant ratio of gen and nitrogen concentration is

$$n(O_2)/n(N_2) = 0.2683 \tag{12}$$

when there is a dissociation of oxygen,

$$\frac{n(O) + 2n(O_2)}{n(N_2)} = 0.5365 \tag{13}$$

ther words, the law of vertical distribution ne mass density in the homosphere leads to

$$\rho = 1.34\rho_{N_2} \tag{14}$$

must be pointed out that the vertical dis- ution of N_2 is practically unaffected by proc- s replacing mixing since its molecular mass = 28 almost corresponds to the mean mo- lar mass of the air.

the *heterosphere,* where the mean molecu- mass is not constant, its variation must be wn in order to obtain a relation between sure and temperature, and (12), (13), and are no longer valid. The definition of H vs that

$$\frac{dH}{H} = \frac{dT}{T} - \frac{dm}{m} - \frac{dg}{g} \tag{15}$$

and if the gradient of the scale height is written as follows:

$$\beta = dH/dz \tag{16}$$

(7) leads to

$$\frac{dp}{p} = -\frac{1}{\beta}\frac{dH}{H} \tag{17}$$

$$\frac{d\rho}{\rho} + \frac{dg}{g} = -\frac{1+\beta}{\beta}\frac{dH}{H} \tag{18}$$

and

$$\frac{dn}{n} + \frac{dg}{g} = -\frac{1+\beta}{\beta}\frac{dH}{H} - \frac{dm}{m} \tag{19}$$

If the gradient of the scale height is a constant, integration of (17), (18), and (19) leads to

$$\frac{p}{p_0} = \left(\frac{H}{H_0}\right)^{-1/\beta} \tag{20}$$

$$\frac{\rho g}{\rho_0 g_0} = \frac{nmg}{n_0 m_0 g_0} = \left(\frac{H}{H_0}\right)^{-(1+\beta)/\beta} \tag{21}$$

Thus, in any atmospheric region where a linear variation of scale height is used as first approximation, equations 20 and 21 represent the variation of pressure and density. Furthermore, the mean molecular mass being constant in the homosphere, the concentration of each constituent can be obtained from measurements of the vertical distribution of the pressure or density. But, in the heterosphere, it is impossible to obtain the concentrations of constituents from measurements of pressure and density. A direct measurement is required for each constituent in order to know the composition of the heterosphere.

In the homosphere, the variation of H gives the variation of the temperature but leads only to the variation of T/m in the heterosphere. Information about the temperature could be obtained if the vertical distribution of molecular nitrogen were known, since the mean molecular mass of N_2 ($M = 28$) is not very much different from the mean molecular mass of the air. In other words, the variation of H with $M = 28$ or 29; i.e., molecular nitrogen in diffusion equilibrium or in mixing should give fairly good estimates of the atmospheric temperature.

Since the temperature is the fundamental

parameter, its vertical distribution is the basis of the nomenclature of the upper atmosphere.

A description of the atmosphere— Before describing the atmosphere above 50 km, i.e., the atmospheric regions corresponding to the ionosphere, it is best to summarize our knowledge of the regions below. Starting from the definition used in meteorology that the lowest region heated by the earth's surface is the *troposphere,* and its upper boundary is the *tropopause,* where the temperature gradient changes, the next region is the *stratosphere.* This region corresponds to a positive gradient of the temperature and extends up to the temperature peak detected in the neighborhood of 50 km. Thus, these two lowest regions of the atmosphere can be described as follows:

Earth's surface	Temperature 273°K ± 20°K
Troposphere	Temperature decreases with height
Tropopause	Temperature minimum, 210°K ± 20°K
	Altitude, 13 ± 5 km, decreasing from equator to pole
Stratosphere	Temperature increases with height
Stratopause	Temperature maximum, 273°K ± 20°K
	Altitude, 50 ± 5 km

The temperature and its gradient vary with latitude, time of day, and season. The localization of the source of heating and the process of heat transport determine the vertical distribution of the temperature. In the troposphere, the heat source is the earth's surface and convection is the principal process of heat transport. Absorption of solar ultraviolet radiation by ozone and emission of infrared radiation in the stratosphere show that the heat budget involves radiative processes.

Above the stratopause the temperature decreases rapidly up to about 85 km. This region is called the *mesosphere,* and its upper boundary, corresponding to a minimum of temperature, the *mesopause.* It is a relatively unstable region in which absorption processes of solar radiation are unimportant compared with the heat-loss processes.

Above the mesopause all ultraviolet radiation of wavelengths shorter than 1750 A is gradually absorbed, and a fraction of the absorbed energy is used for heating the atmosphere. Since molecular oxygen and nitrogen cannot radiate, the only possibility is atomic oxygen subject to an infrared emission at 63 μ. Since other sou of heating such as conduction or arrival particles at the top of the earth's atmospl are possible, it is easy to conceive an incr of temperature with height (detected by increasing scale height) and to define *thermosphere* as the upper atmospheric reg with positive gradient of temperature.

Thus, the parameter temperature descr the regions above 50 km as follows:

Mesosphere	Temperature decreases with hei
Mesopause	Temperature minimum 190°K 25°K
	Altitude 85 ± 5 km
Thermosphere	Temperature increases with hei
Thermopause	Should be the beginning of isothermal layer

Convection in the lower thermosphere conduction in the upper thermosphere must the principal sources of heat transport, the temperature gradient should be related to laws of convection and conduction affect the vertical distribution of heating due to absorption of the solar radiation.

Above a certain altitude simple laws dedu from the statical equation (1) and the equat of state (6) no longer apply to the atmosph gas because dynamic processes involving effects of the magnetic field modify the stat picture.

Observational data—Atmospheric tempe tures and winds have been observed up to km by rocket grenade experiments. But in thermosphere, no direct measurement of temperature exists. Pressure data have been tained up to 120 km; above that altitude o density data are available. Thus, an atm pheric model in which pressure, density, conc tration, and temperature are related can given only below 100 km. In Table 1 we sh an atmospheric model for the homosphere tween 50 and 100 km. The temperature at stratopause is of the order of 273°K, and temperature at mesopause is about 190° Comparing such a model with observatio data of temperatures at the stratopause, th is a variation indicating that $T = 273°K \pm 20°$ At the level of the mesopause observatio data are less precise, but large variations m occur also, and low temperatures such as 160 are not excluded.

BLE 1—*Atmospheric data between 50 and 100 km*

i- e, n	Temperature, °K	Pressure, mm Hg	Density, g cm^{-3}
).0	274	6.7×10^{-1}	1.1×10^{-6}
2.5	274	4.9×10^{-1}	8.3×10^{-7}
5.0	274	3.6×10^{-1}	6.1×10^{-7}
7.5	263	2.7×10^{-1}	4.7×10^{-7}
).0	253	1.9×10^{-1}	3.5×10^{-7}
2.5	242	1.4×10^{-1}	2.6×10^{-7}
5.0	232	9.6×10^{-2}	1.9×10^{-7}
7.5	221	6.6×10^{-2}	1.4×10^{-7}
).0	210	4.5×10^{-2}	9.9×10^{-8}
2.5	207	3.0×10^{-2}	6.7×10^{-8}
5.0	203	2.0×10^{-2}	4.6×10^{-8}
7.5	200	1.3×10^{-2}	3.1×10^{-8}
).0	197	8.7×10^{-3}	2.1×10^{-8}
2.5	193	5.7×10^{-3}	1.4×10^{-8}
5.0	190	3.7×10^{-3}	9.0×10^{-9}
7.5	193	2.4×10^{-3}	5.7×10^{-9}
).0	197	1.6×10^{-3}	3.7×10^{-9}
2.5	200	1.0×10^{-3}	2.4×10^{-9}
5.0	203	6.8×10^{-4}	1.5×10^{-9}
7.5	207	4.5×10^{-4}	1.0×10^{-9}
).0	210	3.0×10^{-4}	6.6×10^{-10}

Measurements of the density in the meso-
here have been made by different methods.
variation by a factor of 2 at latitude 58°N
the neighborhood of 70 km is possible, i.e.,
tween 5×10^{-8} and 10^{-7} g cm^{-3}, while
ere is probably a trend of decreasing density
50 km with increasing latitude. If such vari-
ons occur in the mesosphere, variations of
e pressure are therefore possible at 100 km. At
at level, observational data are very different
d correspond to a broad range of a factor of
in the pressure and density. In other words,
a pressure of the order of $(3 \pm 1) \times 10^{-4}$
n Hg is adopted at 100 km, it is not possible
determine the real range of variation. For
ample, a pressure of the order of 4.5×10^{-2}
m Hg at 70 km and a range between 1×10^{-4}
d 4×10^{-4} mm Hg at 100 km require a vari-
ion of more than 70°K near the mesopause.
Present rocket information on rocket densi-
s at 200 km indicates possible variations of
ore than a factor of 10 between a summer day
d a winter night. On the other hand, analyses
satellite observations show that densities at
0 km are not affected to such an extent. In fact,
nsity fluctuations in the neighborhood of 200

TABLE 2—*Approximate values of the density between 100 and 800 km*

Altitude, km	Density, g cm^{-3}	Number density, cm^{-3}
100	4×10^{-10} to 10^{-9}	$\sim 10^{13}$
200	6×10^{-13}	$\sim 10^{10}$
300	6×10^{-14}	$\sim 10^{9}$
400	6×10^{-15} to 10^{-14}	$\geq 10^{8}$
600	8×10^{-16} to 10^{-15}	$> 10^{7}$
800	8×10^{-17} to 10^{-16}	$> 10^{6}$

km are less than 50 per cent. There is no large variation with latitude, but the day-to-day variation related to the solar flux is the most important effect that is well observed above 400 km.

Table 2 lists values of density for heights between 100 and 800 km.

Since the density decreases by a factor of about 10 between 200 and 300 km and also between 400 and 600 km, clearly there is an increase of the scale height. Recalling the fact that the density at 100 km is of the order of 7×10^{-10}g cm^{-3}, it can be concluded that there is a continuous increase of the scale height, i.e. of T/m, from 100 up to 600 km. It must be pointed out that it is not permissible to use constant scale heights to represent the vertical distribution of the density between two heights when it is clear that its exponential decrease from 100 to 600 km shows different values of the exponential factor for the various intervals of 100 km.

Constitution of the thermosphere—It has been shown that exact information about the constitution of the thermosphere cannot be obtained without knowing the simultaneous variation of T and m. Two kinds of structure can be considered a priori.

First, a thermosphere in which atomic oxygen is the principal constituent requires a very small amount of heating by ultraviolet radiation. This is due to the fact that the energy of production of the F layer resulting from the ionization of atomic oxygen corresponds to the whole ultraviolet energy emitted by the sun, and, therefore, the amount available for heating cannot be more than the energy available for the ionization. In that case, the source of the heating

must be a heat flow by conduction from the upper levels in order to reach the high densities observed above 500 km.

Second, a thermosphere in which molecular nitrogen is more important than atomic oxygen is able to absorb the greatest part of the ultraviolet radiations. In that case, only a fraction of the radiation is involved in the ionization processes observed in the F layers, and there is strong heating of the atmosphere at the F_1 peak and below where molecular nitrogen is ionized and recombines rapidly by dissociative recombination.

The conventional method for the analysis of ionospheric data gives a rate of electron production

$$q = \alpha n_e^2 \simeq 300 \quad \text{electrons cm}^{-3}\ \text{sec}^{-1} \qquad (22)$$

at the peak of the F_1 layer. Such a production corresponds to an energy of the order of 0.1 erg cm^{-2} sec^{-1}, which cannot explain the slow decrease of the density above 200 km unless there is some additional heating due to a conductive heat flow at the top of the earth's atmosphere.

If the ultraviolet radiation is more than 10 times the value necessary to maintain the ionization of the F layers, about 90 per cent must be transformed rapidly into heat in the F_1 layer. Such a process is possible when the ionization of a principal constituent such as N_2 disperses very rapidly by dissociative recombination. It has been shown that the gradient of the scale height H is given by the formula

$$\beta \simeq 10^3 E/H^{1/2} \qquad (23)$$

in which E denotes the energy available. If, for example, the scale height is 40 km, 2 ergs is necessary to obtain a gradient of the order of unity, i.e. an increase of the scale height of 1 km/km or an increase of the temperature of the order of 30°K/km below the peak of the F_1 layer.

It must be pointed out that a thermosphere in which molecular nitrogen is an important constituent requires a rapid increase of the temperature above the E layer to maintain a high ratio N_2/O up to the F_2 layer. On the contrary, an atomic oxygen thermosphere requires a continuous increase of the temperature corresponding to a conductive heat flow in additio[n] to the low heating due to solar radiation.

In conclusion, the structure of the thermo[s]phere depends on the energy available in t[he] radiations emitted by the solar chromospher[e].

Solar radiation—In order to know how t[he] heating of the thermosphere can occur by a[b]sorption of solar radiation of wavelengt[hs] shorter than 1750 A it is necessary to consid[er] the radiations emitted by the sun.

The solar continuum below 1750 A does n[ot] play a principal role, and the solar emisssion [is] essentially due to radiations from the chromo[s]phere and lower corona.

If we consider the lines between 1700 A a[nd] 1200 A that are absorbed by molecular oxyg[en] and lead to its dissociation, it is possible [to] consider four spectral ranges (see Table 3).

From Table 3 it is clear that about 3 er[gs] cm^{-2} sec^{-1} is available for the dissociation [of] O_2 in the E layer during the day, and this co[r]responds to a maximum value for heating.

The energy emitted in the X-ray region ca[n]not be more than 1 erg cm^{-2} sec^{-1}, and sin[ce] the absorption coefficient is less than 10^{-18} cm[^{2}] this part of the solar spectrum can be ignor[ed] in the heating of the E layer.

Ultraviolet radiations for which the absor[p]tion coefficient is more than 5 × 10^{-18} cm^2 a[re] absorbed above the peak of the E layer, and [a] heating must result in the F layers if there [is] sufficient energy. According to formula 23 t[he] energy E necessary to increase the scale heig[ht] H = 10 km at 120 km to H = 40 km at 1[...] km is

$$E \sim 10^{-3} H^{1/2} \beta = 2 \text{ ergs cm}^{-2}\ \text{sec}^{-1} \qquad (2\ldots$$

A small value such as 0.2 erg cm^{-2} sec^{-1} wou[ld] lead to a small gradient β of the order of 1 k[m/] 10 km.

The structure of the atmosphere near the [...] peak, therefore, depends on the energy emitt[ed] in the helium lines at 584 A (He I) and at 3[04] A (He II). There is not yet an accurate d[e]terimation of the intensity of He II (λ30[4]). Theoretical estimates give between 0.1 erg cm[$^{-2}$] sec^{-1} and 2 ergs cm^{-2} sec^{-1}, i.e. between lim[its] that lead to different conclusions about t[he] structure of the atmosphere.

Dissociation of oxygen—The rate of dissoc[ia]tion of molecular oxygen by ultraviolet rad[...]

TABLE 3—*Absorption and dissociation of molecular oxygen*

Spectral Range, A mission lines†	Absorption coefficient, k, cm²	Energy,* erg, cm⁻² sec⁻¹	Dissociation rate, sec⁻¹	Absorption peak, $n(O_2)$cm⁻²	Altitude (approx.), km
1217 (Ly α)	1×10^{-20}	3.4	2.1×10^{-9}	10^{20}	75
1310–1265	$(4 \pm 1) \times 10^{-19}$	0.14	4.7×10^{-9}	2.5×10^{18}	100
1670–1640 1335	$(2 \pm 0.5) \times 10^{-18}$	1.6	2.7×10^{-7}	5×10^{17}	105
1570–1390	$(1 \pm 0.3) \times 10^{-17}$	1.0	1.0×10^{-6}	10^{17}	120

* From Rense's measurements (unpublished).
† Effect of continuum at 1750 is not included.

on being of the order of 10^{-6} sec^{-1}, the con-ntration of O_2 decreases by 50 per cent in bout 10 days. Since the recombination of tomic oxygen above 100 km is a very slow rocess, requiring several months, the thermo-phere should be an atomic oxygen atmosphere. has been shown, however, that a photoequi-brium cannot be reached, since dissociated olecules are replaced by molecues coming om below by upward diffusion. In other words, e normal distribution of molecular oxygen bove a certain altitude is by diffusion.

On the other hand, oxygen atoms produced by issociation do not recombine where they are enerated. They must go below 100 km in or-er to recombine. In fact, there is a continuous ransport of oxygen atoms from the F layer own to below the peak of the E layer.

Such vertical transport of molecular and tomic oxygen affects the mean molecular mass, nd it is not permissible to use formula 13 giv-g the oxygen-nitrogen ratio of the air. For hat reason, it is not possible to obtain the ex-ct ratio molecular oxygen-atomic oxygen, de-ending on the atmospheric vertical movements; irect determinations of molecular and atomic xygen are needed. Nevertheless, molecular oxy-en can exist up to the altitudes of the F_2 layer nd, therefore plays a role in the recombination rocesses.

Dissociation of nitrogen—The dissociation of itrogen depends on several processes: a pre-issociation mechanism having a rate coefficient f the order of 10^{-12} sec^{-1} is a very slow process nd cannot be efficient enough to lead to an im-ortant dissociation. But ionization followed by dissociative recombination

$$N_2^+ + e \rightarrow N + N \tag{25}$$

must be considered an important process since N_2 can be ionized in the various ionospheric layers by ultraviolet radiation and X rays.

Another process, the ion-atom interchange process such as

$$O^+ + N_2 \rightarrow NO^+ + N + 1 \text{ ev} \tag{26}$$

$$N_2^+ + O \rightarrow NO^+ + N + 2 \text{ ev} \tag{27}$$

is also a source of atomic nitrogen.

However, when a nitrogen atom is produced it reacts with molecular oxygen according to the process

$$N + O_2 \rightarrow NO + O \tag{28}$$

(coefficient a_1)

which has an activation energy of the order of 6 kcal, and nitric oxide reacts with atomic nitrogen

$$NO + N \rightarrow N_2 + O \tag{29}$$

(coefficient a_2)

with a very small activation energy (less than 0.5 kcal).

It can be shown that the concentration of nitric oxide is given by

$$n(NO) = a_1 n(O_2)/a_2 \tag{30}$$

If we consider numerical values for the rate coefficient a_1 and a_2, (30) can be written (T = temperature in °K)

$$[n(NO)]/[n(O_2)] = 10^{-2} e^{-3050/T} \tag{31}$$

which shows that $n(NO)$ is only a small fraction of the concentration of molecular oxygen, for the exponential factor plays an important role.

As far as atomic nitrogen is concerned its concentration depends on the ionization of molecular nitrogen and atomic oxygen; see reactions 26 and 27. Its maximum concentration is given by

$$n(\mathrm{N}) = \frac{n(\mathrm{N}_2)I_{\mathrm{N}_2} + n(\mathrm{O})I_{\mathrm{O}}}{a_1 n(\mathrm{O}_2)} \tag{32}$$

in which I_{N_2} and I_{O} denote the ionization rates of molecular nitrogen and atomic oxygen, respectively.

In order to determine the concentration of atomic nitrogen, it is necessary to know the exact ionization rates of molecular nitrogen and atomic oxygen in the whole thermosphere. In fact, an exact determination of the vertical distribution of atomic nitrogen requires knowledge of $n(\mathrm{N}_2)$, $n(\mathrm{O})$, and $n(\mathrm{O}_2)$, as well as the temperature.

In order to show the maximum possibilities let us take a high production rate of 2000 nitrogen atoms cm^{-3} sec^{-1} in the E and F_1 layers with the respective scale heights of 10 and 50 km corresponding to about 4×10^9 and 2×10^{10} photons cm^{-2} sec^{-1}. It is then possible to obtain the results given in Table 4.

TABLE 4—*Atomic nitrogen and nitric oxide*

Temperature, °K	$n(\mathrm{N})n(\mathrm{O}_2)$, cm^{-6}	$n(\mathrm{O}_2)$, cm^{-3}	$n(\mathrm{N})$, cm^{-3}	$n(\mathrm{NO})$, cm^{-3}
300	2.5×10^{19}	2.5×10^{11}	10^8	2.5×10^2
500	$3\ \times10^{17}$	10^9	3×10^8	4.0×10^1
750	$3\ \times10^{16}$	10^9	3×10^7	2.5×10^3
1000	10^{16}	10^9	10^7	2.0×10^4

The maximum value of the atomic nitrogen concentration would be obtained in the F_1 layer, and it would be the same order as $n(\mathrm{O}_2)$ between 150 and 180 km if the temperature were sufficiently low. However, steady conditions cannot be assured for atomic nitrogen throughout the whole thermosphere, since the lifetime τ_{N} of a nitrogen atom, which is defined by

$$\tau_{\mathrm{N}} = 0.7/[2a_1 n(\mathrm{O}_2)] \tag{33}$$

varies with height. In the E layer, where t[illegible] temperature is low, there may be some vari[illegible]tion, but conditions are such that there [illegible] no great difference between day and night. B[illegible] in the F_1 layer, where there is a photoequili[illegible]rium, the lifetime of a nitrogen atom may [illegible] shorter than one night and, therefore, there [illegible] a daily variation. As far as the F_2 layer [illegible] concerned, lifetimes become sufficiently long [illegible] allow diffusion to be effective. Since the abs[illegible]lute concentration will vary according to t[illegible] varying boundary conditions in the F_1 lay[illegible] the concentration of atomic nitrogen cannot r[illegible]main constant in the upper levels of the therm[illegible]sphere. Furthermore, $n(\mathrm{N})$ will be subject [illegible] variations associated with solar activity.

Diffusion in the thermosphere—In aeronom[illegible] problems it is possible to find a criterion f[illegible] the diffusion phenomenon by making a compa[illegible]son between a mixing distribution, correspon[illegible]ing to a constant mean molecular mass, and [illegible] diffusion distribution, in which each constitue[illegible] behaves according to its own molecular mas[illegible] a diffusion time associated with a certain al[illegible]tude. In such a case, it is easy to determi[illegible] diffusion times for minor constituents to rea[illegible] vertical distribution in diffusion equilibriu[illegible] but the absolute times must be deduced [illegible] using the continuity equation since diffusi[illegible] proceeds continuously. It is found that the pe[illegible]centage concentration change is always the sa[illegible] for all altitudes but corresponds to differe[illegible] diffusion times. This continuous action of d[illegible]fusion is, however, limited by the mass exchan[illegible] due to mixing, which determines a boundary co[illegible]dition. If we compare the theoretical result f[illegible] argon and the observational data, it is possib[illegible] to deduce that mixing times for argon are n[illegible] less than 1 day and not more than 1 week ne[illegible] 110 km.

Therefore, diffusion begins for minor co[illegible]stituents in the thermosphere above 100 k[illegible] As far as principal constituents are concerne[illegible] diffusion should begin at higher levels. Th[illegible] the density in the thermosphere above a ce[illegible]tain altitude depends on the varying molecul[illegible] mass of the principal constituents. It decreas[illegible] with height according to the increasing ratio [illegible] the concentrations of atomic oxygen and mole[illegible]ular nitrogen, which are the principal co[illegible]stituents.

The composition of the thermosphere—It has
een shown in equations 15 and 18 that observa-
onal data must be described by the following
lations

$$\frac{dH}{H} + \frac{dg}{g} = \frac{dT}{T} - \frac{dm}{m} \quad (34)$$

d

$$\frac{d\rho}{\rho} + \frac{dg}{g} = -\frac{1+\beta}{\beta}\frac{dH}{H} \quad (35)$$

ne variation of the scale height between 100 d 700 km is due to a simultaneous effect of e increase of the temperature and of the de- ease of the mean molecular mass. If there is conductive heat flow above 300 km, it is ear that at highest altitudes

$$(dH/H) + (dg/g) = -(dm/m) \quad (36)$$

ssuming such a possibility, it is necessary to nsider a thermospheric model in which the ating is important at 150 km. Considering a adient of the scale height $\beta = 1$, the energy cessary to maintain such a gradient is 1.8 erg n^{-2} sec $^{-1}$ at 150 km and 0.8 at 120 km. As- ming that such a decrease of the energy cor- sponds to a loss by convection, it is possible deduce the composition and constitution of e thermosphere above 100 km. The beginning diffusion is an important factor, however, and assume as a working hypothesis that an av- age level is 150 km.

If we have the following conditions at 100 n:

$$p = 3 \times 10^{-4} \text{ mm Hg} \qquad T = 200^\circ\text{K}$$

$$\rho = 6.6 \times 10^{-10} \text{g cm}^{-3}$$

BLE 5—*Atmospheric data between 120 km and 150 km if $\beta = 1$*

lti- de, m	H, km	T, °K	p, mm Hg	ρ, g cm^{-3}
20	8.4	261	1.9×10^{-5}	3.2×10^{-11}
30	18.4	571	8.8×10^{-6}	6.8×10^{-12}
40	28.4	880	5.7×10^{-6}	2.8×10^{-12}
50	38.4	1186	4.2×10^{-6}	1.5×10^{-12}

TABLE 6—*Thermosphere between 160 km and 220 km in diffusive equilibrium*

Altitude, km	H, km	T, °K	p, mm Hg	ρ, g cm^{-3}
160	40.6	1240	3.2×10^{-6}	1.1×10^{-12}
180	45.2	1355	2.0×10^{-6}	6.4×10^{-13}
200	49.9	1470	1.3×10^{-6}	3.8×10^{-13}
220	54.7	1580	8.9×10^{-7}	2.4×10^{-13}

corresponding to number densities (cm^{-3}):

$$n(O_2) = 2.2 \times 10^{12} \qquad n(N_2) = 1.1 \times 10^{13}$$

$$n(O) = 1.4 \times 10^{12} \qquad M = 27.4$$

we obtain between 120 and 150 km the results shown in Table 5.

Adopting a small gradient $\beta = 0.2$ between 150 and 220 km in a diffusive equilibrium, the atmospheric parameters are given in Table 6. The effect of diffusion between 150 and 220 km is to decrease the mean molecular mass from $M = 27.4$ to $M = 26.3$ corresponding to the following ratios:

At 150 km $\qquad$ At 220 km

$$\frac{n(O_2) + n(N_2)}{n(O)} = 9.3 \qquad \frac{n(O_2) + n(N_2)}{n(O)} = 3.5$$

$$\frac{\frac{1}{2}n(O)}{n(O_2)} = 0.3 \qquad \frac{\frac{1}{2}n(O)}{n(O_2)} = 0.8$$

Keeping the temperature constant ($T = 1580$°K) above 220 km, the atmospheric data up to 750 km are given in Table 7.

The effect of diffusion between 250 and 750 km is to decrease the mean molecular mass $M = 25.6$ to $M = 16.2$, i.e. to a mass corresponding to that of atomic oxygen. See other parameters in Table 8.

If we have the following concentrations at 250 km

$$n(N_2) = 2 \times 10^9 \text{ cm}^{-3} \qquad n(O) = 7 \times 10^8$$

$$n(O_2) = 3 \times 10^8$$

they become at 750 km

$$n(N_2) = 7 \times 10^4 \text{ cm}^{-3} \qquad n(O) = 4 \times 10^6$$

$$n(O_2) = 1 \times 10^4$$

i.e., an atomic oxygen atmosphere.

TABLE 7—*Atmospheric data between 250 km and 750 km**

Altitude, km	H, km	p, mm Hg	ρ, g cm^{-3}	M
250	56.7	4.9×10^{-7}	1.3×10^{-13}	25.6
300	60.9	1.9×10^{-7}	4.7×10^{-14}	24.2
350	66.3	8.1×10^{-8}	1.9×10^{-14}	22.6
400	72.6	3.8×10^{-8}	8.0×10^{-15}	20.9
450	79.1	1.9×10^{-8}	3.7×10^{-15}	19.5
500	85.3	9.9×10^{-9}	1.8×10^{-15}	18.3
550	90.5	5.5×10^{-9}	9.8×10^{-16}	17.5
600	94.8	3.2×10^{-9}	5.5×10^{-16}	17.0
650	98.2	1.9×10^{-9}	3.2×10^{-16}	16.6
700	101.1	1.1×10^{-9}	1.9×10^{-16}	16.4
750	103.3	6.9×10^{-10}	1.1×10^{-16}	16.2

* A possible effect of atomic hydrogen has been neglected.

It is easy to see that, above 250 km, determination of the density by satellites can be explained in an isothermal atmosphere in which the mean molecular mass decreases.

As far as variations are concerned, it can be said that an increase of the ultraviolet radiation from 1.8 erg cm^{-2} sec^{-1} to 3 erg cm^{-2} sec^{-1} at 150 km would lead to a temperature at the thermopause of 2000°K and consequently a density of 1.7×10^{-15} g cm^{-3} at 650 km instead of 3.2×10^{-16} g cm^{-3} when the temperature is 1580°K. Such large variation of the density at 650 km (a factor of 5) for an increase of the thermopause temperature fro 1600°K to 2000°K corresponds only to an ir crease of 50 per cent of the density at 220 km

In the present state of knowledge, there no difficulty in interpreting the thermospher densities and their variations if an ultraviol radiation such as He II (λ340 A) has an energ flux greater than 1 erg cm^{-2} sec^{-1} and reach values up to 5 erg cm^{-2} sec^{-1}.

A heating by a conductive flow from upp levels, which would explain the vertical distr bution, may also be required. In fact, ultravi let heating is acting in the sunlit atmosphe while variations in density from day to nigl appear to be less important than the variatio due to fluctuations in the solar radiation fro day to day. Since a variable heating leads different densities, it is necessary to study th heat transfer governed by the differential equa tion

$$\frac{\partial T}{\partial t} = \frac{AT^{1/2}}{\frac{5}{2}kn} \frac{\partial^2 T}{\partial x^2} \qquad (37$$

in which A and k are two constants. It shoul be found that the time necessary for a pract cal effect of heating is of the order of 1 day altitudes of the order of 200 km. Equation 3 shows that such a time must increase as th square of the distance in a horizontal plane, an is inversely proportional to the density. In oth words, the thermosphere should react rapidl to a variation of the solar ultraviolet radiatio

TABLE 8—*Collision frequency of neutral particles* (ν_M), *mean free path* (L), *and kinematic viscosity* (μ/ρ)

Altitude, km	Temperature, °K	ν_M, sec^{-1}	L, cm	μ/ρ, cm^2 sec^{-1}
50	274	5.8×10^{6}	7.2×10^{-3}	1.6×10^{2}
60	253	1.7×10^{6}	2.3×10^{-2}	5.0×10^{2}
70	210	4.5×10^{5}	8.2×10^{-2}	1.6×10^{3}
80	197	9.0×10^{4}	4.0×10^{-1}	7.6×10^{3}
90	194	1.6×10^{4}	2.2	4.2×10^{4}
100	200	2.9×10^{3}	1.2×10^{1}	2.4×10^{5}
150	1185	1.8×10^{1}	5.0×10^{3}	2.3×10^{8}
200	1468	5.0	2.0×10^{4}	1.0×10^{9}
250	1580	1.8	5.7×10^{4}	3.1×10^{9}
300	1580	7.0×10^{-1}	1.5×10^{5}	7.8×10^{9}
400	1580	1.4×10^{-1}	7.4×10^{5}	4.0×10^{10}
500	1580	3.6×10^{-2}	2.8×10^{6}	1.5×10^{11}
600	1580	(1.2×10^{-2})	(8.8×10^{6})	(4.7×10^{11})
700	1580	(4.1×10^{-3})	(2.5×10^{7})	(1.3×10^{12})

d therefore is not subject to large variations density from day to night and with latitude. onsequently, it is necessary to study the vertil cooling below 200 km after sunset. For exnple, a diminution of the temperature beeen 150 and 200 km would increase the deny at 200 km and would decrease the density 650 km.

Therefore a permanent conductive heat flow necessary. It must come from the sunlit hemihere or from the top of the earth's atmosphere. When the energy involved in the ultraviolet radiation is known, it will be possible to deduce the times necessary to maintain the structure of a sunlit atmosphere in a dark atmosphere.

For references, see M. Nicolet, The composition and constitution of the upper atmosphere, *Proc. IRE*, *47*, 142, 1959; chapter 2, *Upper Atmosphere,* edited by J. A. Ratcliffe, to be published by Academic Press; also The aeronomic chemical reactions, Symposium at San Antonio, November 1958, in press.

Ionizations and Drifts in the Ionosphere

J. A. Ratcliffe

Cavendish Laboratory
Cambridge University, England

Abstract—Our knowledge of the vertical distribution, and the horizontal irregularities and movements, of electrons in the ionosphere is summarized. The mechanism by which electrons can be moved either by the movement of the surrounding air or by electric fields arising from charges elsewhere in the ionosphere is discussed. The statistical description of a randomly moving distribution function which is commonly used by investigators of the ionosphere is described.

1. Distribution of Electrons

Layers and ledges—If a radio wave emitted from the ground travels vertically and is reflected by the ionosphere so as to reach the ground after time t it is said to have been reflected from an equivalent height h' where $h' = ct$. Since the wave characteristic observed when t is measured, travels with the group velocity, h' is not the same as h, the real height of reflection. From a knowledge of the observed $h'(f)$ curve which gives h' as a function of the wave frequency (f) it is possible to deduce the $h(f)$ curve, and from this the $N(h)$ curve which relates the electron number-density N to the (actual) height h. In recent years $N(h)$ curves have been computed for a wide range of places and times. In particular the calculations have been refined so as to take account of the effect of the earth's magnetic field, and of the electrons low down with plasma frequencies less than the smallest exploring frequency; moreover use has been made of both the ordinary and the extraordinary wave traces on the ionograms.

$N(h)$ curves have also been deduced from experiments in which radio waves are emitted from rockets. Several isolated examples of these are available.

All the recent results lead to the conclusion that the electron density increases nearly monotonically upward, but that near 110 or 120 km there is a weakly marked 'peak' where $dn/dh = 0$. This is called the E-layer peak. Above this, there is a weak 'trough' where N falls below its value at the peak by not more than 10 or 20 per cent, and at heights that may l between 240 and 600 km there is a second pea called the F_2 peak. Sometimes by day, b never by night, there is a 'ledge,' or point inflection, near 170 km, called the F_1 ledg Under extreme conditions it can become a 'pea where $dN/dh = 0$.

Although on an $N(h)$ curve the characte istics that mark the E-layer peak and the ledge may seem insignificant they are much mo noticeable on $h'(f)$ curves, and world-wi studies show that the 'critical frequencies' and fF_1 coresponding to these features vary a regular way as the sun's zenith angle alte It seems, therefore, that the E layer and the ledge are of fundamental importance for ion sphere theory. To a first approximation th behave as though they correspond to the pea of layers resulting from the action of solar ph ton radiations having two different mass-absor tion coefficients.

The cause of the F_2 peak has been the subje of much discussion. It probably results fro the action of 'ambipolar' diffusion of the ele tron-ion plasma through the neutral air, co bined with a complicated process of electr loss which varies with height. The details a probably not important for the present co ference.

Mean gradients of electron density—For t present purpose it is important to estimate t gradients of electron density in the ionosphe The $N(h)$ curves derived from radio soundin are most numerous at heights above about 1 km. Here they correspond to vertical gradien

N/dh) of order 5×10^{-2} to 10^{-1} cm^{-4} by y and about 10^{-2} cm^{-4} by night. In a spe- l investigation of the E layer *Robinson* 959] found values of $dN/dh = 3 \times 10^{-2}$ $^{-4}$ at heights of about 110 km. In the E_s layer found $dN/dh = 1$ to 5×10^{-1} cm^{-4}.

$N(h)$ curves deduced from rocket experi- nts are usually irregular. If smooth curves drawn through them they correspond to lues of dN/dh of the same order as those ntioned above.

Echo-sounding methods fail in the D region, low 90 km, but useful evidence can be de- ved from the scattering of waves incident ver- ally. Although it has often been suggested at there might be a peak of electron density heights near 85 km (the so-called D layer), ere is no experimental evidence for its exist- ce. The experiments indicate that the verti- l electron gradients are of the order 10^{-2} $^{-4}$ at 90 km, 10^{-3} cm^{-4} at 80 km, and 10^{-4} $^{-4}$ at 70 km.

Horizontal gradients of electron density are eatest at sunrise. Extreme magnitudes can be duced from the observation that the rate of crease of electron density observed at one int in the F region can be as great as 5×10^5 $^{-3}$ in 1 hour at moderate latitudes, where 1 ur corresponds to about 1000 km. The hori- ntal gradient is hence about 5×10^{-3} cm^{-4} d even at these times is small compared with e vertical. At other times it is negligible in mparison.

Irregular gradients of electron density—Evi- nce for small-scale irregularities comes chiefly om experiments on scattering and is reviewed sewhere.

It is desirable here, however, to assess the gnificance of the irregularities on the $N(h)$ rves deduced from experiments in rockets. *fister and Ulwick* [1958] have pointed out at, if there were irregularities of electron den- ty concentrated in one horizontal plane, they ould produce different diffraction effects at fferent heights so that a rocket traveling ver- cally might appear to be moving through a stribution of electrons that was irregular in e vertical direction. In practice the rockets so had horizontal components of velocity, so at they would also experience the direct ef- ct of the horizontal variations. It is therefore not safe to suppose that the irregularities shown on the published $N(h)$ curves deduced from rocket soundings are real.

If the irregularities on the published curves were real they would correspond to irregular variations in dN/dh of order 10 cm^{-4}.

2. Horizontal Drift Movements of Electrons

Methods of measurement—Horizontal movements of *irregularities* in the electron density can be detected and measured at the ground by observing radio waves (a) reflected from meteor trails, (b) reflected from the body of the ionosphere, (c) received from radio stars after transmission through the ionosphere. Observations (a) on meteor trails refer to movements at a measurable height. Observations (b) and (c) refer to phenomena that might have been imposed on the reflected wave by electron movements at a series of different heights. Diffraction theory has been applied, in considerable detail, in attempts to relate movements in the wave diffraction pattern at the ground to movements at different levels in the ionosphere.

Waves reflected from the body of the ionosphere, (b) above, exhibit phenomena of (i) irregular fading and (ii) isolated irregularities such as kinks on the $h'(t)$ or $h'(f)$ curve, or isolated bursts of increased amplitude. It is convenient, at any rate to start with, to consider these two phenomena separately, but without suggesting that they are unrelated.

From the irregular fading of waves of types (b) and (c) observed at three closely spaced points it is possible to separate an 'average drift' and a component of 'irregular movement' of the wave pattern at the ground. The precise meaning of these two components is explained in section 4. We are concerned here only with the average drift. There are reasons for supposing that the average drift of the wave pattern at the ground is a measure of the average drift of the ionospheric irregularities *at the level of reflection for case* (b) *or at levels above about 250 km in case* (c).

Drifts in the E region—[*N.B. In all ionospheric work, drifts are described in terms of the direction toward which the movement occurs. This is the opposite of the meteorological*

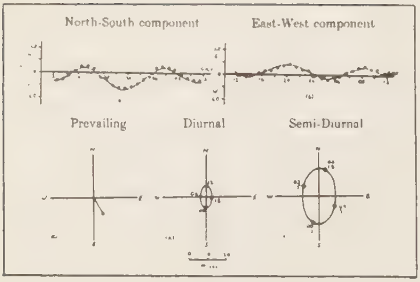

FIG. 1—Average wind components throughout the day for the 12-month period September 1953–August 1954. (*a*) North-south component, (*b*) east-west component, (*c*) prevailing wind: polar presentation; (*d*) diurnal component: polar presentation; (*e*) semidiurnal component: polar presentation.

convention by which winds are described in terms of the direction from which they blow.] Experimental results from methods using reflections from (*a*) meteor trails and (*b*) the body of the ionosphere show that the mean drift in the E region can be analyzed into components (*i*) that are constant throughout 24 hours, (*ii*) that have a period of 24 hours, and (*iii*) that have a period of 12 hours. Average results obtained at Manchester, England, for the year September 1953 to August 1954 are shown in Figure 1. These year-long averages correspond to: (*i*) a constant drift of 15 m sec^{-1} toward the southeast; (*ii*) a drift which rotates in a clockwise sense once in 24 hours directed south at 000 hours, and with magnitude about 10 m sec^{-1}; (*iii*) a drift which rotates in a clockwise sense once in 12 hours, being directed north at 05 and 17 hours, and having a magnitude of about 20 m sec^{-1}. Results from other places in the northern hemisphere agree with these in rough outline, but not in detail.

In the southern hemisphere the direction of rotation of the 24- and 12-hour rotating components are both reversed. The 24-hour component is larger.

In the range of heights from 85 to 110 km the 12-hour rotating component has a direction (θ) which depends on the height, so that $d\theta/dh = 7°$ km^{-1}. The magnitude of the 12-hour component also increases with height, with a gradient of about 1 m sec^{-1} km^{-1}.

The 12-hour rotating component appears to be nearly the same as the 12-hour rotating com- ponent of atmospheric wind deduced by Weeke and Wilkes from theories of atmospheric move ment. Unfortunately, however, their deduction were based on a supposed temperature distri bution that does not now seem reasonable.

The outline given above is based on on year's average. The phases and magnitudes o the different components change through th seasons in a somewhat peculiar way.

Echoes reflected obliquely from auroral ioni zation in the E region give different results They show movements to the west before mid night and to the east after midnight.

Drifts in the F region—The drifts in the F region are predominantly in the east-west direc tion. Below about 400 km at latitude 50°N they are toward the east by day and toward th west by night and have magnitudes of abou 50 m sec^{-1}. Near the magnetic equator the di rection of the drift is reversed: it is toward th west by day and the east by night. This is i accord with the theory which supposes the drif to be caused by the action of electric field [*Martyn*, 1955]. Above about 400 km the drif is also predominantly in the east-west direction but the change-over from east to west occur not at sunrise, but earlier, at about 02 hours.

The magnitude of the F region drift is greate when the magnetic K index is greater. At time of marked magnetic disturbance the drift can b as great as 500 m sec^{-1}. The probability of a re versal of direction near 02 hours increases as K increases.

Random drift velocities—Measurements mad on fading by the close-spaced receiver metho show that there are random velocities super imposed on mean drift velocity (v). If these ar described in terms of the quantity V_o discusse in section 4 it appears that, in the E and F regions, $V_o < V$, and in the D region there i some evidence that V_o may be 2 or 3 times a great as V.

Traveling disturbances—When waves reflecte from the F layer are observed at separate places they often exhibit isolated features tha appear to move, in recognizable form, over con siderable distances. In their most marked form these features are recognizable on the $h'(f)$ curves, or on $h'(t)$ traces in which h' is observe as a function of the time (t) on one frequency

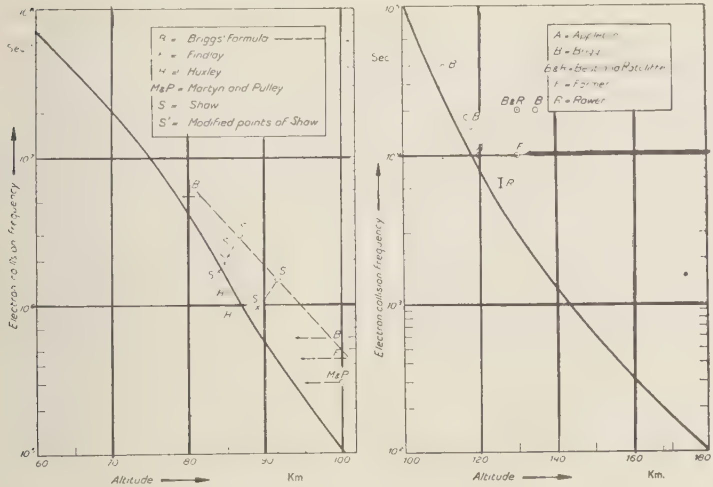

FIG. 2—Electron collision frequency as a function of altitude [*Nicolet*, 1953].

'hey can then be interpreted as distortions of ıe contours of electron density, and it might e thought that they corresponded to some ind of wave traveling through the ionosphere.

These 'traveling disturbances' are frequently ccompanied by 'bursts' of intensity of the re-ected wave of a kind which could be ascribed ɔ focusing by the distorted ionosphere. Fur-her study reveals that these isolated 'bursts' ccur, in less marked form, even when the $h'(f)$ r $h'(t)$ trace is not sensitive enough to show ny abnormality. The large isolated bursts are ndoubtedly associated with the irregularities in he contours. It is reasonable to suppose that he smaller ones are of similar nature.

Although attention has been mainly concen-rated on the traveling disturbances noticeable ı the F region, it is established that corre-ponding disturbances are present in the E re-ion, on a smaller scale. Smaller traveling dis-urbances are also observable in the F region. *Munro* [1958], who has made a detailed tudy of traveling disturbances in the F region, as reached the following conclusions: (a) they ccur on the average about six times during any ne day, but hardly ever at night; (b) in Aus-ralia the movement was predominantly toward he northeast in winter and southeast in sum-ıer, and the average velocity was about 120 m ec^{-1}; (c) the disturbances can extend over distances as great as 100 km and can travel distances of 3000 km.

In both regions the sizes of these disturbances are often of the order of 2 km, and have been seen to travel distances of the order of 50 km without much change.

3. The Causes of Electron Drift

The electrons in the ionosphere are accompanied by positive ions in equal numbers, so that the medium is, on the average, electrically neutral. The electron–positive-ion plasma is immersed in neutral air of density such that the ratio of the number density of neutral molecules or atoms to the number density of the electrons is about 10^9 in the D region, 10^7 in the E region, and 10^3 or 10^4 in the F region.

The electrons collide with neutral molecules with a frequency that is usually denoted by ν and should not be confused with kinematic viscosity for which the same symbol is used. The electron collision frequency at different heights is shown in Figure 2. It is probable that the values of ν near 100-km height are 3 or 4 times smaller than those suggested in this figure by *Nicolet* [1953]. The frequency with which positive ions collide with neutral molecules is about 50 times smaller than the electron collision frequency.

The electrons and ions can be set into mo-

tion either by the impact of the neutral molecules or by an imposed electric field originating, perhaps, in a space charge built up elsewhere in the ionosphere. The motions are subject to the effect of the earth's steady magnetic field. We shall consider the motions of the 'background' electron distribution and of irregularities in it and shall show that they may be different from one another and from the motion of the surrounding neutral air.

Force due to moving air—If the neutral air has a drift velocity C and the electrons have, on the average, zero drift velocity, a drift velocity approximately equal to $2C$ is communicated to an electron at a collision. Since a single electron makes ν collisions per second, the momentum transferred in that time is $2C\nu m$, which is therefore the force exerted on each electron by the drifting neutral air. By the same reasoning the force exerted on ions having the same mass as the neutral molecules is $C\nu m$.

Movements in the absence of collisions—Consider a single electron moving under the action of forces F_x, F_y, F_z along the coordinate axes in the presence of an imposed magnetic field B along the OZ axis. Suppose further that the electron makes no collisions. (The forces could not be caused by the surrounding air if there were no collisions, but for the present purpose that is of no significance.) Then with initial conditions $\dot{x} = \dot{y} = \dot{z} = 0$ it can be shown that the subsequent motion of an electron is described by the equations:

$$\left.\begin{aligned} \dot{x} &= (F_x/eB)\sin\omega t \\ &\qquad + (F_y/eB)(1 - \cos\omega t) \\ \dot{y} &= -(F_x/eB)(1 - \cos\omega t) \\ &\qquad + (F_y/eB)\sin\omega t \\ \dot{z} &= F_z t/m \end{aligned}\right\} \quad (1)$$

with $\omega = Be/m$ written for the angular gyrofrequency of the electron.

If $F_y = F_z = 0$, the motion is as illustrated in Figure 3 and corresponds to a mean drift velocity $\bar{\dot{y}} = -F_x/eB$ along the negative OY direction perpendicular both to the force F_x and to the field B.

If the force F_x is caused by an electric field E_x the mean drift velocity is given by $\bar{\dot{y}} = -E_x/B$ and is independent of e or m. It is therefore the same for electrons and positive ions.

Movements in the presence of collisions with average collision frequency ν—The probability of a time t between collisions is $e^{-\nu t}$. The free motion continues for this time, stops, and is restarted. The average velocities therefore contain the expressions

$$\frac{\int e^{-\nu t}\sin\omega t\,dt}{\int e^{-\nu t}\,dt} = \frac{\omega\nu}{\nu^2+\omega^2}$$

and

$$\left\{1 - \frac{\int e^{-\nu t}\cos\omega t\,dt}{\int e^{-\nu t}\,dt}\right\} = \frac{\omega^2}{\nu^2+\omega^2}$$

and equations 1 give rise to

$$\left.\begin{aligned} \bar{\dot{x}} &= \frac{F_x}{eB}\frac{\omega\nu}{\nu^2+\omega^2} + \frac{F_y}{eB}\frac{\omega^2}{\nu^2+\omega^2} \\ &= \frac{F_x}{m\nu}\frac{\nu^2}{\omega^2+\nu^2} + \frac{F_y}{m\nu}\frac{\nu\omega}{\omega^2+\nu^2} \\ \bar{\dot{y}} &= -\frac{F_x}{eB}\frac{\omega^2}{\nu^2+\omega^2} + \frac{F_y}{eB}\frac{\omega\nu}{\nu^2+\omega^2} \\ &= -\frac{F_x}{m\nu}\frac{\nu\omega}{\nu^2+\omega^2} + \frac{F_y}{m\nu}\frac{\nu^2}{\nu^2+\omega^2} \\ \bar{\dot{z}} &= \frac{F_2}{eB}\frac{\omega}{\nu} = \frac{F_z}{m\nu} \end{aligned}\right\} \quad (2$$

If $F_y = F_z = 0$

$$\left.\begin{aligned} \bar{\dot{x}} &= \frac{F_x}{eB}\frac{\omega\nu}{\nu^2+\omega^2} \\ \bar{\dot{y}} &= -\frac{F_x}{eB}\frac{\omega^2}{\nu^2+\omega^2} \end{aligned}\right\} \quad (3$$

Collisions have resulted in: (*a*) reducing the velocity $\bar{\dot{y}}$, (*b*) reducing $\dot{z}$ to a steady mean value instead of one which increases continuously and (*c*) introducing a velocity $\bar{\dot{x}}$. The reason for the changes in $\bar{\dot{y}}$ and $\bar{\dot{x}}$ can be seen by considering the motion when ν is constant and equal to ω, as represented in Figure 4.

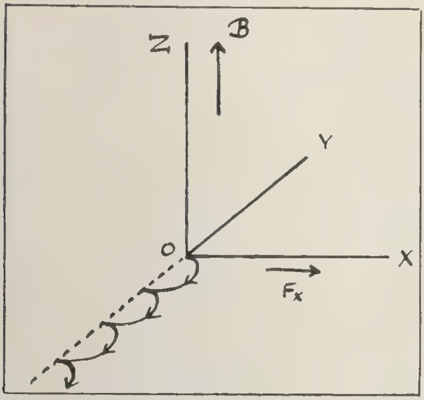

FIG. 3—Motion of an electron without collisions.

Electrons alone moving. The Hall effect in a etal slab—In a metal only the electrons move. f $E_y = E_z = 0$ the current density is given by riting $F_x = eE_x$,

$$j_x = ne\bar{\dot{x}} = \frac{ne^2E_x}{B}\frac{\nu\omega}{\nu^2 + \omega^2} \quad (4)$$

$$j_y = ne\bar{\dot{y}} = -\frac{ne^2E_x}{B}\frac{\omega^2}{\nu^2 + \omega^2} \quad (5)$$

nd it is not in the direction of E_x. If the metal in the form of a slab, bounded by planes arallel to the XZ plane, no current can flow the OY direction. Charges are built up on he surfaces, and they produce a polarization eld E_y just sufficient to reduce j_y to zero.

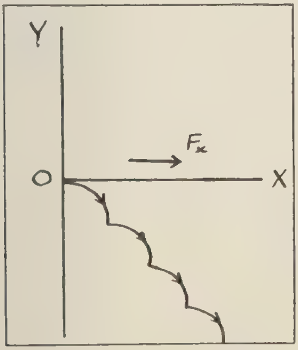

FIG. 4—Motion of an electron, collision and gyro frequencies equal.

This requires

$$j_y = \frac{ne^2}{B}\left\{-\frac{E_x\omega^2}{\nu^2 + \omega^2} + \frac{E_y\nu\omega}{\nu^2 + \omega^2}\right\} = 0 \quad (6)$$

and

$$j_x = \frac{ne^2}{B}\left\{\frac{E_x\nu\omega}{\nu^2 + \omega^2} + \frac{E_y\omega^2}{\nu^2 + \omega^2}\right\} \quad (7)$$

Equation 6 gives

$$E_y = (\omega/\nu)E_x \quad (8)$$

Substitution into (7) gives

$$j_x = (ne^2/m\nu)E_x \quad (9)$$

The current is now just what it would have been if no magnetic field had been present. The existence of the field E_y is the Hall effect. The force per unit volume on the positive ion lattice is

$$neE_y = (ne\omega/\nu)E_x = (ne^2/m\nu)BE_x$$

and this is also equal to $j_x \times B$, the force calculated in the ordinary way.

Ions and electrons both moving in an unbounded medium—If a magnetic field B_z and an electric field E_x are applied to an unbounded medium in mutually perpendicular directions it is usual to write

$$\bar{\dot{x}} = tE_x \quad (10)$$

$$\bar{\dot{y}} = hE_x \quad (11)$$

where t and h are the 'transverse' and 'Hall' mobilities, respectively. Equations 3 show that, for electrons embedded in neutral air,

$$t = \frac{1}{B}\frac{\nu\omega}{\nu^2 + \omega^2} = \frac{\nu}{m(\nu^2 + \omega^2)} \quad (12)$$

$$h = -\frac{1}{B}\frac{\omega^2}{\nu^2 + \omega^2} = \frac{-\omega}{m(\nu^2 + \omega^2)} \quad (13)$$

and, with V_x, V_y, V_z written for $\bar{\dot{x}}$, $\bar{\dot{y}}$, $\bar{\dot{z}}$,

$$\begin{Bmatrix} V_x \\ V_y \\ V_z \end{Bmatrix} = \begin{Bmatrix} t & h & 0 \\ -h & t & 0 \\ 0 & 0 & \dfrac{e}{m\nu} \end{Bmatrix} \begin{Bmatrix} E_x \\ E_y \\ E_z \end{Bmatrix} \quad (14)$$

The velocity of the electrons is not, in general, along the direction of the field E.

Similar expressions govern the velocity of the ions, but, since both ν and ω are different for ions and electrons, the magnitudes of t and h are also different. The ions and electrons thus move, in general, in different directions, with different velocities V_i and V_e. There is one direction, θ, in which the resolved parts $(V_i)_\theta$ and $(V_e)_\theta$ of the velocities are the same. This is the direction in which the ion-electron plasma moves bodily; there is no component of current in this direction. In a direction perpendicular to θ there is a current density j given by

$$j = (V'_i - V'_e)ne$$

where the primes represent the components of the velocities perpendicular to the θ direction. It can be shown that the velocity of bodily movements in the θ direction is just what would be calculated by taking the force to be that produced by the magnetic field acting on the current.

It can also be shown that, if $E_y = E_z = 0$ and θ represents the angle measured from OX, then

$$\tan\theta = (h_e - h_i)/(t_e + t_i) \qquad (15)$$

In the ionosphere it may be supposed that, approximately, $\nu_e/\nu_i = 50$, $m_i/m_e = 4.5 \times 10^4$, $B = 0.45$ gauss. Figure 5 then shows the orientation and magnitudes of the drift velocities and currents produced by an electric field E perpendicular to the magnetic field, at a pressure such that $\omega_e/\nu_e = 10$.

Magnitudes in the ionosphere—Figure 6 shows

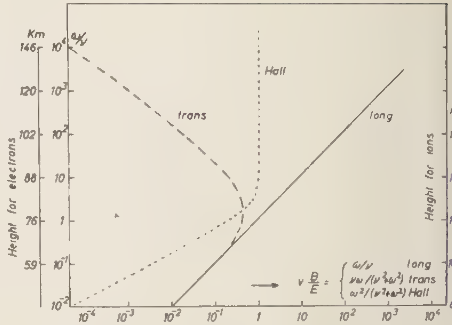

FIG. 6—Drift velocities of ions in the presen of a magnetic field as a function of ω/ν. Dri along the magnetic field B, full line. Drift parall to E and perpendicular to B, dashed line. Dri perpendicular to E and B, dotted line.

how the transverse (t) and Hall (h) mobiliti vary with ω/ν, and it also shows the heights a model ionosphere appropriate to the give values of ω/ν for electrons and ions separatel Figure 7 shows the magnitudes of t and h f electrons and ions plotted against height.

If the ionosphere were uniform and if a for **F** (caused by a wind in the neutral air) or field **E** acted perpendicular to **B** as show the electrons and ions would move as indicate

It is important to consider the relative ea with which winds and electric fields can move t electron-ion plasma in the ionosphere. The for is calculated by first deducing the current densit **j** and then writing the total force as **F** + **j**

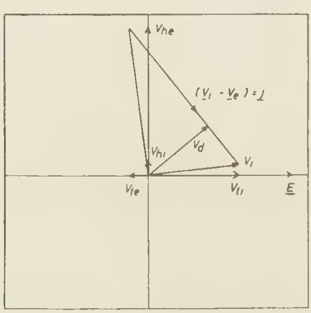

FIG. 5—Drift velocities for ions and electrons in an electric field E, perpendicular to the magnetic field, at a pressure such that $\omega_e/\nu_e = 10$.

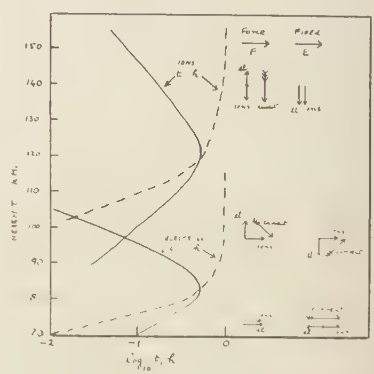

FIG. 7—Currents resulting from differing transverse and Hall mobilities as a function of altitud

eference to Figure 7 will show what happens. irst consider the case where a force is applied by wind. At low levels (70 km) the wind moves ie electrons and ions together and there is current. At high levels (140 km) there is a irrent perpendicular to **F**, and this, in the eld **B**, experiences a force that can be shown be just equal and opposite to **F**, so that there no movement. At intermediate levels the irrent is inclined to **F** so that the resultant rce is not entirely along **F**.

A bounded homogeneous ionosphere—In the ase just considered there was no limitation on ie current flow that could take place at any ngle to the applied electric field. In the case of bounded plasma there will generally be some mit on the directions of current flow; there ust be no flow of current across the bounaries. If equations 2 lead to a current flow cross the boundaries, a space charge will be t up which will produce a field just adequate stop the flow of current across the boundary; is does not imply that there will be no drift the boundary, and, unless an additional meanical force is provided, the boundary of the lasma will move.

The total electric field to be used in equaon 14 is now the sum of the applied field and ie polarization field to prevent current flow cross the boundaries; in some cases this polariation field may be much greater than the aplied field, and the drift velocity, v_d, will be orrespondingly enhanced.

An inhomogeneous ionosphere—The ionohere presents a still more complicated probm, as the decrease of collision frequency with eight makes the plasma inhomogeneous and ie nature of the ionosphere limits to some exnt the possible directions of current flow.

If the ionosphere were considered as a series concentric spherical shells the currents and olarization fields would be different in each iell. But it is shown in Figure 6 that at most eights the mobility along the magnetic field is uch larger than either t or h. Thus a solution hich implies differences of electrostatic potenal at different points of a line of B must be nsatisfactory. The high value of the longitudial mobility will make the lines of B very early equipotentials. The polarization fields et up at one level may be partly short-circuited by the ionization at other levels, and the problem of the electric fields throughout the ionosphere must be considered as a whole. In particular a polarization field set up in E region, where the conductivity per ion pair is a maximum, will be carried by the lines of B to the F region, as originally pointed out by Martyn.

The movement of an irregularity in the ionosphere—All the discussion so far has been concerned with the movements of the ionization in a uniform layer; this drift would not be detectable in general, although it may have important implications for the world-wide distribution of the ionization. The majority of methods of measuring ionospheric drifts take advantage of the existence of irregularities in the region. It is not at all obvious that such irregularities will move in the same way as the background ionization or with the neutral air if there is a wind.

Martyn [1953] attempted to study the behavior of a cylindrical irregularity in a uniform homogeneous plasma with the axis of the cylinder along the geomagnetic field. He was unable to find a satisfactory solution to his problem and concluded that such an irregularity would be unstable. *Clemmow, Johnson, and Weekes* [1955] studied the same problem and concluded that there is a steady-state solution in which the cylinder moves with a velocity dependent on the ratio λ of the ionization in the cylinder to

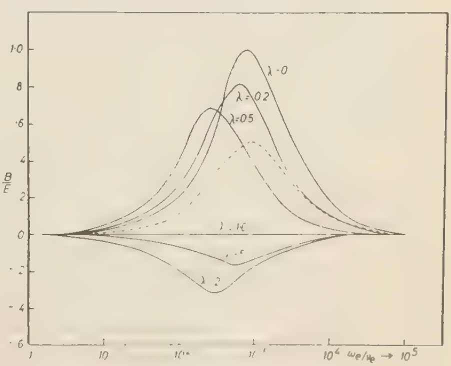

FIG. 8—Drift velocity, parallel to the applied electric field, of a cylindrical irregularity (full line) as a function of the ratio of electron density in the cylinder to that in the surrounding plasma. Drift of the surrounding plasma (dotted line).

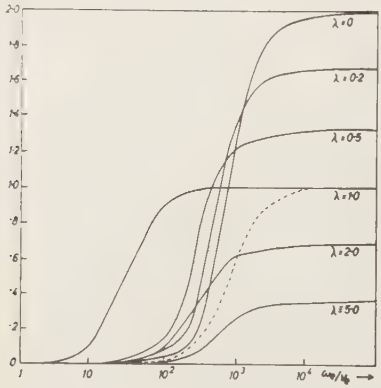

FIG. 9—Drift, perpendicular to the applied electric field, of a cylindrical irregularity (full line) compared with the drift of the surrounding plasma (dotted line).

that in the plasma and on the value of ω_e/ν_e.

In Figures 8 and 9 the values of vB/E for movement parallel to E and perpendicular to E are plotted together with the drift velocities for the background ionization. A similar solution was found for an infinite slab with the magnetic field in the plane of the slab, and in this case a time-varying solution of the equations for small departures from the plasma density was possible; it showed that the slab did in fact move with the steady-state velocity, changing its form only slowly. No steady-state solution was found for any three-dimensional irregularity where the high mobility parallel to B seems to imply that the irregularity will change its form rapidly with time. No solution has yet been obtained for an inhomogeneous plasma.

Summary—An ionized layer or an irregularity in such a layer may be moved either by a wind in the neutral gas or by an applied electric field. In comparing the relative efficiencies of these two cases we may compare the velocities of drift resulting from a wind of velocity $\mathbf{C}_0$ and from an electric field $\mathbf{E} = \mathbf{C}_0 \times \mathbf{B}$. It should be noted that, for the drift of an irregularity shown in Figures 8 and 9, the velocity components are relative to the air. If there is a wind $\mathbf{C}_0$, contributing $\mathbf{C}_0 \times \mathbf{B}$ to $\mathbf{E}$, the velocity relative to the fixed observer is $(\mathbf{V} + \mathbf{C}_0)$.

The discussion presented in this paper leads to the conclusions:

1. In F region ($\omega_e/\nu_e > 10^4$): (*a*) a wind is very inefficient in causing drift of a layer; th induced field $\mathbf{C}_0 \times \mathbf{B}$ produces a drift $-\mathbf{C}_0$, an the ionization does not move. (*b*) An electri field, due to polarization changes, causes a dri E/B. (*c*) A cylindrical irregularity, with its ax along $\mathbf{B}$, moves perpendicular to $\mathbf{E}$ with a ve locity proportional to E/B and dependent o λ. If λ is equally distributed above and belo unity the average drift would be nearly E/I scatter of the estimated drifts could be due t different values of λ.

Figure 9 shows that a wind could caus movement of an irregularity of the order of C provided that the ionization in the irregularit was appreciably different from that in the plasma drifts for $\lambda \gtrless 1$ would be in opposite direction

2. In E region ($10 < \omega_e/\nu_e < 10^4$): (*a*) $\mathbf{C}_0$ an $\mathbf{E}$ are roughly equally efficient in producin drift of a layer. It must be remembered tha $\mathbf{E}$ is not necessarily equal to $\mathbf{C}_0 \times \mathbf{B}$ and ma be much larger, owing to polarization charge (*b*) A cylindrical irregularity now has componen of velocity parallel and perpendicular to I both components depend rather markedly on λ and the resulting drift velocity for differen values of λ is difficult to estimate. Much scatte in apparent drifts would arise from differen values of λ.

3. In D region ($\omega_e/\nu_e < 10$): The electro magnetic effects are now of little importanc and the efficient method of moving the laye or an irregularity would be by a wind.

4. THE STATISTICAL DESCRIPTION OF A RAN DOMLY MOVING DISTRIBUTION FUNCTION

In ionospheric work, measurements are mad on the irregular diffraction pattern formed ove the ground by the downcoming radio wave. Th pattern is described by means of a nomencla ture illustrated below for the case of one spac dimension. It can be extended to two and thre dimensions. It has become common, in iono spheric work, to describe the statistical prope ties of the ionospheric irregularities in the sam way.

Let $f\ (x, t)$ be a randomly moving diffractio pattern in one dimension (x).

The speed of fading S is defined by

$$S = \overline{\left|\frac{\partial f}{\partial t}\right|} \div \bar{f}$$

is the mean rate of change of f, observed at ixed point, and normalized to the mean value f.

The mean gradient G is defined analogously

$$G = \overline{\left|\frac{\partial f}{\partial x}\right|} \div \bar{f}$$

The drift velocity V—If the observer moves th a velocity V the speed of fading (S) that observes will alter. The value of V that gives its smallest value is called the drift velocity the pattern.

The characteristic velocity V_c—Consider a anging pattern for which the drift velocity is zero. It is convenient to define a velocity $= S/G$ such that the observed fading speed ild have been produced by a 'frozen' unanging sample of the pattern moving past the server with velocity V_c. In the actual pattern nsidered there is no mean drift and the fading ses because the pattern changes irregularly. ie fading could have had the same statistical ture if the pattern had not changed but had oved with a constant drift velocity V_c.

The quantities V and V_c are not measured directly; they are usually deduced from fading records made at three different receiving points.

References

Clemmow, P. C., M. A. Johnson, and K. Weekes, A note on the motion of a cylindrical irregularity in an ionized medium, in *The Physics of the Ionosphere,* pp. 136–139, Physical Society, London, 1955.

Martyn, D. F., Electric currents in the ionosphere. III. Ionization due to winds and electric fields, *Phil. Trans. Roy. Soc. London, A, 246,* 306–320, 1953.

Martyn, D. F., Interpretation of observed $F2$ 'winds' as ionization drifts associated with magnetic variations, in *The Physics of the Ionosphere.* pp. 161–165, Physical Society, London, 1955.

Munro, G. H., Travelling ionospheric disturbances in the F region, *Australian J. Phys., 11,* 91–112, 1958.

Nicolet, M., The collision frequency of electrons in the ionosphere, *J. Atmospheric and Terrest. Phys., 3,* 200–211, 1953.

Pfister, W., and J. C. Ulwick, An analysis of rocket experiments in terms of electron-density distributions, *J. Geophys. Research, 63,* 315–333, 1958.

Robinson, B. J., *Repts. Progr. Phys.,* in press, 1959.

The Natural Occurrence of Turbulence

R. W. Stewart

University of British Columbia
Vancouver, B. C., Canada

Abstract—In order to make the scientific meaning of the word 'turbulence' clear, it is proposed that a fluid be called turbulent if each component of the vorticity is distributed irregularly and aperiodically in time and space, if the flow is characterized by a transfer of energy from larger to smaller scales of motion, and if the mean separation of neighboring fluid particles tends to increase with time. Whether or not a flow is turbulent is not simply a matter of Reynolds number, since the *stability* of the flow is a criterion of at least equal importance.

From the results of experimental work in recent years of a number of people (Anderson, Frenkiel and Katz, Kellogg, Liller and Whipple, Malkus) it seems reasonable to infer that, with the exception of strong inversion layers, the atmosphere may be assumed to be turbulent everywhere, although the intensity of the turbulence varies widely in both time and space. If the Kolmogoroff similarity theory of locally isotropic turbulence is accepted, the most important parameter in the turbulent field is the energy dissipation ϵ.

The phenomenon of turbulence is one that, by its very nature, lends itself only too readily to inexact thinking by individuals and inexact communication between individuals. The word itself, in common with such terms as 'force' and 'work,' antedates its scientific use. Like those words it now has two parallel meanings, one scientific and one colloquial. Unfortunately, unlike the expressions of mechanics, the scientific definition of 'turbulence' has never been so clear and unequivocal as to avoid confusion with the colloquial meaning of the word.

I think that we can hardly do better, in a conference of this kind, than to start by trying clearly to define what it is we are talking about. I therefore propose to start by inventing a definition of turbulence which will, I hope, be acceptable to my fluid dynamics colleagues. To start with, turbulence is a *condition,* not a *thing,* and perhaps in our definition we should follow the practice of pathology and describe a syndrome that will define turbulence.

I shall therefore essay the following: 'A fluid is said to be turbulent if each component of the vorticity is distributed irregularly and aperiodically in time and space, if the flow is characterized by a transfer of energy from larger to smaller scales of motion, and if the mean separation of neighboring fluid particles tends to increase with time.' This definition excludes all two-dimensional flows, as well as such phenomena as vortex streets, whirlpools, convectio cells, and internal waves. I think that flu dynamicists would agree that these are n what they have in mind when they discuss tu bulence.

While I am concerned with definitions, the is another term that warrants some attentio namely 'eddy.' The dictionary says 'whirlpoo but that is not what we have in mind. In t usage of those working on problems in tu bulence an eddy simply means a volume fluid moving more or less coherently with r spect to the mean flow. This eddy motion nee not be, and usually is not, of a rotating chara ter. The term can frequently be interchange with the cumbersome expression 'scale of m tion.'

Alternatively, and adding somewhat to t confusion, in theoretical discussions 'eddy' often shorthand for 'Fourier component of t velocity field' or 'Fourier component with certain scalar wave number.' These usages d scribe different things, and so one may, wit out embarrassment, ask what is meant by 'edd in any given context.

Traditionally turbulent flow has always bee contrasted with laminar flow, and whether not a given flow will be turbulent is considere to be a matter of Reynolds number, which essence is the ratio of the inertial terms to t viscous terms in the Eulerian equation of flu

tion. In geophysical cases, however, the Reyn-s number is rarely an important parameter. he exception may be with such troublesome ssibilities as convection currents in the earth's ntle.) An example can be taken from the d of oceanography. In many deep ocean sins the water is very nearly in adiabatic uilibrium—so nearly so that modern meas-ement techniques cannot with certainty es-blish whether or not the structure is stable *ational Academy of Sciences–National Re-rch Council*, 1959]. Currents in the deep ean are believed to be very weak, of the order 1 cm/sec. Now if we form a Reynolds number such a flow in the bottom kilometer of water find that it comes to about 10^7, or as great as t of a river 3 meters deep moving at 6 knots, ich is obviously fully turbulent. However, if ere is a small potential density gradient such t over the kilometer of depth the potential nsity changes by only 1 part in 10^6—about limit of precision of our knowledge of the abatic gradient—then it is unlikely that more n the bottom few tens of meters are turbu-t.

This illustrates an important fact about tur-lence in nature: by and large it is *stability* t determines whether or not a given volume air, or of water, is turbulent. It would be y unusual if the velocity gradient were not ficiently great to sustain turbulence, although course the turbulent intensity might be ex-dingly low. We may say with some confidence t, if air or water is unstable or in neutral bility on a large scale, it will be turbulent. nost never will the velocity gradient be so all that turbulence will be inhibited by too a Reynolds number.

The situation when the structure is stable, wever, is very much more difficult, and it uld be most unwise to attempt to be too gmatic. It is known that, if the velocity dient is sufficiently great, the regime will be bulent in spite of gravitational stability. It also known that for much weaker velocity dients the flow is almost purely laminar. In ermediate cases, as the velocity gradient in-eases with a given density gradient, we find ccessively the formation of internal waves, the eaking of internal waves, and the onset of bulence. The criteria involved, and even the tails of the phenomena, are still the subject of active research and some controversy [see, for example, *Ellison*, 1957, and *Townsend*, 1958*a*].

In the atmosphere another effect is of great importance. If the gas is fairly opaque to its own radiation, and if density is purely a function of temperature, the density of the gas may be determined almost completely by the radiation balance. Thus an apparently stable structure may in practice not behave stably since, for example, a rising volume of air may be warmed by radiation sufficiently rapidly that the cooling by expansion is canceled, and the motion may be more nearly isothermal than adiabatic. This topic has been considered theoretically by *Townsend* [1958*b*]. Radiation may act in the opposite direction too, of course, and *Goody* [1956] has shown that radiation greatly reduces the ability of unstable density structures, if determined by temperature, to drive convection currents.

This brings us to the point where we can discuss the natural occurrence of turbulence, as defined above. It seems that, wherever the density structure is neutral or unstable, we should consider the fluid to be turbulent, since in the situations we are considering it is inconceivable that the very small velocity gradients required would not be present. In these cases we can attempt to predict the intensity of the turbulence even if we are unable to make observations. Extensive experimental work in recent years, together with theoretical treatments, in particular those of *Malkus* [1956] and *Malkus and Veronis* [1958], have given us some confidence in such situations. It should be noted that the definition of turbulence I am employing can include movements of very low intensity, which would be classified as nonturbulent if one were to use as a criterion an arbitrary level of fluctuating velocity, e.g., the 1 ft/sec chosen by *Anderson* [1957].

With stability, however, we are on much less secure ground. We must first look to our criteria of turbulence. The mere fact that there is a transport of momentum vertically by a shearing stress is not sufficient to establish the existence of turbulence, since any mechanism for the production of internal waves transports momentum. Nor is the transport of physical properties of the fluid conclusive: this can occur by the breaking of internal waves followed by

severe stretching in a laminar shear flow and molecular mixing. Similarly, the existence of fluctuations in properties may be due either to turbulence or to breaking internal waves.

For firm evidence of the existence of turbulence we must look for evidence of the actual turbulent velocities. This can be done by means of probing instruments such as an aircraft [*J. S. Malkus*, 1954] or the gustsonde [*Anderson*, 1957] or by observing the dispersal of tracer impurities [*Frenkiel and Katz*, 1956; *Kellogg*, 1956]. The behavior of a tracer is one of the best critical tests for turbulence. Since the situation can usually be watched for a considerable period of time the characteristic diffusive behavior of turbulence can be observed even when the turbulent intensity is so low that an instrument which measures instantaneous velocity may give little or no response.

The statistical analysis by *Anderson* [1957] reveals that, in mid-latitudes at least, intense turbulence is a rather scattered phenomenon in the atmosphere. It tends to occur in layers a few tens or hundreds of meters thick separated by generally more extensive layers which are characterized as nonturbulent by applying his 1 ft/sec criterion. He finds virtually no turbulent layers above 15 km. On the other hand, all the smoke-puff experiments reported by *Kellogg* [1956] show the characteristic diffusive properties of turbulent flow. They extend over an altitude range from about 7.5 km to about 20 km. As Kellogg calculates the turbulent velocities to lie in the range from 4 to 10 cm/sec, there is no conflict with Anderson. It is clear, however, that turbulence is the usual condition of the atmosphere even in the highly stable stratosphere, provided that one does not set an arbitrary lower limit to the intensity that will be described as turbulence.

At higher levels we are faced with a great paucity of data. We have, however, the excellent observations of *Liller and Whipple* [1954] on the movements of visual meteor trails in the 100-km region. The cross correlations calculated from these observations have all the characteristics of rather low Reynolds number turbulence. It seems reasonable to infer that, with the exception of strong inversion layers, the atmosphere may be assumed to be turbulent everywhere, although the intensity of the turbulence varies widely both in time and in space.

This situation may be contrasted with tha in the ocean, where, except for the surface laye above the thermocline, the bottom few meters and coastal regions, there is no really convincing evidence that the water is turbulent. Th difference lies in the fact that the velocity gradients are much lower in the ocean, the stabilit comparatively high, and no radiation effect occur.

Quantitatively our information is far fron complete. The important parameters in an turbulent field are:

(*a*) Energy dissipation, ϵ.
(*b*) Energy density, E.
(*c*) Characteristic scale, L.
(*d*) Degree of anisotropy.
(*e*) Orientation of anisotropy.

The list is in approximate order of the difficulty of measurement.

These are not all independent, of course. I L is suitably defined we have a well establishe law:

$$\epsilon = E^{3/2}/L$$

The dissipation is also related to the energ density and the anisotropy parameters throug the mean flow shear.

If we accept Kolmogoroff's similarity theor of locally isotropic turbulence [see *Batchelo* 1953], then by far the most important parameter in the turbulent field is the dissipation ϵ Although a degree of caution is still in orde [see, for example, *Kraichnan*, 1958], the validity of this similarity theory seems sufficientl probable that we are justified in using it wit some confidence. (*Kraichnan* [1959] himsel points out that his very different conceptua formulation of the turbulence problem lead to results only slightly different from those obtained from Kolmogoroff's assumptions.) As i now well known, the similarity theory leads t the result that the range of the wave numbe spectrum, which does not contribute importantly either to the Reynolds stress or to th viscous dissipation, must have the universa form

$$E(k) = K\epsilon^{2/3}k^{-5/3}$$

where $E(k)$ is the spectral energy density a wave number k and K is an absolute dimensionless constant.

Laboratory studies indicate that this law re-ains valid to wave numbers about as high as

$$k_{1\mathrm{im}} = 0.2(\epsilon/\nu^3)^{1/4}$$

Gifford [1957] finds values for ϵ ranging om about 2 cm² sec⁻³ in the lower few meters about 0.02 cm² sec⁻³ in the stratosphere, for ich we may calculate

$$k_{1\mathrm{im}} = 1\ \mathrm{cm}^{-1} \quad \text{near the surface}$$

d

$$k_{1\mathrm{im}} = 0.1\ \mathrm{cm}^{-1} \quad \text{in the stratosphere}$$

Experimental studies in the atmosphere show at, at the low-wave-number end, the $k^{-5/3}$ law redicted by the similarity theory holds to wave mbers even lower than would be expected hen the assumptions upon which the theory is ased are examined. [See *Ellison*, 1956; *Taylor*, 957].

All phenomena dominated by the high-wave-mber part of the turbulent energy spectrum n thus be predicted from knowledge of the ngle parameter ϵ *Batchelor* [1952] and others ave calculated the expected behavior of a oud of particles immersed in a turbulent fluid ith such a spectral behavior. The analysis of *ifford* [1957] shows that at the very least atchelor's predictions are not inconsistent ith observations of smoke puffs in the atmos-here.

Batchelor [1959] and *Batchelor, Howells, and ownsend* [1959] have recently deduced theo-etically the spectral distribution of the local ncentration fluctuations of an inert contami-ant, using the same assumptions.

Summary—The atmosphere is probably tur-ulent everywhere except in strong inversion yers, although the intensity may be very low. The $k^{-5/3}$ spectral behavior predicted by the milarity theory seems sufficiently reliable that may be used to predict behavior of phenom-na that depend upon the high-wave-number art of the turbulent spectrum.

References

NDERSON, A. D., Free-air turbulence, *J. Meteorol., 14,* 477–494, 1957.

ATCHELOR, G. K., Diffusion in a field of homogeneous turbulence, II, The relative motion of particles, *Proc. Cambridge Phil. Soc., A, 48,* 345–362, 1952.

BATCHELOR, G. K., *The Theory of Homogeneous Turbulence,* Cambridge University Press, 197 pp., 1953.

BATCHELOR, G. K., Small-scale variation of converted quantities like temperature in turbulent fluid, Part 1, General discussion and the case of small conductivity, *J. Fluid Mech., 5,* 113–133, 1959.

BATCHELOR, G. K., I. D. HOWELLS, AND A. A. TOWNSEND, Small-scale variation of converted quantities like temperature in turbulent fluid, Part 2, The case of large conductivity, *J. Fluid Mech., 5,* 134–139, 1959.

ELLISON, T. H., Atmospheric turbulence, in *Surveys in Mechanics,* Cambridge University Press, 475 pp., 1956.

ELLISON, T. H., Turbulent transport of heat and momentum from an infinite rough plane, *J. Fluid Mech., 2,* 456–466, 1957.

FRENKIEL, F. N., AND I. KATZ, Studies of small-scale turbulent diffusion in the atmosphere, *J. Meteorol., 13,* 388–394, 1956.

GIFFORD, F., JR., Relative atmospheric diffusion of smoke puffs, *J. Meteorol., 14,* 410-414, and Further data on relative atmospheric diffusion, same issue, 475–476, 1957.

GOODY, R. M., The influence of radiative transfer on cellular convection, *J. Fluid Mech., 1,* 424–435, 1956.

KELLOGG, W. W., Diffusion of smoke in the stratosphere, *J. Meteorol., 13,* 241–250, 1956.

KRAICHNAN, R. H., Irreversible statistical mechanics of incompressible hydromagnetic turbulence, *Phys. Rev., 109²,* 1407–1422, 1958.

KRAICHNAN, R. H., *N. Y. U. Inst. Math. Sci. Research Rept. HSN-1,* 27, 1959.

LILLER, W., AND F. L. WHIPPLE, High-altitude winds by meteor-train photography, in *Rocket Exploration of the Upper Atmosphere,* a special supplement to vol. 1 of the *Journal of Atmospheric and Terrestrial Physics,* edited by R. L. F. Boyd and M. J. Seaton, pp. 112–130, 1954.

MALKUS, J. S., Some results of a trade-cumulus cloud investigation, *J. Meteorol., 11,* 220–237, 1954.

MALKUS, W. V. R., Outline of a theory of turbulent shear flow, *J. Fluid Mech., 1,* 521–539, 1956.

MALKUS, W. V. R., AND G. VERONIS, Finite amplitude cellular convection, *J. Fluid Mech., 4,* 225–260, 1958.

NATIONAL ACADEMY OF SCIENCES–NATIONAL RESEARCH COUNCIL, *Publication 600, Physical and Chemical Properties of Sea Water,* 202 pp., 1959.

TAYLOR, R. J., Space and time correlations in wind velocity, *J. Meteorol., 14,* 378–379, 1957.

TOWNSEND, A. A., Turbulent flow in a stably stratified atmosphere, *J. Fluid Mech., 3,* 361–372, 1958*a*.

TOWNSEND, A. A., The effects of radiative transfer on turbulent flow of a stratified fluid, *J. Fluid Mech., 4,* 361–375, 1958*b*.

Dynamics of the Upper Atmosphere

P. A. Sheppard

Imperial College,
London, England

Abstract—The mean temperature and motional structure of the stratosphere, mesosphere, and lower ionosphere are described, and the thermodynamics of these regions is considered briefly. Possible disturbances on the mean motion are discussed. It is concluded that vertical convection is a very unlikely cause of such disturbances, that slantwise convection undoubtedly will release potential energy, thus supporting such disturbances, and that small-scale turbulence, though not likely generally, will probably be produced locally (in time and space) in the vicinity of jets in the large-scale baroclinic disturbances.

1. Scope

After noting the observed or inferred global fields of mean temperature and mean zonal motion between 20 and 100 km, and a suggested distribution of radiative heat sources and sinks with which the fields of temperature and composition may be associated, I shall consider the kinds of disturbed motion that appear to be possible as a result of the field of temperature. Argument will be largely based on an appropriate extrapolation of our knowledge and understanding of disturbed motions in the troposphere and lower stratosphere. Hydromagnetic motions will not be discussed.

2. The Fields of Mean Temperature and Zonal Mean Motion, 20–100 Km

A self-consistent evaluation of observations of temperature and zonal (east to west) motion is achieved through the thermal wind equation: mean motion nearly geostrophic, and its variation with height proportional to the meridional temperature gradient (1 m sec^{-1} km^{-1} corresponds to about 0.2°K/100 km in mid-latitudes). The best evaluation to date is due to *Murgatroyd* [1957] and is reproduced in Figure 1. Meridional temperature gradients in a few isobaric surfaces, extracted from Murgatroyd's tabulations, are shown in Figure 2. The main features of these diagrams are as follows:

The temperature increases from winter pole to summer pole below the stratopause: stratopause, temperature maximum at 50–55 k mesopause, temperature minimum at about km. The mesosphere is between the stratopau and the mesopause.

The temperature increases from summer p to winter pole in the mesosphere.

The lowest temperature is at the mesopau summer pole.

The lapse rate in the mesosphere is 3.5° 5°K/km (6°K/km near the summer pole); i versions are above and below.

The maximum annual temperature range at the stratopause and the mesopause pole.

The winter westerly jet is near the stra pause at about 55° latitude; the summer ea erly jet is near the stratopause at about 4 latitude.

Winter easterlies are in the thermosphere, i creasing rapidly with height; summer weste lies, in the thermosphere, increasing less rapid with height.

Vertical shears in the mesosphere and low thermosphere are about 3 m sec^{-1} km^{-1}.

If it appears odd to discuss the dynamics the upper atmosphere using the field of me motion (or temperature) as a starting point, should be remarked that the field of mean m tion is likely to be the outcome, in more th detail, of the field of disturbances associat with it. This at least is true for the troposphe and lower stratosphere and is a reasonable a sumption therefore for the higher levels treat here.

The molecular (kinematic) viscosity of t

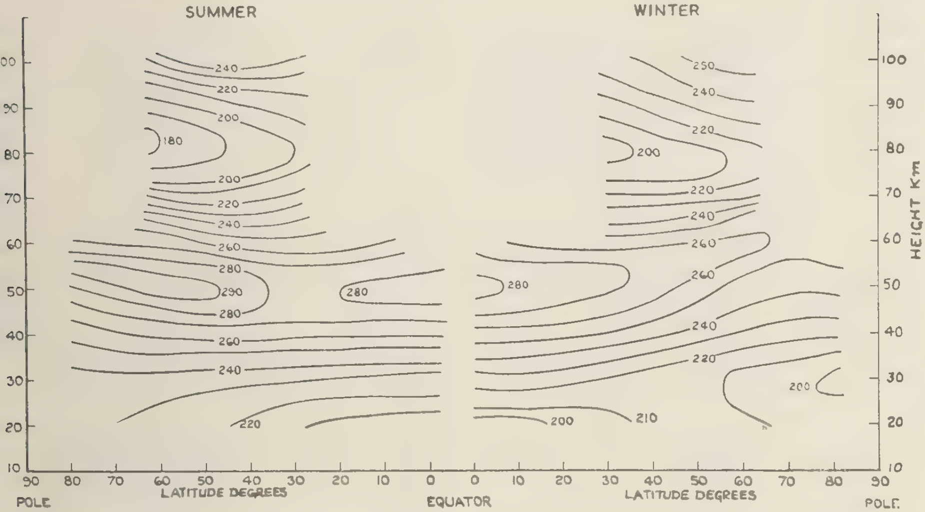

FIG. 1a—Summer and winter temperature (°K) as a function of latitude and height z.

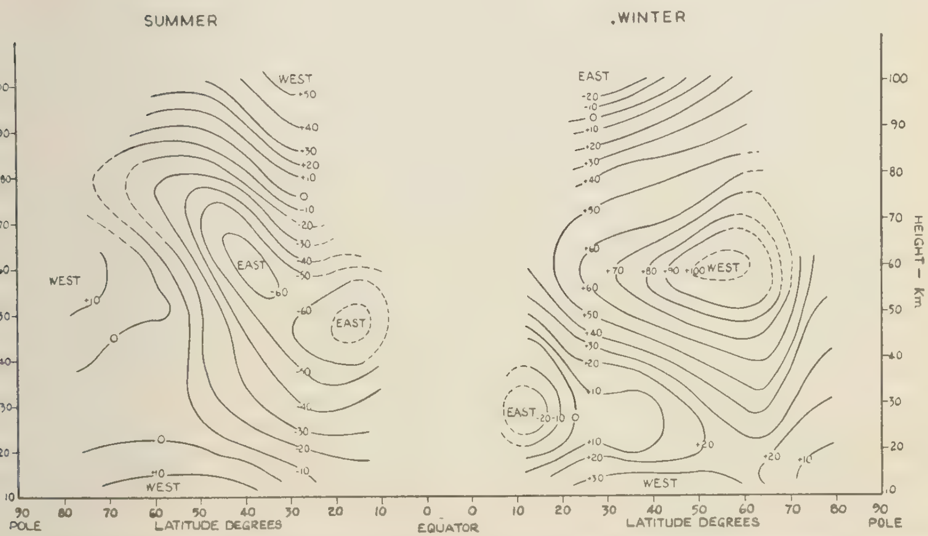

. 1b—Summer and winter zonal winds U (m/sec, wind from west positive) as a function of latitude and height z.

Wind and temperature related by thermal wind equation, i.e. motion geostrophic. After Murgatroyd. produced by permission of Royal Meteorological Society.

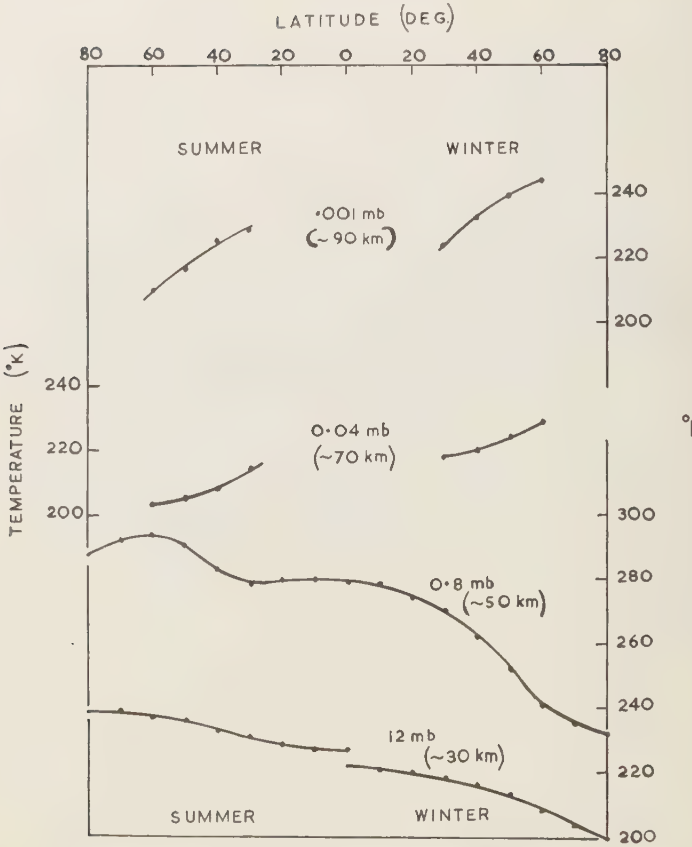

Fig. 2—Meridional temperature variation in selected isobaric surfaces for summer and winter.

air is not a determinative factor in the pattern of energy-containing motions in the troposphere, and, though it increases by several orders to about 10^5 cm^2/sec at 100 km, it is still unlikely to be very important up to this level and will be disregarded.

3. Thermodynamic Background

Murgatroyd and Goody [1958] have computed the distribution of radiative heat sources and sinks from 20 to 90 km, from solar absorption by O_2 and O_3, and from atmospheric emission by CO_2 and O_3. Above about 50 km they find a heat source, ~5°K/day, over the summer pole, where in the upper mesosphere the atmosphere is coldest, and a heat sink, ~−15°K/day, over the winter pole. There is little departure from radiative equilibriu through lower latitudes.

If this picture is correct, heat must be tran ported from summer pole to winter pole (u like the troposphere, where transport is fro equator to pole both seasons). Nonradiati vertical transfer of heat is mostly required the winter hemisphere in high latitudes. The r quirement to transport heat from low temper ture to high temperature is difficult to satis on dynamical grounds.

4. Possible Disturbances on Mean Motion

4.1. *Vertical convection in the mesosphere*- The mean lapse rate (see above) is less than ha the dry adiabatic lapse rate (≃10°K/km) ar

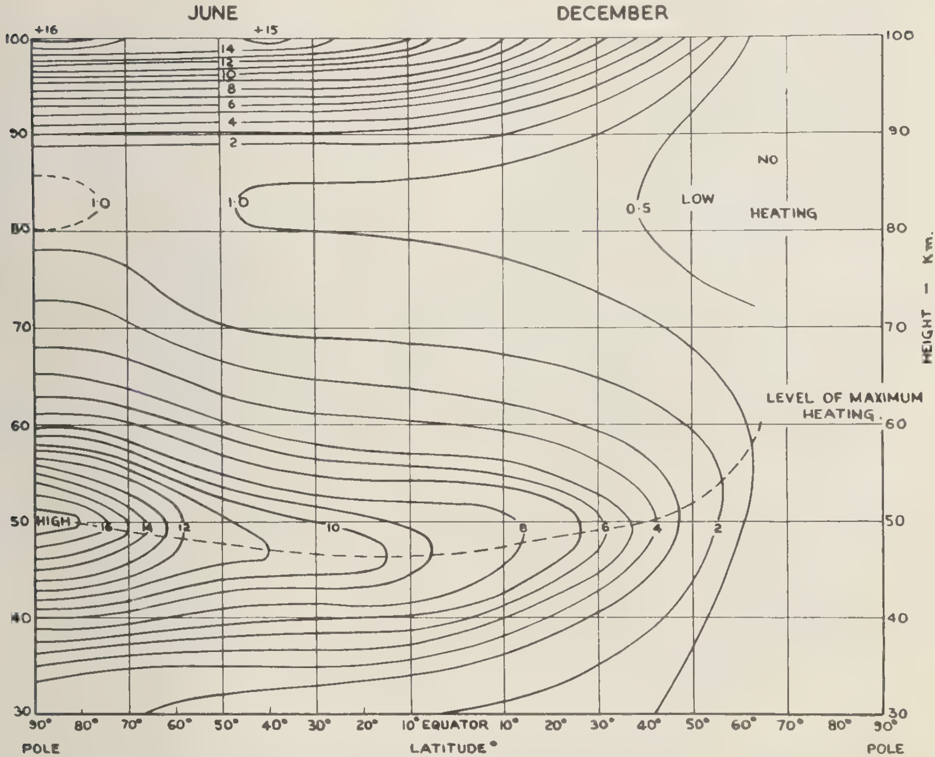

FIG. 3—Heating due to absorption of solar radiation (°K/day) as a function of latitude, height, and season. After Murgatroyd. Reproduced by permission of Royal Meteorological Society.

where approaches it. Yet the assumption has ;en been made that convection is probable in e mesosphere. We therefore ask: (1) Is the tical lapse rate for convection in the meso- here less than the dry adiabatic? (2) Can the tical lapse rate for convection be reached ally and temporarily?

Regarding question 1, chemical association in cending air: e.g., $O_3 + O_2 \rightarrow O + 2O_2$ through one-rich air being brought upward, would duce the critical lapse rate below the dry iabatic (like water vapor condensation in the oposphere). But order-of-magnitude calcula- ns show the possible effect to be utterly gligible. *Goody* [1956] has examined the ef- ;t of radiative transfer of heat on the critical ose rate for convection. This, however, works the opposite sense, as does thermal conductiv- in the classical Rayleigh-Jeffreys cellular otion problem of fluid heated from below. The increase in the critical lapse rate for convection over layers of any significant depth is found to be negligible below 100 km. We have no reason therefore for adopting other than the dry adiabatic lapse rate as a criterion for convection.

Regarding question 2 above, there is a diurnal variation of temperature, different at different levels, from the absorption of solar radiation by O_3 and O_2. The magnitude of this absorption, expressed in equivalent temperature rise per day, has been evaluated by *Murgatroyd* [1957] and is shown in Figure 3. The diurnal variation of temperature will of course be less than the values in Figure 3, because of atmospheric emission, but the figure indicates the order of magnitude. Although the diurnal heating decreases upward from about the stratopause level and so destabilizes the mesosphere around the period of maximum temperature, the amount

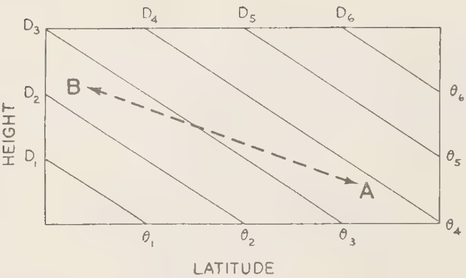

FIG. 4—Slantwise convection or baroclinic instability. The rectangle represents a meridional (vertical) cross section of a layer of atmosphere, with height greatly exaggerated relative to latitude. The sloping lines $\theta_1, \theta_2 \cdots (D_1, D_2 \cdots)$ are the intersections with the vertical plane of surfaces of constant potential temperature (θ) or constant potential density (D); $\theta_1 < \theta_2 \cdots$, $D_1 > D_2 > \cdots$. The system is stable for vertical displacements of particles but unstable for displacements along surfaces whose slope is less than that of the θ, D surfaces, e.g. for a particle displacement from A toward B or B toward A, since buoyancy is evidently created thereby. The horizontal temperature gradient is reflected by a vertical shear of wind (section 2) which gives rise to a characteristic structure of the velocity and temperature fields in a growing disturbance [see *Eady*, 1949]. This structure is evident in the long waves and cyclone waves of the troposphere.

of destabilization is entirely insufficient to produce a dry adiabatic lapse rate at any level—a differential heating of several degrees per kilometer would be required.

Another possible source of local destabilization is differential advection of temperature at different levels by large-scale disturbances. This process occurs in the troposphere but mainly because of boundary action to which no analogue appears in the mesosphere. Since, moreover, the horizontal gradients of temperature in the mesosphere are only of the order of 10°K/1000 km (see Fig. 1), the large-scale disturbances, even if of appropriate structure (which seems unlikely), could hardly destabilize the lapse rate locally to the dry adiabatic.

There is therefore no reason to expect disturbances on the mean field of flow from vertical convection in the mesosphere.

4.2. *Slantwise convection* (*long waves and cyclones*) *in the upper atmosphere*—The thermal field (see Figs. 1*a*, 2) is essentially similar to the troposphere—a meridional temperatur gradient (not necessarily of the same sense), an a statically stable lapse rate—under whic energy is released by large-scale slantwise co vection in extratropical latitudes along surfac of smaller slope than that of the isentrop (constant potential density) surfaces. Figure shows schematically the nature of this so-calle baroclinic instability.

The growth rate of baroclinic disturbances i inversely proportional to the Richardson num ber of the mean field [*Eady*, 1949] and th dominant disturbance, that with maximu growth rate, for mesosphere conditions woul probably be a few thousand kilometers hor zontally. The thermosphere above and strato sphere below are larger Richardson numbe regimes, but these regions should also be baro clinically unstable, though with smaller growt rates of disturbances. Calculations of some o the properties of such disturbances for condi tions between 20 and 80 km have been made b *Fleagle* [1958]. Since they convert potential t kinetic energy they would not transport hea in the sense suggested by the radiative source sink distribution referred to in section 3. The would, however, almost certainly generat frontal zones and jets—not necessarily the jet of the mean flow field (section 2)—with verti cal shear many times the maximum of th mean flow field (see section 4.3).

Baroclinic disturbances are weak or nonex istent in low latitudes, and the link between th momentum and heat transfer fields of the high level extratropical disturbances of the two hemi spheres may perhaps be effected by a meridiona circulation, i.e. vertical overturning [*Sawye* 1958].

In the troposphere the pattern of the genera circulation arising from baroclinic and simpl convective systems is substantially affected b surface friction, one aspect of which is th emergence of surface easterlies (trades) in lo latitudes, of surface westerlies in middle lati tudes, and of direct (energy-producing) and in direct (energy-consuming) meridional circula tions in low and middle latitudes, respectivel [*Sheppard*, 1958]. The interaction betwee layers aloft of different stability and opposit meridional gradient of temperature may per haps provide some analogy with surface fric

n. Without resolving that problem it would apear that numerical experiments on model sospheres are now both possible and very de-able.

4.3. *Small-scale turbulence*—For the mean lds of section 2, representative values of the chardson number

$$\frac{g}{\theta}\frac{\partial \theta}{dz} \Big/ \left(\frac{\partial U}{\partial z}\right)^2$$

ould be: mesophere 20, lower thermosphere ; and so shear turbulence is not to be ex-cted as a universal phenomenon in these gions unless stability has less influence here an in the troposphere.

Townsend [1958] has shown that the effect the exchange of heat by atmospheric radia-on is always to increase the critical value of e Richardson number, because radiative 'con-iction' diminishes the negative buoyancy of oving elements in a stable temperature gra-ent. Turbulence may therefore be more readily aintained in the mesosphere and lower thermo-here, where radiative conduction is relatively gh, than in the troposphere, but the increase the critical Richardson number is unlikely to e sufficient to allow turbulence generally in ese layers.

It would appear more likely that the requi-te shear to overcome the stability is produced poradically, in certain parts (in the region of e jets) of the large-scale baroclinic disturb-nces, as seems to happen in the troposphere lso.

5. Interaction between Different Kinds of Motion

I have said nothing of gravity waves, such as air tides, or of orographically induced motions. We know a good deal about tidal motion at 80 to 100 km, where there is a large-amplitude, mainly semidiurnal, wave, but the possibility of its reaction on the types of motion discussed above does not yet appear to have been considered. Again, we have considerable knowledge and some understanding of orographically induced motions up to and somewhat beyond the tropopause, but the energy density of this motion at ionospheric levels has not, I believe, been estimated or inferred from any observation.

References

Eady, E. T., Long waves and cyclone waves, *Tellus, 1,* 33, 1949.

Fleagle, R. G., Inferences concerning the dynamices of the mesosphere, *J. Geophys. Research, 63,* 137, 1958.

Goody, R. M., Influence of radiative transfer on cellular convection, *J. Fluid Mech., 1,* 424, 1956.

Murgatroyd, R. J., Winds and temperatures between 20 km and 100 km—a review, *Quart. J. Roy. Meteorol. Soc., 83,* 417, 1957.

Murgatroyd, R. J., and R. M. Goody, Sources and sinks of radiative energy from 30 to 90 km, *Quart. J. Roy. Meteorol. Soc., 84,* 225, 1958.

Sawyer, J. S., Report of discussion on 'Dynamical state of the upper atmosphere,' *Weather, 13,* 281, 1958.

Sheppard, P. A., The general circulation of the atmosphere, *Weather, 13,* 323, 1958.

Townsend, A. A., Effects of radiative transfer on turbulent flow of a stratified fluid, *J. Fluid Mech., 4,* 361, 1958.

Visual and Photographic Observations of Meteors and Noctilucent Clouds

P. M. Millman

National Research Council
Ottawa, Ontario, Canada

Abstract—The visible paths of meteors appear generally in the region from 110 km to 60 km above sea level. The relations between meteor height and meteor velocity, brightness, and angle of the path to the vertical are discussed. Persistent meteor trains show a height distribution similar to that of meteors and reveal differential wind motions of various types, as well as giving evidence of a rapid increase in the train diameter during the first few minutes. A vertical spacing of about 6 km between major wind currents seems typical. Noctilucent clouds exhibit velocities comparable to those of meteor trains and often reveal a pattern of roughly parallel lines with a spacing of 9 km.

The purpose of this brief review is to present the evidence contributed by visual and photographic data to the general study of the motions of the upper atmosphere. Meteors may be considered convenient test objects, which produce so-called 'trains,' that is, a residue left along the meteor path. The residue may be visible for some time by means of optical and radio detection techniques.

Since meteor trains are in general produced somewhere along the visible path of a meteor, it is necessary first to discuss typical meteor heights. The best observational data in this field have come from the photographic meteor program at the Harvard Observatory [*Whipple*, 1943; *Jacchia*, 1952; *Hawkins and Southworth*, 1958]. In addition to published records, Dr. F. L. Whipple and Dr. L. G. Jacchia have kindly placed unpublished material at my disposal.

The three chief parameters that determine the height of a meteor path in the atmosphere are, in order of importance: (1) the geocentric velocity of the meteor, V_∞; (2) the absolute brightness of the meteor at maximum light, M_{pm}; (3) the inclination of the meteor path to the vertical, angle Z.

In general, the faster meteors appear and disappear higher than the slower ones. The average effect of velocity is illustrated in Table 1, which lists mean height corrections for reducing meteor heights to those corresponding to a standard velocity of 40 km/sec.

Table 1—*Height correction for reduction to a standard V_∞ = 40 km/sec*

Meteor velocity V_∞, km/sec	Height correction, km
10	
	+17
15	
	+11
20	
	+6
25	
	+4
30	
	+3
35	
	+1
40	
	−1
45	
	−3
50	
	−5
55	
	−7
60	
	−8
65	
	−10
70	
	−12
75	

In Figure 1 are plotted the average values for the beginning, maximum light, and end meteor paths for various absolute luminositi The luminosity unit used is the stellar magr tude of the meteor at maximum light as

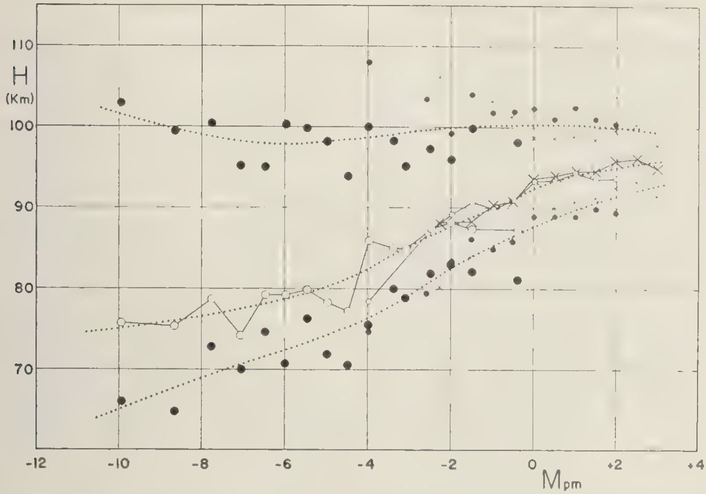

FIG. 1—The mean height of the beginning, maximum light, and end of meteor paths plotted against he absolute luminosity of the meteor, compiled from 808 meteors photographed at Harvard Observaory stations. All values reduced to a standard velocity of 40 km/sec.

vould appear in the zenith at a distance of 100 m. The figure summarizes the results of the ccurate reduction of 808 meteors photoraphed at the Harvard Observatory. All eights have been reduced to a standard velocy of 40 km/sec by use of Table 1.

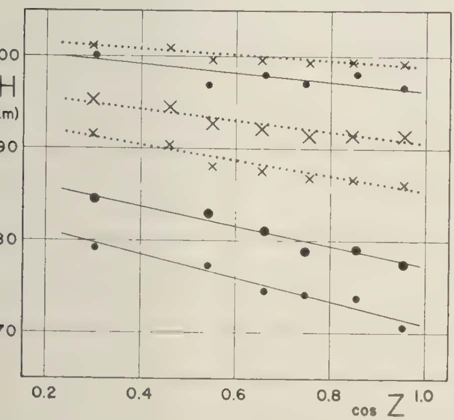

FIG. 2—The height of beginning, maximum ght, and end of meteor paths plotted against e inclination Z of meteor path to the vertical: osses indicate meteors of zero absolute magnide; dots, -5 absolute magnitude. All values reuced to a standard velocity of 40 km/sec.

The effect of the inclination of the meteor path is illustrated in Figure 2, where heights are plotted against cos Z. Mean values reduced to 40 km/sec are shown for two groups of meteors, those of absolute magnitude zero (crosses) and −5 (dots), respectively.

It will be noted that, if V_∞, M_{pm}, and Z are known for any meteor, a fair approximation to the height of its visible path may be made by means of Table 1 and Figures 1 and 2.

The most comprehensive listing of visual meteor trains has been made by *Dr. C. P. Olivier* [1942, 1947, 1957] in three papers. These contain information on a total of 2073 meteor trains with durations ranging all the way from a few seconds up to, in rare cases, several hours. More than 900 trains with durations of 5 minutes or more are listed, and 52 of them lasted an hour or longer. The material is very heterogeneous in quality, and most of the height determinations are by visual methods and are not as accurate as the photographic results summarized above. For somewhat more than 120 trains for which heights were available, *Olivier* [1957] found the mean heights given in Table 2. A more detailed study of these height data by a number of investigators has revealed, for the night trains, a major maximum in frequency

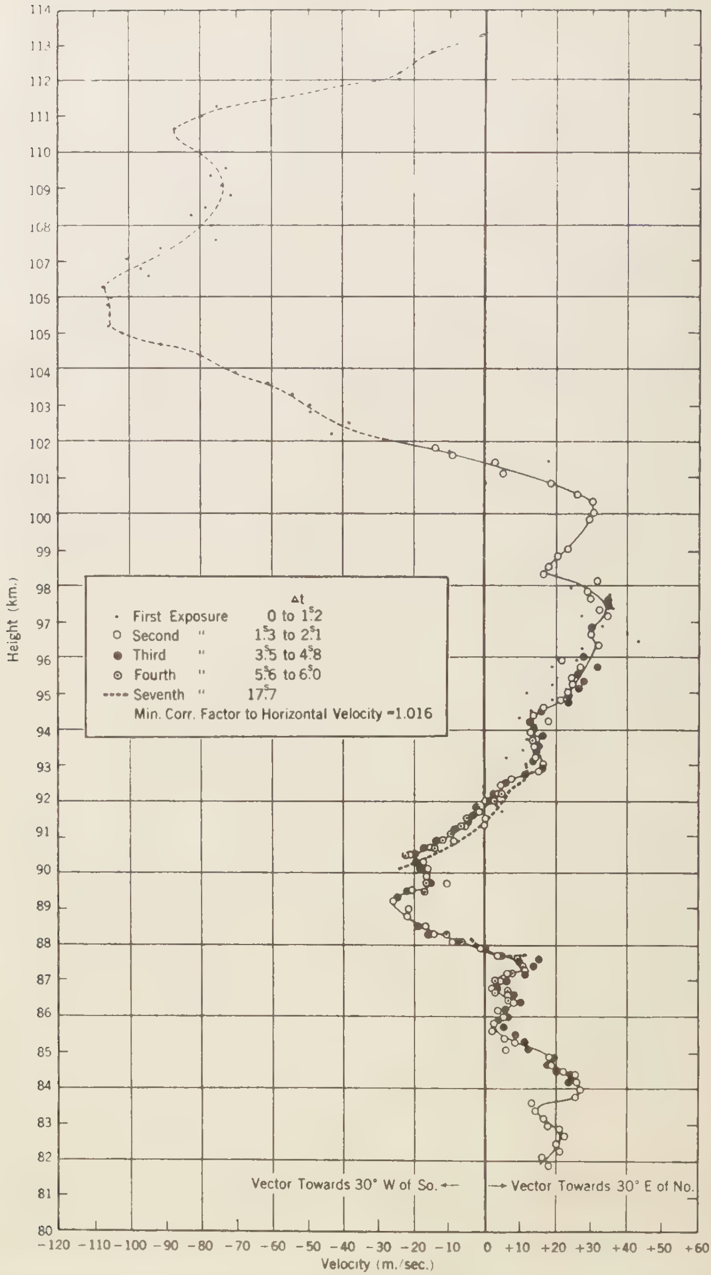

FIG. 3—A typical example of meteor train drifts determined photographically at the Harvard Observatory by Liller and Whipple.

TABLE 2—*Mean heights and drift velocities of persistent meteor trains* [*Olivier, 1957*]

	Height, km		Drift velocity, m/sec
	Beginning	End	
ght trains	102	78	56
ilight trains	77	45	48
y trains	45	27	

ar 90 km height with the lowest points near km; and a second smaller maximum near 60 n with end points near 40 km.

No very significant general conclusions con- rning the directions of train drifts can be awn from Olivier's material. Where informa- n is available train drifts are predominantly rizontal, normal drifts being about 50 m/sec, ough vertical motions are observed in excep- nal cases [*Olivier*, 1933]. *Fedynsky* [1950] s found a mean horizontal drift of 70 m/sec r trains observed in Tadjikstan. R. F. Hughes npublished) has studied 48 trains photographed at Harvard; they had an average duration of 5 seconds. He found that the height of maximum train intensity corresponded closely with maximum meteor light and that 25 per cent of the trains exhibited two primary maxima of intensity, the mean height difference of the two maxima being 7 km.

Liller and Whipple [1954] have published photographic determinations of the drifts of 5 meteor trains with durations from a few seconds to more than 40 seconds. These gave an average horizontal wind speed of 68 m/sec. One of the most characteristic features of the train drifts was the appearance of differential motions, the autocorrelation function for these motions dropping to zero at a height difference of 5.2 km. Maximum wind shears from 25 to 90 m/sec per km of height difference were normal, the average maximum wind shear being over 50 m/sec per km of height difference.

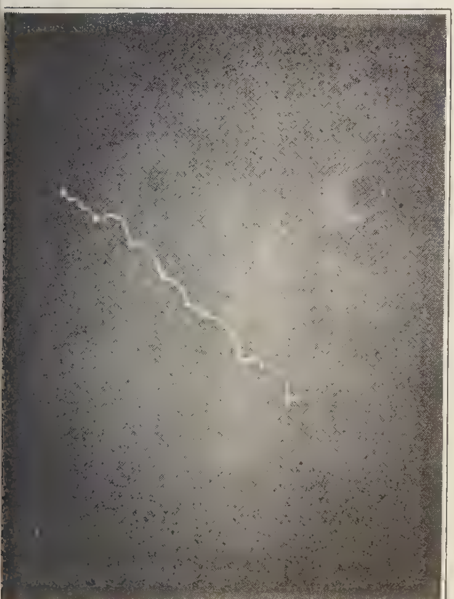

FIG. 4—Photograph of a meteor train taken out 60 seconds after passage of the meteor. ength of train approximately 19°. Photo by F. L. rube, May 3, 1939.

FIG. 5—Four successive photographs of a meteor train, taken at 15-second intervals from 45 to 90 seconds after the meteor's passage. Photos by A. Asnis, May 20, 1944.

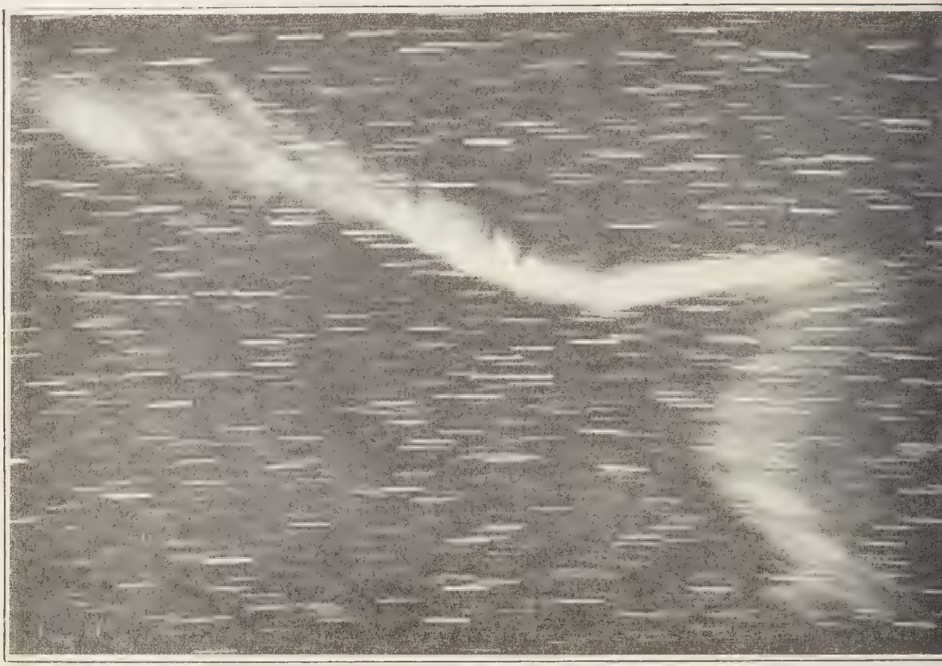

FIG. 6—Photograph of a meteor train, plate exposed from 135 to 195 seconds after passage of meteo
Photo by F. Capen, Jr., April 26, 1956.

The decay rate for the train luminosity was found to be a minimum at about 92 km height; this finding has been confirmed by a photometric study of a photographic train by G. S. Hawkins and W. E. Howard (in press). Figure 3, reproducing the drifts for one of the meteor trains studied by Liller and Whipple, illustrates a typical combination of major wind currents and smaller drift irregularities or turbulence.

The special photographic measures of meteor trains referred to above give results about the development of trains for the interval from 1 second to 1 minute after the passage of the meteor. Visual observations, supplemented by the occasional amateur photograph, follow the train development in general over the interval from 1 minute to 1 hour after the meteor has appeared.

Examination of some hundreds of drawings and visual photographs of the long-enduring trains demonstrates that the most characteristic feature of their development is a fairly consistent change with time from the initial straight line in the upper atmosphere to a snake-li form produced by the differential wind curren This change in form shows that the major wi motions revealed by the accurate photograph results are not short-lived phenomena but least semipermanent features of the structu of the upper atmosphere at these heights. Typ cal examples of long-enduring meteor trains a illustrated in Figures 4, 5, and 6.

P. M. Millman and H. Bernstein (unpu lished) have summarized the general chara teristics of some 50 long-duration trains f which detailed drawings are available. Seven distinct types of differential wind currents we found, typical examples being the S, Z, and forms, a square form, trains with one sha bend, those showing evidence of a narrow j stream, and general irregular diffuse patche These seven forms are illustrated schematical in Figure 7. For 40 selected trains the avera spacing between major wind currents moving opposite directions was 8.3 km along the m teor path; this corresponds to an average heig

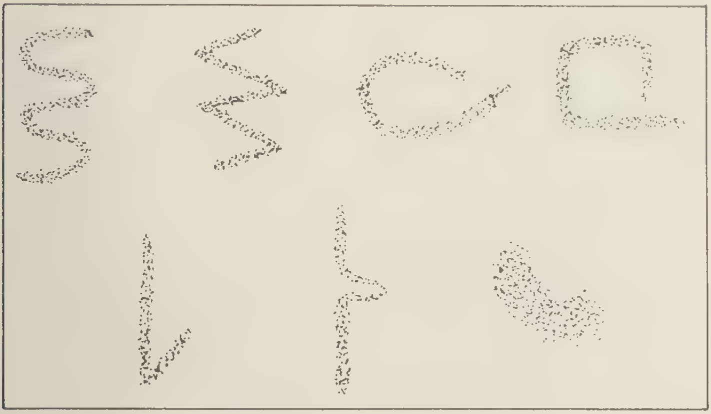

FIG. 7—Schematic representation of typical forms of persistent meteor trains.

difference in the atmosphere of about 6 km. Average differential velocity between currents was 30 m/sec.

In addition to the deformation from a straight line, visually observed trains of long duration exhibit a fairly rapid blurring of small details and a general increase in diameter with time. These characteristics indicate diffusion effects. For 31 meteor trains in the above study the average diameter after 3 minutes was more than 2000 meters. *Trowbridge* [1907], one of the pioneers in the study of meteor trains, noted that they sometimes appeared double, and he ascribed this form to the development of a hollow cylinder of luminosity.

Good quantitative measures of diffusion coefficients derived from visual meteor trains are not numerous. *Hawkins* [1957] has studied a train which was both visually observed and recorded with a Super-Schmidt camera at the Sacramento Peak Observatory. The train lasted between 5 and 6 minutes and had a total diam-

FIG. 8—Noctilucent clouds photographed in the USSR, July 6/7, 1951.

eter of 300 meters after 33 seconds, 600 meters after 240 seconds, and 1040 meters after 330 seconds. Diffusion coefficients between 40 and 800 m^2/sec were found for assumed heights near 90 km. These values are one or two orders of magnitude higher than the diffusion coefficients computed by *Greenhow and Neufeld* [1955] from a study of underdense radio meteor echoes. The difference is probably due to the effects of turbulence, which become increasingly evident for the longer-duration trains.

The Sacramento Peak train exhibited the double form referred to above, but this had disappeared after 5 minutes when the train had attained a diameter of 800 meters. Hawkins concluded that the maximum possible size of eddies dissipating the train was 75 meters during the first 33 seconds and 150 meters during the first 240 seconds, but that at 300 seconds turbulent eddies with diameters of about 230 meters were present.

A phenomenon of the upper atmosphere that gives some information about motions at great heights is noctilucent clouds. Their general characteristics have been summarized by *Vestine* [1934]. They result from the reflection of sunlight by high-lying particles of some type. The mean height of these clouds is never far from 82 km, coinciding with the temperature minimum of the upper atmosphere. Motions of these clouds tend to be toward the southwest quadrant of the sky, with more motion toward the west than toward the south. Velocities have been measured in the range of 30 to 70 m/sec, and 50 m/sec can be taken as an average round figure. On certain occasions, however, velocities between 100 and 200 m/sec have been noted.

Noctilucent clouds normally exhibit elements of a regular structure, sometimes taking the form of a series of long parallel wave crests with a spacing of 9 km between successive cres The crests are sometimes crossed by a secc system of parallel lines at right angles to t first. An example of noctilucent clouds, pho graphed on the night of July 6/7, 1951, is produced in Figure 8.

References

Fedynsky, V. V., Meteor trains and noctiluc clouds in the upper atmosphere, *Meteoritica* 95–112, 1950.

Greenhow, J. S., and E. L. Neufeld, The diffusi of ionized meteor trails in the upper atm phere, *J. Atmospheric and Terrest. Phys.,* 133–140, 1955.

Hawkins, G. S., A hollow meteor train, *Sky a Telescope, 16,* 168–169, 1957.

Hawkins, G. S., and R. B. Southworth, T statistics of meteors in the earth's atmosphe *Smithsonian Contribs. to Astrophys., 2,* 3 364, 1958.

Jacchia, L. G., *Harvard Coll. Observatory a Numerical Analysis Lab. of Mass. Inst. Techn Tech. Rept. 10,* 1952.

Liller, W., and F. L. Whipple, High-altitu winds by meteor-train photography, *Special Su plement to J. Atmospheric and Terrest. Ph 1,* 112–130, 1954.

Olivier, C. P., Heights and train-drifts of Leo meteors of 1932, *Proc. Am. Phil. Soc., 72,* 2 227, 1933.

Olivier, C. P., Long enduring meteor trains, *Pr Am. Phil. Soc., 85,* 93–135, 1942.

Olivier, C. P., Long enduring meteor tra (second paper), *Proc. Am. Phil. Soc., 91,* 3 327, 1947.

Olivier, C. P., Long enduring meteor trai (third paper), *Proc. Am. Phil. Soc., 101,* 2 315, 1957.

Trowbridge, C. C., Physical nature of mete trains, *Astrophys. J., 26,* 95–116, 1907.

Vestine, E. H., Noctilucent clouds, *J. Roy. Astr Soc. Can., 28,* 249–272, 303–317, 1934.

Whipple, F. L., Meteors and the earth's up atmosphere, *Revs. Mod. Phys., 15,* 246–2 1943.

Measurements of Turbulence in the 80- to 100-Km Region from the Radio Echo Observations of Meteors

J. S. GREENHOW AND E. L. NEUFELD

Jodrell Bank Experimental Station
University of Manchester, England

Abstract—Measurements of irregular winds at heights of 80 to 100 km, using radio echoes from meteor trails, are described. Large irregularities with a vertical scale of 6 km, a horizontal scale of the order of 150 km, and a time constant of 6×10^3 sec are observed. The rms wind velocity associated with these irregularities is 25 m sec^{-1}. Turbulent wind shears of the order of 10 m sec^{-1} km^{-1} are found, although occasionally shears as high as 100 m sec^{-1} km^{-1} are observed. Lower limits for the scale and time constant of the smallest eddies are determined.

INTRODUCTION

Measurements of turbulence at heights of 80) 100 km, using radio echoes from meteor ails, are described. The wind velocity is meas-red simultaneously at two points of variable paration along a meteor trail. [*Greenhow and eufeld,* 1959*a*]. Wind shears, and the fall-off correlation between the wind velocity at two oints in space as their separation is increased, an be measured. This enables the dimensions f the large-scale irregularities to be deter-ined. The time constant of these irregularities iven by autocorrelation curves derived from e time variation of the turbulent wind com-onent can also be found. Information about e small eddies can be obtained from observa-ons of the behavior of long-duration meteor choes.

THE LARGE-SCALE IRREGULARITIES

Dimensions—The scale of the large eddies is etermined by investigating the fall-off in cor-elation between the turbulent wind velocities t two points (Fig. 1) as their separation is in-reased. In addition to the turbulent winds, egular periodic and prevailing components are lso present. In order to allow for them, the ean horizontal wind during any hour is ob-ained by averaging approximately 100 indi-idual velocities obtained each hour. The devia-ons of the individual radial wind velocity easurement u_0 and u_c at two points on a me-eor trail X and Y, from the radial components $_r$ of the steady wind, are then obtained for each echo pair in that hour. This gives for the turbulent wind components δu_0 and δu_c at 0 and C

$$\delta u_0 = \bar{u}_r - u_0 \qquad \delta u_c = \bar{u}_r - u_c$$

The lateral correlation coefficient g is then given

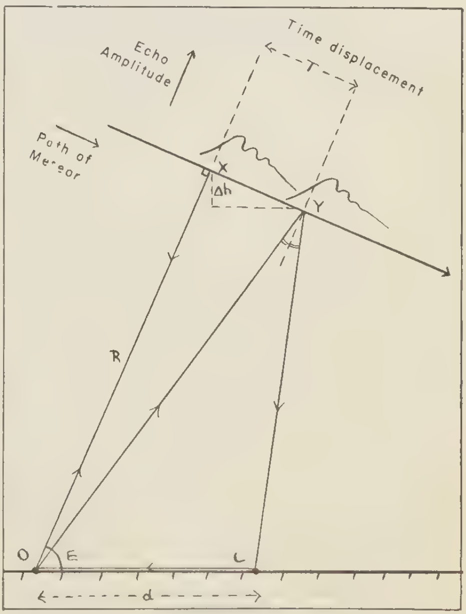

FIG. 1—Diagram illustrating the reception of radio echoes from two different reflecting points on a single meteor trail, using spaced receiving stations at 0 and C. $d = 3.6$ or 20 km.

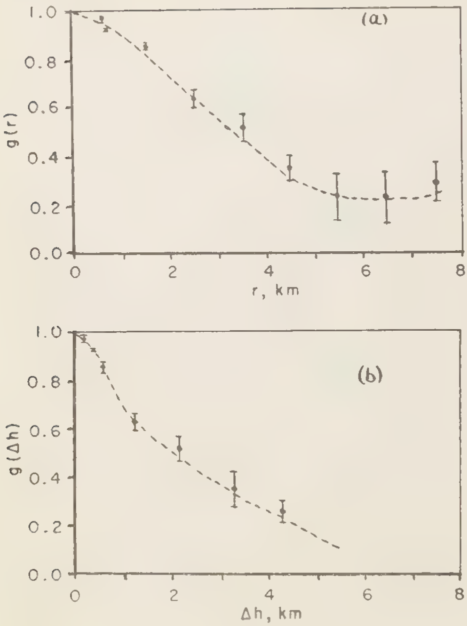

FIG. 2—(*a*) Variation of velocity correlation g with spatial separation of the reflecting points r. (*b*) Variation of g with height separation Δh of the reflecting points.

by

$$g(r) = \frac{\Sigma\ \delta u_0\ \delta u_c}{(\Sigma\ \delta u_0^{\ 2}\ \Sigma\ \delta u_c^{\ 2})^{\frac{1}{2}}} \qquad (1)$$

Approximately 900 echo pairs have been obtained, and for each pair values of δu_o and δu_o have been determined, together with the spatial separation r and height separation Δh of the radio echo reflecting points.

The correlation coefficient $g(r)$ is plotted as a function of spatial separation r in Figure 2(*a*). $g(r)$ decreases from unity at zero separation to 0.2 at a separation of 5 km. For values of $r > 5$ km, instead of decreasing through zero to small negative values as expected for the case of isotropic turbulence, $g(r)$ remains practically constant. This behavior is explained in terms of the anisotropy of the large-scale turbulence. The maximum value of r occurs for a meteor traveling horizontally, but for such a meteor the height difference between the reflecting points falls to zero. When the variation of correlation coefficient with height, irresp tive of the horizontal separation of the refle ing points, is plotted, the unusual behavior the correlation is removed; Fig. 2(*b*). Ext polation of the curve to zero shows that vertical extent of the large-scale irregularitie of the order of 6 km. Thus the apparent lev ing-off in $g(r)$ can be explained if the turl lence is anisotropic, with the fall-off in cor lation mostly in the vertical rather than in horizontal direction.

If echo pairs of the same height separat but different horizontal separations are co pared, an estimate of the rate of fall in cor lation horizontally can be made. It is fou that the horizontal scale of the turbulence is the order 100 to 200 km, an order of magnitu greater than the vertical depth.

Scales of the order of a few kilometers the large irregularities have also been dedu by *Manning and Eshleman* [1957] from obs vations of long-duration meteor echoes.

The root mean square turbulent wind velo and wind shear—The rms turbulent wind veloc V_1 may be determined by measuring the dev tions of the individual meteor drift velocit from the mean drift velocity. The results ha been grouped in hourly intervals for wh $V_1 = (\sum \delta u_c^2/n)^{1/2}$, where n is the number individual meteor drifts and $\delta u_c = \bar{u}_r$ — V_1 varies between approximately 15 and 45 sec^{-1}, with a median value of 25 m sec^{-1}. surprising result is that the turbulent veloc does not vary significantly with wind gradie Figure 3(*a*), or with the mean wind veloc Figure 3(*b*). The median value of the turbul wind shear is 10 m sec^{-1} km^{-1}, Figure 4, althou values exceeding 100 m sec^{-1} km^{-1} are obser occasionally. Between any two points separa by 0.4 km there is a 7 per cent probability observing a shear greater than 40 m sec^{-1} km These measurements are comparable with th of *Liller and Whipple* [1954], obtained fr photographic meteor observations.

Time constant of the large-scale irregularitie Fluctuations of the wind velocity with time a fixed point are observed, and the time const of the fluctuations, given by the interval o which the autocorrelation function falls to ze determines the time constant of the large-sc turbulence t_1 (Fig. 5).

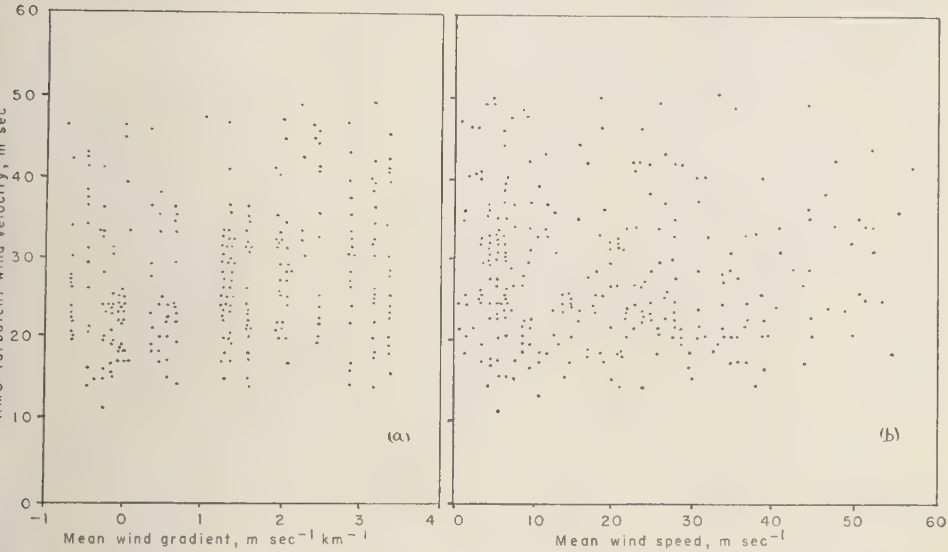

'IG. 3—Scatter diagram showing the rms turbulent velocity to be independent: (*a*) of gradient of the mean wind; (*b*) of the mean wind velocity.

The autocorrelation function $g(\tau)$ which orrelates the turbulent velocity u_s at time s ith the velocity $u_{s+\tau}$ at time $s + \tau$ is given by

$$g(\tau) = \frac{\Sigma u_s u_{s+\tau}}{[\Sigma u_s^2 \; \Sigma u_{s+\tau}^2]^{1/2}} \qquad (2)$$

'he variation of $g(\tau)$ with τ for the turbulent wind component has been determined for a number of continuous 24- and 48-hour runs. [*Greenhow and Neufeld*, 1959*b*]. The mean value of t_1, determined from a number of such autocorrelation curves, is found to be approximately 6×10^3 sec.

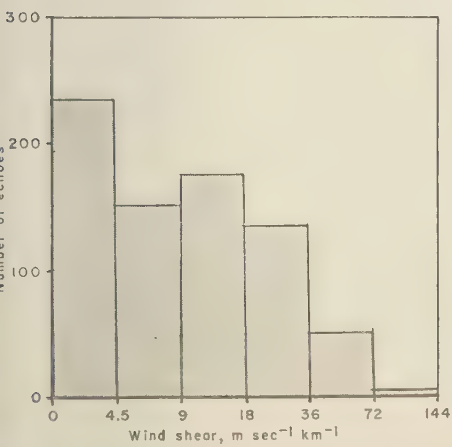

FIG. 4—Distribution of turbulent wind shears measured over a height difference of 0.4 km.

The Turbulence Power

In any turbulent system there exists a whole spectrum of eddy sizes from the largest of scale L, lifetime t_1, and rms velocity V_1 to the smallest of scale η, time constant t_2, and rms velocity V_2. Equations of the form $L = V_1 t_1$ and $\eta = V_2 t_2$ relate the length, velocity, and time parameters of eddies of any size. Measurements of the correlation coefficient show that the vertical scale of the large eddies is approximately 6 km, and the horizontal size may be as high as 100 to 200 km. The time constant of the large eddies, determined from the autocorrelation function concerned with the time variations of wind velocity at a fixed point, is found to be 6×10^3 sec. The rms turbulent velocity is 25 m sec^{-1}. Combining these values of velocity and time, we obtain 150 km for the length parameter of the large eddies. This is in agreement with the horizontal scale suggested by the

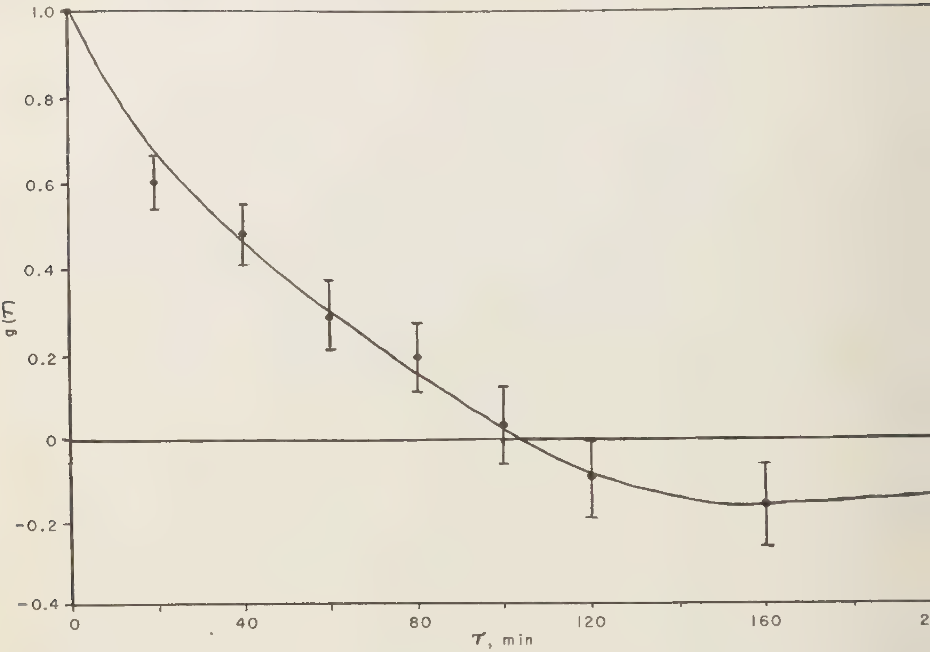

FIG. 5—The autocorrelation function $g(\tau)$ for the time variation of the irregular wind compon measured at a single station.

correlation curves, rather than the more apparent 7-km vertical dimension, which is primarily responsible for the loss of correlation. Thus an equation of the form $L = V_1 t_1$ holds for $L = 150$ km, $V_1 = 25$ m sec^{-1}, and $t_1 = 6 \times 10^3$ sec, and these values have been taken as appropriate to the large eddies.

Energy is supplied to the turbulence at a rate

$$\epsilon = V_1^2/t_1 \quad \text{erg } g^{-1} \text{ sec}^{-1} \tag{3}$$

(ϵ is the turbulence power), and substitution of the above values of V_1 and t_1 gives $\epsilon \sim 10^3$ erg g^{-1} sec^{-1}.

SMALL-SCALE TURBULENCE

From turbulence theory—The energy supplied to the turbulence is finally dissipated in the form of heat by viscous forces. From theories of homogeneous turbulence [*Batchelor*, 1953] the length and time scales of the smallest eddies, which are responsible for most of the dissipation, should depend only upon the rate of supply of energy and the kinematic viscosity. Thus

$$\eta = (\nu^3/\epsilon)^{1/4}$$

$$t_2 = (\nu/\epsilon)^{1/2}$$

η and t_2 can therefore be determined if ϵ a ν are known. ν is the kinematic viscosity. Ho ever, it does not follow from the observati described in this paper that we are necessa concerned with homogeneous turbulence in 90-km region. Indeed, it seems possible fr other contributions in this volume [*Hines*, 19 that the large-scale irregularities may repres some type of regular wave motion. Thus the energy contained in these irregularities not necessarily passed down through eddies smaller size before being dissipated by visc forces. If a value of $\epsilon = 10^3$ ergs g^{-1} sec^{-} assumed, equations (4) and (5) will give mi mum values of the time constant and dimensi of the small energy-dissipating eddies.

Taking $\nu = 2 \times 10^5$ cm^2 sec^{-1}, we find t $\eta = 17$ m, $t_2 = 14$ sec, and $V_2 = 1.2$ m sec

Time delays in the appearance of enduring ieteor echoes—An estimate for a lower value f t_2 can be obtained from the delays in appearnce of discrete radio-echo components from right meteor trails. An initially linear meteor rail should become completely rough at radio avelengths in about the time constant of the mall eddies. As the trail distorts, echoes from arts of the trail removed from the specular reion can therefore be delayed in appearance as uch as to a time t_2 (although large-scale turulence would normally cause the echoes to ppeared earlier). Delays of 30 sec have been oberved showing that $t_2 \gtrsim 30$ sec.

The effects of eddy diffusion on meteor echo luration—The effect of eddy diffusion is to reluce the volume electron density at the center f a meteor trail more rapidly than for molecuar diffusion alone. The time for which the elecron density remains greater than the critical lectron density at a given wavelength can be ound from inspection of the echo characterisics; 200 sec is an average maximum value for bright meteor. If a reasonable initial linear lectron density is assumed, this time can also e used to set a lower limit to t_2, applying exsting theories of eddy diffusion and meteor cho duration [*Booker and Cohen*, 1956]. The ninimum value of the time constant of the smallest eddies, determined in this way, is found to be 10 sec. Minimum values of this order are consistent with the observed behavior of enduring meteor echoes when observed by means of a narrow pulse radar [*Greenhow and Neufeld*, 1959*c*].

References

Batchelor, G. K., *Homogeneous Turbulence*, Cambridge University Press, 197 pp., 1953.

Booker, H. G., and R. Cohen, A theory of long-duration meteor echoes based on atmospheric turbulence with experimental confirmation, *J. Geophys. Research, 61*, 707–733, 1956.

Greenhow, J. S., and E. L. Neufeld, *Proc. Phys. Soc. London B*, (in press), 1959*a*.

Greenhow, J. S., and E. L. Neufeld, *Proc. Phys. Soc. London, B*, (in press), 1959*b*.

Greenhow, J. S., and E. L. Neufeld, Turbulence at altitudes of 80 to 100 km and its effects on long-duration meteor echoes, *J. Atmospheric Terrest. Phys.*, (in press), 1959*c*.

Hines, C. O., An interpretation of certain ionospheric motions in terms of atmospheric waves, *J. Geophys. Research, 64*, 2210–2211, 1959.

Liller, W., and F. L. Whipple, High-altitude winds by meteor-train photography, *J. Atmospheric and Terrest. Phys., Spec. Supplement, 1*, 112–130, 1954.

Manning, L. A., and V. R. Eshleman, Discussion of the Booker and Cohen paper, 'A theory of long-duration meteor echoes based on atmospheric turbulence with experimental confirmation,' *J. Geophys. Research, 62*, 367-371, 1957.

Outline of Some Topics in Homogeneous Turbulent Flow

STANLEY CORRSIN

The Johns Hopkins University
Baltimore, Maryland

Abstract—Following general remarks on the homogeneous turbulence problem, and an indication of kinematic and dynamic relations in the isotropic case, outlines are given of the phenomena of spectral transfer and tendencies toward isotropy. A discussion of Reynolds numbers is followed by detailed comparisons of some characteristic lengths. There are, finally, an outline of some theories on spectral turbulent energy transfer and a mention of static pressure fluctuations.

Note—This sketchy account is chiefly for orientation in the homogenous turbulence problem; many important points are omitted. Figures are qualitative only. References, aside from sporadic ones in the text and footnotes, are in the bibliography at the end of the paper. Text references to one of the first two books are preceded by *GKB* or *AAT*, respectively.

A. The statistical mechanical nature of the turbulence problem—In isopycnic, Newtonian fluid motion, the history of flow from any prescribed initial conditions is given by four equations:

Three Navier-Stokes equations for momentum (Newton's second law):

$$\frac{\partial u_i}{\partial t} + u_k \frac{\partial u_i}{\partial x_k} = -\frac{1}{\rho}\frac{\partial p}{\partial x_i} + \nu \nabla^2 u_i \qquad (1)^1$$

One continuity equation for mass:

$$\partial u_i / \partial x_i = 0 \qquad (2)$$

u_m are turbulence velocities only; we take mean velocities zero, mean pressure gradient zero.

Since the turbulent motion is random, we seek a statistical description rather than velocity field history at each point in space-time. Presumably the initial conditions should also be statistical. At every point in space-time, the random vector field satisfies equations 1 and 2. Hence, the ideal goal of a general theory is predict the complete *functional probability de sity* of the velocity field following some rath simple class of initial conditions.

Some difficulties in attempting to apply cla sical statistical mechanics to turbulence are:

(*a*) No descrete particles can be identifie hence we need a function space as phase spac This can be ameliorated if we can introduce spectral cutoff.

(*b*) No one has discovered a Lagrange Hamiltonian density that will lead via Ham ton's principle to the Navier-Stokes equation

(*c*) Even if we had such a density, we st have no technique for deriving a Liouvi theorem when the phase space is a functi space.

(*d*) System is always dissipative, i.e., *not equilibrium*. Hence, a homogeneous field mu be statistically nonstationary, and a stationa field must be inhomogeneous.

Eberhard Hopf [1952, 1957] introduced t *probability functional* of the velocity field f any time *t*. From the Navier-Stokes equatio he obtained a function-functional, integrodiffe ential equation which no one appears to kno how to cope with. His work is valuable as a ge eral formulation of the turbulence problem.

B. The lesser goals of actual turbulence the

[1] This is the Eulerian form. The Lagrangian form, wherein we follow the fluid particles, is more natural for describing dispersion phenomena. Unfortunately the viscous terms have an almost prohibitively complex nonlinear structure in the Lagrangian system.

[2] Oldroyd (*Proc. Cambridge Phil. Soc., 43* 1 1947), Rosen (*J. Chem. Phys., 21* (7), 1953), a Herivel (*Proc. Roy. Irish Acad., 56, A* (4), 195 have gotten the Navier-Stokes equations throu a restricted variation, however.

—Evidently the functional problem is far re information than we would want (or could dle). In the absence of a mean velocity field, may be interested in such physically motied properties as: (*a*) the kinetic energy of turbulence; (*b*) the 'average eddy size,' and er scales; (*c*) the distribution of energy with pect to eddy size, i.e. the power spectrum; the probability densities of velocity and ocity derivatives at a single space point; mean square displacement of a fluid parе; (*f*) relative displacement statistics for particles; plus many quantities that occur the equations we deduce for the more obusly interesting functions. These, and many ers, are accessible to experiment through the -wire anemometer.[3]

Two classes of 'reduced information' statisti- functions are convenient for describing nogeneous random fields:

. The correlation functions

$$\equiv \overline{u_i(\mathbf{x}, t)u_j(\mathbf{x} + \xi_1, t + \tau_1) \cdots u_s(\mathbf{x} + \xi_{n-1}, t + \tau_{n-1})}$$

2. The multipoint probability densities in ce time

$$P^{(n)}[u_i, u_j^{(1)}, u_k^{(2)}, \cdots, u_s^{(n-1)}]$$

n dealing with differential equations, it is en convenient to work with some integral nsforms of these functions, e.g. their Fourier nsforms: (1) the spectral functions; (2) the racteristic functions.

Apparently no one has yet succeeded in forlating differential equations for the simple obability densities (or the characteristic funcns), and so homogeneous turbulence theory s dealt exclusively with correlation functions d their Fourier transforms, the spectral funcns). Heisenberg and Kraichnan deal initially h the Fourier transform of the instantaneous ocity field, rather than that of the (averaged) relation. Kraichnan actually makes his theoical postulates on the statistical behavior of se random Fourier elements.

Unfortunately, no finite number of correlation equations is determinate because of the nonlinearity of the Navier-Stokes equations; the equation for nth order correlation must involve the $(n + 1)$st correlation. Of course the spectral equations show the same difficulty.

The infinite array must be truncated at some finite stage and sealed-off with the assumption: Herein lie all the theories!

Some categories of assumptions are:

(*a*) Keep the first n equations and neglect $\mu^{(n+2)}$ in the nth.

(*b*) Keep the first n equations and assume a simple *ad hoc* expression for $\mu^{(n+2)}$ in terms of lower-order correlations.

(*c*) Keep the first n equations and use dimensional and/or physical arguments to assume a form for $\mu^{(n+2)}$. (Most of the theories keep only the first equation, and that one only for the degenerate correlation with $\tau = 0$.)

(*d*) Assume complete or partial similarity of the space correlation functions as time goes on. This gives some peripheral information on time-dependent coefficients, but not on the functions themselves.

C. Some Eulerian kinematics—For a three-dimensional, homogeneous scalar field, the auto-correlation field is

$$\mu(\xi) \equiv \overline{\theta(\mathbf{x})\theta(\mathbf{x} + \xi)} = \iiint_{-\infty}^{\infty} e(\mathbf{k}) \cos(\mathbf{k}\cdot\xi)\, dV_k(\mathbf{k}) \tag{3}$$

where $e(\mathbf{k})$ is the spectral density,

$$e(\mathbf{k}) = \frac{1}{8\pi^3} \iiint_{-\infty}^{\infty} \mu(\xi) \cdot \cos(\mathbf{k}\cdot\xi)\, dV_\xi(\xi) \tag{4}$$

Evidently

$$\mu(0) = \overline{\theta^2} = \iiint_{-\infty}^{\infty} e(\mathbf{k})\, dV_k(\mathbf{k}) \tag{5}$$

For an isotropic three-dimensional scalar field,

$$\left.\begin{aligned} e(\mathbf{k}) &= \text{fn}\,(k) \quad \text{only} \\ \mu(\xi) &= \text{fn}\,(\xi) \quad \text{only} \end{aligned}\right\} \tag{6}$$

It is helpful to visualize these as spherically symmetric clouds.

Each spectral point $e(\mathbf{k}_0)\, dV_k(\mathbf{k}_0)$ corresponds

[3] A good account of this instrument is given by vasznay in art. F2 of *Physical Measurements Gas Dynamics and Combustion*, Princeton Unisity Press, 1954.

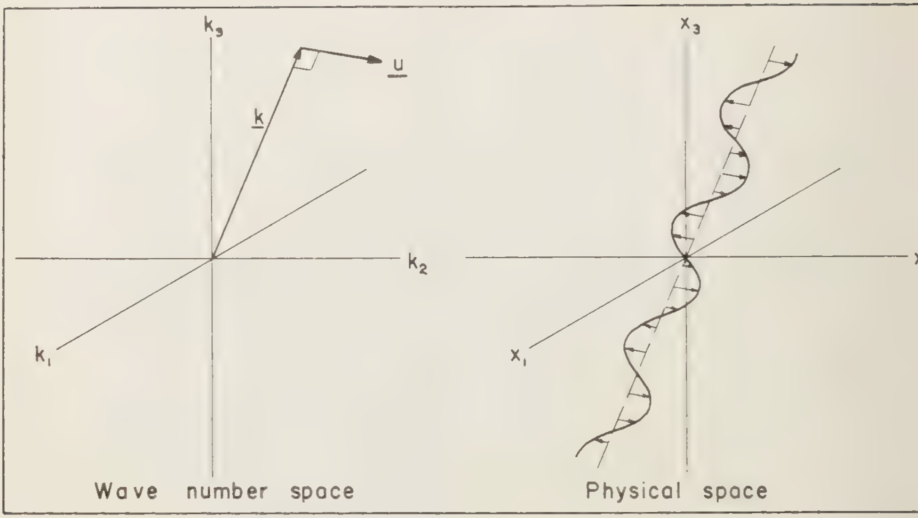

FIG. 1—Representation of shear waves.

to a wave in physical space (θ space), with nodal planes perpendicular to $\mathbf{k}_a$ and wavelength $\Lambda_a = 2\pi k_a^{-1}$.

For a homogeneous vector field, like velocity $\mathbf{u}(\mathbf{x})$, the correlation and spectral density are second-rank tensors:

$$\mu_{ik}(\boldsymbol{\xi}) \equiv \overline{u_i(\mathbf{x})u_k(\mathbf{x}+\boldsymbol{\xi})} = \iiint_{-\infty}^{\infty} f_{ik}(\mathbf{k}) \cdot \exp\,[i(\mathbf{k}\cdot\boldsymbol{\xi})]\, dV_k(\mathbf{k}) \tag{7}$$

$$f_{ik}(\mathbf{k}) = \frac{1}{8\pi^3} \iiint_{-\infty}^{\infty} \mu_{ik}(\boldsymbol{\xi}) \cdot \exp\,[-i(\mathbf{k}\cdot\boldsymbol{\xi})]\, dV_\xi(\boldsymbol{\xi}) \tag{8}$$

Each Fourier element is a shear wave filling the whole physical space, with nodal planes perpendicular to $\mathbf{k}$, wavelength $\Lambda = 2\pi k^{-1}$, and vector direction $\mathbf{u}$ (that of velocity in physical space), Figure 1.

A helpful illustration is the simple case of an infinite field of shear waves all of identical wavelength, uniformly distributed in direction of nodal planes, and (independently) uniformly distributed in direction of velocity vectors. The spectrum is then a tensor uniformly distributed over a hollow spherical shell in wave-number space.

Figure 2 is a schematic attempt at illustrating a related simpler case: a two-dimensional sh wave field with a finite number of elements. simplicity the spectrum is drawn as the di (vector) transform of the actual velocity field

This may help to rationalize the (apologe use of the term eddies in describing spec structure ('big eddies', 'small eddies'). It is of pointed out that the traditional (i.e., be modern turbulence theory) use of the term e implies a spatially local blob of fluid, usu swirling; this seems inconsistent with its to characterize spectral regions since a si spectral element fills the entire physical sp Assume, however, that we identify a wh spherical shell in k space (a cylinder if Fig as the 'eddies of size k^{-1}' (never referring a single eddy).

If we restrict ourselves to a statistic isotropic velocity field (of which the forego illustration is a degenerate case), the class mathematical forms permissible for $\mu_{ik}(\xi)$ $f_{ik}(\mathbf{k})$ is severely limited. Statistical isotropy the random vector field requires that all avera functions be invariant to arbitrary rotat and reflections of the configuration; e.g., averaged functions of u_a and u_b are equal to same functions of u_c and u_d in Figure 3.

Omitting details, it is sufficient here to rem that the purely kinematic constraints of isotr

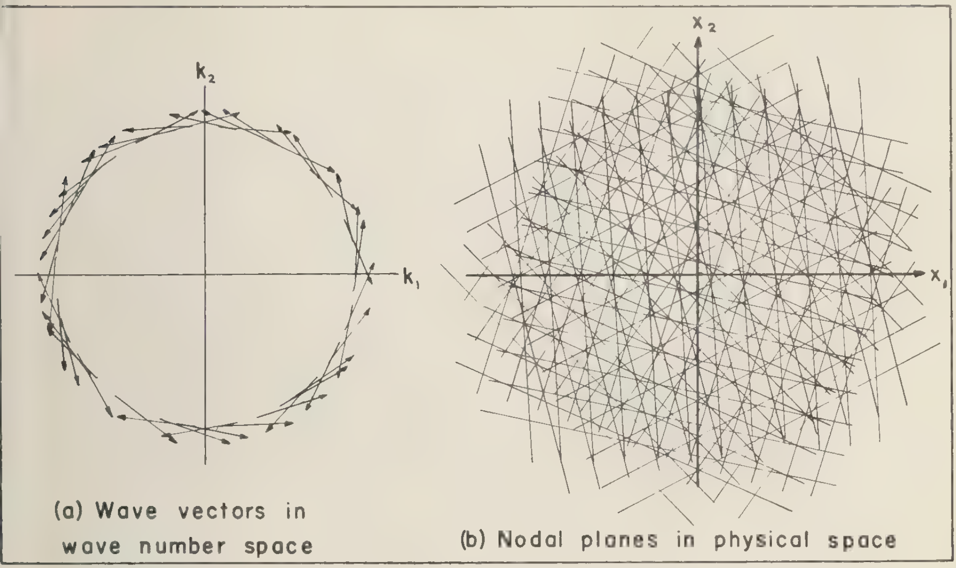

FIG. 2—Sample from an isotropic collection of equal shear waves in two dimensions.

and constant density lead, for example, to the special form

$$f_{ik}(\mathbf{k}) = \left[\delta_{ik} - \frac{k_i k_k}{k^2} \right] \frac{A(k)}{2} \tag{9}$$

where δ_{ik} is the Kronecker delta tensor.

$$A(k) \equiv f_{ii}$$

is spectral energy density, and is a spherical cloud. The spherical integral over a k shell is convenient:

$$\mathcal{E}(k) \equiv 4\pi k^2 A(k)/2 \tag{10}$$

We note that

$$\begin{aligned} \frac{1}{2}\overline{u_i u_i} &= \frac{1}{2}\iiint_{-\infty}^{\infty} f_{ii}(\mathbf{k})\, dV_k(\mathbf{k}) \\ &= \int_0^{\infty} \mathcal{E}(k)\, dk \end{aligned} \tag{11}$$

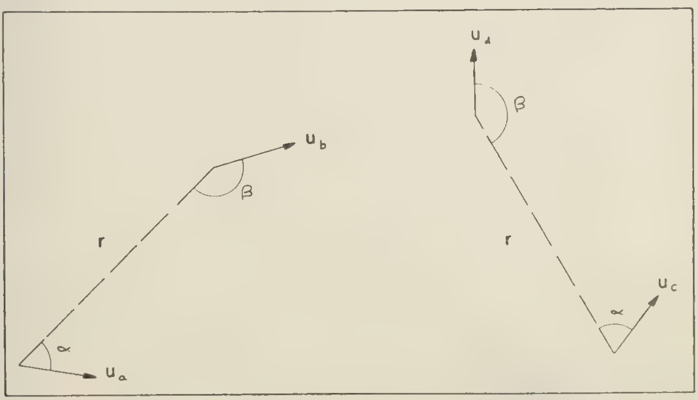

FIG. 3—Velocity components in an isotropic field.

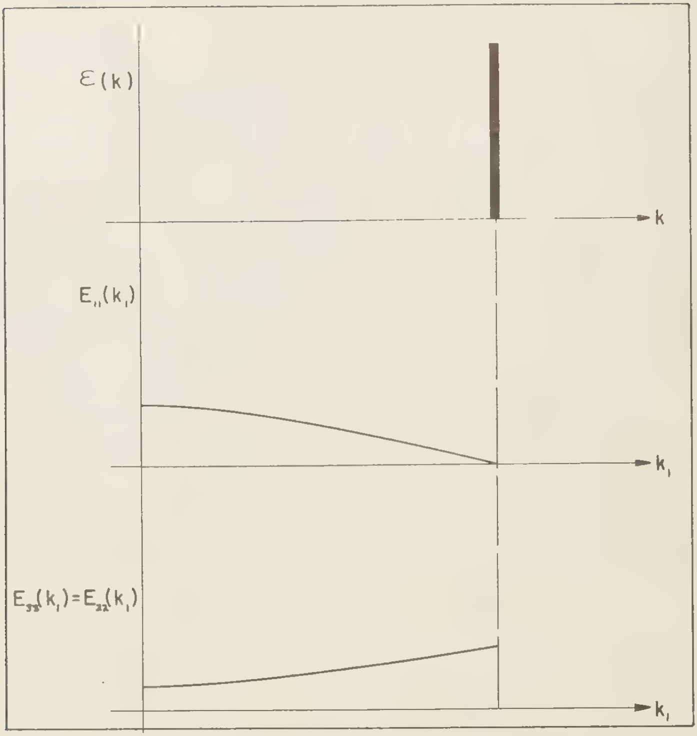

Fig. 4—A 'Dirac type' three-dimensional isotropic spectrum and the two corresponding kinds of one-dimensional spectra.

$\mathcal{E}(k)$ is called the *three-dimensional spectrum.* It is, of course, a function of only one variable at each instant of time.

The spectra we measure most easily with the hot-wire anemometer are the one-dimensional spectra in flow direction, e.g.,

$$E_{11}(k_1)$$

$$= 2\int_{-\infty}^{\infty}\int_{-\infty}^{\infty} f_{11}(k_1, k_2, k_3)\, dk_2\, dk_3 \qquad (12)$$

$$= \int_0^{\infty} \mu_{11}(\xi_1, 0, 0) \cos(k_1\xi_1)\, d\xi_1 \qquad (13)$$

$E_{11}(k_1)\, dk_1$ is the integral over a slab dk_1 thick of contributions to $\overline{u_1^2}$ only.

It turns out that a simple (Dirac) spherical shell energy density $A(k)$ corresponds to Figure 4. Thus, any three-dimensional spectrum split into differential width functions contributes a series of distributed parabolas to the two basi[c] one-dimensional spectra (Figure 5).

Analogous kinematic restrictions apply t[o] velocity correlation tensors and spectra of a[ll] orders.

D. Simplest dynamical equations for isotrop[ic] correlations and spectra—From the Navier-Stoke[s] equation it is simple to deduce equivalent simpl[e] looking scalar equations for the correspondin[g] spectral function:

For the trace of the correlation tenso[r] $F(\xi, t) \equiv \mu_{ii}(\xi, t)$,

$$\frac{\partial F(\xi, t)}{\partial t} = \nabla \cdot \mathrm{S}(\xi, t) + 2\nu\nabla^2 F(\xi, t) \qquad (1\text{4})$$

where $S_j \equiv S_{iji}$ is a partial contraction of th[e] triple correlation

$$S_{ijk} \equiv \overline{u_i(\mathbf{x})u_j(\mathbf{x})u_k(\mathbf{x}+\xi)}$$

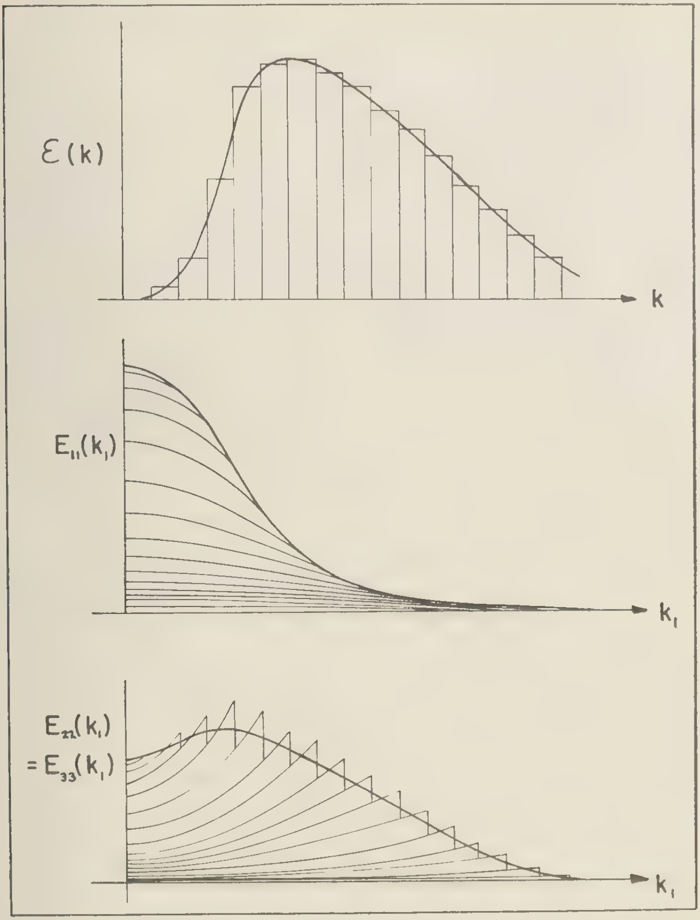

FIG. 5—Extension of Figure 4 to a continuous $\epsilon(k)$.

or the three-dimensional spectrum

$$\frac{\partial \mathcal{E}(k, t)}{\partial t} = T(k, t) - 2\nu k^2 \mathcal{E}(k, t) \qquad (15)$$

hich is of lower order than (14). We note that

$$\int_0^\infty T\, dk \equiv 0$$

To make either equation determinate an dditional relation is needed. The hypotheses re most often made on the form of

$$W(k, t) \equiv -\int_0^k T\, dk'$$

(in terms of $\mathcal{E}$) since it has a simple physical interpretation: the net rate of flux of turbulent energy out through the spherical shell of wave number k.

Equations for correlation and spectrum functions in space time, and/or at more than two points, have also been derived.

For $\xi = 0$ in (14) [or integrating (15) from 0 to ∞], we get the equation for the energy decay of isotropic turbulence,

$$\frac{1}{2}\frac{d\overline{q^2}}{dt} = 3\nu\left[\frac{\partial^2 F}{\partial \xi^2}\right]_{\xi=0} \qquad (16a)$$

$$= \epsilon(t) \qquad (16b)$$

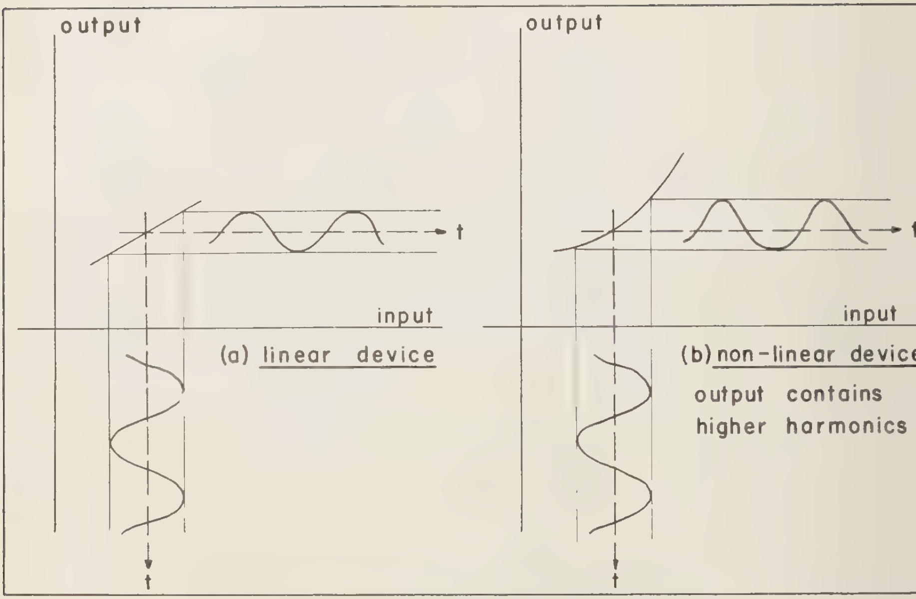

FIG. 6—Illustration of 'spectral transfer' due to nonlinearity.

$$\equiv -5\nu \frac{\overline{q^2}}{\lambda^2} \qquad (16c)$$

Equation 16*b* says only that the rate of disappearance of turbulent energy is equal to the viscous dissipation rate when no source term exists; (16*c*) is merely the definition of a characteristic length λ. Directly from the Navier-Stokes equation, the corresponding form of (16) is

$$\frac{1}{2}\frac{d\overline{q^2}}{dt} = -\nu\overline{\left(\frac{\partial u_i}{\partial x_k}\right)\left(\frac{\partial u_i}{\partial x_k}\right)} \qquad (16d)$$

It can also be shown that the dissipation rate is proportional to the mean square vorticity.

The *integral scales* characterize the energy-bearing eddies. Taylor defined, for example,

$$L \equiv \frac{1}{\overline{u^2}} \int_0^\infty \mu_{22}(\xi_1, 0, 0)\, d\xi_1 \qquad (17)$$

and Batchelor, in his *Homogeneous Turbulence*, has shown that this can be expressed as

$$L = \frac{3\pi}{4} \frac{\int_0^\infty k^{-1}\mathcal{E}\, dk}{\int_0^\infty \mathcal{E}\, dk} \qquad (18)$$

which rationalizes the term 'average eddy s

E. Nonlinearity and spectral transfer—A cer trait of the flows we call turbulent is the average transfer of energy from smaller larger wave numbers. This arises because phenomenon (via the Navier-Stokes equati is inherently *nonlinear*.

Perhaps the simplest illustration of a spec transfer due to nonlinearity is in an instantane system whose input-output curve is not a stra line, e.g. quasi-static response of a vacuum t Figure 6 illustrates the effect with an in whose spectrum is a single line.

A more pertinent illustration is the sir nonlinear differential equation

$$\frac{\partial\theta}{\partial t} + \theta\frac{\partial\theta}{\partial x} = 0$$

If we choose the initial state

$$\theta(x, 0) = B\cos(kx)$$

we find higher harmonics appearing as time on: a series development in t starts like

$$\theta(x, t) \approx B\cos(kx) + (B^2/2)kt\sin(2kx)$$

Qualitative insight into the analytical ructure of a spectral transfer is gained by oking at the spectral structure when θ is ken as a Fourier series,

$$\theta(x, t) = \sum_{k=1}^{\infty} B_k(t) \cos [kx + \varphi_k(t)]$$

he spectral equation is

$$\partial \mathcal{E}_\theta / \partial t = T_\theta \tag{21}$$

hich is the transform of the correlation equation

$$\partial \mu_\theta / \partial t = -(\partial / \partial \xi) M_\theta \tag{22}$$

hese are equivalent to (15) and (14), respecively.

$$\left.\begin{aligned} \mathcal{E}_\theta(k, t) &\equiv \tfrac{1}{2} B_k^2 \\ \mu_\theta(\xi, t) &\equiv \overline{\theta(x)\theta(x+\xi)} \\ M_\theta(\xi, t) &\equiv \overline{\theta^2(x)\theta(x+\xi)} \end{aligned}\right\} \tag{23}$$

To see the mathematical structure of T_θ, we rite M_θ as a Fourier series

$$I_\theta(\xi, t) = \sum_{k=1}^{\infty} [\alpha_k(t) \cos (k\xi) + \beta_k(t) \sin (k\xi)] \tag{24}$$

alculation reveals that

$$\left.\begin{aligned} {}_k &= \frac{B_k}{4} \left\{ \sum_{p=1}^{k} B_p B_{k-p} \cos (\varphi_k - \varphi_p - \varphi_{k-p}) \right. \\ &\qquad \left. + 2 \sum_{q=1}^{\infty} B_q B_{k+q} \cos (\varphi_k + \varphi_q - \varphi_{k+q}) \right\} \\ {}_k &= -\frac{B_k}{4} \left\{ \sum_{p=1}^{k} B_p B_{k-p} \sin (\varphi_k - \varphi_p - \varphi_{k-p}) \right. \\ &\qquad \left. + 2 \sum_{q=1}^{\infty} B_q B_{k+q} \sin (\varphi_k + \varphi_q - \varphi_{k+q}) \right\} \end{aligned}\right\} \tag{25}$$

There are two important features: (*a*) energy ransfer always involves interaction among three Fourier components; (*b*) phase relations are imortant, even though the energy spectrum itself ontains no phase.

Geometrically, spectral transfer appears in he (empirical) fact that relatively coherent lobs of fluid are drawn into ever more convoluted strings and/or sheets (statistical surface stretching). In a two-dimensional, binary, scalar field, for example, the results of turbulent convection may look like Figure 7.

This is the whole story in mixing of a passive scalar; in the dynamic spectral transfer it is only part of the story. The inherent nonlinearity precludes the analytical use of (random) superposition for constructing complex flows out of simple solutions to the Navier-Stokes equations.

F. Tendencies toward isotropy—It is found experimentally that roughly homogeneous turbulence that is receiving no energy tends to become isotropic. For example, a square-mesh grid set across a uniform flow is a very nonisotropic turbulence generator (Fig. 8). Yet, some 40 to 50 mesh lengths downstream, its turbulence is roughly isotropic.

If this turbulence is then sent through an axisymmetric contraction, the preferential strain field (acting most directly on vorticity) introduces strong anisotropy. As is indicated in Figure 9 the cartesian components approach equipartition in the uniform flow region afterward [*Uberoi*, 1956; *Mills and Corrsin*, 1959]. It can be shown that in this region the intercomponent transfer depends on the static pressure fluctuations, which is not surprising since pressure is a scalar, but there is no theory that can predict even the signs of these transfer terms.

Empirically, this approach toward *gross isotropy* is slow in the sense that its rate is about the same as the rate of energy decay.

The local isotropy concept of Kolmogorov (at high enough Reynolds number, the turbulent small structure may be isotropic even when large structure is not) is based on the idea that the nonlinear spectral cascade is an orientation-losing process. This postulate has intuitive appeal as well as some direct and indirect experimental support [*GKB*: Townsend, 1948*b*; Corrsin, 1949; Laufer, 1950]. Of course, the mean strain rate in all shear flows must tend to make the structure anisotropic in all parts of the spectrum. If the spectral energy transfer process destroys orientation, however, local isotropy can still be expected in spectral regions where the local transfer time

$$\tau(k) \equiv [k^3 \mathcal{E}]^{-1/2} \tag{26}$$

is much smaller than the characteristic time of

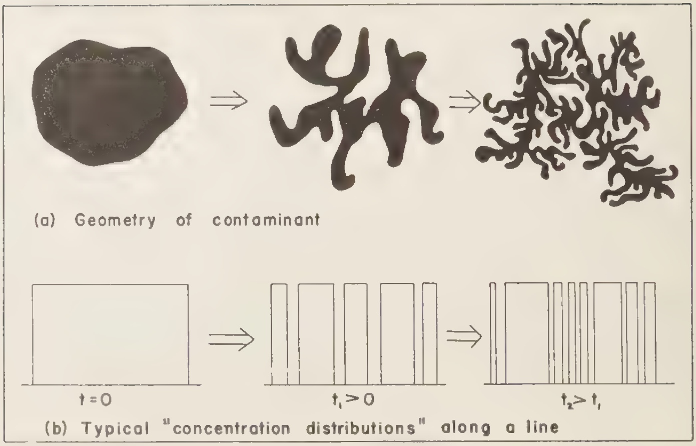

FIG. 7—Spectral transfer in convective mixing with no molecular diffusion.

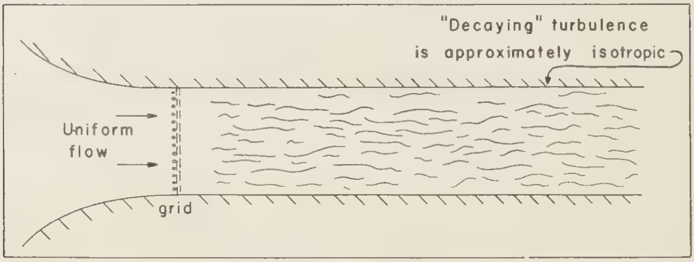

FIG. 8—Conventional method of generating approximately isotropic turbulence.

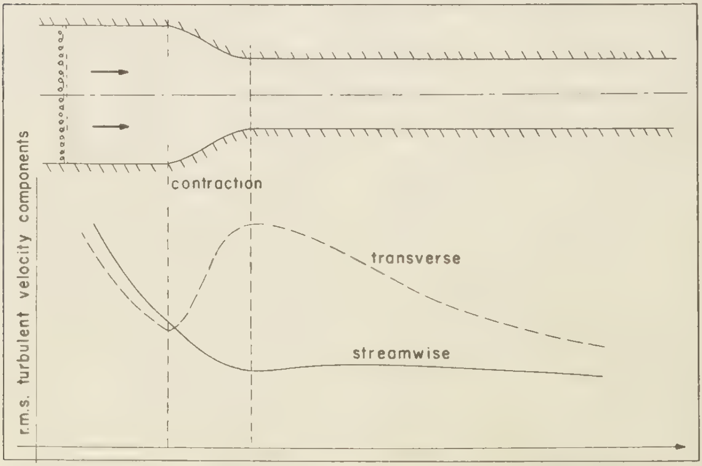

FIG. 9—Root-mean-square turbulent velocity fluctuations during gross strain and afterward.

gross shear strain,

$$\left|\frac{\partial \bar{U}}{\partial y}\right|^{-1}$$

sort of argument leads to possible in-
lities as necessary conditions for local
opy [*Corrsin*, 1957, 1958; *Uberoi*, 1957].

Reynolds numbers; inertial, isotropic region—
n the Navier-Stokes equations, it can be
vn that a basic dimensionless parameter in
ous flow is the ratio of the magnitudes of
ia forces to viscous forces: the Reynolds
ber,

$$\frac{\rho \dfrac{U}{D/U} D^3}{\mu(U/D)\ D^2} = \frac{UD}{\nu} \tag{27}$$

re U and D are characteristic velocity and
th, respectively.

homogeneous turbulence there are no
acteristic mean flow velocities or lengths,
turbulence parameters are appropriate. A
mon choice is

$$R_\lambda \equiv (u'\lambda/\nu) \tag{28}$$

(due to G. I. Taylor). An alternative physical interpretation is

$$R_\lambda \sim \frac{\text{(turbulent kinetic energy)}}{\text{(dissipation in time)}(\lambda/u')} \sim \frac{\overline{u^2}}{\nu(u^2/\lambda^2)(\lambda/u')} \tag{29}$$

(λ/u') is a time characterizing the turbulent strain and vorticity. From (16c) we see that λ^2/ν is a characteristic decay time. We note that

$$\frac{\lambda^2/\nu}{\lambda/u'} = R_\lambda \tag{30}$$

Alternatively, it seems plausible to use

$$R_L \equiv u'L/\nu \tag{31}$$

since L is an average eddy size. Since they are monotonically related ($R_\lambda \sim R_L^{1/2}$, section I), the choice is not important.

It is helpful to introduce the notion of a *spectral Reynolds number*,

$$\mathcal{R}(k) \equiv \frac{v_k l_k}{\nu} = \frac{1}{\nu}\left[\frac{\mathcal{E}}{k}\right]^{1/2} \tag{32}$$

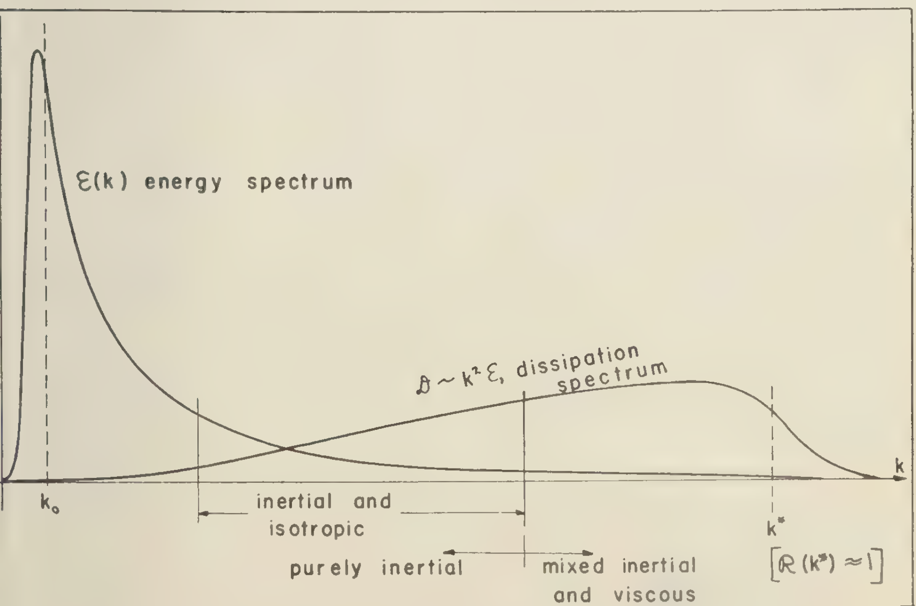

FIG. 10—Spectral ranges in turbulence of moderate Reynolds number.

to reveal the relative importance of inertial and viscous effects in different parts of the spectrum. Since $\mathcal{E}(k)$ must decrease at high enough k, $\mathcal{R}(k)$ also decreases, and for small enough eddies we must have a region in which viscous forces are important (Fig. 10).

If the lower boundary of the *mixed* range is at very large k, there may be a spectral region which is both inertial and isotropic. For such a region Kolmogorov [*GKB*, Kolmogorov, 1941*a*] postulated that $\mathcal{E}(k)$ depends only on the rate of energy flux through this part of the spectrum. But this must equal the total dissipation rate ϵ. The only form dimensionally possible is

$$\mathcal{E}(k) = N\epsilon^{2/3}k^{-5/3} \tag{33}$$

In the next section it is shown that the numerical constant N is of the order of unity.

H. Relations among some characteristic scales—To obtain a wave number k^* characterizing the dissipation spectrum, Kolmogorov postulated $k^* = k^*(\epsilon, \nu)$ only. Hence

$$k^* \equiv (\epsilon/\nu^3)^{1/4} \tag{34}$$

The inverse quantity $\eta \equiv k^{*-1}$ is often called the 'Kolmogorov microscale.' The corresponding characteristic velocity is

$$v^* \equiv (\epsilon\nu)^{1/4} \tag{35}$$

so that the corresponding Reynolds number

$$v^*/(k^*\nu) \equiv 1 \tag{36}$$

by definition.

The ratio η/λ follows from introducing Taylor's isotropic expression for ϵ, (16*b*, *c*), into (34):

$$\frac{\eta}{\lambda} = \frac{1}{(15)^{1/4}R_\lambda^{1/2}} \doteq \frac{0.5}{R_\lambda^{1/2}} \tag{37}$$

To estimate the relation between η and the mean free path l in a gas, we introduce the kinetic theory result $\nu \approx lc$ into (36); c is essentially sound velocity:

$$l/\eta \approx v^*/c \tag{38}$$

the Mach number of the dissipative eddies. Introducing (35) and Taylor's form for ϵ gives

$$l/\eta \approx (0.5/R_\lambda^{1/2})(u'/c) \tag{39}$$

To have negligible 'slip' effect in the dissipation phenomenon, we must have

$$R_\lambda^{1/2} \gg \tfrac{1}{2}(u'/c)$$

It is noteworthy that (36) is the cond
$\mathcal{R}(k^*) = 1$. Introducing (33) into this, we ob
the estimate $N = 1$.

A more elaborate approach involves rep
ment of the actual spectrum at extremely
Reynolds numbers with a purely ine
spectrum

$$\mathcal{E} = N\epsilon^{2/3}k^{-5/3}$$

truncated at $k_0(\approx L^{-1})$ and at $k^*(\gg$
Estimating the total dissipation in this
i.e.,

$$\epsilon = 2\nu \int_0^\infty k^2\mathcal{E}\,dk$$

$$\approx 2N\nu\epsilon^{2/3} \int_{k_0}^{k^*} k^{1/3}\,dk$$

we arrive at $N \approx \frac{2}{3}$ (neglecting $k_0^{4/3}$ relativ
$k^{*4/3}$). This appears paradoxical, estima
dissipation with a nondissipative form, bu
can be justified as long as the true $\mathcal{E}(k)$ decr
sufficiently rapidly for $k > k^*$.

A similar calculation for energy,

$$\tfrac{1}{2}\overline{q^2} = \int_0^\infty \mathcal{E}\,dk \approx \tfrac{2}{3}\epsilon^{2/3} \int_{k_0}^{k^*} k^{-5/3}\,dk$$

is one way of establishing a rough conne
between λ and L. Neglecting $k^{*-2/3}$ relativ
$k_0^{-2/3}$, we get

$$\lambda/L \approx 8/R_\lambda$$

which is of the same order as experime
results (obtained at too small a Reynolds num
of course).

In most turbulent shear flows we can iden
a shear zone width Δ, like the 'thickness'
boundary layer or jet. There are still no the
for predicting a relation between turbul
scales and this mean flow dimension. Wit
being precise about definitions (since the r
are a bit different in the different types of s
flows anyway), laboratory data indicate
integral scales are roughly proportional t
independent of Reynolds number:

$$L_s \approx J\Delta$$

ere $1/20 < J < 1/2$, depending on the direc-n in which the scale is measured and the rticular choice of velocity component [*AAT*, hubauer and Klebanoff, 1951; Favre, Gaviglio, d Dumas, 1957, 1958; *Grant*, 1958].

There is a strong temptation to use (the more cessible) Eulerian integral scale as character-ic length in estimating a turbulent diffusivity. is is wrong in principle: Lagrangian correlation termines the dispersive motion of fluid par-les. Yet it seems to work moderately well in actice. For flows with complete dynamic nilarity, all lengths should remain propor-onal, so this success is less surprising. There still no theory connecting the Eulerian and agrangian statistical functions, except for some niting forms.

I. Some assumptions for isotropic spectral ansfer—Consider (15) in the form

$$\frac{\partial \mathcal{E}}{\partial t} = -\frac{\partial W}{\partial k} - 2\nu k^2 \mathcal{E} \tag{45}$$

he simplest assumption is Kovasznay's [*GKB*' ovasznay, 1949] that $W(k)$ depends on $\mathcal{E}(k)$ the same wave number. Dimensionally,

$$W = C_K k^{5/2} \mathcal{E}^{3/2} \tag{46}$$

nd hence (45) becomes, with C_K a numerical onstant,

$$\frac{\mathcal{E}}{t} = -\tfrac{3}{2} C_K k^{3/2} \mathcal{E}^{3/2} \cdot \left\{\frac{5}{3} + \frac{k}{\mathcal{E}}\frac{\partial \mathcal{E}}{\partial k}\right\} - 2\nu k^2 \mathcal{E} \tag{47}$$

he theoretical results turn out to be remarkably ell behaved [*Reid and Harris*, 1959], leading to $-5/3$ inertial region, and a literal cutoff at $= k^*$.

Obukhov [*GKB*, Obukhov, 1941] reasoned in nalogy to the way in which turbulence in a hear flow drains energy out of the mean motion, ith terms like $\overline{uv}\, \partial \overline{U}/\partial y$. In effect, he postu-ted that the small structure $(k > k_a)$ sees the rge structure $(k < k_a)$ as a quasi-mean motion. ence the transfer rate from the $(k < k_a)$ part f the spectrum to the $(k > k_a)$ part is propor-ional to the product of rms strain rate of the ower part by energy in the upper part:

$$V(k) \doteq C_0 \left\{\int_k^\infty \mathcal{E}\, dk'\right\}\left\{\int_0^k k''^2 \mathcal{E}\, dk''\right\}^{1/2} \tag{48}$$

where C_0 is a constant. This theory is more general than Kovasznay's. The solution behaves like $k^{-5/3}$ in the inertial range, but $\mathcal{E}(k)$ unfortunately increases with k at large k.

Heisenberg [*GKB*, Heisenberg, 1948*a*] chose a form for W analogous to the viscous term:

$$W(k) = 2\nu_T(k) \int_0^k k'^2 \mathcal{E}\, dk' \tag{49}$$

He assumed that the *turbulent viscosity* at a particular k depends on the smaller eddies only. Then, dimensionally,

$$\nu_T(k) = C_H \int_k^\infty [k''^{-3}\mathcal{E}]^{1/2}\, dk'' \tag{50}$$

with C_H a constant. Substitution of (49) and (50) into (45), integrated from 0 to k, gives Heisenberg's final equation. It has been subjected to considerable mathematical study [*GKB*: Bass, 1949; Chandrasekhar, 1949*a*]. It yields $k^{-5/3}$ behavior in the inertial range and k^{-7} behavior for $k > k^*$.

Von Kármán [*GKB*, von Kármán, 1948*b*] has presented a dimensionally inspired form that includes the foregoing ones.

It is rather drastic to assume C_K, C_0 or C_H constant in the theories mentioned above. This implies no effect of viscosity on the inertial transfer even in spectral regions with important viscous forces. Generally speaking, dimensional approaches like these may be more successful when they are generalized to include a *three* wave number interaction (see, for instance, *GKB*, section 5.2). For example, the big eddies (by their strain-rate) cause energy to transfer from small eddies to still smaller ones.

Kraichnan [1956*b*, 1958*a*] has presented a new theory which goes farther toward coping with triplet interactions. His hypotheses are applied to the time correlations of the instantaneous spectral elements in wave number space. Restricting consideration to stationary, isotropic turbulence maintained by a random forcing field, he makes two central postulates: (*a*) triple correlation coefficients among any three interacting spectral components are $\ll 1$; (*b*) for any three spectral components that interact directly (i.e., whose vector wave numbers form a triangle in **k** space), the direct interaction completely overrides the multitude of indirect interactions.

His results are somewhat different from those of most previous theories. For example, in the inertial spectral range

$$\mathcal{E}(k) \sim \epsilon^{1/2} u'^{1/2} k^{-3/2} \qquad (51)$$

instead of $\sim k^{-5/3}$. Furthermore, his dissipative microscale (k_d^{-1}) differs from the Kolmogorov scale:

$$k_d/k^* \approx R_\lambda^{-1/6} \qquad (52)$$

Published spectral measurements do not seem adequate to resolve the difference in inertial exponent. Furthermore, no laboratory spectra appear to have been measured at large enough Reynolds number for an isotropic inertial range to exist [*Corrsin*, 1958].

Possibly unfavorable to the Kraichnan's theory is the fact that the spectral Reynolds number (32) gives

$$\mathcal{R}(k_d) = \text{fn}(R_\lambda) \neq 1 \qquad (53)$$

On the other hand, introduction of (51) into an estimate of the skewness factor

$$S \equiv \overline{(\partial u/\partial x)^3}/[\overline{(\partial u/\partial x)^2}]^{3/2}$$

gives a dependence on $R_\lambda(\sim R_\lambda^{-1/3})$ which is qualitatively better than the prediction (independent of R_λ) which follows from the Kolmogorov inertial spectrum (33). S is directly connected with spectral transfer, hence is important. *Reid* [1956*a*, 1956*b*] has estimated its Reynolds number dependence according to the Heisenberg and Obukhov theories.

J. The quasi-normal postulate—Rendering finite sequence of correlation equations dete minate by actually neglecting the highest-ord correlation is a rather drastic procedur Millionshtchikov [*GKB*, Millionshtchikov, 194 proposed instead that the highest order (onl be replaced by lower-order correlations as thoug the field were normal (Gaussian). In particula $\mu^{(4)}$ can thus be eliminated from the $\mu^{(3)}$ equatic in terms of $\mu^{(2)}$ by using the equivalent of

$$\overline{abcd} = \overline{ab}\,\overline{cd} + \overline{ac}\,\overline{bd} + \overline{ad}\,\overline{bc} \qquad (5$$

Uberoi [1953, 1954] has found this to be rough true for the large structure in grid-generat turbulence.

This postulate has recently been exploit most fruitfully by *Proudman and Reid* [195 and by *Tatsumi* [1957]. To the power spectru equation, they add one for the Fourier tran form of the three-point triple correlation wi the quadruple expressed in terms of double These equations have been solved (omittin viscous terms) to see what happens for a sm time after the turbulence spectrum has a pr scribed form. Tatsumi begins with a Dir spectrum at $t = 0$ (Fig. 2). His first term f series development in t is sketched qualitative in Figure 11.

Proudman and Reid begin with a 'final perio spectrum. Their initial transfer function ar small t spectrum are sketched in Figure 12.

Although the use of the quasi-normal postula seems at the moment to have less physic

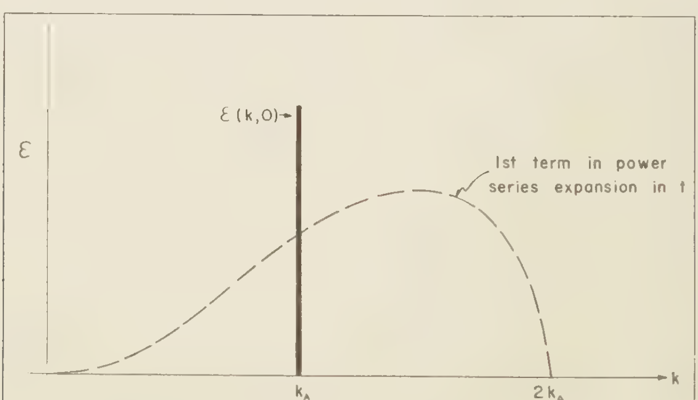

FIG. 11—Tatsumi analysis.

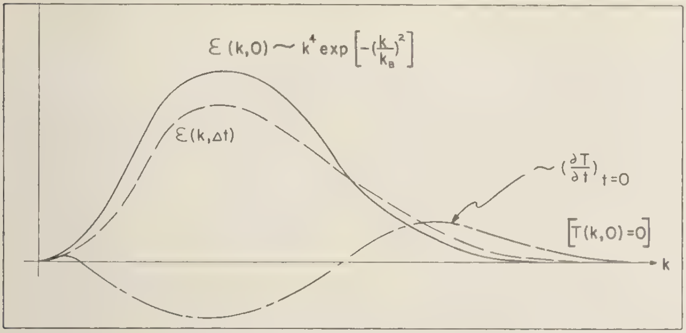

FIG. 12—Proudman-Reid analysis.

onale than some of the other theories, its ention of the triple interactions should give n edge over the double-interaction theories.

K. More on restricted spectral regions—In lition to the particularly simple forms deduced Kolmogorov and Kraichnan for the isotropic, rtial region in the spectrum, some attention been devoted to the *viscous region*, $k \gg k^*$. has been pointed out that Heisenberg's theory es $\mathcal{E} \sim k^{-7}$ in this region.

The experimental evidence is still not clear $k \gg k^*$. *Betchov* [1957] reports $\mathcal{E} \sim k^{-6}$. wnsend [*GKB*, Townsend, 1951*b*] has analyzed theoretical models based on the convective etching of randomly oriented (*a*) vortex ments and (*b*) vortex sheets. Both of these to exponential forms, rather more comfort- e than a power law, since it permits the stence of all spectral moments. His experi- nts seem to favor the sheets.

In stationary turbulence it is obvious both ysically and mathematically, from (15), that cannot have a fully viscous region such that T can be neglected for $k \gg k^*$. The Townsend models represent a mechanism attributable to the nonlinear terms in the Navier-Stokes equations. For decaying isotropic turbulence, however, $\partial\mathcal{E}/\partial t \neq 0$, and the spectrum develops as indicated in Figure 13, so it is conceivable that, for $k \gg k^*$,

$$\partial\mathcal{E}/\partial t \approx -2\nu k^2 \mathcal{E} \qquad (55)$$

whence

$$\mathcal{E} \sim (\nu k^2 t)^2 \exp\left[-2\nu k^2 t\right] \qquad (56)$$

This is identical in form with the final period solution [*GKB*], $R_\lambda \to 0$. This case is actually a random Stokes flow.

L. Static pressure fluctuations—Heisenberg [*GKB, Heisenberg*, 1948*a*], Obukhov [*GKB, Obukhov*, 1949*a*], Batchelor [*GKB, Batchelor*, 1951], and *Uberoi* [1953, 1954] have made predictions on the form of the Eulerian two-point pressure correlation function and on the value of the mean square pressure gradient fluctuation, all in isotropic turbulence. Batchelor also estimated

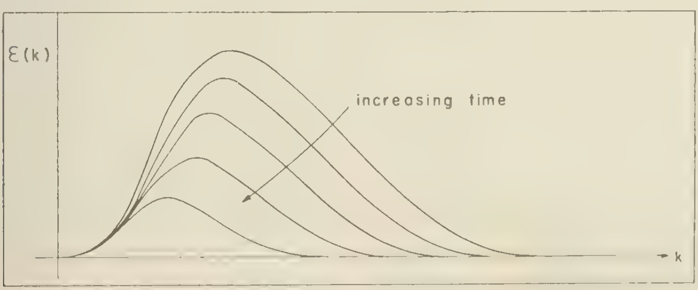

FIG. 13—Sequential spectra in decaying isotropic turbulence.

rms pressure fluctuation:

$$p' \approx 0.6\rho \overline{u}^2$$

No direct measurements of p' have been made in grid turbulence, but Uberoi calculated p' from quadruple velocity correlation measurements and found satisfactory agreement.

In shear flow the situation may be different. At the wall in a turbulent boundary layer *Harrison* [1958] measured

$$p' \approx 0.005\rho \overline{U}_\infty^2 = 0[2\rho \overline{u}^2]$$

Willmarth's [1959] measured value is approximately half of this.

Symbols

$A = f_{ii}$, spectral energy density.
$B =$ Fourier amplitude of a scalar.
$c =$ sound velocity in a gas.
C_K, C_0, $C_H =$ undetermined numerical constants in spectral transfer theories.
$D =$ a characteristic length.
$e =$ base of natural logarithm.
$e(\mathbf{k}) =$ spectral density of θ.
$E_{mn}(k_s) =$ any 'one-dimensional' spectrum of turbulence.
$\mathcal{E}(k) =$ the 'three-dimensional' spectrum of turbulence.
$f_{ik}(\mathbf{k}) =$ the spectral density of turbulence.
$F = \mu_{ii}$, trace of the correlation tensor.
$J =$ an empirical numerical factor.
$\mathbf{k} =$ (vector) wave number (magnitude $= k$).
$k^* = 1/\eta$, the Kolmogorov dissipation wave number.
$k_0 = 1/L$, wave number of 'energy-bearing eddies'.
$k_d =$ the Kraichnan dissipation wave number.
$l =$ mean free path in a gas.
$l_k = k^{-1}$.
$L =$ a particular integral scale of isotropic turbulence.
$L_s =$ any one of the integral scales in a turbulent shear flow.
$M_\theta =$ two-point triple correlation of $\theta(x)$.
$N =$ the dimensionless coefficient of the Kolmogorov inertial spectrum.
$p =$ static pressure fluctuation.
$P =$ probability density.
$q = (\mathbf{u}\cdot\mathbf{u})^{1/2} \equiv (u_j u_j)^{1/2}$, magnitude of turbulent velocity vector.
$R_\lambda \equiv u'\lambda/\nu$, a turbulence Reynolds number.
$R_L \equiv u'L/\nu$, a turbulence Reynolds number
$\mathcal{R}(k) = (1/\nu)(k^{-1}\mathcal{E})^{1/2}$, spectral Reynolds num
$S = \overline{(\partial u/\partial x)^3}/[\overline{(\partial u/\partial x)^2}]^{3/2}$, skewness facto $\partial u/\partial x$.
$S_{ijk}(\xi) =$ two-point triple correlation (tenso turbulent velocity.
$t =$ time.
$T(k) =$ a spectral transfer function.
$\mathbf{u}$ or $u_i =$ turbulent velocity vector (ma tude $= q$).
u, $v =$ cartesian components of $\mathbf{u}$ in x ar directions.
$u' \equiv (\overline{u^2})^{1/2}$, rms value of the u component component, in isotropic turbulence).
$U =$ a characteristic velocity.
$\overline{U} =$ mean velocity component in x directio
$\overline{U}_\infty =$ free stream velocity outside of a boun layer.
$v_k = (k\mathcal{E})^{1/2}$, characteristic velocity associ with 'eddies of wave number k'.
$v^* = (\nu\epsilon)^{1/4}$, the Kolmogorov dissipation velo
$dV(\mathbf{k})$, $dV(\xi) =$ differential volume elemen $\mathbf{k}$ and ξ spaces.
$W(k) = \int_0^k T\, dk'$.
$\mathbf{x}$ or $x_i =$ coordinate vector.
x, $y =$ two cartesian components.
$\delta_{ik} = \begin{Bmatrix} 1 \text{ if } i = k \\ 0 \text{ if } i \neq k \end{Bmatrix}$, the 'Kronecker delta or 'unit tensor'.
$\Delta =$ a characteristic thickness of a mean s flow.
$\epsilon =$ the rate of viscous dissipation of turbu kinetic energy, per unit mass.
$\eta = (\nu^3\epsilon^{-1})^{1/4}$, the Kolmogorov (dissipa microscale ($= k^{*-1}$).
$\theta =$ a scalar field or variable.
$\lambda =$ Taylor's dissipation scale.
$\Lambda =$ wavelength.
μ, $\mu^{(n)} =$ correlation functions.
$\mu_{ik}(\xi) =$ correlation tensor function of ho geneous turbulent velocity field.
$\mu =$ viscosity coefficient.
$\nu = \mu/\rho$, kinematic viscosity.
$\xi =$ vector difference in coordinate (ma tude $= \xi$).
$\rho =$ density.
$\tau =$ time difference.
$\tau(k) = (k^3\mathcal{E})^{-1/2}$, characteristic spectral time
$\varphi_k =$ phase angle.

Bibliography

Books

ACHELOR, G. K., *Homogeneous Turbulence,* Cambridge University Press, 1953.

ONSEND, A. A., *The Structure of Turbulent Shear Flow,* Cambridge University Press, 1956.

LMOGOROV, A. N., A. M. OBUKHOV, A. M. YAGLOM, AND A. S. MONIN, *Sammelband zur statistischen Theorie der Turbulenz,* Akademie-Verlag, Berlin, 1958.

Papers and Reports

he following selected list gives some papers ch are not in the bibliographies of the first books. I have *not* included NACA Reports ch were listed as NACA Technical Notes (the inal form of publication) in these books.

CHELOR, G. K., AND I. PROUDMAN, The large-ale structure of homogeneous turbulence, *Phil. rans. Roy. Soc., A, 248,* (949), January 1956 brief account in 'The singularity in the spec-um of homogeneous turbulence,' by Batchelor, *roc. Symposium Appl. Math.,* VII, McGraw-Hill Book Co., 1957).

SS, J., Space and time correlations in a turulent fluid, I and II, *Univ. Calif. Publs. Statistics, 2* (3) and (4), Berkeley, 1954.

CHOV, R., An inequality concerning the production of vorticity in isotropic turbulence, *J. Fluid Mech., 1* (5), November 1956.

CHOV, R., On the fine structure of turbulent ows, *J. Fluid Mech., 3* (2), November 1957.

NCH, G., AND H. FERGUSON, Remarks on Chandrasekhr's results relating to Heisenberg's heory of turbulence, *Phys. of Fluids, 2* (1), anuary-February 1959.

RGERS, J. M., AND M. MITCHNER, On homogeneous non-isotropic turbulence connected with notion having a constant velocity gradient, *Proc. Koninkl. Ned. Akad. Wetenschap., B, 56,* 228–35 and 343–354, 1953.

ANDRASEKHAR, S., A theory of turbulence, *Proc. Roy. Soc., A, 229* (1), 1955.

ANDRASEKHAR, S., Theory of turbulence, *Phys. Rev., 102* (4), 15, 1956.

OPER, R. D., AND M. LUTZKY, Exploratory investigation of the turbulent wakes behind bluff bodies, *David Taylor Model Basin Rept. 963,* October 1955.

RRSIN, S., Some current problems in turbulent shear flows, chapter 15, *Proc. 1st Symposium on Naval Hydro.,* National Academy of Sciences–National Research Council, 1957.

RRSIN, S., Local isotropy in turbulent shear flow, *NACA Research Memo. RM 58B11,* May 1958.

AYA, A., Contribution à l'analyse de la turbuence associée à des vitesses moyennes, *Pubs. Sci. tech. ministère air, 345,* Paris, 1958.

NSTEIN, H. A., AND H. LI, The viscous sublayer along a smooth boundary, *J. Eng. Mech. Div., Proc. Am. Soc. Civil Engrs.,* no. *EM2,* April 1956.

FAVRE, A., J. GAVIGLIO, AND R. DUMAS, Quelques mesures de correlation dans le temps et l'espace en soufflerie, *Recherche aéronaut.,* no. 32, March/April 1953.

FAVRE, A., J. GAVIGLIO, AND R. DUMAS, Space-time double correlations and spectra in a turbulent boundary layer, *J. Fluid Mech., 2* (4), June 1957.

FAVRE, A., J. GAVIGLIO, AND R. DUMAS, Further space-time correlations of velocity in a turbulent boundary layer, *J. Fluid Mech., 3* (4), January 1958.

GRANT, H. L., The large eddies of turbulent motion, *J. Fluid Mech., 4* (2), June 1958.

HARRISON, M., Pressure fluctuations on the wall adjacent to a turbulent boundary layer, *David Taylor Model Basin Rept. 1260,* December 1958.

HOPF, E., On the application of functional calculus to the statistical theory of turbulence, *Proc. Symposium on Appl. Math.,* VII, McGraw-Hill Book Co., 1957. This is a brief account of the original paper, Statistical hydromechanics and functional calculus, *J. Rat. Mech., 1* (1), 1952.

JAIN, P. C., A theory of homogeneous isotropic turbulence, *Appl. Sci. Research,* A, *8,* 219–227, 1959.

KRAICHNAN, R. H., Relation of fourth-order to second-order moments in stationary isotropic turbulence, *Phys. Rev., 107* (6), 1957.

KRAICHNAN, R. H., Irreversible statistical mechanics of incompressible hydromagnetic turbulence, *Phys. Rev., 109,* March 1, 1958*a*.

KRAICHNAN, R. H., Higher order interactions in homogeneous turbulence theory, *Phys. of Fluids, 1* (4), July–Aug. 1958*b*.

KRAICHNAN, R. H., Interpretation of a dynamical approximation for isotropic turbulence, *New York Univ., Inst. of Math. Sci., Research Rept. HSN-1,* March 1959*a*.

KRAICHNAN, R. H., The structure of isotropic turbulence at very high Reynolds number, *J. Fluid Mech., 5* (4), May 1959*b*.

LAURENCE, J. C., Intensity, scale and spectra of turbulence in mixing region of free subsonic jet, *NACA, Rept. 1292,* 1956 (originally *NACA TN 3561* and *TN 3576*).

LIEPMANN, H. W., Aspects of the turbulence problem, *Z angew. Math. u. Phys., 3* (5) and (6), 1952.

LIN, C. C., A critical discussion of similarity concepts in isotropic turbulence, *Proc. 4th Symposium Appl. Math.,* American Mathematical Society, 1951, McGraw-Hill Book Co., 1953.

LIN, C. C., A simplified formulation of the similarity concepts in istotropic turbulence, *J. Aeronaut. Sci., 20* (4), April 1953.

MALKUS, W. V. R., Outline of a theory of turbulent shear flow, *J. Fluid Mech., 1* (5), November 1956.

MEECHAM, W. C., Relation between time symme-

try and reflection symmetry of turbulent fluids, *Phys. of Fluids, 1* (5), September-October 1958.

Miller, D. R., and E. W. Comings, Static pressure distribution in the free turbulent jet, *J. Fluid Mech., 3* (1) October 1957.

Milliat, J. P., Étude de l'ecoulement turbulent dans un divergent, *Proc. 6th Congr. l'Assoc. intern. de recherches hydrauliques,* 1955 (more detail is given in Milliat's doctoral thesis, University of Grenoble, 1955).

Mills, R. R., Jr., A. L. Kistler, V. O'Brien, and S. Corrsin, Turbulence and temperature fluctuations behind a heated grid, *NACA Tech. Note 4288,* August 1958.

Mills, R. R., Jr., and S. Corrsin, Effect of a contraction on turbulence and temperature fluctuations generated by a warm grid, *NASA Memo. 5-5-59 W,* May 1959.

Munch, G., and A. D. Wheelon, Space-time correlations in stationary isotropic turbulence, *Phys. of Fluids, 1* (6), 462–468, 1958.

Obukhov, A. M., and A. M. Yaglom, On the microstructure of atmospheric turbulence—a review of recent work in the USSR, *J. Roy. Meteorol. Soc., 85* (364), April 1959.

Pearson, J. R. A., The effect of uniform distortion on weak homogeneous turbulence, *J. Fluid Mech., 5,* (2), February 1959.

Phillips, O. M., The irrotational motion outside a free turbulent boundary, *Proc. Cambridge Phil. Soc., 51* (1), 1955.

Phillips, O. M., The final period of decay of non-homogeneous turbulence, *Proc. Cambridge. Phil. Soc., 52* (1) 1956.

Proudman, I., and W. H. Reid, On the decay of a normally distributed and homogeneous turbulent velocity field, *Phil. Trans. Roy. Soc., A, 247* (926), November 1954.

Reid, W. H., The skewness factor according to Obukhoff's transfer theory, *J. Aeronaut. Sci., 23* (4), 1956*a*.

Reid, W. H., Two remarks on Heisenberg's theory of isotropic turbulence, *Quart. Appl. Math., 14* (2), July 1956*b*.

Reid, W. H., On the approach to final period of decay in isotropic turbulence according to Heisenberg's transfer theory, *Proc. Natl. Acad. Sci., U. S., 42* (8), 1956*c*.

Reid, W. H., One-dimensional equilibrium spectra in isotropic turbulence, *Brown Univ. Div. Appl. Math., Tech, Rept. 27* (for ONR), May 1959.

Reid, W. H., and D. L. Harris, The similarity spectra in istropic turbulence, *Phys. of Fluids, 2* (2), March–April 1959.

Reis, F. B., Studies of correlation and spec homogeneous turbulence, Ph.D. dissert Massachusetts Institute of Technology, 1

Reynolds, O., On the dynamical theory of in pressible viscous fluids and the determin of the criterion, *Phil. Trans. Roy. Soc., A* (1), 1895.

Ruetenik, J. R., and S. Corrsin, Equilibriu bulent flow in a slightly divergent chann *Jahre Grenzschichtforschung,* edited b Gortler and W. Tollmein, F. Vieweg und Braunschweig, 1955.

Sandborn, V. A., Experimental evaluation o mentum terms in turbulent pipe flow, *N TN 3266,* January 1955.

Stewart, R. W., Irrotational motion asso with free turbulent flows, *J. Fluid Mech.,* December 1956.

Tani, I., and Y. Kobashi, Experimental s on compound jets, *Proc. 1st Japan Natl. C for Appl. Mech.,* 1951, Science Council of J 1952.

Tatsumi, T., The theory of decay process compressible isotropic turbulence, *Proc. Soc., A, 239,* 16–45, 1957.

Tsuji, H., Experimental studies on the chara tics of isotropic turbulence behind two *J. Phys. Soc. Japan, 10* (7), 1955.

Tsuji, H., Experimental studies on the spe of isotropic turbulence behind two gri *Phys. Soc. Japan, 11* (10), 1956.

Uberoi, M. S., Quadruple velocity correlation pressure fluctuations in isotropic turbu *J. Aeronaut. Sci., 20* (3), 1953 (errata, *ibi* (2), 1954; details in *NACA TN 3116,* Ja 1954).

Uberoi, M. S., Effect of wind-tunnel contr on free-stream turbulence, *J. Aeronaut. S* (8), 1956.

Uberoi, M. S., Equipartition of energy and isotrophy in turbulent flows, *J. Appl. Ph* (10), 1957.

Willmarth, W. W., Wall pressure fluctuati a turbulent boundary layer, *NACA TN* 1958 (see also *J. Acoust. Soc. Am., 28* (6) vember 1956).

Willmarth, W. W., Space-time correlation spectra of wall pressure in a turbulent bou layer, *NASA Memo. 3-17-59 W,* March 1

Zijnen, van der Hegge B. G., Measureme turbulence in a plane jet of air by the dif method and by the hot-wire method, *App Research, A, 7,* 293, 1957.

The Motion of Fluids with Density Stratification

R. R. Long

The Johns Hopkins University
Baltimore, Maryland

Abstract—The mathematical complications of the theory of fluids with density stratification in a gravity field stem from the generation of vorticity in such fluid systems. Even if the fluid starts from rest and can be considered frictionless, anything but the most trivial subsequent motion is rotational. Then the solution of the problem involves solution of the Navier-Stokes equations. In one particular but important case these equations can be integrated once to yield a second-order partial differential equation in the stream function, but even here the governing equation is nonlinear. It is tractable, however, in some interesting cases. A few of them are discussed and compared with experiment.

Under many circumstances flow of a stratified fluid is characterized by the presence of strong velocity concentrations or jets. This phenomenon as observed in the laboratory and in atmosphere and oceans is discussed. The problem is approachable theoretically by means of boundary-layer theory. This approach is current research, and only a few results can be given.

Introduction—Studies of fluids with stable nsity variation, i.e. stratified fluids, have nost universal application. Except in very allow layers,[1] an incompressible fluid with nsity *decrease* in the direction of the gravity rce is unstable and the heavier fluid will fall wn, displacing the lighter fluid. Ultimately, stable density variation in the vertical axis sults. Almost invariably, then, fluid systems all fields of fluid mechanics are stratified iid systems. This does not mean that the abilizing effect of density stratification will ways be important. Any conceivable flow past airfoil, for example, will be almost unaffected the ever-present stability of the atmosphere. ıt in geophysics and astrophysics, stability has cided importance, as we shall see.

In this paper we deal only with incompressle fluids. Since we have met to discuss the nosphere, in which the material is a gas, this atement deserves some explanation. Let us nsider a special case [*Long*, 1956*a*]. If we ve steady, frictionless, nonconducting, nonradiating, two-dimensional motion of a stratified, perfect gas, we can show that the equations of motion are identical to those of a liquid[2] if

$$\left|\frac{q^2 - U_0^2}{2c_0^2}\right| \ll 1 \tag{1}$$

$$\left|\frac{g(z - z_0)}{c_0^2}\right| \ll 1 \tag{2}$$

$$-\frac{1}{\theta_0}\frac{d\theta_0}{dz_0} = \frac{1}{\rho_0}\frac{d\rho_0}{dz_0} \tag{3}$$

where in an undisturbed region of flow (upstream) all quantities have subscript zero; q is the speed, z is distance in the vertical, U is the horizontal velocity, c is the speed of sound, θ is potential temperature in the gas (i.e. the temperature of the parcel if reduced adiabatically to some standard pressure), ρ is density in the liquid. The first condition is the one normally arising in aerodynamics. If the free stream speed drops from U_0 to zero at a stagnation point of an airfoil, and if U_0 is near or above the speed of sound, compressibility is important. I think it is likely that condition 1 is met in ionospheric motions. The second condition arises from the expansion of a parcel as it rises in a gas. This

[1] If we neglect friction and conduction, a liquid always unstable if the density increases with ight [*Prandtl and Tietjens,* 1934, pp. 17, 35]. friction and conduction are included, disturbces need not grow if the depth of the layer is fficiently small (see, for example, *Stommel,* 47).

[2] *Batchelor* [1953] obtained qualitatively similar results under conditions that are in some ways more general.

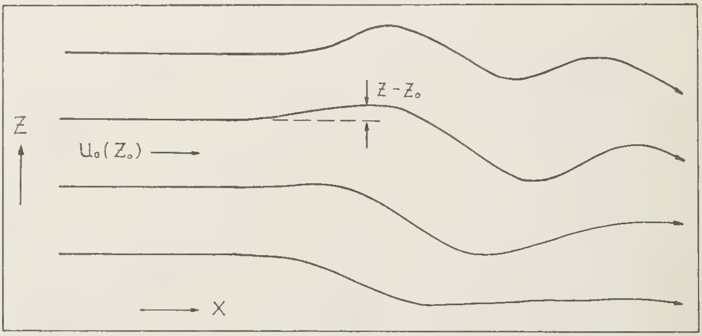

FIG. 1.

condition is probably troublesome since the ratio in (2) is about 1 if $z - z_0$ is 10 km. We shall see later, however, that the stability of the ionosphere may tend to reduce the vertical scale of the motion to values below 10 km. The third condition states that the percentage change of density in the liquid must be replaced by the percentage change of potential temperature in a gas.

In this simple type of motion at least we have a reasonable basis for assuming that the ionosphere will behave like an incompressible fluid. It seems unlikely that time dependence, friction, conduction, etc., will render this assumption seriously deficient.

In most of the discussion below we confine attention to nonturbulent fluids for several reasons. One is that much of this work has been related to laboratory experiments in which turbulence is absent. Second, the problem is at best a very difficult one and, perhaps, calls for the utmost in simplification to begin with. It is curious, however, that laminar, stratified, shear flows may be more complicated in one sense than turbulent flows (at high Reynolds numbers). Thus *Batchelor* [1953] showed that a turbulent atmosphere is characterized by fewer nondimensional members than a laminar one. (The simplification results from the unimportance of the Reynolds number when it is large.) But the overwhelming advantage of nonturbulent flow is that we can write down a determinate set of equations.

Any application of this paper to the ionosphere depends on several factors. I suppose that it is an unsettled question whether the ionosphere or parts of it may be considerec laminar motion.[3] *Goody* [1954], for exam states that separation of gases begins at 8 100 km, with increasing predominance of lig components above this. Turbulence, theref is decreasing rapidly as we go into the i sphere. If it becomes laminar there shoulc connections between the phenomena of paper and phenomena of the ionosphere turbulent, there will still be qualitative simi ties if the turbulent friction forces fit into virtual viscosity concept [*Townsend*, 1956] some fluid systems, jets and wakes for exam this gives useful results.

Equations of motion—internal Froude n ber—We take, as the equations of a nonrad ing liquid in an absolute coordinate system

$$du/dt = -(1/\rho)p_x + \nu\nabla^2 u$$

$$dv/dt = -(1/\rho)p_y + \nu\nabla^2 v$$

$$dw/dt = -(1/\rho)p_z - g + \nu\nabla^2 w$$

$$-(1/\rho)(d\rho/dt) = \nabla \cdot \mathbf{v}$$

$$dT/dt = \kappa\nabla^2 T$$

$$\rho = \rho_0(1 - \alpha T)$$

where we have assumed a linear dependenc density on temperature T (or, in later exp

[3] An important question in this connection is value of the relevant nondimensional nun (Richardson number) which just permits the istence of turbulent motion in a stratified f This has been the object of a number of invest tions [*Richardson*, 1920; *Ellison*, 1957; *Towns* 1958].

ıtal work, on salinity $-T$). ν is the co-ficient of viscosity, and κ the coefficient of duction (or diffusion). In the horizontal ations of motion we see that we may replace y the constant ρ_0 if we neglect αT compared h 1. Since αT is $\Delta\rho/\rho_0$, where $\Delta\rho$ is $\rho - \rho_0$, is justified if the vertical scale of the mo-ı is not too large. Again, as we point out er, this seems to be the case. In the vertical ation of motion we have a different situa-ı. We can neglect $\rho_0 \alpha T\, dw/dt$ compared with dw/dt, for example, with no new approxi-tion. If we neglect $\rho_0 \alpha T g$ compared with $\rho_0 g$ would be neglecting a term that is of the ne order as, or, more usually, much larger n, dw/dt. For example, if we put $\Delta\rho/\rho_0 =$ 0, $\alpha T g$ corresponds to a *vertical* acceleration 100 cm/sec².

In the equation of continuity the term $/\rho) d\rho/dt$ is the rate of change of density lowing a parcel. For a liquid this can change y by the very slow process of conduction and liation and is negligible. Our simplified equa-ns are then

$$du/dt = -\chi_x + \nu \nabla^2 u \tag{7}$$

$$dv/dt = -\chi_y + \nu \nabla^2 v \tag{8}$$

$$dw/dt = -\chi_z + \tau + \nu \nabla^2 w \tag{9}$$

$$\nabla \cdot \mathbf{v} = 0 \tag{10}$$

$$d\tau/dt = \kappa \nabla^2 \tau \tag{11}$$

ıere $\tau = \alpha g T$ and $\chi = p/\rho_0 + gz$. The ap-oximation involved is called the Boussinesq proximation [*Boussinesq*, 1903]. Physically have made two assumptions: (1) that the ertia of a parcel of a given volume varies with acceleration and is not sensibly affected by e slight variations of density from parcel to rcel; (2) that the pressure distribution in the ıid is primarily hydrostatic. The vertical ac-lerations are much less than g and are, in ct, of the order of 'modified gravity,' $g' = g$ ρ/ρ_0. This is precisely the acceleration of a rcel if displaced such a distance vertically at the density difference between it and its vironment is $\Delta\rho$.

If we nondimensionalize the equations, tak-g typical parameters U for velocity and L for length, we get the usual nondimensional numbers of fluid mechanics plus

$$F_i'^2 = U^2/g(\Delta\rho/\rho)L$$

where we have used $\Delta\rho$ as a typical (constant) density difference. This number is the ratio of the inertia force to the 'buoyancy' force of gravity. It is called the internal Froude number or the Richardson number [*Batchelor*, 1953]. It should be distinguished from the ordinary Froude number [*Rouse*, 1938]

$$F^2 = U^2/gL = F_i'^2(\Delta\rho/\rho)$$

which arises in problems with a free surface, e.g. water waves.

Layered systems—An idealization of a fluid with a continuous density distribution and, perhaps, with a basic continuous velocity distribution is a system of two superimposed fluids, each with a different uniform density and velocity, as in Figure 2. It is reasonable to suppose that the discontinuous system will be similar to the continuous one in some respects. We consider two types of flows: (1) an infinitesimal, arbitrary, time-dependent disturbance of the two-fluid system; (2) finite long-wave disturbances.

1. If we disturb the two-fluid system slightly we notice that since each layer is homogeneous and without vorticity ($dU/dz = 0$) the subsequent motion will be irrotational in each layer. The velocity components normal to the interface must be the same in each layer and equal to the normal velocity of the interface, but the tangential components can be discontinuous [*Lamb*, 1932, p. 373]

We assume perturbation velocity potentials

$$\varphi = C \exp\left[kz + i(\sigma t - kx)\right]$$

$$\varphi' = C' \exp\left[-kz + i(\sigma t - kx)\right]$$

since these satisfy Laplace's equation and die out at infinity in the respective layers. Two conditions must be satisfied, the kinematic condition at the interface, and the dynamic condition that pressure be continuous across the interface. This can be done readily if we assume infinitesimal amplitudes of the waves. The result is a relationship between the various

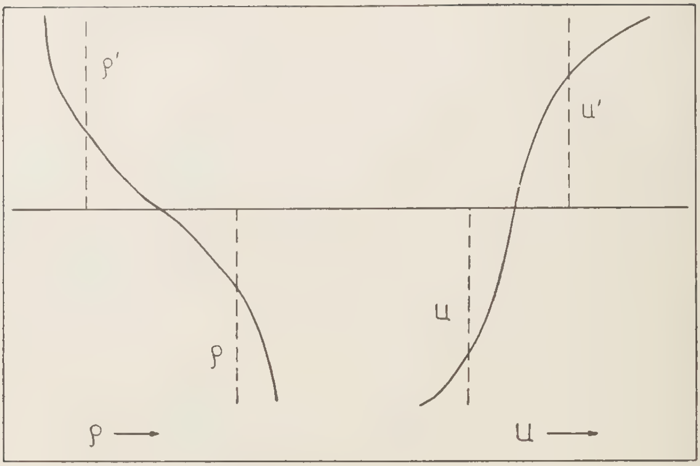

FIG. 2.

constants:

$$\frac{\sigma}{k} = \frac{\rho U + \rho' U'}{\rho + \rho'} \pm \sqrt{\frac{g}{k}\frac{\rho - \rho'}{\rho + \rho'} - \frac{\rho\rho'}{(\rho + \rho')^2}(U - U')^2}$$

Notice that we have not yet used the Boussinesq approximation. If we do that now we get a clear picture in a special case of the way in which the approximation affects the solution of a given problem. We get

$$\frac{\sigma}{k} = \frac{U + U'}{2} \pm \sqrt{\frac{g'}{2k} - \frac{(U - U')^2}{4}}$$

If the density difference is zero, $g' = 0$, and σ has an imaginary part. Waves of all wave numbers will grow. This illustrates the useful physical principle that velocity shear tends to be destabilizing. If $\rho' > \rho$, so that g' is neg[…] the growth rate of the waves increases a[…] have stronger instability. On the other ha[…] $g' > 0$, the density distribution is stabl[…] the longer waves are stabilized. The solut[…] still unstable, however, for sufficiently […] waves if there is any shear. If the shear is […] all waves are stable. These two opposing e[…] of shear and density difference are fundam[…] in the theory of stratified fluids.

2. Finite disturbances of any fluid s[…] are very difficult to analyze. In this case, […] is zero, we have a water-wave problem. […] here only a few simple, finite wave pa[…] have been investigated. However, if we are[…] ing to make the hydrostatic assumption, […] is equivalent to considering disturbances o[…] long length, that is, of finite amplitude but[…] very gradual slope of interface, some im[…]

FIG. 3.

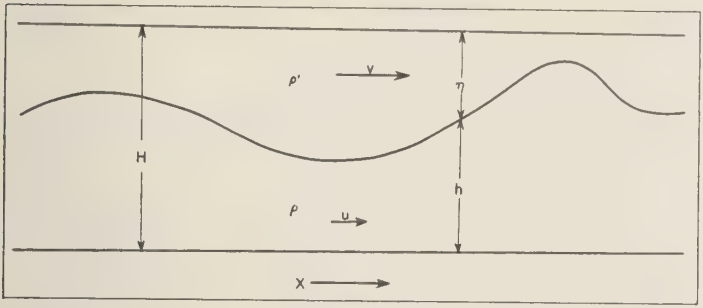

FIG. 4.

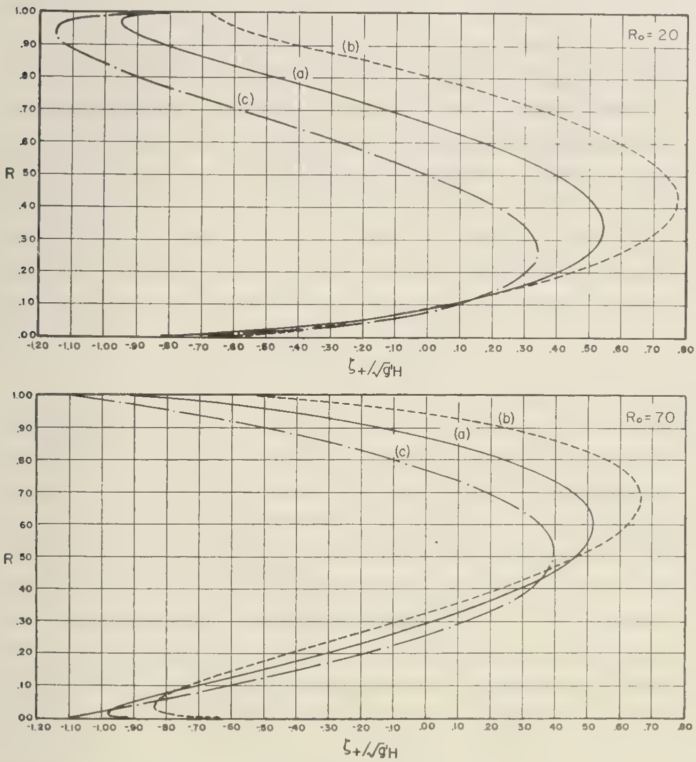

FIG. 5.

t results can be obtained. In particular, we d that all water-wave disturbances of this ıd tend to steepen in the direction of propa- tion and eventually break. In the case of tual water waves such breaking is a common currence, but only if the initial disturbance sufficiently large. If the disturbance is small, it can propagate without change of shape as a solitary wave of elevation, resembling the wave on the left side of Figure 3. In the latter case the hydrostatic approximation is invalid [*Lamb*, 1932, p. 423].

In the two-fluid problem two results have been obtained, one for the hydrostatic case and

one for the solitary wave [*Keulegan*, 1953; *Long*, 1956*b*, 1956*c*].

Let $h/H = R$, and let R_0 be the undisturbed value. Move the coordinate system with the lower fluid so that the upper has a relative speed toward the right of v_0. The speed of propagation of a nondimensional height R, denoted by ζ_+, is shown in Figure 5 for two cases. A qualitative description is:

(*a*) If there is no shear the wave advances on two resting fluids. The speeds of propagation are given by the curves labeled (*a*) in Figure 5. If the lower fluid is shallower, a moderate elevation moves faster than a depression and will steepen and break and then travel as a surge or bore just as in the single-fluid system of Figure 3. If the lower fluid is deeper, a moderate depression moves faster than an elevation, as shown in Figure 6; this phenomenon does not occur in water waves, In the first case if we move with the breaking wave we get a hydraulic jump as in Figure 7. In the second case we get what might be called a hydraulic drop, shown in Figure 8. We see from Figure 5, however, that the speed of propagation is not a monotonic function of height. A large initial elevation will steepen in its lower parts

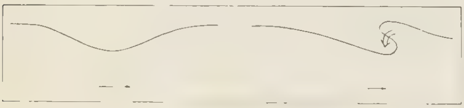

FIG. 6.

FIG. 7.

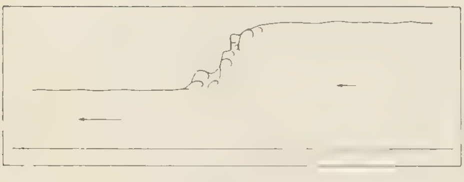

FIG. 8.

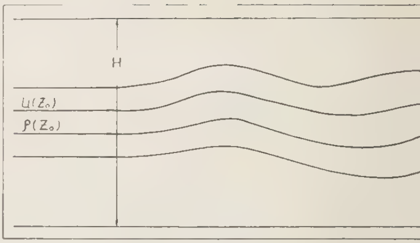

FIG. 9.

and flatten out above. Presumably this m that a surge or bore of only limited heig possible.

(*b*) If the upper fluid moves in the d tion of wave propagation we get curves (*l* Figure 5. This causes a shift of the maxi wave speed to greater interface height, pe ting larger waves of elevation to break ward.

(*c*) If the upper fluid moves against th rection of wave propagation there is a shi maximum wave speed to smaller inte heights.

The investigations of the solitary wave a interface of two fluids have two interestin sults. One is that a wave of elevation can p gate without change of shape only if R_0 < If $R_0 > 1/2$ the solitary waves are of depres The second approximation to the solitary yields limits on the wave amplitude, sugge the possible development of hydraulic jum drops for large initial disturbances.

Steady motions in a continuously stra perfect liquid—If there is a continuous ve distribution of density and velocity, the v city that exists and is generated makes it n sary in general to deal with the primitive, linear equations of motion even if the flu frictionless and nonconducting. There is on ception, namely, steady, two-dimensional tion [*Long*, 1953, 1955]. It is then possib integrate the equations of a perfect liqu yield an equation in the stream functi analogous to that of potential flow for an trary basic density and velocity distributio is even possible in this case to do this wit appeal to the Boussinesq approximation. assume an undisturbed region sufficientl upstream, as in Figure 9. The integration y

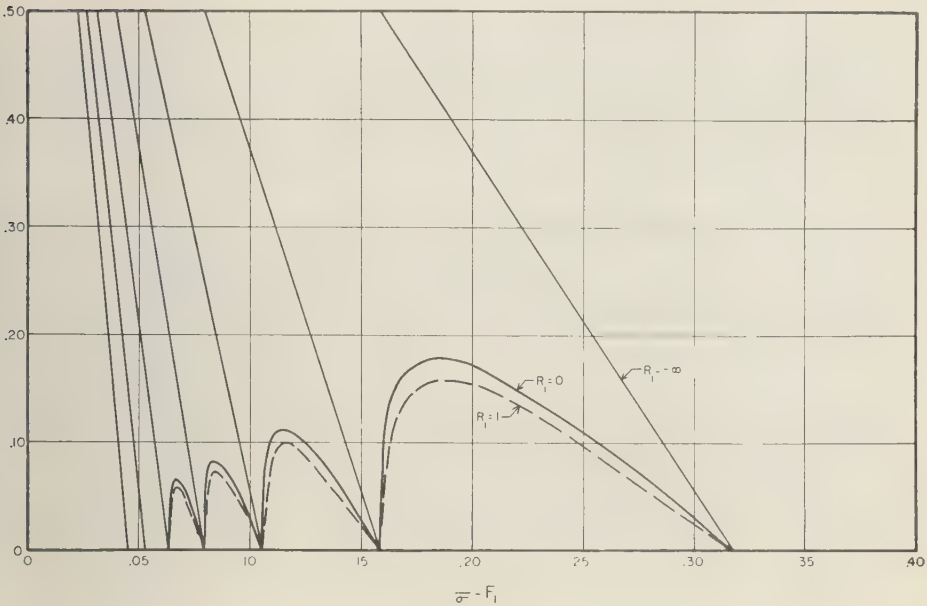

FIG. 10.

$$ {}^2 z_0 + \tfrac{1}{2}[(\nabla z_0)^2 - 1]\frac{d}{dz_0}(\ln U^2\rho) - \frac{g}{U^2\rho}\frac{d\rho}{dz_0}(z_0 - z) = 0 \qquad (12)$$

here z_0 is the height of the streamline in the disturbed region and $U(z_0)$ is the velocity the undisturbed region. If $U^2\rho$ is constant d ρ is linear in z_0, equation 12 is linear,

$$\nabla^2\delta + \sigma^2\delta = 0 \qquad \delta = z - z_0$$

$$\sigma^2 = g\left|\frac{1}{\rho}\frac{d\rho}{dz_0}\right| / U^2 = \text{constant} \qquad (13)$$

nce ρ usually varies very slowly, this is close the case of a uniform basic flow and can be roduced in the laboratory.

There is no problem in solving the linear odel for flow over barriers of infinitesimal ight, and we find a more or less complicated ave motion in the lee of the barrier. It is vious that internal wave motions should be characteristic feature of stratified fluids: if particle is pushed down in such a fluid it ids itself lighter than its environment and ses with an acceleration $g\Delta\rho/\rho_0$. It comes back to its original level, then overshoots until it is in a region where it is heavier than its environment. It accelerates downward, and one complete cycle of an oscillation is completed.

If the barrier is of finite height we have greater difficulties. One approach is to assume a very long barrier so that, in $\nabla^2\delta$, $\partial^2\delta/\delta x^2$ is negligible. Then equation 12 is

$$(\partial^2\delta/\partial y^2) + \sigma^2\delta = 0$$

A solution is

$$\delta = \beta(x)\frac{\sin\sigma(H - z)}{\sin\sigma(H - \beta)} \qquad (14)$$

where we have satisfied two conditions, that the upward displacement of a streamline $\delta = z - z_0$ vanishes at a plane rigid top $z = H$, and that the bottom with a nearly constant height β (x) is the streamline z_0 $(x, z) = 0$. Equation 14 leads to Figure 10. If $F_1 > 1/\pi$ the height β may be anything up to the total depth. Except for the exceptional values of $F_1 = 1/p\pi$, $p = 1, 2, \cdots$, there is a maximum barrier for each value of F_1 given by the distance from the $\beta = 0$ line to the first sloping line above is denoted by $R_1 = -\infty$. As the ob-

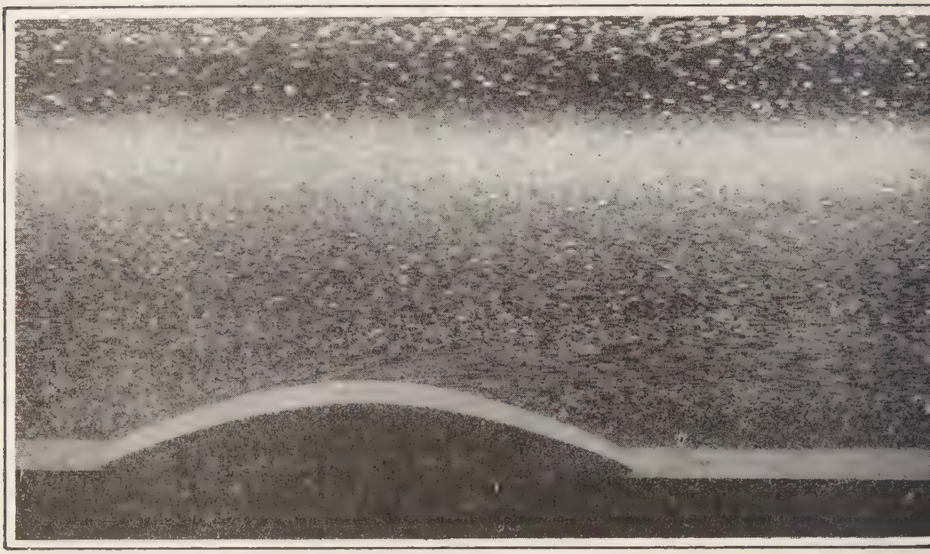

FIG. 11.

stacle nears its maximum size the velocity tends to infinity at some points of the fluid. If the obstacle is close to its maximum size we will have tremendous shears, and one might expect a breakdown into turbulence, so that the solution may exist but be unstable. Moreover, we may show from the solution that a high obstacle means negative velocities if $F_i = 1/\pi$ at some levels, and it follows that this is accompanied by an increase of density with height locally. 'Overturning instability' will result. The heights β at which this occurs are given by the solid curves labeled $R_i = 0$ in Figure 10.

In the regions above the solid curves, if F_i decreases, the unstable solutions show a finer and finer microstructure of flow consisting of alternate 'jets' one on top of the other. If we take L to be a typical length of the phenomenon, H/L is approximately the number of jets in either direction. Let us now construct an internal Froude number

$$F_i' = u/\sqrt{g(\Delta'\rho/\rho_0)L}$$

where $\triangle^1\rho/\rho_0$ is the percentage density difference across one jet. This is approximately

$$\Delta'\rho/\rho_0 = (L/H)(\Delta\rho/\rho)$$

so that

$$F_i' = F_i(H/L) = F_i n$$

The solution now shows that F_i' is appro mately a constant as n becomes large (bou aries go to infinity, for example).

$$F_i' \sim \tfrac{1}{3}$$

These jets occur in experiments as shown Figure 11 and in the same number as forec by theory, despite the fact that the experimen conditions correspond to overturning instabil or even nonexistence in the theory. But e when we have stability in the experiment microstructure (wave structure) decreases size in the same way. Applied to the ionosphe if F_i' is taken as $\sqrt{U^2/SL^2}$, where

$$S = (g/\theta)(d\theta/dz)$$

putting $U = 5 \times 10^4$, $S = 4 \times 10^{-4}$, F_i' 1/3, L becomes 7×10^5. This suggests a mic structure of motion in the ionosphere extrem small compared with its total depth. Since I insensitive to S we get about the same va for the troposphere, in rough agreement w observation.

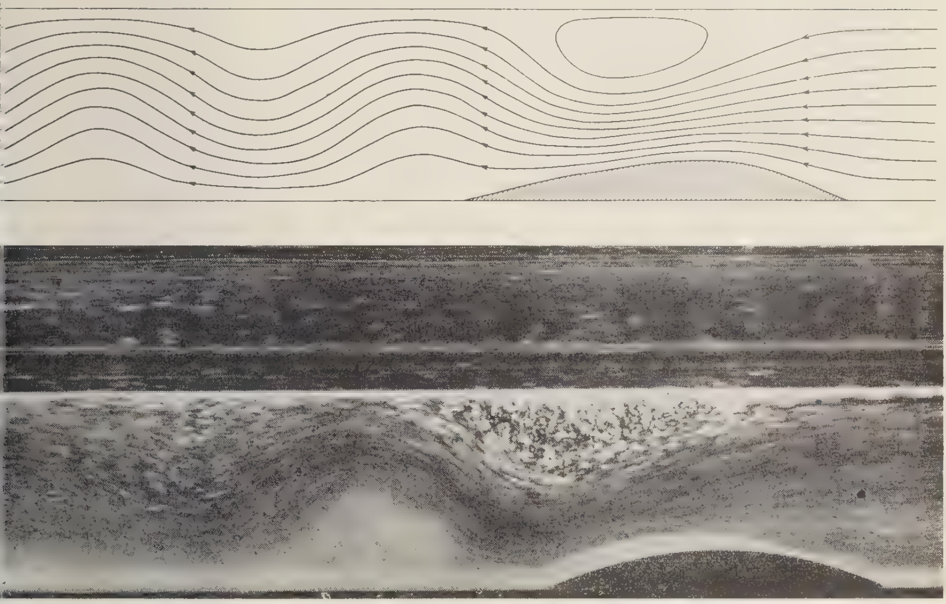

FIG. 12.

Another approach to the finite-obstacle prob-m is to solve for the infinitesimal obstacle, hose height is proportional, say, to an infini-simal a. Then, in the solution, let a be a nite quantity. The resulting solution still tisfies the linear equation 13 and the condi-on that the top plane surface be a streamline, ut the kinematic condition at the obstacle is o longer met. However, the curve $z_0\ (x, z) = 0$ an be taken as a new bottom, and it is found at there is now a barrier of reasonable shape at increases in size with a. It can be made bitrarily high if $F_i > 1/\pi$, but if less than is we get maximum obstacles of the same eneral size as those in the case of the infi-itely long obstacle. The resulting motion is avelike, with decreasing structure as F_i de-reases in the manner indicated above. This ow can be compared with experiment, and, as nown in Figures 12 and 13, theory and experi-ent are in good agreement if the solution ex-ts and is stable. But even in the unstable egion the two are qualitatively similar in the ense that the waves are in the right place and re of the right number. In regions where the heory indicates overturning instability we see turbulent eddies in the experiment. These, of course, cause a rapid reduction in wave amplitude downstream whereas the theory predicts no damping.

If the obstacle size is increased above the point of nonexistence, alternate jets appear of the size and number predicted by the long-wave theory. They propagate far upstream, as seen in Figure 11.

Concentrations in stratified flow—The experiments mentioned above suggest that the jets are a fundamental phenomenon and merit separate investigation. We now approach the jet phenomenon by considering an experiment in which we withdraw fluid from a slit at the end of a long channel. As we might expect, slow withdrawal produces such large concentrated shears that friction is obviously of paramount importance. Fast flows, however, can be discussed from the viewpoint of perfect fluid theory. If the basic density gradient is linear and we assume that the flow upstream from the sink ultimately becomes uniform, we are again led to

$$\nabla^2\delta + \sigma^2\delta = 0$$

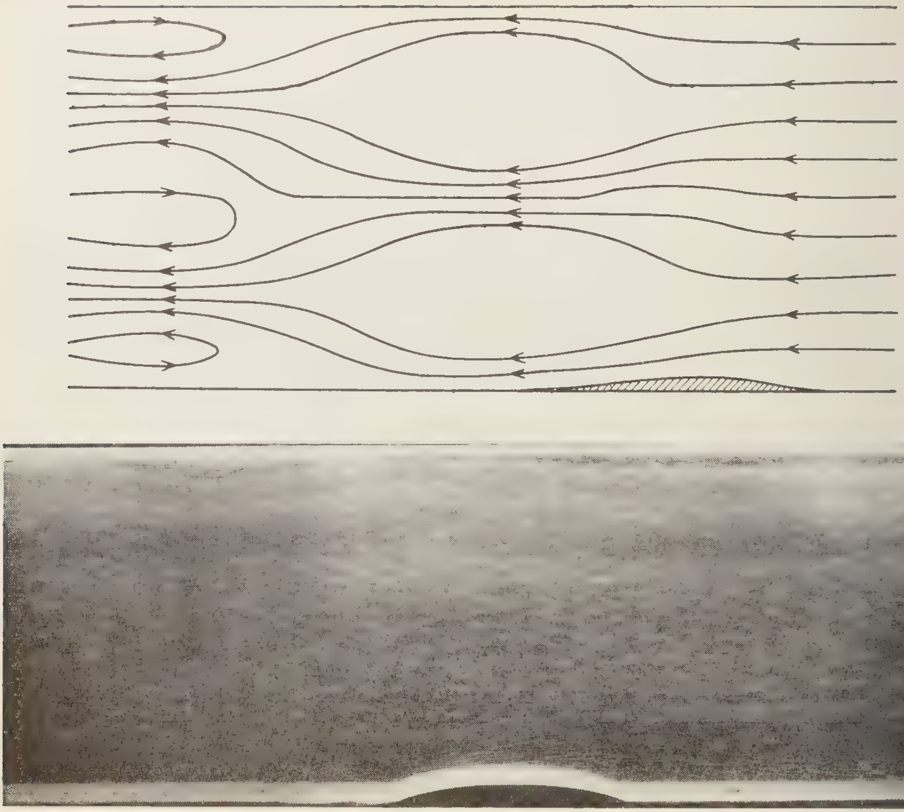

FIG. 13.

if we adopt the Boussinesq approximation. The bottom is at $z = 0$, the top at $z = H$, and there is a wall at $x = 0$, with a sink at $z = H/2$. The solution is

$$\delta = \sum_{n=1}^{\infty} (-1)^{n+1} \frac{H}{n\pi} \cdot \exp\left[\frac{4\pi^2 n^2}{H^2} - \sigma^2\right]^{1/2} \times \sin 2n\pi \frac{y}{H}$$

The corresponding motion is only a slight modification of potential flow if F_i is sufficiently large. If F_i decreases, the sink draws more and more from its own level until at $F_i = \frac{1}{2}\pi$ a jet forms in the middle of the channel of maximum speed $3U$ and two counter currents of speed $u = -U$ at the top and bottom of the channel. This motion exists at great distances from the sink and corresponds to a critical v of F_i. Below this no solution exists. This v F_i corresponds to the speed of a long w with nodal surface at the level of the sink, the jet results from the propagation upstr against the current of this wave.

The fact that U goes to zero means tha have again a reversal of the density grad and that this perfect fluid flow is unstab certain regions. This is sufficient to disco a further search by perfect fluid theory steady, frictionless flow below $F_i = \frac{1}{2}\pi$ any case, as F_i gets very small the experim motion is laminar and we have a very int jet approaching the sink. Friction is cert important in this regime and diffusion to κ is not too small. The viscous approach is rent research, and results are meager. F

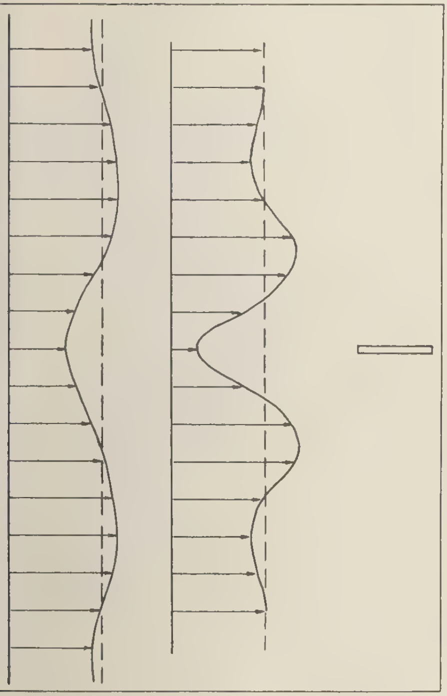

FIG. 14.

:al reasons suggest that we return to the mul-
ɔle jets (or wake) of the obstacle experiment.
stead of the obstacle at the bottom, how-
er, we move a flat plate in a stratified fluid,
idway between top and bottom, so slowly that
e disturbance vanishes at top and bottom. We
ay then consider that we deal with an infinite
iid. As expected, a system of jets occurs ahead
d behind. These are steady with respect to
e obstacle. In this coordinate system we have
flow pattern ahead of the plate as shown in
gure 14.

Since, in our case, κ is so very small, we as-
me that $d\tau/dt = 0$, or, for steady state,

$$\tau = \tau(\psi)$$

here ψ is the stream function. Upstream in
e experiment τ is linear and $\psi = -Uz$, so
at if $\tau = kz$

$$\tau = -(k/U)\psi$$

eglecting variations perpendicular to the x-z plane, the equations are

$$uu_x + wu_z = -\chi_x + \nu u_{zz}$$
$$uw_x + ww_z = -\chi_z + \nu w_{zz} - (k/U)\psi$$
$$u = -\psi_z \qquad w = \psi_x$$

if we neglect variations with respect to x compared to vertical variations in the viscous terms. Adopting the boundary-layer hypothesis that $\nu u_{zz} \sim wu_z$

$$w \sim \nu/z$$

and from continuity

$$u \sim \nu x/z^2$$

But

$$\chi \sim \nu^2 x^2/z^4$$

whence

$$ww_z/\chi_z \sim z^2/x^2 \ll 1$$

Our equations are then

$$uu_x + wu_z = -\chi_x + \nu u_{zz}$$
$$(k/U)\psi = -\chi_z$$

Introducing the stream function and eliminating χ we get

$$-\psi_z\psi_{zzx} + \psi_x\psi_{zzz} + (k/U)\psi_x - \nu\psi_{zzzz} = 0$$

This must be solved subject to finiteness and symmetry conditions and the condition that $u \to U$ at $|z| \to \infty$. If we integrate the x equation, moreover, we get the integral condition that

$$J = \int_{-\infty}^{\infty} (\chi + u^2)\, dz$$

is a constant.

The problem can be solved if the flow is arbitrarily slow so that the nonlinear terms can be neglected. The solution is of the form

$$\psi = -U_z + JU^{1/2}\nu^{-1/2}k^{-1/2}x^{-1/2}f(\eta)$$

where

$$\eta = z/(x^{1/4}\nu^{1/4}U^{1/4}k^{-1/4})$$

The equation for f is

$$4f^{\mathrm{IV}} + f'\eta + 2f = 0$$

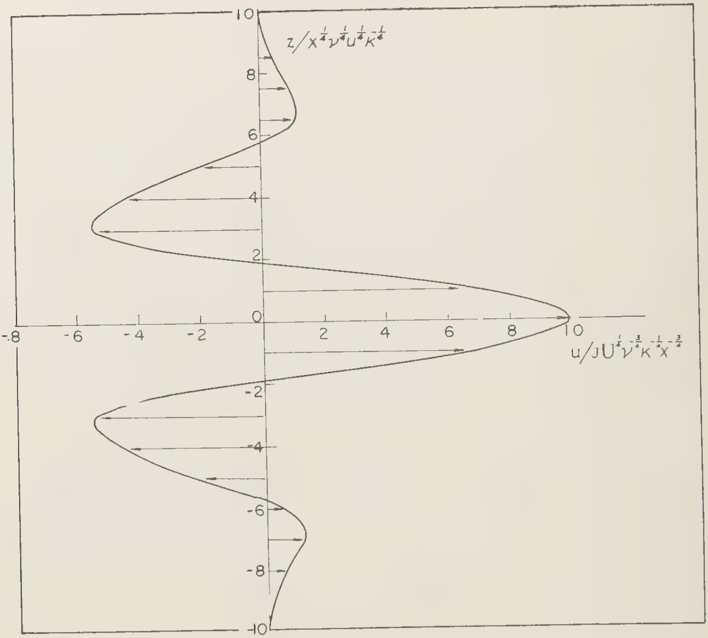
$z/x^{\frac{1}{4}}\nu^{\frac{1}{4}}U^{\frac{1}{4}}\kappa^{-\frac{1}{4}}$
10
8
6
4
2
0
-2
-4
-6
-8
-10
-8
-6
-4
-2
2
4
6
8
10
$u/JU^{\frac{1}{4}}\nu^{-\frac{3}{4}}\kappa^{-\frac{1}{4}}x^{-\frac{3}{4}}$

Fig. 15.

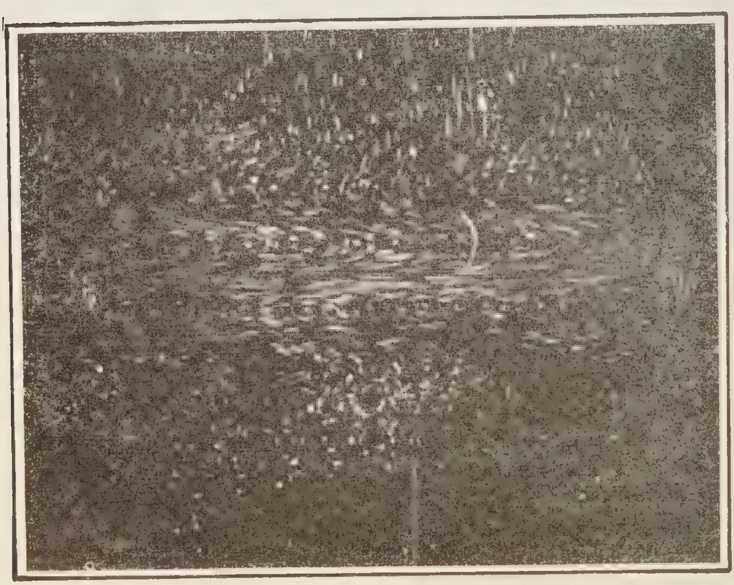

Fig. 16.

is may be integrated numerically very
idily. The profile of the horizontal velocity
shown in Figure 15. Figure 16 is an experi-
ntal photograph with the same general fea-
ces. Current experimental work suggests that
ere is quantitative agreement between ex-
riment and theory if the plate moves slowly
ough.

References

tchelor, G. K., The conditions for dynamical similarity of motions of a perfect-gas atmosphere, *Quart. J. R. Meteorol. Soc., 79,* 224, 1953.

ussinesq, J., *Théorie analytique de la chaleur, 2,* 172, Gauthier-Villars, Paris, 1903.

lison, T. H., Turbulent transport of heat and momentum from an infinite rough plane, *J. Fluid Mech., 2,* 456-466, 1957.

ody, R. M., *The Physics of the Stratosphere,* Cambridge University Press, 1954.

eulegan, G. H., Hydrodynamic effect of gales on Lake Erie, *U. S. Nat. Bur. Stds. J. Res., 50,* 99-109, 1953.

mb, Sir Horace, *Hydrodynamics,* Dover Publications, New York, 1932.

ng, R. R., Some aspects of the flow of stratified Fluids. I. A theoretical investigation, *Tellus, 5,* 42-58, 1953.

Long, R. R., Some aspects of the flow of stratified fluids. III. Continuous density gradients, *Tellus, 7,* 341-357, 1955.

Long, R. R., Models of small-scale atmospheric phenomena involving density stratification, in *Fluid Models in Geophysics,* U. S. Govt. Printing Office, Washington, D. C., pp. 135-147, 1956*a*.

Long, R. R., Solitary waves in one- and two-fluid systems, *Tellus, 8,* 460-471, 1956*b*.

Long, R. R., Long waves in a two-fluid system, *J. Meterol., 13,* 70-74, 1956*c*.

Prandtl, L., and O. G. Tietjens, *Fundamentals of Hydro and Aeromechanics,* McGraw-Hill Book Company, New York, 1934.

Richardson, L. F., The supply of energy from and to atmospheric eddies, *Proc. Roy. Soc. London, 97,* 354-373, 1920.

Rouse, H., *Fluid Mechanics for Hydraulic Engineers,* McGraw-Hill Book Company, New York, 1938.

Stommel, H., A summary of the theory of convective cells, *Ann. N. Y. Acad. Sci., 48,* 715-726, 1947.

Townsend, A. A., *The Structure of Turbulent Shear Flow,* Cambridge University Press, 1956.

Townsend, A. A., Turbulent flow in a stably stratified atmosphere, *J. Fluid Mech., 3,* 361-372, 1958.

Radio Scattering in the Lower Ionosphere

H. G. Booker

Cornell University
Ithaca, New York

Abstract—Radio-scattering phenomena at the 80- to 90-km level observed in the frequency range 30 to 100 Mc/sec indicate the presence of irregularities of electron density with scales in the range from 20 to 60 meters (corrugation wavelengths from 120 to 360 meters). The irregularities are approximately isotropic, and the scattered power is inversely proportional to about the sixth power of scale. The power law involved may, however, vary somewhat with the state of the atmosphere. The fading of the radio waves is consistent with random motions of the irregularities with velocities of the order of 25 m/sec. Similar observations of the sporadic-E phenomena occurring at a height of about 110 km show that the scattered power is inversely proportional to something like the eighteenth power of scale while the velocity of irregularities, if interpreted as random, is around 5 m/sec.

1. *Introduction*—In this paper an attempt is made to describe certain aspects of radio scattering in the ionosphere likely to be of quantitative interest in connection with atmospheric turbulence. The scattering phenomena available for consideration are the following:

(a) Fading of regular ionospheric echoes: the fading that still exists when interference has been eliminated between waves multiply reflected between the earth and the ionosphere or between waves doubly refracted in the presence of the earth's magnetic field.

(b) The phenomenon of spread F: the situation in which a pulse incident upon the ionosphere is reflected as an irregular echo of duration far in excess of that of the incident pulse.

(c) The sporadic-E phenomenon: a phenomenon of intermittent reflection at E-region levels that is sometimes almost mirrorlike, but more often involves only partial reflection or backscattering.

(d) Aspect-sensitive echoes: echoes that appear to come from a direction nearly normal to that of the earth's magnetic field. Backscattering from auroral ionization is of this type.

(e) Meteor echoes: echoes from the ionization trails of meteors either before or after the trails have been distorted by atmospheric motions.

(f) Scattering from below the E region: echoes that appear to be associated with irregularities of ionization density below the m E region.

(g) Scintillation phenomenon: a phenon non of twinkling involved in transmissi through the ionosphere from discrete sources cosmic noise or from radio transmitters in sat lites.

The above phenomena are described and lustrated in chapter 5 of *Atmospheric Explo tions* [Houghton, 1958].

All the scattering phenomena mentioned capable of giving information about irregula ties of electron density in the ionosphere t may be associated with atmospheric turbulen For yielding quantitative information likely be of interest in connection with the fluid m chanics of the ionosphere, however, some of phenomena are of greater importance th others. Phenomena (a) and (b) involve, addition to scattering by irregularities of el tron density, rather violent phenomena of fraction, reflection, and dispersion. These co plications make it difficult to use phenome (a) and (b) at present to derive reliable inf mation on the possible effect of atmosphe turbulence. Phenomenon (c) is in princi more promising, but suffers from the dis vantage that, in spite of more than a quar of a century of study, ionospherists are una to assign a basic cause. Phenomenon (d) see to be due to irregularities of electron dens

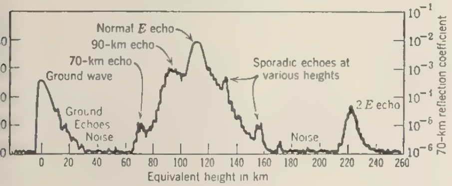

FIG. 1—Variation of echo amplitude with equiva-
nt height, showing echoes from an equivalent
ight less than 100 km [*Gardner and Pawsey,*
58].

igned along the earth's magnetic field, and ay have nothing to do with atmospheric tur- lence at all. However, the size of the irregu- rities along the earth's magnetic field that ems to be required to explain auroral echoes om E-region levels is of the order of tens of eters. It has been difficult to think of a phe- menon other than atmospheric turbulence at might produce irregularities of this size. A od theory of atmospheric turbulence at iono- heric levels would be very helpful in attempts explain phenomena (a) through (d), but esent knowledge of these phenomena scarcely elds quantitative guides to the fluid mechanics the ionosphere associated with radio scatter- g.

Phenomena (e) and (g) contain a good deal information that may be relevant to atmos- eric turbulence. Scattering from ionized me- or trails is of two types, that occurring while e trails are still substantially straight and at occurring after they have been distorted atmospheric motions. Echoes from distorted meteor trails are dealt with elsewhere in this symposium. Echoes from straight trails are of interest primarily as a cause of interference in the study of phenomenon (f).

Phenomenon (f) is illustrated in its simplest form by directing a radar vertically upward at a frequency of the order of 1 or 2 Mc/s under conditions of very low noise level. The echoes obtained from various ranges are illustrated qualitatively in Figure 1. The pulse transmitted by the radar is recorded by the receiver in diminished form at the extreme left of the diagram. Since no substantial degree of vertical beaming is employed, terrain echoes are received horizontally and may be seen at ranges between 10 and 30 km. The main echo from the E region of the ionosphere occurs at the range of 110 km. An echo that has involved two reflections from the E region, with an intermittent reflection from the ground, may be seen at a range of 220 km. Sporadic echoes from meteor trails are shown at ranges of approximately 130, 160, and 170 km. The echoes that are of interest in connection with atmospheric turbulence are those coming from heights between about 70 and 100 km. These echoes are shown peaking at a height of about 90 km, with a subsidiary peak at 70 km. In Figure 1, echo strength is shown on a logarithmic scale. The vertical scale at the right indicates the amplitude reflection coefficient for a horizontal plane surface at a height of 70 km that would be required to produce any particular echo strength.

The backscattering from a level of the order

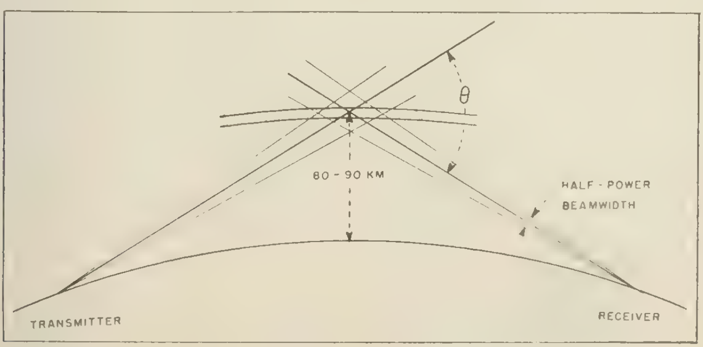

FIG. 2—Geometry of radio scattering.

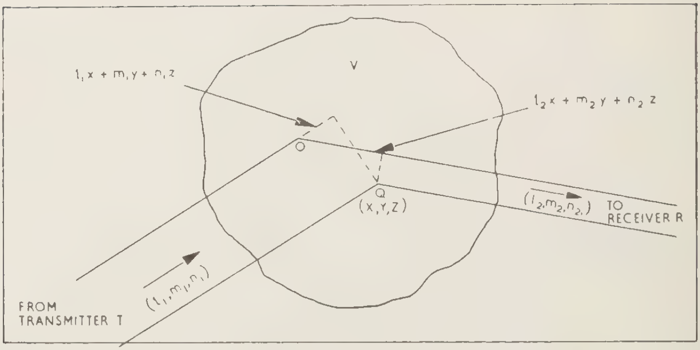

FIG. 3—Geometry of scattering.

of 90 km indicated in Figure 1 produces a phenomenon of long-distance propagation that is of interest in the frequency range from 30 to 100 Mc/s. Over this range long-distance transmission by means of reflection from the regular E and F regions is not usually possible. By training two narrow beams in the same part of the ionosphere in the vicinity of 80 to 90 km as is indicated in Figure 2, however, it is possible to use phenomenon (f) to communicate over ranges of the order of 1000 to 2000 km. The interpretation of observations of radio scattering made in this way is particularly interesting in connection with possible atmospheric turbulence at heights of the order of 80 to 90 km.

Phenomenon (g) is concerned with the effect of irregularities of electron density upon radio waves transmitted through the ionosphere from top to bottom. The scattering involved is in directions close to the direction of propagation of the main wave. The phenomenon may also be described in terms of the irregular phase variation produced in the transmitted wave by irregularities of electron density. Among the difficulties involved in interpreting data of this sort is the fact that a wide range of heights is potentially involved. It is difficult therefore to assign to a particular height or range of heights information derived from scintillation phenomena that might be associated with ionospheric turbulence. The relevant facts are described in another paper [*Booker*, 1958].

In this paper we shall devote our attention to phenomenon (f). We shall first derive t theory that has been developed for interpreti the phenomenon and then, in the light of t theory, examine the available observations.

2. *Scattering by isotropic and nonisotro irregularities*—Suppose that linearly polariz radiation from an isotropic transmitter of pow P located at T falls on a volume v of the m dium where there are irregularities (see Fig. and let us calculate the scattered power ceived at a point R. We shall suppose that t distances from T to v and from R to v are la compared with the linear dimensions of the pa of the medium from which scattering is imp tant. We shall also assume that the irregula ties make no first-order change in the fi strength of the incident wave at any po (Born's approximation).

The field strength at a point Q of v at a d tance r_1 from T is

$$E_0 = \left(\frac{\zeta P}{2\pi}\right)^{1/2} \frac{\exp(-jkr_1)}{r_1}$$

where k and ζ are the propagation constant a characteristic impedance of the medium in absence of irregularities. An increment $\Delta\epsilon$ in capacitivity ϵ of the medium at Q produces additional electric moment per unit volume

$$\Delta P = E_0 \Delta\epsilon$$

At point R at a distance r_2, this increase electric moment in an element of volume causes a field whose polarization potential

$$\frac{1}{\ldots\epsilon} \Delta P \frac{\exp(-jkr_2)}{r_2}\, dv$$

$$= \frac{1}{4\pi} E_0 \frac{\Delta\epsilon}{\epsilon} \frac{\exp(-jkr_2)}{r_2}\, dv$$

om (2). Hence the total polarization potential roduced at R by irregularities $\Delta\epsilon/\epsilon$ at the arious points of v is

$$= \frac{1}{4\pi} \int_v E_0 \frac{\Delta\epsilon}{\epsilon} \frac{\exp(jkr_2)}{r_2}\, dv$$

$$= \frac{1}{4\pi} \left(\frac{\zeta P}{2\pi}\right)^{1/2} \int_v \frac{\Delta\epsilon}{\epsilon} \cdot \frac{\exp\{-jk(r_1 + r_2)\}}{r_1 r_2}\, dv \qquad (3)$$

om (1). To handle the quantity

$$\exp\{-jk(r_1 + r_2)\}/r_1 r_2$$

is convenient to choose a reference point O the volume v. Let O be distant r_1^0 from T ad r_2^0 from R. Since it is assumed that the linear mensions of the important part of v are small mpared to r_1^0 and r_2^0, the product $r_1 r_2$ in the enominator may be replaced by $r_1^0 r_2^0$. We ay now write

$$= \frac{1}{4\pi} \left(\frac{\zeta P}{2\pi}\right)^{1/2} \frac{\exp\{-jk(r_1^0 + r_2^0)\}}{r_1^0 r_2^0}\, I \qquad (4)$$

here

$$= \int_v \frac{\Delta\epsilon}{\epsilon} \exp[-jk\{(r_1 - r_1^0) + (r_2 - r_2^0)\}]\, dv \qquad (5)$$

To transform the integral I, let (l_1, m_1, n_1) a unit vector in the direction of incidence and (l_2, m_2, n_2) a unit vector in the direction of attering. Let the corodinates of the element volume dv at Q be (x, y, z). On the assumption at T and R are at a great distance (see Fig. 3), e have

$$\begin{cases} r_1 - r_1^0 = l_1 x + m_1 y + n_1 z & (6) \\ r_2 - r_2^0 = -(l_2 x + m_2 y + n_2 z) & (7) \end{cases}$$

so that

$$(r_1 - r_1^0) + (r_2 - r_2^0) = (l_1 - l_2)x + (m_1 - m_2)y + (n_1 - n_2)z \qquad (8)$$

Hence

$$I = \int_v \frac{\Delta\epsilon}{\epsilon} \exp[\{jk(l_2 - l_1)x + (m_2 - m_1)y + (n_2 - n_1)z\}]\, dx\, dy\, dz \qquad (9)$$

$$= p\{k(l_2 - l_1), k(m_2 - m_1), k(n_2 - n_1)\} \qquad (10)$$

where

$p(l, m, n)$ is the Fourier transform of

$$(\Delta\epsilon/\epsilon)\,(x, y, z) \qquad (11)$$

We shall actually require $|I^2|$. Now, by Kinchine's theorem, $|p^2|$ is the Fourier transform of

$$\int_v \frac{\Delta\epsilon^*}{\epsilon}(X, Y, Z) \frac{\Delta\epsilon}{\epsilon} \cdot (X + x, Y + y, Z + z)\, dX\, dY\, dZ \qquad (12)$$

and this is equal to

$$v \overline{\left|\frac{\Delta\epsilon}{\epsilon}\right|^2} \rho(x, y, z) \qquad (13)$$

where ρ is the autocorrelation function of $\Delta\epsilon/\epsilon$ defined by

$$\rho(x, y, z) = \frac{\int_v \frac{\Delta\epsilon^*}{\epsilon}(X, Y, Z) \frac{\Delta\epsilon}{\epsilon}(X + x, Y + y, Z + z)\, dX\, dY\, dZ}{\int_v \left|\frac{\Delta\epsilon}{\epsilon}(X, Y, Z)\right|^2 dX\, dY\, dZ} \qquad (14)$$

and $\overline{\left|\frac{\Delta\epsilon}{\epsilon}\right|^2}$ is the mean square fractional deviation of ϵ given by

$$\overline{\left|\frac{\Delta\epsilon}{\epsilon}\right|^2} = \frac{1}{v} \int_v \left|\frac{\Delta\epsilon}{\epsilon}\right|^2 dv \qquad (15)$$

Let $P(l, m, n)$ be the Fourier transform of $\rho(x, y, z)$, the autocorrelation function of $(\Delta\epsilon/\epsilon)$

(x, y, z). Then it follows from (10) and (13) that

$$|I|^2 = v \left|\frac{\Delta\epsilon}{\epsilon}\right|^2 P\{k(l_2 - l_1),$$

$$\cdot k(m_2 - m_1), k(n_2 - n_1)\} \qquad (16)$$

If χ is the angle between the direction of scattering and the direction of E_0, the scattered field at R is

$$E = k^2 \sin\chi \Pi = \frac{1}{4\pi}\left(\frac{\zeta P}{2\pi}\right)^{1/2} k^2 \sin\chi$$

$$\cdot \frac{\exp\{-jk(r_1^0 + r_2^0)\}}{r_1^0 r_2^0} I$$

from (4). The scattered power density at R is therefore

$$\frac{|E|^2}{2\zeta} = \frac{P}{(4\pi)^3} k^4 \sin^2\chi \frac{1}{(r_1^0)^2(r_2^0)^2} |I|^2$$

The power scattered per unit solid angle in the direction of R is therefore

$$(r_2^0)^2 \frac{|E|^2}{2\zeta} = \frac{P}{4\pi(r_1^0)^2} \frac{\pi^2 \sin^2\chi}{\lambda^4} |I|^2$$

where λ is the radio wavelength. Hence the power scattered in the direction of R per unit solid angle, per unit incident power density, is

$$\frac{\pi^2 \sin^2\chi}{\lambda^4} |I|^2$$

The power scattered per unit solid angle, per unit incident power density, per unit volume, is therefore

$$\sigma = \frac{1}{v} \frac{\pi^2 \sin^2\chi}{\lambda^4} |I|^2$$

$$= \left|\frac{\Delta\epsilon}{\epsilon}\right|^2 \frac{\pi^2 \sin^2\chi}{\lambda^4} P\{k(l_2 - l_1),$$

$$\cdot k(m_2 - m_1), k(n_2 - n_1)\} \qquad (17)$$

from (16).

The direction of the vector

$$(l_2 - l_1, m_2 - m_1, n_2 - n_1) \qquad (18)$$

is the external bisector of the angle between the direction of incidence and the direction of scattering. This defines what may be called the 'mirror direction' for the directions of i cidence and scattering. Planes perpendicu to the vector (18) are able to 'mirror' the directi of incidence into the direction of scatteri Now the irregularities $(\Delta\epsilon/\epsilon)(x, y, z)$ in t medium may be Fourier-analyzed into pla stratified fractional deviations of ϵ havi sinusoidal profiles, and these are continuou distributed both with regard to direction a corrugation wavelength. It is this Four analysis of $(\Delta\epsilon/\epsilon)(x, y, z)$ that is described the functions $p(l, m, n)$ and $P(l, m, n)$. Wh the result (17) implies, therefore, is that scatt ing in a particular direction depends on t Fourier content of the irregularities in the as ciated mirror direction. It also depends on t presence in the mirror direction of corrugati wavelengths such as to produce constructi interference in the direction of scatteri For a scattering angle θ (see Fig. 2), the must be important Fourier content of sca

$$\frac{\lambda}{4\pi \sin(\theta/2)} \qquad (1$$

in the mirror direction associated with t directions of incidence and scattering.

3. *Application of scattering theory to t ionosphere*—We may assume that, apart fro irregularities, the electron density N in t ionosphere is a function of height only. From t electron density at a particular height, arrive at the plasma wavelength λ_N in accordan with the equation

$$\lambda_N^2 = \pi/r_e N \qquad (2$$

where r_e is the classical radius of the electro In terms of the charge e and the mass m of electron and the vacuum inductivity μ_v, t expression for the classical radius of the electr is

$$r_e = \mu_v e^2/4\pi m \qquad (2$$

and its numerical value is

$$r_e = 2.8 \times 10^{-15} \quad \text{meter} \qquad (2$$

Neglecting the effect of collisional frequen and of the earth's magnetic field, the dielectr constant at a particular location is

$$\epsilon/\epsilon_v = 1 - (\lambda^2/\lambda_N^2) \qquad (2$$

where ϵ_v is the vacuum capacitivity. In the applications in which we are interested, the radio wavelength λ is small compared with the plasma wavelength λ_N, so that no distinction need be drawn between the wavelength in the ionosphere and the vacuum wavelength.

We assume that, in the ionosphere, there are irregularities of electron density that result in a mean square departure of electron density from mean denoted by $\overline{(\Delta N)^2}$. By taking differentials in equations 20 and 23 we may deduce that

$$\overline{|\Delta\epsilon/\epsilon|^2} = (\lambda/\lambda_N)^4\overline{(\Delta N/N)^2} \quad (24)$$

and consequently that

$$\overline{(\Delta\epsilon/\epsilon)^2} = (1/\pi^2)r_e^2\lambda^4\overline{(\Delta N)^2} \quad (25)$$

Substitution from equation 25 into equation 17 gives

$$\sigma = r_e^2\overline{(\Delta N)^2}\sin^2\chi \cdot P\left[\frac{2\pi}{\lambda}(l_2 - l_1), \frac{2\pi}{\lambda}(m_2 - m_1), \frac{2\pi}{\lambda}(n_2 - n_1)\right] \quad (26)$$

This equation gives the power scatter per unit solid angle per unit incident power density and per unit volume for a radio wavelength λ in an ionosphere for which the mean square departure of electron density from the mean is $\overline{(\Delta N)^2}$, (l_1, m_1, n_1) is a unit vector in the direction of incidence, and (l_2, m_2, n_2) is a unit vector in the direction of scattering, while χ is the angle between the direction of scattering and the direction of the electric vector in the incident wave.

Some simple autocorrelation functions are shown in the first line of Tables 1 and 2, and their Fourier transforms are shown in the second line. The autocorrelation functions shown in Table 1 are nonisotropic; those in Table 2 are isotropic. In the third line of each table are shown the scattering coefficients derived from equation 26. In the case of the isotropic scattering coefficients we have to evaluate the expression

$$(l_2 - l_1)^2 + (m_2 - m_1)^2 + (n_2 - n_1)^2 \quad (27)$$

in terms of the scattering angle θ. This may be done with the aid of Figure 4, in which (l_1, m_1, n_1) and (l_2, m_2, n_2) are unit vectors in the directions of incidence and scattering, and the difference of these vectors is a vector whose magnitude is the square root of expression 27. From the geometry of Figure 4 it follows that the value of expression 27 is

$$[2\sin(\theta/2)]^2 \quad (28)$$

Use of this value for (27) converts the expressions in the second line of Table 2 into the expressions in the third line in accordance with equation 26. It should be noted that any pair of the autocorrelation functions in the tables may be convolved by multiplying the corresponding pair of Fourier transforms.

It will be observed that, apart from the dipole scattering factor $\sin^2\chi$ associated with scattering by an individual electron, each of the scattering formulas given in the third line of Table 2 shows a dependence on direction of scattering and on wavelength of the form

$$\sigma \propto \frac{1}{\left\{1 + \left(\frac{4\pi L}{\lambda}\sin\frac{\theta}{2}\right)^2\right\}^{n/2}} \quad (29)$$

In practice it is usually possible to assume that L is large compared with λ, and there is then a range of values of the scattering angle θ such that

$$\sin(\theta/2) \gg (\lambda/4\pi L) \quad (30)$$

In these circumstances relation 29 reduces to

$$\sigma \propto \left(\frac{\lambda}{\sin(\theta/2)}\right)^n \quad (31)$$

Experiments made under the conditions illustrated in Figure 2 usually satisfy equation 31 for an appropriate value of n.

All the isotropic scattering functions depend on the scattering angle θ and the radio wavelength λ in the combination

$$(1/\lambda)\sin(\theta/2) \quad (32)$$

Since the wavelength λ is inversely proportional to the frequency f, we may say that the scattering is a function of

$$f\sin(\theta/2) \quad (33)$$

In other words, if the frequency f and the scattering angle θ are changed in such a way as to keep expression 33 constant, there is no

TABLE 1—*Nonisotropic scattering formulas*

$\rho(x, y, z)$	$\exp\left\{-\frac{1}{2}\left(\frac{x^2}{a^2} + \frac{y^2}{b^2} + \frac{z^2}{c^2}\right)\right\}$	$\exp\left\{-\left(\frac{x^2}{a^2} + \frac{y^2}{b^2} + \frac{z^2}{c^2}\right)^{1/2}\right\}$
$P(l, m, n)$	$(2\pi)^{3/2} abc \exp\{-\tfrac{1}{2}(a^2 l^2 + b^2 m^2 + c^2 n^2)\}$	$\frac{8\pi abc}{\{1 + (a^2 l^2 + b^2 m^2 + c^2 n^2)\}^2}$
σ	$(2\pi)^{3/2} r_e^{\,2} \overline{(\Delta N)^2} \sin^2\chi\, abc$ $\exp[-\{2\pi^2/\lambda^2\}\{a^2(l_1 - l_2)^2 + b^2(m_1 - m_2)^2 + c^2(n_1 - n_2)^2\}]$	$\frac{8\pi r_e^{\,2} \overline{(\Delta N)^2} \sin^2\chi\, abc}{[1 + \{4\pi^2/\lambda^2\}\{a^2(l_1 - l_2)^2 + b^2(m_1 - m_2)^2 + c^2(n_1 - n_2)^2\}]^2}$

TABLE 2—*Isotropic scattering formulas*

$P(x, y, z)$ $r = (x^2 + y^2 + z^2)^{1/2}$	$\exp\left(-\frac{1}{2}\frac{r^2}{L^2}\right)$	$\exp\left(-\frac{r}{L}\right)$	$\frac{r}{L} K_1\left(\frac{r}{L}\right)$	$\left(1 + \frac{r}{L}\right)\exp\left(-\frac{r}{L}\right)$
$\rho(l, m, n)$ $k = (l^2 + m^2 + n^2)^{1/2}$	$(2\pi)^{3/2} L^3 \exp(-\tfrac{1}{2}k^2 L^2)$	$\frac{8\pi L^3}{(1 + k^2 L^2)^2}$	$\frac{6\pi^2 L^3}{(1 + k^2 L^2)^{5/2}}$	$\frac{32\pi L^3}{(1 + k^2 L^2)^3}$
σ	$(2\pi)^{3/2} r_e^{\,2} \overline{(\Delta N)^2} \sin^2\chi L^3$ $\exp\left\{-\frac{1}{2}\left(\frac{4\pi L}{\lambda}\sin\frac{\theta}{2}\right)^2\right\}$	$\frac{8\pi r_e^{\,2} \overline{(\Delta N)^2} \sin^2\chi L^3}{\left\{1 + \left(\frac{4\pi L}{\lambda}\sin\frac{\theta}{2}\right)^2\right\}^2}$	$\frac{6\pi^2 r_e^{\,2} \overline{(\Delta N)^2} \sin^2\chi L^3}{\left\{1 + \left(\frac{4\pi L}{\lambda}\sin\frac{\theta}{2}\right)^2\right\}^{5/2}}$	$\frac{32\pi r_e^{\,2} \overline{(\Delta N)^2} \sin^2\chi L^3}{\left\{1 + \left(\frac{4\pi L}{\lambda}\sin\frac{\theta}{2}\right)^2\right\}^3}$

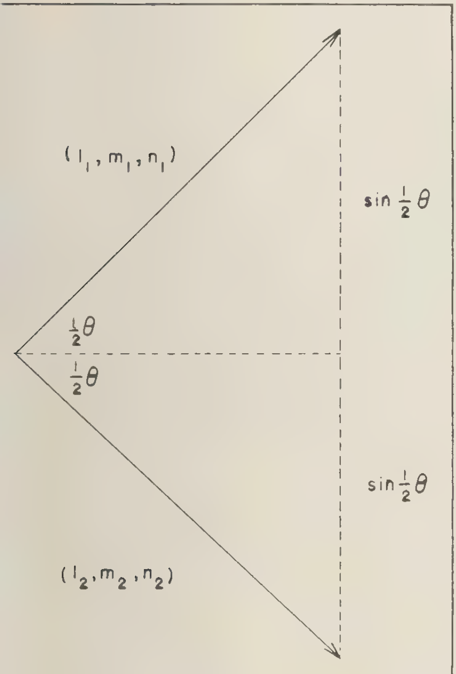

FIG. 4—Illustrating the calculation of expression 27 in terms of the scattering angle θ.

hange in the scattering apart from the dipole cattering factor $\sin^2 \chi$.

4. *Scatter communication experiments*—In rinciple it would be desirable to arrange for a arrow transmitting beam and a narrow reeiving beam to intersect in the ionosphere, hereby defining a common volume the scattering properties of which could be studied. If it vere feasible to vary the position of the reeiver in space at will, it would then be possible o map out the scattering diagram of the volme of ionosphere under study and to compare he results with theoretical formulas such as hose given in Tables 1 and 2. An experimental rogram of this sort is of course quite impracical. However, the fact that simple scattering ormulas involve functions of expression 33 nakes it possible to perform roughly the same xperiment at a fixed scattering angle θ by arying the frequency f. A number of experinents of this type have been carried out in onnection with VHF scatter communication. The most recent experiments have been carried out by the Central Radio Propagation Laboratory of the National Bureau of Standards [*Blair*, 1959]. The experimental arrangement was of the type indicated in Figure 2. The transmitters and receivers had a separation of about 1300 km, and five frequencies were used which were approximately 30, 40, 50, 74 and 108 Mc/s. The axes of the antenna beams were elevated at an angle 4.6° above the horizon, so that they intersected at a height of about 85 km above the earth. Each beam was approximately conical, with a beamwidth of about 6°. The common ionospheric volume involved in the transmitting and receiving beams was thus substantially the same on all five frequencies. Numerous other precautions were taken to ensure that measurements made on the five frequencies could be satisfactorily compared with one another.

It is unlikely that the whole of the common volume of the transmitting and receiving beams was equally important in causing scattering. As indicated in Figure 1, there is a marked variation of scattering with height, with a maximum in the vicinity of 90 km. Under these circumstances scattering would be principally confined to a layer of thickness perhaps 10 km centered at a height of 90 km. In earlier experiments [*Bailey, Bateman, and Kirby*, 1955] using pulse transmission, the height of scattering could be deduced from the delay time involved. Heights were of the order of 90 km at night and somewhat less (possibly 80 km) during the day. The scattering can therefore be pictured as coming from a layer that cuts across the common volume of the transmitting and receiving beams somewhat as indicated in Figure 2, the height being 80 to 90 km.

Results obtained during December 1957 are shown in Figure 5, and those obtained during June 1958 in Figure 6. It will be observed that the scattered power received is at a maximum during the middle of the day. This is almost certainly associated with the fact that the ionization in the 80- to 90-km level is caused by incoming radiation from the sun and therefore maximizes at midday. At night one would expect that ionization in the 80- to 90-km level of solar origin would disappear by recombination, and it is known from measurements of the absorption of radio waves at lower frequencies that this is substantially true. At the 90-km

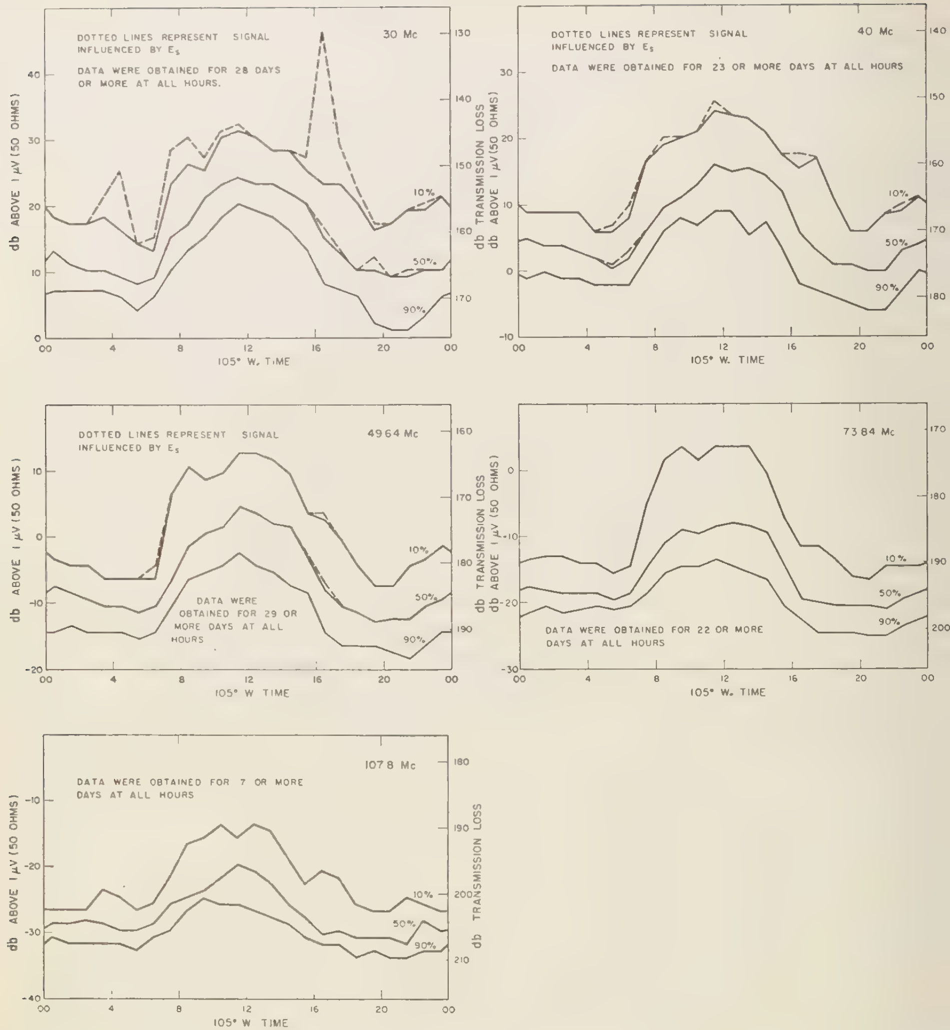

FIG. 5—Received signal intensity equaled or exceeded 10, 50, and 90 per cent of the time for Decemb 1957. (Values adjusted to 2-kw transmitter power.) [From *Blair,* 1959, by permission.]

level, however, some ionization is maintained at night by incoming meteors.

In analyzing data such as those shown in Figures 5 and 6 from the point of view of atmospheric turbulence, the effect of meteors causes confusion. In so far as a meteor trail becomes diffused by atmospheric motions it is as relevant to a study of turbulence as ionization of solar origin. But scattering by a fresh meteor trail before it has diffused should be eliminate from the data. Scattering by undiffused mete trails can easily be recognized. When the sign is examined aurally a Doppler whistle associate with the creation of the trail can be heard. Th number of such whistles normally varies fro about 10 per minute at 0600 local time to every few minutes at 1800 local time. Thu in the few hours before dawn, the number of u

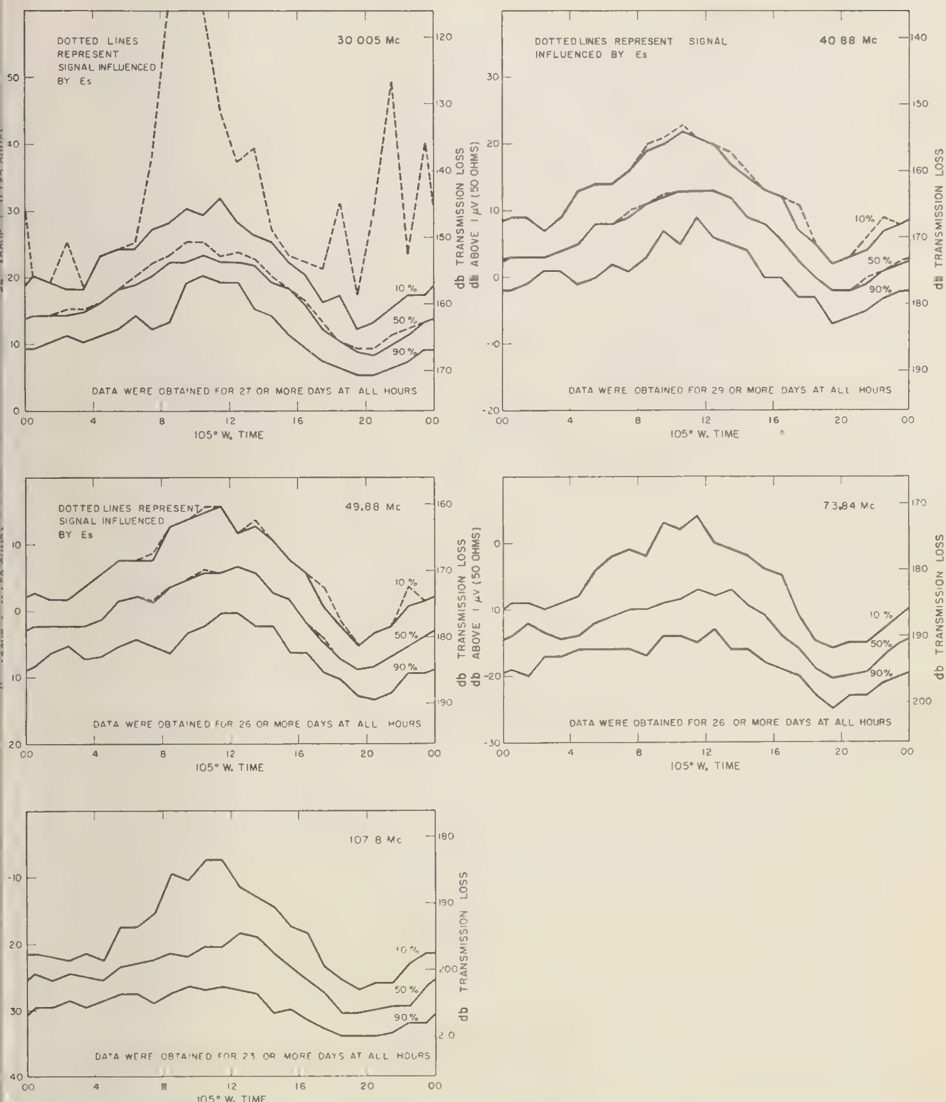

IG. 6—**Values of received signal intensity equaled or exceeded 10, 50, and 90 per cent of the time for June 1958.** (All values adjusted to 2-kw transmitter power.) [From *Blair*, 1959, by permission.]

ffused meteor trails occurring in the common olume of the antennas is large and the solar ontribution to the ionization is negligible. An alysis of atmospheric turbulence requires the everse of this situation. This is to be found at idday and for an hour or two thereafter, when e solar contribution to ionization is large and the number of undiffused meteor trails is small.

The frequency dependence of the scattered signal is illustrated in Figure 7. Both received power and frequency are shown on logarithmic scales so that the straight lines in the diagrams imply a power-law dependence on frequency or wavelength of the type indicated in equation

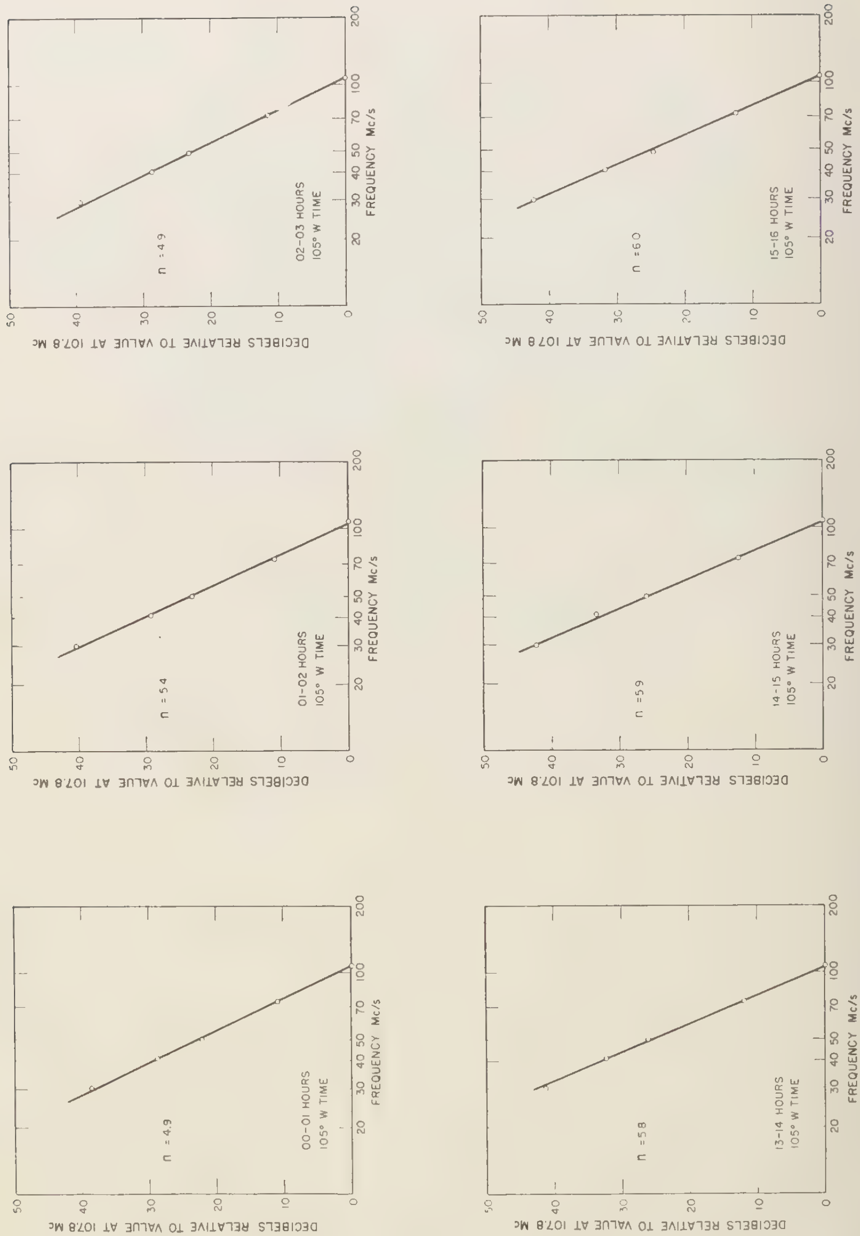

FIG. 7—Dependence of signal intensity on frequency for 10 days of June 1958. [From *Blair*, 1959, by permission.]

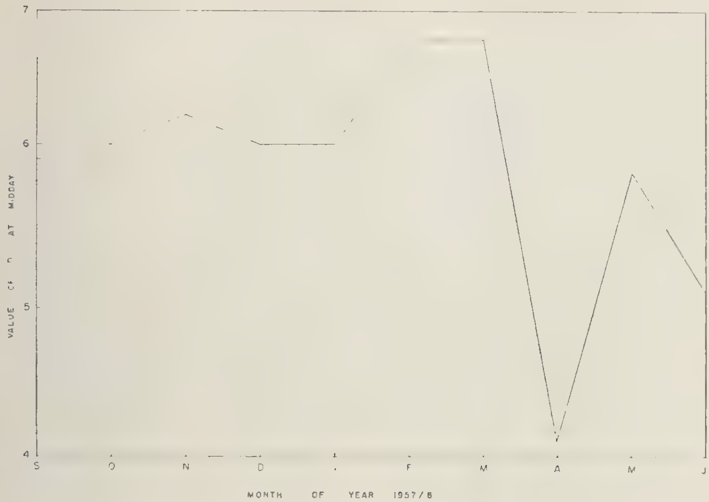

FIG. 8—Midday values of n in equation 31 for various months.

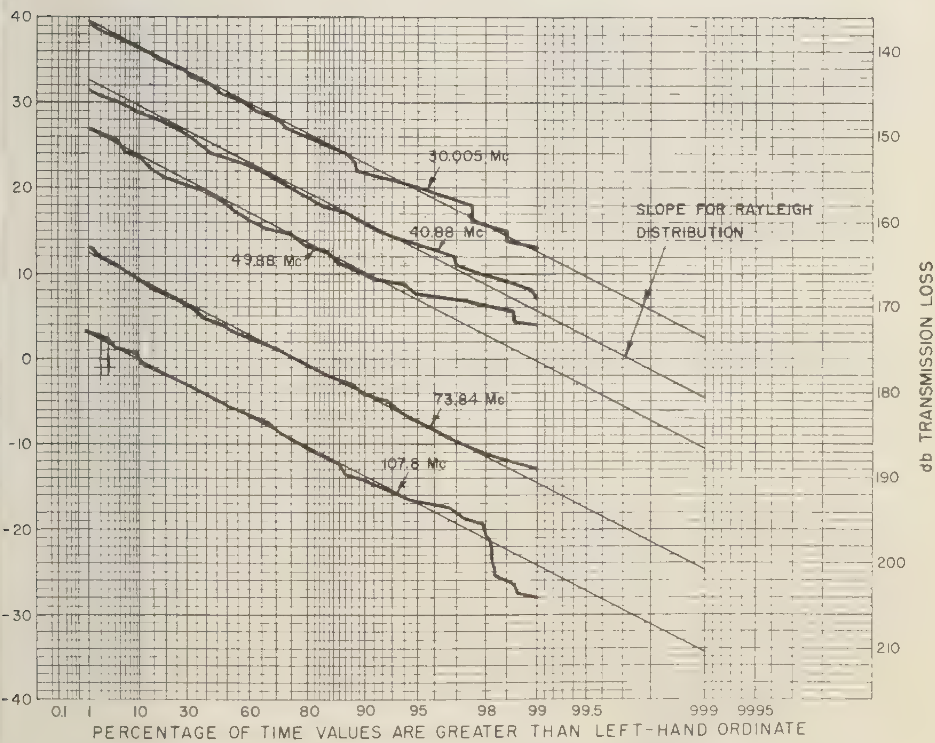

FIG. 9—Amplitude distribution of signal intensity values received during period of 1150 to 1200 hours, 105° W time June 27, 1958. [From *Blair*, 1959, by permission.]

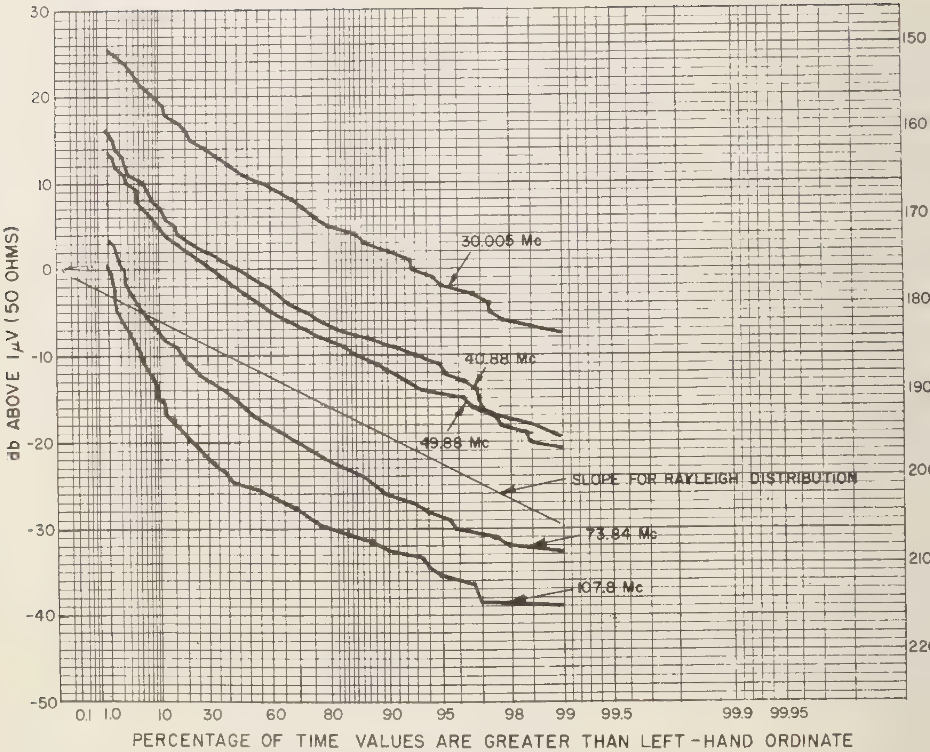

FIG. 10—Amplitude distribution of signal intensity values received during period of 0000 to 0010 hours 105° W time June 28, 1958. [From *Blair*, 1959, by permission.]

31. The values of n to be used in equation 31 are shown in the diagrams of Figure 7.

The value of n obtained by the method indicated in Figure 7 varies with time of day, being larger in the daytime than at night, presumably because of the effect of undiffused meteor trails at night. For an undiffused meteor trail a value of n equal to unity would be expected. It is reasonable to assume, therefore, that the values of n to be considered in relation to atmospheric turbulence are the ones obtained at midday or shortly thereafter. The midday values for the months from September 1957 to June 1958 are shown in Figure 8. It will be observed that some variation in the value of n occurs. April 1958 appears in particular to be anomalous possibly owing to the effect of a meteor shower. If the data are to be used to assess a single integral value of n, however, the value appears to be 6.

Experiments similar to the above have b carried out for radio scattering at troposph levels for which a much greater range of quency is available. The value of n obtai in these experiments was 5. There is some v ability in the value of n in this case too, an has been suggested [*Bolgiano,* 1958] that may be associated with variation in the stabi of the atmosphere.

The scale of the irregularities being inve gated in this experiment is given by express 19 on inserting the appropriate value of scattering angle θ (about 10°). It follows t the scale of the irregularities involved is ab 6 wavelengths. Inserting the values of wa length corresponding to the frequencies in we deduce that the range of scales for which result $n = 6$ is appropriate is from about to 60 meters. These figures are to be compa

on the one hand with the mean free path (3×10^{-3} meter at 80 km and 2×10^{-2} meter at 90 km) and on the other hand with the size of visual distortions in meteor trails (a few kilometers).

For an experiment of the type illustrated in Figure 2, the mirror direction referred to at the end of section 2 is in the vertical direction. Thus, the Fourier components of the irregularities important in producing the scattering involve corrugations about 6 wavelengths in scale in the vertical direction. However, experiments of this type also indicate irregularities in the horizontal direction. This may be appreciated by using a pair of receiving systems that may be moved relative to each other laterally to the direction of the transmitter. The random nature of the irregularities produces fading of the received signal, which is identical for the two receivers provided that they are sufficiently close together, but as they are moved apart the fading becomes uncorrelated. The correlation decreases to 0.5 for a spacing of about 4 wavelengths normal to the path. This implies that irregularities in the horizontal direction are roughly 4 wavelengths in scale, and those in the vertical direction are roughly 6 wavelengths in scale. The irregularities are therefore approximately isotropic.

Random motion of the irregularities of electron density causing the scattering should produce a probability distribution in the strength of the received signal that is approximately Rayleigh in type, except in so far as scattering by undiffused meteor trails affects the distribution. The probability distribution obtained at midday is shown in Figure 9; it follows the Rayleigh distribution closely. At midnight, however, the distribution is as shown in Figure 10, and the departure from the Rayleigh distribution is presumably due to undiffused meteor trails. If at midday we use the fading data to estimate the Doppler spread arising from irregular motion of the scatterers, the velocity obtained is about 25 m/sec.

The dotted lines in Figures 5 and 6 indicated that the phenomenon of sporadic E is observed from time to time in the frequency range 30 to 100 Mc/s. If this is a scattering phenomena, it is to be thought of as taking place at a height of about 110 km, where the mean free path is about 0.4 meter. From the fact that sporadic E is more marked at the lowest frequency used (30 Mc/s), it follows that the frequency variation involved in sporadic E is more rapid than that involved in the regular 80- to 90-km scattering phenomena. The data indicate for sporadic E a value of n of the order of 18. The fading rate for sporadic E is comparatively slow, indicating perhaps an irregular velocity of around 5 m/sec.

References

Bailey, Bateman, and Kirby, Radio transmission at VHF by scattering and other processes in the lower ionosphere, *Proc. IRE, 43,* 1181–1230, 1955.

Blair, J. C., Frequency dependence of VHF ionospheric scattering, *Natl. Bur. Standards Tech. Note 9,* April 1959. (Essentially the same material as in *Natl. Bur. Standards Rept. 6049.*)

Bolgiano, R., A meteorological interpretation of wavelength dependence in transhorizon propagation, Ph.D. thesis Cornell University, 1958. (to be published).

Booker, H. G., The use of radio stars to study irregular refraction of radio waves in the ionosphere, *Proc. IRE, 46,* 298–314, 1958.

Gardner, F. F., and J. L. Pawsey, Study of the ionospheric *D*-region using partial reflections, *J. Atmospheric and Terrest. Phys., 3,* 321, 1953.

Houghton, H. G., *Atmospheric Explorations,* John Wiley & Sons, chapter V, 1958.

Large-Scale Movements of Ionization in the Ionosphere

D. F. Martyn

C.S.I.R.O., Camden
New South Wales, Australia

Abstract—The complexity of the causes of variations in and motions of ionization in the ionosphere is stressed, as is the difficulty of differentiating real and virtual motions. An instability mechanism for deviations in ionization density is suggested, for which the predicted temporal and spatial morphologies appear to be consistent with those of the occurrence of sporadic E, spread F, and radio-star scintillations.

Radio echo-sounders (ionosondes) tell us the height distributions of the electron densities (N) below the ionization peaks in the principal regions of the ionosphere. It is a safe assumption that the values of N thus obtained are also those of the positive ions, since the regions must be electrically neutral to a very high approximation. The peaks of those densities vary in height in the course of the solar and lunar day, and are also perturbed during magnetic storms. The causes of the height variations are complex. On the one hand, the layers should move in rhythm with the solar zenith distance, being lowest at, or soon after, noon, when the sun's ionizing radiation penetrates most deeply. On the other hand, the electrodynamic forces associated with the solar and lunar tides, and with the disturbance magnetic variations, cause vertical motions whose amplitudes and phases are not yet precisely known in all parts of the world. Damping these effects is diffusion, which tends to produce an ionization distribution similar to that of the atmosphere itself; its influence is important only in the F region, at heights of about 250 km or more, where the diffusion time can be measured in hours or less. Yet a further cause of apparent vertical motion of the $N(h)$ profile is the height gradient of the efficiency of the ionization destruction processes. In the F region, where ionization decays according to an attachment law

$$\partial N/\partial t = -\beta N$$

there is clear evidence that the decay process decreases exponentially with height, resulting in an apparent upward movement of residual ionization. All these processes appear to opera in the highest (F) region of the ionosphere, a the resulting $N(h)$ distribution reflects the b ance between them.

From this it will be clear that observation the variations of $N(h)$ profiles cannot give directly the actual vertical velocity of ioni tion drift. This can only be inferred on assum tions whose plausibility is now fairly well est lished.

It is equally difficult to assess horizontal io zation velocities. On hydrodynamical reason it is safe to assume that horizontal wind velo ties will be larger than vertical velocities by factor comparable with (earth radius)/(la height), i.e. by about 20. Nevertheless we ha no means of observing horizontal motion o uniform layer. We can and do observe horizon movements of perturbations. These have b studied extensively by workers in many parts the world, in both the E and the F regions. shall not attempt to review these results he as their significance is still unclear, and it is yet possible to say whether they show real m tion of ionization or are manifestations of ho zontally traveling waves.

Save in the lowest regions of the ionosph it is impossible to ignore the effect of elect dynamic forces upon the motion of ionizati The main electric currents flow at heig slightly above 100 km, but the associated el tric polarization field is communicated to higher ionospheric regions along the highly c ducting geomagnetic field lines. This means t flow perturbations in the dynamo region will reflected in corresponding perturbations

gher regions. Indeed, in the F region the upling between the plasma and neutral gas is strong that electrical perturbations from be-v can set the whole mass in motion in a time ich less than a day.

In the F region large perturbations of ioniza-on density occur, producing the phenomena spread F and the scintillations of radio stars. seems unlikely that these notable phenomena which have well marked morphological associa-on with the ionospheric current systems) could directly due to *local* turbulence. There is a echanism, however, which could produce these enomena as a result of turbulence in lower gions. Any such turbulence must produce a cal perturbation of the polarization field that ill transfer upward in such a way as to pro-ice a perturbation of ionization in the upper gion. *Such a perturbation is unstable if on e underside of an ionized region drifting up-ard.* To understand this consider a sphere of nization density $N + \Delta N$ embedded in a edium of density N drifting with velocity V cross a magnetic field H. The sphere becomes olarized and drifts, *relatively to the medium,* ith velocity

$$v = -V\epsilon/(3 + \epsilon)$$

where $\epsilon = \Delta N/N$ and may have any numerical value. The effect of this, on the underside of an onized region drifting upward, is to cause a najor perturbation; a small positive perturba-ion moves downward into regions of lower den-sity, so becoming a large local perturbation; in other words, an ionized region is unstable in these circumstances. In the F region, where the Hall conductivity is small, the sphere moves like a solid; there is no interchange of ionization with the matrix medium at the boundary. A necessary criterion for instability therefore is that the lifetime of the ionization be comparable with or greater than the time necessary for the sphere to drift across an appreciable portion (scale height) of the ionized region. This condition is satisfied in the F region.

In the E region the most prominent irregularity is sporadic E (E_s), which has a morphology complex in both time and space. At first sight it would seem unlikely that the above ideas could apply to E_s, since the lifetime of E ionization is only a few minutes, and the drift velocities are low (less than a few hundred centimeters per second). Here, however, the Hall conductivity becomes important. A perturbation no longer can move like a solid body; there is constant interchange of ionization with the medium at the walls. In other words, a perturbation travels as a kinematic wave. The relevant ionization lifetime becomes that necessary to travel from the center of the perturbation to its walls; this travel distance is about 0.5 km or less, as against the 50 km necessary in the F region. It seems likely, therefore, that the instability criteria examined above for the F region may be applicable also to the E region, and that sporadic-E ionization, particularly at low and moderate latitudes, may be due to small turbulent or meteoric perturbations enhanced by the above processes. Certainly the predicted temporal and spatial morphologies of instability in the E and F regions appear to be consistent with the known morphologies of the occurrence of E_s, spread F, and radio-star scintillations.

Reference

Martyn, D. F., The normal F region of the ionosphere, *Proc. IRE, 47,* 147–155, 1959.

Scattering of Waves and Microstructure of Turbulence in the Atmosphere

A. M. Oboukhov

Institute of the Physics of the Atmosphere
Academy of Sciences, Moscow

Abstract—The paper deals with a brief survey of the theory of scattering of waves by turbulent inhomogeneities. Experiments on the study of scattering phenomena of sound by turbulence in the surface layer of the atmosphere are discussed. These experiments were carried out to obtain some information on the turbulent spectrum; their results are compared with the data of meteorological measurements in the surface layer. Applying the method of scattered radio waves to the study of turbulence in the ionosphere is discussed.

Inhomogeneities of the atmosphere due to turbulence result in the scattering of waves of different types (sound, radio) as they propagate through the atmosphere. The propagation of sound is affected by random inhomogeneities in the spatial distribution of wind and temperature (and to a less extent humidity). The fluctuations in the refractive index at VHF are mostly due to turbulent variations of temperature and humidity (fluctuations of pressure are of practically no importance). The scattering of radio waves in the ionosphere is due to microinhomogeneities in the field of electron density, which may also have a turbulent character.

1. During the past decade great interest has arisen among radio engineers in the problem of the scattering of radio waves in connection with the observed phenomenon of VHF propagation beyond the horizon. Owing to scattering by turbulent inhomogeneities some portion of radiated energy reaches the shadow zone and ensures the reliable reception of signals (Fig. 1). A series of important investigations of the theory of this phenomenon were carried out by *Booker and Gordon* [1950] and *Villars and Weisskopf* [1954], and many other reports, both experimental and theoretical, were published in *Proc. IRE*, *43* (10), 1955. The works of *Megaw* [1950, 1957] suggesting the statistical method of investigation using the theory of turbulence are of great interest. The literature on this problem is extensive (see the bibliography in *Vysokovsky*, 1958).

In spite of different approaches and different terminology, one can speak, at present, abo establishing a certain unique point of view general questions of the theory of wave scatte ing in media with random inhomogeneities. T differences in theoretical results published a usually due to the choice of different statisti models (correlation functions) for the descri tion of turbulence. Some of these models we only preliminary and of somewhat formal cha acter. Among the most recent researches t very interesting results on the theory of VH tropospheric propagation obtained by Silverm should be noted. *Silverman* [1956] used in l theory the conclusions of the modern theory turbulence and experimental data about t microstructure of the temperature field in t atmosphere. Similar results were obtained *Batchelor* [1955].

A phenomenon similar to the VHF trop

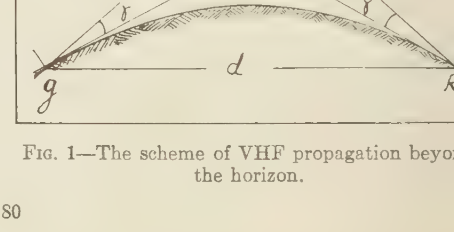

Fig. 1—The scheme of VHF propagation beyo the horizon.

spheric propagation has been observed also for sound [*Pridmore-Brown and Ingard,* 1955]. Since 1941 a series of works has been published in the USSR which deal with the development of the theory of the scattering of sound by turbulence [*Oboukov,* 1941; *Blokhintsev,* 1946; *Tatarskiy,* 1953].

For geophysicists and specialists in the theory of turbulence, the phenomenon of the scattering of waves by turbulent inhomogeneities is of interest as a means of obtaining information about the turbulent structure, particularly of the upper layers that are not available for direct investigation.

In the present paper an attempt is made to give a brief statement of the theory of this phenomenon as a foundation for the interpretation of pertinent observations. The results of some experiments carried out at the Institute of Physics of the Atmosphere (Academy of Sciences, USSR, in 1958) on detailed investigations of the scattering of sound in the turbulent atmosphere are also described. These experiments may serve as a model for similar ones with radio waves for the purpose of investigating the microstructure of turbulence in the upper layers of the atmosphere.

2. We proceed now to the theoretical consideration of the problem of the scattering of waves. For simplicity we shall restrict ourselves to the case of the scattering of a wave described by a scalar potential φ (sound). It should be mentioned that the same method is applied to electromagnetic waves, and, as a result of this, very similar equations are obtained for the intensity of the scattered wave. For the intensity of the scattered radio waves there is a factor that takes the polarization effect into account; this factor, however, in cases of practical interest is close to unity.

The initial equation is

$$\Delta\varphi - \frac{n^2}{c_0^2}\cdot\frac{\delta^2\varphi}{\delta t^2} = 0 \qquad (2.1)$$

where

c_0 = the standard value of the propagation velocity.

n = the refractive coefficient.

The dependence of the monochromatic wave on time is determined by the multiplier $e^{-i\omega t}$ (ω is the cyclic frequency). For the sake of simplicity we shall not write the multiplier. In the case of a monochromatic wave it follows from equation 2.1 that

$$\Delta\varphi + k^2(1 + \mu)^2\varphi = 0 \qquad (2.2)$$

where $k = \bar{n}(\omega/c_0)$; $\bar{n}$ is the mean value of the refractive index, $\mu = (n - \bar{n})/\bar{n}$ is the relative fluctuation of the refractive index. Under actual atmospheric conditions the fluctuations of the refractive index are small so that $\mu \ll 1$ (for sound $\mu \simeq 10^{-3} - 10^{-4}$, for radio waves in the troposphere $\mu \simeq 10^{-6} - 10^{-7}$). In connection with this, equation 2.2 is solved by the perturbation method by means of μ:

$$\varphi = \varphi_0 + \varphi_1 + \cdots \qquad (2.3)$$

In the first approximation φ_0 describes the direct wave, φ_1 describes the scattered wave. It follows from (2.2) that φ_1 satisfies the nonhomogeneous wave equation:

$$\Delta\varphi_1 + k^2\varphi_1 = -2\mu k^2\varphi_0 \qquad (2.4)$$

Assume that μ is different from zero only within a certain finite volume V (the scattering volume), and a radiator and a receiving set are situated far from this volume. In this case the solution of equation 2.3 for the potential of the scattered wave φ_1 can be approximately represented as:

$$\varphi_1(P) = \frac{A(M_0)}{2\pi R^2}\iiint_v \exp\left[i(\mathbf{k}, \boldsymbol{\varrho})\right] \cdot\mu(\mathbf{M}_0 + \boldsymbol{\varrho})\, dv\varrho \qquad (2.5)$$

where M_0 is the center of the scattering volume, A the amplitude of the incident wave, P the point of observation of the scattered field (receiving set), $R = r_pM_0$ the distance between these points, $\mathbf{k} = \mathbf{k}'' - \mathbf{k}'$ the difference between wave vectors of the direct wave ($\mathbf{k}''$) and the scattered wave ($\mathbf{k}'$), $\boldsymbol{\varrho}$ the variable radius vector from the center of the scattering volume M_0. Further, we shall call $\mathbf{k}$ the vector of scattering, and the angle between $\mathbf{k}''$ and $\mathbf{k}'$ the angle of scattering θ (Fig. 2).

Thus, the amplitude of the scattered wave (2.5) is determined (in the approximation of Fraunhofer's diffraction) by a Fourier component of the field of μ (the fluctuations of the refractive index) corresponding to the plane

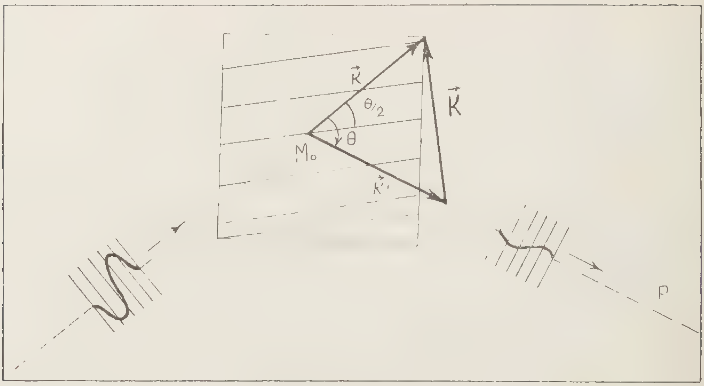

FIG. 2—Geometrical characteristics of scattering.

'wave' with a wave vector $\mathbf{k}$. Note that

$$|\mathbf{k}| = 2k \sin \theta/2 \qquad (2.6)$$

This is the condition established by Breggs.

A corresponding scale of inhomogeneities of the field μ, due to which the scattering occurs in the direction θ, is determined as

$$l = \frac{2\pi}{|\mathbf{k}|} = \frac{\lambda}{2 \sin \theta/2} \qquad (2.7)$$

Equations 2.5 and 2.6 show that by observing the scattering effect at different angles and different wavelengths we actually make a 'spectral analysis' of the spatial structure of the fluctuations in the refractive index.

3. The situation, however, is complicated by the fact that the fluctuations in the index in the actual atmosphere are of very irregular and 'random' character, owing to the turbulence. Therefore, to describe them we use a statistical method with the help of the correlation function. It is natural to assume the field μ in the considered region to be statistically homogeneous and the correlation function to be dependent here on the vector $\boldsymbol{\varrho}$ alone, which determines the reciprocal position of the observation points M and M'

$$\overline{\mu(M)\mu(M')} = B(\boldsymbol{\varrho}) \qquad (3.1)$$

In actual calculations most authors consider the fluctuating field to be isotropic, and this essentially simplifies the investigation, since in that case the correlation function is dependent only on the distance ρ between the observati[on] points. The introduction of the hypothesis [of] isotropy nevertheless requires special co[n]firmation by appropriate experiments, a[nd] may not always be applicable. We shall r[e]strict ourselves to a hypothesis of homogenei[ty] (without assuming isotropy beforehand).

Different components of the Fourier spectru[m] are not statistically correlated; this follo[ws] from the general theory of statistically hom[o]geneous fields [*Yaglom*, 1949]. The measure [of] intensity of these components is the 'spectr[al] density' $\Phi(\mathbf{p})$ determined as the Fourier tran[s]form of the correlation function of the fie[ld]

$$\Phi(\mathbf{p}) = \frac{1}{(2\pi)^3} \iiint_{-\infty}^{+\infty} \cos(\mathbf{p}, \boldsymbol{\varrho}) B(\boldsymbol{\varrho})\, dv_{\boldsymbol{\varrho}} \qquad (3.$$

where $\Phi(\mathbf{p}) \geq 0$. The spectral description [of] turbulence appears to be more convenient [in] some respects and to have a clearer physic[al] interpretation than the correlation functio[n].

Computing the mean square of the amplitu[de] of the scattered wave $\overline{\varphi\varphi^*}$ with the help [of] equation 2.5 we obtain the value proportion[al] to the mean energy of the scattered field E[...] This characteristic can be observed directl[y]. It appears here that

$$\frac{E_s}{E_0} = \frac{V \cdot k^4}{(2\pi)^2 R^2} \Phi(\mathbf{k}) \qquad (3.$$

where E_0 is the energy of the incident wave [in] the region of scattering. (In the case of electr[...]

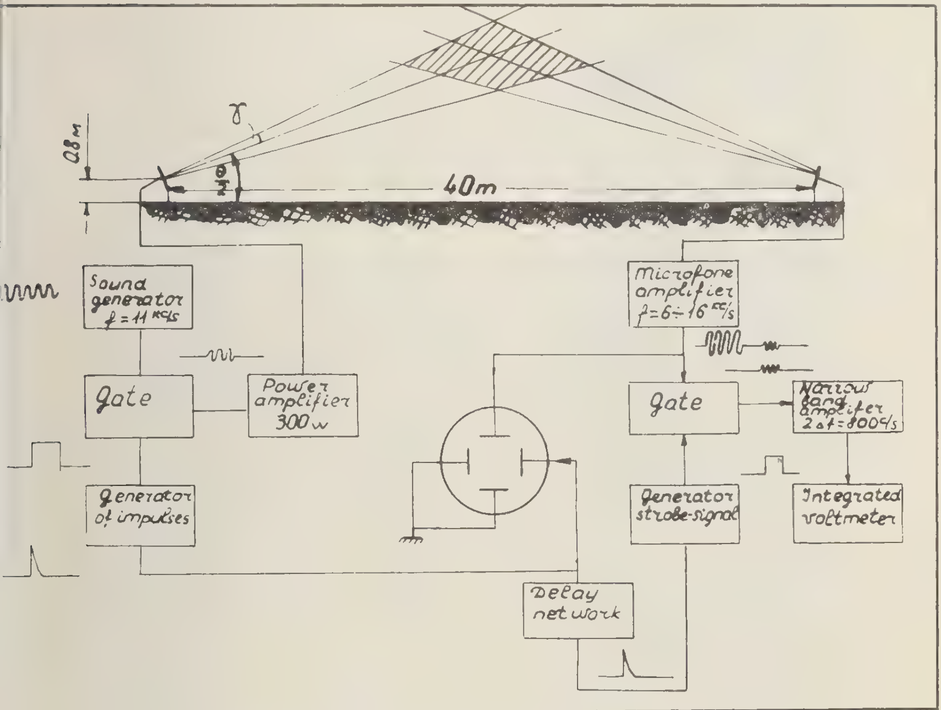

FIG. 3—The scheme of the experiment on the scattering of sound.

ıgnetic waves a factor $\sin^2 \chi$ enters the right rt of (3.3), where χ is the angle between the ctrical vector in the incident wave and the ıttering direction.)

Thus, the measurement of the mean intensity the scattered field enables us to determine spectral function of the turbulent fluctuans in the refractive index for the values of a ve vector $\mathbf{k} = \mathbf{k}'' - \mathbf{k}'$ corresponding to an tual experiment. *Silverman* [1956] applied uation 3.3 to the problem of VHF scattering the troposphere, assuming that the turbulent viations of temperature and humidity are ponsible for the fluctuations in the refractive dex and satisfy the 2/3 law (in accordance th the works of *Oboukhov* [1949], *Yaglom* 49], and *Corrsin* [1951]. Consequently, to scribe the turbulent pulsations of the refractive dex n, instead of the correlation function, we the structure function of the form

$$\overline{[n(M) - n(M')]^2} = C_n^{\,2} \rho^{2/3} \qquad (3.4)$$

where C_n^2 is the structure characteristic of the turbulent fluctuations in the refractive index. It is expressed through the corresponding characteristics of microstructure of the fields of temperature and humidity. (A short description of the contemporary theory of microstructure of the meteorological fields and some actual data are given in the review by *Oboukhov and Yaglom*, 1959.) It may be shown that the spatial spectral function corresponding to the locally isotropic field characterized by the structure function (3.4) is

$$\Phi(\mathbf{p}) = 0.033 \cdot C_n^{\,2} \cdot |p|^{-11/3} \qquad (3.5)$$

with the help of which an equation for the intensity of the scattered field (given in Silverman's article) can easily be obtained:

$$\frac{E_1}{E_0} = \frac{\text{Const}}{R^2} \cdot \frac{v \cdot C_n^{\,2}}{\lambda^{1/3}} (\sin \theta/2)^{-11/3} \qquad (3.6)$$

The experiment does not contradict equation 3.6.

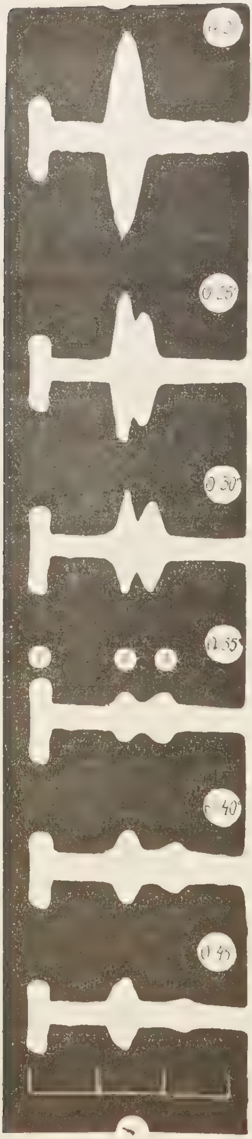

FIG. 4—The direct and the scattered impulse on the screen of the cathode oscillograph.

It should be noted, however, that the microstructure of turbulence in a free atmosphere has not been investigated very thoroughly.

4. To study the regularities of the scattering of waves by turbulent inhomogeneities, so experiments on the scattering of sound in surface layer of the atmosphere were carr out at the Institute of Physics of the Atmosph (Academy of Sciences of the USSR) in 19 Some results of these investigations have b published by *Kallistratova* [1959]. The experim tal work was conducted in an open place in steppe. The scheme of the experiment is sho in Figure 3. A powerful electrostatic sou transducer and a microphone with a narr directional pattern (the beam width γ = 1. were used. The distance between the tra ducer and the microphone was equal to $2R$ = meters. Signals of wavelength λ = 3 cm w used in the work. Sequences of wave pack (impulses of 20 waves) were used instead monochromatic radiation. This system enab one to separate the scattered signal from direct one because of the delay in transmiss time (Fig. 4). (In working with sound it difficult to avoid the effect of the direct sig 'leaking' to the receiving set due to the s lobes of the radiation pattern.) A special el tronic mechanism made it possible to separate scattered signal and to measure its amplitu In each series of measurements of the depende of the amplitude of the scattered signal upon angle of scattering, θ ranged from 25° up to 5 About 60 series of measurements under differ meteorological conditions and at different tin of day were carried out. Experiments w accompanied by meteorological measureme at the mast (wind and temperature were measu at several levels). The data of these measu ments were used in the analysis of the experim tal material of the acoustic measurements. estimate of the structural characteristics the refractive index for sound was made. the basis of investigations carried out bef [*Oboukhov*, 1951; *Tatarsky* 1956], the cor lation between the characteristics of wind microstructure, temperature, and rameters characterizing the meteorological c ditions were established. Figure 5 illustra the manner in which the observed effect values of the amplitude of the scattered sig (divided by the amplitude of the incident wa for the angle of scattering θ = 25° depend the 'meteorological factor'

$$M = \sqrt{(V_*^2/c^2)\cos^2(\theta/2) + 0.06(T_*^2/T^2)} \qquad (4$$

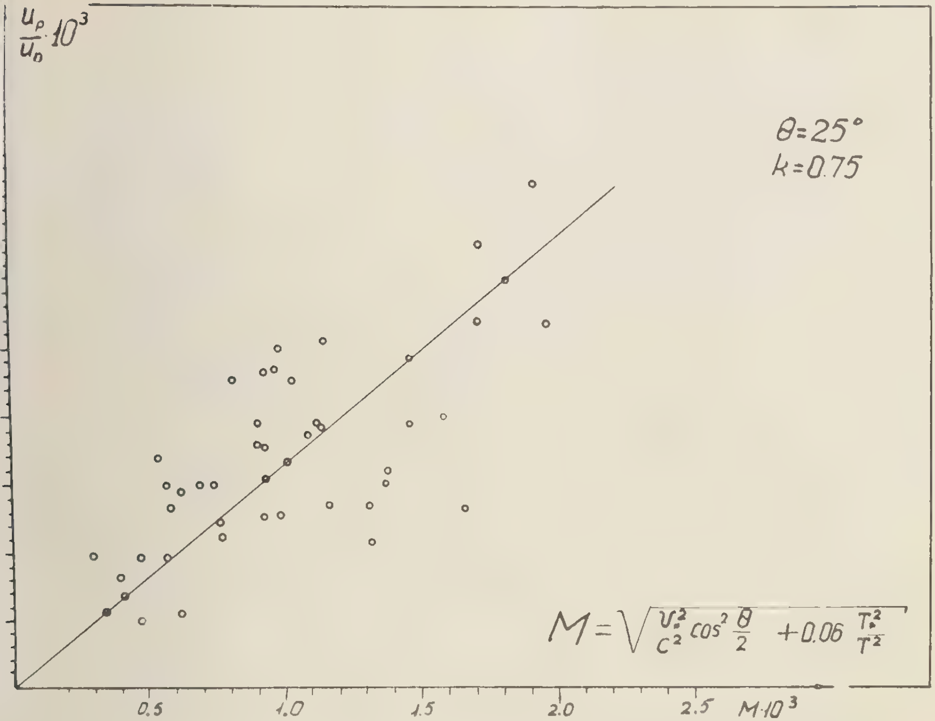

FIG. 5—The dependence of the amplitude of the scattered wave upon the meteorological factor M.

here V_* and T_* are the parameters in log-ithmic laws approximating the dependence the mean wind velocity and temperature on the height in the surface layer of the mosphere:

$$\bar{V}(Z) = \frac{V_*}{H} \ln Z/Z_0 \tag{4.2}$$
$$T = T_* \ln Z/Z_0 + T_0$$

The results for the angles of 25° and 30° tained from the theoretical equation

$$\frac{U_s}{U_0} = \frac{\text{Const } R\gamma^3 M^2}{\lambda^{1/3}} (\sin \theta/2)^{-16/3} \tag{4.3}$$

e in satisfactory agreement with observations.[1]

So, for example, if $\theta = 25°$ the coefficient of proportionality between U_s/U_0 and M determined empirically is equal to 1.6, and its theoretical value according to equation 4.3 appeared to be 3.8. Taking into account inaccuracy in determination of the magnitude of the 'scattering volume' and some numerical coefficients, the difference cannot be considered important.

Figure 6 illustrates the dependence of the scattering effect upon the angle θ (indicatrix) obtained experimentally. Log sin $\theta/2$ is plotted along the abscissa axis. The ratio of the effective amplitude of the scattered signal to that of the

[1] The volume of scattering and the structure efficient for the refractive index are determined om the following equation:

$$V = \frac{R^3\gamma^3}{\sin\theta}; \quad C_n^{\ 2} = \frac{1}{H^2 Z^{2/3}} \cdot \left(\frac{V_*^{\ 2}}{C^2} \cos^2\frac{\theta}{2} + 0.06\frac{T_*^{\ 2}}{T^2}\right)$$

U_s and U_0 are the effective amplitudes of the scattered and direct sound waves.

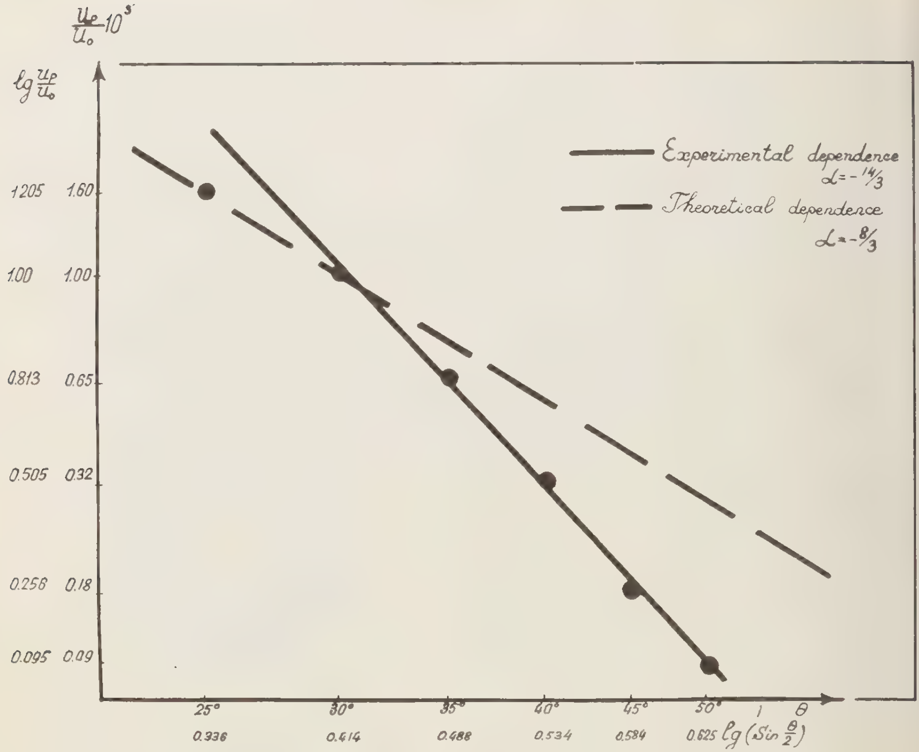

Fig. 6—The dependence of scattering upon the angle θ.

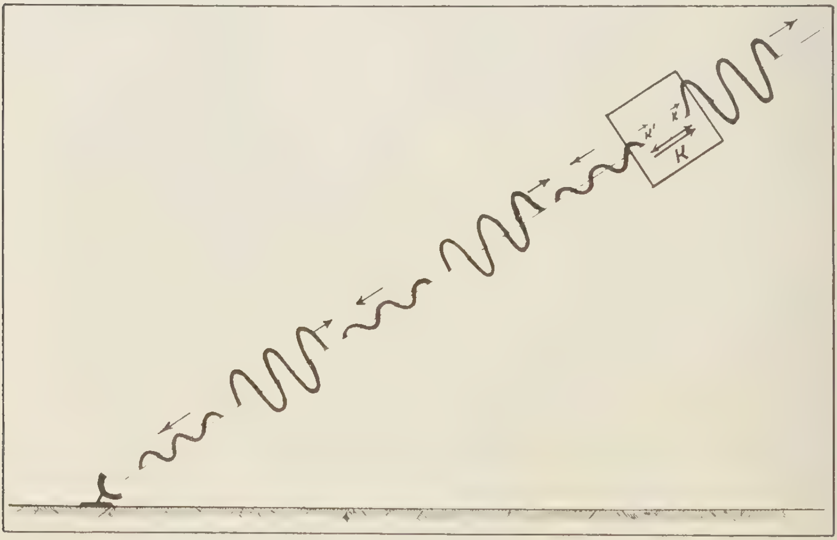

Fig. 7—The scheme of sounding by an inclined ray.

nt signal U_s/U_0 is plotted along the ordinate . It was reduced to some standard meteoro-gical conditions (also in log scale). The dashed given in this figure shows the theoretical catrix of scattering. If the angles θ are large, intensity of scattering obtained is somewhat than it should be according to Kolmogoroff's trum (the $\frac{2}{3}$ law). This may be explained by fact that, in the region of the turbulent trum that is responsible for the scattering wave for which $\lambda = 3$ cm for angles greater n 25° to 30° (the scale of inhomogeneities ectively $l = \lambda/(2 \sin \theta/2) = 7 \sim 3.5$ cm), ous effects come into play (the internal e of turbulence, characterizing the viscosity ts in the atmosphere, is of the order of n).

his experiment demonstrates the possibility detecting scattered sound waves in the osphere. In view of this a new method of tral analysis is likely to be put into practice g observations of the scattering effect at erent angles and different wavelengths. . It can be assumed that the method of ttered waves may be helpful for obtaining rmation about the spectrum of turbulent omogeneities in the ionosphere—fluctuations lectron density. Short waves[2] that can pass ough the ionosphere and undergo only partial ttering can be used in this case.

Note that experiments carried on in accordance h a routine scheme (Fig. 1) with different quencies and angles of scattering supply rmation about the spectral distribution of omogeneities only along the vertical (the ction of the scattering vector **k**). It is, principle, impossible to distinguish the cases statistically isotropic and essentially non-ropic stratified structure of the medium. One can try to test the hypothesis of isotropy changing the direction of the radiator and receiving set from the baseline horizontally. e scattering vector will acquire a horizontal nponent. Finally, it seems of great interest study the effect of backscattering (the radio ation principle) by turbulent inhomogeneities. is method, in particular, was applied by V. V. Kostarev with his collaborators for the study of tropospheric inhomogeneities [*Gorelik and Kostarev*, 1959]. By utilizing this last method the hypothesis of isotropy can be tested by an inclined sounding from a single point (Fig. 7). Here, we shall not dwell on the technical difficulties in the detection and measurement of very weak signals. It should be said that at the present moment modern radio technique has developed enormously in this respect, but holds even greater promise.

[2] $\lambda < \lambda_{kp}$ (the critical wavelength).

References

Batchelor, G. K., *Cornell Univ. Sch. Eng. Tech. Rept. 26,* 1955.

Blokhintsev, D. I., *Acoustics of Heterogeneous (Nonhomogeneous) Atmosphere,* Moscow, 1946.

Booker, H. G., and W. E. Gordon, *Proc. IRE, 38* (4), 1950.

Corrsin, S., On the spectrum of isotropic temperature fluctuations in an isotropic turbulence, *J. App. Phys., 22,* 469–473, 1951.

Gorelik, A. G., and V. V. Kostarev, *DAN SSSR, 125* (1), 59, 1959.

Kallistratova, M. A., *DAN SSSR, 125* (1), 69, 1959.

Megaw, E. C. S., Scattering of electromagnetic waves by atmospheric turbulence, *Nature, 166,* 1100–1104, 1950.

Megaw, E. C. S., Fundamental radio scatter propagation theory, *Proc. IEE,* pt. C, *104,* 441–455, 1957.

Oboukhov, A. M., *DAN SSSR, 30,* 611, 1941.

Oboukhov, A. M., *Izvest. A. N. SSSR,* Geographical and geophysical series, *13* (1), 58, 1959.

Oboukhov, A. M., *Izvest. A. N. SSSR,* Geophysical series, no. 3, 49, 1951.

Oboukhov, A. M., and A. M. Yaglom, On the microstructure of atmospheric turbulence, *Quart. J. Roy. Meteorol. Soc., 85,* 81–90, 1959.

Pridmore-Brown, D. C., and U. Ingard, *J. Acoust. Soc. Am., 27* (1), 36, 1955.

Silverman, R. A., Turbulent mixing theory applied to radio scattering, *J. Appl. Phys., 27,* 699–705, 1956.

Tatarskiy, V. I., *ZhETF, 25* (½), 74, 1953.

Tatarskiy, V. I., *Izvest. A N. SSSR,* Geophysical series, no. 6, 689, 1956.

Villars, F. M. H., and V. F. Weisskopf, *Phys. Rev., 94,* 232, 1954.

Vysokovsky, D. M., Some problems on the far atmosphere distribution of ultra-short radio waves, *A. N. SSSR,* Moscow, 1958.

Yaglom, A. M., The law of probability and its application, II, no. 3, 292, 1957.

Yaglom, A. M., *DAN SSSR, 69* (6), 743, 1949.

Effect of a Magnetic Field on Turbulence in an Ionized Gas

J. W. Dungey

*A. W. R. E., Aldermaston
Berkshire, England*

Abstract—The problem is formulated using the equations of motion for each constitutent of the gas. Approximations are discussed, and idealizations are adopted appropriate to the ionosphere. A physical picture is given for the generation of irregularities in electron density by shear flow in the neutral air. Given the motion of the air, the electron density can be calculated, and this calculation is carried out in the linear approximation for an arbitrary Fourier component.

Introduction—The magnetic field probably plays an important role in the generation of irregularities in the E layer, but this aspect of the problem presents less difficulty than the turbulence itself. The effect of the magnetic field can be worked out from classical laws of physics as follows.

Maxwell's equations are valid anywhere except in very fundamental research:

$$\operatorname{div} \mathbf{H} = 0 \qquad (1)$$

$$\partial \mathbf{H}/\partial t = -c \operatorname{curl} \mathbf{E} \qquad (2)$$

$$\operatorname{div} \mathbf{E} = 4\pi\rho \qquad (3)$$

$$c \operatorname{curl} \mathbf{H} - \partial \mathbf{E}/\partial t = 4\pi \mathbf{j} \qquad (4)$$

where

$\mathbf{H}$ = magnetic field,

$\mathbf{E}$ = electric field in Gaussian units.

charge density, $\rho = \sum_i n_i e_i$, where n_i = particle density of ith constituent; e_i = charge.

current density, $\mathbf{j} = \sum_i n_i e_i \mathbf{u}_i$, where u_i = fluid velocity of ith constituent.

Neglect of rate of ionization etc.—The equation of continuity

$$\partial n_i/\partial t = -\operatorname{div}(n_i \mathbf{u}_i) \qquad (5)$$

is valid for each constituent separately, except that terms should be added to represent 'reactions' such as ionization, recombination, dissociation, and charge exchange. These are omitted in this paper, because we are interested in faster processes.

Each constituent has an equation of motion

$$\frac{\partial u_i}{\partial t} + (\mathbf{u}_i \cdot \nabla)\mathbf{u}_i = \sum_j \frac{m_j \nu_{ij}}{m_i + m_j}(\mathbf{u}_j - \mathbf{u}_i)$$
$$+ \frac{e_i}{m_i}\left(\mathbf{E} + \mathbf{u}_i \wedge \frac{\mathbf{H}}{c}\right) + \mathbf{g} - \frac{\nabla p_i}{n_i m_i} \qquad ($$

(viscosity is neglected here), where ν_{ij} = f quency for particles of ith constituent of collisio with particles of jth constituent; $\mathbf{g}$ = gravi p_i = partial pressure.

These equations, when supplemented well posed initial, boundary, or periodic conditions, determine the solution of the proble

Approximations that are usually valid—T magnetic field at the ground is close to a dip field, and variations are relatively small.

(i) The same may be assumed in the ionosphe

The following approximations are based numerical values and can be checked m convincingly at the end. Let a = length sca Then corresponding to the weakness of magne variations, from (i)

$$\operatorname{curl} \mathbf{E} \ll |\mathbf{E}|/a$$

We shall put

$$\mathbf{E} = -\nabla\phi$$

(This approximation implies that the inducta of any current circuit is small and is least g for large-scale phenomena.) The displacem current is small (it is important only at ra frequency):

$$4\pi j \approx c \operatorname{curl} \mathbf{H} \quad (4') \qquad \operatorname{div} \mathbf{j} \approx 0$$

(ii) $\rho \ll e n_e$, n_e = electron density.

(iii) $\rho|\mathbf{E}| \ll \mathbf{j} \wedge \mathbf{H}/c$

Idealization

(a) No negative ions.

(b) Only one species of positive ions, sub-ipt p.

(c) Only one species of neutral molecule, bscript n.

(d) From (ii), $n_p \approx n_e$. (9)

(e) Neglect collisions between electrons and sitive ions (not valid in F layer).

Numerical values

$H \sim 0.4$ gauss, $n_p \approx n_e < 3.10^6$ cm^{-3}.

$$= \frac{\nu_{np}}{n_p} \sim 10^{-9} \text{ cm}^3 \text{ sec}^{-1},$$

$$\Omega_p = \frac{eH}{m_p c} \sim 140 \text{ sec}^{-1}.$$

$$= \frac{\nu_{ne}}{n_e} \sim 10^{-8} \text{ cm}^3 \text{ sec}^{-1},$$

$$\Omega_e = \frac{eH}{m_e c} \sim 7.10^6 \text{ sec}^{-1}$$

arge of electron $= -e$; Ω_p and Ω_e are here ch taken positive).

$\nu_{np}^{-1} > 5$ minutes; neglect the effect of col-ons on the motion of the neutrals, which ll be inexorable.

Write

$$\frac{m_n \nu_{pn}}{+ m_p} = \nu_p(\approx \tfrac{1}{2}\nu_{pn}),$$

$$\frac{m_n \nu_{en}}{m_n + m_e} = \nu_e(\approx \nu_{en}).$$

For the charged particles, (6) now has the form

$$+ (\mathbf{u}_i \cdot \nabla)\mathbf{u}_i = \nu_i(\mathbf{u}_n - \mathbf{u}_i)$$

$$+ \frac{e_i}{m_i}\left(\mathbf{E} + \mathbf{u}_i \wedge \frac{H}{c}\right) + \mathbf{g} - \frac{\nabla p_i}{n_i m_i} \qquad (6')$$

Note $\nu_e/\nu_p \sim 20$, but $m_p\nu_p/m_e\nu_e \sim 1500$.

Equations derived from (6′)—It is convenient think of the weakly ionized gas as a totally ized gas superposed on a neutral gas. The tral gas only feels the effect of the electro-gnetic field via collisions with charged ticles. The equation of transfer of momentum the totally ionized component is obtained by multiplying the two equations 6′ by n_e times the corresponding mass and adding. Put

$$(m_p + m_e)\mathbf{u}_t = m_p\mathbf{u}_p + m_e\mathbf{u}_e$$

and

$$(m_p\nu_p + m_e\nu_e)\mathbf{U} = m_p\nu_p\mathbf{u}_p + m_e\nu_e\mathbf{u}_e$$

Then with approximation (iii)

$$n_e(m_p + m_e)(\partial\mathbf{u}_t/\partial t + (\mathbf{u}_t\cdot\nabla)\mathbf{u}_t)$$

$$+ \frac{m_p m_e}{(m_p + m_e)e^2}(\mathbf{j}\cdot\nabla)(\mathbf{j}/n_e)$$

$$= n_e(m_p\nu_p + m_e\nu_e)(\mathbf{u}_n - \mathbf{U})$$

$$+ \mathbf{j} \wedge \mathbf{H}/c + n_e(m_p + m_e)\mathbf{g}$$

$$- \nabla(p_p + p_e) \qquad (10)$$

The last term on the left-hand side arises from the inertial terms in (6′) and is usually small.

A form of Ohm's law can be obtained by eliminating $\mathbf{u}_n$ from the two equations 6′. Neglecting $m_e\nu_e$ compared with $m_p\nu_p$, and ν_p compared with ν_e (after the subtractions have been carried out), it can be written

$$\mathbf{E} = \mathbf{j}/\sigma_0 + \mathbf{j} \wedge \mathbf{H}/(n_e ec) - \mathbf{U} \wedge \mathbf{H}/c$$

$$- (n_e e)^{-1}\nabla p_e - m_e\nu_e g/e\nu_p$$

$$+ m_e(e\nu_p)^{-1}(\nu_e(\partial u_p/\partial t + (\mathbf{u}_p\cdot\nabla)u_p)$$

$$- \nu_p(\partial\mathbf{u}_e/\partial t + (\mathbf{u}_e\cdot\nabla)\mathbf{u}_e)) \qquad (11)$$

where

$$\sigma_0 = n_e e^2/m_e\nu_e.$$

Equation 11 exhibits the physics and is useful for some problems. Only the first three terms on the right-hand side are usually important. Note that

$$\mathbf{u}_t = \mathbf{u}_p - \frac{m_e}{m_p + m_e}\frac{\mathbf{j}}{n_e e}$$

$$\mathbf{U} = \mathbf{u}_p - \frac{m_e\nu_e}{m_p\nu_p + m_e\nu_e}\frac{\mathbf{j}}{n_e e}$$

The 'induced field' in (11) is $\mathbf{U} \wedge \mathbf{H}/c$, but this differs from $\mathbf{u}_p \wedge H/c$ or $\mathbf{u}_t \wedge H/c$ by only a small multiple of the 'Hall field' $\mathbf{j} \wedge \mathbf{H}/n_e ec$.

In the following we shall consider problems

in which (10) reduces to

$$n_e(m_p\nu_p + m_e\nu_e)(\mathbf{U} - \mathbf{u}_n) = \mathbf{j} \wedge \mathbf{H}/c \qquad (12)$$

which expresses the condition that the ionized gas drifts with such a speed that collisions with the neutral gas just balance the electromagnetic force.

Substitute for $\mathbf{U}$ in (11) and leave out the small terms; then

$$\mathbf{E} = \frac{\mathbf{j}}{\sigma_0} + \frac{\mathbf{j} \wedge \mathbf{H}}{n_e ec} + \frac{\mathbf{H} \wedge \mathbf{j} \wedge \mathbf{H}}{n_e m_p \nu_p c^2} - \frac{\mathbf{u}_n \wedge \mathbf{H}}{c} \qquad (13)$$

The third term on the right-hand side represents a reduction of conductivity in directions perpendicular to $\mathbf{H}$. The extra dissipation is due to the collision dissipation of the drift expressed by (12).

Unfortunately we shall need to solve (13) for $\mathbf{j}$. It is then useful to solve (6′) for $\mathbf{u}_i$ after omitting terms as in (12) and (13). Distinguishing components parallel and perpendicular to $\mathbf{H}$ by subscripts $_\parallel$ and $_\perp$ gives

$$(u_i - u_n)_\parallel = (e_i/m_i\nu_i)E_\parallel \qquad (14)$$

$$(\nu_i^2 + \Omega_i^2)(\mathbf{u}_i - \mathbf{u}_n)_\perp = \frac{\nu_i e_i}{m_i}\left(\mathbf{E} + \mathbf{u}_n \wedge \frac{\mathbf{H}}{c}\right) + \frac{e_i^2}{m_i^2 c}\left(\mathbf{E} + \mathbf{u}_n \wedge \frac{\mathbf{H}}{c}\right) \wedge \mathbf{H} \qquad (15)$$

The two terms on the right-hand side of (15) are perpendicular to each other, and the ratio of their magnitudes is ν_i/Ω_i. The ν's decrease with height; the Ω's hardly vary.

$\nu_e = \Omega_e$ at about 80 km.

$\nu_p = \Omega_p$ at about 140 km.

Below 80 km, $(\mathbf{u}_p - \mathbf{u}_n)$ and $(\mathbf{u}_e - \mathbf{u}_n)$ are nearly antiparallel.

From 80 to 140 km, $(\mathbf{u}_p - \mathbf{u}_n)$ and $(\mathbf{u}_e - \mathbf{u}_n)$ are nearly perpendicular.

Above 140 km, $(\mathbf{u}_p - \mathbf{u}_n)$ and $(\mathbf{u}_e - \mathbf{u}_n)$ are nearly parallel.

The current density $\mathbf{j}$ can be obtained from (14) and (15) with n_e.

In several kinds of problem, E is then determined by the approximations (7) and (8) together with well posed boundary or periodicit conditions.

Irregularities in electron density due to turbulence—The neutral air tries to carry th ionized gas with it in its motion, but the magnetic field resists the motion of ionized gas acros the lines of force. This effect is exhibited b (13) with $\mathbf{E} = 0$. Then $\mathbf{j}$ has a positive componen in the direction of $\mathbf{u}_n \wedge \mathbf{H}$. Putting this into th right-hand side of (12) shows that the componen of $\mathbf{U}$ in the direction of $\mathbf{u}_n$ is less than $\mathbf{u}_n$. Consequently a solenoidal $\mathbf{u}_n$ can give rise to irregularities in electron density. This is illustrate in Figure 1, in which the sloping lines are line of force. Whereas $\mathbf{u}_n$ is solenoidal, $\mathbf{U}$ is far fron solenoidal, and the ionized gas is being compresse locally. A crude estimate of the strength o the irregularities gives

$$\frac{\delta n_e}{n_e} \sim \frac{\Omega_e\Omega_p}{(\nu_e^2 + \Omega_e^2)^{1/2}(\nu_p^2 + \Omega_p^2)^{1/2}}$$

which seems plausible for this mechanism A more detailed investigation by Howells (i the press) shows that the mechanism is differen when $\Omega_e > \nu_e$ but $\nu_p > \Omega_p$. The irregularitie then depend most on the component of vorticit (curl $\mathbf{u}_n$) parallel to $\mathbf{H}$. It is a little more complicated, however, as can be seen from the simplifie case where the magnetic field is uniform an $(\mathbf{H}\cdot\nabla)\mathbf{u}_n = 0$. Then

$$\text{curl}\,(\mathbf{u}_n \wedge \mathbf{H}) = \mathbf{u}_n\,\text{div}\,\mathbf{H} + (\mathbf{H}\cdot\nabla)\mathbf{u}_n - \mathbf{H}\,\text{div}\,\mathbf{u}_n - (\mathbf{u}_n\cdot\nabla)\mathbf{H} =$$

assuming again that $\mathbf{u}_n$ is solenoidal.

Then $-\nabla\phi = \mathbf{E} = -\mathbf{u}_n \wedge \mathbf{H}/c$, and fror (14) and (15) $\mathbf{u}_p = \mathbf{u}_e = \mathbf{u}_n$ and no irregularitie are produced. In order to get irregularitie some variation of $\mathbf{u}_n$ in the direction of $\mathbf{H}$ i needed. Then $\mathbf{E}$ is no longer perpendicular t $\mathbf{H}$, and, because the conductivity parallel to I is relatively large, a smaller electric field needed to prevent the build-up of space charg The problem is susceptible of a linear treatme and can be discussed in terms of one Fourie component.

A Fourier component—Assume that the u perturbed n_e is uniform and that the irreg larities have $\delta n_e \ll n_e$. Then a linear treatme is permissible neglecting terms with $(\mathbf{u}\cdot\nabla)n$ and it is sufficient to consider a Fourier com

ent varying as exp ($i\mathbf{k}\cdot\mathbf{x}$). We shall use (12) get an approximation for $\partial n_e/\partial t$:

$$/\partial t = -\operatorname{div}(n_e\mathbf{u}_e) \approx -\operatorname{div}(n_e\mathbf{U})$$

$$\approx (m_p\nu_p c)^{-1}\operatorname{div}(\mathbf{j}\wedge\mathbf{H}) \quad (16)$$

m (7)

$$\mathbf{E} = -i\phi\mathbf{k} \quad (17)$$

,

$$j_q = \sigma_{qr}(\mathbf{E} + \mathbf{u}_n \wedge \mathbf{H}/c)_r \quad (18)$$

ere σ_{qr} is a tensor obtainable from (14) and). Equation (8) now requires

$$ik_qk_r\sigma_{qr}\phi = k_q\sigma_{qr}(\mathbf{u}_n \wedge \mathbf{H})_r/c \quad (19)$$

w let $\mathbf{H}$ have the z direction, and let $\mathbf{k}$ be pendicular to the x direction ($k_x = 0$):

$$v(\mathbf{j}\wedge\mathbf{H}) = i\mathbf{k}\cdot\mathbf{j}\wedge\mathbf{H} = -iHk_yj_k \quad (20)$$

$$\sigma_{qr} = \begin{vmatrix} \sigma_1 & \sigma_2 & 0 \\ -\sigma_2 & \sigma_1 & 0 \\ 0 & 0 & \sigma_0 \end{vmatrix}$$

ite (V_x, V_y, V_z) for $\mathbf{u}_n$; $k_yV_y + k_zV_z = 0$. m (18)

$$= \sigma_1V_yH/c + \sigma_2(-i\phi k_y - V_xH/c) \quad (21)$$

from (19)

$$^2\sigma_1 + k_z^2\sigma_0)\phi$$

$$= -(k_yH/c)(\sigma_1V_x + \sigma_2V_y) \quad (22)$$

nce

$$^2\sigma_1 + k_z^2\sigma_0)(-i\phi k_y - V_xH/c)$$

$$= (H/c)(k_y^2\sigma_2V_y - k_z^2\sigma_0V_x)$$

nce from (16), (20), and (21)

$$\approx \frac{-iH^2}{m_p\nu_pc^2}\left\{\left(\sigma_1 + \frac{k_y^2\sigma_2^2}{k_y^2\sigma_1 + k_z^2\sigma_0}\right)k_yV_y - \frac{k_z^2\sigma_0\sigma_2}{k_y^2\sigma_1 + k_z^2\sigma_0}k_yV_x\right\} \quad (23)$$

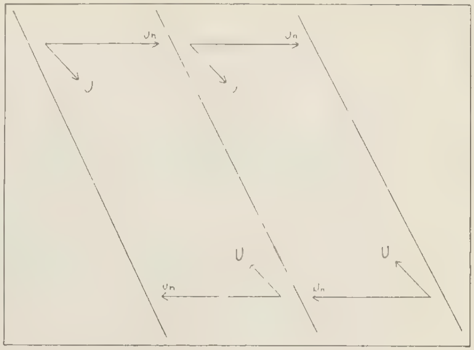

FIG. 1—Effect of shear flow.

The first term on the right-hand side represents the effect described by Figure 1, and the second effect of vorticity parallel to $\mathbf{H}$. The latter is seen to vanish in the simplified case where $k_z = 0$, but so long as k_z is comparable to k_y, (23) may be approximated by

$$\frac{\partial n_e}{\partial t} \sim \frac{-iH^2}{m_p\nu_pc^2}(\sigma_1k_yV_y - \sigma_2k_yV_x) \quad (24)$$

because σ_0 is never less than σ_1.

When $\nu_p \gg \Omega_p$, the contribution of the positive ions to the conductivity can be neglected, and it is found from (15) that

$$\frac{\partial n_e}{\partial t} \sim \frac{n_e\Omega_e\Omega_p}{\nu_p(\nu_e^2\Omega_e^2)}(\nu_ek_yV_y + \Omega_ek_yV_x)$$

When $\nu_p \ll \Omega_p$, the positive ion contribution to σ_1 is most important, giving

$$\partial n_e/\partial t \sim n_ek_yV_y$$

This must lead to strong irregularities with $\delta n_e \sim n_e$, and diffusion should be taken into account by a pressure term in (12). Diffusion is most important at short wavelengths. Howells includes it in his treatment and discusses the spectrum of the irregularities in considerable detail. The spectrum is, of course, important for scattering experiments.

Note on Some Observational Characteristics of Meteor Radio Echoes

P. M. Millman

National Research Council, Ottawa
Ontario, Canada

Abstract—Attention is called to the observational evidence for meteor echoes from portions of the path well removed from the position of minimum range. Fading periods for echoes observed at Ottawa are given.

I should like to call attention to certain experimental results that must be taken into account in any discussion or attempted explanation of meteor radar echoes. Our observational data at Ottawa consist chiefly of range-time records of meteor echoes made with essentially omnidirectional antenna systems at a frequency of 32 Mc/s. Examples of such records are shown in Figures 1 and 2, where time appears as the x coordinate, and range, or distance from the observer, as the y coordinate.

In dealing with the brighter group of visual meteors, objects represented by masses ranging from 0.1 to 10 grams which enter the atmosphere at speeds from 20 to 60 km/sec, it is important to recognize that a radar echo may be recorded from positions on the meteor path well removed from the point where a perpendicular from the observer meets it. In fact, for this group of meteors, observed at the given frequency, there is no particular preference for the position of minimum range in the production of an echo.

The echoes produced from parts of the meteor path well removed from the minimum-range position may appear within small fractions of a second (<0.1 sec) of the passage of the meteor head, but there is a statistical relation giving increasing mean delays of several seconds in the appearance of the echo as we move along the meteor path in either direction away from the position of minimum range.

With the passage of time, an echo, which originally may have been produced from all portions of a sizable segment of a meteor path (10 to 40 km in length), degrades into a number of discrete echoes at specific ranges. These exhibit irregular or semiregular fading, a gradually disappear after durations rangi from 10 to 300 seconds. In other words, so mechanism operates to produce very quickly apparent roughness of the meteor trail th makes possible the nonspecular reflection radio waves at the 10-meter wavelength sca The general features of this nonspecular refl tion appear the same even when the ioniz trail is viewed from several widely diverg directions. [*Millman*, 1950; *Millman and M Kinley*, 1949].

In a study of 6193 meteor echoes recorded 32 Mc/s with high time discrimination dur one 24-hour period at Ottawa, Rao and Millm (unpublished) found semiregular fading peri to be generally present. The echoes were vided on the basis of duration as shown in accompanying tabulation.

Duration, sec	No. of Echoes
<0.2	1558
0.2 to 0.4	2408
>0.4	2227

A frequency distribution of the fading peri for the meteors with durations greater than second gave approximately a Gaussian distri tion with a most probable fading period of (second, or a fading frequency of 20 cps.

References

Millman, P. M., and D. W. R. McKinley, Th station radar and visual triangulation of teors, *Sky and Telescope, 8*, 114–116, 1949.

Millman, P. M., Meteoric ionization, *J. R Astron. Soc. Can., 44*, 209–220, 1950.

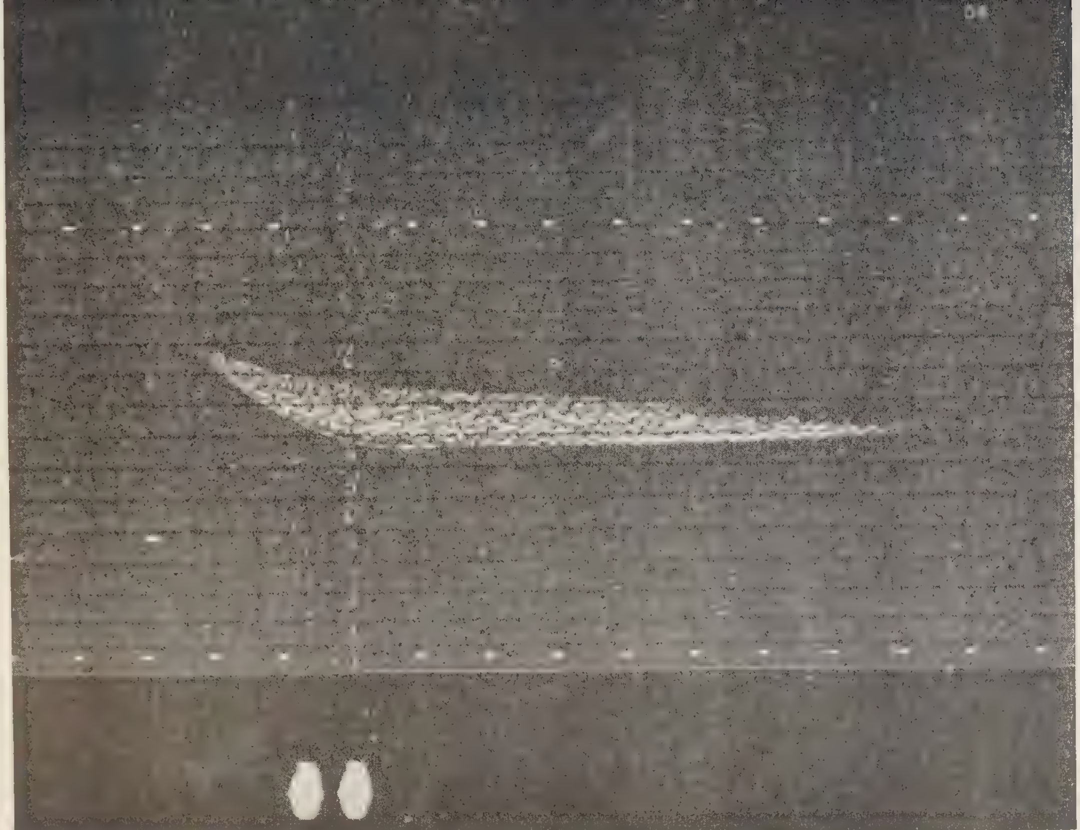

FIG. 1—Meteor echo recorded at 6 hr, 33 min, 57 sec, UT, on December 10, 1958, at the Springhill Meteor Observatory, Ottawa, with the high-powered 32 Mc/s meteor radar. The seconds markers appear along the x coordinate, and 20-km range intervals are indicated in the y coordinate. The echo extends from a range of about 240 km to 170 km, and lasts for 11 seconds. There is indication of a double head echo. The meteor was visually observed as of magnitude −2 and was nonshower. Visual markers appear at the bottom.

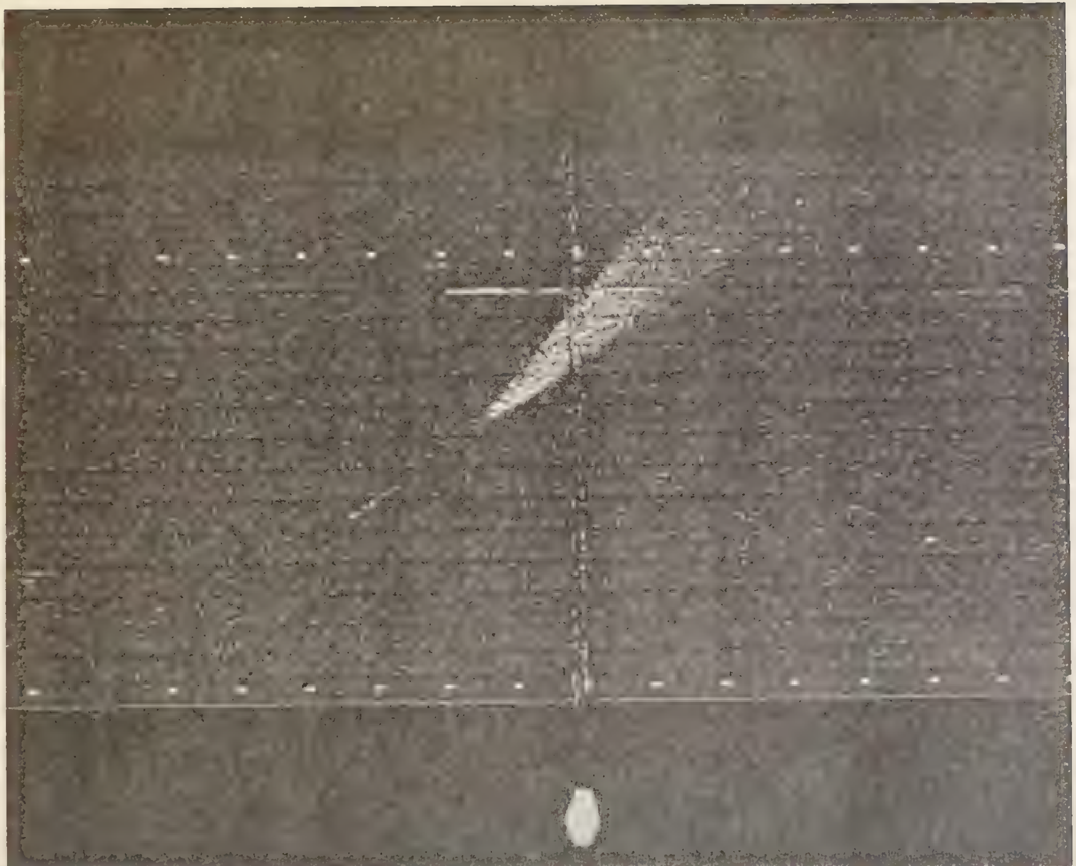

FIG. 2. Meteor echo recorded at 8 hr. 00 min. 32 sec, UT, on December 11, 1958, at the Springhill Meteor Observatory, Ottawa. This echo is remarkable for its extent in range. The head echo starts at a range of 150 km, and the enduring portion of the echo is still faintly visible at the top of the record at a range of 400 km. This meteor

On the Structure of Turbulence in Electrically Neutral, Hydrostatically Stable Layers

H. A. PANOFSKY

Pennsylvania State University
University Park, Pennsylvania

ummary—At levels of the order of 100 ers, in unstable layers smoke from stacks nders both vertically and horizontally, but table layers it meanders horizontally only, a minimum of vertical spreading. Thus, si-horizontal eddies are indicated, in stable rs, with dimensions of the order of 100 ers.

a the 'stable' stratosphere, turbulence is fre- ntly recorded with instruments sensitive to tuations of air speed. According to Clodman published), such turbulence is usually not by the plane crew, indicating the absence of tical gust velocities. Again, quasi-horizontal ies of the same scale are indicated.

'here is also some evidence for larger eddies with large horizontal and small vertical dimensions. This comes from the recorded wind speeds determined in flights across the streamlines of the winds at levels of the order of 13 km. The wind profiles along such flights show irregularities in the horizontal direction, the scale of which is 30 to 60 km, and the magnitude 5 to 10 m sec^{-1}.

In summary, stable layers can be characterized by a whole spectrum of large quasi-horizontal eddies which can be produced by the large-scale variations of mean wind in the horizontal. It is likely that these eddies eventually decay into small, isotropic eddies, but the range of wave numbers within any inertial subrange is presumably small.

On the Similarity of Turbulence in the Presence of a Mean Vertical Temperature Gradient

A. S. Monin

Institute of Physics of the Atmosphere
Academy of Sciences, Moscow, USSR

Abstract—The frequency spectrum of vertical turbulence components is considered in the case of a vertical temperature gradient. Similarity methods are employed, one to describe the energy and inertia ranges, another (Kolmogoroff) to describe the inertia and dissipation ranges. It is proposed that, since both theories hold in the inertia range, a relation can be determined between the two unknown universal functions involved.

Let us consider as an example the time spectrum of vertical velocity $S(\omega)$ (ω = frequency) in the surface layer of the atmosphere. The spectrum can be divided into three parts: energy range, inertia range, and dissipation range. There are two theories of similarity for atmospheric turbulence. The first one is valid for all the spectrum outside the dissipation range. According to this theory, turbulence is determined by the following parameters: friction velocity v_t, vertical turbulent heat flux q (it is more convenient to use $q/c_p\rho$, where c_p = heat capacity, ρ = density), and the Archimedes parameter g/t_0 (g = acceleration of gravity, t_0 = mean temperature). The corresponding scales of length, velocity, and temperature are

$$\left.\begin{aligned} L &= \frac{v_t^3}{n(g/t_0)(-q/c_p\rho)} \\ V &= v_t/n \\ T_t &= -(1/nv_t)(q/c_p\rho) \end{aligned}\right\} \qquad (1)$$

(n = von Kármán constant). Dimensionless characteristics determined by means of scales (1) must be universal functions of dimensionless height $\zeta = z/L$. For instance, the mean wind velocity must have a form

$$U(z) = \frac{v_t}{n}\left[f\left(\frac{z}{L}\right) - f\left(\frac{z_0}{L}\right)\right] \qquad (2)$$

where z_0 = roughness and $f(\zeta)$ = some universal function. According to the energy balance equation the rate of dissipation equals

$$\epsilon = \frac{v_t^3}{nL}[f'(\zeta) - 1] \qquad (3$$

The spectrum $S(\omega)$ will have the form

$$S(\omega) = \frac{v_t^2 z}{U} f_1\left(\frac{\omega z}{U}, \frac{z}{L}\right) \qquad (4$$

Plotting log $[(U/v_t^2z)\ S(\omega)]$ against log $[\omega z/U$ we obtain universal curves for each value of th stability parameter z/L.

The second similarity theory is the we known theory of locally isotropic turbulen by Kolmogoroff. It is valid for the range statistical equilibrium, i.e., for inertia and di sipation range. According to this theory turbu lence is determined by the viscosity ν, by th rate of dissipation ϵ, and (if the temperatu field is taken into account) by $\eta = x\ \overline{(\nabla t}$ (x = the thermal conductivity). In general th Archimedes parameter g/t_0 does influence th structure of turbulence too (Oboukhov ha published an article about it); but we sha neglect the dependence upon g/t_0 here.

Considering the time spectra we must tak into account additionally the mean velocity U because the frequency ω is not an invaria characteristic; it depends upon the mean velocit Without going into the details, we can expre $S(\omega)$ in the inertia range as follows:

$$S(\omega) = \frac{U^4}{\epsilon} f_2\left(\frac{\omega U^2}{\epsilon}\right) \qquad ($$

The function $f_2(x)$ must be universal; it expected to be proportional to $x^{-5/3}$.

In the inertia range we can use both theories [illegible] similarity. Therefore we can obtain the [illegible]ation between universal functions f_1 and f_2 [illegible] equations 4 and 5:

$$f_1(x, \zeta) = \left(\frac{U}{v_t}\right)^2 \frac{U^3}{\epsilon z} f_2\left(\frac{U^3}{\epsilon z} x\right) \qquad (6)$$

[illegible]ere U/v_t and $U^3/\epsilon z$ are some functions of ζ [illegible]cording to equations 2 and 3.

Plotting log $[(\epsilon/U^4)\, S(\omega)]$ against log $(\omega U^2/\epsilon)$ in the inertia range we must obtain a universal curve for all the cases. This curve is expected to be the straight line with the slope $-5/3$.

Both the predictions (4) and (5) are in good agreement with measurements of time spectra of vertical velocity made in the Institute of Physics of the Atmosphere, Academy of Sciences, USSR. In particular the measurements are decisively in favor of the '$-5/3$' law against the '$-3/2$' law for spectrum proposed by Kraichnan.

On the Spectrum of Electron Density Produced by Turbulence in the Ionosphere in the Presence of a Magnetic Field

I. D. Howells

Cavendish Laboratory
Cambridge, England

Abstract—The work described in this paper starts from Dungey's results, and obtains approximate equations for number density of ionization, under the action of turbulence, diffusion, and a magnetic field, in various limiting cases. The principal result is that this mechanism cannot be expected to produce irregularities that are strongly elongated along the magnetic field. A form is obtained for the spectrum function of number density below 140 km.

This paper extends Dungey's work, making use of his model and approximations. The notation is essentially the same, but we use subscripts + and − for ions and electrons, and

$\mathbf{u}$	= neutral gas velocity.
$\mathbf{B}$	= magnetic induction (constant and uniform).
$-\nabla\phi$	= electric field.
γ	= coefficient of ambipolar diffusion.
$\Omega_\pm$	$= eB/m_\pm, \qquad n_+ = n_- = n.$

The equations are (in mks units)

$$m_\pm \nu_\pm(\mathbf{u}_\pm - \mathbf{u}) = \mp e\nabla\phi \pm \mathbf{u}_\pm \times e\mathbf{B} - kT\frac{\nabla n}{n} \qquad (1)$$

$$\frac{\partial n}{\partial t} + \nabla\cdot(n\mathbf{u}_+) = \frac{\partial n}{\partial t} + \nabla\cdot(n\mathbf{u}_-) = 0 \quad (2)$$

which implies

$$\nabla\cdot n(\mathbf{u}_+ - \mathbf{u}_-) = 0 \qquad (3)$$

The idea for solution is to find $\mathbf{u}_\pm$ from (1), and to substitute into (3) to obtain an equation for ϕ in terms of n. Except in special cases, no exact solution for ϕ appears possible; but in certain limiting cases we can obtain simple approximate solutions and estimate their error. The resulting approximate value of $\mathbf{u}_+$ can then be used in the first of (2).

Case I. $\Omega_+ \ll \nu_+$ (heights well below 140 km).

In this case we can state that the ion velocity is close to $\mathbf{u}$, and write

$$\mathbf{u}_+ = \mathbf{u} - \gamma(\nabla n/n) + \mathbf{v}$$

where $\mathbf{v}$ is small compared with $\mathbf{u}$, and can b expressed in terms of $\mathbf{u}$, n, and ϕ. From the firs of (2), the equation for n is then (since $\nabla\cdot\mathbf{u} = 0$

$$\frac{\partial n}{\partial t} + \mathbf{u}\cdot\nabla n + \nabla\cdot(n\mathbf{v}) = \gamma\nabla^2 n \qquad (4$$

If the ionization is initially uniform ($n = n_0$ the term $\nabla\cdot(n\mathbf{v})$ is important because it lead to the production of irregularities. It can b replaced by $n_0\nabla\cdot\mathbf{v}$ (since $n - n_0 \ll n_0$, b Dungey's work), and further approximated as:

$$n_0\nabla\cdot\mathbf{v} \simeq \begin{cases} n_0\dfrac{\Omega_+\Omega_-}{\nu_+\nu_-}\dfrac{\partial u_3}{\partial x_3} & \text{if} \quad \Omega_- \ll \nu \\ n_0\dfrac{\Omega_+}{\nu_+}\left(\dfrac{\partial u_2}{\partial x_1} - \dfrac{\partial u_1}{\partial x_2}\right) & \text{if} \quad \Omega_- \gg \nu \end{cases}$$

taking the 3-axis in the direction of $\mathbf{B}$.

But, for the distortion of irregularities onc they have been produced, the term $\nabla\cdot(n\mathbf{v})$ not important, and they rapidly lose any direc tional dependence that they acquired in the production. Extending the idea of an equilibriu range we find that the spectrum function proportional to

$$n_0^2\left(\frac{\Omega_+\Omega_-}{\nu_+\nu_-}\right)^2 \quad \text{or} \quad n_0^2\left(\frac{\Omega_+}{\nu_+}\right)^2,$$

and that the only other parameters are those the turbulence: the energy dissipation ϵ, an the kinematic viscosity (Prandtl number $\simeq\frac{1}{2}$ Thus, in the inertial subrange the form of th spectrum function $\Gamma(k)$ [*Batchelor*, 1959], must b

$$\Gamma(k) \propto \begin{cases} \left(\dfrac{\Omega_+\Omega_-}{\nu_+\nu_-}\right)^2 n_0^{\,2} k^{-1} & \text{if} \quad \Omega_- \ll \nu_- \\ \left(\dfrac{\Omega_+}{\nu_+}\right)^2 n_0^{\,2} k^{-1} & \text{if} \quad \Omega_- \gg \nu_- \end{cases}$$

In approximate calculation gives 10 per cent or the departure from isotropy.

If there is a gradient of ionization density, he extra contribution to the spectrum is the ame as if there were no magnetic field, and in articular will show a $k^{-5/3}$ variation in the nertial subrange. It is possible that the k^{-1} law ould be dominant, especially at the greater eights.

Case II. $\Omega_+ \gg \nu_+$ (heights above 140 km).

The charged particles now move approximately long the magnetic lines of force, and the equation is found to be approximately

$$\frac{\partial n}{\partial t} + \frac{\partial(nu_3)}{\partial x_3} + \frac{\nu_+}{\Omega_+}\left(u_2 \frac{\partial n}{\partial x_1} - u_1 \frac{\partial n}{\partial x_2}\right) = \gamma \frac{\partial^2 n}{\partial x_3^{\,2}} + \gamma\left(\frac{\nu_+}{\Omega_+}\right)^2\left(\frac{\partial^2 n}{\partial x_1^{\,2}} + \frac{\partial^2 n}{\partial x_2^{\,2}}\right) \quad (5)$$

If we start with no large gradients, the last term on each side of the equation can be neglected. Irregularities can now be produced by the $\partial(nu_3)/\partial x_3$, and they will be of fractional order unity. Consideration of the movement of Fourier components in wave-number space indicates that greatly elongated irregularities will not be produced (and so the neglected terms need never be introduced). A reasonable upper limit for possible elongation should be 2 to 1.

These arguments do not preclude the existence of strongly elongated irregularities, at any height, but indicate that they cannot be produced by the usual kind of turbulence.

A more complete account of this work is to be published.

Reference

Batchelor, G. K., Small-scale variation of convected quantities like temperature in turbulent fluid, *J. Fluid Mech., 5,* 113–133, 1959.

Evidence of Elongated Irregularities in the Ionosphere

B. Nichols

Cornell University
Ithaca, New York

Abstract—Radio observations of backscatter from ionospheric irregularities under both auroral and nonauroral conditions indicate the presence of small-scale irregularities, elongated along the earth's magnetic field. These elongated irregularities have been found at heights from 80 to 300 km. The most precise measurements available are related to echoes from auroral ionization at a height of about 100 km. These indicate scales of tens of meters along the earth's magnetic field and tens of centimeters normal to the field.

Introduction—Radio observations in recent years have provided strong evidence of the existence of irregularities in electron density in the ionosphere that are elongated in the direction of the earth's magnetic field. This paper briefly summarizes that part of the evidence that has been obtained by backscatter radar measurements at radio frequencies above the critical frequency of the ionospheric layers. In all cases only a small fraction of the transmitted energy is scattered back to the receiver by the irregularities. The echoes received are spread in range as compared with the transmitted pulse and have probability amplitude distributions of the Rayleigh type—as would be expected if the echoes were being received by scattering from many irregularities adding in random phase.

The theory of radio scattering from small irregularities has been discussed by *Booker* [1959]. Regardless of the mechanism responsible for their production, the irregularities mainly responsible for *backward* scatter will have a scale size equal to the radio wavelength divided by 4π and will be oriented in a direction perpendicular to the direction of incidence of the radio beam. Since the observations described here have been made at wavelengths from 0.5 to 15 meters, they give evidence about the small-scale irregularities of electron density in the ionosphere.

Information about the irregularities can be obtained, of course, only when they are large enough to give detectable echoes. At times of aurora the irregularities are strong, and considerable information on the character of echoes from auroral ionization has been obtained. There are other occasions when backscatter echoes are obtained in the absence of any of the other phenomena usually associated with aurora. Accordingly, this brief survey considers both the data from auroral echoes and the data from what for present purposes will be called "nonauroral" echoes.

Auroral echoes—The most striking feature of radio echoes from auroral ionization is that the incident radio beam must be directed almost perpendicular to the earth's magnetic field at the height concerned. This fact in itself shows that the small-scale irregularities are elongated along the earth's magnetic field. Unfortunately, this perpendicularity requirement limits our knowledge of the extent of the ionization, since at high latitudes—where the aurora is most common—the heights at which perpendicularity can be achieved lie in the range 80 to 130 km.

Although auroral echoes have been investigated at many frequencies, the most precise statements can be made as a result of measurements at wavelengths less than a meter [*Presnell, Leadabrand, Dyce, Schlobohm, and Berg*, 1959; *Fricker, Ingalls, Stone, and Wang*, 1957; *Chapman, Blevis, Green, and Serson*, 1957]. At such short wavelengths it has been possible to use highly directive antennas and to determine quite closely the heights and angles involved. It has been found that it is not necessary to direct the radio beam exactly perpendicular to the earth's magnetic field, but the perpendicularity requirement becomes more stringent as the frequency is increased. The degree of aspect

nsitivity involved can be explained if the irgularities responsible for these echoes have mensions of the order of some tens of meters ong the magnetic field and some tens of centieters across the magnetic field. At College, laska [*Presnell and others,* 1959], two kinds of hoes have been observed. One type, seen ainly at night, comes from a relatively rericted region of space, from single or multiple iroral arcs. A second type, seen mainly during ie day, appears to arise from ionization that is latively homogeneous over a wide region of pace (500 by 800 km in extent).

At relatively low geomagnetic latitudes it is ossible to achieve perpendicularity with the irth's magnetic field at higher altitudes, but ie number of occasions on which aurora can be oserved at these latitudes is small. However, n several occasions [*Schlobohm, Leadabrand, yce, Dolphin, and Berg,* 1959], at a wavength of about 3 meters, auroral echoes have een observed from a geomagnetic latitude of 3°. The heights of the irregularities responsible or the echoes lay between 200 and 300 km. ince the requirement of perpendicularity was reserved, it is clear that elongated irregularies exist in that height range as well as at eights near 100 km.

The times of occurrence of auroral echoes orrelate closely with magnetic disturbances, nd the drift motions of the irregularities in onization bear a close relation to the ionospheric urrent system [*Nichols,* 1959] The speeds of hese motions, however, are a power of 10 faster han the usual speeds measured in the ionophere. On the other hand, the echoes from ieteor trails occurring in the same region as the urora indicate that the drift motions in the ieteor trail have their normal value [*Bowles,* 955]. The fast drift speeds of the auroral onization are probably caused by the increased lectric fields that drive the current system reponsible for the magnetic disturbances.

Nonauroral echoes—Aspect-sensitive radio choes from the ionosphere have also been oberved at times when no other indication of urora was present [*Leadabrand,* 1955; *Gallaher,* 1956; *Weaver,* 1958]. The aspect sensiivity observed has the same character as that lescribed for auroral echoes; i.e., the echoes are btained only from regions where the radio beam is approximately perpendicular to the earth's magnetic field. The measurements have been made at longer wavelengths (10 to 20 meters), and the broad antenna beams involved make it difficult to state precisely the heights of the irregularities responsible for the backscatter. However, the heights are found to lie within the E and F layers of the ionosphere.

The echoes observed occurred quite regularly, and at Stanford could be detected nearly every night. The occurrence of the echoes had little correlation with geomagnetic disturbances. The F-region echoes were quite closely associated with the appearance of spread F. The E-region echoes correlated closely with sporadic-E activity. In all cases the irregularities responsible for the backscatter must have been considerably elongated along the earth's magnetic field to explain the aspect sensitivity observed, although the exact dimensions are not known. The relative speeds of the irregularities [*Gallagher,* 1956] were about 45 m/sec, much slower than those found in auroral echoes.

Echoes of a similar type have been observed in Texas [*Heritage, Weisbrod, Fay, and Morgan,* 1959]. There a wavelength of 1.5 meters was used, and echoes were observed at receivers separated from the transmitter. The scattered signals were observed only from receiving sites that approached or corresponded to the position for specular transmission from ionization elongated along the lines of the earth's magnetic field.

References

Booker, H. G., Radio scattering in the lower ionosphere, *J. Geophys. Research, 64,* 2164–2177, 1959.

Bowles, K. L., Some recent experiments with VHF radio echoes from aurora and their possible significance in the theory of magnetic storms and auroras, *School of Elec. Eng., Cornell Univ., Research Rept. E. E. 248,* Ithaca, N. Y., 1955.

Chapman, J. H., B. C. Blevis, F. D. Green, and H. V. Serson, *Defence Research Telecommunications Establishment, Rept. 44-2-1,* Ottawa, 1957.

Fricker, S. J., R. P. Ingalls, M. L. Stone, and S. C. Wang, UHF radar observations of aurora, *J. Geophys. Research, 62,* 527–546, 1957.

Gallagher, P. B., Analysis of a new type of radio scattering from the ionospheric E-region, *Radio Propagation Lab. Stanford Univ., Tech. Rept. 107,* Stanford, Cal., 1956.

Heritage, J. L., S. Weisbrod, W. J. Fay, and L. A. Morgan, Further aspects of 200-Mc H-scatter signals, *Paper Presented at Spring Meeting of URSI,* Washington, D. C., May 4–7, 1959.

Leadabrand, R. L., Radio echoes from auroral ionization detected at relatively low geomagnetic latitudes, *Radio Propagation Lab., Stanford Univ., Tech. Rept. 98,* Stanford, Cal., 1955.

Nichols, B., Auroral ionization and magnetic disturbances, *Proc. IRE, 47,* 245–254, 1959.

Presnell, R. I., R. L. Leadabrand, R. B. Dyce, J. C. Schlobohm, and M. R. Berg, VHF and UHF auroral investigations at College, Alaska, *Stanford Research Inst., Final Rept., Part I, Contract AF 30(602)-1762,* Menlo Park, Cal., 1959.

Schlobohm, J. C., R. L. Leadabrand, R. B. Dyce, L. T. Dolphin, and M. R. Berg, High-altitude 106.1-Mc radar echoes from auroral ionization detected at a geomagnetic latitude of 43°, *Stanford Research Inst., Final Rept., Part II, Contract AF 30(602)-1762,* Menlo Park, Cal., 1959.

Weaver, P. F., Interpretation of some backscatter echoes in terms of field-aligned irregularities in the F region, *School of Elec. Eng., Cornell Univ., Research Rept. E. E. 389,* Ithaca, N. Y., 1958.

Geomorphology of Spread F and Characteristics of Equatorial Spread F

R. W. H. Wright

University College of Ghana
Achimota, Ghana

Abstract—Between magnetic latitudes 20°N and 20°S there is a well defined region where spread F is a normal occurrence on magnetically quiet days. Equatorial spread F is a night-time phenomenon that begins between 1900 and 2200 by a characteristic doubling of the layer and an increase in virtual height, indicating a vertical velocity. Later in the night, after 2300, the records show group retardation and no stratification. The occurrence of equatorial spread F is decreased by magnetic activity.

Radio-star scintillations in equatorial regions are correlated strongly with spread F and have the same diurnal variation and the same anticorrelation with magnetic activity. The phenomenon of 'flutter' (rapid fading of long-distance, high-frequency stations) shows the same variations. Measurements using the spaced receiver method indicate that, in the equatorial region, the irregularities in the F layer are greatly elongated along the lines of the earth's magnetic field.

Four examples of typical equatorial spread F records are shown in Figure 1. The first two of these are typical of equatorial spread F soon after it is formed. It is characterized by: (1) no signs of group retardation at all; (2) stratifications; (3) no well defined minimum height; (4) wide spread in both heights and frequency; (5) usually occurring between 1900 and 2200. The second two are typical of records observed later in the night and are characterized by: (1) group retardation visible but wide spread particularly at higher frequencies; (2) sharply defined minimum height; (3) no stratification; (4) usually occurring from 2300 onward.

Dr. Bowles of the C.R.P.L. would only refer to the early night type shown by the first two records as true equatorial spread F. They are treated here merely as the same type. The first type is very likely produced by irregularities at the bottom of the F layer, and the second by irregularities near the nose or maximum of the layer.

Figure 2 shows a series of records illustrating the behavior of reflections from the layer as spread F develops. It will be seen that the layer doubles before the spread echoes develop. This is almost inevitable before spread F, echoes being reflected from a layer tilt that develops just before spread F occurs. Hence a vertical velocity of the layer is indicated. This is shown more clearly in Figure 3, which shows how the minimum virtual height of the F layer varies with time on days when spread F develops, and also on days when no spread F develops. It should be emphasized that these are virtual heights only. True heights were not available; also, in the presence of spread F it is very difficult to determine true heights. The way in which spread F develops on the days when it does occur is shown in the bottom curve, based upon a quantitative estimate of the degree of spread F on a scale of 3. The middle graph shows the difference of heights on F and non-F days. It is clear that there is a greater rise of the bottom of the F layer on days on which spread F develops. This could be due to: (1) vertical drift of ionization, (2) eating away of the bottom of the layer by a recombination process; (3) a large divergence of the horizontal velocities in the lower layers. The second possibility is ruled out, as it would be even greater at the lower levels that exist on days when spread F does not occur. The first process seems by far the most likely. It appears to fit in nicely with Dr. Martyn's mechanism for the production of spread F underneath the layer at 1900 when the layer is rising. Later, when the layer starts to come down and the bottom of the layer be-

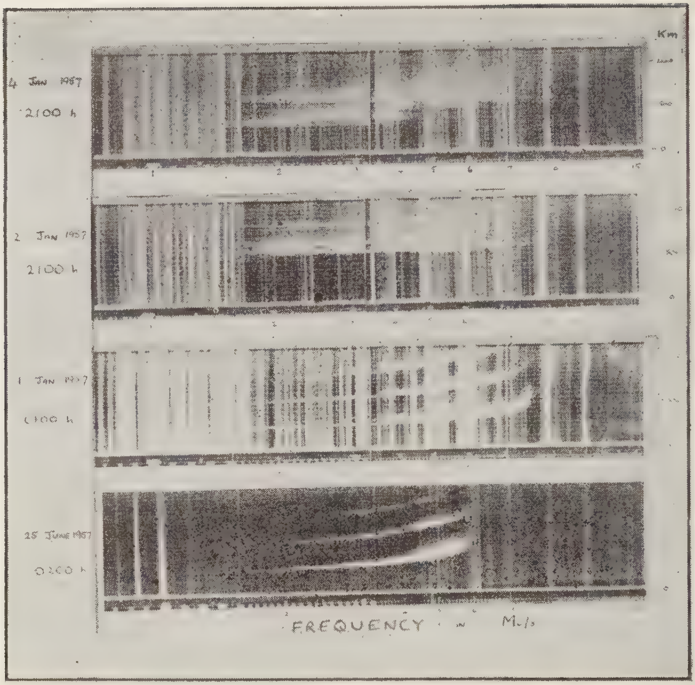

Fig. 1—Typical equatorial spread F records.

comes stable and sharply defined again, spread F is observed only at the nose or maximum of the layer.

We can now turn to the geomorphology of the spread F. We have taken the magnetically quiet days during the month of September and have examined the *routine reductions* of the records for as many stations as possible. Figure 4 shows the occurrence of spread F plotted against magnetic dip. It is important to note here the very great risks involved in using the routine reductions, as Briggs has shown. However, an amazingly consistent picture comes out from the graph. It is clear that in the regions between magnetic dip 40°S and 40°N or magnetic latitudes 20°N and 20°S there is a well defined region where spread F is a normal occurrence on quiet days. This we may call the equatorial belt of spread F. It is worth noting that at very high latitudes, also, there is evidence that spread F occurs on quiet days. As these stations are near the auroral zone it is possible that even on 'quiet days' the conditions are magnetically fa from undisturbed.

It may be relevant to consider that th equatorial type of sporadic E occurs in a bel between 5°N and 5°S magnetic latitude.

We have also observed that at equatorial sta tions the occurrence of spread F is reduced o magnetically disturbed days. In temperat latitudes the position is reversed. Figure shows this for all the stations examined in Fig ure 4 and illustrates that in the same belt fron 20°S to 20°N magnetic latitude the occurrenc of spread F is *decreased* by magnetic activity Outside this belt the reverse is true. Magneti storms therefore act to prevent the formatio of equatorial spread F.

There is some evidence that the rise in heigh of the F layer on quiet days at 1900 is limited t a similar belt. Equatorial sporadic E is also de creased on magnetically disturbed days.

Up to this point we have really considere spread F only. Radio-star scintillation is a fu

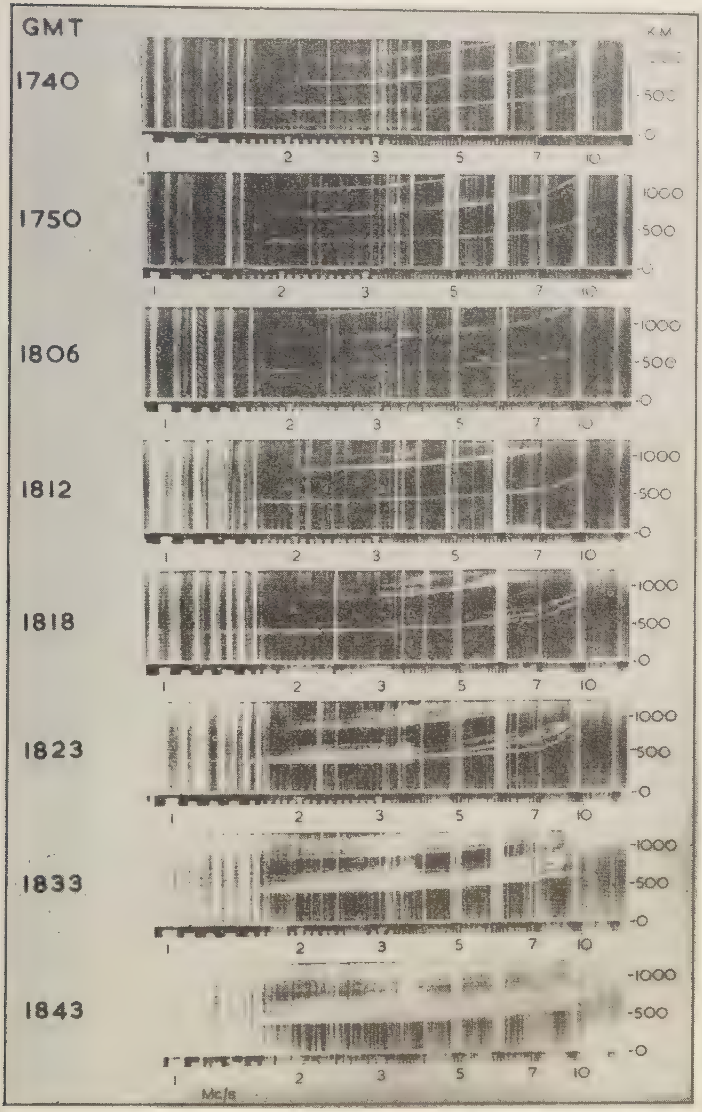

FIG. 2—Records of the behavior of reflections from the F layer as spread F develops.

ther phenomenon that has been observed in equatorial regions. It has the following properties:

1. Its diurnal variation is the same as that of spread F.

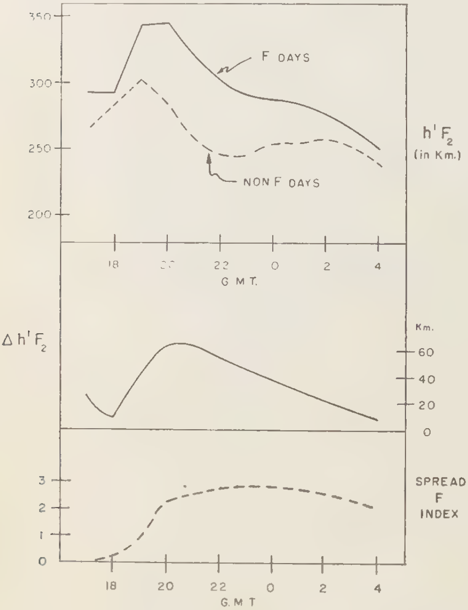

FIG. 3—Variation of the minimum virtual height of the F layer with time, on F and non-F days.

2. It is very strongly marked at the equato In fact, the scintillations are often so strong 50 Mc/s that all evidence of the presence of strong radio star may be scintillated out.

3. It is strongly anticorrelated with magnet activity, especially at sunspot maximum. Ma netic storms reduce the likelihood of scintill tions, and scintillation is a normal phenomen on quiet days. It also correlates strongly wi spread F.

We have also recorded in Accra, West Afric the signal strength of the BBC stations on and 21 Mc/s. The phenomenon known as flutt is observed, starting around 1900 and diminis ing considerably by midnight. It is a rapid fa ing of the signal of about 10 to 40 cycles/se The quality of the signal is ruined. The effect strongly correlated with spread F, and antico related with magnetic activity. During a ma netic storm the quality of the signal received considerably improved.

Finally, the irregularities in the F layer ha been examined by the three-spaced-receive method. A full analysis of the fading patter indicates that the diffraction pattern on th ground has irregularities that are elongated a curately along the magnetic meridian with a axial ratio of 11 to 1. An important fact in th connection is that the measurements made Walthair and Singapore using the same meth do not appear to show anything like th

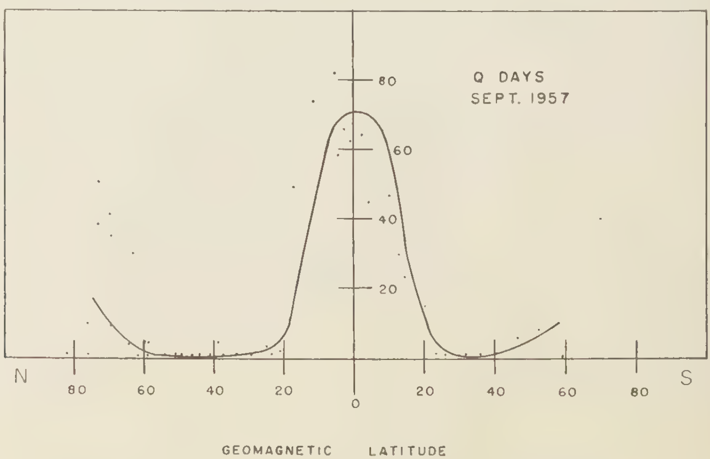

FIG. 4—Occurrence of spread F plotted against magnetic dip.

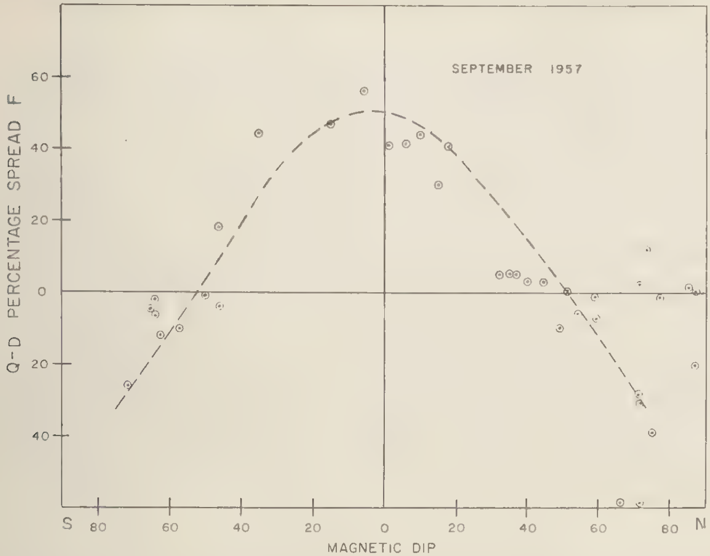

FIG. 5—Relative occurrence of spread F on magnetically quiet and disturbed days.

ongation. Both these stations are approximately at 10°N magnetic latitude. If those measurements are correct, the phenomenon of large horizontal elongation along the lines of force in the equatorial region is limited to a very narrow belt.

Journal of Geophysical Research Volume 64, No. 12 December, 19

Eddy Diffusion and Its Effect on Meteor Trails

J. S. Greenhow

Jodrell Bank Experimental Station
University of Manchester, England

Abstract—Information about the small-scale turbulence at heights near 90 km has been obtained from photographic meteor trails. The time constant of the smallest eddies is found to be approximately 30 sec, and the turbulence power to be 70 ergs g^{-1} sec^{-1}.

The effects of eddy diffusion on meteor trails at heights of about 90 km have been investigated by making use of the visual and photographic observations summarized by Millman. Trail radii, defined as the standard deviation r of an assumed Gaussian distribution of intensity acros any diameter, have been estimated. The resul are shown in Figure 1, together with the theo retical variation of r for various values of amb polar diffusion and eddy diffusion. AG is th

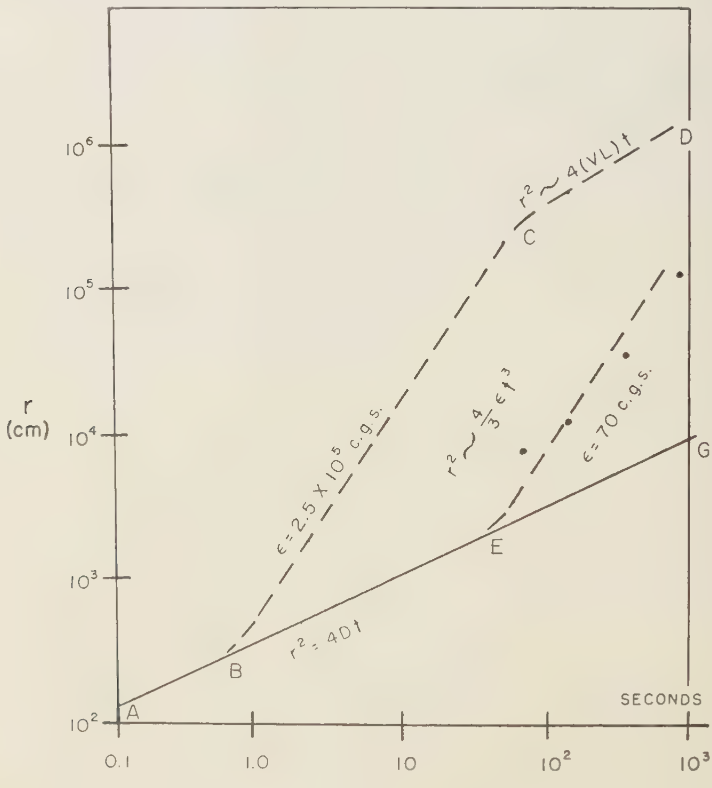

Fig. 1—Trail radius r as a function of time.

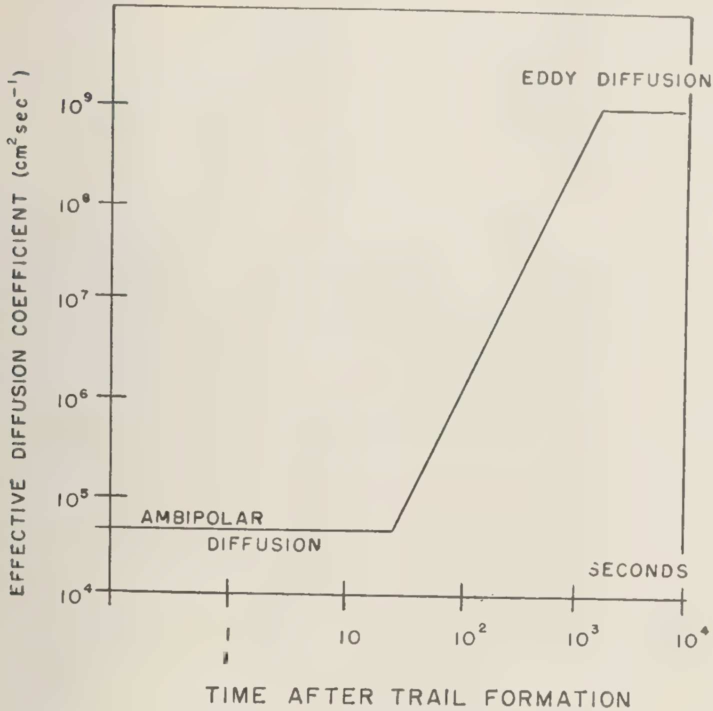

FIG. 2—Effective diffusion coefficient as a function of time.

riation expected for ambipolar diffusion given ove by $r^2 = 4Dt$ (for $D = 4 \times 10^4$ cm² $^{-1}$). *ABCD* is the variation expected for nogeneous turbulence with a turbulence power $\epsilon = 2.5 \times 10^5$ ergs g^{-1} sec^{-1} [deduced by *oker and Cohen,* 1956]. After a time $t_1 = 0.4$, the time constant of the Kolmogorov small-le turbulence, the trail radius begins to in-ease in the manner $r^2 = 4/3\ \epsilon t^3$ up to a time the time constant of the large-scale turbu-ce. After this time the radius once more in-ases in the manner $r^2 = 4D_e t$. D_e is the eddy fusion coefficient $D_e = VL$, where V and L the velocity and scale associated with the ge-scale turbulence. The measured values of are also shown in the figure. These points lie ich more closely on the line *EF,* which cor-ponds to turbulence power of only 70 ergs g^{-1} sec^{-1}. They also give a value of 30 sec for the time constant of the small-scale turbulence, leading to a small-scale dimension of 20 m and velocity of 0.7 m sec^{-1}. The variation of effective diffusion coefficient with time after trial formation is given in Figure 2. If the large-scale turbulence has a time constant of the order 10^3 sec, as indicated earlier, the effective diffusion coefficient would increase from the ambipolar value of 4×10^4 cm² sec^{-1} at a time of 30 sec to the eddy diffusion coefficient of 10^9 cm² sec^{-1} at a time of 1000 sec.

REFERENCE

BOOKER, H. G., AND R. COHEN, A theory of long duration meteor echoes based on atmospheric turbulence with experimental confirmation, *J. Geophys. Research, 61,* 707–733, 1956.

An Interpretation of Certain Ionospheric Motions in Terms of Atmospheric Waves

C. O. Hines

Defence Research Board, Ottawa, Canada

Abstract—Internal atmospheric waves, subject to gravitational and compressional forces, have characteristics in close accord with measurements of ionospheric motions revealed by meteor trails. They are also consistent with other types of observational evidence on movement in the ionosphere. Many of the observations may therefore find their proper interpretation in terms of these waves.

Adiabatic internal gravitational waves in a nonviscous compressible isothermal atmosphere are governed by the dispersion equation

$$\omega^4 - \omega^2 C^2(K_x^2 + K_z^2) + i\gamma g\omega^2 K_z + (\gamma - 1)g^2 K_x^2 = 0 \qquad (1)$$

where C is the speed of sound, γ the ratio of specific heats, g the acceleration due to gravity, ω the circular wave frequency, K_x the horizontal propagation number, and K_z the vertically upward propagation number. The last three quantities derive from an assumed form of solution

$$(\rho - \rho_0)/\rho_0 \propto (p - p_0)/p_0 \propto U_x \propto U_z \propto \exp i(\omega t - K_x x - K_z z)$$

in which ρ is the density, ρ_0 its unperturbed value, p the pressure, p_0 its unperturbed value, U_x the horizontal component of atmospheric velocity, and U_z the corresponding vertical component. Both ρ_0 and p_0 vary as $\exp -\gamma gz/C^2$. One permitted solution of the dispersion equation is $K_x = k_x$ (real) and $K_z - i\gamma g/2C^2 = k_z$ (real), with

$$\omega^4 - \omega^2 C^2(k_x^2 + k_z^2) - \gamma^2 g^2 \omega^2/4C^2 + (\gamma - 1)g^2 k_x^2 = 0 \qquad (2)$$

Thus a solution of the basic equation exists in which $(\rho - \rho_0)/\rho_0$, $(p - p_0)/p_0$, U_x, and U_z all have an exponential growth with height, being proportional to $\exp \gamma gz/2C^2$, and in this solution mean wave-energy density and flux are independent of height. The phase variations are governed by (2). [See *Hines*, 1955, 1956, for th basic relations and derivation.]

These solutions correspond in their propertie to the large-scale motions revealed by meteo trails. At the appropriate periods (~100 mir from the observations of J. S. Greenhow an E. L. Neufeld, this symposium) and vertical scale sizes (~6 km, from the same and othe sources), equation 2 leads to the conclusio $k_z \sim 18k_x$ (for $C = 300$ m/s, $g = 9.5$ m/s²) which indicates that the horizontal structur size is of the order 18×6 km $= 108$ km, con sistent with Greenhow and Neufeld's observa tions. Associated equations show that $U_x \sim 18U$ which is also consistent with the anisotropy o motion revealed by meteors. Finally, the ex ponential growth with height predicted by th theory is consistent with available meteor data particularly with the photographic data o *Liller and Whipple* [1954].

Viscous effects tend to damp out waves whos scale size is sufficiently small. At periods of 10 min, at the 90-km level, this would occur at scale size of the order of 1 km. Smaller scal sizes could occur at higher frequencies, but thes could not be much less than a few hundre meters at the 90-km level. The minimum per mitted scale increases with height, and this con clusion too is in accord with the observations o *Liller and Whipple* [1954].

The same type of wave could be responsibl for the wavelike irregularities revealed by noc tilucent clouds, although the pertinent period there are only of the order 5 min.

The same type of wave might also be relevan in the explanation of E- and F-region 'drift

easurements. They would provide an irregular attern of ionization variation, if enough modes ere superimposed, and this might be expected exhibit random velocities in a drift analysis. addition to the random motions of the pat- ern, the velocity of any very-long-period mo- on (such as that of the tides) would be ex- ected to be superimposed. This would over- ome the difficulty, stressed by Mr. Ratcliffe at is meeting, which arises in interpreting the bserved linking-together of 'meteor' and 'drift' easurements of tidal winds.

Finally, these same waves seem likely to pro- ide the mechanism that produces large-scale raveling disturbances. The wave numbers and eriods associated with such disturbances are onsistent with the dispersion equation quoted bove. The associated ionization variations vould be strongly influenced by the magnetic ield, and must be examined in detail. Previous implified examinations [*Hines*, 1955, 1956], ased on the possibility of a resonance motion, do not now appear to be particularly pertinent, and a more thorough analysis has been initiated. t should lead to a new set of preferred wave arameters, which can then be compared with he observed parameters.

At meteor heights, the observed velocities of atmospheric motion produce nonlinear forces of about one-tenth the magnitude of the strongest inear forces. This suggests that wave interaction may be strong at those levels, and it can be speculated that a cascade process of energy transfer exists in the wave sequence analogous to that considered in turbulence theory.

Two sources of energy can be thought of readily. If the cascade process does work, the known atmospheric tides might provide the energy input end of the wave sequence. Otherwise, it seems necessary to look for a source in the lower atmosphere, with energy propagation upward (phase propagation downward). Since the amplitude grows with height, only small amplitudes ($\sim$1 cm/sec in velocity) need be sought in the lower atmosphere.

These waves have been discussed briefly elsewhere [*Hines*, 1955, 1956, 1959*a*, 1959*b*] and will be described more fully in a forthcoming paper.

References

Hines, C. O., Hydromagnetic resonance in ionospheric waves, *J. Atmospheric and Terrest. Phys.*, *7*, 14–30, 1955.

Hines, C. O., Electron resonance in ionospheric waves, *J. Atmospheric and Terrest. Phys.*, *9*, 56–70, 1956.

Hines, C. O., Turbulence at meteor heights, *J. Geophys. Research*, *64*, 939–940, 1959*a*.

Hines, C. O., Motions in the ionosphere, *Proc. IRE*, *47*, 176–186, 1959*b*.

Liller, W., and F. L. Whipple, High altitude winds by meteor-train photography, in *Rocket Exploration of the Upper Atmosphere*, edited by R. L. F. Boyd and M. J. Seaton, special supplement to *J. Atmospheric and Terrest. Phys.*, *1*, Pergamon Press, London, 1954.

On the Influence of the Magnetic Field on the Character of Turbulence in the Ionosphere

G. S. GOLITSYN

Institute of the Physics of the Atmosphere,
Academy of Sciences,
Moscow, USSR

Abstract—The influence of the earth's magnetic field on the character of turbulence in the ionosphere is considered on the basis of the equations of magnetohydrodynamics. The estimates given show that its influence in the lower ionosphere up to heights of 150 to 200 km can be neglected. At heights greater than 200 km the influence of the earth's magnetic field must be considered in the dynamics of the medium. The fact that the gases are highly rarefied constitutes an additional problem in formulating a theory of turbulence for the upper regions of the ionosphere. It is shown here that the ratio of Kolmogoroff's inner scale of turbulence to the mean free path of neutral molecules decreases with the decrease in number of particles n as $n^{1/4}$, reaching the value of the order 30 or less at the height of 250 km. Therefore, the theory of turbulent motions at such heights should not entirely neglect the molecular structure of the medium.

A great variety of physical conditions is characteristic of the upper atmosphere along the vertical. At a height of 80 to 100 km and above, the atmosphere becomes noticeably conductive and various processes there begin to be influenced by the earth's magnetic field. In the present paper we consider the question of the influence of the magnetic field on the nature of turbulent motions in the ionosphere. It seems reasonable for this purpose to use the equations of magnetohydrodynamics for an incompressible viscous fluid:

$$\frac{\partial \mathbf{v}}{\partial t} + (\mathbf{v}\nabla)\mathbf{v} = -\frac{\nabla p}{\rho} + \frac{1}{4\pi\rho}[\text{rot }\mathbf{H}\cdot\mathbf{H}] + \nu\Delta\mathbf{v} \quad (1)$$

$$\frac{\partial \mathbf{H}}{\partial t} = \text{rot }[\mathbf{vH}] + \nu_m\Delta\mathbf{H} \qquad \nu_m = c^2/4\pi\sigma \quad (2)$$

$$\text{div }\mathbf{v} = 0 \quad (3)$$

$$\text{div }\mathbf{H} = 0 \quad (4)$$

The parameter ν_m is the so-called magnetic viscosity, which is inversely proportional to the conductivity of the medium σ (in the Gaussian system of units the dimension of σ is equal to sec^{-1}). The remaining notation is the conventional one.

Let us consider some consequences of thes equations. Given the characteristic scale c motion L and the characteristic velocity U the ratio of terms on the right side of equatio 2 has the order of magnitude

$$UL/\nu_m = R_m \quad (5$$

The number R_m is the so-called magnetic Reyn olds number. It is useful to keep in mind i connection with the Reynolds number of hydro dynamics:

$$R_m = R(\nu/\nu_m) \quad (5$$

If, for the kind of motion considered, R_m much greater than unity, the term of equatio 2 describing the dissipation of fields can b neglected and the well known theorem abou frozen-in fields is valid. According to th theorem, movements of the force lines of th magnetic field are impossible with respect t the medium. The field then has the same chang of scale as the other quantities. The role of th field in the dynamics of the medium can b characterized (see equation 1) by a parameter

$$\eta = H^2/8\pi p \quad ($$

The influence of the field is negligible if $\eta \ll$

Let us consider the second extreme case whe $R_m \lesssim 1$. In equation 2 the term describing th

ssipation of the field due to finite conductivity ceeds the one describing the inductional crease of the field due to the movements in e fluid. Here the change of scale of the field determined mainly by the conductivity of e fluid and is equal, in order of magnitude, to $= \nu_m/U$. Let us estimate the influence of the ld here. In the Navier-Stokes equation the rm ∇p is of the order of magnitude p/L; the rm $(1/4\pi)$[rot $\mathbf{H}\cdot\mathbf{H}$] is of the order $H^2/8\pi L_1 =$ $U/8\pi\nu_m$; and their ratio is equal to the number

$$K = H^2UL/8\pi\nu_m p = \eta R_m \qquad (7)$$

ne influence of the magnetic field is negligible $K \ll 1$.

We turn now to a consideration of turbulence a conductive medium in the presence of a agnetic field. If the influence of the field on e minimum scales of turbulence is not imrtant, it may be assumed that dissipation of rbulent energy is the result of the effect of scosity. The small-scale turbulence will then of the usual character and will be similar to ual atmospheric turbulence. For the inner inimum) scale of turbulence l_0 in a well veloped turbulent flow, the Reynolds number l_0/ν is equal to unity in order of magnitude. this case condition 5 becomes

$$\nu/\nu_m \gg 1 \qquad (8)$$

hen $\eta \ll 1$ the influence of the field can be glected. If η is greater than unity, or has this der of magnitude, the usual representation of e theory of turbulence can be expected to se its validity, since in this case the strong agnetic field stabilizes the movements at ales greater than l_0.

Let us consider a medium with poor conducvity. The influence of the field on turbulence, obtained from condition 5, is not essential if

$$\nu\eta/\nu_m \ll 1 \qquad (9)$$

The criteria 8 and 9 have been applied to the real conditions of the upper atmosphere for the purpose of clarifying the question whether the earth's magnetic field influences the character of turbulence. The results for different heights are shown in Table 1. The magnetic field was assumed to be 0.5 gauss in these estimates. The rest of the quantities, approximated to the first significant figure, were taken from *Mitra* [1952]. The latest data obtained from rocket and sputnik measurements were not used in our estimates as they would not change our results essentially. From Table 1 it is seen that up to a height of about 200 km the earth's magnetic field does not affect the small-scale turbulence. At greater heights an effect may exist, but the mean free path is of the order of magnitude of a kilometer; therefore, the scale of corresponding eddies is too large to be of interest in the study of the scattering of radio waves.

Thus we know the order of magnitude of the product u_0l_0: it is equal to the kinematic viscosity ν. However, we cannot say anything concrete separately about the scales and velocities of the minimum eddies. For these we need to know some other characteristics of turbulence from experiment. In the scientific literature there are indirect conclusions about the behavior of the turbulence power per unit mass ϵ along the vertical and estimates of its value [*Booker*, 1956; *Matuura and Nagata*, 1958]. Knowing ϵ we can determine the values of u_0 and l_0 separately. In accordance with the dimensional theory

$$l_0 = (\nu^3/\epsilon)^{1/4} \qquad (10)$$

As ϵ has a very weak influence in this relation, we neglect its dependence upon height. This increases the value l_0. Indeed, according to

TABLE 1

z, km	νm, cm²/sec	ν, cm²/sec	η	λ, cm	Criterion 8 or 9
80	$7\cdot10^{15}$	$2\cdot10^{3}$	$2\cdot10^{-5}$	$0\cdot4$	$\nu\eta/\nu_m = 5\cdot10^{-18} \ll 1$
100	$2\cdot10^{15}$	10^{5}	10^{-3}	6	$\nu\eta/\nu_m = 5\cdot10^{-14} \ll 1$
150	10^{11}	$2\cdot10^{7}$	$0\cdot1$	$5\cdot10^{2}$	$\nu\eta/\nu_m = 2\cdot10^{-5} \ll 1$
200	$5\cdot10^{9}$	$2\cdot10^{8}$	1	10^{4}	$\nu\eta/\nu_m = 0\cdot04 \ll 1$
250	$7\cdot10^{8}$	$2\cdot10^{9}$	5	10^{5}	$\nu/\nu_m = 3 \quad \eta > 1$
300	10^{9}	$8\cdot10^{9}$	20	$4\cdot10^{5}$	$\nu/\nu_m = 8 \quad \eta \gg 1$

Booker [1956] the value of ϵ increases from 5.10^{-4} w/kg in the troposphere up to 10^3 w/kg at the height of about 200 km, and its ratio, to the power 1/4, is equal to 37. Taking into account that $\nu \sim n^{-1}$, where n is the number of molecules per cubic centimeter and that the mean free path is also $\lambda \sim n^{-1}$, the following ratio may be obtained:

$$\frac{l_0}{\lambda} = \frac{l_{0s}}{\lambda_s}\left(\frac{\epsilon_s}{\epsilon}\right)^{1/4}\left(\frac{n}{n_s}\right)^{1/4} \tag{11}$$

where the quantities with the subscript s are defined at the surface of the earth. Thus, the ratio l_0/λ decreases with decrease in density as $n^{1/4}$.

The value $n_s = 2.1 \cdot 10^{19}$ cm^{-3}; at the height of 100 km $n = 4 \cdot 10^{13}$ and $(n_s/n)^{1/4} = 30$; at the height of 250 km $n = 3 \cdot 10^9$ and $(n_s/n)^{1/4} = 300$. The additional decrease of the ratio l_0/λ is the result of the growth of ϵ. At the surface of the earth $\lambda \approx 10^{-5}$ cm and $l_0 \approx 0.1$ cm; therefore $l_0/\lambda \approx 10^4$. Under these conditions the molecular length scale may be entirely neglected in developing a theory of turbulence. At a height of 250 km the value l_0/λ decreases to 30, or perhaps to even smaller values, owing to the growth of ϵ. This situation reveals itself still more clearly when turbulence in interstellar gases is considered [*Kaplan*, 1955]. On the other hand, it may be obvious that, in order to ensure the mechanism of viscous dissipation, l_0 should be much larger than the mean free path, since the gradients of velocities are small and a large number of collisions of molecules must occur for their equalization. This contradiction makes it necessary to be cautious in applying the known results of the theory of turbulence that are true and valid for the dense troposphere to the rarefied gases. To formulate a theory of turbulence for the rarefied gases, we should, apparently, also take the mean free path as a length scale. It may be shown that to assume this is equivalent to taking into account the compressibility of fluids (the viscosity ν has the order of magnitude of the product of the speed of sound and the mean free path).

The practical conclusion is that, in spite of reasonable expectation to the contrary, turbulence in the lower ionosphere (at heights of 100 to 150 km) is apparently similar to ordinary atmospheric turbulence, and the influence of the earth's magnetic field may be taken into account as a small correction.

I should like to thank Professor A. M. Oboukhov and Dr. A. S. Monin for helpful discussions.

References

Booker, H. G., Turbulence in the ionosphere with applications, *J. Geophys. Research, 61,* 673–705, 1956.

Kaplan, C. A., Structural, correlation and spectral functions of interstellar gas turbulence, *Astron. J. USSR, 32,* 255–264, 1955.

Matuura, N., and T. Nagata, *Rept. Ionosphere Research Japan, 12* (2), 147, 1958.

Mitra, S. K., *The Upper Atmosphere,* Calcutta, 1952.

Magnetohydrodynamics of the Small-Scale Structure of the F Region

J. P. DOUGHERTY

Cavendish Laboratory
Cambridge, England

Abstract—The influence of the E region on Martyn's model for the explanation of radio-star scintillations and spread F is briefly discussed.

Starting from the general formulation de-[vel]oped by *Dungey* [1959], if, in the F region, we [ne]glect inertial, gravitational, and partial pres-[su]re terms (as well as motivation by neutral gas [m]otions), the velocity vectors for ions and [ele]ctrons are given by 'mobility matrices' [op]erating on the electric field, as described by [Ra]tcliffe [1959]. Furthermore, for the F region, [th]e Larmor frequency exceeds the collision [fr]equency for both kinds of particles to such an [ex]tent that the formulas reduce to

$$\mathbf{U}_i \simeq \mathbf{U}_e \simeq \mathbf{E}\times\mathbf{B}/B^2$$
$$+ \text{ arbitrary velocity 'parallel' to } \mathbf{B} \qquad (1)$$

[to] a very close approximation, together with [th]e condition

$$\mathbf{E}\cdot\mathbf{B} \simeq 0 \qquad (2)$$

From (1), $\mathbf{E} + \mathbf{U}\times\mathbf{B} = 0$, so that, although [th]e conductivity across the field tends to zero, [w]e have a 'freezing-in' theorem for the field [li]nes just as in the classical case of very large [is]otropic conductivity. So long as curl $\mathbf{E} = 0$, [th]is motion of the field lines merely 'permutes [th]e lines of force' without actually changing [th]e magnetic field, but it is a useful way of [p]icturing the state of affairs since we can regard [ea]ch tube of force as containing the same ioni-[z]ation throughout its motion. The equation of [e]quilibrium for production, loss, and transport [b]y gravitational and pressure terms is satisfied [w]ithin each tube independently.

It should be noted that such tubes all dip [d]own into the 'dynamo' region of the ionosphere, [w]here collisions are more frequent, and (1) [a]nd (2) cease to hold. It is here that the large-[sc]ale electric fields in the ionosphere are generated. Consequently the electric field to be found in any flux tube, and hence the motion of the flux tube, are controlled from this level. That this is so for the large-scale motions of the F region was pointed out by Martyn some years ago, but it seems to the present author that the same is true for small-scale motions. On the other hand, *Martyn's* [1959] claim of the unstable nature of the motion of cylindrical irregularities is based on the calculation of their behavior in an infinite medium, as worked out by *Clemmow, Johnson, and Weekes* [1955]; an *infinite* cylinder moves relatively to the background essentially because surface charges accumulate and require the electric field to be different inside from outside. It must be emphasized that this is an effect arising from the difference between $\mathbf{U}_i$ and $\mathbf{U}_e$, in other words, from the incompleteness of the 'freezing-in'; and, although, as the collision frequency tends to zero, the results of Clemmow and co-workers tend to a definite limit, nevertheless, if one begins with ν *exactly* zero, the motion of an infinite cylinder is found to be indeterminate. This suggests that in the F region the surface charge effect is a very weak one, in which case the E-region control that Martyn neglected is what settles the apparent indeterminacy instead. If this is so, and the dynamo field is at first taken to be very smooth, then such cylinders, or indeed irregularities of an even more complicated kind, move simply as if imbedded in the F region and do not exhibit instability.

If the E-region electric fields have irregular parts due to turbulent driving winds, then, as *Farley* [1959] has shown in detail, such fields are well transmitted into the F region even if of quite small length-scale. Using again the

concept of particles frozen to moving lines of force, we see that irregular motions are produced in the F region, but it must be remembered that, so long as curl $\mathbf{E} = 0$, the plasma motions so induced are divergence-free, so that production of irregularities in this way, suggested by *Dagg* [1957], is restricted to an effect depending on the mean gradient. On the other hand, disturbances involving changes of $\mathbf{B}$ (i.e. of the Alfvén type) can induce changes in density. Such disturbances may propagate downward from the outer ionosphere and account for some of the radio-star scintillations.

Note added later—The author did not have time to refer to the extension of this notion to the consideration of complete tubes of force terminating in the ionosphere at both ends, and to the recent work of Helliwell [*Helliwell and Morgan*, 1959] on whistler propagation, supporting the existence of tubes of density differing slightly from their surroundings, whose motion would arise partly from E-region control at the ends of the tubes and partly from the gravitational and pressure effects, so far neglected. The reader is referred to *Gold's* [1959] detailed description of these ideas. Unstable motions of such tubes arising in the way Gold has explained may be found, on detailed investigation, to explain the interesting morphologic features that Martyn has described. The prese author wished merely to question Martyn mechanism for explaining the instability.

References

Clemmow, P. C., M. A. Johnson, and K. Weeke Motion of a cylindrical irregularity in an ioniz medium, *Proc. Ionosphere Conf.*, The Physic Society of London, p. 136, 1955.

Dagg, M., The origin of the ionospheric irregula ties responsible for radio star scintillation a spread *F*. II: Turbulent motion in the dynar region, *J. Atmospheric and Terrest. Phys.*, 139, 1957.

Dungey, J. W., Effect of a magnetic field on tu bulence in an ionized gas, *J. Geophys. Researc 64,* 2188-2191, 1959.

Farley, D. T., A theoretical study of electrosta fields in the ionosphere, *Cornell Univ. Resear Rept., EE 441,* Oct. 15, 1959.

Gold, T., Motions in the magnetosphere of t earth, *J. Geophys. Research, 64,* 1219–12 1959.

Helliwell, R. A., and M. G. Morgan, Atmo pheric whistlers, *Proc. IRE, 47,* 200–208, 19

Martyn, D. F., Large-scale movements of ioniz tion in the ionosphere, *J. Geophys. Researc 64,* 2178–2179, 1959, or *Nature, 183,* 1382, 1959

Ratcliffe, J. A., Ionization and drifts in the ion sphere, *J. Geophys. Research, 64,* 2102–21 1959.

Electrodynamic Stability of a Vertically Drifting Ionospheric Layer

J. A. Fejer

Defense Research Telecommunications Establishment
Ottawa, Canada

Abstract—The electrodynamic stability of a vertically drifting ionospheric layer is examined under certain simplifying assumptions. No evidence of instability is found.

The suggestion has been made [*Martyn*, 1959, d in this symposium] that 'the ionization on e undersurface of the F region is essentially stable if it is moving upward under the in- ence of electrodynamic drift.' The suggestion as supported by reasoning based on a result *lemmow, Johnson, and Weekes*, 1955] relating the motion of an irregularity in ionization nich has the shape of a circular cylinder with axis parallel to a uniform magnetic field. The utral gas was assumed stationary, and a uni- rm electric field perpendicular to both the is of the cylinder and the magnetic field was ostulated. Clemmow, Johnson, and Weekes ow that the velocity of the cylindrical irregu- rity, which in this special case moves without stortion, generally differs from the drift veloc- y of the surrounding uniform ionization.

Martyn suggests that this velocity difference n be responsible for a growth of the difference tween the ionization density of the medium d that of the irregularity if the medium has a ight gradient of ionization. The irregularity visualized drifting into a region of the sur- unding medium where the difference between e ionization densities of the medium and of e irregularity is accentuated.

It is clear that a horizontally stratified layer rifts without distortion of shape, and there- re an irregularity in which the electron density a function of the height only will not drift lative to the layer. Martyn considers a field- igned cylindrical irregularity on the magnetic quator in a vertically drifting layer to illustrate is point. Unfortunately, the problem of such a linder in a horizontally stratified layer is not sy to treat mathematically. Since it is known that an irregularity in the horizontal stratification does not cause instability, it might be interesting to consider a vertically elongated irregularity, where the mechanism postulated by Martyn would be expected to operate.

Assume a uniform magnetic field $\mathbf{B}$ in the y direction and a uniform electric field $\mathbf{E}_0$ in the x direction of a cartesian coordinate system. Let the electron density be independent of y, and assume that the irregularity is situated between the planes $x = 0$ and $x = \epsilon$, where the electron density is N' and the electron density in the surrounding medium is N. The assumed

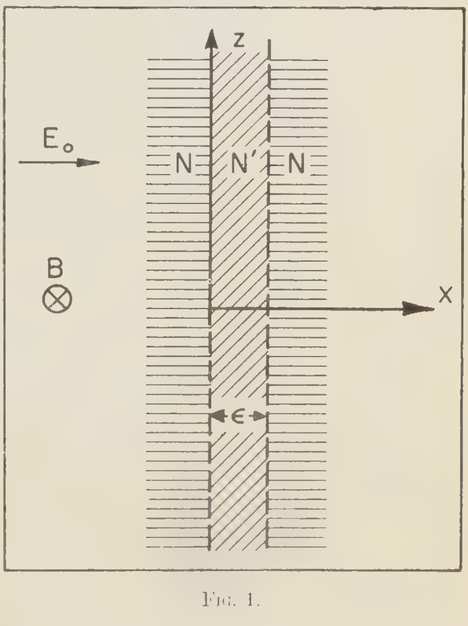

Fig. 1.

irregularity is thus infinitely elongated in the z direction (height). Let N be an arbitrary function of the height z, and let

$$N' = \lambda N \tag{1}$$

where λ is a constant so that N'/N is independent of height.

In the F region with the electric field everywhere perpendicular to the magnetic field it is a good approximation to write for the current density

$$\mathbf{j} = \sigma \mathbf{E} \tag{2}$$

where the conductivity σ is small but not negligible. The electrons and ions move almost together with a drift velocity

$$\mathbf{v} = \mathbf{E} \times \mathbf{B}/B^2 \tag{3}$$

In the first approximation one can write

$$\operatorname{div} \mathbf{j} = 0 \tag{4}$$

$$\operatorname{curl} \mathbf{E} = 0 \tag{5}$$

Equations 2, 4, and 5 determine the initial distribution of $\mathbf{E}$ and $\mathbf{j}$ in space. The conductivity σ is proportional to the electron density and is known initially as a function of position. At infinity we have $\mathbf{E} = \mathbf{E}_0$.

We can then use the equation

$$\partial N/\partial t = -\operatorname{div}(N\mathbf{v}) \tag{6}$$

together with (3) to determine new values of the electron density an instant later and repeat the whole procedure.

Applying this method to the vertically elongated irregularity yields

$$\mathbf{E}' = \mathbf{E}_0/\lambda \qquad ($$

where $\mathbf{E}'$ is the electric field inside the irregularit

A glance at equations 6, 3, and 1 makes clear that

$$\partial N/\partial t = \partial N'/\partial t \qquad ($$

and the electron density difference between t irregularity and the surrounding medium do not change with time.

The assumption λ = constant is not vital the above argument. Equation 7 and therefo equation 8 will remain approximately va while the horizontal dimension ϵ of the irreg larity is much smaller than the vertical exte of the layer and while λ is not very small or ve large at any height.

Summing up, it may be stated that the d ference between N and N', as seen from a syste stationary with respect to the neutral mediu does not change with time. This appears indicate that, at least for the special case vertically elongated irregularities treated he the instability suggested by Martyn does n occur, although according to equations 3 a 7 the drift velocity in the irregularity is differe from that in the medium.

References

Clemmow, P. C., M. A. Johnson, and K. Week Motion of a cylindrical irregularity in an ioniz medium, *Proc. Ionosphere Conf.*, Physical S ciety (London), p. 136, 1955.

Martyn, D. F., The normal F region of the ion sphere, *Proc. IRE*, *47*, 147-155, 1959.

Effect of Density Variation on Fluid Flow

CHIA-SHUN YIH

Department of Engineering Mechanics, University of Michigan
Ann Arbor, Michigan

Abstract—The effect of density variation on the flow of an incompressible and inviscid fluid is twofold. On the one hand, the inertia of the fluid changes in direct proportion to the density. On the other hand, the body force acting on a fluid element also changes in direct proportion to the density. Since body force is not the only force acting on the fluid, the inertia effect and the gravity effect of density variation do not cancel each other, and many interesting phenomena occur in the flow of a heterogeneous fluid that do not occur in the flow of a homogeneous fluid.

In this paper it is shown that the inertia effect can be simply evaluated for steady flows. If the velocity in the steady flow of a heterogeneous fluid in the absence of gravity is multiplied by the square root of the density, the result represents a dynamically possible flow of a homogeneous fluid. At the other extreme, when the gravitational effect dominates the flow, it has been shown both analytically and experimentally that the motion of a fluid is confined to the layer at which it originates. As usual, it is when the inertia effect and the gravity effect are comparable that the solutions of stratified flows become difficult, even if the flow is assumed to be steady and the fluid inviscid. From one series of such solutions and the supporting experiments one sees that, on the one hand, infinitely many modes of stationary internal waves of finite amplitude are dynamically possible (apart from the consideration of generation), and, on the other hand, physically significant solutions of stratified flows may involve velocity discontinuities.

troduction—In the flow of an incompressible inviscid fluid, inhomogeneity of the fluid af- s the flow in two ways. First, a change of ity always involves a proportional change he inertia per unit volume of the fluid. Sec- , a density change always involves a change ody force per unit volume in a gravitational . Although this body force is proportional he density in a uniform gravitational field, it nfortunately not the only force acting on fluid. Thus the flow pattern of an inho- eneous fluid may differ considerably from of a homogeneous fluid even though the ndary conditions are the same.

n this paper it will be shown that the inertia t of density change can be simply evaluated steady flows, and that, when the flow is weak therefore dominated by the gravitational t, it is confined to the level at which the urbance causing the motion is situated. A es of exact solutions for flow into a sink, in ch both inertia and gravity effects are taken account, will be given for all Froude num- , however small. The results of supporting eriments will be cited to show that the analytical solutions for Froude numbers less than $1/\pi$ are not physically significant, and that the possibility for velocity discontinuities must sometimes be provided for in order to obtain a physically significant analytical solution.

Inertia effect in steady flows—Since the fluid is considered to be incompressible, the density ρ satisfies the equation

$$D\rho/Dt = 0 \tag{1}$$

in which

$$\frac{D}{Dt} = \frac{\partial}{\partial t} + u_i \frac{\partial}{\partial x_i}$$

is the operator for substantial differentiation, with t denoting the time and u_i the velocity component in the direction of the cartesian coordinate x_i. The summation convention is adopted, so that

$$u_i \frac{\partial}{\partial x_i} = u_1 \frac{\partial}{\partial x_1} + u_2 \frac{\partial}{\partial x_2} + u_3 \frac{\partial}{\partial x_3}$$

The condition for continuity is

$$\frac{\partial \rho}{\partial t} + \frac{\partial(\rho u_i)}{\partial x_i} = 0 \tag{2}$$

From equations 1 and 2 it follows that the continuity equation for an incompressible fluid (even of variable density) can be written

$$\partial u_j/\partial x_j = 0 \qquad (3)$$

Euler's equations of motion for an inviscid fluid are

$$\rho \frac{Du_i}{Dt} = -\frac{\partial p}{\partial x_i} + \rho g_i \qquad (i = 1, 2, 3) \qquad (4)$$

if g_i is the body force per unit mass in the x_i direction. If $(x_1, x_2, x_3) = (x, y, z)$, and the y axis is vertical, $(g_1, g_2, g_3) = (0, -g, 0)$.

Since the inertia effect exclusively is under examination, the term ρg_i in equation 4 can be omitted, and we have, for steady flows,

$$\rho u_j \frac{\partial u_i}{\partial x_j} = -\frac{\partial p}{\partial x_i} \qquad (5)$$

which, because of equation 1, can be written as [*Yih*, 1958]

$$\sqrt{\rho}\, u_j \frac{\partial \sqrt{\rho}\, u_i}{\partial x_j} = -\frac{\partial p}{\partial x_i} \qquad (6)$$

Furthermore, for steady flows the equation of continuity can be written as

$$\frac{\partial(\sqrt{\rho}\, u_j)}{\partial x_j} = 0 \qquad (7)$$

also by virtue of equation 1. Thus with

$$u_i' = \sqrt{\rho}\, u_i \qquad (8)$$

the governing equations become

$$u_j' \frac{\partial u_i'}{\partial x_j} = -\frac{\partial p}{\partial x_i} \qquad \frac{\partial u_j'}{\partial x_j} = 0$$

which are the equations governing the flow o homogeneous fluid of density equal to uni Hence, in the absence of a gravitational fie the general flow *pattern* of an inhomogene fluid is identical to that of homogeneous fl under similar boundary conditions. Only the locity is different. The velocity for the in mogeneous fluid can be obtained from that the homogeneous fluid through division of latter by $\sqrt{\rho}$. Furthermore, it can be sho from equation 9 that in the associated flow fi u_i' irrotationality will persist, provided t gravity effect is negligible and the flow is stea This is not true of the actual flow field u_i.

In the presence of a gravitational field, conclusions reached are true if the flow is tirely horizontal, or if the flow is so rapid t gravity effect, though present, is negligible.

Gravity effect—For very weak steady n tions the situation is entirely different. Iner effect is now negligible, and the motion is dor nated by gravity effect. The equation of c tinuity can now be written, with (x, y, z) (x_1, x_2, x_3) and (u, v, w) for (u_1, u_2, u_3),

$$v \frac{\partial \rho}{\partial y} = 0$$

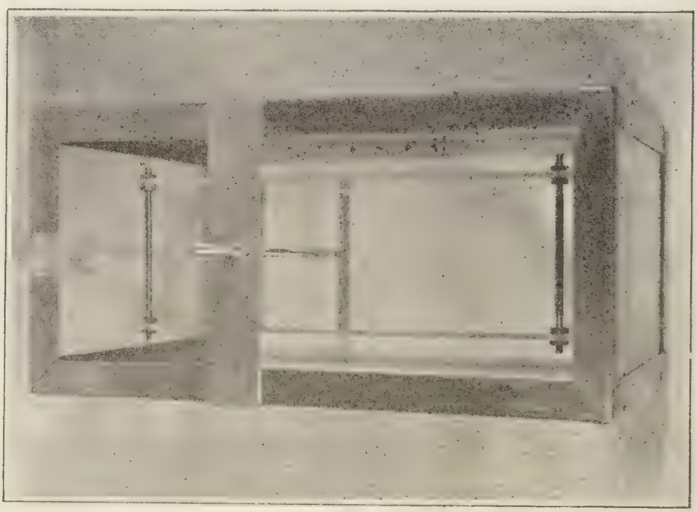

FIG. 1—Apparatus for demonstrating the gravity effect of density stratification.

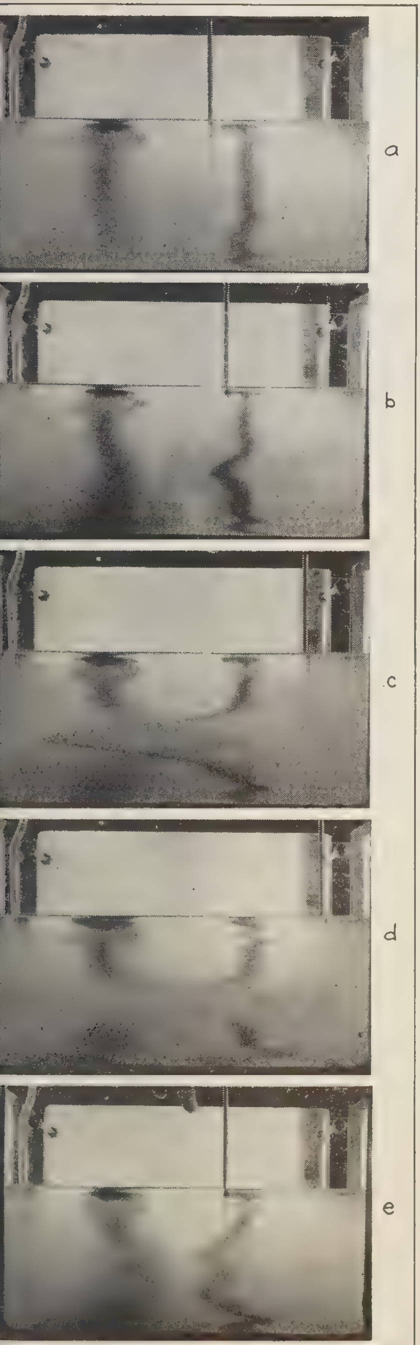

IG. 2—Development of dye streaks, showing confinement of the motion to the range of els at which the paddle is situated.

from which it follows that

$$v = 0 \tag{10}$$

since the fluid is stratified in the direction of y. Furthermore, from the equations of motion

$$\frac{\partial p}{\partial x} = 0 \qquad \frac{\partial p}{\partial y} = -gy \qquad \frac{\partial p}{\partial z} = 0$$

It follows that

$$\frac{\partial \rho}{\partial x} = 0 \qquad \frac{\partial \rho}{\partial z} = 0 \tag{11}$$

Equations 10 and 11 state that for steady weak motions the effect of gravity is to inhibit vertical motion and horizontal density gradients completely.

If the motion is two-dimensional to start with, $w = 0$, and the motion is only in the x direction, with no change in u or ρ with respect to x. This result is directly similar to a result of *Proudman* [1916] for weak steady axisymmetric motions relative to a strong general rotation.

The conclusions of this section are generally supported by the results of a simple experiment. Figure 1 shows the apparatus used. The two partition walls do not extend the full length of the container, so that as the paddle moves the stratified fluid realized by layers of salt water of different density can circulate around. Figure 2*a* shows the vertical dye streaks, one in the inner channel, and the clearer one in one of the outer channels. Figures 2*b* to 2*d* show the development of streaks as the paddle was moved to the right. Finally, Figure 2*e* shows the return of the dyed particles as the paddle is moved back to a place near its original position. Aside from obvious viscous effects, the conclusions of this section are largely supported by the results of this simple experiment. The striking feature is that a little stratification is sufficient to make the effect of the moving paddle felt far upstream and downstream.

Stationary waves of finite amplitude—The equation governing steady two-dimensional flows of a stratified fluid can be derived from equations 1, 3, and 4, with u_s equal to zero, and has been given by *Long* [1953]:

$$\nabla^2\psi + \frac{1}{\rho}\frac{d\rho}{d\psi}\left(\frac{\psi_x^2 + \psi_y^2}{2} + gy\right) = H(\psi) \tag{12}$$

in which

$$\nabla^2 = \frac{\partial^2}{\partial x^2} + \frac{\partial^2}{\partial y^2}$$

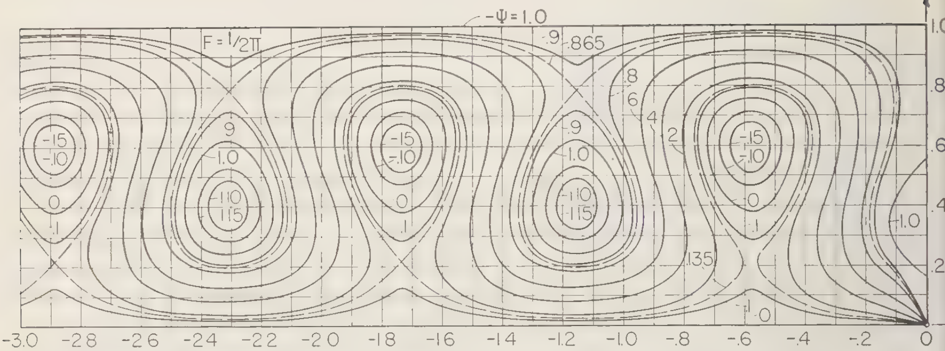

Fig. 3—Pattern of stratified flow into a sink, corresponding to a formal solution of equation 18 $F = 3/4\pi$, with upstream waves.

ψ is the stream function, and subscripts indicate partial differentiation. Through the transformation [*Yih,* 1958]

$$\psi' = \int \sqrt{\rho}\, d\psi \tag{13}$$

which is suggested by equation 8, Long's equation can be put in the simpler form

$$\nabla^2\psi' + \frac{d\rho}{d\psi'}\, gy = H_1(\psi') \tag{14}$$

in which the function $H_1(\psi')$ depends on upstream conditions.

For flows with an upstream velocity (horizontal) U such that $U^2\rho$ is constant (A^2, say) and with the linear density variation upstream

$$\rho = \rho_0 - \beta y \tag{15}$$

equation 14 becomes

$$\nabla^2\psi' + \frac{g\beta}{A^2}\psi' = -\frac{g\beta}{A} y \tag{16}$$

If d is a representative length, the dimensionless variables

$$\Psi = \frac{\psi'}{Ad} \qquad \xi = \frac{x}{d} \qquad \eta = \frac{y}{d} \tag{17}$$

can be used for convenience. Equation 16 then becomes

$$\Psi_{\xi\xi} + \Psi_{\eta\eta} + F^{-2}\Psi = -F^{-2}\eta, \tag{18}$$

in which $F = A/d\sqrt{g\beta}$ is the Froude number. In his paper of 1953, Long stated: 'This [the case of constant $U^2\rho$ and linear variation of ρ with y upstream] the only case I have been able to discover f which the differential equation governing t motion of a stratified fluid is exactly linear.'

Infinitely many other cases for which t governing equation is exactly linear will now given. These correspond to stationary period waves of finite amplitude. If

$$\Psi = -\eta - \frac{2}{\pi}\sum_{n=1}^{N} \sin n\pi\eta[A_n \cos (F^{-2} - n^2\pi^2)^{1/2}\xi + B_n \sin (F^{-2} - n^2\pi^2)^{1/2}\xi] \quad (1$$

$$\rho = \rho_0 - (\beta d)\eta - \frac{2\beta d}{\pi} \cdot \sum_{1}^{N} \sin n\pi\eta[A_n \cos (F^{-2} - n^2\pi^2)^{1/2}\xi + B_n \sin (F^{-2} - n^2\pi^2)^{1/2}\xi] \quad (2$$

with $F^{-1} > N\pi$, the governing equation is aga equation 18, the solution of which is giv exactly by equations 19 and 20 for flow betwe two parallel horizontal boundaries at distance apart. The 'upstream condition' is now period The waves represented by equations 19 and were actually found by Long as lea waves bo analytically and experimentally. The only diffe ence is that Long did not realize that for these waves the governing equation is exact linear without the benefit of the stringent u stream conditions $U^2\rho$ = constant and $\rho =$ $-\beta y$.

The occurrence of velocity discontinuities From Figure 2 it has been seen that, but for t effect of viscosity, steady weak motions wou

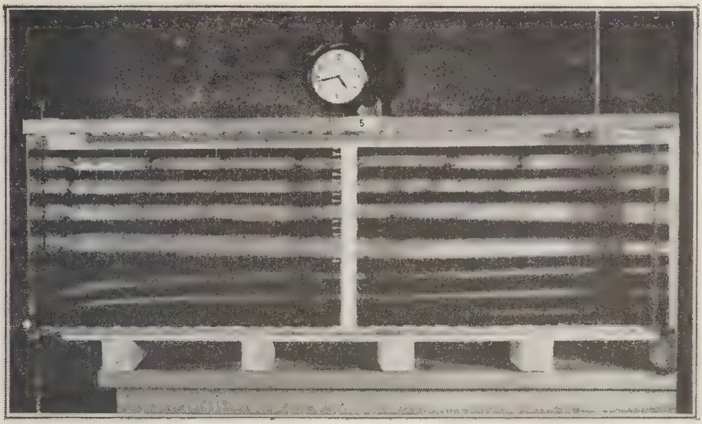

4—Actual pattern of stratified flow into a sink when the Froude number F is below the critical number $1/\pi$. (Courtesy of Dr. W. R. Debler.)

elop velocity discontinuities (at the levels of edges of the paddle). In a study of stratified between two horizontal boundaries into a [*Yih*, 1958], a solution for equation 18 was nd for $F > 1/\pi$. For Froude numbers less n the critical value $1/\pi$, either waves would ur upstream or a velocity discontinuity would elop. For $F = 1/2\pi$, a solution[1] of equation 18 with upstream waves gives the flow pattern in Figure 3, whereas the experiments of *Debler* [1959] showed that these waves do not occur upstream, that a velocity discontinuity occurs between a moving layer and an essentially stagnant layer (Fig. 4), and that the Froude number based on the thickness of the moving layer is approximately $1/\pi$. Hence, for an analytical solution to be physically significant, the possibility of the occurrence of velocity discontinuities may have to be provided for.

Acknowledgment—The work described in this paper has been sponsored by the Office of Ordnance Research, U. S. Army. The assistance of Mr. William O'Dell in producing Figure 3 is greatly appreciated.

References

DEBLER, W. R., Stratified flow into a line sink, to be published in *Proc. Am. Soc. Civil Engrs.*, 1959.

LONG, R. R., Some aspects of the flow of stratified fluids. I. A theoretical investigation, *Dept. Civil Eng., Johns Hopkins Univ., Tech. Rept. 2*, 1953.

PROUDMAN, J., On the motion of solids in a liquid possessing vorticity, *Proc. Roy. Soc. London, A, 92*, 408–424, 1916.

YIH, C.-S., On the flow of a stratified fluid, *Proc. Third Natl. Congr. Appl. Mechanics*, pp. 857–861, 1958.

The general solution (entirely formal) is

$$= -\eta - \frac{2}{\pi} \cdot \left\{ \sum_{n=1}^{N} \frac{\sin n\pi\eta}{n} [\cos (F^{-2} - n^2\pi^2)^{1/2}\xi + B_n \sin (F^{-2} - n^2\pi^2)^{1/2}\xi] + \sum_{n=N+1}^{\infty} \frac{\sin n\pi\eta}{n} \exp (n^2\pi^2 - F^{-2})^{1/2}\xi \right\}$$

$$= \rho_0 - (\beta d)\eta - \frac{2\beta d}{\pi} \cdot \left\{ \sum_{n=1}^{N} \frac{\sin n\pi\eta}{n} [\cos (F^{-2} - n^2\pi^2)^{1/2}\xi + B_n \sin (F^{-2} - n^2\pi^2)^{1/2}\xi] + \sum_{n=N+1}^{\infty} \frac{\sin n\pi\eta}{n} \exp (n^2\pi^2 - F^{-2})^{1/2}\xi \right\}$$

in which

$$(N + 1)\pi \geq F^{-1} \geq N\pi$$

and the B's are arbitrary.

Turbulence in Shear Flow with Stability

A. S. MONIN

Institute of Physics of the Atmosphere
Academy of Science, USSR

Abstract—The turbulence energy balance is considered under conditions of mean-flow shear and varying density stratification, and it is concluded that: in a stable atmosphere the total turbulence energy is reduced; the maximum of the spectrum shifts to smaller scales; and, at heights large compared with the mixing length, the effects of the surface are negligible, the turbulence tends to be homogeneous, and the shear to be constant. On the other hand, when the atmosphere is unstable, the total energy and scale tend to increase, the surface always exerts an important influence, turbulent mixing is very intensive, and shear tends toward zero.

The main parameters of the mean flow are the mean velocity profile $U(z)$ (z = height) and mean potential temperature profile $\theta(z)$. Potential temperature is the most convenient characteristic of stratification because it is invariant under adiabatic vertical displacements of fluid particles. The vertical gradient of potential temperature is given by

$$\frac{\partial \theta}{\partial z} = \frac{\theta}{T}\left(\gamma_a + \frac{\partial T}{\partial z}\right)$$

where T = molecular temperature, and $\gamma_a \approx 10°$ C/km, so-called adiabatic gradient.

Neutral stratification corresponds to θ = constant; stable, to $\partial\theta/\partial z > 0$; unstable, to $\partial\theta/\partial z < 0$. Thermal instability means that vertical displacements of fluid particles are being accelerated by Archimedes forces.

The most important characteristics of turbulence are the kinetic energy per unit mass

$$b = \tfrac{1}{2}(\overline{u'^2} + \overline{v'^2} + \overline{w'^2})$$

the scale of turbulence or mixing length l (mean distance from the place of birth of an eddy to the place of its disappearance), and the energy spectrum $E(k)$.

In the presence of shear, turbulence cannot be isotropic and homogeneous. In fact there are specific directions in space—directions of mean wind and of shear; it is also clear that turbulence must be inhomogeneous along the vertical.

Let us consider the influence of shear and stability from the point of view of energy balance. The changes of turbulent energy are to shear, viscosity, and stability. The en balance equation can be written as follows:

$$\frac{db}{dt} = k\left(\frac{\partial U}{\partial z}\right)^2 - \epsilon - k_t \frac{g}{\theta}\frac{\partial \theta}{\partial z}$$

Here k, k_t = the coefficients of turbulent ing for momentum and heat, g = accelera of gravity, ϵ = rate of dissipation. The term describes the production of turbulent ergy by shear, the second dissipation, the t the exchange between kinetic energy of tu lence and potential energy of stratification.

In the stationary case the energy equa takes a form of

$$\epsilon = k\left(\frac{\partial U}{\partial z}\right)^2\left(1 - \frac{k_t}{k} Ri\right) \qquad Ri = \frac{g}{\theta}\frac{\partial\theta/}{(\partial U/}$$

It leads to the well known existence crite of turbulence given by Richardson:

$$Ri \leq Ri_{cr} \quad (= k/k_t)$$

Parameters of turbulence can be estimated parameters of the mean flow:

$$l \sim \frac{U}{\partial U/\partial z} \qquad \epsilon \sim \frac{(\delta U)^3}{l}$$

where δU = the difference of mean velociti a vertical separation of l.

In the case of stable stratification ($\partial\theta/\partial z$ > eddies are working against Archimedes fo and lose some part of their energy. This e

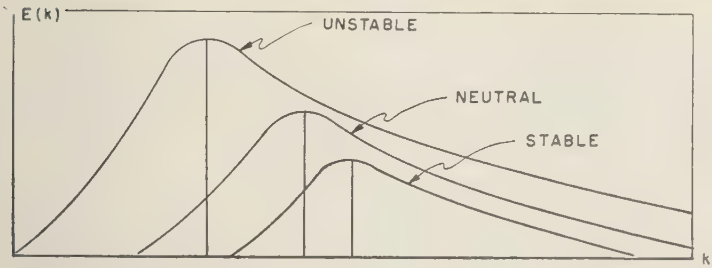

FIG. 1—The effect of stability on the spectrum of turbulence.

ost essential for large eddies. As a result, energy b and the scale l diminish as com- d with the neutral case with the same ; the energy spectrum changes: total en- reduces and the maximum shifts to smaller s (Fig. 1). The mixing length l is small. At eights $z > l$ the presence of the wall is not tial and turbulence tends to be homogeneous along vertical; shear tends to be constant.

In the case of unstable stratification the turbulence has an additional source of energy in the potential energy of stratification. Large eddies have a right to exist. Total energy b and scale l increase with instability. The presence of the wall is always important. Turbulent mixing is very intensive so that shear tends to zero.

Turbulent Spectra in a Stably Stratified Atmosphere

R. BOLGIANO, JR.

Cornell University
Ithaca, New York

Abstract—After noting the discrepancy between the predictions of turbulence theory and the empirical evidence from radio experiments, the author suggests that this may be the result of modification of the turbulent spectra by the effects of buoyancy in stably stratified layers. He points out that in such situations kinetic energy of turbulence is converted, over a wide range of scales, to potential energy of the resulting density deviations, that this potential energy is subsequently destroyed by the action of further turbulent mixing and molecular diffusion, and, finally, that the primary effect is to reduce the viscous dissipation rate significantly below that which normally would be estimated on the basis of large-scale turbulent motions. Universal forms are predicted for the kinetic energy and density fluctuation spectra, and in the *buoyancy* subrange (the part of the equilibrium range that reflects the anisotropy induced by the density gradient) the energy spectrum is found to be proportional to $k^{-11/5}$, the density spectrum to $k^{-7/5}$.

A problem that has arisen often in recent years in connection with ionospheric studies is the frequency, or wavelength, dependence of scatter propagation. In accordance with the single-scattering (Born) approximation, the scattering cross section σ is given by *Batchelor*, [1957]

$$\sigma \propto \{\overline{\delta N^2}/\lambda^4\} F_N(\mathbf{k}) \qquad (1)$$

where $\overline{\delta N^2}$ is the mean-square deviation of refractive index, λ is the radio wavelength, and $F_N(\mathbf{k})$ is the density of contributions to $\overline{\delta N^2}$ in vector wave-number space. The wave number at which F_N is to be evaluated is the difference between the propagation vectors of the incident and scattered waves. Its magnitude is given by

$$k_{scattered} = \{4\pi/\lambda\} \sin \theta/2 \qquad (2)$$

θ being the angle through which the energy is scattered.

If the scattering wave number falls in the (isotropic) inertial subrange, σ should, for the ionosphere, exhibit a $\lambda^{11/3}$ ($k^{-11/3}$) dependence. As has been pointed out previously in this symposium, scaled radio experiments seldom indicate such a form. The magnitude of the exponent is found to vary from time to time, usually falling in the range 4 to 7. A similar discrepancy arises in tropospheric propagation studies [*Bolgiano*, 1959], where a strong positive correlation has been detected between the magnitude of the exponent and the value of th Richardson number that describes the layer o the atmosphere through which the princip propagation occurs [*Bolgiano*, 1958]. A possib explanation for this variability of the wav length dependence, as well as for the excessi values of the exponent, may lie in the modifica tion of the turbulent spectra, both in shape an in the scale at which molecular dissipation se in, due to the effects of buoyancy forces in stably stratified portion of the atmosphere.

The thesis set forth here is that the buoyanc forces, which act to oppose vertical motio (when the medium is characterized by a lap of mean potential density, $\bar{\hat{\rho}}$), serve not only remove kinetic energy from the turbulent fie at the driving scales but also, because of th very anisotropy inherent in the unique natu of the vertical direction, to 'bleed' the turbulen over a wide range of scales. In the equation conservation of energy of the turbulen [*Townsend*, 1958],

$$\partial/\partial t(\tfrac{1}{2}\overline{u_i u_i}) = -\overline{u_i u_j}\,\partial U_i/\partial x_j - \partial/\partial x_j(\overline{\tfrac{1}{2}u_i u_i u_j} + \overline{p u_j}/\hat{\rho}_0) - (g/\hat{\rho}_0)\,\overline{\delta\hat{\rho} w} - \epsilon \qquad ($$

the third term on the right describes the buo ancy effects; $\delta\hat{\rho}$ is the fluctuation in potent density from its mean value, induced by vertic

ion. A positive value of the covariance $\overline{\delta\hat{\rho}w}$ esponds to a downward flux of heat, in eement with the positive gradient of potential perature that accompanies such a situation. e now write

$$\overline{\delta\hat{\rho}w} = \int_{\mathbf{k}\ space} \mathcal{R}\{\Phi_{z\hat{\rho}}(\mathbf{k}')\}\ d\mathbf{k}' \qquad (4)$$

real part of $\Phi_{z\hat{\rho}}(\mathbf{k})$ is a measure of the con- utions to the heat flux at the vector wave nber $\mathbf{k}$. Since this cospectrum is not, in eral, zero for the axisymmetric structure ored by the uniqueness of the vertical direc- , it is in fact quite reasonable to assume it tive throughout that k interval in which structure remains anisotropic. This hypoth- leads to interesting consequences, of which following are important examples.

he contributions to the conversion of kinetic rgy to potential energy (i.e., the potential rgy of the instantaneous density deviation ern) at a given scale can now be written

$$g/\hat{\rho}_0 \mathcal{R}\{\Phi_{z\hat{\rho}}(\mathbf{k})\} \qquad (5)$$

is, energy is extracted from the turbulence r a range of sizes, as previously suggested. urther consequence of the distributed energy version is the gradual reduction in the rate nertial transfer of turbulent energy across spectrum, toward the high-wave-number . The net result is that the viscous dissipation ϵ may be smaller, perhaps by a very sizable centage, than the rate of generation of bulent energy as given by the first term on the t in the energy conservation equation. That

$$\epsilon \ll \overline{u_i u_j}\ \partial U_i/\partial x_j \sim u^3/l \qquad (6)$$

re u and l refer to the energy containing ies of the turbulence. This possible difference veen the rates of generation and of viscous ipation of turbulent energy is a most signi- nt characteristic of the stably stratified ation.

is important to note that the same fluid ions that, by working against the forces of yancy, convert kinetic energy to potential rgy also generate deviations of potential sity (or temperature) from the mean dis- ution. Mean square fluctuations are produced at a rate $\chi_{\hat{\rho}}$ given by

$$\chi_{\hat{\rho}} \equiv \overline{\delta\hat{\rho}w}\ \partial\bar{\hat{\rho}}/\partial z \qquad (7)$$

and are subsequently mixed by the convective motions of the turbulence. This process results in the continuous break-up of density deviations into smaller-scale components and the ultimate destruction of these deviations (and of the potential energy they represent) through the diffusive effects of molecular motion. Thus, the kinetic energy extracted from the field of turbulence and stored in the form of a distribution of density fluctuations finally achieves the same fate as that which is transferred through the spectrum inertially and dissipated by viscosity.

In the part of the spectrum beyond the wave numbers at which the major contributions are are made to $\overline{\delta\hat{\rho}w}$, $\chi_{\hat{\rho}}$ is essentially constant; yet, for what may be a sizable wave-number interval, the structure remains anisotropic under the influence of the density gradient. This entire tail of the spectrum may be expected to achieve a state of statistical equilibrium under these circumstances, for which the governing parameters are: $\chi_{\hat{\rho}}$, $g/\hat{\rho}_0$, ϵ, ν, κ and k, where κ is the thermal conductivity. The following forms can then be predicted for the kinetic energy and density fluctuation spectra respectively (summed over all directions in wave-number space):

$$E(k) \sim \epsilon^{11/4}\chi_{\hat{\rho}}^{-5/4}(g/\hat{\rho}_0)^{-5/2} \cdot G\{\nu\chi_{\hat{\rho}}(g/\hat{\rho}_0)^2/\epsilon^2,\ \nu/\kappa,\ k/k_B\} \qquad (8)$$

$$\Gamma_{\hat{\rho}}(k) \sim \epsilon^{7/4}\chi_{\hat{\rho}}^{-1/4}(g/\hat{\rho}_0)^{-5/2} \cdot G_{\hat{\rho}}\{\nu\chi_{\hat{\rho}}(g/\hat{\rho}_0)^2/\epsilon^2,\ \nu/\kappa,\ k/k_B\} \qquad (9)$$

in which G and $G_{\hat{\rho}}$ are unknown universal functions and k_B is the wave number given by

$$k_B \equiv \chi_{\rho}^{3/4}(g/\hat{\rho}_0)^{3/2}/\epsilon^{5/4} \qquad (10)$$

If the Reynolds number is sufficiently large, the equilibrium spectrum may divide into three distinct subranges: (1) the *buoyancy* subrange—those larger, anisotropic eddies directly influenced by the density stratification; (2) the inertial subrange in which the anisotropy has been erased and the usual universal equilibrium theory [*Batchelor*, 1953*a*] is applicable; and (3) the dissipation subrange at the high-wave-number end of the spectrum, where molecular

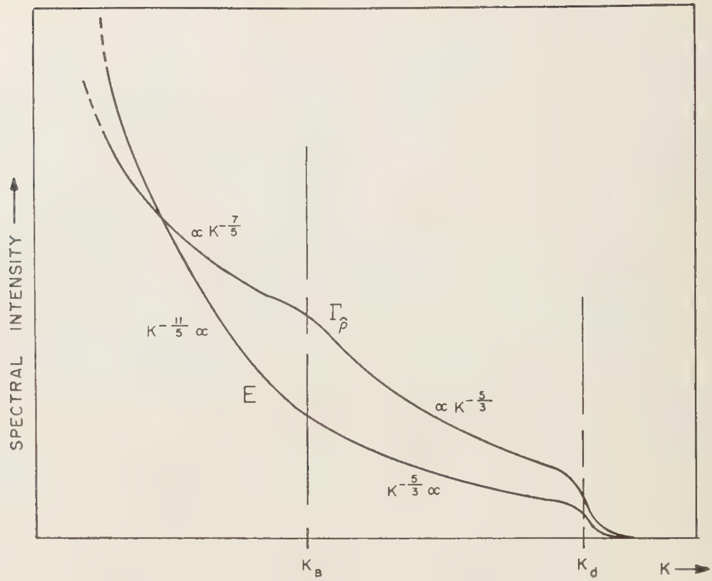

Fig. 1—Spectral forms in a stably stratified atmosphere.

effects dominate. The first two intervals are then separated by the wave number k_B, the second and third by the viscosity cutoff, $k_d = (\epsilon/\nu^3)^{1/4}$.

Under these circumstances more specific predictions can be made. In the buoyancy subrange the rate of inertial transfer of turbulent energy across the spectrum is so much in excess of ϵ and the local dissipation is so small that ϵ, ν, and κ may be dropped from the list of governing parameters. One is thus led to:

$$\left.\begin{aligned} E(k) &\sim \chi_{\hat{\rho}}^{2/5}(g/\hat{\rho}_0)^{4/5}k^{-11/5} \qquad (11)\\ \Gamma_\rho(k) &\sim \chi_{\hat{\rho}}^{4/5}(g/\hat{\rho}_0)^{-2/5}k^{-7/5} \qquad (12)\end{aligned}\right\} (k_1 \ll k \ll k_B)$$

where k_1 represents the scale of the energy containing eddies. In the inertial subrange ($k_B \ll k \ll k_d$) the usual $k^{-5/3}$ forms apply. Resultant typical spectra are shown in Figure 1.

Notice should be taken of the fact that k_B and k_d are influenced oppositely by variation of the stability $(\partial\bar{\hat{\rho}}/\partial z)$. Increasing lapse of density tends to increase $\chi_{\hat{\rho}}$ but to decrease ϵ. Consequently k_B becomes larger whereas k_d becomes smaller. It is conceivable that under sufficiently stable conditions the inertial subrange disappears entirely and the whole structure is anisotropic. Of course, under neutral conditions, the buoyancy subrange is nonexistent.

Two further properties of the buoyancy su range are of some interest. First, the value Richardson's number characterizing a given si eddy may be calculated, according to *Batchel* [1953*b*], as

$$Ri = gL\delta\hat{\rho}/(\hat{\rho}_0 U^2) \sim gk^{-1/2}\Gamma_{\hat{\rho}}^{1/2}/(\hat{\rho}_0 kE) \quad (1$$

On substitution of the forms for $\Gamma_{\hat{\rho}}$ and appropriate to the buoyancy subrange, it found that Ri is of order unity throughout t interval, a not surprising result since buoyan forces presumably dominate the structure here

Second, the relative diffusion of two particl separated a distance r, corresponding to a sca lying within the buoyancy subrange, shou proceed according to

$$\overline{r^2} \sim \chi_{\hat{\rho}}(g/\hat{\rho}_0)^2 t^5 \quad (1$$

This may be compared with the t^3 law noted Batchelor earlier in this session as descripti of the inertial subrange.

References

Batchelor, G. K., *The Theory of Homogeneo Turbulence,* University Press, Cambridge, 1 pp., 1953*a*.

Batchelor, G. K., Dynamical similarity of m

ons of a perfect-gas atmosphere, *Quart. J. Roy. Meteorol. Soc.*, *79*, 224–235, 1953*b*.
CHELOR, G. K., Wave scattering due to turbulence, *Naval Hydrodynamics, Publ. 515*, National Academy of Sciences–National Research Council, 1957.
GIANO, R., JR., A meteorological interpretation f wavelength dependence in transhorizon propagation, a paper presented before the Combined Technical Session, URSI-IRE Joint Meeting, Washington, D. C., April 1958. J. Res., pt. D., Nat. Bur. Stds., in press.
BOLGIANO, R., JR., Wavelength dependence in transhorizon propagation, *Proc. IRE*, *47*, 331–332, 1959.
TOWNSEND, A. A., 1958 turbulent flow in a stably stratified atmosphere, *J. Fluid Mech.*, *3*, 361–372, 1958.

Relation of Turbulence Theory to Ionospheric Scatter Propagation Experiments

A. D. WHEELON

Space Technology Laboratories, Inc.
Los Angeles, California

Summary—After a brief historical introduction the author considers the statistical behavior of ionospheric scatter signals. The random fading of the signals is taken to be suggestive of a scatter process, and predictions as to amplitude distribution (Rayleigh) and as to space or time correlations, made on this basis, are found to be in fair agreement with empirical results. It is noted that no attempts have as yet been made to predict the correlation coefficients.

The scattering of electromagnetic waves by turbulent irregularities is discussed next. The Born approximation (single scattering) is employed. This together with the far-field approximation leads to an expression for the received power in terms of the spectrum of mean square deviations in electron density. Neglecting polarization effects and assuming isotropy and homogeneity of electron density deviations within the common volume, the received power is given by

$$P_R = P_T r_0^2 A_R G_R \frac{b}{R^2} \cdot \csc\frac{\theta}{2}\, \Gamma\left(\frac{4\pi}{\lambda}\sin\frac{\theta}{2}\right) \Big/ \left\{4\pi\left(\frac{4\pi}{\lambda}\sin\frac{\theta}{2}\right)^2\right\}$$

where P_R and P_T are the received and transmitted powers, respectively, r_0 is the classical radius of the electron, A_R and G_R are the effective area and gain of the receiving antenna, b is the vertical depth of the scattering layer, R_2 is the distance from the scattering volume to the receiver, θ is the angle through which the energy is scattered, λ is the radio wavelength, and $\Gamma(k)$ is the spectral representation as a function of wave-number magnitude only of the contributions to the mean square deviations in electron density. It is noted that this expression is the only linkage, so far, between turbu lence theory and the results of radio exper ments. Caution is advised in applying it b cause of the unsubstantiated assumptions en ployed in its derivation.

The author then considers the spectrum c electron density deviations and its relation t turbulence. It is pointed out that, for typic VHF experiments, knowledge is required of th spectrum in the difficult transition region be tween the inertial and dissipation subrange Three theories purporting to account for th fluctuations of electron density are discusse The first, directly related to the dynamic pre sure fluctuations, is discounted. The other tw are the turbulent mixing theories proposed b Oboukhov and Corrsin and by Villars an Weisskopf. It is claimed that they differ co ceptually in the manner by which they a count for the primary mixing of the mea gradient of electron density. The spectrum, how ever, is found to depend upon the square the mean gradient in each case.

Signal level and scattering heights are take up next. On the grounds of the turbulent mixin arguments the received power is also found to b proportional to the square of the mean gradie of electron density. Evidence of a very shar gradient in the daytime at 70 km and a som what weaker gradient at 85 km at all times reported. Pulse transmissions, able to resolv this height difference, are said to support the arguments, as is the diurnal variation of sign level. Similar seasonal and annual variatio are explained in terms of gradient changes u der solar control.

Recent National Bureau of Standards da on frequency dependence are referenced th show a spectral form which does, on occasio

icate agreement with the inertial subrange diction of one or the other of the missing ories. There is, at other times, evidence of stantial accord with the results of *Batchelor, wells, and Townsend* [1959] for the case in ich electron diffusivity is large compared with ematic viscosity ($D \sim 2\nu$ in the lower iono- ere). It is also noted that these new data, le indicating variations in spectral form diur- ly and seasonally, give no evidence of change exponent over the 3.5:1 frequency range ered. As for distance dependence, the author nts to the complexity introduced by vertical homogeneity in the mean gradient of electron density. He believes that satisfactory experimental results have yet to be published.

Finally, the author explains some features of sudden ionospheric disturbances—loss of 6 Mc/s signal; enhancement of 50 Mc/s scatter transmission; and attenuation, followed by enhancement, of 28 Mc/s scatter signals—in terms of increased attenuation (inversely proportional to frequency squared) and transient increases in the mean gradient of electron density.

Reference

Batchelor, G. K., I. D. Howells, and A. A. Townsend, *J. Fluid Mech., 5,* 134, 1959.

Traveling Disturbances Originating in the Outer Ionosphere

K. Bibl and K. Rawer

*Ionosphären-Institut Breisach,
Deutsche Bundespost, Germany*

Abstract—Some observations that have been obtained with variations of the classical echo-sounding method must be interpreted as resulting from perturbation and/or oscillation phenomena occurring in the outer ionosphere. The vertical velocity component of 'traveling disturbances' coming from outside and propagating through the ionosphere is determined as 115 ± 35 m/sec. Oscillation-like phenomena have a large range of quasi-periods, between 1/4 and 12 hours.

Introduction—Disturbances visible as large deformations of the echo traces have been observed by comparison of distant stations [*Munro,* 1948, 1950; *Beynon,* 1948]. They were first interpreted in terms of a horizontal displacement. Then one of us found similar disturbances moving along the traces of the ionogram from high to low frequencies [*Bibl,* 1952, 1953]. Such phenomena seem to have been seen for the first time by Wells [*Wells, Watts, and George,* 1946].

Our interpretation of the phenomenon was that some perturbation moves across the site of the observing station, the motion having a vertical component. Different models have been suggested for the form of the perturbation, one being a pressure wave [*Bibl, Harnischmacher, and Rawer,* 1955]. Recently, *Akasofu* [1956] attempted a theoretical explanation of our results by applying magnetohydrodynamic equations. He identified the phenomenon from its velocity as a 'retarded sound wave.' This is the degeneration of a neutral sound wave in the plasma case. Its displacement is approximately guided along the magnetic lines of force. Akasofu concluded further, from our observations, that the amplitude of the observed wave is too large to admit the simple treatment of classical acoustics, which supposes small amplitudes.

As the disturbance normally begins at the high-frequency end of the echo trace, there can be little doubt that the corresponding shock wave originates above the F_2 ionization peak, in the outer ionosphere.

A new method of recording—The disturbances were first observed in time lapse moving p tures (Fig. 1). It is somewhat difficult to ide tify them in isolated ionograms, but they c be very clearly seen in a moving picture. F cently one of us [*Bibl,* in press] has used t technique of direct recording of various chara teristics for these observations. This technic was introduced by Uyeda and *Nakata* [195

A record of minimum virtual height can obtained from the usual panoramic display si ply by omitting on the screen the deflection c responding to frequency. The frequency of t ionosonde is still varied; the spot remains m of the time in one of the minimum height po tions. A continuously moving film thus gives record like that shown in Figure 2. From t daytime record it can be seen that the mi mum height of the *F* region varies rapidly. addition, fringes can be seen on this figure d scending from large virtual heights toward t bottom of the layer. As height increases dow ward in our records, the fringes go upwa (Fig. 2). They correspond to a deformation the trace or its luminosity and are manifes tions of the 'traveling disturbance.' It was ea to identify some of them with disturbances v ble on the movie film (numbers on Figs. 2 a 3). It may be noted that the oscillation-l variations of the $h'F_2$ level (intermediate le of the record) also seem to be related to t traveling disturbances.

Another interesting record is obtained by su pressing the height deflection after gating one the echoes. Minimum and maximum usable f quency of the echo are then recorded. For t

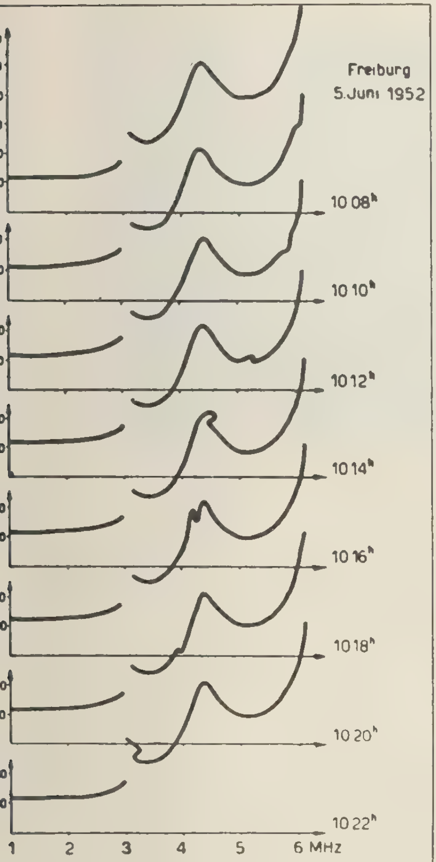

'IG. 1—A series of ionograms obtained with 2-
nute intervals. A deformation of the echo trace
irst seen at 1010 h at a frequency higher than
MHz. It moves along the echo trace reaching
F_1 cusp at 1014 h. The low-frequency end of
F trace (3 MHz) is reached at 1022 h.

ce reflected from the F region, the lower it is given by the blanketing LUF (in dayne); the upper limit can be identified with 'top frequency.' This is approximately the layer critical frequency of the extraordinary nponent. In these records the traveling dis-bances can also be seen by the variations of ninosity shifting along the trace. We can see nges going downward in Figures 3 and 4. (This ft corresponds to a decrease of electron den-y with time.) Figure 3 was obtained simul-neously with Figure 2; the same individual disturbances as marked in Figure 2 can easily be identified. In Figure 4, again a daytime record, some other disturbances are marked which also were first noted on the corresponding movie film.

Not all fringes appearing on such records are really associated with a traveling disturbance. The vertical ones simply arise from interference. But it seems to us that the analysis of the moving pictures may in the near future be replaced by study of the $h'(t)$ record in combination with the F-region top-frequency record. Some experience, of course, will still have to be obtained in correlating these with normal records.

Analysis employing true height—In the past the velocity of the traveling disturbances could only be estimated from the time variation of the virtual height [*Bibl,* 1952, 1953]. Now we have made a true height analysis for some disturbances, using the original quarter-hourly ionograms. The method of *Schmerling* [1958] has been used for this reduction. Besides this we have followed the individual disturbances on the movie film. After identification by replaying slowly and stopping from time to time, the time was noted at which each disturbance passed various frequencies. These curves were then combined with the curve of true height versus frequency, calculated from the ionograms. By elimination of the frequency, the true height of the disturbance is obtained as a function of time. One example is given in Figure 5. About half of all analyzed cases (including that of Fig. 5) gave a slightly concave curve, indicating a decrease of velocity with decreasing height. The other half of the analyzed cases gave a straight line corresponding to a constant velocity.

The number of observations is not yet sufficient to give results valid for all seasons, but the cases in the spring of 1959 that were analyzed gave a rather well defined velocity of 115 m/sec (median value) with a dispersion of about ± 35 m/sec (standard deviation). These results were obtained at altitudes between about 300 and 150 km.

It seems to us that this sort of disturbance very often decreases considerably in amplitude when it approaches the E-region level. In fact, most disturbances disappear in the zone between F and E regions. This should be quite normal for a sound wave traveling in the direction of

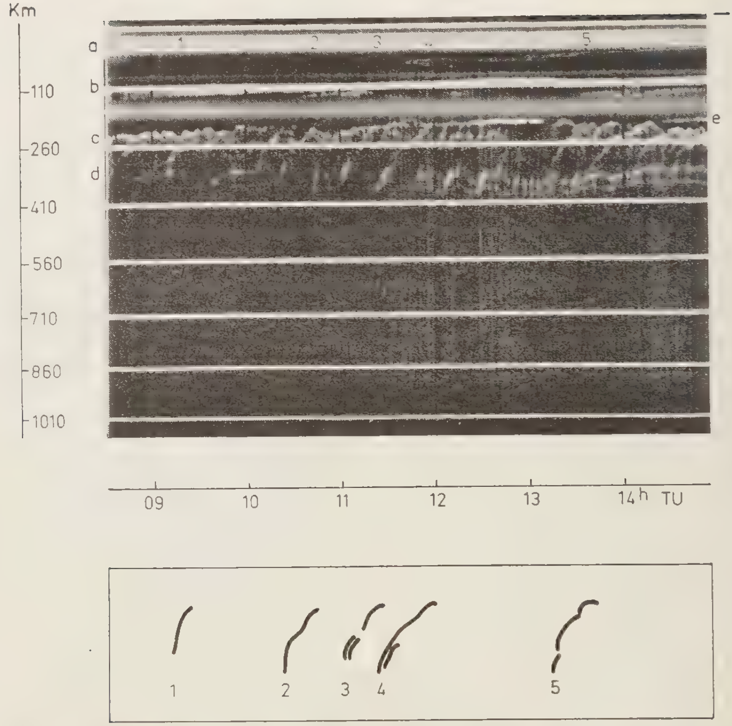

FIG. 2—Typical daytime height record: virtual height (downward) as a function of time. Horizo tal straight lines: height markers, 150 km distant. The characteristic echo levels are well marked: = direct signal; $b = h'E$ and $h'E_s$; $c = h'F$; $d = h'F_2$; $e = h'2E_s$. (b lies just on the second heig marker.) The traveling disturbances can be seen asinclined fringes clearly visible between $h'F_2$ and h' Five typical disturbances are indicated on the drawing below the original record.

rapidly increasing atmospheric density. (Even with constant energy flux, the relative disturbance should vary inversely with the absolute density.) In other cases the generation of a sporadic-E layer of the 'sequential type' seems to be associated with the disturbance.

These are all daytime results. The traveling disturbances are rare at night but appear quite regularly in the daytime.

In these disturbances we observe the consequences of some still unknown phenomenon that occurs in the outer ionosphere. An explanation is sought in terms of shock wave phenomena in a plasma.

Oscillations in the F region—From Figure 2 it can be seen that oscillation-like variations occur in the $h'F_2$ level and are still clearly visible in the $h'F$ level. They may be due to shock waves of a more or less periodic form. It ma also be that they are somewhat like a true osci lation with well defined period. In order to i vestigate this problem, one of us has used superposed epochs analysis for the ionospher characteristics f_0F_2 and F_2-3000-MUF [*Bil* 1958]. This analysis applied to the routine da of some ionospheric stations in Europe and Africa resulted in quasiperiods of some hour (We are indebted to the directors of these st tions, Professor Dieminger, Professor Lahay and Ingenieur Herrink, for providing us wi the complete data.) A large number of mo recent data (collection made possible by a gra of Deutsche Forschungsgemeinschaft) have bee indicated by points in Figure 6 (circles for r peated oscillations on the superposed epoc diagram). The abscissa of the diagram is ge

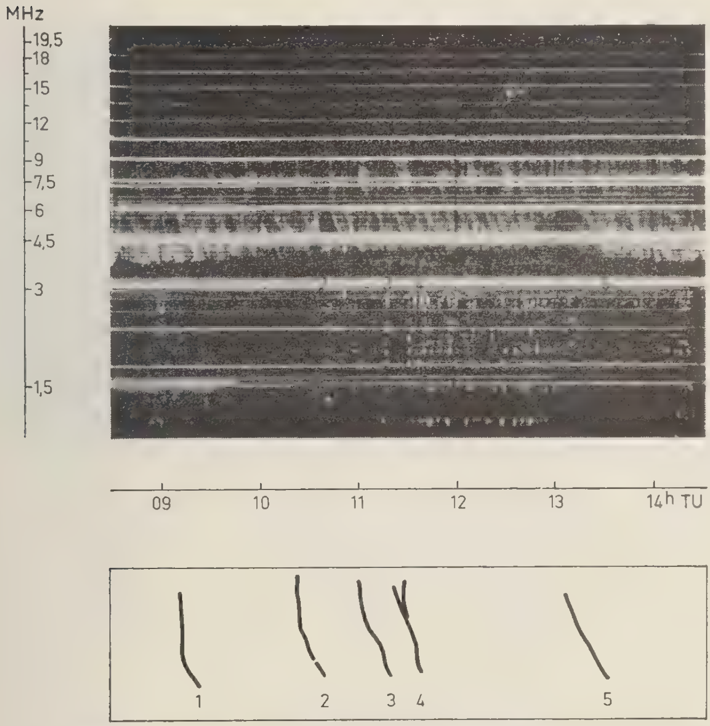

Fig. 3—Typical daytime frequency record (gated for F echoes): frequency (upward) as a function time. Same period as represented in Figure 2. Horizontal straight lines: frequency markers (multis of 1.5 MHz). (The bright horizontal bands come from interference with broadcast services.) In lower frequency range only some white points are visible. They come from interference. The lower quency limit of F echoes is well marked. This is the blanketing limit. Just before no. 5 this limit is her high as a consequence of sporadic-E blanketing. (The corresponding 2 E_s trace can be seen on gure 2.) The upper frequency limit, less clearly visible, lies at about 9 MHz. A number of traveling turbances can be seen as white fringes, all inclined in the same direction. Five typical disturbances, same as in Figure 2, are indicated on the drawing below the original record.

gnetic latitude. For Freiburg we have also roduced the quasi-periods visible on the $h'(t)$ ords. It can be seen that the triangles corponding to these observations fill up the ice below the points found by the supersed epochs method in a continuous manner. is means that in temperate latitudes the asi-period is not very well defined, values beeen 1/4 and 12 hours being observed. The persion of the points obtained with the supersed epochs method near the equator is conerably smaller; the most probable value lies tween 4 and 5 hours.

For comparison we have indicated (as crosses) some of the points obtained as quasi-periods from magnetic micropulsations by *Obayashi* [1958]. He identifies them with a true oscillation of the outer ionosphere, viz., standing Alfvén waves along the magnetic line of force (toroidal oscillations). In spite of the large dispersion of our points, there can be no doubt that there is a great difference between them and the phenomenon related to the magnetic micropulsations. Following Obayashi's reasoning, one might think that perhaps poloidal oscillations (modified Alfvén waves in the outer ionosphere) could explain our observations, but Obayashi calculates the same orders of time con-

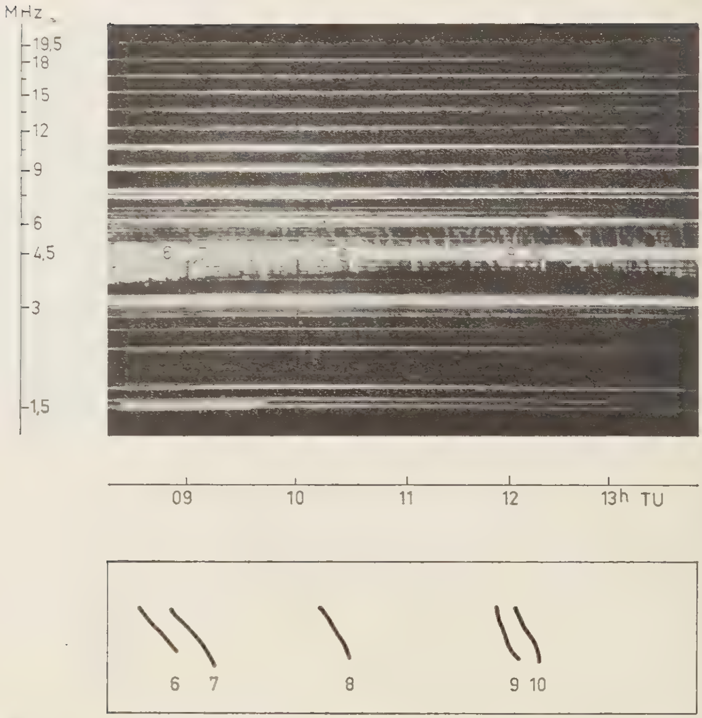

FIG. 4—Another daytime frequency record. The fringes are less regular in direction than in Figu 3. Some traveling disturbances, all first identified on the movie film, are indicated on the drawing ju below the original record.

stant for both forms. Therefore no adequate explanation can as yet be given.

Conclusions—In the past the ionosphere has been considered a series of different, well separated layers. During recent years we have learned from rocket results that there is no deep gap between the layers and that we should consider the ionosphere as an entity. Now from satellites and whistler observations we are learning more about the outer ionosphere. Our routine observations of the ionosphere can become more and more significant if we attempt to interpret them as relating to the lower end of this large ionization belt surrounding the earth, which we call now 'the outer ionosphere.' These routine observations are also important, of course, in that they allow a continuous observation of phenomena. We believe that they should be studied in more detail.

Note—Since this paper was not prepared specifically for this conference, some explanato remarks are necessary.

For many studies of oscillation in the F r gion a true height analysis is not necessar since the dependence of the oscillation frequen on time and season, and the dependence of t phase on height, are not changed by the tr height transformation. The relative amplitu can be measured by the variation of maximu electron density and F_2-3000 MUF. T monthly statistical distribution of f_oF_2 is f from being normal at all stations of the worl This phenomenon has not been explained phy ically. The variation of the maximum usab frequency is even larger over the 3000-km pat (The F_2-3000 MUF is a good measure of t form of the layer; a large MUF means a sha low, low altitude layer with high electron de sity; a small MUF characterizes a thick lay at great height, which is less highly ionized

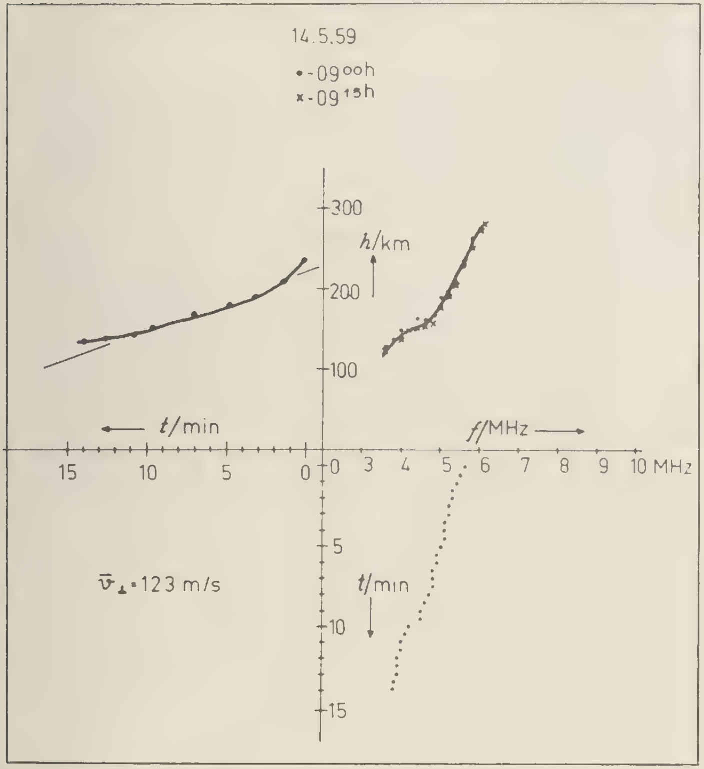

ɢ. 5—True velocity of an individual traveling disturbance. Bottom at right: development of the disance as obtained from the movie film. (Frequency where the trace was deformed as a function me.) Top at right: true height obtained from quarter-hourly ionograms with the Schmerling ique (record before and after the disturbance). Top at left: true height as a function of time, ined by combination of the two right-hand diagrams.

temperate zones the fluctuation of the layer le measured by F_2-3000 MUF is about 20 cent; near the equator the fluctuation is t 44 per cent. These very large-scale (1– km) variations have superposed on them eling disturbances starting always down- l at the moment or a little before the MUF hes the minimum value. Several traveling es per hour are possible. The direction of movement of the ionization seems always to *cross* the direction of the lines of the mag- field.

r all studies of motion, the difference be- n successive measured values must be com- d with the monthly mean of these differ- s.

References

Akasofu, S., Dispersion relation of magnetohydrodynamic waves in the ionosphere and its application to the shock wave, *Rept. Ionosphere Research Japan, 10,* 24–40, 1956.

Beynon, W. J. G., Evidence of horizontal motion in region F_2 ionization, *Nature, 162,* 887, 1948.

Bibl, K., Phénomènes dynamiques dans les couches ionosphériques, *Compt. rend., 235,* 734–736, 1952.

Bibl, K., Die Ionosphärenschichten und ihre dynamischen Phänomene, *Z. Geophysik,* pp. 136–141, 1953.

Bibl, K., Zur Dynamik der Ionosphäre, *Z. Geophysik, 1,* 1–33, 1958.

Bibl, K., Some results of directly recorded ionospheric characteristics, *J. Atmospheric and Terrest. Phys.,* in press.

Bibl, K., E. Harnischmacher, and K. Rawer,

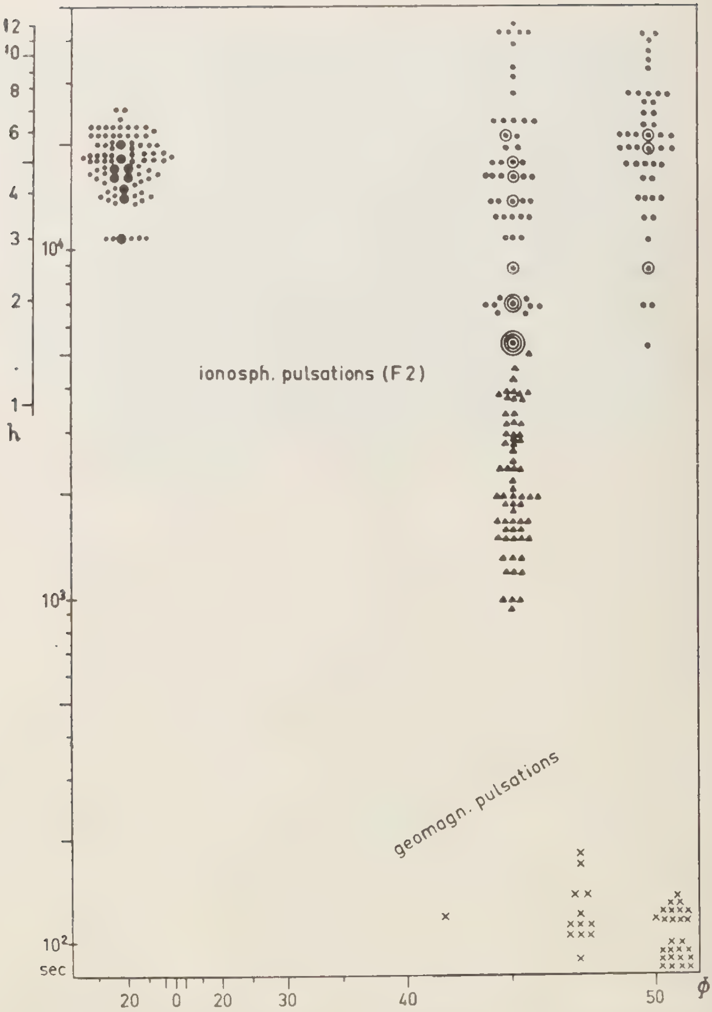

FIG. 6—Quasi-period of ionospheric pulsations as a function of geomagnetic latitude ϕ. Points circles from superposed epochs analysis of routine observations (circles for repeated oscillations). angles from continuous virtual height records (read at the $h'F$ level). The crosses are taken from O ashi's paper; they correspond to geomagnetic micropulsations.

Some observations of ionospheric movements, in *The Physics of the Ionosphere,* London, pp. 113–118, 1955.

MUNRO, G. H., Short-period changes in the *F*-region of the ionosphere, *Nature, 162,* 886, 1948.

MUNRO, G. H., Travelling disturbances in the ionosphere, *Proc. Roy. Soc. London, A 202,* 208, 1950.

NAKATA, Y., Short period variations in the ionosphere, *J. Radio Research Lab. Tokyo, 1,* 1–82, 1954.

OBAYASHI, T., Geomagnetic forms and the e outer atmosphere, *Rept. Ionosphere Res Japan, 12,* 301–335, 1958.

SCHMERLING, E. R., An easily applied metho the reduction of *h'-f* records to *N-h* profil cluding the effects of the earth's magnetic *J. Atmospheric and Terrest. Phys., 12,* 1958.

WELLS, H. W., J. M. WATTS, AND D. E. G Detection of rapidly moving ionospheric c *Phys. Rev., 69,* 540–541, 1946.

Hydromagnetic Theory of Geomagnetic Storms[1]

A. J. DESSLER

Missiles and Space Division, Lockheed Aircraft Corporation
Palo Alto, California

AND

E. N. PARKER

Enrico Fermi Institute for Nuclear Studies, University of Chicago
Chicago, Illinois

Abstract—A hydromagnetic theory is presented which explains the average characteristics of geomagnetic storms. The magnetic storm is caused by a sudden increase in the intensity of the solar wind. Stresses are then set up in the geomagnetic field by the solar plasma impinging upon the geomagnetic field and becoming trapped in it. These stresses, which are propagated to the earth as hydromagnetic waves, account for the observed average magnetic storm variations. The sudden commencement of the magnetic storm is due to a hydromagnetic wave generated by the impact of the solar plasma on the geomagnetic field. The initial phase of the magnetic storm, during which the magnetic field is above average intensity, is due to the increased solar wind pressure. During the initial phase, instability causes small plasma clouds to become imbedded in the magnetic field. They break up and diffuse into the magnetic field to form a belt of trapped particles from the sun (principally protons and electrons). The trapped protons set up stresses, mainly due to centrifugal force, which account for the main phase of the magnetic storm. The recovery from the main phase is attributed to the relief of the stress on the geomagnetic field by the transfer of the energy of the trapped protons to neutral hydrogen by means of ion-atom charge exchange. The correct recovery time for the magnetic storm is predicted from the measured cross section of the ion-atom charge-exchange process and the hydrogen density values around the earth deduced from the scattering of solar Lyman-α radiation.

INTRODUCTION

their calculations on the geomagnetic s to be expected from 1000 km/sec clouds nized gas from the sun, *Chapman and ro* [1932] demonstrated that the initial of a geomagnetic storm can be explained y by solar plasma pushing inward on the agnetic field. The main phase, on the other , has proved to be more difficult to explain. interplanetary space was presumed to be uum, Chapman and Ferraro formulated theory of the main phase accordingly, showed that the main phase could be ex- ed in terms of an equivalent ring current. that time, it has been shown that inter- tary space [*Behr and Siedentopf*, 1953] and pace inside the geomagnetic field above the ionosphere [*Storey*, 1953] contain enough ionized gas to be good electrical conductors. In the presence of high electrical conductivity, the magnetic field is frozen into the gas, so that the deformation of the elastic geomagnetic field during a storm becomes a question of the stresses that the gas is able to exert on the field. The geomagnetic storm becomes a problem in hydromagnetic theory.

In this paper, we shall present a hydromagnetic theory that accounts for the average characteristics of geomagnetic storms. Following the descriptions by *Chapman and Bartels* [1940] and *Chapman* [1951], these average characteristics may be summarized as follows:

(*a*) The sudden commencement is characterized in low and temperate latitudes by an increase in H, the horizontal component of the earth's magnetic field. This increase in H is typically 20 to 30 γ ($1\ \gamma = 10^{-5}$ gauss). The increase in

[1] resented at the meeting of the American hysical Union, May 4-7, 1959, Washington, .

H is largest at equatorial stations and has a rise time of 1 or 2 minutes.

(*b*) The initial phase is the period during which H is above its initial undisturbed value. The initial phase lasts about 2 to 8 hours.

(*c*) The main phase is the period following the initial phase during which H is much more below the initial undisturbed value than the initial phase is above it. A main-phase decrease of about 50 to 100 γ may be taken as a typical figure. After the minimum is reached, H slowly recovers toward its normal value. During the main phase, the rate of recovery increases with time. That is, the main phase is characterized by a saucer shape in the H vs. time curve (d^2H/dt^2 is positive during the main phase). The main phase of the magnetic storm, which generally lasts from 12 to 24 hours, tends to be noisy. Often large positive and negative excursions with amplitudes of the order of several hundred gamma and periods of about $\frac{1}{2}$ hour occur in the magnetic field. These excursions are not shown in the averaged magnetic storm data.

(*d*) The recovery phase follows the main phase and is characterized by an exponential recovery toward the initial undisturbed value of H (d^2H/dt^2 is negative during the recovery phase). The recovery phase has a recovery time constant of about 1 day, although a 2- or 3-day recovery time is not uncommon. Quite often there are no magnetic disturbances during the recovery phase other than the slow recovery.

Almost all magnetic storms display smoothed characteristics which fall within a factor of 3 of the numbers given in the above description of average magnetic storm characteristics. The theory as developed in this paper will be compared with these average storm parameters. Auroral phenomena are not explained.

In the first section of this paper we shall describe a physical model, and in the following sections we shall make detailed calculations of its implications.

I. The Model

Ordinarily, the earth's dipole field is confined to a distance of about 6 to 10 earth radii by the impact pressure of solar plasma on the geomagnetic field [*Dungey*, pp. 229–236, 1954; *Hoyle*, 1956; *Parker*, 1958*a*]. The distance at which the ordered dipole field is terminated
that at which the magnetic pressure, $B^2/(2$
(mks units), falls below the impact pressure
the solar plasma, ρv^2, where ρ is the plas
mass-density and v is the plasma velocity relat
to the earth. A magnetic storm is initiated
the collision between the earth's magne
field and a relatively dense plasma cloud
stream that has been ejected from the sun. T
interplanetary magnetic field [*Colgate*, 19
Petschek, 1958], as well as the plasma interacti
with the normal interplanetary gas [*Kahn*, 19
pp. 115–116, 1957; *Parker*, 1958*b*, 1959], w
maintain a sharp leading edge on the fast clo
from the sun. It has been experimentally demo
strated [*Patrick*, 1959] that the hydromagne
shock thickness is less than the collision me
free path. The largest shock thickness to
considered is the ion cyclotron radius in t
interplanetary magnetic field (approximately
km for a 1000 km/sec proton in an interplaneta
field of 1 γ).

The rise time of such a shock front would
of the order of 10 seconds. All other predictio
of shock thickness yield even faster rise tim
The sharp onset is probably smoothed somewh
by attenuation of the higher-frequency Four
components in the lower ionosphere [*Dessl*
1959*a*].

The impact of the plasma cloud on the g
magnetic field will initially compress the ma
netic field on one side of the earth and gener
a hydromagnetic wave. It is readily shown th
however irregularly one pushes in on the ma
netic field, the field intensity will be increas
more or less uniformly all around the ea
[*Parker*, 1958*a*]. The increase in intensity
carried around the earth by the hydromagne
wave in about 10 seconds [*Green and othe*
1959; *Francis and others*, 1959], in agreeme
with observation [*Gerard*, 1959]. (The ea
estimates of the hydromagnetic propagati
time [*Dessler*, 1958*a*] were much too large,
subsequent quantitative studies have show
Since the plasma will push closest to the ea
in the equatorial region of the dipole fi
where $B^2/(2\mu_0)$ is a minimum, and since
hydromagnetic wave generated by the plas
impact will be refracted somewhat toward
equatorial region, we should expect the intens
of the sudden commencements to be enhanc

ıe equatorial region. The point here is that ·omagnetic waves carry the effect of the ıct down to the bottom of the ionosphere. gularities in the ionosphere will lead to l differences in hydromagnetic wave propaga- so that sudden commencement and initial se features recorded at neighboring surface netic observatories may be quite different. he currents generated by the impact of r plasma on the geomagnetic field remained 'rom the earth, as suggested in the Chapman- ·aro theory, sudden-commencement and ial-phase features would be rather uniform ınd the earth. Thus, the hydromagnetic roach explains the relationship between the pman-Ferraro theory of sudden commence- ıt and initial phase, and the observation of *ɔush and Vestine* [1955] that 'substantial ·ents associated with the sudden commence- ıt and the initial phase flow in or near the ·gion.'

he boundary between the geomagnetic l and the plasma cloud is unstable [*Dungey*, 229–236, 1954; *Parker*, 1958*a*] in a manner ewhat analogous to the classical hydro- amic Helmholtz instability. Pieces of plasma penetrate the geomagnetic field and rapidly ık up and diffuse into the field [*Parker*, 1957]. ıs, a belt of trapped particles will be produced hin the earth's magnetic field. The initial se of a magnetic storm is that phase during ch the solar plasma cloud pushes against earth's field and before appreciable diffusion he plasma into the geomagnetic field takes :e. The main phase commences when an reciable amount of the plasma cloud diffuses the geomagnetic field.

he trapped particles from the solar plasma ments exert three stresses on the geomagnetic l, two of which decrease H while the third ls to increase it. These three stresses may easily visualized if we consider a single ticle trapped in the geomagnetic field. If particle is injected in the equatorial plane ı a velocity $w_\perp$ normal to field and a velocity parallel to the field, the particle will possess nstant diamagnetic moment $\mu = \frac{1}{2}mw_\perp^2/B$, will oscillate back and forth across the ıtorial plane with a velocity $w_\parallel$ as it crosses equatorial plane. In its north-south oscilla- · motion, the particle's guiding center follows the trajectory $r = b \cos^2 \lambda$, which traces a line of force in a dipole field, r being the distance from the center of the earth to the particle, b the distance to the point where the particle crosses the equatorial plane, and λ the latitude angle of the particle. Thus, the following three stresses may be written:

1. The diamagnetic moment is repelled from the earth's field with a force $F_m = -\mu \nabla B = 3mw_\perp^2/(2b)$.
2. The curvature of the line of force that constitutes the guiding center for the particle leads to an outward centrifugal force $F_c = 3mw_\parallel^2/b$ as the particle crosses the equatorial plane. It is easily seen (see section II) that the force is a maximum at the equatorial plane because there the radius of curvature is a minimum and $w_\parallel$ a maximum.
3. In its small cyclotron orbit in the earth's field, the particle exerts a centrifugal force that tends to spread the magnetic field locally. This spreading produces a field change outside the orbit which is, of course, just that which would be produced by a dipole moment $\frac{1}{2}mw_\perp^2/B$.

Note that in each case the stress depends only on the particle energy. If we do not invoke particle acceleration in the vicinity of the earth, the particles are supplied directly from the solar wind with their kinetic energies unchanged, and the protons have 2×10^3 times the energy carried by the electrons. If we consider particle acceleration near the earth resulting from the Fermi mechanism due to the hydromagnetic waves in the geomagnetic field [*Dessler*, 1958*b*], then again the protons will have much more energy than the electrons, since the Fermi mechanism is relatively ineffective for the electrons [*Parker*, 1958*b*]. Thus, in this presentation, we neglect the electron contribution and confine our discussion to the stresses produced by the protons.

In this paper, we adopt the position that the main-phase decrease in H is primarily due to the stretching outward of the geomagnetic lines of force by the centrifugal force term F_c of the protons. Akasofu (private communication) has independently come to a similar conclusion. The net effect of the motion perpendicular to the field is of lesser importance, as will be shown in section II. It will also be shown in that section

that the fractional change $\Delta B/B_0$ in the magnetic field intensity at the surface of the earth is related to the total particle energy parallel to the magnetic field $E_\parallel$ by

$$E_\parallel/E_m \approx -\Delta B/(2B_0)$$

for the simple case of particles moving along the lines of force near the equatorial plane. E_m is the total geomagnetic energy external to the earth, and

$$E_m = (4\pi/3)a^3(B_0^2/\mu_0)$$

where a is the radius of the earth and B_0 is the field intensity at the surface at the equator. Taking $B_0 = 3 \times 10^{-5}$ w/m² (0.3 gauss), we have

$$E_m = 8 \times 10^{17} \quad \text{joules}$$

Thus, for example, a storm decrease of $\Delta B = 100\ \gamma$ requires a total particle energy $E_\parallel = 1.3 \times 10^{15}$ joules. In order to match the observed pattern of average vertical intensity magnetic storm variations over the earth's surface, most of the particles must be trapped between 3 and 5 earth radii (section III). The particles then occupy a volume of the order of 10^{22} m³, indicating a mean energy density of 1.3×10^{-7} joules/m³. As an example, if we suppose simply that the particles are protons with the solar wind velocity of the order of 10^3 km/sec, we require a particle concentration of 10^8 protons/m³.

The diamagnetic repulsion or F_m term as a cause of the main phase was considered by *Alfvén* [1955] for temporarily trapped solar particles. The first suggestion that the main phase might be due to completely trapped particles is due to *Singer* [1957].

The third stress term, the local spreading of the magnetic field due to the cyclotron orbit of the particles, is important in the region immediately beneath the particles' mirror points on the earth's surface. During the main phase, the diamagnetic moment will reduce the absolute value of the vertical intensity beneath the mirror points. If the bulk of the magnetic storm particles are trapped between 3 and 5 earth radii (the vicinity of the outer Van Allen belt), the reduction in the magnitude of the vertical intensity will occur between about 55° latitude and the auroral zone (~67° latitude). Elsewhere, the

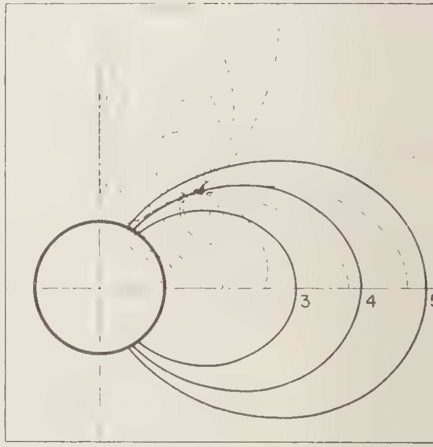

FIG. 1—Magnetic field (dotted lines) from tip of a belt of trapped protons centered earth radii and mirrored 1 earth radius ab the surface of the earth. The lines do not pe trate very far into the earth because of the electrical conductivity of the earth's interior. aid in making this drawing, a laboratory m was set up using permanent magnets.

magnitude of the vertical intensity will slightly increased by this effect. These cha are schematically suggested in Figure 1. S effects are observed [*Chapman and Bartels*, 1 p. 287]. The magnitude of the reductio calculated in section III.

In order to explain the recovery phas means of removing most of the trapped part in about 1 day is required. The trapped ticles to be removed are protons with ene probably below 12 kev (or velocities less 1500 km/sec, corresponding to a sun-e travel time of 1 day). It has been pointed that charge exchange between protons neutral atmospheric hydrogen atoms will effectively remove protons trapped in the magnetic field with energies less than 50 [*Stuart*, 1959]. Thus, charge exchange betw the magnetic storm protons and neutral at pheric hydrogen atoms provides the mecha for the recovery phase. The cross section the charge-exchange reaction $P_f + H_t \rightarrow H_f +$ between protons, P, and hydrogen atoms, where the subscripts f and t refer to fast thermal velocities respectively, has measured over a wide range of energies

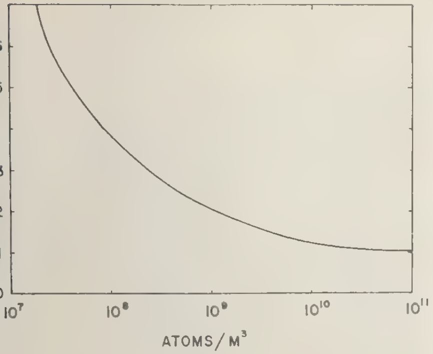

ɪɢ. 2—Distribution of neutral hydrogen atoms
ınd the earth. The radial distance is measured
ı the center of the earth. (After *Johnson*,
.)

others, 1958]. In this reaction, a fast (perhaps
) km/sec) proton picks up an electron from
ıermal hydrogen atom and becomes a fast
:ral atom. Then the original proton is no
er coupled to the magnetic field and ceases
contribute to the storm. From the cross-
ion measurements, it is found in section IV
the lifetime of a proton (with less than 20
energy) moving in a neutral atomic hydrogen
is independent of the proton's energy. The
ime is inversely proportional to the number
sity of neutral hydrogen atoms. Therefore,
time for recovery from the main phase of a
netic storm may be calculated solely from
ıowledge of the distribution of the atmos-
ic neutral atomic hydrogen. Using the
ber density of neutral hydrogen given by
ıson [1959] and shown in Figure 2, the correct
ı-phase recovery time of about 1 day follows.
rom our model of the initial phase, a great
netic storm should inject protons more
ly into the geomagnetic field (where the
ber density of hydrogen atoms is greater)
ı a moderate storm. Also, a great magnetic
n may heat the ionosphere [*Dessler*, 1959*a*,
b], thereby increasing the scale height and
ospheric density far from the earth. Both
e effects will increase the probability for
ped protons to undergo charge exchange by
easing the average number density of hydro-
atoms in the vicinity of the protons. There-
we should expect the recovery time to be
ter for a great magnetic storm than for a

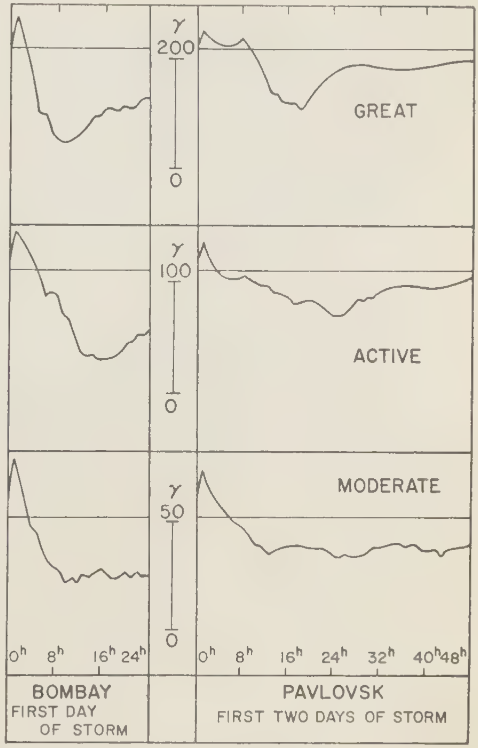

FIG. 3—Averaged magnetic storm variations of the horizontal magnetic intensity as measured from the time of the sudden commencement. The magnetic storms are divided into three intensities. Note that the great magnetic storms recover much faster than the moderate storms. (*After Chapman*, 1927.)

moderate one. This variation of recovery time with the severity of the storm is observed, as shown in Figure 3.

To recapitulate, we have the following model for a geomagnetic storm: (*a*) The sudden commencement is initiated by the impact of solar plasma on the geomagnetic field. The effect of the impact is carried down to the lower ionosphere by hydromagnetic waves. The sharp leading edge of the solar plasma is produced by the weak magnetic field and plasma normally present in interplanetary space. (*b*) The initial phase is due to the increased solar wind pressure on the geomagnetic field. This continues until the diffusion of plasma (trapping of protons) in the geomagnetic field becomes important.

(c) The main phase is due to the stresses set up in the geomagnetic field by trapped protons from the solar wind. The major stress term comes from the centrifugal force of the trapped particles as they oscillate back and forth along the lines of force through the equatorial plane. (d) The recovery phase is due to the relief of the main-phase stress through the transfer of the energy of the trapped protons to neutral hydrogen by means of the ion-atom charge-exchange process.

II. Geomagnetic Effects of Trapped Particles

In this section it will be our purpose to write down the general methods of calculating the magnetic effects of charged particles moving in a magnetic field imbedded in a background plasma. We will apply the general method to the formal calculation of the geomagnetic effects of a stationary distribution of charged particles injected into the geomagnetic field at a distance of 4 earth radii from the earth's center.

1. *General discussion*—In the following discussion, 'plasma' will be used to denote the equilibrium background gas and 'particles' will refer to the nonequilibrium injected component. The stresses exerted by charged particles on the magnetic field in which they are moving can be calculated from the equivalent hydrostatic pressure of the particle motions. Thus, if we have a distribution of charged particles with an equivalent pressure P_2 in a magnetic field B in which there is a tenuous plasma with pressure P_1, the mass motion $\mathbf{v}$ of the particles and the magnetic field strength are related by the familiar hydromagnetic equation of motion

$$\rho\, d\mathbf{v}/dt = -\nabla(P_1 + P_2 + B^2/2\mu_0) + (\mathbf{B}\cdot\nabla)\mathbf{B}/\mu_0 \qquad (1)$$

where ρ is the gas density. When the collision rate is sufficiently low, as it is throughout most of the geomagnetic field, so that the thermal motions may be anisotropic, we must use the more general equation

$$\rho\, (d\mathbf{v}/dt)_\perp = -\nabla_\perp(P_\perp + B^2/2\mu_0) + \{[(\mathbf{B}\cdot\nabla)\mathbf{B}]_\perp/\mu_0\} \cdot[1 + (P_\perp - P_\parallel)/(B^2/\mu_0)] \qquad (2)$$

in which we distinguish between the pressu $P_\perp$ and $P_\parallel$ respectively perpendicular and para to the magnetic field.

If the particle distribution is stationary, have $d\mathbf{v}/dt = 0$, and (1) or (2) becomes an eq tion for the magnetic field in terms of the p ticle pressures. As (1) and (2) are nonlin partial differential equations, their gene solutions are exceedingly difficult. In order expedite our exposition, we shall restrict o selves to the special case where the plas enmeshed in the field is either in hydrosta equilibrium or sufficiently tenuous so that exerts only negligible stresses on the magn field. Then the only stresses exerted on field are those of the additional charged p ticles, and the calculation is greatly simplifi It can be proved in a formal way that the eff $\Delta\mathbf{B}$ of the additional particles can be calcula from a suitable integral over the individ particle trajectories.

Suppose therefore that we consider a st magnetic field in which the background plas is either in hydrostatic equilibrium (this wo follow if the surfaces of equal density coinc with the geopotential surfaces) or else tenuous that the total force that the plas exerts on the field is small compared with total stress, of the order of $B^2/(2\mu_0)$, carried the field. Then everywhere between the traj tories of the individual additional charged p ticles we must have $\nabla \times \mathbf{B} = 0$ (the possibi that $\nabla \times \mathbf{B}$ is parallel to $\mathbf{B}$ is excluded by nonconnecting terrestrial atmosphere), so t $\mathbf{B}$ is expressible as $\mathbf{B} = -\nabla\psi$, where $\nabla^2\psi =$ It is not true, of course, that $\nabla \times \mathbf{B}$ vanishes the individual trajectories, because each ad tional particle transports a charge, and we m satisfy Maxwell's equation

$$\mu_0\mathbf{j} = \nabla \times \mathbf{B}$$

where $\mathbf{j}$ is the current density. Thus, let enclose each additional particle trajectory b tube of small cross section. In the space outs the tubes the field satisfies Laplace's equati The derivatives of the field on the surfaces the tubes are related by the condition (3), so, together with the assumption that the f must vanish at infinity, they uniquely determ the solution of Laplace's equation outs Consider then the integral expression

$$) \equiv [\mu_0/(4\pi)] \int d^3\mathbf{r}'\mathbf{j}(\mathbf{r}') \times (\mathbf{r} - \mathbf{r}')/|\mathbf{r} - \mathbf{r}'|^3 \quad (4)$$

$d^3\mathbf{r}'$ is an element of volume and $\mathbf{j}(\mathbf{r}')$ is urrent density of each additional particle tory. Since (4) is simply the Biot-Savart or the trajectory currents $\mathbf{j}(\mathbf{r})$, it obviously ies Laplace's equation at all points outside urfaces enclosing the individual trajectories, t obviously satisfies (3) on each trajectory. efore, it is the change in the magnetic produced by the additional particles. To ay be added any field $\mathbf{B}$ which satisfies ace's equation throughout the entire region. $\mathbf{B}$ is small compared with $\mathbf{B}$, then the par- rajectories, and hence $\mathbf{j}(\mathbf{r}')$, can be calculated ing $\Delta\mathbf{B}$. And $\Delta\mathbf{B}$ can then be calculated (4).

recapitulate, we have shown that the etic effect of the stresses P_2 produced by ional charged particles introduced into the agnetic field can be calculated from the ral (4) taken over the detailed individual ional particle trajectories (calculated in nperturbed field), provided that: (1) the ional particle distribution is such as to ationary in time; (2) the background plasma tic and exerts no forces on the field; (3) the ional particles are sufficiently few so that $\ll \mathbf{B}$. If we give up any one of these three tions we cannot use (4). Clearly, therefore, alculations in this paper apply only to an zed sort of geomagnetic storm. It must be asized that, in the actual case, partial tion of one or more of these conditions lead to effects quantitatively different from calculated here.

Particle motion—The motion of the in- ual additional particles in the geomagnetic may be calculated, of course, using the well n guiding center approximation, since the tron radius, $R = mw_\perp/(qB)$ due to the ity $w_\perp$ perpendicular to the field is small ared with the scale of the field. $w_\perp^2/B$ is a ant of the motion. It can be shown that, g to dipole repulsion, the particle drifts the velocity

$$_1 = [mw_\perp^2/(2qB^4)]\mathbf{B} \times \nabla(B^2/2) \quad (5)$$

the surface of a magnetic shell. This may be written simply as

$$u_1 = -w_\perp R/(2l) \quad (6)$$

in terms of the scale l of the variation of $|\mathbf{B}|$, where

$$1/l = \nabla_\perp \ln B \quad (7)$$

The motion $w_\parallel$ of the particle *along* the lines of force is subject to the acceleration

$$dw_\parallel/dt = -(w_\perp^2/2B)\, \partial B/\delta s$$

as a consequence of the convergence or divergence of the lines of force. We denote distance measured along a line of force by s. The curvature k of the lines of force leads to the centrifugal force $mw_\parallel^2k$, which is balanced by the Lorentz force of the drift

$$\mathbf{u}_2 = [mw_\parallel^2/(qB^4)]\mathbf{B} \times [(\mathbf{B}\cdot\nabla)\mathbf{B}] \quad (8)$$

More simply,

$$u_2 = mw_\parallel^2k/(qB) \quad (9)$$

The centrifugal force is exerted against the magnetic field and obviously tends to increase the field density on the side away from the center of curvature.

The hydromagnetic equation (1), or (2), is the quantitative expression for the sum of all the particle stresses [*Parker*, 1957]. The current $\mathbf{j}(\mathbf{r})$ appearing in (4) is $ne(\mathbf{u}_1 + \mathbf{u}_2)$ plus the cyclotron motion about the lines of force, whose magnetic effect is most easily represented by the magnetic moment per unit volume.

3. *Magnetic effects of particle motion perpendicular to* **B**—Consider a magnetic field in the z direction with an intensity which is a function only of the distance $\varpi = (x^2 + y^2)^{1/2}$ from the z axis. Into this field we introduce $2\pi bn$ particles in the form of a uniform ring of radius b around the z axis in the $z = 0$ plane. We suppose that the particles all have a velocity $w_\perp$ perpendicular to the field, and, besides circling the field with a speed $w_\perp$, they all drift in a ring around the axis with the velocity u_1. It is readily shown that the drift u_1 plus the diamagnetic moment results in a magnetic effect $\Delta B(z)$, at a distance z along the axis from the plane of the ring, where

$$\Delta B(z) = \frac{\mu_0 n b m w_\perp^2}{4B(b)(b^2 + z^2)^{3/2}} \cdot \left\{ \frac{b}{l} + \frac{b^2 - 2z^2}{b^2 + z^2} \right\} \quad (10)$$

The scale l is, of course, now defined as

$$1/l = d \ln B(\varpi)/d\varpi$$

The first term in the braces is the contribution of u_1; the second term is the diamagnetic moment.

In the equatorial plane of the geomagnetic field we have

$$B(b) = B_0(a/b)^3$$

and

$$l = -b/3$$

so that

$$\Delta B(z) = \frac{-\mu_0 n b^4 m w_\perp^2 (2b^2 + 5z^2)}{4B_0 a^3 (b^2 + z^2)^{5/2}} \qquad (11)$$

Thus, the relative field perturbation at the origin (the center of the earth, neglecting the fact, of course, that the earth is itself a conducting, and therefore a diamagnetic, body) is

$$-\Delta B/B_0 = 2E_\perp/(3E_m) \qquad (12)$$

where $E_\perp$ is the sum of the particle kinetic energies, $2\pi b n(\frac{1}{2} m w_\perp^2)$, and E_m is the external geomagnetic field energy. The diamagnetic moment produces an increase which cancels one-third of the decrease due to u_1 (the second term in the braces in equation 10).

The effect of a diamagnetic earth is estimated in part 5 of this section.

4. *Magnetic effects of particle motion parallel*

If the particle speed is $w_\parallel$ along the line of forc the centrifugal force is $m w_\parallel^2 k$. The drift perpendi cular to the lines of force as a consequence o the centrifugal force is given by (8). Note tha the centrifugal force for a trapped particle is maximum when $\theta = \pi/2$, since $w_\parallel$ and k ar maxima there.

Suppose that the additional particles ar distributed uniformly around the earth in shell generated by rotating the line of forc (equation 13) about the geomagnetic dipo axis. An element of arc length along the lin of force is

$$ds = b \sin\theta (1 + 3\cos^2\theta)^{1/2}\, d\theta$$

and the field density is

$$B = B(b)(1 + 3\cos^2\theta)^{1/2}/\sin^6\theta$$

Thus, if there are $\mathfrak{N}$ additional particles per un length of line at the equatorial plane, there ar $n(\theta)\, d\theta$ particles in between θ and $\theta + d\theta$, whe

$$n(\theta) = \mathfrak{N}\, ds/d\theta$$

The current due to the centrifugal force of th particles in $d\theta$ is

$$j_\phi(\theta)\, d\theta = q u_2 n(\theta)\, d\theta/(2\pi r \sin\theta)$$

$$= -\frac{3}{2\pi} \frac{\mathfrak{N} m w_\parallel^2 (1 - \cos^4\theta) \sin\theta\, d}{b B(b)(1 + 3\cos^2\theta)^{3/2}}$$

The resulting distortion on the geomagnet axis at a distance z from the center of the earth

$$\Delta B(z) = \frac{\mu_0}{2} \int d\theta j_\phi(\theta) \frac{r^2 \sin^2\theta}{[r^2\sin^2\theta + (z - r\cos\theta)^2]^{3/2}} = -\frac{3\mathfrak{N} m w_\parallel^2 b \mu_0}{B(b) 4\pi}$$

$$\cdot \int \frac{dx(1 + x^2)(1 - x^2)^4}{(1 + 3x^2)^{3/2}[b^2(1 - x^2)^2 - 2bz(1 - x^2)x + z^2]^{3/}}$$

to **B**—Now consider the effect on the geomagnetic field of the centrifugal force of particle motion along the lines of force. The lines of force of a dipole satisfy the relation

$$r = b\sin^2\theta \qquad (13)$$

where b is the radial distance from the center of the earth at the equatorial plane (i.e., $\theta = \pi/2$). It is readily shown that the curvature k of such a line is

$$k = \frac{3(1 + \cos^2\theta)}{b\sin\theta(1 + 3\cos^2\theta)^{3/2}} \qquad (14)$$

where $x = \cos\theta$.

If the additional particles moving along th lines of force are all near the equatorial plan and have a total number N, then

$$\Delta B(z) = \frac{-3N m w_\parallel^2 \mu_0}{4\pi B(b)(b^2 + z^2)^{3/2}} \qquad (1$$

which at the origin reduces to

$$\Delta B/B_0 = -2E_\parallel/E_m \qquad (1$$

On the other hand, suppose that the addition particles are spread uniformly along the lin

orce between the latitudes $\pm\lambda$. The effect ne origin is then

$$0) = -\frac{3\mathfrak{N} m w_{\parallel}^2 \mu_0}{2\pi b^2 B(b)} \int_0^{\sin\lambda} \frac{dx(1 - x^4)}{(1 + 3x^2)^{3/2}}$$

$$= \frac{\mathfrak{N} m w_{\parallel}^2 \mu_0}{4\pi b^2 B(b)} \left\{ \frac{\sin\lambda(5 - \sin^2\lambda)}{(1 + 3\sin^2\lambda)^{1/2}} + \frac{1}{3^{1/2}} \ln [3^{1/2} \sin\lambda + (1 + 3\sin^2\lambda)^{1/2}] \right\} \qquad (17)$$

total number of particles is

$$) = 2\mathfrak{N} \int_0^{\pi/2-\lambda} d\theta\,(ds/d\theta)$$

$$= \mathfrak{N} b\{\sin\lambda(1 + 3\sin^2\lambda)^{1/2} + (1/3)^{1/2} \ln [3^{1/2}\sin\lambda + (1 + 3\sin^2\lambda)^{1/2}]\}$$

s, in the limit, as $\lambda \rightarrow \pi/2$, we have

$$/2) = \mathfrak{N} b\{2 + (1/3)^{1/2} \ln (2 + 3^{1/2})\} = 2.76 b\mathfrak{N}$$

$$\Delta B(0) = -N(\pi/2) m w_{\parallel}^2 / b^3 B(b) = -2E_{\parallel}/(3E_m) \qquad (18)$$

Effect of a diamagnetic earth—As mentioned ier, we neglect the fact that the earth is ctively perfectly diamagnetic below a depth ibout 260 km for short-period phenomena as a geomagnetic storm [*Chapman*, 1951, 6]. The diamagnetic effect was neglected to plify the calculations. As we will now show, ever, neglecting this effect leads us to overnate the trapped particle energy density essary to cause the main phase decrease at most, 1/3.

uppose that a uniform external field is ressed across a perfectly diamagnetic earth radius a. Taking the impressed field to be roximately uniform, and of magnitude ΔB from the earth, the field in the vicinity of the h is derivable from the scalar potential

$$\psi(r, \theta) \approx -\Delta B[r + a^3/(2r^2)] \cos\theta$$

ch fits the boundary condition $\partial\psi/\partial r = 0$ at a (i.e., the normal component of the resultant l is zero on the surface of the earth). The l at the earth's surface is given by

$$-\nabla\psi|_{r=a} = \tfrac{3}{2}\Delta B \sin\theta$$

For a given impressed field, ΔB, the change at the equator ($\theta = \pi/2$) is (3/2) ΔB. Thus, we have probably somewhat overestimated the trapped particle energy density. However, since the field decreases as $\sin\theta$ away from the equator, we note that at $\theta = 42°$ the resultant field and the applied ΔB are equal. The resultant field becomes negligible in the polar regions. Therefore, equations 12 and 16, which were derived neglecting the diamagnetic earth, give essentially the correct results. If the magnitude of the main-phase decrease were given for a latitude of 48° (colatitude $\theta = 42°$), equations 12, 16, and 18 would not require any correction for a diamagnetic earth.

6. *General magnetic effect of trapped particles*—Now consider the problem of calculating the magnetic effect at the origin as a consequence of a belt of trapped particles crossing the equatorial plane at $b = 4$ earth radii and mirroring at 2 earth radii. The shell is a figure of rotation given by (13). For simplicity, we shall suppose every particle to have a velocity w, so that, in terms of the pitch angle α,

$$w_{\perp} = w \sin\alpha \qquad w_{\parallel} = w \cos\alpha \qquad (19)$$

For a given particle, with an angle of pitch α_1 as it crosses the equatorial plane, we have the usual adiabatic invariant expression

$$\sin^2\alpha(\theta) = [B(\theta)/B_1] \sin^2\alpha \qquad (20)$$

where $B_1 = B_0(a/b)^3$ is the field density in the equatorial plane. If the particle mirrors at $\theta = \theta_2$ [i.e., $\sin\alpha(\theta_2) = 1$], then

$$\sin^2\alpha_1 = B_1/B(\theta_2) = \sin^6\theta_2/(1 + 3\cos^2\theta_2)^{1/2}$$

For particles crossing the equatorial plane at $b = 4a$ and mirroring at $2a$, the mirror positions are $\theta = \pi/4$ and $3\pi/4$, and the minimum pitch angle at the equator is $\alpha_{\min} = 16°20'$ or 0.285 radian. Any particles which were injected into the geomagnetic field with smaller pitch angles are quickly lost by charge exchange, as they mirror below $2a$ where the atomic hydrogen densities are relatively high. The minimum pitch angle $\alpha_2(\theta)$ for any value of θ is then given by

$$\sin^2\alpha_2(\theta) = \sin^2\alpha_{\min}(1 + 3\cos^2\theta)^{1/2}/\sin^6\theta$$

Now the actual particle velocity distribution in the geomagnetic field is certainly not exactly isotropic (section IV). For instance, Fermi acceleration by hydromagnetic waves in the geomagnetic field will systematically change the distribution. We are not prepared at the present time, however, to state the actual distribution in any quantitative way. Therefore, as the simplest illustrative model, we shall assume that the particle distribution is isotropic, except for the gaps $\alpha < \alpha_2(\theta)$ and $\alpha > \pi - \alpha_2(\theta)$, where there are no particles. This assumption greatly simplifies the following mathematics, because the pitch angle distribution which is proportional to $\sin \alpha$ in an isotropic distribution does not vary with the field density along the lines of force. Thus the number of particles $f\, d\alpha$ per unit length of field with pitch angles in the interval α to $\alpha + d\alpha$ is simply proportional to the cross section of the field, or

$$f(\theta, \alpha)\, d\alpha = \begin{cases} C[B_1/B(\theta)] \sin \alpha \quad \text{for} \\ \quad \alpha_2(\theta) < \theta < \pi - \alpha_2(\theta) \\ \quad \text{zero otherwise} \end{cases}$$

where C is a constant proportional to the total number of particles. The total number of particles in $(\theta, \theta + d\theta)(\alpha, \alpha + d\alpha)$ is

$$\psi(\theta, \alpha)\, d\theta\, d\alpha = f(\theta, \alpha)\, d\alpha\, ds \tag{21}$$

or

$$\psi(\theta, \alpha) = Cb \sin^7 \theta \sin \alpha$$

As a consequence of the drift velocity u_1, given in (6), of the particles in $d\theta$, we have a circular current in the azimuthal direction

$$j^{(1)}(\theta)\, d\theta = \frac{-1}{2\pi r \sin \theta} \cdot \int_{\alpha_2(\theta)}^{\pi - \alpha_2(\theta)} d\alpha \psi(\theta, \alpha)\, d\theta e u_1(\theta, \alpha)$$

or

$$j^{(1)}(\theta) = \frac{-Cmw^2 \sin^4 \theta k(\theta)}{4\pi B(\theta)} \int_{\alpha_2(\theta)}^{\pi - \alpha_2(\theta)} d\alpha \sin^3 \alpha$$

$$= \frac{-Cmw^2 \sin^4 \theta k(\theta) \cos \alpha_2(\theta)[1 - \frac{1}{3} \cos^2 \alpha_2(}{2\pi B(\theta)}$$

Similarly the drift velocity u_2, given in (yields

$$j^{(2)}(\theta) = \frac{-Cmw^2 \sin^4 \theta k(\theta)}{2\pi B(\theta)} \cdot \frac{2}{3} \cos^3 \alpha_2(\theta)$$

The magnetic field at the origin due to current loop $j(\theta)\, d\theta$ at $(b \sin^2 \theta, \theta)$ is, from (easily shown to be

$$d\beta = \mu_0 j(\theta)/(2b)$$

so that we have the fields

$$\beta^{(1)} = \frac{-Cmw^2 \mu_0}{4\pi b} \int \frac{d\theta \sin^4 \theta k(\theta) \cos \alpha_2(\theta)[1 - \frac{1}{3} \cos^2 \alpha_2(\theta)]}{B(\theta)} \quad (2$$

and

$$\beta^{(2)} = \frac{-Cmw^2 \mu_0}{6\pi b} \cdot \int \frac{d\theta \sin^4 \theta k(\theta) \cos^3 \alpha_2(\theta)}{B(\theta)} \quad (2$$

as a consequence of the dipole repulsion a motion along the lines of force, respectively.

Now consider the field arising from t cyclotron motion of the particles and ch acterized by the diamagnetic moment μ. It c be shown that a ring of dipoles of total mome Q and radius a results in a field P at a distan z along the axis from the ring, given by

$$P = -Q \frac{(a^2 - 2z^2) \cos \phi - 3az \sin \phi}{(a^2 + z^2)^{5/2}}$$

where ϕ is the angle between the dipoles and t axis of the ring. In our case the dipoles a directed along the geomagnetic lines of for so that

$$\sin \phi = 3 \sin \theta \cos \theta/(1 + 3 \cos^2 \theta)^{1/2}$$

and

$$\cos \phi = (3 \cos^2 \theta - 1)/(1 + 3 \cos^2 \theta)^{1/}$$

Thus the particles in $d\theta$ contribute the field

$$d\beta^{(3)} = \frac{Cmw^2 \sin \theta (1 + 3 \cos^2 \theta)^{1/2} \mu_0}{8\pi b^2 B(\theta)} \cdot \int_{\alpha_2}^{\pi - \alpha_2} d\alpha \sin$$

rying out the integration over α, and then grating over θ, yields

$$_{3)} = \frac{Cmw^2\mu_0}{4\pi b^2}\int \frac{d\theta \sin\theta(1 + 3\cos^2\theta)^{1/2}}{B(\theta)} \cdot \cos\alpha_2(\theta)(1 - \tfrac{1}{3}\cos^2\alpha_2(\theta)) \quad (24)$$

'he limits of integration in (22), (23), and) are the extreme mirror points. In our case y are $\theta = \pi/4$ and $3\pi/4$. The integration st be done numerically, and it is necessary write out the functional dependence of the egrands in full. Thus

$$= \frac{-Cmw^2b\mu_0}{4\pi B_0a^3}\int \frac{d\theta \sin^9\theta(1 + \cos^2\theta)}{(1 + 3\cos^2\theta)^2}$$

$$1 - \sin^2\alpha_{\min}(1 + 3\cos^2\theta)^{1/2}/\sin^6\theta]^{1/2}$$

$$2 + \sin^2\alpha_{\min}(1 + 3\cos^2\theta)^{1/2}/\sin^6\theta] \quad (25)$$

$$) = \frac{-2Cmw^2b\mu_0}{4\pi B_0a^3}\int d\theta \frac{\sin^9\theta(1 + \cos^2\theta)}{(1 + 3\cos^2\theta)^2} \cdot[1 - \sin^2\alpha_{\min} \cdot(1 + 3\cos^2\theta)^{1/2}/\sin^6\theta]^{3/2} \quad (26)$$

l

$$) = \frac{Cmw^2b\mu_0}{12\pi B_0a^3}\int d\theta \sin^7\theta[1 - \sin^2\alpha_{\min} \cdot(1 + 3\cos^2\theta)^{1/2}/\sin^6\theta]^{1/2} \cdot[2 + \sin^2\alpha_{\min} \cdot(1 + 3\cos^2\theta)^{1/2}/\sin^6\theta] \quad (27)$$

e total number of particles is

$$= 2Cb\int d\theta \sin^7\theta[1 - \sin^2\alpha_{\min} \cdot(1 + 3\cos^2\theta)^{1/2}/\sin^6\theta]^{1/2} \quad (28)$$

Numerical integration of (28) yields $Cb =$ $2N$. We then obtain the numerical results m (25), (26), and (27):

$$\beta^{(1)}/B_0 = -0.51E/E_m$$

$$\beta^{(2)}/B_0 = -0.41E/E_m$$

l

$$\beta^{(3)}/B_0 = +0.24E/E_m$$

ere E is the total particle energy, $\tfrac{1}{2}Nmw^2$. te that the particle motion parallel to the field contributes $\beta^{(2)}$, which is 1.52 times larger than the contribution $\beta^{(1)} + \beta^{(3)}$ of the motion perpendicular to the field. It is obvious, of course, that, had we chosen a particle velocity distribution emphasizing the motion perpendicular to the geomagnetic field, we could have made $\beta^{(2)}$ smaller than $\beta^{(1)} + \beta^{(3)}$ simply by making $E_\parallel$ extremely small, even though $E_\parallel$ is more effective than $E_\perp$ in producing a decrease of the geomagnetic field. There is, of course, reason to believe that such a pancake distribution does not exist (section IV).

The parallel and perpendicular components of the particle motion contribute the respective energies

$$E_\parallel = \tfrac{1}{3}Cbmw^2\int d\theta \sin^7\theta \cos^3\alpha_2(\theta) \quad (29)$$

and

$$E_\perp = Cbmw^2\int d\theta \sin^7\theta \cdot \cos\alpha_2(\theta)[1 - \tfrac{1}{3}\cos^2\alpha_2(\theta)] \quad (30)$$

so that for our particular case

$$E_\parallel = 0.28E \quad \text{and} \quad E_\perp = 0.72E$$

It follows that we may write

$$\beta^{(2)}/B_0 = -1.46E_\parallel/E_m$$

and

$$[\beta^{(1)} + \beta^{(3)}]/B_0 = -0.375E_\perp/E_m$$

again showing how much more effective motion along the lines of force is than perpendicular motion.

In Figure 4 we have plotted the integrands of (25), (26), and (27) to show the contribution to the field as a function of θ. In Figure 5 we have plotted the integrands of (28), (29), and (30) to show the distribution of the particles and their parallel and perpendicular kinetic energies.

III. Reduction in the Magnitude of the Vertical Magnetic Intensity by Trapped Particles

The mean behavior of the vertical magnetic intensity is described by *Chapman and Bartels* [1940, p. 287], who state that the changes in vertical intensity are small and positive from

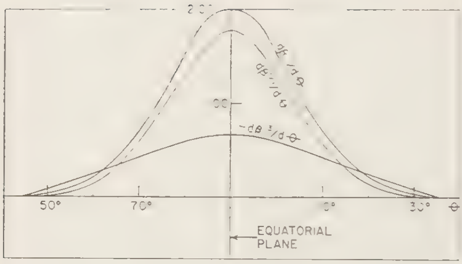

FIG. 4—The contribution $d\beta^{(n)}$ to the field at the origin, from the particles in $(\theta, \theta+d\theta)$, plotted in units of mw^2Cb/B_0a^3. The field $\beta^{(2)}$ is due to the particle motion parallel to the geomagnetic field, and $\beta^{(1)}$ and $\beta^{(3)}$ are due to the motion perpendicular.

the equator (where the change is zero) up to about 55° northern latitude; there they change sign (to negative) and increase numerically toward the auroral zone. A further change of sign, to positive values, occurs at or within the auroral zone (~67° latitude). The change in vertical intensity decreases toward the pole. The average decrease in vertical intensity near 60° magnetic latitude is very roughly 3 to 4 γ. Since the auroral zone moves toward the equator during a severe magnetic storm, it is probable that this zone of decreased vertical intensity also moves toward the equator.

As stated previously and as schematically illustrated in Figure 1, the diamagnetic moment of trapped particles reduces the vertical intensity of the geomagnetic field beneath the mirror points. The observed decrease in vertical intensity seems to center at about 60° latitude.

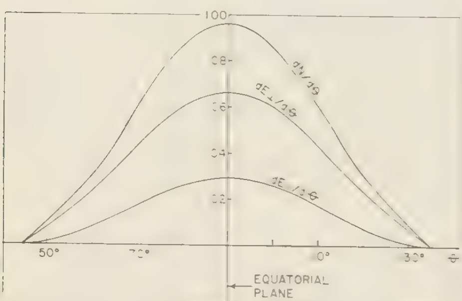

FIG. 5—The distribution of the particles and the parallel and perpendicular kinetic energies in units of $2Cb$ and $CB\ mw^2$ respectively.

The magnetic field line which passes through t latitude crosses the equator at 4 earth radii fr the center. Thus, in order to match the obser magnetic storm average variations in verti intensity, it is required that the major part the magnetic storm protons be injected at ab 4 earth radii.

In order to estimate the decrease in verti intensity, let us assume that the magne storm protons are injected between about and 5 earth radii. Protons that mirror belo earth radii are quickly removed either atmospheric collisional loss or by charge excha with neutral hydrogen (section IV). Thus, have a belt of trapped protons extending do to within 1 earth radius above the surface the earth at a latitude of about 60° (Fig. The tips of the belt shown in Figure 1 are resp sible for reducing the vertical magnetic intens The total particle energy was estimated in s tion I to be about 1.5×10^{15} joules. If α is fraction of the total particle energy in the t where the particles are mirroring, the effect perpendicular particle energy is 1.5×10 joules. The geomagnetic field in the tips (a earth radii) is 6×10^{-6} w/m², so that the effect magnetic moment, which is the perpendicu particle energy divided by the geomagne field, is $3 \times 10^{20}\alpha$ amp m². The field on surface of earth, 7×10^6 m below the tip, accordingly approximately $7 \times 10^{-8}\alpha$ w/ Assuming that the fraction of the total num of particles contained in the tip over the po of ground observation is of the order of $\alpha = 1$ (see Fig. 1), we arrive at a rough estimate 7 γ for the decrease of the vertical intensi Thus, the agreement with observation is sa factorily within observational error and large uncertainty in the choice of the mo parameters. When more detailed informati is available from observation, a more quantitat calculation will be possible.

IV. LIFETIME OF MAGNETIC STORM PROTO IN THE GEOMAGNETIC FIELD

The lifetime between charge-exchange co sions for a proton moving with a constant veloc v in a neutral atomic hydrogen gas of const number density n is simply the length of ti required for a proton to sweep out a cylinder volume $1/n$. The lifetime, τ, is then given

$(Qvn)^{-1}$, where Q is the charge-exchange s section. Over a range of proton energies about 100 ev to 20 kev, Q was measured found to be inversely proportional to the on's velocity [*Fite and others*, 1958], so that independent of particle energy in this energy ge and varies only with n. At higher energies, cross section falls much faster than $1/v$. rting the measured value for the product we obtain $\tau = 10^{13}/n$ seconds, where n is iber of hydrogen atoms per cubic meter. s, for a lifetime of 1 day ($\sim 10^5$ seconds), ust be 10^8 H atoms/m^3. The distribution [atoms vs. altitude, as calculated by *Johnson* 9], is shown in Figure 2. The hydrogen ity is given as 10^9/m^3 at 2 earth radii, and 0^8/m^3 at $3\frac{1}{2}$ earth radii. Therefore, we find 10^8 atoms/m^3 is a reasonable average num- density along the path of a proton that is ored near 2 or 3 earth radii.

he curve shown in Figure 2 represents the er limit for the density of the hydrogen d around the earth. More refined calculations reduce these density values by as much as ctor of 2 (F. S. Johnson, private communica-). If the hydrogen density is found to be r than shown in Figure 2, it will be required *most* of the magnetic storm protons be ored near 2 earth radii in order to provide fficiently high number density of hydrogen ns along the proton's trajectory. The dis- ution of proton pitch angles will no longer sotropic. As the pitch angle distribution is known, however, the calculations made in ons II and III used an isotropic distribution implicity.

spection of Figure 2 shows that the density ydrogen atoms increases very rapidly below rth radii, so that any protons mirroring w this level will be removed relatively kly. It is observed that severe magnetic ns have shorter recovery phases than mild (Fig. 3). This observation may be explained ne or both of the following: (1) Since the wind is blowing harder during a severe n, the magnetic storm protons will be ted more deeply into the geomagnetic than during a mild storm. The greater entration of hydrogen atoms closer to the yields a shorter lifetime for the magnetic n protons injected during a severe storm. (2) Ionospheric heating by hydromagnetic waves could be severe enough to increase the scale height in the F region and above, thus increasing the atmospheric density far from the earth [*Dessler*, 1959*a*, 1959*b*]. A severe magnetic storm will cause more ionospheric heating than a mild storm, because of the larger magnetic fluctuations during a severe storm. Therefore, during a severe magnetic storm, Figure 3 may have to be revised to show a greater density of H atoms far from the earth. This greater density of H atoms would increase the probability for magnetic storm protons to undergo charge exchange, thereby shortening the recovery phase for a severe magnetic storm.

Acknowledgments—We are indebted to Dr. F. S. Johnson for many valuable suggestions during the preparation of this paper. We also wish to thank Mr. M. I. Green for setting up the laboratory model used to draw Figure 1.

References

Alfvén, H., On the electric field theory of magnetic storms and aurorae, *Tellus, 7,* 50–64, 1955.

Behr, A., and H. Siedentopf, Untersuchungen über Zodiakallicht und Gegenschein nach lichtelectrischen Messungen auf dem Jungfraujoch, *Z. Astrophys., 32,* 19–50, 1953.

Chapman, S., On certain average characteristics of world-wide magnetic disturbance, *Proc. Roy. Soc. London, A, 115,* 242–267, 1927.

Chapman, S., *The Earth's Magnetism,* John Wiley & Sons, New York, 127 pp., 1951.

Chapman, S., and J. Bartels, *Geomagnetism,* Oxford University Press, London, 1049 pp., 1940.

Chapman, S., and V. C. A. Ferraro, A new theory of magnetic storms, *Terrestrial Magnetism and Atmospheric Elec., 37,* 147–156, 1932.

Colgate, S. A., A description of a shock wave in free particle hydrodynamics with internal magnetic fields, *Univ. Calif. Radiation Lab. Rept., UCRL 4829,* 1957.

Dessler, A. J., The propagation velocity of world-wide sudden commencements of magnetic storms, *J. Geophys. Research, 63,* 405–408, 1958*a*.

Dessler, A. J., Large amplitude hydromagnetic waves above the ionosphere, *J. Geophys. Research, 63,* 507–511, 1958*b*.

Dessler, A. J., Ionospheric heating by hydromagnetic waves, *J. Geophys. Research, 64,* 397–401, 1959*a*.

Dessler, A. J., Upper atmosphere density variations due to hydromagnetic heating, *Nature, 184,* 261–262, 1959*b*.

Dungey, J. W., Electrodynamics of the outer atmosphere, *The Physics of the Ionosphere,* The Physical Society, London, 406 pp., 1954.

FITE, W. L., T. R. BRACKMAN, AND W. R. SNOW, Charge exchange in proton-hydrogen-atom collisions, *Phys. Rev., 112,* 1161–1169, 1958.

FORBUSH, S. E., AND E. H. VESTINE, Daytime enhancement of the size of sudden commencements and initial phase of magnetic storms at Huancayo, *J. Geophys. Research, 60,* 229–316, 1955.

FRANCIS, W. E., M. I. GREEN, AND A. J. DESSLER, Hydromagnetic propagation of sudden commencements of magnetic storms, *Journal of Geophys. Research, 64,* 1643–1645, 1959.

GERARD, V. B., The propagation of world-wide sudden commencements of magnetic storms, *J. Geophys. Research, 64,* 593–596, 1959.

GREEN, M. I., W. E. FRANCIS, AND A. J. DESSLER, Refraction of hydromagnetic waves in the geomagnetic field. *Bul. Am. Phys. Soc., 4,* 360, 1959.

HOYLE, F., Suggestion concerning the nature of the cosmic-ray cutoff at sunspot minimum, *Phys. Rev., 104,* 269–270, 1956.

JOHNSON, F. S., The structure of the outer atmosphere including the ion distribution above the *F*-2 maximum, *Lockheed Tech. Rept., LMSD 49719,* Sunnyvale, Calif., 29 pp., April, 1959.

KAHN, F. D., The collision of two highly ionized clouds, *Gas Dynamics of Cosmic Clouds,* Interscience Publishers, New York, pp. 115–116, 19

KAHN, F. D., Collision of two ionized strea *J. Fluid Mech., 2,* 601–615, 1957.

PARKER, E. N., The gross dynamics of a hyd magnetic gas cloud, *Suppl. Astrophys. J., 3,* 76, 1957.

PARKER, E. N., Interaction of the solar wind w the geomagnetic field, *Phys. Fluids, 1,* 171–1 1958*a*.

PARKER, E. N., Suprathermal particles, III: el trons, *Phys. Rev., 112,* 1429–1435, 1958*b*.

PARKER, E. N., Plasma dynamical determinati of shock thickness in an ionized gas, *Astroph J., 129,* 217–223, 1959.

PATRICK, R. M., Production of very high spe shock waves, *Bul. Am. Phys. Soc., 4,* 283, 19

PETSCHEK, H. E., Aerodynamic dissipation, *Re Modern Phys., 30,* 966–972, 1958.

SINGER, S. F., A new model of magnetic stor and aurorae, *Trans. Am. Geophys. Union,* 175–190, 1957.

STOREY, L. R. O., An investigation of whistli atmospherics, *Phil. Trans. Roy. Soc., A, 2* 113–141, 1953.

STUART, G. W., Satellite-measured radiation, *Ph Rev. Letters, 2,* 417–418, 1959.

(Manuscript received August 13, 1959.)

Geomagnetic Effects of High-Altitude Nuclear Explosions[1]

A. G. MCNISH

National Bureau of Standards
Washington 25, D. C.

Abstract—Two high-altitude nuclear explosions detonated near Johnston Island in August 1958 produced distinct geomagnetic effects at Honolulu, Palmyra Island, Fanning Island, Jarvis Island, and Apia. No other operating magnetic observatories reported discernible effects. The effects at the first four observatories are attributed to overhead currents caused by increased ionization of the atmosphere by γ rays and their secondaries from the detonations. The effects at Apia are attributed to charged particles from the detonations and Compton electrons released from the air around the detonation.

ntroduction—Two high-altitude nuclear ex-sions detonated in the vicinity of Johnston and, "Teak" on August 1 and "Orange" on gust 12, 1958, produced unusual geomagnetic ects which were recorded by a number of con-tional magnetographs operating at the time. e magnetographs were located at Honolulu, waii (Ho), Palmyra Island (Pa), Fanning and (Fa), Jarvis Island (Ja), and Apia, Sa-a (Ap). The first and last of these stations regular magnetic observatories of the U. S. ast and Geodetic Survey and the New Zealand teorological Service, respectively. The other ree were set up in connection with the IGY ogram to study the equatorial electrojet. eir operation was continued beyond the IGY riod, partly at the suggestion of the present iter, to obtain more complete information on electrojet and to detect any effects that ght be caused by the atomic tests under way the close of the IGY.

These were the only stations at which a arly discernible geomagnetic effect occurred. e records at the station next nearest to the tonation point, Guam, at a distance slightly er 4000 km, was entirely free of perturbations ich began at the time of the explosions.

In this paper evidence will be presented to ow that the effects at all stations except Apia e due to electric currents flowing in the lower ionosphere because of enhanced ionization caused by high-energy quanta from the explosions and their associated scattered quanta. The effects at Apia, as has been suggested by others [*Cullington*, 1958; *Kellogg and others*, 1959] are undoubtedly due to charged particles. These, it will be shown, may include some particles produced initially by the explosion, in the case of Teak, but in both cases probably, at least at first, consist mainly of Compton electrons released by the prompt γ radiation.

Time of detonations—Two of the five observatories where effects were recorded had rapid-run magnetographs in operation, one at a speed of 1/15 mm/sec (Ho) and the other at 1/20 mm/sec (Ap). The onset of disturbance was very sudden at both these stations and simultaneous to within the time resolution obtainable. Since Ap is about 2000 km farther from the detonation point than Ho, it must be concluded that the effect was propagated at, or close to, the speed of light. The very excellent photographic recording at Ho permitted measurement of the time of onset of the disturbance to ± 1 sec. This estimate was found to agree with the announced times of the detonations [*AEC*, 1959*a*], which were for Teak, August 1, at 10:50:05, GMT, and for Orange, August 12, at 10:30:08, GMT. The time scales for the magnetographs at the other stations permit no precise determination of the time of onset, but, within the limits of uncertainty, it was the same at those stations also.

Charge particles originating at the detonation

[1] Most of the material in this paper was origi-lly presented at a staff meeting of the NBS at e Laboratories at Boulder, Colo., on March 9, 59.

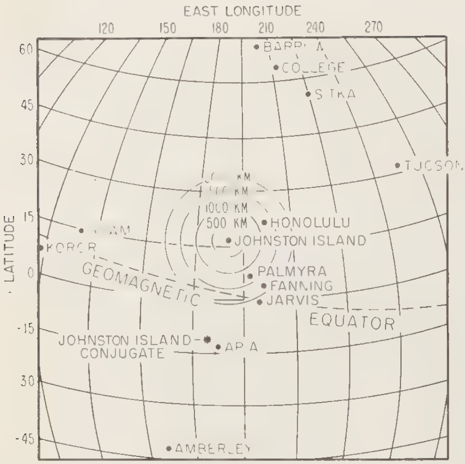

Fig. 1—Location of magnetic stations in Pacific area.

point could not have arrived in the vicinity of Ho in such a short time, 1 second or less. The spiraling radius of even the most energetic particles released by the explosion would be only a few kilometers at the most, too little for them to travel this distance in simple flight. Trapped particles would require several minutes to drift this distance. Therefore, if the geomagnetic effects at Ho, Pa, Fa, and Ja were caused by increased ionization overhead the ionizing agent must have been γ rays and neutrons, together with their secondaries, released from the detonations.

No such considerations apply for the effects at Apia, which is to the southeast of the geomagnetic conjugate point of Johnston Island. (See Fig. 1. The conjugate point shown was computed from the first-degree harmonics. Greater precision seems uncalled for.) Electrons and ions from the detonations could travel along the magnetic lines of force to the conjugate area with nearly the speed of light.

Form of the perturbations—The perturbations at all the stations east of Johnston Island were very similar in form from station to station and for both Teak and Orange. The recordings at Ho are typical (Fig. 2). All three components of the geomagnetic field, declination D, horizontal intensity H, and vertical intensity Z, were affected. (Since the field changes were

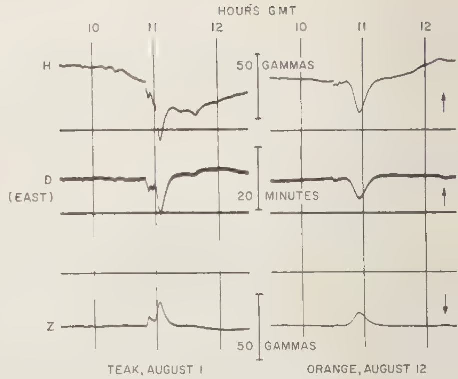

Fig. 2—Recordings of magnetic changes Honolulu, Hawaii, for Teak, August 1, and Orang August 12, 1958.

small, changes in D, H, and Z may be treated orthogonal vectors.) All three componen changed suddenly at the onset of perturbati and retained most of this change for sever minutes, after which additional change in ea element took place in the same sense as t initial change, attained a maximum in a fe minutes, and then returned to approximate predisturbance values.

The total duration of the perturbations these stations seemed to be less than 50 mi utes. This judgment is based on examination the D and Z records at these stations. The records at all stations were subject to so natural perturbation which was evident befo both events, particularly for Teak. Therefo in reducing the recordings, it was assumed th all effects of the detonations were over in minutes, and changes in the components we corrected for natural perturbations by linear i terpolation between the preperturbation val and the value 50 minutes later. The effect doing this was trivial on all components exce H.

There were some significant differences b tween the perturbations due to Teak and tho due to Orange at all stations. It should be bor in mind that the two explosions were set off different altitudes: Teak was at a height 'over 200,000 feet' (60 km), and Orange 'about 100,000 feet' (30 km [*AEC*, 1959 *b*]. Ho, for Teak, the second change in the co ponents began at about 10 minutes after ons

attaining its maximum at about 13 minutes. turn to approximately predisturbance values all components had occurred about 30 min- s after t_0. For Orange the corresponding times e about 15, 25, and 50 minutes. At Ho the erage difference between the perturbed and perturbed values of the components between onset and beginning of the second change was about 6 times as great for Teak as for Orange, although the maximum of the perturbation was about the same for both.

The effects at the other eastward stations were very similar to those at Ho, although there were some significant differences. At Fa

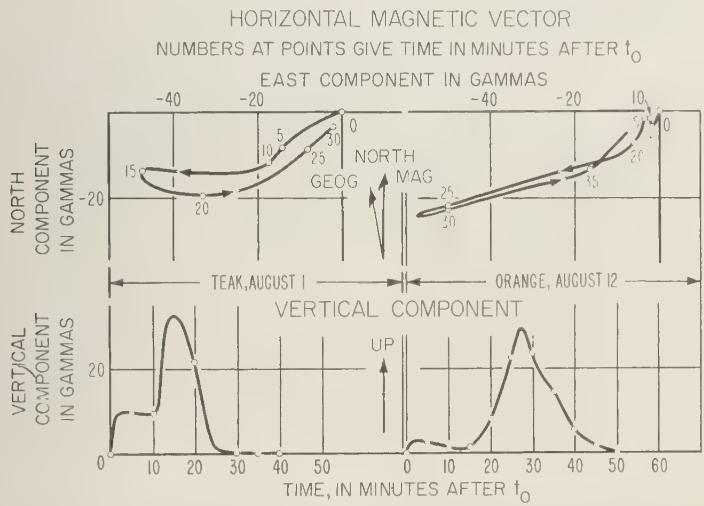

. 3—Geomagnetic field changes at Honolulu due to high-altitude nuclear bombs Teak, August 1, and Orange, August 12, 1958.

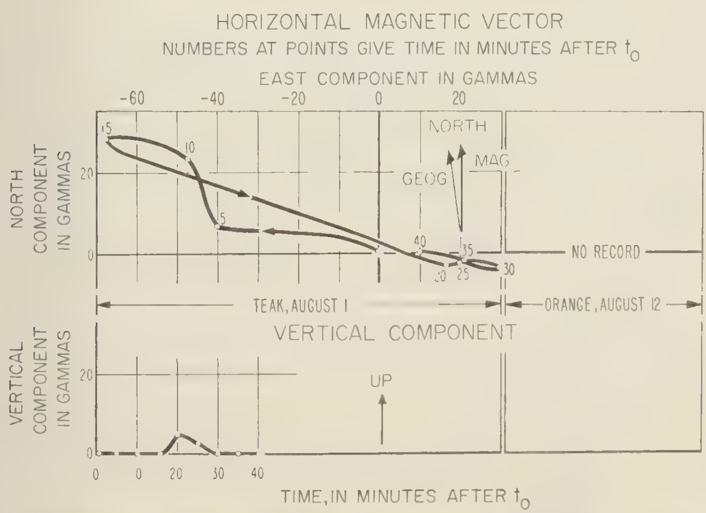

. 4—Geomagnetic field changes at Palmyra Island due to high-altitude nuclear bombs Teak, August 1, and Orange, August 12, 1958.

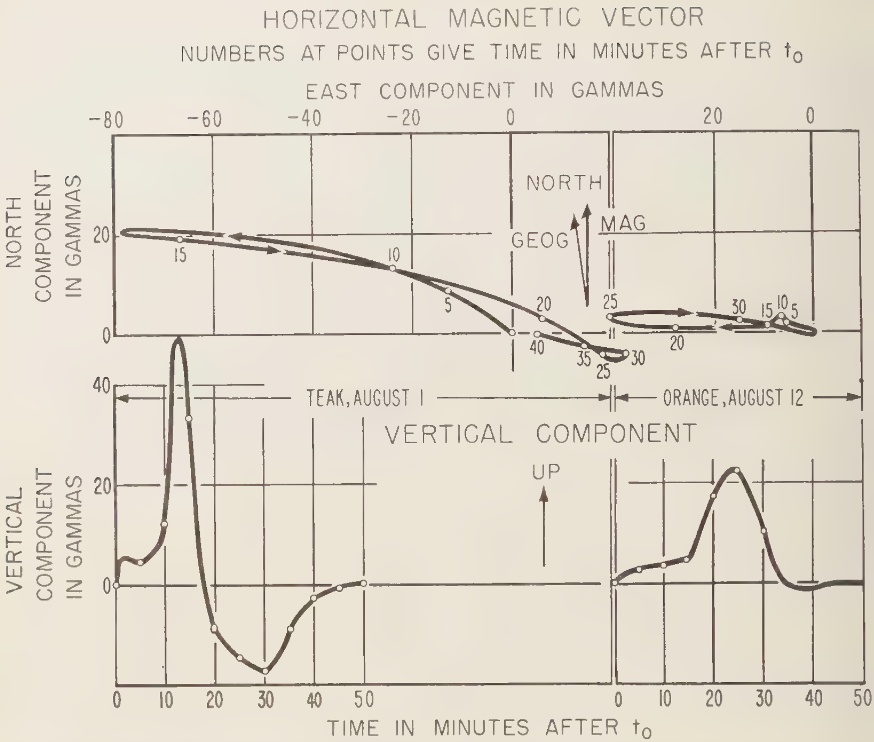

FIG. 5—Geomagnetic field changes at Fanning Island due to high-altitude nuclear bombs Tea
August 1, and Orange, August 12, 1958.

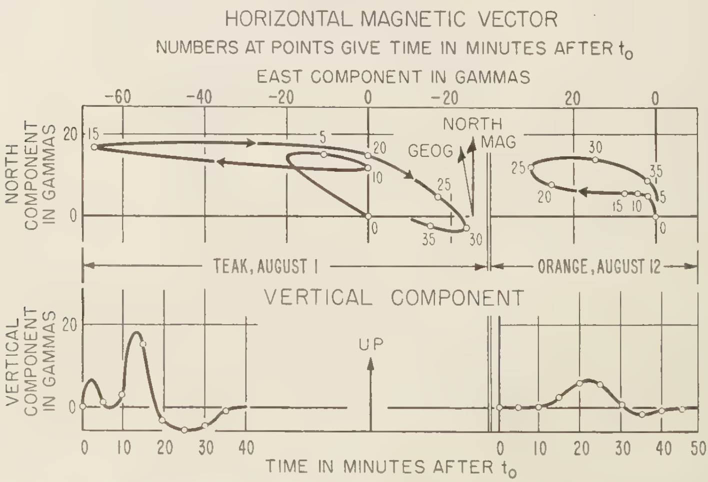

FIG. 6—Geomagnetic field changes at Jarvis Island due to high-altitude nuclear bombs Tea
August 1, and Orange, August 12, 1958.

e initial effects were of approximately the me magnitude for both events; at Ja the inil effect was very small for Orange as conasted with the 6 to 1 ratio at Ho. The maxi-um effect at Fa and Ja was only half as great r Orange as for Teak as contrasted with a 1 to ratio at Ho. (The magnetograph at Pa was t operating during Orange.) At all three of ese stations there was an aftereffect for Teak ginning about 18 minutes after t_0, when the anges in the components reversed sense with spect to the initial and maximum changes in e components. This was not discernible for range at any of the eastward stations or at o for Teak.

The changes in Z at the eastward stations are special interest. At most of the stations they nformed in respect to time with changes in agnitude of the horizontal vector. At Pa the change was very small for Teak (no record r Orange). At Ja the Z changes were smaller r both events than at the other stations; in ct, the initial part of the disturbance was mpletely lacking in Z for Orange. The main ange is always representable by an upward-rected vectorial component.

Vector plots of the disturbance (see Figs. 3, 5, and 6; the plots are extended beyond the timed points in accordance with the magnetic recordings) in the horizontal plane show that the disturbance vector at each station described a narrow loop, the main axis of which was directed approximately toward the place of detonation. The vector for the aftereffect at Pa, Fa, and Ja, as noted above in connection with Teak, was oppositely directed. The Z changes were directed upward, so that the disturbance vector at each station when resolved on a vertical plane through the main axis of the loop for that station had an upward component. Interestingly, the angle of the vector with respect to the horizontal plane at Ho was approximately the same as that for the average diurnal variation vector at that station for the corresponding time during the daylight hours. A similar comparison cannot be made for the other eastward stations because of absence of complete data from them.

The effects at Apia were very different. The disturbance lasted considerably longer, nearly 2 hours, and the field changes were very erratic. Also the patterns of the changes for the two events were dissimilar. For both, the onset was sharp. For Teak all three components exhibited both positive and negative changes during the first minute after the detonation, and the maxi-

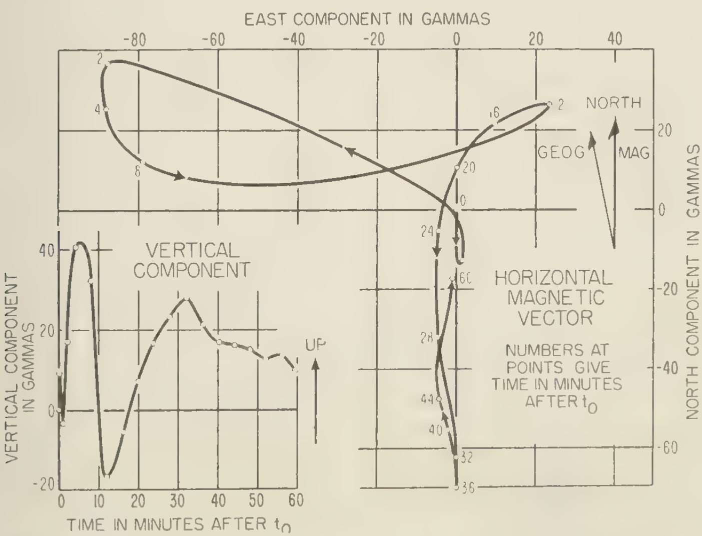

FIG. 7—Geomagnetic field changes at Apia due to high-altitude nuclear bomb Teak, August 1, 1958.

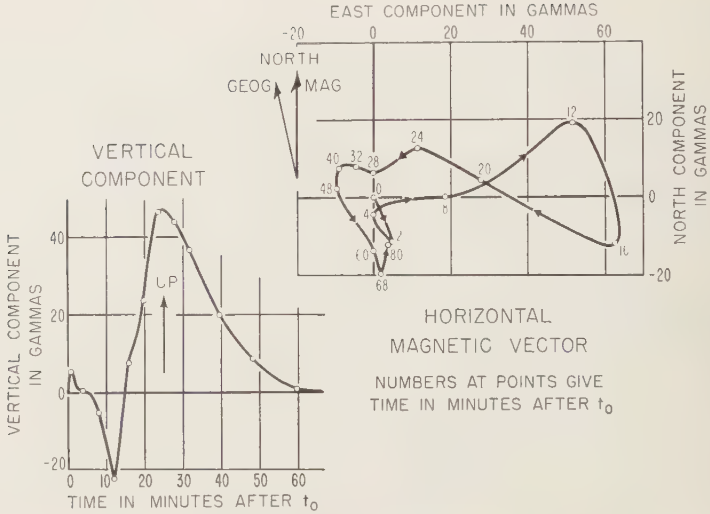

Fig. 8 –Geomagnetic field changes at Apia due to high altitude nuclear bomb Orange, August 12, 195

mum value for the horizontal component of the perturbation vector was attained in 2 minutes. For Orange the initial changes did not reverse sense and were followed by a quiescent period of about 5 minutes before the more severe changes began. It is noteworthy that this quiescent period was equal to the time difference between the beginning of the second phase of Teak and Orange effects at Ho.

Vector plots of the disturbances at Apia (Figs. 7 and 8) show that for Teak the horizontal vector described three loops, first to the west, then to the east, and then to the south, returning roughly to the origin after each excursion. For Orange only one well defined loop was described and that toward the east. Changes in Z did not correspond closely to changes in the horizontal plane as they did for the eastward stations.

Interpretations of the perturbations—It is usual to attribute most geomagnetic fluctuations to the effects of electric current sheets in the lower layer of the ionosphere at a height of about 90 to 95 km. At lesser heights the ionosphere is ordinarily not sufficiently conducting to permit currents to flow because of low electron density and high collision frequency. At greater heights the collision frequency is so low that d-c conductivity is greatly reduced because of spiraling of electrons around the magneti lines of force. Associated with such electric cur rents in the ionosphere are currents induced i the earth which enhance the horizontal com ponent of the geomagnetic fluctuations and di minish the vertical component. This model i particularly appropriate if the geomagneti fluctuations exhibit similarity over considerabl distances on the earth's surface as compare with the height of the current sheet (90 to 9 km). This is true for the perturbations observe at the eastward stations for both Teak an Orange.

The relative intensity of the current shee which would give rise to the observed perturba tions can be represented by plotting the dis turbance vectors for each station on a ma after rotation through 90° in a clockwise direc tion. If this is done for the vectors at variou times after t_0 for both Teak and Orange, representation suggestive of a circular flo around Johnston Island is obtained from th data from the eastward stations (Figs. 9 an 10). For neither event do the current vecto for Apia fit into this flow. For this reason th effects at Apia are attributed to local disturbanc associated with the geomagnetic conjugate poi and effects at the eastward stations to a separat general circulation.

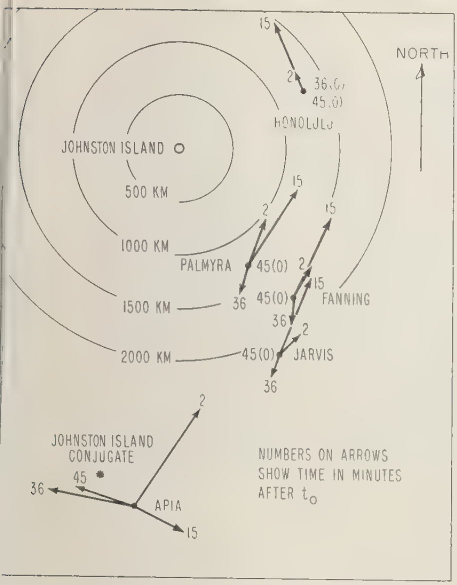

ig. 9—Vectors for overhead current sheet to pro-
uce geomagnetic effects of Teak, August 1, 1958.

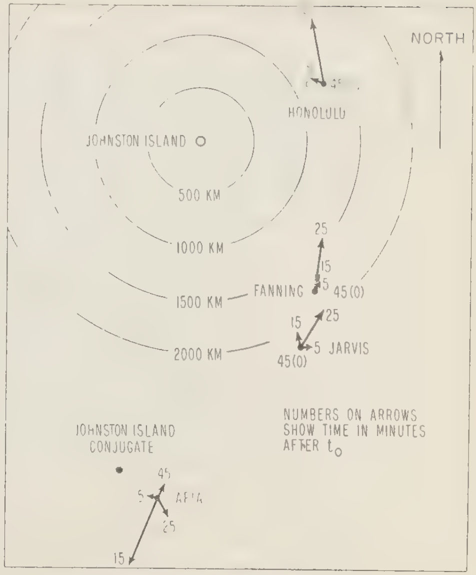

Fig. 10—Vectors for overhead current sheet to produce geomagnetic effects of Orange, August 12, 1958.

In an independent analysis of these perturba-
ons, *Matsushita* [1959] has attributed them to
rong electric currents flowing in the vicinity
f Johnston Island rather than over the sta-
ons affected. This does not seem to be a plausi-
le explanation, for several reasons: (1) Such
fects should decrease with distance from the
urce approximately as an inverse cube. On the
ntrary, the effects for Teak were greater at
a, Fa, and Ja than they were at Ho even
ough all these stations except Pa are farther
om Johnston Island than Ho is. (2) The Z
anges should be directed downward, not up-
ard, as they are. Actually, the ratio of hori-
ntal to vertical changes at the maximum were
the ratio of 5 to 3 at Ho, 14 to 1 at Pa, 8 to 5
Fa, and 4 to 1 at Ja for Teak, with similar
tios for Orange, showing that the vertical ef-
cts were not negligible. (3) Distinct effects
ould have been observed at Guam amounting
about 10 gammas for Teak and 3 gammas for
range, assuming an inverse cube law. (4) After-
fects at the eastward stations should not have
en lacking at Honolulu.

The current-sheet model seems somewhat
ore attractive. Such a sheet could be caused by ionization of the lower ionosphere above the eastward stations. The mechanism whereby this ionization could be produced will be discussed in detail in a following section. For present considerations it will be assumed that such ionization is possible.

Since the Z changes were everywhere upward for the eastward stations it must be assumed that the current sheet extended beyond the remotest station, Ja, for both events, though not much beyond Ja for Orange as the Z changes associated with Orange at that station were small. The electromotive forces to produce these currents can be accounted for by a classical theory of geomagnetism.

The Stewart-Schuster theory of the geomagnetic diurnal variations attributes them to electric currents flowing in the lower ionosphere. The electromotive forces driving the currents are induced in the ionosphere by horizontal tidal winds across the vertical component of the earth's permanent magnetic field. The principal term in the velocity potential is a semidiurnal one (see Figs. 11 and 12). If the ionosphere were uniformly ionized two current systems

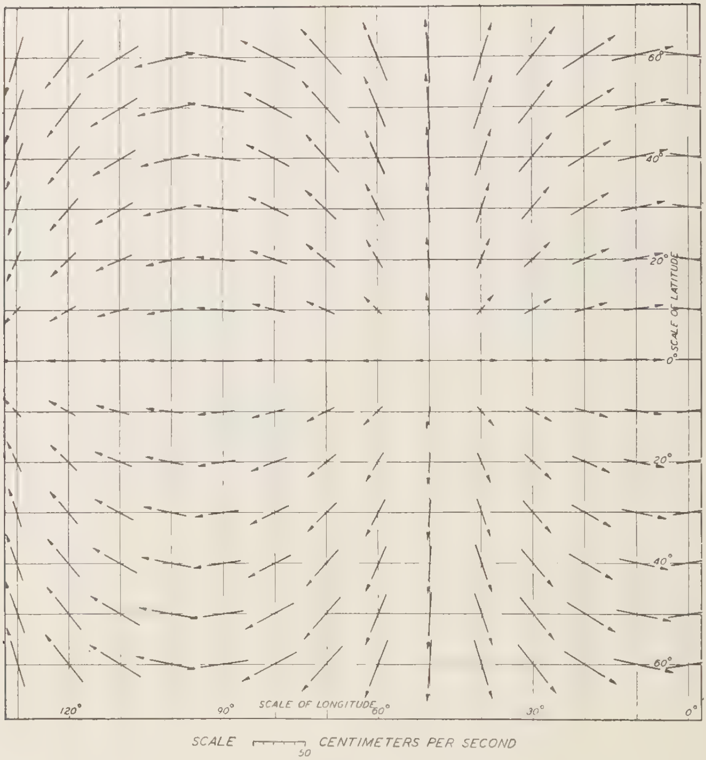

FIG. 11—Air velocities arising from semidiurnal atmospheric tides.

would result, one centered near the 11-hour meridian and one near the 23-hour meridian, but since the d-c conductivity of the lower ionosphere at night is smaller by a factor of 100 or so than in the daytime only the daylight current system is distinct. Lengthy series of observations at several magnetic observatories, however, reveal a vestige of the night-time system. Therefore, it may be assumed that, since it was about 2300 local time at Johnston Island when the detonations occurred, a system of electromotive forces was available for producing the circular current provided that the ionosphere was made conducting over a large area by radiations from the nuclear processes.

Several special characteristics of the diurnal variation current system should be discussed. The system of electromotive forces induced in the ionosphere do not form a closed circuit but are patterned as arcs extending northward and southward from evening toward morning point on the equator. The strongest electromotiv forces are built up in high latitudes, where th product of the tidal wind velocities and th vertical magnetic field is greatest. The electro motive forces in equatorial regions are small This system of electromotive forces produce accumulations of electric charge near the equato at intervals of 90° in longitude. The resultin electrostatic gradient along the equator cause closing of the current loops. The d-c conductivit along the equator (actually the dip equato where the magnetic field is horizontal) is en hanced by vertical electric polarization built u by differential ion-electron drift. This gives ris to the equatorial electrojet.

Since ionization produced by the detonation was asymmetrical with respect to the equato the southern part of the current system was no excited for either event. This is probably th

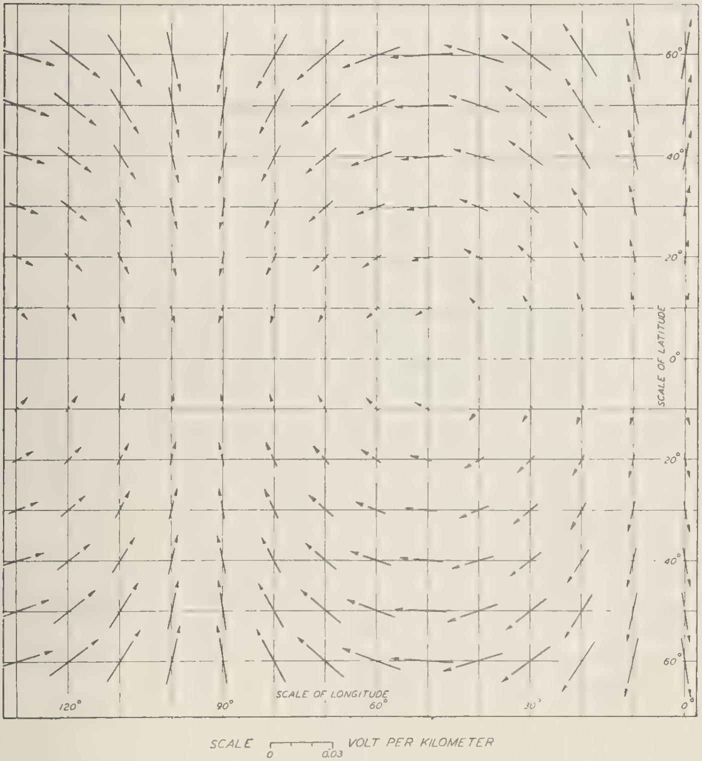

FIG. 12—Electromotive forces in atmosphere due to semidiurnal atmospheric tides.

eason that the current vectors at Fa and Ja re not parallel with the equator, as they are or the normal diurnal variation currents. Also, ecause of the limited duration of the disturbnce it is likely that the vertical electric polariation necessary for the electrojet was not built p. The aftereffect recorded at Pa, Fa, and Ja or Teak may be attributed to redistribution of he electric charge built up in the equatorial egion during the main part of the disturbance.

The effects at the eastward stations were such s would have been caused during daylight ours by a solar flare. The explanation offered ere for these artificial perturbations is essenially the same as that proposed by *McNish* 1937] some time ago, and now generally acepted, to account for the effects of a solar lare on the geomagnetic field: the effects were uch as would be expected if the sun had hone briefly over an area 2000 to 3000 km in radius about Johnston Island. A similar explanation has been proposed by *Maeda* [1959].

The relatively small changes in Z at Pa are inconsistent with the Z changes at the other stations. As the diurnal variation in Z at Pa does not seem to be small, it is not reasonable to attribute this to freakish distribution of electric currents induced in the ocean. Possibly the Z change at Pa may be affected by intense currents flowing near Johnston Island.

The effects at Apia were of a different nature. Morphologically, they were different from those at the other stations, resembling more closely the type of disturbance frequently observed near the auroral zone to which Birkeland assigned the term 'polar elementary storms' more than 50 years ago. That auroras were seen in the vicinity of the geomagnetic conjugate point on both occasions is strong evidence that these artificial perturbations were similar in origin to

the polar disturbances. It is therefore plausible to attribute these effects to electrons and ions emitted from the detonation area which spiraled along the lines of magnetic force to the conjugate area.

Whether the effects at Apia are due to electric currents caused to flow as a result of convective circulation from local heating of the ionosphere by the incoming particles or to magnetohydrodynamic waves from the detonation area is a matter of speculation.

It has been shown [*Kompanects*, 1959] that nuclear explosions in the atmosphere give rise to electromagnetic fields which are propagated as atmospherics, presumably caused by Compton electrons released by the γ rays. Since both Teak and Orange appear to have been detonated at a height where the atmosphere is sufficiently dense for the Compton process to be of importance, such a wave may have been generated by both explosions and have been guided along the lines of force to the vicinity of Apia. This may account for the sharp initial effects observed there. It is not suggested here that the main effects are due to this initial wave.

Insufficient observational data are available to delineate with tolerable uniqueness a current system in the region that would give rise to the effects. It is striking that Apia, which was farthest from the detonation area of any of the stations affected, exhibited the strongest effects.

Mechanism of ionization—Information has been released [*AEC*, 1959b] that the weapons detonated were in the megaton range and that Teak was detonated above 60 km and Orange about 30 km. It was possible to arrive at approximately these conclusions from the geomagnetic effects before these figures were given. For purposes of discussion it will be assumed that the yields of Teak and Orange were 1 megaton each. All weapon information used in this discussion is drawn from the AEC publication, *The Effects of Nuclear Weapons*. Since both Teak and Orange appear to have been fusion weapons, some of this background information may be incorrect. Such misinformation cannot alter the conclusions substantially, however.

The γ ray dosage during the first minute after detonation of a 1-kt weapon is about 10^6 roentgens at about 60 meters (p. 349, *op. cit.*). Scaling this up by a factor of 10^3 (the scaling

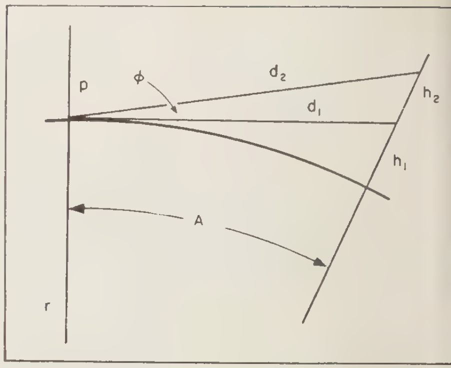

FIG. 13—Ray geometry.

factors given on p. 350 do not appear to be a[p]plicable) gives a dosage of 2.3 r at Ho and 0.8 [r] at Ja, allowing for only inverse distance square[s] and no atmospheric absorption. Taking the a[t]mospheric density as 1.2×10^{-8} g/cm^3 at [9]... km, this corresponds to the production of 5 [$\times$] 10^4 ion pairs/cm^3 at Ho and 2×10^4 ion pair[s]/cm^3 at Ja, since 1 r $= 1.6 \times 10^{12}$ ion pairs/... Since the normal ion density of the E layer [is] only about 10^5, this would be enough to accou[nt] for the initial effects. At lesser heights, where t[he] air density is greater, greater ionization wou[ld] be produced.

Consider a ray originating at a point p in t[he] atmosphere directed toward another point ... with the angular distance A between p and ... Let ϕ be the angle the ray makes with the hor[i]zon plane (Fig. 13). It can be shown that t[he] air mass per unit area through which the ra[y] must pass to arrive at q is approximately

$$m = r\rho_0 \sec\varphi \int_0^A \exp\left\{-\frac{rA\tan\varphi}{H} - \frac{rA^2}{2H}\right\} d\ldots$$

where r is the radial distance from the earth['s] center to p, H the scale height of the atmo[s]phere, and ρ_0 its density at p. This equation ma[y] be put into usable form by completing t[he] square in the integral. Then

$$m = \rho_0 \sec\varphi \sqrt{\frac{\pi r H}{2}}$$

$$\cdot \exp\left\{\frac{r\tan^2\varphi}{2H}\right\} \left[\operatorname{erf}(x)\right]_{\tan\varphi\sqrt{r/(2H)}}^{(A+\tan\varphi\sqrt{r/2H}\ldots}$$

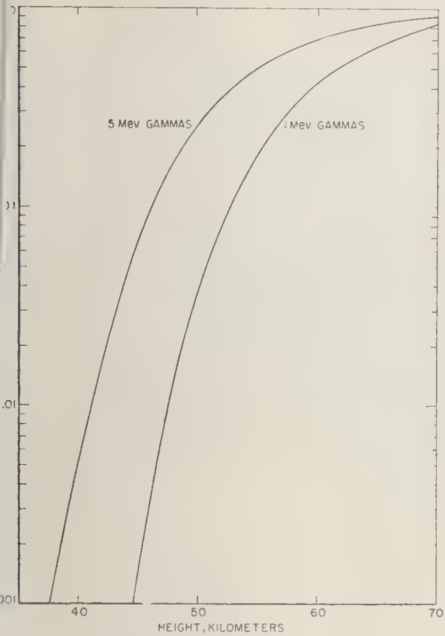

G. 14—Air attenuation for horizontal rays as a function of height.

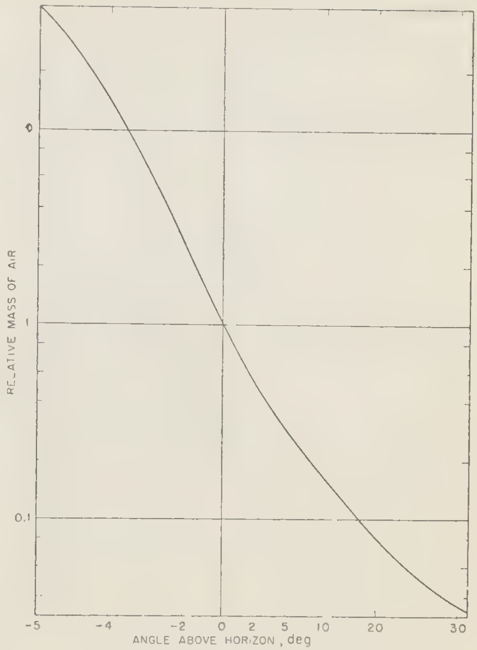

FIG. 15—Variation in air mass as a function of angle.

For the special case in which $\phi = 0$.

$$m = \rho_0 \sqrt{\frac{\pi r H}{2}} \left[\operatorname{erf}(x)\right]_0^{A\sqrt{r/2H}}$$

nce $r \gg H$ this approximation is a good one. ysically this means that most of the absorp- on occurs close to p, that is, for small values A.

The intensity of γ-ray flux of a given energy a distance d is given by

$$I = (I_0/d^2)e^{-\mu d}$$

here I_0 is the intensity at unit distance and μ e linear absorption coefficient. For the air nsity at the surface of the earth the absorp- on reduces the intensity to $1/e$ of its value at a stance of 300 meters for 5-mev γ rays and 5 meters for 1-mev γ rays.

The equations given above permit calculation absorption for rays from detonations at vari- s altitudes and angles. This is most easily ac- mplished by considering the absorption of rizontal rays passing to very great distances d the variation of air mass encountered as ϕ anges (Figs. 14 and 15). The absorption for horizontal rays varies rapidly with height up to about 50 km. Above about 60 km absorption is unimportant. The air mass through which a ray must pass varies rapidly with ϕ. For $\phi = -3°$ the air mass through which the ray passes is 10 times as great as for a horizontal ray. Therefore the reduction in intensity for a horizontal ray must be raised to the tenth power to give that for a 3°-ray. For rays with positive ϕ the air mass is considerably reduced relative to that for a horizontal ray. For example, at $\phi = 15°$ the air mass is only 0.1 as great as for a horizontal ray. The reduction in intensity for a horizontal ray, then, must be raised to the 0.1 power.

If it is assumed that the heights given for the detonations are correct, direct radiations from Orange ($h = 30$ km) would have been reduced to negligible intensities even at Ho, if they traveled in straight lines, and those from Teak ($h > 60$ km) would have been negligible at Ja. However, this is not the mechanism for propagation of γ radiation in an absorbing medium.

The absorption equation given above applies for the diminution of intensity for γ rays of a

given energy, not for the total flux of radiation. When any quantum engages in collision (except for pair formation, which can be ignored here) it gives rise to a Compton electron and a scattered quantum of lower energy. The angles between the incident quantum, the scattered quantum, and the Compton electron are such as to conserve momentum.

The Klein-Nishina formula permits calculation of the differential cross section for various angles of scatter. Graphs for the scattered angle θ with respect to the direction of the primary ray as a function of the differential cross section have been computed [*Nelms,* 1953] for various γ-ray energies. Forward scatter predominates for high-energy quanta. For 5-Mev quanta, half of the rays are scattered within a cone about the direction of the primary ray the elements of which make an angle of 20° with the axis. All azimuths of scatter within this cone are equally probable. If the direction of the primary ray is tangential to the earth, half of the scattered rays will be scattered toward the earth and half away from it. For tangential primary rays scattering at an angle θ, one-fourth of the secondaries will have an earthward component greater than $\theta\sqrt{2}$. The secondaries, which are nearly as energetic as the primaries for small θ, in turn are scattered, giving rise to tertiaries, etc. At each scatter half of the quanta will be lost, owing to their having an upward component. Thus the number of quanta proceeding around the earth will be decreased by a factor of 2 approximately for each free path with a degradation in energy. This scattering mechanism seems adequate for producing intense ionization as far from the detonation point as was observed.

Near the detonation point considerable numbers of quanta going away from the earth undoubtedly gave rise to secondaries directed approximately tangential to the earth. For Orange, which was detonated low in the atmosphere, these outward-going primaries, that is those with large positive values of ϕ, must have been responsible for most of the effects.

Exact calculation of the energy that can be propagated by this scattering process would be laborious, and pointless unless the actual spectral distribution of the quanta were given, but some rough estimates can be made. For 5-Mev quanta the energy loss may be about 80 pe cent, considering scattering in unfavorable d rections. However, it appears that radiatio could get to the affected areas after two o three scatters. This would diminish its itensit somewhat. The calculations made before, i which ionization was computed allowing onl for inverse distance effects, assumed that th weapons were of 1-megaton yield. Since th gave only enough ionization for the effects with out the scatter mechanism, it must be assume to allow for scatter, that the yield was sever megatons for both weapons.

The announced approximate height fo Orange, 30 km, seems a bit too low for muc radiation to arrive at the affected area. Th minimum plausible height would be about 10 k greater.

The larger effects which attained their max mum at the eastward stations 15 to 25 minut after the explosions can be explained with le importance being attached to the scatterin mechanism. They occurred several minutes aft the initial effects, when radiation was bein emitted from the residue of the atomic processe Although this radiation is less intense and le penetrating than the initial radiation it may b presumed that the debris had ascended to co siderable heights so that direct rays from th debris could travel farther toward the affecte areas before engaging in scattering.

That the onset for the larger effects was minutes later for Orange than for Teak is prob ably due to the lesser height at which Orang was detonated; additional time was require for the debris from Orange to ascend to th same height. Taking the heights as announce this would indicate that the debris from Orang was ascending at about 6 km/min, which woul place the Orange debris at a height of 120 k at onset of the larger effects and the Tea debris at the same height, assuming the sam rate of rise.

As was pointed out before, following th first impulse on the record, the magnetic fie at Ap was relatively quiescent for the first minutes of Orange as contrasted with the larg effects which set in almost immediately fo Teak. This, too, is attributable to the differen in height for the two detonations. As reporte Teak was detonated at a height of 60 kn

erefore electrons emitted during the first min- could have penetrated the small mass of nosphere above the detonation. On the other nd, only Compton electrons produced in the nosphere by the upward-directed prompt γ liation could have arrived at Ap initially en Orange was detonated. Five minutes after onation of Orange the debris must have been a height of 60 km also, at the rate of rise eviously computed.

There is further evidence of widespread ioni- tion of the lower ionosphere in connection th these detonations. During Teak, blackouts radio communication were observed promptly er the detonations even for circuits passing closer to the detonation point than 3000 n [*Obayashi and others,* 1959]. Such wide- read effects seem to be explicable only by the attering mechanism.

References

EC Release B-39, March 10, 1959*a*.

AEC Release B-94, June 15, 1959*b*.

Cullington, A. L., A man-made or artificial aurora, *Nature, 182,* 1365–1366, 1958.

Kellogg, P. J., E. P. Ney, and J. R. Winkler, *Nature, 183,* 358–360, 1959.

Kompaneets, A. S., Radio emission from an atomic explosion, *Soviet Phys. JETP, 35* (8), 1076–1080, 1959.

McNish, A. G., Terrestrial magnetic and ionospheric effects associated with bright chromospheric eruptions, *Terrestrial Magnetism and Atmospheric Elec., 42,* 109–122, 1937.

Maeda, H., Geomagnetic disturbances due to nuclear explosions, *J. Geophys. Research, 64,* 863–864, 1959.

Matsushita, S., On artificial geomagnetic and ionospheric storms associated with high-altitude explosions, *J. Geophys. Research, 64,* 1149–1161, 1959.

Nelms, A. T., Graphs of the Compton energy-angle relationship and the Klein-Nishina formula from 10 kev to 500 Mev, *NBS Circ. 542,* August 1953.

Obayashi, T., S. C. Coroniti, and E. T. Pierce, *Nature, 183,* 1477–1478, 1959.

(Manuscript received September 11, 1959.)

Artificial Auroras Resulting from the 1958 Johnston Island Nuclear Explosions

J. M. MALVILLE

High Altitude Observatory
University of Colorado, Boulder, Colorado

Abstract—Beta decay electrons traveling along magnetic lines of force are shown to be capable of accounting for the artificial aurora which appeared at the conjugate point of Johnston Island after the explosion of August 1. Dissociative recombination and ion-atom interchange are suggested as the primary exciting mechanisms of the oxygen forbidden lines in the artificial auroral rays and may account, when combined with collisional de-excitation, for the observed violet color of the rays. The high-altitude arc may be a form of auroral afterglow and may result from a process similar to that which enhances the oxygen red lines in twilight.

Introduction—The nuclear tests in August ıd September 1958 at Johnston Island and in onnection with project Argus in the South Atntic have demonstrated the ability of hightitude explosions to initiate artificial auroral, eomagnetic, and ionospheric disturbances. The eomagnetic and ionospheric effects of the Johnon Island shots of August 1 and 12 have been nalyzed by *Matsushita* [1959].

Two distinct types of aurora were observed fter the Johnston Island explosions. A red uroral cloud drifting overhead from the direcon of Johnston Island was observed at Maui, Iawaii, 25 minutes after the explosion, and imıediately after the explosion bright auroral ays near the magnetic conjugate point of ohnston Island were observed by the staff of ıe Apia observatory. The Apia aurora bears ıe closer resemblance to natural auroras and, ı the sense that the nature of the exciting articles as well as something about their energy known, represents a controlled geophysical xperiment. This paper will discuss some aspects f the Apia aurora as inferred from the visual bservations reported in the open literature.

Observations—As reported by *Cullington* 1958*a*] bright auroral rays were observed from pia essentially coincident with the explosion of ugust 1. The rays lasted approximately 6 ıinutes and were 'at first violet covered with ed and gradually changed to green.' The rays ere followed by a red glow which continued or another 8 minutes. In addition, a 'crimson' arc was observed north of the conjugate point with a magnetic latitude of perhaps 7°.

The aurora of August 12 lasted 17 minutes but was more diffuse (no rays were observed) and less intense than that of the first [*Cullington*, 1958*b*].

Character of the explosions—It has been reported in the popular press [*Time*, 1959] that the shots of August 1 and 12 were thermonuclear detonations exploded at altitudes of 40 and 20 miles, respectively. The diameter of the fireball on August 1 was reported to be 11 miles after 0.5 second.

For our calculations we shall assume that a 20-kt fission bomb was used as a trigger for the 10^3-kt fusion reaction. Although the fusion reaction should release energetic instantaneous electrons, we shall consider for our calculations only β decay electrons resulting from the fission fragments of the 20-kt trigger bomb. A 20-kt explosion releases a total energy of 2×10^{13} calories, or 8.37×10^{20} ergs. Approximately 10 per cent of the total energy is in the form of residual nuclear radiation [*Glasstone*, 1957]. The residual radiation, defined as that emitted after 1 minute from the time of the explosion, amounts to 8.37×10^{19} ergs. The decay with time of the residual activity may be described for the first 200 days by the equation [*Glasstone*, 1957]

$$A = A_0 t^{-1.2} \tag{1}$$

where A_0 is the activity at 1 minute and t is in

minutes. We evaluate A_0:

$$8.37 \times 10^{19} = A_0 \int_1^\infty t^{-1.2}\, dt = A_0\, 10.2$$

Thus $A_0 = 16.8 \times 10^{18}$ ergs/min $= 27.9 \times 10^{16}$ ergs/sec.

Origin of auroras—If the fission fragments are distributed uniformly through the fireball, we can calculate the electron flux from the 11-mile-diameter sphere of August 1, assuming that two-thirds of the residual radiation is in the form of β decay electrons. An effective upper limit on the electron flux can be computed by assuming that all the β decay electrons have energies of 0.5 Mev; the corresponding flux at 1 minute after the explosion at the surface of the sphere is 6×10^9 electrons/cm²/sec. If, then, the focusing effect of the magnetic field is negligible, 6×10^9 electrons/cm²/sec is the maximum electron current that could appear field-oriented at the magnetic conjugate point of Johnston Island.

The height, h, of a dipole line of force above the earth's surface is given by

$$h = b \cos^2 l - a \tag{2}$$

where l = geomagnetic latitude, a = earth's radius, and

$$b = a \sec^2 l_0 \tag{3}$$

The geomagnetic latitude of Johnston Island is 14.3°, and its magnetic latitude (dip) is 16°; the maximum heights of the line of force for an explosion at 60 km are 477 and 589 km, respectively. The equivalent lengths of the dipole lines of force in terms of centimeters of air at standard temperature and pressure, obtained by a graphical integration along the lines c force, are given in Table 1. The correspondin values of electron energy thresholds are take from *Bates* [1954], but because of the effects c electron scattering these values are only ap proximate. For an explosion at a magnetic lat tude of 14.3° and a height of 70 km or less th minimum energy required for electrons to b able to penetrate into the opposite hemisphe is 0.5 Mev, and our use of this value in calcu lating the upper limit on the electron current i justified. The equivalent depth of the atmos phere at various heights and the correspondin electron energy thresholds [*Bates*, 1954; *Bate and Griffing*, 1953] are given in Table 2. Onl rarely do natural auroras occur down to height of 70 km, and then they are generally type auroras appearing at the time of breakup c auroral arcs into rays. The average height c the lower borders of natural auroras lies betwee 100 and 110 km, indicating that the electron in the Apia aurora had energies in excess c those in natural auroras by factors of at leas 20 to 50.

The upper limit of 6×10^9 electrons/cm²/se on the electron current in the Apia auroral ray does not appear greatly in excess of that fo natural auroras. Electron fluxes of 10^8 electrons cm²/sec and possibly greater by a factor of 1 have been inferred from auroral X-ray measure ments by *Winckler and others* [1958], and pro ton fluxes of 10^7 to 10^8 protons/cm²/sec hav been estimated from Hα intensities in moderatel bright auroral arcs [*Chamberlain*, 1954]. Ele tron currents of 10^{10} to 10^{12} electrons/cm²/se have been suggested by *Chamberlain* [1955] i connection with his ray discharge theory. How ever, the excitation efficiency of an electric-field accelerated electron stream with its larg number of low-velocity electrons would be sig nificantly less than that of the electron strean considered here in connection with the Api

TABLE 1—*Equivalent lengths of dipole lines of force for* $l_0 = 14.3°$

Height near conjugate point, km	h = 60 km: L, cm air STP	h = 60 km: E, Mev	h = 70 km: L, cm air STP	h = 70 km: E, Mev
60	1250	3	770	1.7
70	770	1.7	285	0.75
85	640	1.5	155	0.5
h_{max}	630	1.5	143	0.48

TABLE 2—*Equivalent depths of the atmospher*

Height, km	L, cm air STP	E, kev
70	50	250
100	0.7	21
110	0.25	12

ora. In natural auroras in the absence of an tric-field-accelerating mechanism we should ect the electron and proton fluxes to be ghly equal in magnitude and for bright au-ll rays to equal perhaps 10^7 to 10^8 electrons/ /sec.

he observed violet color of the Apia auroral s departs significantly from the color of ıral auroras. It is undoubtedly due to the ; negative system of N_2^+. Naturally occurring et auroras are observed only as sunlit au-as where the enhancement of the N_2^+ band em results from resonant scattering by sun-t. Whereas in normal auroras the N_2^+ band 3914 A has roughly the same intensity as [] 5577 A, in violet auroras, according to *rmer* [1954], 3914 A may be enhanced rela-e to the green line by a factor of 7. This en-cement in the Apia aurora may result en-ly from the increased energies of the incident trons. The forbidden [OI] lines in auroras most likely excited by two processes: (*a*) in region above 100 km by direct collisional itation by electrons; (*b*) below 100 km by isional electronic excitation and, in addition, ion-atom interchange and dissociative re-nbination:

$$O^+ + N_2 \rightarrow NO^+ + N \qquad (4)$$

$$NO^+ + e \rightarrow O + N \qquad (5)$$

l by dissociative recombination of O_2^+:

$$O_2^+ + e \rightarrow O^* + O^* \qquad (6)$$

tsushita [1959] has estimated that the main roral display of August 1 occurred at a ght of 70 to 90 km above the conjugate nt, in which case dissociative recombination ıld be the primary mechanism for the ex-ation of the [OI] lines. The ionization cross tion of N_2 and O_2 should be similarly depend- on electron energy. On the other hand, the cess of dissociative recombination requires atively slow electrons, and consequently, if N_2^+ band system results from the simul-eous ionization and excitation of N_2, an in-ase in energy of the incident electrons should ance the N_2^+ auroral emissions relative to se of the atomic dissociation products. Di-t electronic excitation of the forbidden [OI] es should still operate at the 70- to 90-km level, but it should be negligible compared with the ionization and excitation of N_2; the ratio of the concentrations of O and N_2, $N(O)/N(N_2)$, drops from approximately unity at 140 km to approximately 10^{-4} at 75 km. Collisional de-excitation would be a significant supression mechanism for the [OI] lines below 90 km, and would be a second agent contributing toward an effective enhancement of the N_2^+ first nega-tive system. Such a supression of the oxygen red lines in low-altitude type B auroras has been observed by *Hunten* [1955].

The red color 'covering' the violet rays may result from the mutual neutralization of N_2^+ by O^- or O_2^- as is possibly the case in type B auroras [*Malville*, 1959]. The gradual change from violet and red to green merely reflects the fading of intensity of the rays, red and violet having higher color thresholds than green.

In order that red color be perceived the au-rora must have an emission rate of at least 100 kilorayleighs, where the rayleigh is defined as $4\pi \times 10^6$ quanta/cm²/sec/sterad [*Hunten, Roach, and Chamberlain*, 1956]. The transition be-tween aurora and night airglow lies somewhere around 1 kilorayleigh. A red auroral ray with a diameter of 0.1 km would then have a volume emission rate of at least 10^7 quanta/cm³/sec, and would disappear entirely when the volume emission rate dropped below 10^5 quanta/cm³/sec. Thus after 6 minutes the electron current in the rays must have become less than 2×10^7 elec-trons/cm²/sec. According to equation 1, after 6 minutes the residual activity would have de-creased by a factor of $6^{-1.2} = (8.6)^{-1}$, which would indicate that the radius of the fission cloud had increased by a factor of $(11.6)^{1/2} = 3.37$, in order that the ray current drop by a factor of 10^2.

The red glow which persisted 8 minutes after the disappearance of the rays may have had a line-of-sight thickness of 10 km, requiring a volume emission rate of 10^5 quanta/cm³/sec, which is equal to the emission rate at which rays disappeared. The complete fading of the glow after 8 minutes implies another hundred-fold decrease of the emission rate and an in-crease of the surface area of the fission cloud during the 14-minute period by a factor of ap-proximately 40.

The 'crimson' arc which had a magnetic lati-

tude of about 7° and a corresponding height of perhaps 400 km may have had its origin in ion-atom interchange and dissociative recombination:

$$O^+ + N_2 \rightarrow NO^+ + N \quad (4)$$

$$NO^+ + e \rightarrow N + O^* \quad (5)$$

and in this sense would be a form of auroral afterglow. This type of process has been shown by *Chamberlain* [1958] to be capable of accounting for the slow decay of the oxygen red line in the twilight. The rate of the reactions 4 and 5 is strongly dependent upon the concentration of N_2, and the existence of the arc after 400 seconds implies, according to Chamberlain's theory, a lower border of the oxygen red line emission at about 175 km. This is lower than the presumed height of the arc but nevertheless suggests a clear separation of the red glow and the higher arc.

Conclusions—Electrons resulting from the β decay of the fission fragments of a 20-kt trigger fission bomb are capable of accounting for the artificial aurora observed from Apia after the Johnston Island explosion of August 1, 1958. The distinctive violet color of the rays indicates a strong enhancement of the N_2^+ band system relative to the oxygen green line and may imply that dissociative recombination rather than direct electronic excitation was the primary exciting mechanism for the forbidden O I. lines. The low altitude of the rays suggests a close association between the Apia rays and type B auroras, where the red coloration results possibly from the mutual neutralization of N_2^+ by O^- or O_2^-. The high-altitude 'crimson' arc may result from a combination of the processes of ion-atom interchange and dissociative recombination and in this respect may be similar to the twilight enhancement of the oxygen red lines in the airglow.

Acknowledgments—It is a pleasure to th J. W. Chamberlain, S. Matsushita, and J. W. W wick for very stimulating discussions on problem.

References

BATES, D. R., The physics of the upper atm phere, *The Earth as a Planet,* edited by G Kuiper, University of Chicago Press, Chic pp. 567–643, 1954.

BATES, D. R., AND G. GRIFFING, Scale height terminations and auroras, *J. Atmospheric Terrest. Phys., 3,* 212–216, 1953.

CHAMBERLAIN, J. W., The excitation of hydro in aurorae, *Astrophys. J., 120,* 360–366, 1

CHAMBERLAIN, J. W., Discharge theory of aur rays, *The Airglow and the Aurorae,* edited E. B. Armstrong and A. Dalgarno, Pergar Press, London, pp. 206-221, 1955.

CHAMBERLAIN, J. W., Oxygen red lines in the glow, *Astrophysical J., 127,* 54–66, 1958.

CULLINGTON, A. L., A man-made or artificial rora, *Nature, 182,* 1365–1366, 1958*a*.

CULLINGTON, A. L., Apia aurorae, Address gi in Samoa, Canterbury Astronomical Soci Sept. 16, 1958*b*.

GLASSTONE, S., *The Effects of Nuclear Weap* United States Atomic Energy Commission, 1

HUNTEN, D. M., Some photometric observat of auroral spectra, *J. Atmospheric and Ter Phys., 7,* 141–151, 1955.

HUNTEN, D. M., F. E. ROACH, AND J. W. CHAM LAIN, A photometric unit for the airglow aurora, *J. Atmospheric and Terrest. Phys* 345–346, 1956.

MALVILLE, J. M., Type B aurorae in the antar *J. Atmospheric and Terrest. Phys.,* in press, 1

MATSUSHITA, S., On artificial geomagnetic ionospheric storms associated with high-altit explosions, *J. Geophys. Research, 64,* 1149–1 1959.

STÖRMER, C., Sunlit aurorae, *Proc. Conf. on Aur Physics,* edited by N. C. Gerson, T. J. Kenes and R. J. Donaldson, Jr., *Geophys. Research per 30,* Air Force Cambridge Research Cer pp. 95–115, 1954.

TIME, *73,* 56, June 29, 1959.

WINCKLER, J. R., L. PETERSON, R. ARNOLDY, R. HOFFMAN, *Phys. Rev., 110,* 1221-1231, 195

(Manuscript received August 13, 1959; rev September 12, 1959.)

Application of Hansen's Theory to the Motion of an Artificial Satellite in the Gravitational Field of the Earth

PETER MUSEN

Theoretical Division, Goddard Space Flight Center
National Aeronautics and Space Administration
Silver Spring, Maryland

Abstract—In order to draw geophysical and geodetic conclusions from the motion of the artificial satellite, we need an accurate theory that will permit the easy inclusion of any gravitational term. This articles contains a theory of Hansen's type adaptable to the use of large computing machines. The form of the disturbing function suggests the use of the process of iteration. The computations can be carried out to any desired order compatible with the accuracy of the geodetic parameters. The theory as written is valid for zonal harmonics of all orders in the earth's gravitational field. A program based on this theory was developed by Dr. Herget and his collaborators and was used by the Vanguard Computing Center to produce the numerical theories of several satellites.

troduction—This paper contains a theory of sen's type for the artificial satellite. The ry was developed by the author at the est of Dr. Paul Herget, Director of the innati Observatory, during the author's as- tion with the Vanguard Computing Center consultant and during his stay at the innati Observatory.

ansen's theory was chosen because it is ly numerical and permits the full use of computing machines. The basic idea con- in the introduction of a fictitious satellite ribing an auxiliary ellipse of constant shape ccordance with Kepler's laws. The position e real satellite is determined by its deviation the position of the auxiliary satellite. The tion vectors have the same direction, but ifferent times. Let $\mathbf{r}$ be the position vector of al satellite, and $\bar{\mathbf{r}}$ the position vector of the liary satellite. Hansen's development then ends on the parameter ν and on the pseudo- e z defined by the vectorial equation

$$\mathbf{r}(t) = (1 + \nu)\bar{\mathbf{r}}(z)$$

pseudotime z represents the time at which position vector of the auxiliary satellite has direction possessed by the real satellite at e t.

he notations in this article in general agree those used by *E. W. Brown* [1896].

wo scalar equations for absolute values and for unit vectors are

$$r = (1 + \nu)\bar{r} \tag{1}$$

$$\mathbf{r}^0(t) = \bar{\mathbf{r}}^0(z) \tag{2}$$

We assume that the auxiliary ellipse is rotating in the osculating orbit plane uniformly with respect to the eccentric anomaly of the fictitious satellite; then $\nu\bar{r}$ and $\delta z = z - t$ can be interpreted respectively as perturbations of the radius vector and of time. They are determined by a *single* Hansen function W. We introduce two systems of rectangular coordinates: One (xyz) is fixed in space, the other (XYZ) is rigidly connected with the osculating orbit plane. The X and Y axes are in the orbit plane; the Z axis stands normal to that plane. The intersection of the X axis with the celestial sphere is called the 'departure point.'

The motion of both satellites consists of the motion in the osculating plane (XY) combined with the rotation of that plane about the instantaneous radius vector. In order to obtain the absolute velocity no effect of rotation is to be added, because the instantaneous axis of rotation coincides with the radius vector. The fictitious forces produced by the rotation of the system (XY) either disappear or are normal to the orbit plane, and the equation of the motion of the satellite with respect to the (XY) system

takes the simple form

$$\ddot{\mathbf{r}} + \mathbf{r}/r^3 = \text{grad}\ \Omega$$

i.e., it has the same form as in an inertial system. Such moving systems of coordinates are called 'ideal' by Hansen. The position of the moving system can be determined by three Eulerian angles:

i, the inclination to the earth's equator.
θ, the longitude of the ascending note.
σ, the angular distance of the node from the departure point.

But in our theory instead of Euler's angles we will introduce parameters analogous to the parameters of Olinde Rodrigues in the theory of the rotation of a rigid body.

The angular distance of the osculating perigee from the departure point will be designated by χ. We shall introduce the conventional osculating elliptic elements defined as follows:

$a =$ the osculating semimajor axis.
$e =$ the osculating eccentricity.
$n = a^{-3/2}$ the osculating mean motion.
$h = 1/\sqrt{a(1 - e^2)}$.

These elements are time-dependent in general. The theory depends on time-independent constants of integration: a_0, e_0, π_0, σ_0, i_0, θ_0, $n_0, = a_0^{-3/2}$, h_0, and g_0, the mean anomaly at the epoch.

The osculating elements assume values that are always close to but not identical with the values of these integration constants.

The main differences between Hansen's classical lunar theory and our exposition are the following:

1. The eccentric anomaly of the fictitious satellite is used as the independent variable, instead of time.

2. The existence of fast computing machines permits the replacement of Hansen's development into Maclaurin series by the method of iterations.

3. Of the four parameters that determine the position of the orbit plane, two differ from Hansen's.

4. The rotation matrix is used instead of the development of polar coordinates.

The effect of the motion of the earth's axis is neglected. It is mainly secular and can [b]e obtained, if necessary, as an additional corre[c]tion. The periodic irregularities produced [b]y this motion are so small that they can be ne[g]lected.

Disturbing function—The differential equatio[ns] in polar coordinates r, v in the (XY) system ha[ve] the same form as in the fixed system:

$$\frac{d^2r}{dt^2} - r\left(\frac{dv}{dt}\right)^2 + \frac{1}{r^2} = \frac{\partial\Omega}{\partial r}$$

$$\frac{d}{dt}\left(r^2\frac{dv}{dt}\right) = \frac{\partial\Omega}{\partial v}$$

We define the disturbing function as t[he] negative of the difference between the gravit[a]tional potential and the potential of a spheri[cal] earth of the same mass. In this theory the d[is]turbing function Ω is taken in the form of [an] expansion in zonal harmonics which we wr[ite] explicitly to the fourth order:

$$\Omega = \frac{k_2}{r^3}(1 - 3\psi^2) + \frac{k_3}{r^4}(3\psi - 5\psi^3) + \frac{k_4}{r^5}(3 - 30\psi^2 + 35\psi^4)$$

where ψ is the sine of the geocentric latitude,

$$\psi = \sin i \sin(v - \sigma)$$

The first harmonic is absent from (5) becau[se] the origin is taken at the center of mass.

The position of the perigee of the auxilia[ry] ellipse in the system (XY) is defined by [the] equation

$$\pi = \pi_0 + y\,\Delta E \qquad \Delta E = E - E_0$$

The motion of the auxiliary satellite in [the] ellipse is defined by the system of equations

$$\bar{r}\cos\bar{f} = a_0(\cos E - e_0)$$

$$\bar{r}\sin\bar{f} = a_0\sqrt{1 - e_0^2}\sin E$$

$$\bar{r} = a_0(1 - e_0\cos E)$$

$$E - e_0\sin E = g_0 + n_0 z$$

$$= g_0 + n_0(t - t_0) + n_0\,\delta z$$

The polar angle of the fictitious satellite w[ith] respect to the X axis is

$$\bar{f} + \pi_0 + y\,\Delta E$$

ld according to (2)

$$v = \bar{f} + \pi_0 + y\,\Delta E$$

t us define the constants σ_0, θ_0 is such a way at the expressions

$$2N = \sigma_0 + \theta_0 - \sigma - \theta - 2\alpha\,\Delta E \qquad (11)$$

$$2K = \sigma_0 - \theta_0 - \sigma + \theta + 2\eta\,\Delta E \qquad (12)$$

not contain any constant terms. The secular tion y, α, η must be determined in such a way at the development of the coordinates conns no secular terms, but only periodic. This quirement is equivalent to the requirement at $2N$, $2K$, and $n_0\,\delta z$ consist of periodic terms ly. We have

$$\left.\begin{aligned} \sigma &= \sigma_0 - (\alpha - \eta)\,\Delta E - (N + K) \\ \theta &= \theta_0 - (\alpha + \eta)\,\Delta E - (N - K) \end{aligned}\right\} \qquad (13)$$

$$- \sigma = \bar{f} + (\pi_0 - \sigma_0) + (y + \alpha - \eta)\,\Delta E + (N + K)$$

e expressions

$$) = \sigma_0 - (\alpha - \eta)\,\Delta E$$

$$) = \theta_0 - (\alpha + \eta)\,\Delta E \qquad (14)$$

$$) = (\pi_0 - \sigma_0) + (y + \alpha - \eta)\,\Delta E$$

e the mean values of the corresponding ments. We have

$$\psi = \sin i \sin (f + (\omega) + N + K) \qquad (15)$$

By introducing four parameters:

$$\left.\begin{aligned} &= \sin \tfrac{1}{2}i \cos N, \quad \lambda_3 = \cos \tfrac{1}{2}i \sin K \\ &= \sin \tfrac{1}{2}i \sin N, \quad \lambda_4 = \cos \tfrac{1}{2}i \cos K \end{aligned}\right\} \qquad (16)$$

$$\lambda_1^2 + \lambda_2^2 + \lambda_3^2 + \lambda_4^2 = 1$$

e can represent (15) in the form

$$= 2(\lambda_1\lambda_4 - \lambda_2\lambda_3) \sin (\bar{f} + (\omega)) + 2(\lambda_2\lambda_4 + \lambda_1\lambda_3) \cos (\bar{f} + (\omega)) \qquad (17)$$

ich leaves only $\bar{f} + (\omega)$ in the argument. e introduction of four interindependent rameters is convenient from the standpoint symmetry. However, the number of indepennt parameters is only three. We can introduce ree independent parameters:

$$\left.\begin{aligned} p &= \frac{\lambda_1}{\lambda_4} = tg\tfrac{1}{2}i \frac{\cos N}{\cos K} \\ q &= -tg\tfrac{1}{2}i \frac{\sin N}{\cos K} = -\frac{\lambda_2}{\lambda_4} \\ s &= \frac{\lambda_3}{\lambda_4} = tgK \end{aligned}\right\} \qquad (17')$$

instead of λ_1, λ_2, λ_3, λ_4. These parameters, like the λ parameters, leave only $\bar{f} + (\omega)$ in the argument in (15). The system (p, q, s) is definitely preferable for the polar satellites. Putting

$$\begin{aligned} l &= (\bar{r}/a_0) \cos (\bar{f} + (\omega)) \\ &= \tfrac{1}{2}(1 + \sqrt{1 - e_0^2}) \cos (E + (\omega)) \\ &\quad + \tfrac{1}{2}(1 - \sqrt{1 - e_0^2}) \cos (E - (\omega)) \\ &\quad - e_0 \cos (\omega) \end{aligned} \qquad (18)$$

$$\begin{aligned} m &= (\bar{r}/a_0) \sin (\bar{f} + (\omega)) \\ &= \tfrac{1}{2}(1 + \sqrt{1 - e_0^2}) \sin (E + (\omega)) \\ &\quad - \tfrac{1}{2}(1 - \sqrt{1 - e_0^2}) \sin (E - (\omega)) \\ &\quad - e_0 \sin (\omega) \end{aligned} \qquad (19)$$

we can represent (15) in the form convenient for further development:

$$\psi = 2(a_0/\bar{r})(\lambda_1\lambda_4 - \lambda_2\lambda_3)\,m + 2(a_0/\bar{r})(\lambda_2\lambda_4 + \lambda_1\lambda_3)\,l \qquad (20)$$

We have also

$$\frac{a_0}{\bar{r}} = \frac{2}{\sqrt{1 - e_0^2}} (\tfrac{1}{2} + \beta \cos E + \beta^2 \cos 2E + \beta^3 \cos 3E + \cdots) \qquad (21)$$

$$e = \sin \varphi$$

$$\beta = tg\tfrac{1}{2}\varphi$$

We have to distinguish the E entering into the development of the perturbations from the 'elliptic' E in (7) to (10) and in (18) to (21). The partial derivative $\partial\Omega/\partial E$ which enters the differential equations for perturbations is taken with respect to the elliptic E.

For this reason it is convenient to use the notation F for E in (18) to (21). Each step of the process of iteration leads to the series of

the form

$$\Omega^* = \sum C \cos(iE + 2j\omega + kF)$$
$$+ \sum S \sin[iE + (2j+1)\omega + kF] \quad (22)$$

for Ω. We have for the partial derivative with respect to the elliptic E

$$\partial\Omega/\partial E = \overline{\partial\Omega^*}/\partial F$$

where the 'bar' operation means, in Hansen's notation, the replacement of F by E.

Perturbations in the orbit plane—The perturbations of the radius vector and of the mean anomaly are the only perturbations in the orbit plane that enter Hansen's theory. The equations determined the basic function W in our case evidently take the form [*Hansen*, 1838]

$$\frac{dW}{dt} = h_0 \frac{\partial\Omega}{\partial v}\left\{2\frac{\bar{\rho}}{r}\cos(\bar{f} - \bar{\varphi}) - 1 + 2\frac{h^2}{h_0^2}\cdot\frac{\bar{\rho}}{a_0}\cdot\frac{\cos(\bar{f} - \bar{\varphi}) - 1}{1 - e_0^2}\right\}$$
$$+ 2h_0\frac{\bar{\rho}}{r}\sin(\bar{f} - \bar{\varphi})\cdot r\frac{\partial\Omega}{\partial r}$$
$$+ \frac{y}{\sqrt{1 - e_0^2}}\left[\frac{\bar{\rho}}{a_0}\cdot\frac{\partial W}{\partial F} - \left(W + 1 + \frac{h_0}{h}\right)e_0 \sin F\right]\frac{dE}{dt} \quad (23)$$

and

$$\overline{W} = W|_{F=E}$$

$\bar{\rho}$ and $\bar{\varphi}$ are the radius vector and the true anomaly, which can be eliminated in favor of eccentric anomaly F by means of the usual formulas:

$$\bar{\rho}/a_0 = 1 - e_0 \cos F$$
$$(\bar{\rho}/a_0)\cos\bar{f} = \cos F - e_0$$
$$(\bar{\rho}/a_0)\sin\bar{f} = \sqrt{1 - e_0^2}\sin F$$

The eccentric anomaly F, together with $\bar{\rho}$ and $\bar{\varphi}$, is introduced as an artificial device in order to facilitate the integration and to keep the elliptic motion separated from the perturbations. After the integration is done there is no need for such a separation and we replace F by E again. In fact, (23) is equivalent to the combination of the equation for areal velocity and the two equ tions for the Laplacian vector. Using the gener ization of *Hill's* formula [1881]:

$$\frac{dn_0\,\delta z}{dt} = n_0\frac{\overline{W} + \nu^2}{1 - \nu^2} - \frac{y}{\sqrt{1 - e_0^2}}\left(\frac{\bar{r}}{a_0}\right)^2\cdot\frac{d}{d}$$

and the equation

$$n_0\frac{dt}{dE} + \frac{dn_0\,\delta z}{dE} = \frac{\bar{r}}{a_0}$$

which arises from the differentiations of Keple equation, we deduce

$$\frac{dn_0\,\delta z}{dE} = \frac{\overline{W} + \nu^2}{1 + \overline{W}}\cdot\frac{\bar{r}}{a_0} - \frac{1 - \nu^2}{1 + \overline{W}}\cdot\frac{y}{\sqrt{1 - e_0^2}}\left(\frac{\bar{r}}{a_0}\right)^2 \quad (2$$

and

$$n_0\frac{dt}{dE} = \frac{\bar{r}}{a_0}\cdot\frac{1 - \nu^2}{1 + \overline{W}}\left(1 + \frac{y}{\sqrt{1 - e_0^2}}\cdot\frac{\bar{r}}{a_0}\right.$$

Taking into consideration that

$$\frac{\partial\Omega}{\partial v} = \frac{\partial\Omega}{\partial\bar{f}} = \frac{\bar{r}}{a_0\sqrt{1 - e_0^2}}\cdot\frac{\partial\Omega}{\partial E} - \frac{e_0 \sin E}{\sqrt{1 - e_0^2}}\, r\frac{\partial\Omega}{\partial r} \quad ($$

and eliminating $\partial\Omega/\partial v$ from (23), we deduce following equation, analogous to the equation planetary perturbations [*von-Zeipel*, 1902]

$$\frac{dW}{dE} = N\Lambda r\frac{\partial a_0\Omega}{\partial r} + M\Lambda\frac{\partial a_0\Omega}{\partial E} + \frac{Sy}{\sqrt{1 - e_0^2}} \quad ($$

where

$$(1 - e_0^2)M = \frac{h^2}{h_0^2}[-2 + 2e_0\cos E$$
$$+ 2\cos(F - E)$$
$$- e_0\cos(F - 2E) - e_0\cos F]$$
$$+ \frac{1}{1 + \nu}[2e_0^2 - 2e_0\cos E$$
$$+ e_0^2\cos(F + E)$$

$$(2 - e_0^2) \cos (F - E) - e_0 \cos F]$$

$$1 - \tfrac{1}{2}e_0^2 + 2e_0 \cos E$$

$$\tfrac{1}{2}e_0^2 \cos 2E \tag{27}$$

$$- e_0^2)N = \frac{h^2}{h_0^2} [+2e_0 \sin E$$

$$- e_0 \sin F + e_0 \sin (F - 2E)]$$

$$+ \frac{1}{1 + \nu} [-2e_0 \sin E$$

$$- (2 - e_0^2) \sin (F - E)$$

$$+ e_0^2 \sin (F + E)]$$

$$+ e_0 \sin E - \tfrac{1}{2}e_0^2 \sin 2E \tag{28}$$

$$= \frac{1 - \nu^2}{1 + W}\left(1 + \frac{y}{\sqrt{1 - e_0^2}}\cdot\frac{\bar{r}}{a_0}\right) \tag{29}$$

$$= \frac{\bar{p}}{a_0}\cdot\frac{\partial W}{\partial F} - \left(W + 1 + \frac{h_0}{h}\right) e_0 \sin F \tag{30}$$

erturbations of the position of the orbit plane—ng the equations of the theory of the varia-n of constants:

$$\sin i \frac{d\theta}{dt} = h \frac{\partial \Omega}{\partial Z} r \sin (v - \sigma)$$

$$\frac{d\sigma}{dt} = \frac{d\theta}{dt} \cos i$$

l taking (11) and (12) into consideration, have:

$$= -\alpha \frac{dE}{dt} - \tfrac{1}{2}h \frac{\partial \Omega}{\partial Z} r\cdot \mathrm{ctg}\, \frac{i}{2}\cdot \sin (v - \sigma)$$

$$= +\eta \frac{dE}{dt} + \tfrac{1}{2}h \frac{\partial \Omega}{\partial Z} r\cdot \mathrm{tg}\, \frac{i}{2}\cdot \sin (v - \sigma)$$

rom these last two equations and from

$$\frac{di}{dt} = h \frac{\partial \Omega}{\partial Z} r \cos (v - \sigma)$$

easily deduce:

$$= +\alpha\lambda_2 \frac{dE}{dt}$$

$$+ \tfrac{1}{2}a_0 h(1 + \nu) \frac{\partial \Omega}{\partial Z} (\lambda_4 l - \lambda_3 m)$$

$$\frac{d\lambda_2}{dt} = -\alpha\lambda_1 \frac{dE}{dt}$$

$$+ \tfrac{1}{2}a_0 h(1 + \nu) \frac{\partial \Omega}{\partial Z} (-\lambda_3 l - \lambda_4 m)$$

$$\frac{d\lambda_3}{dt} = +\eta\lambda_4 \frac{dE}{dt}$$

$$+ \tfrac{1}{2}a_0 h(1 + \nu) \frac{\partial \Omega}{\partial Z} (\lambda_2 l + \lambda_1 m)$$

$$\frac{d\lambda_4}{dt} = -\eta\lambda_3 \frac{dE}{dt}$$

$$+ \tfrac{1}{2}a_0 h(1 + \nu) \frac{\partial \Omega}{\partial Z} (-\lambda_1 l + \lambda_2 m)$$

But in our case

$$r \frac{\partial \Omega}{\partial Z} = \frac{\partial \Omega}{\partial \psi} \cos i$$

and eliminating dt by means of

$$\frac{dt}{dE} = \frac{\bar{r}}{a_0 n_0} \Lambda$$

we obtain

$$\frac{d\lambda_1}{dE} = +\alpha\lambda_2 + \tfrac{1}{2}\cdot\frac{h}{h_0}$$

$$\cdot \frac{a_0}{\sqrt{1 - e_0^2}} \frac{\partial \Omega}{\partial \psi} \cos i(\lambda_4 l - \lambda_3 m)\Lambda$$

$$\frac{d\lambda_2}{dE} = -\alpha\lambda_1 + \tfrac{1}{2}\cdot\frac{h}{h_0}$$

$$\cdot \frac{a_0}{\sqrt{1 - e_0^2}} \frac{\partial \Omega}{\partial \psi} \cos i(-\lambda_3 l - \lambda_4 m)\Lambda \tag{31}$$

$$\frac{d\lambda_3}{dE} = +\eta\lambda_4 + \tfrac{1}{2}\cdot\frac{h}{h_0}$$

$$\cdot \frac{a_0}{\sqrt{1 - e_0^2}} \frac{\partial \Omega}{\partial \psi} \cos i(\lambda_2 l + \lambda_1 m)\Lambda$$

$$\frac{d\lambda_4}{dE} = -\eta\lambda_3 + \tfrac{1}{2}\cdot\frac{h}{h_0}$$

$$\cdot \frac{a_0}{\sqrt{1 - e_0^2}} \frac{\partial \Omega}{\partial \psi} \cos i(-\lambda_1 l + \lambda_2 m)\Lambda$$

From (31) and (17) we can deduce the equa-

tions

$$\frac{dp}{dE} = -\alpha q + \tfrac{1}{2}\frac{h}{h_0}\frac{a_0}{\sqrt{1-e_0^2}}\frac{\partial\Omega}{\partial\psi}$$
$$\cdot \cos i[(1+p^2)l$$
$$+ (pq - s)m]\Lambda + \eta ps$$
$$\frac{dq}{dE} = +\alpha p + \tfrac{1}{2}\frac{h}{h_0}\cdot\frac{a_0}{\sqrt{1-e_0^2}}\frac{\partial\Omega}{\partial\psi}$$
$$\cdot \cos i[(pq + s)l$$
$$+ (1+q^2)m]\Lambda + \eta qs \qquad (32)$$
$$\frac{ds}{dE} = +\eta(1+s^2) + \tfrac{1}{2}\frac{h}{h_0}\frac{a_0}{\sqrt{1-e_0^2}}\frac{\partial\Omega}{\partial\psi}$$
$$\cdot \cos i[(ps - q)l$$
$$+ (qs + p)m]\Lambda$$

Constants of integration; determination of $\overline{W}$ *and* $n_0\,\delta z$—The real constants of integration are the six elements $a_0, e_0, g_0, \theta_0, i_0, \omega_0 = \pi_0 - \sigma_0$. They do not have any simple kinematical or geometrical meaning; in particular, no moment of time exists for which these elements are osculating. This system is unique; it must be compatible with the observations and is obtained as the result of the process of orbit correction repeated several times. All the auxiliary constants of integration that appear in the solution are determined as functions of the six basic constants in such a way that the process of iteration does not introduce any secular terms in the expressions for $n_0\,\delta z$, $1+\nu$, $\lambda_1, \lambda_2, \lambda_3, \lambda_4$. In connection with this remark, it is necessary to point out that not every integral requires an additive constant, but only those integrated series that consist of terms of the form

$$A \cos(iE + 2j\omega).$$

If the integrated series consists of terms of the form

$$A \sin(iE + 2j\omega)$$
$$A \cos[iE + (2j+1)\omega],$$
$$A \sin[iE + (2j+1)\omega]$$

no integration constant is added.

The differential equations 26, 24, and 31, or 26, 24, and 32, constitute the basic system which is solved by the method of iterations, starting with $n_0\,\delta z = 0$, $1 + \nu = 1$, $\lambda_1 = \sin\tfrac{1}{2}i_0$, $\lambda_2 = \lambda_3 = 0$, $\lambda_4 = \cos\tfrac{1}{2}i_0$, or with $p = tg$ ½
$q = s = 0$ if we are using p, q, s instead o
parameters.

The program for the multiplication
numerical Fourier series was developed
Herget and his collaborators. It permits us
obtain a final approximation in a very sh
time. At each step of the process of iterat
we determine y in such a way that no term
the form $A \sin F$ is present in (26); otherw
the integration will produce a secular term
W and a term of mixed type in $\overline{W}$. For a simi
reason, the constants α and η are determi
in such a way that no constant terms appear
the right-hand sides of (31). The second a
third equations of (31) are especially conveni
for the determination of α and η. Each step
the process of iteration leads to the series
dW/dt consisting of terms of the form

$$A \sin(iE + 2j\omega)$$
$$A \sin(iE + 2j\omega \pm F) = A \sin(iE + 2j\omega$$
$$\cdot \cos F \pm A \cos(iE + 2j\omega) \sin$$
$$A \cos[iE + (2j+1)\omega]$$
$$A \cos[iE + (2j+1)\omega \pm F]$$

and, in connection with the general rema
about the additive constants of integration,
is evident that in the series for W this consta
takes the form

$$C_0 + C_1 \cos F$$

and W has the form

$$W = \sum C \cos(iE + 2j\omega + kF)$$
$$+ \sum S \sin[iE + (2j+1)\omega + kF]$$
$$+ C_0 + C_1 \cos F \qquad k = -1, 0, +1 \quad (3$$

The series for W takes the form

$$\overline{W} = C_0 + C_1 \cos E + \sum C \cos(iE + 2j$$
$$+ \sum S \sin[iE + (2j+1)\omega] \qquad (3$$

Equation 26 can be written in the form

$$\frac{dn_0\,\delta z}{dE} = \overline{W}\frac{\bar r}{a_0} + \left(\frac{\nu^2 - \overline{W}^2}{1+\overline{W}}\cdot\frac{\bar r}{a_0}\right.$$
$$\left. - \frac{y}{\sqrt{1-e_0^2}}\cdot\frac{1-\nu^2}{1+\overline{W}}\cdot\frac{\bar r^2}{a_0^2}\right) \qquad (3$$

ich is more convenient for the application he method of iteration, because the values of nd $\overline{W}$ in the parentheses can be taken from previous approximation. Substituting (34) the first term of the right-hand side of), we determine C_0 and C_1 in such a way that constant term and the term having E as argument disappear. This leaves only iodic terms in $n_0\ \delta z$, with no constant term no term having E as the argument, because h terms are already contained in Kepler's ation.

Determination of h/h_0 and $1 + \nu$—The expres- for W, after the constants C_0 and C_1 are ermined, can be written in the form

$$W = X + Y \cos F + Z \sin F \quad (36)$$

s the part of W independent of F; Y can be ained by putting $F = 0$ in the part containing . Eliminating $\bar{\varphi}$ and $\bar{\rho}$ from the equation *nsen*, 1838]

$$= -1 - \frac{h_0}{h} + 2\frac{h}{h_0}\cdot\frac{\bar{\rho}}{a_0}$$

$$\cdot\frac{1 + e\cos(\bar{\varphi} + \pi_0 + y\,\Delta E - \chi)}{1 - e_0^{\ 2}}$$

means of

$$\bar{\rho}\cos\bar{\varphi} = a_0(\cos F - e_0)$$

$$\bar{\rho}\sin\bar{\varphi} = a_0\sqrt{1 - e_0^{\ 2}}\sin F$$

$$\bar{\rho} = a_0(1 - e_0\cos F)$$

l comparing the result with (36), we deduce

$$= -1 - \frac{h_0}{h} + 2\frac{h}{h_0}\cdot\frac{1}{1 - e_0^{\ 2}}$$

$$- 2\frac{h}{h_0}\cdot\frac{ee_0\cos(\pi_0 + y\,\Delta E - \chi)}{1 - e_0^{\ 2}}$$

$$= 2\frac{h}{h_0}\cdot\frac{e\cos(\pi_0 + y\,\Delta E - \chi) - e_0}{1 - e_0^{\ 2}}$$

follows from these two last equations that

$$X + e_0 Y = -1 - (h_0/h) + 2(h/h_0)$$

tting

$$h_0/h = 1 + \Delta$$

we obtain, after some easy transformations

$$\Delta = -\tfrac{1}{3}(X + e_0 Y) + \tfrac{2}{3}(\Delta^2 - \Delta^3 + \cdots) \quad (37)$$

and

$$h/h_0 = 1 + \tfrac{1}{2}(\Delta + X + e_0 Y) \quad (38)$$

No additional integration is required to obtain h/h_0. The perturbations of the radius vector can be obtained from the equation

$$\overline{W} = -1 - \frac{h_0}{h} + 2\frac{h_0}{h}\cdot\frac{1}{1 + \nu}$$

which can be put in the form

$$\nu = \tfrac{1}{2}(\Delta - \overline{W}) - \tfrac{1}{2}(\Delta + \overline{W})\nu \quad (39)$$

which is more convenient for the application of the method of iteration. Again, in the determination of $1 + \nu$ the additional integration is avoided.

Determination of λ parameters—Each step of the process of iteration leads to the equations

$$\begin{aligned} \lambda_1 &= \sin\tfrac{1}{2}i_0 + \tfrac{1}{2}(A + B) + \delta\lambda_1 \\ \lambda_2 &= \delta\lambda_2 \\ \lambda_3 &= \delta\lambda_3 \\ \lambda_4 &= \cos\tfrac{1}{2}i_0 + \tfrac{1}{2}(A - B) + \delta\lambda_4 \end{aligned} \quad (40)$$

where $\delta\lambda_1$, $\delta\lambda_2$, $\delta\lambda_3$, $\delta\lambda_4$ are the series obtained by the formal integration of (31). They do not contain any constant terms, and their form is

$$\begin{aligned} \delta\lambda_1 &= \sum C\cos(iE + 2j\omega) + \sum S\sin[iE + (2j + 1)\omega] \\ \delta\lambda_2 &= \sum S\sin(iE + 2j\omega) + \sum C\cos[iE + (2j + 1)\omega] \\ \delta\lambda_3 &= \sum S\sin(iE + 2j\omega) + \sum C\cos[iE + (2j + 1)\omega] \\ \delta\lambda_4 &= \sum C\cos(iE + 2j\omega) + \sum S\sin[iE + (2j + 1)\omega] \end{aligned} \quad (41)$$

and $\frac{1}{2}(A + B)$ and $\frac{1}{2}(A - B)$ are the constants of integration.

Evidently, only the form of $\delta\lambda_1$ and $\delta\lambda_4$ admits

such additive constants. Two conditions must be satisfied:

1. The principal term in the latitude must have the form $\sin i_0 \sin (\bar{f} + (\omega))$. We had

$$\psi = 2(\lambda_1\lambda_4 - \lambda_2\lambda_2)\sin(\bar{f} + (\omega)) + 2(\lambda_2\lambda_4 + \lambda_1\lambda_3)\cos(\bar{f} + (\omega)) \tag{42}$$

and, consequently, the constant part in the development of $2(\lambda_1\lambda_4 - \lambda_2\lambda_3)$ is $\sin i_0$.

2. In addition

$$\lambda_1^2 + \lambda_2^2 + \lambda_3^2 + \lambda_4^2 = 1 \tag{43}$$

These two conditions determine A and B. Substituting (40) into (42) and (43) we obtain

$$\tfrac{1}{2}(A^2 - B^2) + A(\cos\tfrac{1}{2}i_0 + \sin\tfrac{1}{2}i_0) + B(\cos\tfrac{1}{2}i_0 - \sin\tfrac{1}{2}i_0) + \text{const. in } 2(\delta\lambda_1 . \delta\lambda_4 - \delta\lambda_2 . \delta\lambda_3) = 0$$

$$\tfrac{1}{2}(A^2 + B^2) + A(\cos\tfrac{1}{2}i_0 + \sin\tfrac{1}{2}i_0) - B(\cos\tfrac{1}{2}i_0 - \sin\tfrac{1}{2}i_0) + \text{const. in } (\delta\lambda_1^2 + \delta\lambda_2^2 + \delta\lambda_3^2 + \delta\lambda_4^2) = 0$$

or

$$\begin{aligned} A^2 + 2A(\cos\tfrac{1}{2}i_0 + \sin\tfrac{1}{2}i_0) + (11) &= 0 \\ B^2 - 2B(\cos\tfrac{1}{2}i_0 - \sin\tfrac{1}{2}i_0) + (12) &= 0 \end{aligned} \tag{44}$$

where

$$(11) = \text{const. in } [(\delta\lambda_1 + \delta\lambda_4)^2 + (\delta\lambda_2 - \delta\lambda_3)^2]$$

$$(12) = \text{const. in } [(\delta\lambda_1 - \delta\lambda_4)^2 + (\delta\lambda_2 + \delta\lambda_3)^2]$$

Equations 44 can be solved by the method of successive approximations if the satellite is not a polar one. For polar satellites the system (p, q, s) is preferable because we can simply put

$$p = \mathrm{tg}\tfrac{1}{2}i_0 + \delta p$$

$$q = \delta q$$

$$s = \delta s$$

where δp, δq, δs are the series deduced by the formal integration.

Decomposition of the matrix of rotation—The matrix representing a rotation about the x a for the angle α has the form

$$A_1[\alpha] = \begin{bmatrix} +1 & 0 & 0 \\ 0 & +\cos\alpha & -\sin\alpha \\ 0 & +\sin\alpha & +\cos\alpha \end{bmatrix}$$

and the matrix representing a rotation abo the z axis is

$$A_3[\alpha] = \begin{bmatrix} +\cos\alpha & -\sin\alpha & 0 \\ +\sin\alpha & +\cos\alpha & 0 \\ 0 & 0 & +1 \end{bmatrix}$$

The transformation from the system rigi connected to the moving ellipse to the equator system requires a triple rotation, and the tra formation matrix can be represented as t product of three matrices:

$$\Gamma = A_3[\theta]\cdot A_1[i]\cdot A_3[\pi_0 + y\,\Delta E - \sigma]$$

But

$$\theta = (\theta) - N + K$$

$$\pi_0 + y\,\Delta E - \sigma = (\omega) + N + K$$

and consequently

$$\Gamma = A_3[(\theta)]\cdot A_3[K - N]\cdot A_1[i] \cdot A_3[N + K]\cdot A_3[(\omega$$

Taking (16) into consideration, we can represe Γ after some easy transformations in the form

$$\Gamma = A_3[(\theta)]\cdot\begin{bmatrix} \lambda_{11} & \lambda_{12} & \lambda_{13} \\ \lambda_{21} & \lambda_{22} & \lambda_{23} \\ \lambda_{31} & \lambda_{32} & \lambda_{33} \end{bmatrix}\cdot A_3[(\omega)]$$

where

$$\lambda_{11} = +\lambda_1^2 - \lambda_2^2 - \lambda_3^2 + \lambda_4^2,$$

$$\lambda_{12} = -2(\lambda_3\lambda_4 + \lambda_1\lambda$$

$$\lambda_{13} = 2(\lambda_1\lambda_3 - \lambda_2\lambda_4)$$

$$\lambda_{21} = 2(\lambda_3\lambda_4 - \lambda_1\lambda_2),$$

$$\lambda_{22} = -\lambda_1^2 + \lambda_2^2 - \lambda_3^2 + \lambda$$

$$\lambda_{23} = -2(\lambda_1\lambda_4 + \lambda_3\lambda_2)$$

$$_{} = 2(\lambda_3\lambda_1 + \lambda_2\lambda_4),$$

$$\lambda_{32} = 2(\lambda_4\lambda_1 - \lambda_2\lambda_3),$$

$$\lambda_{33} = -\lambda_1^2 - \lambda_2^2 + \lambda_3^2 + \lambda_4^2$$

ne further analytical development of the atrix Γ is not presented. It was found that from e standpoint of expedience the substitution numerical values of $\lambda_1, \lambda_2, \lambda_3, \lambda_4$ evaluated from e series is preferable. The position vector of e satellite with respect to the equatorial stem is given by the formula

$$\mathbf{r} = (1 + \nu)\Gamma \cdot \begin{bmatrix} a_0 (\cos E - e_0) \\ a_0\sqrt{1 - e_0^2} \sin E \\ 0 \end{bmatrix}$$

he numerical computation of perturbations for given moment of time is made by the method iteration. Starting from Kepler's equation

$$E - e_0 \sin E = g_0 + n_0(t - t_0) + n_0\ \delta z$$

nd, from the series for $n_0\ \delta z$, we compute E nd $n_0\ \delta z$ by the method of iterations, using $_0\ \delta z = 0$ as the first approximation. After the nal value of E is reached, we compute $n_0\ \delta z$, $+ \nu$, λ's from the corresponding series; finally e compute the equatorial coordinates of the atellite.

Conclusion—The theory described here is a umerical one; it permits the full use of the rge capacity of modern machines; and it has een the basis for the Vanguard programs eveloped by Herget and his collaborators. It hould be noted that the Vanguard orbit elements ather than the conventional osculating elements re the constants of integration of the present heory. The computation can be carried out o any desired order compatible with the accuracy f the basic data. Hansen's theory permits the easy inclusion of any source of the gravitational nature which might become important in the future, and the same program can be used for all cases.

Despite all these features, the disadvantages of the numerical treatment under certain conditions must also be pointed out. The numerical procedures are not satisfactory if the eccentricity is smaller than ≈ 0.05 or larger than ≈ 0.6. In the limit of small eccentricities the determination of the motion of the perigee is difficult because the eccentricity appears as a divisor. In elongated orbits the difficulty is caused by the presence of $1 - e_0^2$ in the denominator and by the slow convergence of the series for $a_0/\bar{r}$. For these two extreme cases some sort of analytical development would be preferable. In connection with the problem of analytical development the results obtained by *Brouwer* [1958] and by *Kozai* [1959] deserve to be mentioned.

The problem of handling the critical inclination also remains. Work on these problems is being continued.

References

Brown, E. W., *An Introductory Treatise on the Lunar Theory,* Cambridge University Press, 1896.

Brouwer, D., Outlines of general theories of the Hill-Brown and Delaunay types of orbits of artificial satellites, *Astron. J., 63,* 433–438, 1958.

Hansen, P. A., Fundamenta nova investigationis orbitae verae quam Luna perlustrat, pp. 1–331, Gotha, 1938.

Hill, G. W., Note on Hansen's theory of perturbations, *Am. J. Math., 4,* 256–259, 1881.

Kozai, Y., The motion of a close earth satellite, in press, 1959.

von-Zeipel, H., Angenährte Jupiterstörungen für die Hecuba-gruppe, Academy of Science of St. Petersburg, p. 7, 1902.

(Manuscript received October 7, 1959.)

The Scintillation of Radio Signals from Satellites

K. C. Yeh

Department of Electrical Engineering

and

G. W. Swenson, Jr.

Departments of Electrical Engineering and Astronomy
University of Illinois
Urbana, Illinois

Abstract—Signals from satellites $1957\alpha_2$ and $1958\delta_2$, recorded during a 20-month period, are analyzed to determine the diurnal and seasonal variations of the incidence of scintillation. Marked diurnal effects are noted, scintillation being much more frequent at night. Night-time scintillation correlates with the occurrence of ionospheric 'spread F' and apparently originates in inhomogeneities at heights of about 220 km and, in most cases, at latitudes greater than 40°N. Daytime scintillation appears to originate in smaller, inhomogeneous regions below 220 km and more widely distributed in latitude.

Introduction—Immediately after the launch-
g of satellite $1957\alpha_2$ (sputnik I) it was noted at at times the amplitudes of both 20- and -Mc/s signals fluctuated rapidly and irregu-ly, at rates of the order of several fluctua-ns per second [*Kraus and Albus,* 1958; *War-ck,* 1958]. Observations in Australia [*Slee,* 58] suggested a correlation between scintilla-n of satellite signals and radiation from smic sources, though this suggestion was not pported by a report from Alaska [*Parthasar-hy and Reid,* 1959]. With 20 months' data ailable, partly from $1957\alpha_2$ (sputnik I) but ainly from $1958\delta_2$ (sputnik III), it is now ssible to attempt a somewhat more complete alysis of the phenomenon.

Method of analysis—When no scintillation is esent the signal received on a linear dipole ex-bits regular sinusoidal amplitude variations re-lting from Faraday rotation of the resultant ectric vector. The same has also been observed connection with the radio echoes from the oon [*Browne, Evans, and Hargreaves,* 1956]. other occasions the sinusoidal fading is rtly or completely obscured by scintilla-n. For purposes of analysis each amplitude cord is arbitrarily assigned a 'scintillation in-x' on the basis of visual inspection in accord-ce with the following criteria:

Index	*Character of Signal*
0	Regular Faraday fading
1	Faraday fading with superimposed scintillation
2	Faraday fading completely obscured by scintillation

Typical examples are given in Figure 1.

In order to investigate temporal variations of scintillation the visually assigned scintillation indices are added for all passages occurring within a selected 2-hour period of the day. The sum is divided by 200 times the number of passages to arrive at a 'percentage scintillation' for the period in question. This quantity is plotted versus time of day for four 3-month periods during the first year of life of sputnik III ($1958\delta_2$). The results are discussed in the next section.

It should be cautioned that on some occasions there occurs the phenomenon illustrated in Figure 2, in which the signal builds up in amplitude during the satellite's approach toward the station, then suddenly decreases to inaudibility in less than a second. This evolution is accompanied by very rapid, irregular fading. While the satellite recedes from the station the reverse effect is sometimes noted, the signal suddenly increasing from below the noise level to a peak value comparable in amplitude with

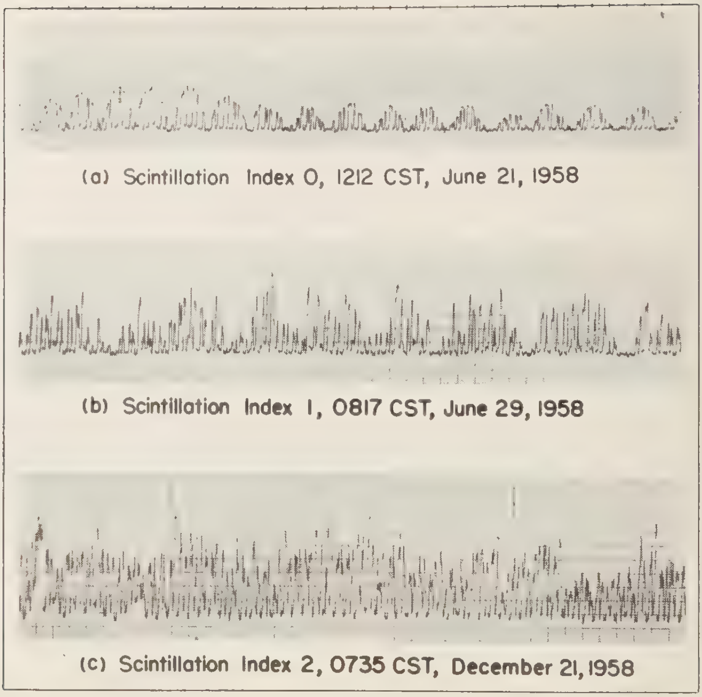

FIG. 1—Examples of satellite signal scintillation. From top to bottom the scintillation indices are spectively 0, 1, and 2. One-second time ticks are shown at the top. 1958δ_2.

signals received from directly overhead. Sometimes two such sudden increases or decreases are observed in less than 4 minutes. As such phenomena are observed only when the satellite is below the height of maximum electron density it is apparent that ionospheric reflections are involved. The sudden changes in signal strength can be explained by skip-distance focusing by the ionosphere. The skip distances for a typical occurrence have been computed using a parabolic model ionosphere and a modification of the formula given by *Rawer* [1948]. The results are illustrated in Figure 3. Curve D_2 gives ground distances, as a function of takeoff angle, over which a satellite signal can be propagated with one reflection from the ionosphere; curve D_1, with one ionospheric reflection and one ground reflection. These curves were computed using electron density profiles furnished by the National Bureau of Standards for the time of the passage illustrated in Figure 2. Both the sudden decreases in signal strength indicated by the minima in these curves were actu observed, at approximately the expected tances.

A particular effort has been made to excl such ionospherically reflected signals from statistical study of scintillation.

Diurnal and seasonal variations—The diu and seasonal variations of radio star scint tion have been discussed extensively and l been summarized by *Booker* [1958]. Maxin incidence of scintillation generally occurs sho after local midnight. A secondary maximun midday has been noted in Australia and Can but not in England. Although the seasonal v ation in England is slight, it is as strong as diurnal variations in Australia.

The diurnal and seasonal variations of s tillation of 20 Mc/s signals from satellite 195 as observed from Urbana, Illinois, are s marized in Figure 4. It should be noted these histograms may be contaminated b number of extraneous influences since, in

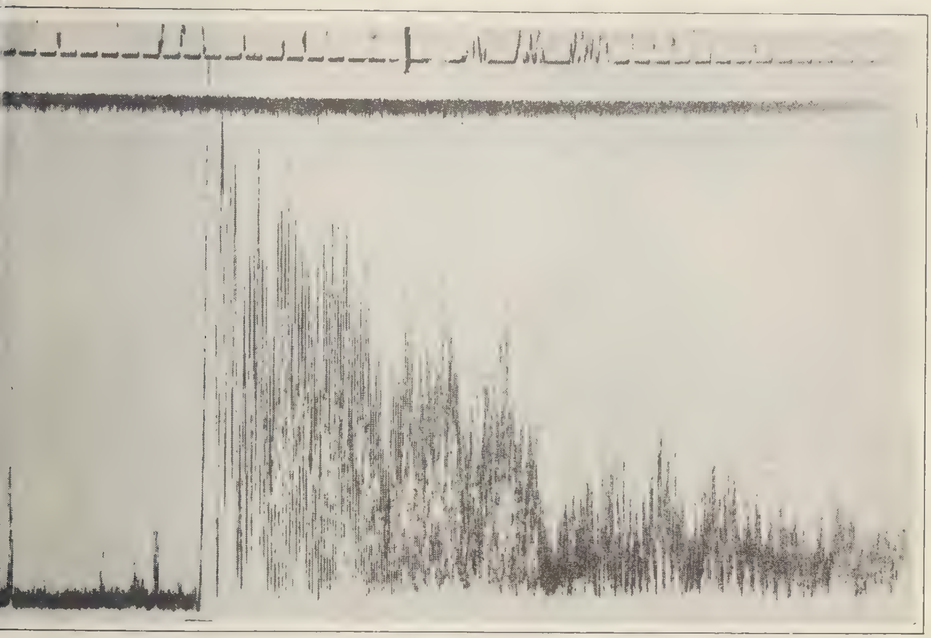

G. 2—Sudden decrease in signal strength at $23^h27^m10^s$ CST, October 13, 1957, for satellite 1957α. Time increasing from right to left. One-second time ticks are shown at the top.

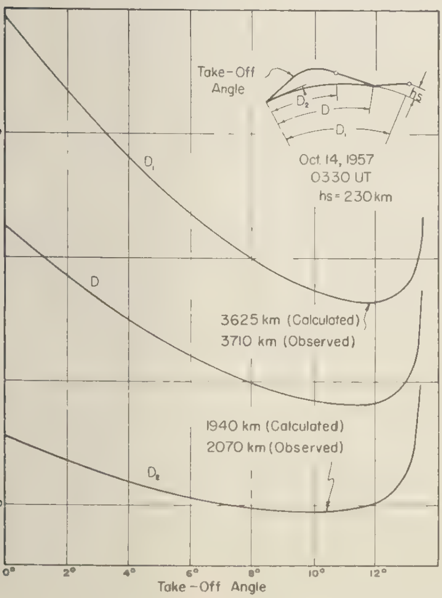

G. 3—Ground distances as a function of take-off angle.

eral, the several observations averaged into each 2-hour interval occurred on successive days. These influences are as follows:

1. There may be successive 'disturbed' or 'quiet' days which may be atypical over a longer averaging-time.

2. It is known that scintillation of radio stars is a function of the zenith angle of the line of sight from the radiator to the observer. The results presented here are averages of signals from all parts of the sky. In many passages transitions from no scintillation to violent scintillation take place in tens of seconds.

3. The histograms include observations of satellites at various heights. Assuming that a satellite may pass either above or below a scintillation-producing region, the apparent incidence of scintillation may be less than the true incidence. The dependence of scintillation upon height is discussed below.

4. During certain periods of observation only a small number of passages was noted. Intervals containing fewer than ten passages are indicated by question marks on the histograms.

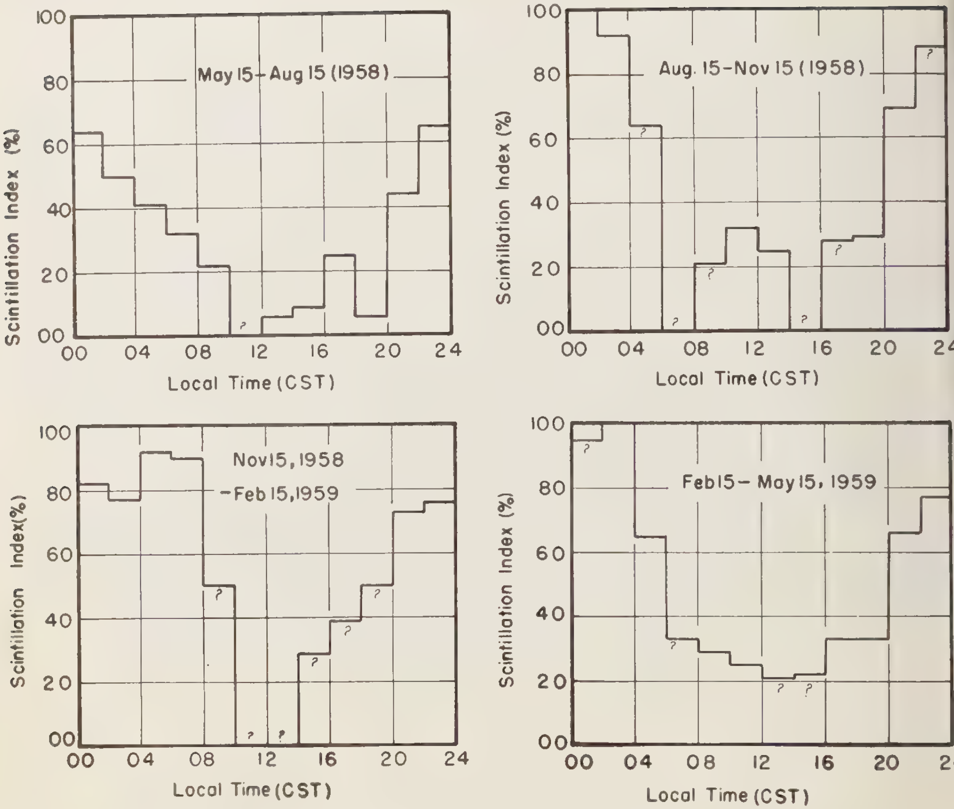

FIG. 4—Diurnal and seasonal variations of 20 Mc/s satellite scintillation. 1958δ_2.

As shown in Figure 4, the night-time maximum has been observed throughout the year. A daytime maximum has also been seen during some seasons. Relatively little seasonal variation has been noted, except that the night-time maximum was comparatively weak during the summer.

During the period May 15 to August 15, 1958, satellite 1958δ_2 was near perigee as it passed over Urbana (40°N latitude) on its northbound passages. The height of perigee was approximately 220 km above the surface of the earth; hence, the reduction in scintillation during this period may have been caused by the low height rather than by seasonal influences. The diurnal variation has been replotted separately for high (above 700 km) and low (200–250 km) passes for the period in question. Figure 5 is the result. Clearly there is much less night-time scintillation for low than high passages, whereas th daytime scintillation is roughly the same fo both heights. It may therefore be inferred tha the inhomogeneities responsible for the nigh time scintillation are near or above 220 km i height. Night passages during September 195 at about 310 km height, were nearly alway accompanied by scintillation, indicating the exis ence of night-time irregularities below abou 300 km. The suggestion is, then, that the in homogeneities responsible for night-time scin tillation lie between about 200 and 300 km.

Geographical locations of irregularities- Scintillation was observed on 20- and 40-Mc/ signals of satellite 1957α_2 (sputnik I) for ever southeastbound (night-time) passage near th University of Illinois. Typically, strong scinti lation was present from the time the satelli rose over the northwestern horizon until

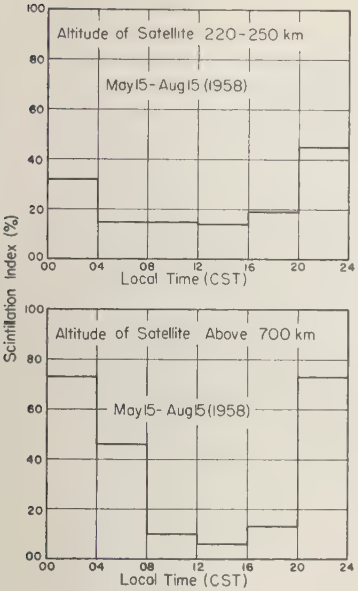

[FI]G. 5—Variation of scintillation with satellite altitude.

[re]ached some point high in the sky. Frequently, [th]en, the scintillation ceased abruptly and regu[la]r Faraday rotation was observed until the [sa]tellite set in the southeast. The subsatellite [lo]cations of these transition points are plotted [in] Figure 6. A typical pass is shown as a line [pa]ssing near Winnipeg and Champaign-Urbana. [T]he points suggest the southern boundary of a [re]gion of ionospheric irregularity extending at [le]ast 15° in latitude. Observation of satellite [1]958δ_2 confirms the existence of this southern [bo]undary for most of the night-time passages; [da]ytime scintillation, however, may be ob[se]rved in any part of the sky.

Scintillation and spread F—A close associa[ti]on of radio star scintillation and 'spread F', as [ob]served on a vertical-incidence sounder, has [be]en remarked by several writers [for example, *[B]riggs*, 1958]. In Figure 6 crosses are used to [de]signate five sounding stations above which [sa]tellites are visible from Champaign-Urbana. [R]ecords made at Urbana of satellite passages [wi]thin 10° of longitude of each of these stations [ha]ve been compared with sounding records in [a]n effort to correlate scintillation with spread [F]. Only one passage was within 10° of Ottawa; [sp]read F was present, as well as scintillation.

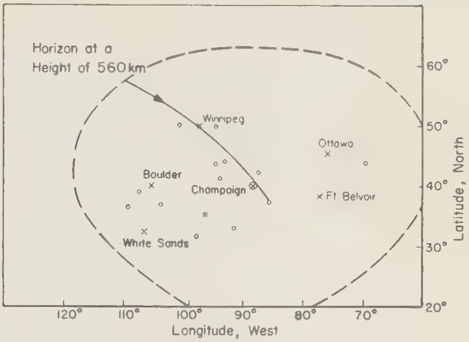

FIG. 6—Subsatellite locations of transitions from scintillation to smooth Faraday fading. Satellite 1957α_2, southeast bound passages.

All nine passages near Winnipeg showed scintillation; spread F was observed in five, polar blackout in two, and normal echoes (neither spread F nor blackout) in two. There appears to be a significant correlation between the occurrences of scintillation and of spread F; unfortunately, only meager data have been available on the occurrence of spread F at the time of recorded satellite passages.

Of the five scintillating passages within 10° of Boulder, spread F was reported in four and no sounding data were available for the fifth. It is interesting to note that for three passages there occurred a transition from scintillation to regular Faraday fading between Boulder and White Sands. In these passages, spread F occurred at Boulder but not at White Sands; this observation is interpreted as support for a definite correlation between scintillation and spread F.

Conclusions—Observation of scintillation of 20-Mc/s satellite signals yields valuable data about ionospheric irregularities. Night-time scintillation originates in a region near 220 km and below 300 km in height and usually north of about 40°N latitude. Daytime scintillation originates in smaller, inhomogeneous patches distributed over wide ranges of latitudes. Seasonal variations of scintillation are slight. Night-time scintillation correlates with spread F as observed on a vertical-incidence sounder.

Acknowledgments—The authors are indebted to their colleagues Dr. E. C. Hayden, Dr. I. R. King, Mr. J. P. McClure, Mr. Victor Gonzales, and Mr. Henri Robe, of the University of Illinois, for their assistance in collecting and analyzing

satellite data. Dr. James Warwick, of the High Altitude Observatory, University of Colorado, very kindly criticized the work and has made his records of 1957α_2 available for inspection. Dr. C. Gordon Little and Mr. Robert S. Lawrence, of CRPL, have made useful suggestions. Ionosphere sounder data were supplied by the National Bureau of Standards and by the Defence Research Telecommunications Establishment of Canada. Satellite orbital data were supplied by the Smithsonian Astrophysical Observatory, the National Aeronautics and Space Administration, and Project Space Track of the U. S. Air Force. The project has been supported financially by the National Science Foundation under Grant Y/32.40/266 of the IGY program.

References

Booker, H. G., The use of radio stars to study irregular refraction of radio waves in the ionosphere, *Proc. IRE, 46,* 298-314, 1958.

Briggs, B. H., The diurnal and seasonal variat of spread *F* ionospheric echoes and scinti tions of a radio star, *J. Atm. and Terrest. Ph 12,* 89–99, 1958.

Browne, I. C., J. E. Evans, and J. K. Hargrea Radio echoes from the moon, *Proc. Phys. S B, 69,* 901, 1956.

Kraus, J. D., and J. S. Albus, A note on so signal characteristics of sputnik I, *Proc. IRE,* 610–611, 1958.

Parthasarathy, R., and G. C. Reid, Sig strength recordings of the satellite 19 (sputnik III) at College, Alaska, *Proc. I 47,* 78–79, 1959.

Rawer, K., Optique géométrique de l'ionosph *Rev. Sci., 86,* 585–600, 1948.

Slee, O. B., Radio scintillations of satellite 19 *Nature, 181,* 1610–1612, 1958.

Warwick, J. W., *IGY satellite rept. series, no* July 30, 1958.

(Manuscript received August 21, 1959.)

Fall-Day Auroral-Zone Atmospheric Structure Measurements from 100 to 188 Km

R. HOROWITZ, H. E. LAGOW, AND J. F. GIULIANI[1]

Goddard Space Flight Center
National Aeronautics and Space Administration
Washington, D. C.

Abstract—The density and pressure of the atmosphere from 100 to 188 km above Fort Churchill, Manitoba, Canada, were determined from the IGY NN 3.15 Aerobee-Hi rocket flight on October 31, 1958, at 2:00 P.M., CST. Two magnetic cold-cathode ionization gages were used to measure pressure and pressure changes on the side of the rolling rocket. Excellent agreement was obtained (*a*) between the two gages throughout flight, and (*b*) between ascent and descent measurements. Measured pressures in the region from 100 to 112.5 km were corrected for a residual gas pressure of approximately 3×10^{-5} mm Hg. An ambient pressure of 10^{-4} mm Hg was obtained at 106 km. The derived pressure of 2.3×10^{-6} mm Hg at 188 km is approximately a factor of 2 lower than the corresponding arctic summer-day value. Densities were measured from 130 to 188 km. The density value of 5.2×10^{-7} g/m^3 at 188 km is approximately 40 per cent lower than the summer-day value. The density profile presented here is in good agreement with the arctic November-day density point obtained at 200 km in 1956. Scale heights (RT/Mg) were derived from the measured pressure and density data vs. altitude, using the hydrostatic equation. The scale-height value obtained at 188 km was 63 km, and the scale-height gradient from 180 to 188 km was 0.5 km/km.

ntroduction—On October 31, 1958, at 2:00 M., CST, Aerobee-Hi rocket NN 3.15F was nched at Fort Churchill, Manitoba, Canada, part of the United States International Geoysical Year rocket program. The rocket was trumented to describe the structure of the nosphere: pressure, density, and scale height, m balloon altitude to peak of flight. Owing the different aerodynamic effects and prese regions involved, the structure experiment s divided into low-altitude and high-altitude asurements. The data shown here give the ucture profile from 100 to 188 km. The lowitude data will be presented separately.

The experiment—The high-altitude structure periment was identical to that flown aboard robee-Hi NN 3.13F and has been described ly by *Horowitz and LaGow* [1958]. Hence, y a brief description of the method and iipment will be given here.

t has been shown [*Havens, Koll, and LaGow,* 52; *Horowitz and Kleitman,* 1953; *Horowitz and LaGow,* 1957] that, when the mean free path of atmospheric molecules is large compared with rocket dimensions, it is possible to use kinetic theory to relate gage pressure to ambient atmospheric pressure and density. Both pressure and density can be measured relatively independently of temperature and average molecular weight of the gas if an absolute pressure gage is mounted on the side of a rapidly rolling rocket having a large angle of attack. Furthermore, ambient density can be determined even in the presence of a residual gas cloud, provided that, on the average, the incoming atmospheric air molecules reach the gage without striking molecules of the gas cloud. Finally, it can be shown that, when the pressure gage is mounted with its axis perpendicular to the axis of the rolling rocket, the ambient atmospheric density is related to the gage pressure by:

$$\rho_a = \Delta P_g/(V_{P_i}\sqrt{\pi}V') \qquad (1)$$

Where

$\rho_a \equiv$ ambient atmospheric density [g/cm^3].

$\Delta P_g \equiv$ change in gage pressure over a roll cycle [dyne/cm^2].

[1] Formerly with the U. S. Naval Research Laboory, Washington, D. C.

V_{P_i} ≡ most probable speed of molecules inside the gage [cm/sec].

V' ≡ maximum velocity ram experienced by the gage during a roll cycle [cm/sec].

Equation 1 can be used if the following conditions exist: (*a*) the pressure inside the gage is low enough so that the mean free path is greater than the gage dimensions; (*b*) the gage mouth is directly exposed to the atmosphere through an orifice; (*c*) the molecules in the upper atmosphere and those leaving the gage have a Maxwellian velocity distribution; (*d*) at any altitude, the average mass of the molecules entering the gage is equal to that of the molecules leaving; (*e*) the rocket's aspect, altitude, and velocity remain essentially constant over a roll cycle.

The two cold cathode magnetic ionization gages had a usable range from 10^{-3} to $\approx 2 \times 10^{-7}$ mm Hg [*Backus*, 1949]. These sensors consisted of a small external magnet with a central rectangular loop of wire for the anode, and were mounted 180° apart on the cylindrical part of the rocket. The 35-cm^3 gage volume was exposed to the atmosphere through a 1-cm-diameter orifice.

The flight gages were calibrated against hot-cathode ionization gages which were checked against a McLeod gage. A typical flight-gage calibration curve is shown in Figure 1. The scatter in the experimental calibration curve increases as the pressure is decreased, reaching a value of 15 per cent at 5×10^{-6} mm Hg and 30 per cent at 7×10^{-7} mm Hg.

Figure 2 shows the gage circuit. A 3000-volt supply was connected in series with the gage and a set of resistors. The a-c voltages out of the medium- and high-gain circuits were proportional to the a-c pressure change in the gage and were in phase with the roll of the rocket. Four neon tubes protected the high-gain cathode follower during heavy gage discharge. The low-gain and direct outputs provided the d-c pressure measurements.

Experimental data—All gage data were obtained via telemetering. In the telemetering system used in this rocket [*Best and others*, 1952] all channels were calibrated sequentially at intervals of 16 seconds by five 1-volt steps applied to the data channel inputs. The stability

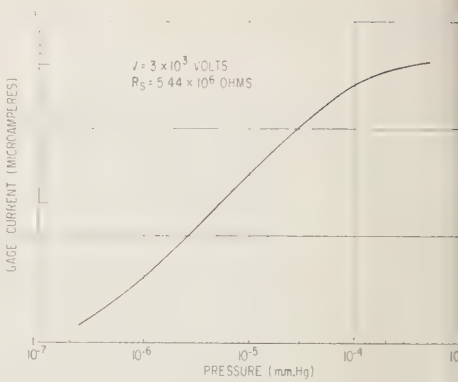

FIG. 1—Typical Philips gage calibration curve.

of the system, together with the calibration made it possible to read absolute voltages wit an error of less than 0.05 volt, and voltag changes occurring in a few seconds with an er ror of less than 0.01 volt.

The Aerobee-Hi NN 3.15F rocket reached a altitude of 188 km 231.7 seconds after takeo Its south and east velocities were measured t be 87 m/sec and 270 m/sec, respectively, an remained essentially constant throughout th portion of flight of interest. The rocket's att tude variation was determined by means o sun, horizon, and magnetic-field detector Viewed from above, the rocket rolled and pr cessed in a counterclockwise direction. In th region where these measurements were mad the rocket roll rate was ~1.6 cps, and the pr cession rate was ~88.2 seconds. The angul momentum vector made an angle of 14° wi the vertical and was 44° east of south. The d ameter of the precession cone was 33°. At 14 seconds, the rocket axis was 31° from the vert cal and 50° east of south.

Figure 3 is a plot of the gages' dc pressur in millimeters of mercury as a function of tin of flight in seconds. For convenience, the tw flight gages were denoted as PGN and PGS. Th asymmetry between ascent and descent ga pressure, noted on previous flights, is attribut to outgassing of metal parts and to gas escapi from the rocket. The straight lines at the e tremities of the curve represent the best es mate of the residual gas pressure as a functi of time.

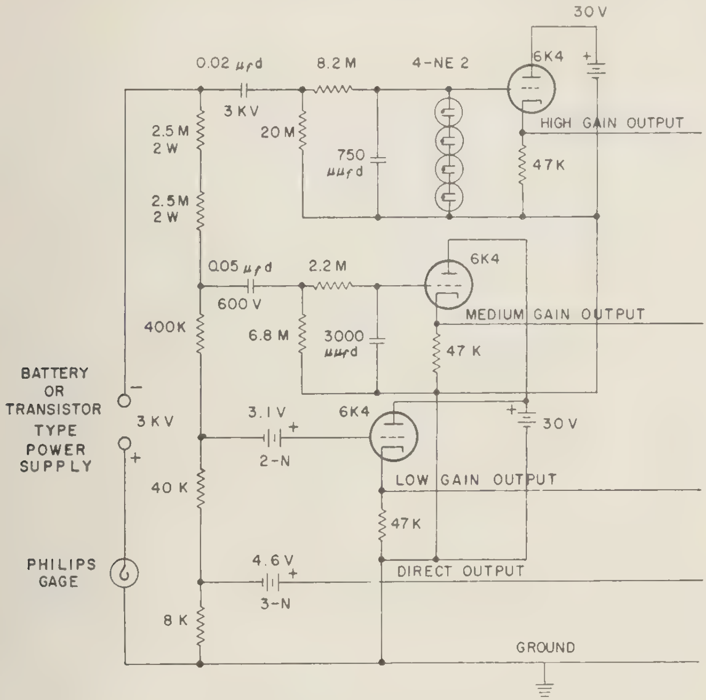

Fig. 2—Schematic of gage circuit.

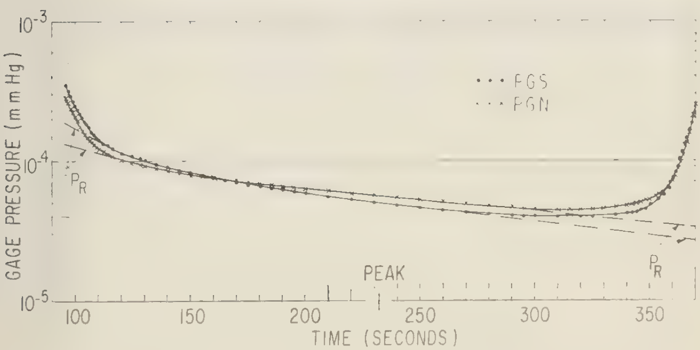

Fig. 3—D-c gage pressures vs. time of flight.

As the rocket rolled, the pressure gages re-rded a-c signals corresponding to the change gage pressure over a roll cycle. Figure 4 ows the measured peak-to-peak change in gage essure in millimeters of mercury as a function time of flight in seconds. Since the gage sig-ls are recorded continuously, data points were obtained for each roll cycle, but, for simplicity, they were not shown that often. The medium-gain outputs were used, since the high-gain channels remained saturated throughout flight, except for short intervals at 150 seconds and at peak. Two important observations should be made about Figure 4:

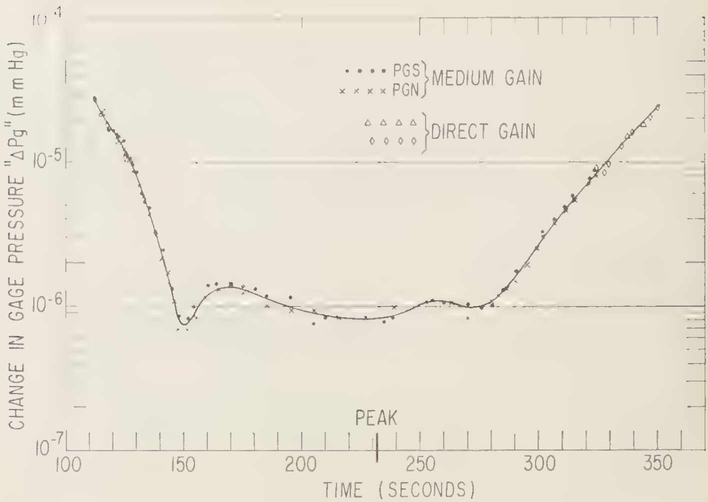

Fig. 4—Variation in gage pressure (ΔP_g) vs. time of flight.

1. Agreement between the roll signals from the two gages is better than 30 per cent throughout flight. Hence, an average curve (solid line) can be taken as representative of ΔP_g vs. time, with an error between this curve and measured points of less than 15 per cent. Therefore, in subsequent discussion of atmospheric density measurements, emphasis will be placed on comparing ascent with descent data. It should be understood, however, that every ascent or descent density datum point represents two independent measurements agreeing with this value to ~15 per cent.

2. The pressure changes, ΔP_g, obtained from the medium-gain a-c coupled circuits are in good agreement with those from the direct outputs. From Figure 2 it is seen that the direct output is just a voltage developed across a known resistor.

Analysis of data—Figure 5 shows atmospheric pressure in millimeters of mercury plotted against altitude in kilometers. Atmospheric pressure values were obtained from gage pressure by subtracting the residual gas pressure; see Figure 3. No correction was necessary for velocity ram, since theory shows [*Horowitz and LaGow*, 1957] that, in the altitude region of interest and for the given gage orientation, gage pressure readings at points displaced 90° in roll from the maximum pressure are true am-

bient pressures, except for thermal transp
tion effects, which were negligible for
temperatures involved. Hence, these amb
pressure measurements are independent of
attitude of the rocket. The scatter in exp
mental points is less than 20 per cent, and
of it is due to the error involved in subtrac
the residual pressure. In fact, the apparent
rate of change of the residual gas at about
seconds makes the determination of the cor
residual pressure uncertain at this time. He
the ascent pressure points should be taken a
indication that, if the residual gas on ascer
estimated in the usual way, agreement is
tained between ascent and descent data. H
ever, the pressure data stand primarily on
good agreement obtained between two i
pendent gages on descent. Above 112.5 km,
pressure curve is based on measured dens
and computed scale heights described be
The Fort Churchill summer-day values m
ured in July 1957 are shown for comparison
the 100- to 125-km region the pressure pro
are seen to differ by less than 30 per c
whereas at 185 km the summer-day value
factor of 2 higher than the corresponding
day value.

Figure 6 is a plot of atmospheric densit
grams per cubic meter as a function of alti
in kilometers. The measured density values f

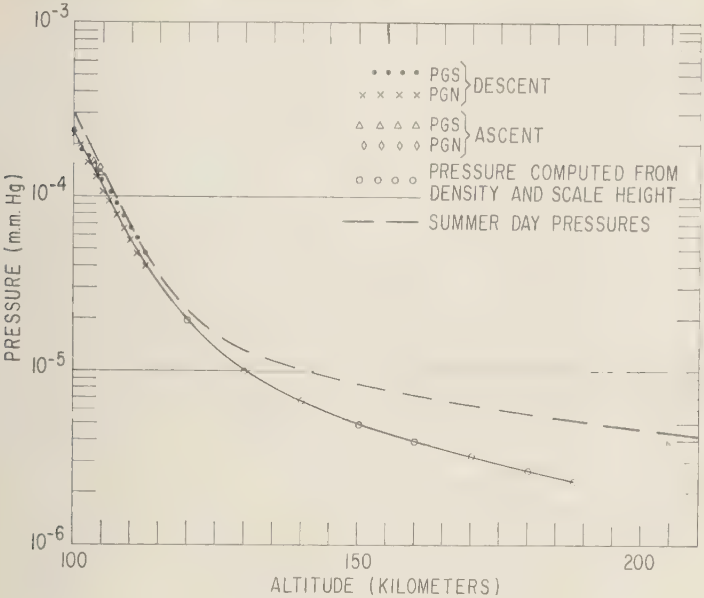

FIG. 5—Pressure vs. altitude.

) to 188 km were obtained from the change gage pressure by means of equation 1. Hence, determination of these density values was ependent of the ambient atmospheric temature. Good agreement was obtained between measured ascent and descent density values h less than 20 per cent scatter between the erimental points. On this flight, density ues from 100 to 130 km were not reduced m the recorded gage pressure changes bese of the increased error in both ΔP_g and the nputed velocity ram into the gage. Instead, lower-altitude density values were obtained m the measured pressure profile. The density ve was then drawn through the computed l experimental points. The authors instrunted Aerobee-Hi NN 3.12F for a daytime ng at Fort Churchill to check out, among er equipment, their IGY high-altitude atspheric structure experiment. The rocket was nched in November 1956, and became unble after about 80 seconds, when it went into at spin. However, the authors were able to ain the peak density value [*LaGow, Horoz, and Ainsworth*, 1958] shown in Figure 6 density profile obtained here 2 years later agrees with this single density point. The summer-day density profile is also shown in Figure 6 for comparison. In the region from 105 to 160 km the difference between the two profiles is less than 20 per cent, whereas at 188 km the summer-day value is about 60 per cent higher than the corresponding fall-day value.

Scale height (RT/Mg) in kilometers vs. altitude in kilometers is shown in Figure 7. The scale-height values were computed from the density vs. altitude curve, using the equation

$$\rho_1/\rho_2 = H_2/H_1 \cdot \exp - [2(h_1 - h_2)/(H_1 + H_2)] \qquad (2)$$

where h_1 and h_2 are altitudes in kilometers, H_1 is the scale height at h_1, ρ_1 is the density at h_1, H_2 is the scale height at h_2, and ρ_2 is the density at h_2. ρ_1, ρ_2, h_1, and h_2 are known. The value for H_1 was taken from the measured atmospheric pressure data; hence H_2 could be computed. To use equation 2 it must be assumed that electrical, magnetic, and tidal forces are small compared with the gravitational force, so that the hydrostatic equation is valid. At 120 km there was a marked increase in the scale-height gradient,

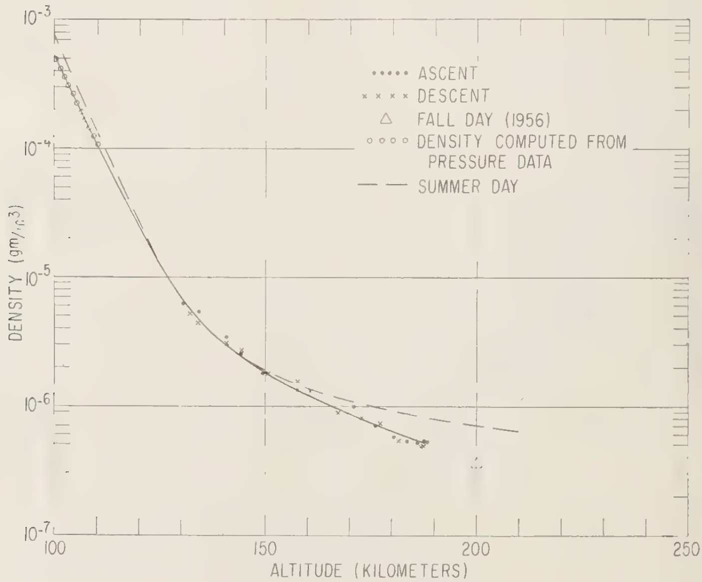

FIG. 6—Density vs. altitude.

which reached a maximum value of 1 km/km. The scale-height value at 188 km was 63 km, and the gradient was ~0.5 km/km. The summer-day scale-height profile is shown for comparison.

Discussion of errors—The accuracy of the pressure data depends upon the following factors:

(*a*) The pressure gage calibration: The pressure standard used during gage calibration had an accuracy better than 10 per cent. The maximum scatter between calibration points down to the minimum gage pressure recorded in flight was less than 15 per cent. Hence, any error in the pressure value due to gage calibration is less than 15 per cent.

(*b*) Location of the ambient pressure points during a roll cycle: For each roll cycle, two ambient pressure points exist, one 90° in roll earlier, the other 90° in roll later, than the maximum ram position. Over a roll cycle, both ambient points agreed to better than ±5 per cent. Hence, errors in pressure values due to locating ambient pressure points are less than 10 per cent.

(*c*) Correction for residual gas pressure: From Figure 3 it is seen that the slopes of residual gas curves are determined on desc where the residual pressures are ~3 × 10^{-5} Hg. Hence, for the descent pressure data u the residual gas should not have introduce error greater than 15 per cent. From the analysis of the authors' remaining IGY ro NN 3.14F, which was fired in the arctic wi at midnight, and contained open and prese hot- and cold-cathode ionization gages, it pears that presealing the pressure gage at uum and opening it at high altitude reduces observed residual gage pressure by at least order of magnitude.

It is concluded from the above that the m ured ambient pressure values are accurate to ter than ±20 per cent.

The accuracy of the density data dep upon the following factors:

(*a*) The a-c gage sensitivity: This quan is determined from the slope of the d-c pres calibration curve, which is known to ±20 cent. Furthermore, it should be noted that a-c gage sensitivity varies with gage press see Figure 1. The agreement between ascent descent density values at times when the

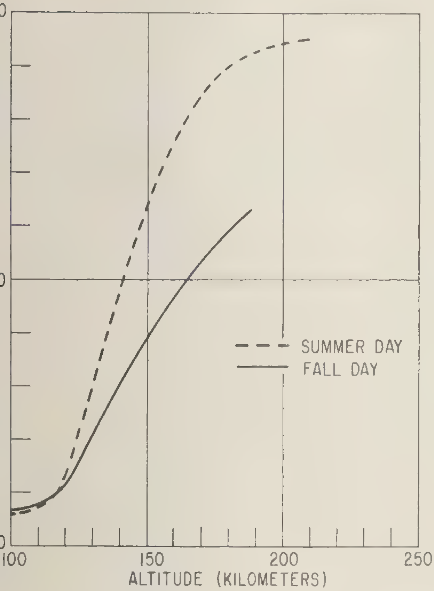

FIG. 7—Scale height vs. altitude.

ssures were different indicates that the a-c sitivity values taken from the d-c calibration ve were proper.

b) Medium-gain circuit sensitivity: From previous discussion in connection with Fig- 4, it was concluded that no significant error sted in the a-c circuit factor used to obtain sity values.

c) Trajectory and aspect: The peak time ue given by radar was independently checked h impact pressures at the lower altitudes, l good agreement was obtained. The rocket pact point was in good agreement with the izontal velocities supplied by radar and VAP. Hence, it is believed that errors in tra- tory data could not affect the plotted density a by more than 10 per cent. Likewise, errors aspect should cause errors in density of less n ±10 per cent. Only pressure changes hav- proper phase relations associated with them re used to obtain the density data.

d) Atmospheric winds: Since the proper se was obtained between the pressure-gage signal and the solar aspect detector signal, l since good agreement was obtained between ent and descent density values, it is concluded that the error in the density values due to atmospheric wind is less than ±10 per cent.

(*e*) Gas composition: A study of the response of the Philips gage to different gases [*Foote*, 1944] showed that, if the gage sensitivity to air ($M = 28.9$) is 1.0, the gage sensitivity to nitrogen and oxygen is ~1.0, to hydrogen 0.55, and to water vapor 1.45. It appears that the maximum composition error could be 50 per cent. For the different assumed gas-composition values at the altitudes involved, however, the error due to atmospheric composition affecting the gage is probably less than 10 per cent.

It should be noted that atmospheric composition affects the density values obtained from the roll pressure signals. This is due to the term $V_{P_i} \equiv$ the most probable speed of molecules inside the gage, which appears in equation 1, relating gage pressure roll signal to atmospheric density. Since

$$V_{P_i} \equiv (2RT/M)^{1/2}$$

the density value is proportional to the square root of the assumed mean molecular mass. For the data presented here, M was assumed to be $= 23.8$. It is seen, however, that values of M from 28 to 20 can introduce errors in the computed density of less than 10 per cent.

It is concluded that, at the altitudes involved, density errors due to gas composition are less than 10 per cent.

(*f*) Incoming charged particles: From the mode of operation of the cold-cathode ionization gage, and from the response of flight ionization gages having ion traps, it is concluded that any error in density due to ions entering the gage is less than 5 per cent.

(*g*) Gas interference: This is included for completeness, since a residual pressure above ambient was detected, and therefore the possibility exists that interference took place, although there is no experimental evidence that the incoming atmospheric molecules were interfered with. Furthermore, it is unreasonable to expect gas interference to affect both gages in exactly the same way. Therefore, if an error exists in the density values due to gas interference, it is probably negligible.

In view of what has been presented, the authors believe that the density values have a maximum error of ±30 per cent.

TABLE 1—*Atmospheric pressure, density, temperature, and scale height*

Altitude, km	Pressure, mm Hg	Density, g/m³	Scale height, km	Temperature, °K for M = 28
100	2.4×10^{-4}	4.9×10^{-4}	6.7	220
110	5.9×10^{-5}	1.1×10^{-4}	7.7	250
120	1.9×10^{-5}	2.5×10^{-5}	11	360
130	9.8×10^{-6}	6.7×10^{-6}	21	690
140	6.6	3.0	31	1010
150	4.9	1.8	39	1270
160	3.9	1.2×10^{-6}	46	1500
170	3.2	8.6×10^{-7}	53	1710
180	2.6	6.4	59	1910
188	2.3×10^{-6}	5.2×10^{-7}	63	2010

Discussion of results—Table 1 summarizes the data. Atmospheric temperatures in degrees Kelvin were computed from scale-height values on the assumption that the gram-molecular weight of the air was equal to 28.9 and remained constant up to 188 km. Temperatures corresponding to other assumed molecular weights can readily be obtained from the values given here simply by multiplying the value given by the ratio of assumed molecular weight to 28.9.

The following observations can be made:

(*a*) At 100 km the atmospheric pressure is 2.4×10^{-4} mm Hg, the density is 4.9×10^{-4} g/m³, and the scale-height value is 6.7 km. The corresponding atmospheric temperature is about 220°K.

(*b*) At 120 km there is a significant increase in the scale-height gradient, which reaches a maximum value of 1 km/km, and starts to decrease at about 150 km. Hence, in the region between 120 and 145 km, there exists a significant heat source, or rapid change in gas composition, or both. The scale-height value obtained at 150 km is 39 km, corresponding to temperatures in the range ~1000° to 1250°K.

(*c*) At 188 km the atmosphere is comparatively hot and dense. The scale-height value of 63 km indicates temperatures between 1500° and 2000°K.

The authors have not followed the usual practice of displaying the error flags along with the measured data points in order to keep the semilog data graphs reasonably clear after they are compressed for publication. Instead, they have stated the accuracy of their measurements. If error flags for the data shown in Figure and 6 were constructed for both summer fall, a region of overlap would be observed tween the measured pressure data in the 1 to 112.5-km region, and between the measu densities in the region from 130 to about km. Hence, the possibility exists that the d time structure of the atmosphere in these gions is essentially the same during fall summer.

Acknowledgments—The authors wish to exp their appreciation to the U. S. National Comr tee for the International Geophysical Year, Canada, and to the U. S. Army, Navy, and Force, all of whom made possible the IGY fi at Fort Churchill. Thanks are due to the ra and DOVAP tracking crews, who supplied ex lent data. The authors wish to thank Mr. J. A worth for his trajectory analysis and for his ch of impact pressure peak time. Finally, they v to extend particular thanks to Mr. H. B. Ben who developed the electronic instrumentation who also greatly assisted the authors in field che outs before rocket launching.

REFERENCES

BACKUS, J., *Theory and Operation of a Phi Ionization Gage Type Discharge, Characteris of Electrical Discharges,* edited by Guthrie Wakerling, McGraw-Hill Book Co., New Y pp. 345–369, 1949.

BEST, N., AND OTHERS, The AN/DKT-7 15 char PPM telemetering transmitter, *U. S. Naval search Lab. Rept. 4016,* 1952.

FOOTE, L. R., Effect of different gases on Phi gages, *Univ. Calif. Radiation Lab., AECD 2* 1944.

HAVENS, R. J., R. T. KOLL, AND H. E. LAGOW, pressure, density, and temperature of the ear

mosphere to 160 kilometers, *J. Geophys. Research, 57*, 62, 1952.
owitz, R., and D. Kleitman, A method for determining density in the upper atmosphere uring rocket flight, *U. S. Naval Research Lab. ept. 4246*, 1953.
owitz, R., and H. E. LaGow, Upper air pressure and density measurements from 90 to 220 ilometers with the Viking 7 rocket, *J. Geophys. esearch, 62*, 57, 1957.
Horowitz, R., and H. E. LaGow, Summer-day auroral-zone atmospheric-structure measurements from 100 to 210 kilometers, *J. Geophys. Research, 63*, 757, 1958.
LaGow, H. E., R. Horowitz, and J. Ainsworth, Arctic atmospheric structure to 250 kilometers, *IGY Rocket Rept. Ser. 1*, National Academy of Sciences, pp. 38–46, 1958.

(Manuscript received August 27, 1959.)

Effects of Pi Meson Decay-Absorption Phenomena on the High-Energy Mu Meson Zenithal Variation near Sea Level[1]

J. A. Smith and N. M. Duller

Department of Physics
University of Missouri
Columbia, Missouri

Abstract—An approximate calculation of the ground-level high-energy mu meson intensities is presented, with curves showing peculiar maxima in the angular vicinity from about 55° to 75° with respect to the vertical at ground-level energies from about 60 bev to 160 bev. The effects are explained in terms of well known pi meson decay-absorption phenomena high in the earth's atmosphere.

Introduction—Recent cosmic-ray experiments ave produced direct evidence that there are ignificantly more mu mesons of very high enrgy incident at large zenith angles than from he vertical direction [*Moroney and Parry,* 954; *Roe and Ozaki,* 1959]. This increase in itensity with zenith angle is in distinct contrast vith the well known variation of the total mu ieson intensity near sea level, which is approxiiately proportional to the square of the cosine f the zenith angle. The purpose of the present aper is to present the numerical results of an pproximate theoretical calculation showing deails of the zenith-angle dependence of the differential and integral intensities of high-energy osmic-ray mu mesons at a depth of 1000 g/cm^2 n the earth's atmosphere.

Although a great amount of theoretical and xperimental work has been done on the general roblem of the cosmic-ray secondary cascades, ery little public attention has been paid to the letailed and explicit forms of the high-energy round-level mu meson zenithal variations. *Buini and Moliere* [1953, 1954] discuss the exonent n in the $\cos^n\theta$ relation for the integral au meson intensity, showing theoretically that becomes negative in the region of mu meson nergies near 100 bev. The definitive work of *Barrett and others* [1952] presents a clear exlanation of the high-altitude decay-absorption phenomena of the parent particles giving rise to mu mesons. The work of many others is mentioned later in context.

The diffusion equation—As in much of the previous work, the now familiar pi meson diffusion equation forms the basis of our investigation. For one familiar with the literature on this general subject, some of the immediate presentation will contain few surprises. (See especially *Barrett and others,* 1952; and *Murayama and others,* 1955.) However, for the purpose of self-containment and convenience in the discussion of the physical causes of the anomalous effects and to permit a sufficiently detailed catalog of the physical approximations used, it is important to review briefly a conventional program of the intensity calculations.

The diffusion equation for pi mesons in the earth's atmosphere expresses the change of the intensity of pi mesons as the difference between the number produced in a thin layer of the atmosphere and the number removed by both absorption and decay in flight in this thin layer. In notation to be defined, it may be written as follows:

$$\frac{dN_\pi}{dy} = \frac{AE_\pi^{-k}}{\cos\theta}\exp\left(\frac{-y}{\lambda_P\cos\theta}\right) - \frac{N_\pi}{\cos\theta}\left[\frac{1}{\lambda_\pi} + \frac{m_\pi c}{\rho(y)\tau_0 E_\pi}\right] \tag{1}$$

In this equation, N_π is a function of E_π, y, and θ, all variables identified by the fact that $N_\pi(E_\pi, y, \theta)\, dE_\pi\, d\Omega$ is meant to be the number

[1] Supported in part by the Research Corporaion, the Alfred P. Sloan Foundation, and US/IGY Project 2.24 of the National Academy of Sciences nd the National Science Foundation.

of pi mesons per second and per square centimeter with kinetic energy E_π in dE_π at vertical atmospheric depth y in grams per square centimeter traveling within solid angle $d\Omega$ at zenith angle θ.

The production factor $AE_\pi^{-k} \exp(-y/\lambda_P \cos\theta)$ is meant to be the increase in N_π produced per gram per square centimeter of atmosphere by the primary nucleons and their energetic n-component progeny, the exponential attenuation of which is controlled by the absorption mean free path λ_P. The derivation of this expression assumes a constant average multiplicity of pi mesons and also assumes that these mesons get a constant average fraction of the producing nucleon kinetic energy. The result is a pi meson differential energy spectrum at production with the same exponent (k) as that assumed for the primary spectrum. The factor A contains the multiplicity and energy partition proportionality parameters, which undoubtedly vary at least slowly with the incident energy [*Ishikawa and Maeda*, 1958; *Kaneko and Okazaki*, 1958] but here are tacitly held constant. It is assumed further that the forward direction of the producing particle is always maintained by the high-energy particles it generates.

The absorption term includes the physically important high-energy pi meson absorption mean free path, λ_π (as opposed to the interaction mean free path), which takes implicit account of the production and propagation of high-energy pi mesons resulting from interactions of other pi mesons with nuclei of the atmosphere.

The decay term includes $\rho(y)$, the density of the atmosphere in grams per cubic centimeter at depth y; m_π, the rest mass of the pi meson (assumed to be 140 Mev/c^2); τ_0, the proper mean lifetime of the pi meson (assumed to be 2.55×10^{-8} sec); and c, the velocity of light. This term arises from the usual radioactive decay relationship giving the number of pi mesons decaying in flight in time dt: $N_\pi\, dt/\tau$. Here τ is the dilated mean lifetime of the pi meson as observed in the laboratory frame of reference. The intervals dt and τ are replaced, respectively, by $dy/c\rho(y) \cos\theta$ and $\tau_0 E_\pi/m_\pi c^2$ because the kinetic energy E_π is always much larger than $m_\pi c^2$ for particles of interest in this discussion.

Before a solution to the diffusion equation can be found one must choose k in the production term and assume a suitable dependence for ρ on atmospheric depth. Usually k is chos between about 2.6 and 3.0. For the prese calculation we will use $k = 8/3$ [*Neher*, 19 *Puppi and Dallaporta*, 1952; *Greisen*, 195 The isothermal atmosphere in which $\rho = \rho_0 y$ is a convenient approximation which can modified slightly at various depths to gi reasonable accuracy. The symbols ρ_0 and refer to ground level and are taken to be 0.001 g/cm³ and 1000 g/cm², respectively.

With the above assumptions and the conditi that $N_\pi = 0$ at $y = 0$, one readily finds t solution:

$$N_\pi(E_\pi, y, \theta) = \frac{AE_\pi^{-8/3} y \exp(-y/\lambda_\pi \cos}{\cos\theta}$$

$$\cdot \sum_{n=0}^{n=\infty} \left(\frac{y}{\lambda' \cos\theta}\right)^n \left[n!\left(n+1+\frac{bj_\pi}{E_\pi \cos\theta}\right)\right]^{-1} \quad ($$

Here, $1/\lambda' = 1/\lambda_\pi - 1/\lambda_P$ and $j_\pi = m_\pi y_0 c/\tau$

The quantity $b = 0.771$ has been included order to improve the approximation introduc by assuming the isothermal atmosphere. T scale height y_0/ρ_0 is clearly too large for calcu tions related to phenomena occurring very hi in a real atmosphere. (See *Rossi*, 1952, Appen VI.) We therefore have replaced y_0/ρ_0 by by_0 such that

$$by_0/\rho_0 = RT_e/(Mg) \quad ($$

The 'effective temperature' T_e for the atmosph above Columbia, Missouri, is calculated the approximate method suggested by *Bar and others* [1952] from data supplied by t United States Weather Bureau. In (3), R is t gas constant, M is the effective molecular wei of air, and g is the acceleration due to gravi The chosen value of b is found from (3) af the calculated temperature $T_e = 220$°K introduced.

In this work we arbitrarily omit the co plications that arise in considering the contri tions to the high-energy mu meson flux from t decay of heavy mesons by taking into acco only the pi mesons produced directly in nucl interactions. The problem of the relative i portance of heavy mesons and directly produ pi mesons as parents of high-energy cosmic- mu mesons has been discussed by several auth [*Barrett and others*, 1952, 1954; *Budini a*

oliere, 1953, 1954; *Sherman*, 1954; *Avan and van*, 1955; *Sreekantan and others*, 1956; *akeman*, 1956; *Randall and Hazen*, 1958].

The evidence on the relative frequency of roduction of pi mesons and heavy mesons ppears to indicate that at the high energies of terest in the present context roughly equal umbers of pi mesons and K mesons are produced *al and others*, 1954; *Franzinetti and Morpurgo*, 957]. It seems inevitable, therefore, that heavy eson processes must be included in any comete description of the decay-absorption cometition effects which give rise to the anomalous nithal variations of energetic mu mesons. ome of the complications and uncertainties that ise in such a description were discussed by *arrett and others* [1952]. Since their work was ublished much has been learned about the heavy eson species, but the difficulties that remain e still appreciable. In principle, at least, it easy to see that, at sufficiently high energy, mospheric decay-absorption phenomena of all eavy mesons whose direct decay products clude mu mesons should play a role similar that of the pi mesons. For other species .g., the K_π) there is an extra decay. Assuming at the absorption mean free path for energetic eavy mesons is not very different from that of e pi mesons, it appears that the larger ratio of st mass to lifetime would suppress only slightly e K meson competition effects, which must arallel almost exactly the pi meson phenomena f the present development.

The differential intensities—The formal exression for the mu meson intensity at ground vel (depth y_0) from the decay of pi mesons of nergy E_π in dE_π is

$$(E_\pi, \theta) = \int_0^{y_0} P_\mu(E_\pi, y, \theta) N_\pi(E_\pi, y, \theta) \frac{dt}{dy} \frac{dy}{\tau} \quad (4)$$

he function $P_\mu(E_\pi, y, \theta)$ is the probability of urvival to ground level (i.e., probability of ot decaying before reaching ground level) for mu meson resulting from the decay of a pi eson at depth y moving in direction θ with nergy E_π.

Various approximate forms of this survival robability are used here, but for convenience nd simplicity they will all be denoted by P_μ. An accurate expression is

$$P_\mu = [yE_\mu/(y_0E_\mu^*)]^{B_\mu/(E_\mu' \cos\theta)} \quad (5)$$

(See *Rossi*, 1952, p. 157.) Here,

$$B_\mu = b_\mu m_\mu y_0 c/\tau_{\mu_0}\rho_0$$

E_μ is the energy of the mu meson at the depth y_0; E_μ^* is the mu meson energy at y; and E_μ' is the energy the mu meson would have had at the top of the atmosphere. Once again the approximation of the isothermal atmosphere has been improved by modification of the scale height for a particular process. In B_μ, y_0/ρ_0 has been replaced by $b_\mu y_0/\rho_0$, with $b_\mu = 0.80$ to correspond to the temperature about halfway to the top of the atmosphere in linear units. The proper mean lifetime of the mu meson is denoted by τ_{μ_0} (assumed to be 2.22×10^{-6} sec).

In the calculation of $f(E_\pi, \theta)$, specific assumptions about the energy losses of the mesons must be used to relate E_μ, E_μ^*, and E_μ' functionally. The results of these assumptions will also be used in transforming from high-altitude pi meson energy (E_π) to ground-level mu meson energy (E_μ) in an approximate way. We assume that $\cos\theta\, dE/dy \equiv a = 2.5$ Mev per g/cm² (the density effect being less important here than in *George*, 1952) and that when a pi meson of energy E_π decays it gives rise to a mu meson of approximate average energy $E_\mu^* = rE_\pi = 0.76E_\pi$ in the same direction as the motion of the pi meson. By the second assumption we are also constraining the depth y to be the depth of origin of the mu meson for the integration of (4). Then,

$$E_\pi = \frac{E_\mu^*}{r} = \frac{1}{r}[E_\mu + a(y_0 - y)\sec\theta] \quad (6)$$

and

$$P_\mu = \left\{\frac{y}{y_0}\left[1 - \frac{a(y_0 - y)\sec\theta}{rE_\pi}\right]\right\}^{B_\mu/(rE_\pi\cos\theta + ay)} \quad (7)$$

With this form of P_μ substituted into (4), one must integrate numerically to find $f(E_\pi, \theta)$. In order to keep the explicit variables and parameters in the result, however, it is convenient to remove P_μ from the integration over depth by assuming an appropriate average value of $y/\cos\theta$ for the appearance of the mu mesons. This is a fairly good approximation

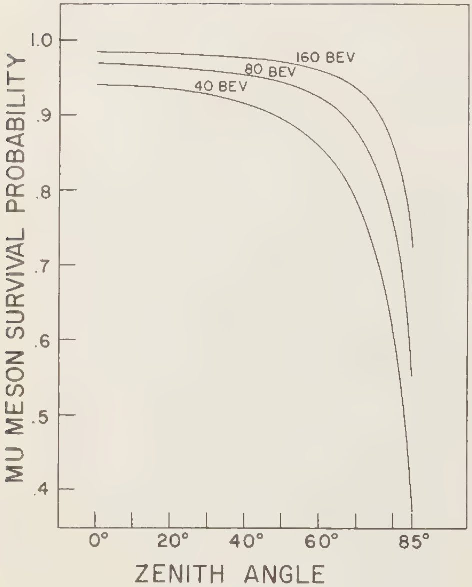

FIG. 1—Plots of P_μ vs. zenith angle θ as expressed in equation 9.

because at high energies P_μ varies slowly with $y/\cos\theta$ except at very large zenith angles. (Beyond 80° our flat atmosphere is a poor approximation to the actual curved atmosphere anyway.) With the choice of $(y/\cos\theta)_{\text{average}} = 100$ g/cm², we have

$$E_\pi = [1/r][E_\mu + ay_0(\sec\theta - 0.100)] \tag{8}$$

and

$$P_\mu = \left\{0.100 \cos\theta \cdot \left(1 - \frac{a(y_0 \sec\theta - 100)}{rE_\pi}\right)\right\}^{B_\mu/[(rE_\pi+100a)\cos\theta]} \tag{9}$$

Figure 1 shows how this form of P_μ varies with energy and zenith angle.

Insignificant error is introduced by integrating to $y = \infty$ instead of $y = y_0$, and the simplification of the resulting expression is helpful. We then have

$$f(E_\pi, \theta) = \frac{AE_\pi^{-11/3}P_\mu\lambda_\pi bj_\pi}{\cos\theta} \cdot \sum_{n=0}^{n=\infty}\left(\frac{\lambda_P - \lambda_\pi}{\lambda_P}\right)^n\left(n + 1 + \frac{bj_\pi}{E_\pi\cos\theta}\right)^{-1} \tag{10}$$

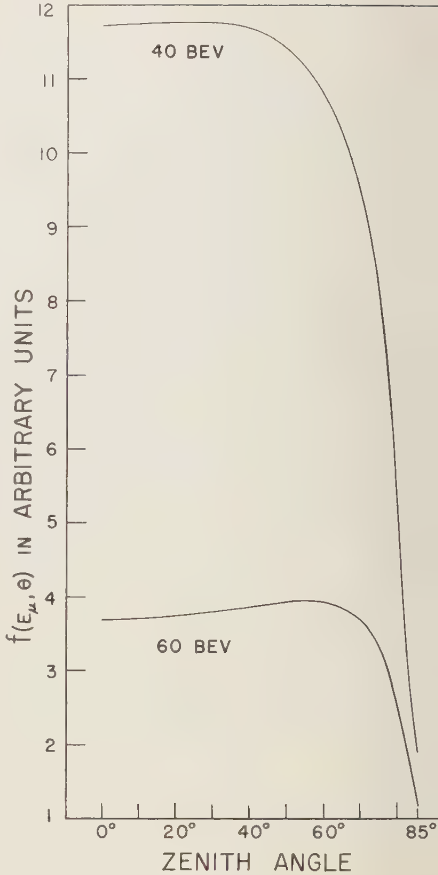

FIG. 2—The differential directional intensity mu mesons at ground-level energies 40 and bev. The curves of Figures 2 to 6 are in arbitr units on the ordinate but are mutually normali

Substitution of (8) into (10) gives the ferential mu meson intensity at ground leve terms of the ground-level mu meson ene This result will be denoted by $f(E_\mu, \theta)$.

In a paper to appear later the authors prop to discuss the effects of different assumed m free paths on the high-energy mu meson in sities. It appears well established that λ_P rem essentially constant near 120 g/cm² even very high energies [*Farrow*, 1957]. On the o hand, the value of λ_π has been the subjec considerable controversy. Some authors h argued theoretically for $\lambda_\pi \simeq \lambda_P/2$ [*Hayak*

d others, 1955; *Murayama and others*, 1955]. efall has adduced evidence from atmospheric ects that $\lambda_P < \lambda_\pi \leq 2\lambda_P$ [*Trefall*, 1955, 1957]. o direct measurements have been made at ry high energies. Anticipating the results of r calculations assuming different (but con- ant) values of λ_π, we can say that, as expected, creasing the value of λ_π has qualitatively the me effect on the curves as increasing the energy: e intensities are decreased, and the maxima in e curves are moved to larger zenith angles. e qualitative character of the curves, however, essentially unchanged with λ_π in the range g/cm² — 240 g/cm². Because the assumption at $\lambda_\pi = \lambda_P = 120$ g/cm² is a convenient and t unrealistic compromise, we use it here. In

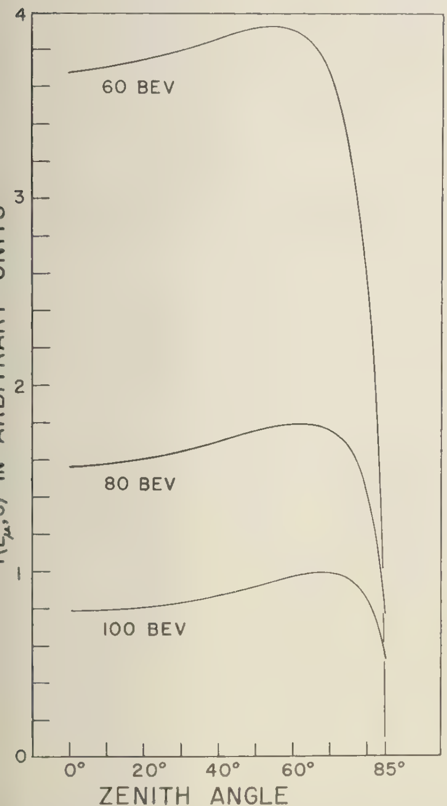

FIG. 3—The differential directional intensity of u mesons at ground-level energies 60, 80, and 0 bev.

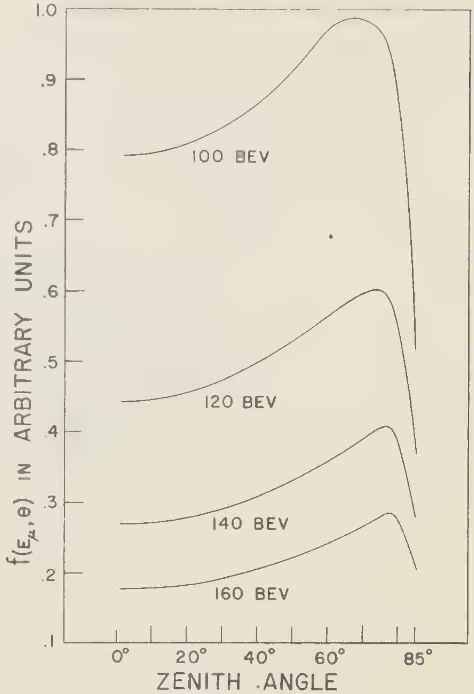

FIG. 4—The differential directional intensity of mu mesons at ground-level energies 100, 120, 140, and 160 bev.

this case, only the term with $n = 0$ in (10) remains and the factor $[(\lambda_P - \lambda_\pi)/\lambda_P]^0$ is formally replaced by unity, as can be seen by solving the original differential equation with $\lambda_\pi = \lambda_P$ from the start.

Figures 2, 3, and 4 show numerical results for $f(E_\mu, \theta)$ vs. θ. Figures 5 and 6 show the dependence on E_μ. The most obvious feature of the curves is the way they rise at large zenith angles. This behavior was anticipated by *Barrett and others* [1952] and by *Budini and Moliere* [1953, 1954]. At low energies the pi mesons decay so quickly that they traverse very little atmosphere, and the resulting mu meson flux (much deeper in the atmosphere) is not affected appreciably by pi meson absorption. At sufficiently high energy, however, the dilation of the pi meson lifetime decreases the decay probability, permitting path lengths in the atmosphere in which interactions can occur. A pi meson starting at depth y and

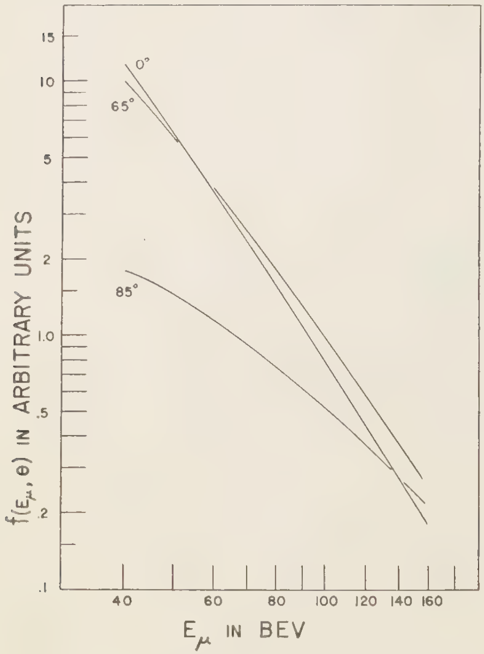

FIG. 5—The results of Figures 2 to 4 plotted as functions of the ground-level mu meson energy at zenith angles 0°, 65°, and 85°.

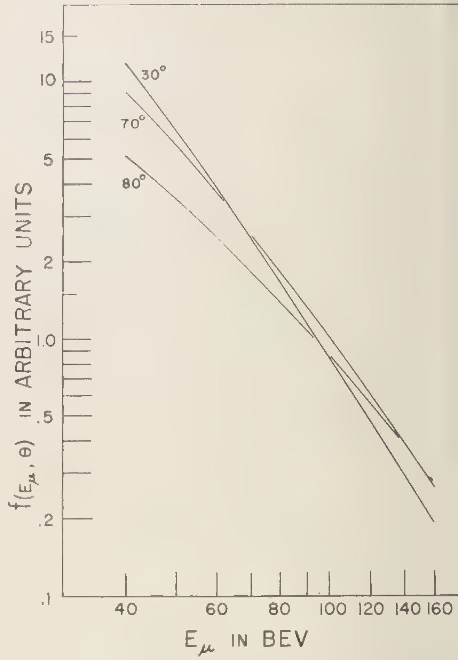

FIG. 6—The results of Figures 2 to 4 plotted functions of the ground-level mu meson energy zenith angles 30°, 70°, and 80°.

moving obliquely at a given energy traverses a less dense atmosphere on the average than another pi meson starting at the same depth with the same energy but moving vertically. Thus the obliquely incident meson traverses fewer grams per square centimeter of atmosphere per unit time and has a greater chance to decay than the vertically incident particle. This effect is enhanced by the production of the obliquely incident mesons at greater altitudes, since an average value of $y/\cos\theta$ for production implies a smaller depth y for larger zenith angle.

Figure 2 shows that according to the present calculations the rise in intensity begins to appear at ground-level mu meson energies near 40 bev. The rise becomes more prominent at higher energies and the maximum in intensity moves to larger zenith angles because the competition effects become more influential and because ionization loss and mu meson decay are relatively less effective at the higher energies. If the rapid changes at large angles are taken seriously, these results have important implications for design of experiments in which telescopes employed to accept particles at angles beyo 50°.

It would be misleading to claim great curacy for the curves presented here. There many simplifying physical assumptions uncertainties in the assumed behavior of cosmic-ray secondaries at very large energ which make the goal of ultimate accuracy realistic for the present treatment. Neverthele the assumptions are believed to be sufficien conservative to give an excellent description the general trends and effects. The comparis with experiment which follow will serve mai to confirm the qualitative features of the pres work.

Experimental results showing the high-ene mu meson zenith-angle dependence at grou level in detail are not yet available. There h have been many pertinent underground periments. The vertical measurements of m

these are summarized by *Barrett and others* [1952] in an intensity-depth curve which indicates a differential ground-level intensity proportional to $E_\mu^{-\alpha}$, with α varying from approximately 3 for E_μ somewhat less than 100 bev and slowly increasing with increasing energy. The agreement of the present calculations as shown in Table 1 is considered reasonable.

TABLE 1—*Magnitudes of the logarithmic slopes* (α) *of the curves in Figures 5 and 6*

Zenith angle	40 bev	60 bev	100 bev	160 bev
0°	2.82	2.85	3.08	3.18
30°	2.74	2.81	3.03	3.17
60°	2.30	2.56	2.85	2.98
70°	2.18	2.42	2.67	2.80
75°	2.00	2.20	2.50	2.72
80°	1.68	1.96	2.25	2.54
85°	1.01	1.33	1.70	2.07

Moroney and Parry [1954] and *Roe and Ozaki* [1959] have made intensity measurements with large magnetic spectrographs at widely separated angles. The Manchester group has also used a large magnet to investigate the vertical intensity at high energies [*Wolfendale*, 1954]. The larger statistical uncertainties in the data of Moroney and Parry above 20 bev make comparison with the present calculations correspondingly less significant, but if their average curves are taken seriously the differential intensities near 50 bev are proportional to $E_\mu^{-\alpha}$ with the following approximate values of α: 2.8 at 0°; 2.6 at 30°; and 2.3 at 60°. Comparison of these numbers with the appropriate results in Table 1 shows general agreement as to magnitude and trend with change in zenith angle. Another pertinent characteristic of the curves in Figures 5 and 6 is the energy at which each curve crosses the curve for $\theta = 0°$. In the present calculations the following approximate cross-over points are observed: 50 bev for 60°; 62 bev for 70°; 72 bev for 75°; 90 bev for 80°; and 140 bev for 85°. (These results for 80° and 85° cannot be taken very seriously because of the 'flat atmosphere' approximation, but they are given to show the trend.) Again using the average curves of Moroney and Parry, the energies at which large zenith-angle differential intensities are equal to the vertical intensity lie roughly between 30 and 60 bev. The more recent results of *Roe and Ozaki* [1959] are statistically much more reliable at energies near 100 bev, however, and these investigators find that the intensities at 0° and 68° are equal 'in the neighborhood of 100 bev.' The present results thus appear to lie roughly between the two sets of experimental data.

Roe and Ozaki also found that in the region 10 to 120 bev the differential intensities at 0° and 68° are proportional to $E_\mu^{-\alpha}$ with $\alpha = 2.70 \pm 0.06$ for the vertical and $\alpha = 2.34 \pm 0.08$ at 68°. *Wolfendale* [1954] reports $\alpha = 3.0 \pm 0.1$ for energies from about 23 to 100 bev. The calculations agree in a general way with a rough average of the experiments, but refined calculations should agree more nearly with the statistically superior results of Roe and Ozaki.

The integral intensities—A first approximation to the total directional intensity of mu mesons above a given energy at ground level may now be calculated by integrating (10) over energy:

$$F(E_{\pi_0}; \theta) = \int_{E_{\pi_0}}^{\infty} f(E_\pi, \theta)\, dE_\pi \qquad (11)$$

When this has been done, the use of (8) for E_{π_0} affords an approximate way to correct for energy losses due to ionization and decay and gives $F(E_{\mu_0}; \theta)$, the intensity of mu mesons at ground level above a given ground-level mu meson energy.

In the integration of (11), again the factor P_μ forces either numerical integration or the use of some appropriate average value of P_μ outside the integral. An approximate average value will be used here, but, since it depends on the forms of the energy integrals which predominate in (11), we may momentarily postpone this issue and write the result of the integration:

$$F(E_{\pi_0}; \theta) = A P_\mu \lambda_\pi \sum_{n=0}^{n=\infty} \left(\frac{\lambda_P - \lambda_\pi}{\lambda_P}\right)^n \left\{\frac{0.600}{E_{\pi_0}^{5/3}} - \frac{1.50(n+1)\cos\theta}{bj_\pi E_{\pi_0}^{2/3}} + \left[\frac{(n+1)\cos\theta}{bj_\pi}\right]^{5/3}\right.$$

$$\cdot \left[\frac{\sqrt{3}\,\pi}{2} - \frac{1}{2} \ln \left\{ \frac{\left[E_{\pi_0}^{1/3} + \left(\frac{bj_\pi}{(n+1)\cos\theta}\right)^{1/3}\right]^2}{\left(\frac{bj_\pi}{(n+1)\cos\theta}\right)^{2/3} - \left(\frac{bj_\pi}{(n+1)\cos\theta}\right)^{1/3} E_{\pi_0}^{1/3} + E_{\pi_0}^{2/3}} \right\} + \sqrt{3}\ \mathrm{arc\ tan} \left\{ \frac{2E_{\pi_0}^{1/3} - \left(\frac{bj_\pi}{(n+1)\cos\theta}\right)^{1/3}}{\sqrt{3}\left(\frac{bj_\pi}{(n+1)\cos\theta}\right)^{1/3}} \right\} \right] \Bigg\} \qquad (1$$

If it is again assumed that $\lambda_\pi = \lambda_P$, only the term with $n = 0$ survives and again the factor $[(\lambda_P - \lambda_\pi)/\lambda_P]^0$ is replaced by unity. Consideration of the integration over energy then leads to pi meson energy $\mathbf{E}_\pi = 1.32E_{\pi_0}$ for the representative value to be used in P_μ. With this, and after inserting the transformation from E_{π_0} to E_{μ_0} using (8), we have $F(E_{\mu_0}; \theta)$, the zenith-angle dependence of mu mesons of energy greater than E_{μ_0} at the depth of 1000 g/cm² in the atmosphere. Plots of this function are presented in Figure 7.

Features similar to those of the differential intensity are again present. The results indicate that apparatus at sea level capable of discriminating against mu mesons of energy less than 40 bev should detect the peculiar zenith-angle depend-

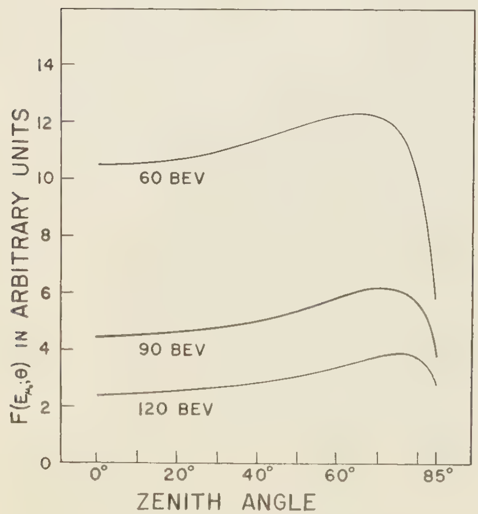

FIG. 7—The total (integral) directional mu meson intensity above ground-level energies 60, 90, and 120 bev.

ence directly. Figure 7 indicates that the to directional intensity above 60 bev at 65° is alm 20 per cent above that at 0°. For all mu meso above 120 bev the increase from the verti to the maximum is about 65 per cent. The resu of Roe and Ozaki can be integrated over ener to show that the integral intensities at 0° a 68° are approximately equal above about 50 b and of course for greater energy the hig intensity is always at the larger zenith ang Comparison of this result with the present c culations shows at least approximate quanti tive agreement and qualitatively confirms t features of Figure 7 at large zenith angles.

Rigorous numerical calculations to replace t averaging assumptions of the present work a apparently needed. Many items will have to included and treated more carefully in a refi theory, but the following are among the most i portant: (1) All important sources of mu meso this will certainly include the heavy mesons a at extremely high energies probably the hypero (2) Possible variation of λ_π and particle prod tion spectra with increase in energy; stud such as those reported by *Ishikawa and Ma* [1958] and *Kaneko and Okazaki* [1958] are sig ficant here. (3) Variation of stopping power w energy at very high energy; detailed resu such as those of *George* [1952] must be tal into account. (4) A more nearly accurate atm phere, especially for large zenith angles.

Interesting and moderately sensitive tests assumptions used in refined calculations app to be feasible in comparisons with statistica significant experiments in the 100-bev and seve hundred bev regions. Unfortunately, go angular resolution seems necessary, especia at large zenith angles. Continued experime with large magnetic spectrographs should sup many of the needed data, but more telesco experiments underground could contribute

ey are designed with special care. For example, periments in which narrow-angle underground lescopes detect mu mesons incident at large nith angles on steeply inclined surface features ould provide useful data.

References

VAN, L., AND M. AVAN, Intensity and angular distribution of the penetrating component of cosmic rays underground, *Compt. rend., 241,* 1122–1124, 1955.

ARRETT, P. H., L. M. BOLLINGER, G. COCCONI, Y. EISENBERG, AND K. GREISEN, Interpretation of cosmic-ray measurements far underground, *Revs. Modern Phys., 24,* 133-178, 1952.

ARRETT, P., G. COCCONI, Y. EISENBERG, AND K. GREISEN, Atmospheric temperature effect for mu mesons far underground, *Phys. Rev., 95,* 1573-1575, 1954.

UDINI, P., AND G. MOLIERE, Die Entwicklung der Nukleonen-Mesonenkomponente in der Atmosphäre, *Kosmische Strahlung,* pp. 380–412, Springer-Verlag, Berlin, 620 pp., 1953.

UDINI, P., AND G. MOLIERE, Concord of cosmic ray components in the atmosphere, *New Research Techniques in Physics,* pp. 56–59, Servicio Gráfico, Rio de Janeiro, 449 pp., 1954.

ARROW, L. A., Mean free path of high-energy nucleons in the atmosphere, *Phys. Rev., 107,* 1687–1694, 1957.

RANZINETTI, C., AND G. MORPURGO, An introduction to the physics of the new particles, *Suppl. Nuovo cimento, 6,* 730–746, 1957.

EORGE, E. P., Observations of cosmic rays underground, *Progress in Cosmic Ray Physics,* pp. 392–451, Interscience Publishers, New York, 557 pp., 1952

REISEN, K., The extensive air showers, *Progress in Cosmic Ray Physics, 3,* 1–137, Interscience Publishers, New York, 420 pp., 1956.

AYAKAWA, S., K. ITO, AND Y. TERASHIMA, Positive temperature effect of cosmic rays, *Progr. Theoret. Phys. Kyoto, 14,* 497–510, 1955.

HIKAWA, G., AND K. MAEDA, The average multiplicity and inelasticity in pi meson production in the atmosphere, *Nuovo cimento, 7,* 53–66, 1958.

KEMAN, D., Production of cosmic ray mesons at large zenith angles, *Canadian J. Phys., 34,* 432-450, 1956.

KANEKO, S., AND M. OKAZAKI, The energy dependence of meson multiplicity in the high-energy interactions, *Nuovo cimento, 8,* 521–532, 1958.

LAL, D., Y. PAL, AND RAMA, On the composition and properties of shower particles produced in high energy interactions, *Suppl. Nuovo cimento, 12,* 347–352, 1954.

MORONEY, J. R., AND J. K. PARRY, Momentum distribution and charge ratio of mu mesons at zenith angles in the east-west plane, *Australian J. Phys., 7,* 423–438, 1954.

MURAYAMA, K., K. MURAKAMI, R. TANAKA, AND S. OGAWA, The atmospheric effects on the intensity of high energy mu mesons, *Progr. Theoret. Phys. Kyoto, 15,* 421–430, 1955.

NEHER, H. V., Recent data on geomagnetic effects, *Progress in Cosmic Ray Physics, 1,* 245–314, Interscience Publishers, New York, 557 pp., 1952.

PUPPI, G., AND N. DALLAPORTA, The equilibrium of the cosmic ray beam in the atmosphere, *Progress in Cosmic Ray Physics, 1,* 315–391, Interscience Publishers, New York, 557 pp., 1952.

RANDALL, C. A., AND W. E. HAZEN, The intensity and angular distribution of mu-mesons 1100 feet underground, *Nuovo cimento, 8,* 878–881, 1958.

ROE, B. P., AND S. OZAKI, Cosmic ray mu meson spectrum (Abstract), *Bull. Am. Phys. Soc., 4,* 8, 1959.

ROSSI, B., *High Energy Particles,* Prentice-Hall, New York, 569 pp., 1952.

SHERMAN, N., Atmospheric temperature effect for mu mesons observed at a depth of 846 MWE, *Phys. Rev., 93,* 208–211, 1954.

SREEKANTAN, B. V., S. NARANAN, AND P. V. RAMANAMURTY, On the angular distribution of penetrating cosmic-ray particles at a depth of 103 MWE below ground, *Proc. Indian Acad. Sci., A, 43,* 113–129, 1956.

TREFALL, H., On the positive temperature effect in the cosmic radiation, *Proc. Phys. Soc. London, A, 68,* 625–631, 1955.

TREFALL, H., On the positive temperature effect in the cosmic radiation and the pi-mu decay, *Physica, 23,* 65–72, 1957.

WOLFENDALE, A. W., Experiments on mu mesons at Manchester and Ceylon, *Suppl. Nuovo cimento, 12,* 107–110, 1954.

(Manuscript received August 21, 1959; revised September 17, 1959.)

A Relationship between the Lower Ionosphere and the [OI] 5577 Nightglow Emission

J. W. McCAULLEY AND W. S. HOUGH

Boulder Laboratories, National Bureau of Standards
Boulder, Colorado

Abstract—The results of a study comparing 5577 A airglow intensity with ionosphere characteristics, using observations near Boulder, Colorado, are presented. The analysis suggests that 5577 variations in airglow intensity can be correlated with variations of an ionospheric stratum. This stratum, as observed by low-frequency sweep soundings, is in the 90- to 110-km region. It is concluded that the observations do not uniquely support any one excitation mechanism for the 5577 emission.

Introduction—During the period of the In- rnational Geophysical Year, data have been cumulated on separate phenomena in the ver ionosphere. They include measurements the zenith intensity of 5577 nightglow tained at Fritz Peak, Colorado, 39°55′N, 5°29′W; and virtual height vs. frequency cords made with the low-frequency sounder Sunset, Colorado, 40°02′N, 105°28′W. The stance between the two stations is 13.2 km.

The purpose of this study was to find corre- ions between these data and to investigate ysical behavior in the lower ionosphere, be- v 110-km height.

The height of the 5577 nightglow emission s been established by rocket measurements *ousey,* 1958] and ground measurements *oach, Megill, Rees, and Marovich,* 1958] to in the 90- to 110-km region.

The ionospheric data from the 90- to 110-km gion recorded every 15 minutes have been idied and compared with the green-line zenith ensities recorded during a corresponding pe- d.

Observations—The airglow observations were de at the Fritz Peak Observatory by an all- y scanning photometer which eliminates the otometric effect of astronomical light, using birefringent filter of a type described by *Dunn d Manring* [1955]. The 5577 zenith intensities re recorded as galvanometric deflections on ntinuous strip records and reduced to absolute intensities in rayleighs.[1] These intensities were recorded 2 minutes after the quarter hour.

Ionosphere observations were made at Sunset Field Site with a low-frequency sweep sounder using an antenna spanning 3400 feet across a small valley between two steep hillsides. The vertical-incidence instrument is a pulsed radar of unique design almost identical to that described by *Blair, Brown, and Watts* [1953]. The characteristics of the ionosphere obtained are virtual heights and particular frequencies of reflection from 0 to 410 km. The observations were made within 1 minute of each quarter hour. The recorded information of the ionosphere is obtained on 35-mm film during approximately 30 seconds while the operating frequency of the vertical sounder is tuned from 50 kc/s to 2 Mc/s. These ionograms were reduced by inspection to obtain the virtual height vs. frequency characteristics of the reflecting strata.

Analysis—The variations in virtual height (h'), top frequency (f_o), and blanketing frequency (f_b) for each stratum have been compared with the variations in airglow intensity for the three nights included in this study, July 5/6, 1957, September 18/19, 1957, and February 19/20, 1958. These values are given in Tables

[1] If the surface brightness, B, is measured in 10^6 quanta/cm^2 sec ster, the intensity in rayleighs, Q, is $4\pi B$ [*Hunten, Roach, and Chamberlain,* 1956].

1, 2, and 3; the time variation of the data is plotted in Figure 1. After the detailed study of three nights was completed, ten additional nights were inspected. The preliminary values obtained are given in Table 4. We define top frequency as the maximum frequency at which reflection from a stratum is recorded, and blanketing frequency as the frequency at which the stratum becomes partly transparent, as shown in Figure 2.

The sample ionogram, selected to show f_0 and f_b, is not 'typical' of low-frequency ionograms. The more usual night ionogram shows three strata, one within each of the following virtual height ranges—80 to 90 km, 90 to 100 km, and 100 to 120 km. The highest stratum is probably sporadic E (E_s). The lower strata have been given provisional designations until a more complete understanding of the lower ionosphere is reached. D_1 designates the lower and D_2 the higher of these two strata. In the

TABLE 1
Observations of July 5/6, 1957

Time, MST	h', km	f_0, mc	f_b, mc	Δf, mc	Q, rayleighs	k_p
2045	89	0.50	0.19	0.31	640	
2100	92	0.67	0.19	0.49	720	
	91	0.70	0.20	0.50	870	
2130	92	0.61	0.16	0.45	930	
	91	0.62	0.19	0.43	980	2.67
2200	92	0.61	0.20	0.41	930	
	91	0.61	0.19	0.42	820	
2230	91	0.70	0.20	0.50	900	
	91	0.59	0.19	0.40	1110	
2300	91	0.52	0.16	0.36	980	——
	91	0.51	0.16	0.35	900	
2330	92	0.52	0.14	0.38	850	
	91	0.53	0.15	0.38	848	
0000	92	0.51	0.16	0.35	823	
	93	0.57	0.14	0.43	777	
0030	92	0.51	0.15	0.36	797	3.33
	93	0.53	0.18	0.35	720	
0100	97	0.61	0.16	0.45	850	
	94	0.57	0.13	0.44	900	
0130	92	0.71	0.15	0.56	1050	
	93	0.67	0.16	0.52	1030	
0200	93	0.61	0.16	0.45	1050	——
	91	0.58	0.16	0.42	1050	
0230	90	0.71	0.15	0.56	1030	
	92	0.76	0.17	0.59	1260	2.67
0300	94	0.58	0.15	0.43	1130	
	94	0.59	0.13	0.46	...	

TABLE 2
Observations of September 18/19, 1957

Time, MST	h', km	f_0, mc	f_b, mc	Δf, mc	Q, rayleighs	
2015	94	0.68			392	
2030					426	
					392	
2100	105	0.69			460	
					409	
2130					478	1
					426	
2200					392	
	101	0.55			409	
2230	102	0.53			478	
	96	0.54			535	
2300	93	0.54			528	–
	97	0.84	0.72	0.12	563	
2330	95	0.80	0.62	0.18	580	
	95	0.82	0.70	0.12	580	
0000	96	1.06	0.71	0.35	648	
	92	1.03	0.76	0.27	648	
0030	95	1.04	0.82	0.22	580	1
	95	0.87	0.77	0.10	563	
0100	97	0.86	0.73	0.13	580	
	100	0.86	0.68	0.18	545	
0130	100	0.91	0.75	0.16	545	
	98	0.90	0.76	0.14	528	
0200	100	0.77	0.56	0.11	478	–
	98	0.88	0.55	0.33	545	
0230	99	0.74	0.54	0.20	580	
	100	0.80	0.60	0.20	495	
0300	98	0.72	0.65	0.07	443	1
					443	
0330					443	
					443	
0400					375	

sample ionogram only E_s and D_2 strata are p
ent. The intensity of 5577 airglow appear
be correlated with the D_2 stratum.

The virtual height of the D_2 stratum and
intensity of 5577 airglow (Q) have been c
pared, and the result is shown in Figure 3
can be seen that the height of the stratum va
between ≈90 and 110 km. The greater hei
seem to be associated with fall and winter
servations and the lower heights with sp
and summer observations. A correlation
tween h' and Q is suggested when the va
are plotted on an individual night basis; th
shown by the time variation of h' and Q
Figure 1. These variations appear to have
inverse relation. The gross effect is that

TABLE 3
Observations of February 19/20, 1958

e, T	h', km	f_0, mc	f_b, mc	Δf, mc	Q, rayleighs	k_p
)	108	0.80			438	
	110	0.83			361	3.67
)	112	0.74			361	——
	107	0.80			310	
)	107	0.81			285	
	...	...			330	
)	110	0.75			317	
	106	0.75	0.70	0.05	336	
)	106	0.72	0.72	0	352	4.00
	105	0.78	0.73	0.05	374	
)	105	0.80	0.80	0	371	
	102	0.90	0.87	0.03	397	
)	102	0.90	0.87	0.03	...	
	103	1.00	0.70	0.30	...	
)	100	0.80	0.76	0.04	483	——
	102	0.90	0.86	0.04	480	
)	103	0.82	0.70	0.12	534	
	104	0.75	0.65	0.10	662	
)	105	0.77	0.56	0.26	736	
	102	1.02	0.50	0.52	717	
)	101	0.96	0.60	0.36	643	3.00
	103	0.90	0.72	0.28	662	
)	103	0.85	0.45	0.40	666	
	103	0.74	0.40	0.34	662	
)	105	0.63	0.40	0.23	659	
	106	0.63	0.28	0.35	573	
)	105	0.65	0.43	0.22	506	——
	104	0.62	0.33	0.29	509	
)	105	0.70	0.55	0.15	506	2.67
	106	0.72	0.60	0.15	486	
)	106	0.75	0.69	0.06	451	

ual height tends to increase as the airglow ensity decreases.

plot of f_0 and f_b vs. Q (Fig. 4) shows that, low airglow intensities, f_0 and f_b do not differ ificantly in magnitude. As the airglow in- sity increases, however, f_0 tends to remain h while f_b decreases, and the difference in quency becomes relatively large. A com- ison between Q and the frequency difference f), the top frequency minus the blanketing quency, is shown in Figure 5, where it can seen that Δf is small or essentially zero when airglow intensity is less than 200 to 400 leighs. This suggests that a threshold phe- nenon may exist such that, for airglow in- sities greater than 200 to 400 rayleighs, Δf omes significant. It is interesting to note t the most probable zenith airglow intensity

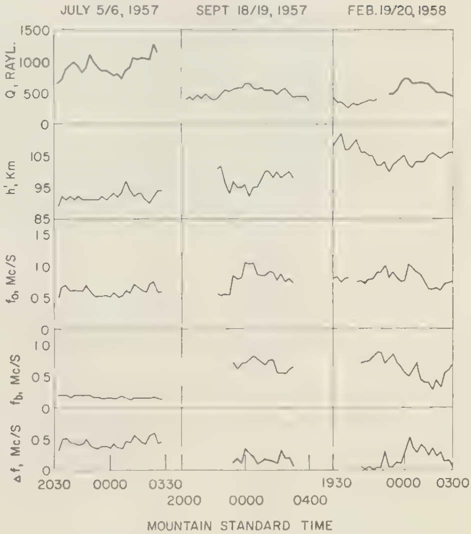

FIG. 1—Variation of 5577 airglow intensity (Q), virtual height (h'), top frequency (f_0), blanketing frequency (f_b), and $\triangle f$ with time for three nights, each 15-minute value (columns 1 through 5 from Tables 1, 2, and 3).

at Fritz Peak is 300 to 350 rayleighs, and values greater than 400 rayleighs occur in about 50 per cent of the observations made during the IGY [*Roach, McCaulley, and Marovich*, 1959].

Discussion—The excitation mechanism of the 5577 airglow line has been discussed in a paper by Tandberg-Hanssen and Roach (Excitation mechanisms of the oxygen 5577 emission in the upper atmosphere; in press) and two possible mechanisms are suggested: (1) a photochemical reaction modified by the mass motions within the region, and (2) an electrical-discharge excitation induced by the mass motions themselves. These mechanisms will be briefly discussed in the light of the data presented in this paper.

The airglow may be considered a purely static phenomenon. A photochemical reaction, then, could not account for the occurrence of an intensity maximum at any time during the night. New evidence [*Roach, Tandberg-Hanssen, and Megill*, 1958a, b] suggests that the 5577 airglow is composed of discrete cells having a diameter of about 2500 km and a translational motion of ≈ 100 m/sec. Using this new evi-

TABLE 4
Ten Additional Nights, 1958

Date	Time, MST	h', km	f_0, mc	f_b, mc	Δf, mc	Q, rayleighs	k_p	Remark
Jan. 21/22	2000					...		
	2100	105	1.10	1.10	0	550	3.00	
	2200	105	1.43	1.31	0.12	440		
Feb. 23/24	2300					270		
	0000					320	2.00	No D_2
	0100					...		
Mar. 17/18	2100	88	0.53	0.43	0.10	320		
	2200	90	0.53	0.53	0	360	4.00	
	2300	95	0.46	0.43	0.03	240		
Mar. 26/27	2000					310		
	2100					390	2.67	No D_2
	2200					360		
May 27/28	0100					...	3.00	
	0200	90	0.44	0.40	0.04	570		
	0300	94	0.48	0.48	0	360	1.67	
Jul. 11/12	2100					...		
	2200					470	3.33	No D_2
	2300					350		
Jul. 13/14	2200	97	0.60	0.60	0	240	3.33	
	2300	96	0.67	0.67	0	250		
	0000					...	4.00	
Aug. 6/7	2000					...		
	2100	90	1.00	1.00	0	280	1.33	
	2200	90	0.75	0.75	0	180		
Aug. 11/12	2000					...		
	2100					280	2.67	No D_2
	2200					200		
Aug. 25/26	2300					140		
	0000	90	0.53	0.43	0.10	240	3.33	
	0100	90	0.64	0.64	0	170		

dence, Tandberg-Hanssen and Roach have presented the possibility that the green-line excitation is a photochemical reaction as proposed by *Chapman* [1930] but modified by translational movements of airglow cells superimposed on turbulence. Assuming excitation due to the Chapman reaction [$O + O + O \rightarrow O_2 + O\,(^1S)$], the transition yield is directly proportional to the cube of the number density of atomic oxygen. Thus, a small change in the number density will produce a relatively large change in the intensity; and, since the distribution of atomic oxygen is peaked near 100 km [*Bates and Nicolet,* 1950], the reaction will be height-sensitive. The apparent decrease in virtual height with increasing airglow intensity, as suggested by Figure 1, is not substantiated by the additional data presented in Figure 3. If the Chapman reaction were responsible for th 5577 emission, the intensity would be expecte to show a maximum at the level of the maxi mum atomic oxygen concentration and to de crease as the cube of the number density o either side.

As a second possibility, Tandberg-Hansse and Roach have invoked environmental effec to account for the 5577 emission. The ionospher is likened to a gas-discharge tube, the essenti feature being the presence of an electric fiel strong enough to accelerate electrons to a energy capable of exciting the oxygen aton The data presented in Figure 5 suggest a rel tionship between $\triangle f$ and Q. This relationshi may have some significance in determining th existence of an excitation process for the 557 emission involving electrons, even though th

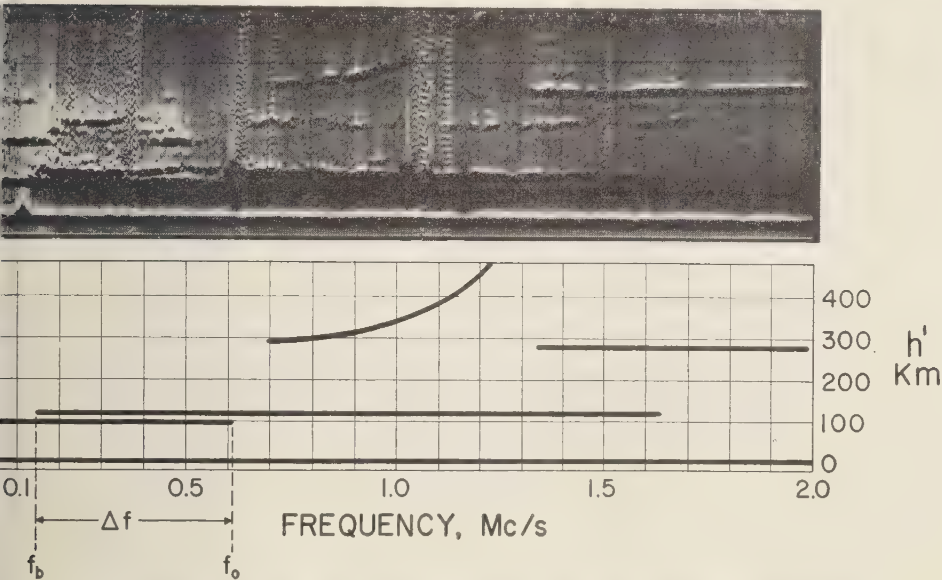

Fig. 2—Sample night-time low-frequency ionogram showing ionosphere characteristics.

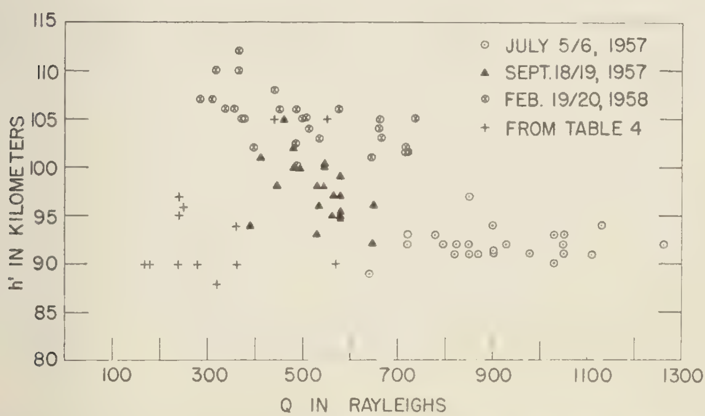

ig. 3—Variation of virtual height of D_2 stratum with 5577 airglow intensity (columns 1 and 5 from Tables 1, 2, and 3; and columns 2 and 6 from Table 4).

hysical interpretation of $\triangle f$ is not definitely ertain. $\triangle f$ may indicate the electron density s. height gradient, the degree of turbulence at ne observed height level, or a combination of oth. These are speculative suggestions, and a ıore comprehensive study to determine the gnificance of $\triangle f$ and its relation to the air-low is in progress.

Conclusion—Evidence has been presented suggesting a relationship between ionosphere variations and 5577 airglow variations in the 90- to 110-km region. Two possible excitation mechanisms for the 5577 emission have been briefly reviewed, and an attempt has been made to fit the observations presented into one or both mechanisms. The conclusion was reached

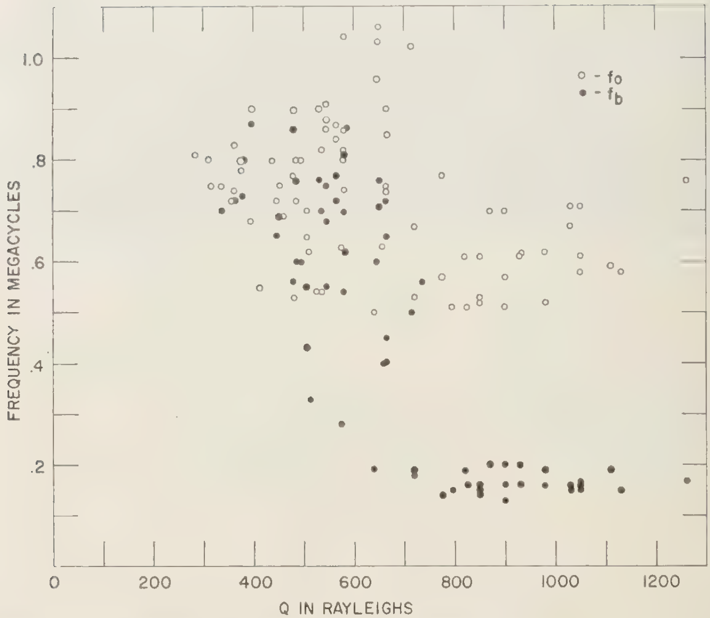

FIG. 4—Variation of top frequency (f_0) and blanketing frequency (f_b) with 5577 airglow intensit (columns 2, 3, and 5 from Tables 1, 2 and 3; and columns 3, 4, and 6 from Table 4.

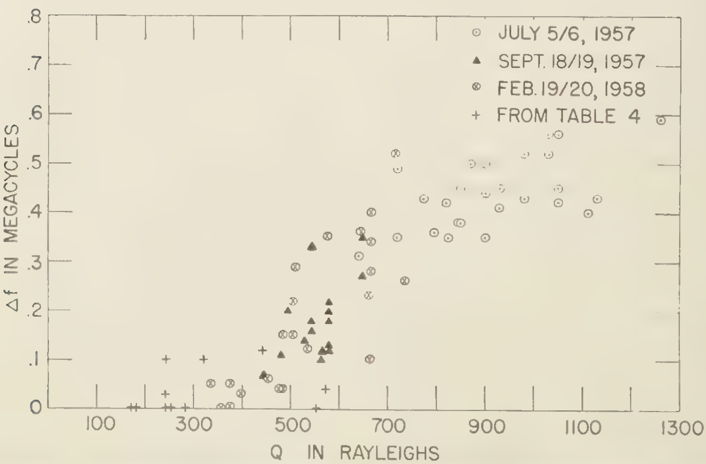

FIG. 5—Variation of $\triangle f$ with 5577 airglow intensity (columns 4 and 5 from Tables 1, 2, and 3; and c umns 5 and 6 from Table 4).

at the observations do not support either pothesis to the exclusion of the other. The nount of data presented is small, and significantly more data must be studied before any finitive interpretation can be made.

Acknowledgment—The research presented in s paper was supported in part by a grant from e National Science Foundation.

References

tes, D. R., and M. Nicolet, The photochemistry of atmospheric water vapor, *J. Geophys. Research, 55,* 301–327, 1950.

air, J. C., J. N. Brown, and J. M. Watts, An ionosphere recorder for low frequencies, *J. Geophys. Research, 58,* 99–107, 1953.

iapman, S., A theory of upper atmosphere ozone, *Mem. Roy. Meteorol. Soc., 3,* 103–125, 1930.

unn, R. B., and E. R. Manring, A recording night sky photometer of high spectral purity, *J. Opt. Soc. Am., 46,* 572-577, 1956.

Hunten, D. M., F. E. Roach, and J. W. Chamberlain, A photometric unit for the airglow and aurora, *J. Atmospheric and Terrest. Phys., 8,* 345–346, 1956.

Roach, F. E., J. W. McCaulley, and E. Marovich, The origin of [OI] 5577 in the airglow and aurora, *J. Research Natl. Bur. Standards, 63D,* 15–18, 1959.

Roach, F. E., L. R. Megill, M. H. Rees, and E. Marovich, The height of nightglow 5577, *J. Atmospheric and Terrest. Phys., 12,* 171–176, 1958.

Roach, F. E., E. Tandberg-Hanssen, and L. R. Megill, The characteristic size of airglow cells, *J. Atmospheric and Terrest. Phys., 13,* 113–121, 1958*a*.

Roach, F. E., E. Tandberg-Hanssen, and L. R. Megill, Movements of airglow cells, *J. Atmospheric and Terrest. Phys., 13,* 122–130, 1958*b*.

Tousey, R., Rocket measurements of the night airglow, *Ann. géophys., 14,* 186–195, 1958.

(Manuscript received July 24, 1959; revised September 8, 1959.)

A Comparison of Sferics as Observed in the Very Low Frequency and Extremely Low Frequency Bands

LEE R. TEPLEY

Stanford Research Institute
Menlo Park, California

Abstract—A large number of sferics were photographically recorded in the very low frequency (VLF) and extremely low frequency (ELF) bands at a UCLA field station in Hawaii. From the characteristic VLF waveforms it was clear that the VLF signals were generated from lightning discharges. It was found that an observable ELF component (slow tail) followed the VLF component in almost all cases. It was also found that about one third of the sferics observed were ELF signals, similar in appearance to slow tails but not preceded by observable VLF oscillations.

Peak amplitudes were measured for both the VLF and ELF components of almost 3000 sferics. The results were tabulated in groups according to (1) whether the sferics were recorded during the day or during the night, (2) whether the polarity of the initial excursion of the ELF signal was positive or negative, and (3) whether the VLF and ELF components appeared together or separately. Amplitude distribution histograms were plotted for all cases. For those sferics possessing both VLF and ELF components, the VLF to ELF peak amplitude ratios were also tabulated separately as in (1) and (2) above, and ratio-distribution histograms were plotted.

The more important results obtained from the histograms were as follows.

1. No significant differences were found between the amplitude distributions for the ELF waveforms that were preceded by VLF oscillations and those that were not. Hence, it is probable that both groups were generated by lightning discharges.

2. For both daytime and nighttime sferics the median value of the ELF amplitude was greater for ELF waveforms of positive polarity than for waveforms of negative polarity.

3. For both daytime and nighttime sferics the median value of the VLF/ELF peak-amplitude ratio was greater for ELF waveforms of negative polarity than for waveforms of positive polarity.

4. The polarity of the ELF waveform was predominantly negative at night and positive during the day (verified by a count of the polarities of almost 6000 additional ELF waveforms).

An attempt is made to explain the experimental results in terms of known properties of lightning discharges, and some of the difficulties in making such an interpretation are indicated.

INTRODUCTION

For the past five years the atmospheric physics group at the Institute of Geophysics of the University of California at Los Angeles has been investigating extremely low frequency electromagnetic wave propagation in the earth-ionosphere waveguide. Some of the earlier results of this work have been described previously [*Holzer and Deal*, 1956; *Holzer*, 1958]. At present the primary objectives of the project are the determination of attenuation and dispersion in the ELF band. The most recent experimental data were obtained in the summer and fall of 1957 from a network consisting of a station near the city of Wahiawa on Oahu, Hawaii; a station at the UCLA campus in Los Angeles, California; and a station at the National Bureau of Standards site near Sterling, Virginia.

The ELF components of radio atmospherics (sferics) were recorded photographically and on magnetic tape simultaneously at the three sites. The results of the ELF data analysis will be reported at a later date by R. E. Holzer and E. A. Smith.

VLF components of sferics were also recorded

photographically at the three stations for purposes of comparison between the VLF and ELF signals. In the present paper the results of this comparison are presented, but the report is restricted to data obtained at the Hawaii station.

Whereas the major part of the project deals with ELF wave propagation, the work to be described here is of interest primarily with respect to lightning discharges. The results seem to imply some unusual characteristics of lighting discharges not fully described in the literature. A completely satisfactory explanation of these results does not appear possible without additional experimentation. Nevertheless, several possible interpretations will be considered in this paper.

Background

In a typical ground-return stroke of lightning, the current rises to its peak value in about 10 μsec and decays to a small fraction of its maximum value in about 100 μsec [*Bruce and Golde,* 1941]. The radiation pulse of the associated electromagnetic field is proportional to the first derivative of the current dipole moment of the discharge column. From observations at 30 to 50 km from the source, it has been observed that a broad energy spectrum is obtained, and the maximum amplitude usually occurs at frequencies between 5 and 10 kc/s [*Florman,* 1955; *Watt and Maxwell,* 1957]. When observed at a considerable distance from the source, the sferic is a superposition of pulses consisting of the direct (or ground) wave and a number of reflected waves from the surfaces of the earth-ionosphere waveguide. The appearance of the composite waveform varies with the nature of the source, the distance between the source and receiver, and propagation conditions in the waveguide. However, at distances greater than 1,000 km the waveform generally consists of a series of either smooth or jagged oscillations of quasi-frequency near 10 kc/s and a total time duration on the order of 1 msec. It has been shown [*Wait,* 1957] that the maximum transmission of the waveguide occurs at frequencies between 10 and 20 kc/s. Hence, the quasi-frequency of the received signal near 10 kc/s is associated with both the frequency of maximum energy at the source and favorable
conditions for transmission of frequencies
this range in the waveguide.

As long ago as 1926 it was observed [*App*
ton and others, 1926] that the main portion
the sferic (as described above) was occasiona
followed by a second oscillation of considerab
lower quasi-frequency and somewhat lower a
plitude. The second oscillation is frequently
ferred to as the 'slow tail.' However, not un
recently was it determined that the maximu
energy of the second oscillation generally c
curred at frequencies below 200 cps. *Holzer a*
Deal [1956] were able to show a close correl
tion between world-wide thunderstorm activi
and the mean energy level in the range of 20
120 cps. Their results imply a very low attenu
tion coefficient for radiation in this frequen
range and also indicate that almost all of t
measured electromagnetic energy in the 20-
120-cps range (which may be interpreted as
superposition of slow tails) originates in ligh
ning discharges over the entire surface of t
earth.

The problem of slow-tail propagation in t
earth-ionosphere waveguide (zero-order mo
theory) was first treated theoretically by *Sch*
mann [1952], later by *Liebermann* [1956], *Wa*
[1958*a, b*], and others. It was found that a r
gion of high transmission exists below 200 c
in addition to the region discussed earlier at
to 20 kc/s. The VLF (Δf = 3 to 30 kc/s) a
ELF (Δf = 10 to 1000 cps) bands include t
two regions of high transmission. [Note: T
VLF band was defined as 3 to 30 kc/s at t
Atlantic City Radio Convention of 1947; ho
ever, the bandwidth of the UCLA equipme
was actually 2.5 to 25 kc/s. There is no stan
ardized nomenclature for frequency ranges b
low 3 kc/s. The definition of the ELF ba
given here corresponds to the bandwidth
the UCLA equipment.] At distances great
than several thousand kilometers, energy
the ELF band propagates almost entirely
the zero-order waveguide mode. Hence, t
propagation of a transient (slow tail) in t
ELF band may be investigated mathematicall
using zero-order mode theory. *Schumann* [195
has made extensive calculations of this typ
using a wide variety of source functions
represent the time variation of current flo
in the discharge channel. For certain types

rce functions, the waveform of the radiated lse can be expressed in a relatively simple thematical form. Other similar source funcns result in complex mathematical expressions m which the change of waveshape with disice can be found only with difficulty. Hence, seems desirable to consider first only the npler mathematical results for comparison th experiment. At least some of these results derived from source functions that are ysically reasonable approximations of the acl time variation of current flow in the disarge channel. Other results are derived from s realistic source-current functions but are ll of value in presenting a general picture waveshape propagation.

In all the relatively simple cases, it is found eoretically that a unidirectional source curit leads to a waveform of only two halfcles, and that the polarities of the half-cycles not change as the pulse moves through the veguide. Attenuation and dispersion cause a crease in amplitude and an increase in time ration for both half-cycles as the distance m the source increases, but otherwise the veshape changes only slightly. It is conceivle that other source functions, representing ysically reasonable discharge currents, could sult in waveforms of greatly different charteristics than those just mentioned. However, seems far more probable that a small change the source current function will result in a nparably small change in the propagated veshape, even if the mathematical expresn for the waveshape is far more complex than fore the change was made. The approximate eservation of waveshape that is predicted eoretically, at least from the simpler theoreti- results, has been verified by observations de at UCLA field stations for the past sevl years. Individual slow-tail waveforms orded simultaneously in Hawaii and in Calimia inevitably show the same general appearce. Hence, it appears that the slow-tail waveape may be utilized to obtain information out the current flow in a lightning-discharge annel many thousands of kilometers distant. particular, the theory predicts that the larity of the initial excursion should indicate direction of current flow. [Note: The direcn of the current flow may also be obtained from the initial excursion of the ground wave as observed in the VLF band. However, the ground wave can only be observed separately at distances on the order of 500 km. At greater distances dispersion results in a superposition of ground and sky waves, and the composite waveform bears little relation to the radiation pulse near the source.]

From the observations at the UCLA field stations it is found that most experimentally observed slow tails fall into one of the two following types.

Type A—This waveform consists of a single large half-cycle sometimes followed by a second half-cycle of substantially lower amplitude and correspondingly longer duration. The waveshape may be obtained theoretically if the source current is taken as a Dirac impulse. It may be expected that any unidirectional current source of sufficiently short duration will produce a qualitatively similar waveform.

Type B—This waveform consists of two halfcycles of comparable amplitude, the second of which is of longer duration than the first. On occasion there seems to be a third half-cycle of substantially lower amplitude and longer duration. However, the third half-cycle may be associated with the ever-present noise background instead of with the preceding two halfcycles. The first two half-cycles of the waveshape may be obtained theoretically if the source current is taken to be unidirectional but of longer duration than the current responsible for the type A waveform. [Note: From consideration of some of the mathematically simpler cases treated by Schumann it appears that as the wave propagates, the second half-cycle may decrease more rapidly in amplitude than does the first. Thus, as the distance from the source increases, the distinction between types A and B waveforms may disappear. Hence, the type A waveform may be associated with a relatively long duration unidirectional current flow in the discharge channel, provided that the waveform is observed at a sufficiently great distance from the source.]

The existence of a third half-cycle is not predicted theoretically from any of the unidirectional source-current functions which were considered by Schumann and which led to the relatively simple mathematical results mentioned

previously. It is conceivable, though unlikely, that a slightly modified source-current function would generate an ELF waveform with an additional half-cycle. Since the UCLA results establish the existence of only two half-cycles, they may be considered to be in agreement with Schumann' theory.

Slow tails with additional half-cycles have been reported by other workers [*Liebermann,* 1956; *Hepburn,* 1957]. Such waveforms could be produced by unusual conditions at the source (such as an oscillating current flow in the discharge channel) or by unusual propagation conditions (such as the anomalous mode hypothesized by Liebermann). Alternatively, additional oscillations may be produced at the receiver by instrumental effects, such as reduced amplification at the lower frequencies.

Instrumentation

In the present paper we are concerned only with data recorded at the UCLA field station on Oahu. The station was set up in an isolated area to minimize the effects of power-line interference with natural signals in the ELF band.

The signal was received on a 20-ft vertical antenna. The base of the antenna was capacitatively coupled to the grid of a cathode follower preamplifier. The input resistance of the cathode follower was 10 megohms. This was shunted by a capacitance of 7500 $\mu\mu$f, giving a low frequency cutoff near 2 cps. At the output of the cathode follower the signal was separated by bandpass filters into its VLF and ELF components, each of which was amplified by battery-operated equipment located at the antenna base. Facilities were also provided at the antenna base to permit a rapid check of the gain and frequency response of the system.

The recording equipment was located in a van 150 ft from the antenna and was coupled to the antenna preamplifiers through shielded cables. The equipment in the van was powered by a 60-cps, 110-volt, gasoline-driven generator. This was accomplished without the introduction of any noticeable 60-cycle interference in the ELF channel. However, a 60-cycle rejector (bridged-T filter) was utilized to eliminate a small 60-cycle component originating from power lines several miles away.

The VLF signal from the antenna preamplifier (Δf = 2500 to 25,000 cps) was passed throu an amplifier and a 50-μsec delay line and w terminated on the horizontal input of one cha nel of a dual-beam oscilloscope. The VLF wav form was displayed in a conventional mann by means of a triggered sweep lasting abo 700 μsec. Before entering the delay line, t VLF signal activated a special triggering ne work that controlled the sweep circuit of t oscilloscope. The sweep was applied to t vertical axis to provide a time base for the VI trace. The 50-μsec time delay was usually su ficient to permit observation of almost the e tire VLF waveform.

The ELF signal from the antenna preamp fier (Δf = 10 to 1000 cps) was passed throu the 60-cycle rejector to the vertical axis of t second channel of the oscilloscope. Both t VLF and ELF signals were recorded phot graphically by means of an oscillographic stri film camera. The time base for the ELF cha nel was provided by the motion of the film (or 20 inches/sec). The ELF signal was al recorded on magnetic tape with a frequenc modulated tape recorder (Δf = 2 to 3000 cp

Because of the slow roll-off characteristics the low-pass cutoff (1000 cps) of the anten preamplifier, a portion of the VLF signal a peared on the ELF channel. Since the film spe was not sufficient to resolve the VLF comp nent, it appeared as a sharp spike. The presen of the spike facilitated the matching of the VI and corresponding ELF signals which otherwi would have been difficult at times, particular when the ELF background was relatively hig

Analysis of Data

General—A considerable amount of data w collected at the UCLA station on Oahu throug out the summer and fall of 1957. Climatologic information indicates that very little thunde storm activity occurred within several thousa miles of Hawaii during most of this peri [*World Meteorological Organization,* 1956 Hence, most of the recorded sferics probab originated from distant thunderstorms. Becau of limitations of time and personnel, only small sample of the data was used for the stati tical analysis presented here. The samples th were analyzed were obtained during the perio of relatively low sferic activity. Hence, it ma

concluded that almost all of the sferics that re analyzed originated at distances on the ler of 3000 miles or more from Hawaii.

Data samples were analyzed for both night d day propagation conditions. Whenever posle, records obtained near noon or midnight re used in order to minimize possible complitions arising from propagation over mixed ht and day paths or from sunrise and sun- effects. The observed rate of occurrence of rics was always much greater at night than ring the day; hence, in order to obtain a nparable number of sferics for both propagan conditions, it was necessary to use a longer ta sample during the day than at night. A tailed analysis was made of one night run 3.4 sec) and four day runs (232 sec) in which ELF peak amplitude and the VLF/ELF ak-amplitude ratio were tabulated for almost 00 sferics. The quantities were tabulated sepately for ELF waveforms of positive and gative polarity. (The term 'positive' as deed here refers to the positive electric vector ected *downward* at the receiver. The definin is in agreement with that used by *Pierce* 955*a*].)

To obtain additional information a count of polarity of ELF waveforms was made from separate runs containing about 5700 strokes.

In Figure 1 sample sections of film are shown m the night run (August 30, 1957, 2:40 a.m.) d from one of the day runs (October 22, 1957, 55 p.m.) which were analyzed in detail. The ward direction in the picture corresponds to direction of positive polarity for signals the ELF channel. The time scale and the ection of increasing time in the ELF channel shown above the film samples. In the VLF annel the sweep begins near the middle of film and terminates at the heavy horizontal e near the top, where the spot on the cathode tube rests. (When the sweep is triggered, spot moves downward in a few microseconds d then returns at a constant speed to its rest- point in about 700 μsec.)

Because of differences in instrumentation the y records and the night records differ in the lowing respects.

1. For the day record an additional channel was ded to the system (by means of an electronic itch) to permit the photographic recording of a WWV time signal, which appears below the ELF trace in the two lower film samples of Figure 1. A sharp spike is superimposed on the WWV time signal. The spike is triggered by the VLF oscillation and serves to determine its arrival time accurately. The time signal was used to permit identification of the same waveform at the UCLA and Hawaii stations.

2. A higher film speed was used during the day to obtain better time resolution (20 inches/sec as compared with 10 inches/sec for the night run). The expanded time base results in a broadening of the ELF waveform in the day record. [Note: As a result of the relatively greater dispersion associated with daylight propagation conditions, the periods of ELF waveforms tend to be longer in the daytime. This may be observed by comparing the day records with the night records in Figure 1, but the effects of dispersion tend to be obscured because of the expanded time base used for the day records.]

3. A slight ripple may be observed on the ELF trace on the day record. The ripple was induced by mechanical vibration of the stripfilm camera and occurred only at the higher film speed.

In addition to the differences between day records and night records associated with the instrumentation for photographic recording, a number of other differences due to propagation effects may be observed. These will be discussed in the following sections.

Classification of waveforms—In order to make the analysis as unbiased as possible, every waveform was placed in a definite category, as indicated in Table 1.

In category 1, peak amplitudes were measured for both VLF and ELF waveforms. The VLF amplitude was determined either from the triggered waveform or from the amplitude of the spike in the ELF channel (see Appendix for details) as observed on the photographic record. The latter method was employed because a large number of VLF signals were too small to trigger the sweep in the VLF channel but were large enough to appear as measurable spikes on the ELF trace. Hence, if amplitudes had not been measured from the spikes it would have been necessary to discard a large part of the waveform data. The minimum spike ampli-

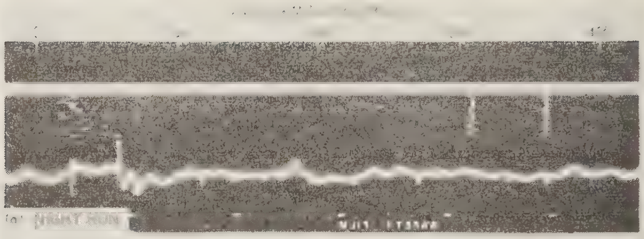

Note the large positive and negative ELF signals at the left and the series of small negative ELF signals at the right

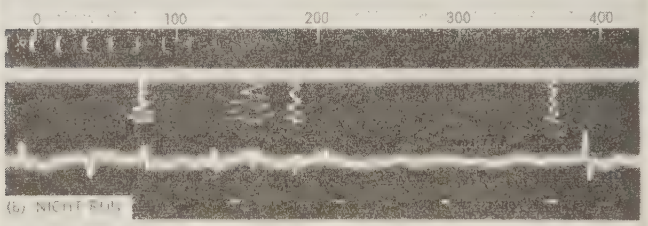

Note the VLF spikes associated with most of the larger slow tails. The smooth VLF oscillation probably indicates propagation from a long distance. This is consistent with the relatively long time delay between the spike and the slow tail

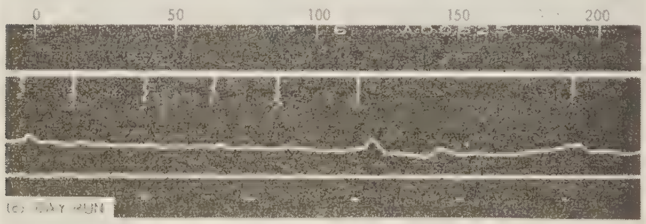

Note that most of the slow tails and the corresponding VLF oscillations are similar in appearance. There is a strong suggestion that all of the signals originated in the same thunderstorm area and possibly were part of a multiple stroke.

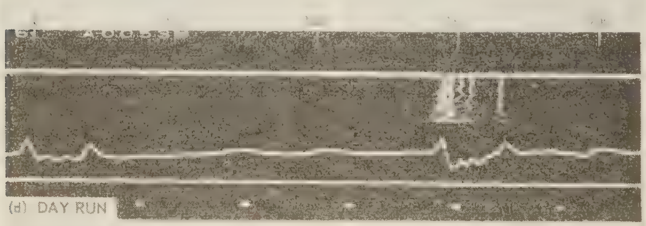

Note the slow tails at the left which are not preceded by VLF oscillations. Also note the series of VLF spikes that appear near the peak of the ELF waveform at the right. The spikes may originate from a leader stroke. This interpretation is consistent with the ragged appearance of the corresponding waveforms in the VLF channel which are superimposed due to multiple triggering. It may be implied that the ELF waveform originates from the initial slow field change which includes the leader stroke. However, the interpretation must be treated with caution since waveforms of this appearance are relatively rare, and the composite waveform may be a superposition of two separate sferics. The leader stroke and the slow tails and spikes immediately to the right appear to constitute a multiple stroke.

FIG. 1—Sample film records.

TABLE 1—*Classification of waveforms*

			ELF polarity						
			Night run (33.4 sec)			Day run (232 sec)			Total number of sferics
ıtegory	VLF waveform	ELF waveform	+	−	?	+	−	?	
1	Measured	Measured	249	732		569	337		1887
2	Not observed (or below 10 mv/m)	Measured	112	380		221	170		883
3	Measured	Not observed (or below 200 μv/m)			13			35	48
4	Measured	Observed but not measured (high background)	7	12		1	1		21
5	Measured	Not observed (high background)			13				13
6	Not measured	Not measured	21	2			2		25
ɔtal number of sferics			389	1126	26	791	510	35	2877

ght run—August 30, 1957, 2:40 A.M. HST.
ıy runs—October 21, 1957, 10:55 A.M. HST.
October 21, 1957, 11:55 A.M. HST.
October 22, 1957, 12:55 P.M. HST.
October 22, 1957, 2:55 P.M. HST.

de which could be measured with reasonable curacy corresponded to a VLF field strength about 10 mv/m. The ELF amplitude was termined from the magnetic tape record as ayed back through a 500-cps low-pass filter nich was used to eliminate completely the ike from the ELF channel. This was particurly desirable in the analysis of the night data, nce dispersion at night is relatively poor and e slow tail is not always completely separated om the VLF oscillation.

In category 2, only the ELF signal was easured; the VLF spike was either not obrved, or observed but not measurable because a combination of ELF background and the ite width of the baseline. In this case, the LF field strength was always below 10 mv/m.

In category 3 only the VLF signal was meased. In this case the field strength of the ELF gnal was always less than 200 μv/m, this ure being typical of the ELF background ring a relatively quiet period.

In categories 4 and 5 only the VLF signal as measured. The ELF signal was either not served, or observed but not measurable because of the relatively high ELF background.

In category 6, neither VLF nor ELF signals were measured because of clipping in either the VLF or the ELF channel or sometimes both.

The following results are immediately apparent from Table 1.

1. *About 98 per cent of the observed sferics possess observable ELF components.* In contrast with the present observations, *Hepburn* [1957] has reported that a much smaller percentage of sferics observed in England possess slow tails (only about 10 per cent by day and an unspecified percentage by night). The disagreement is probably largely due to differences in sensitivities of the recording equipment, since Hepburn's lower limit of measurement was given as 20 mv/m, whereas the lower limit of the present system was 200 μv/m.

2. *About 30 per cent of the observed sferics possess an ELF but not a VLF component.* The following possibilities must be considered in attempting to explain this result.

a. Origin of ELF signals in sources other than lightning discharges. Since the VLF oscillation is characteristic of at least one common type

TABLE 2—*Polarity count*

Date	Time, HST	Polarity +	Polarity −	Number of sferics		Polarity ratio +/−
Night runs						
1957						
July 24	1:50 A.M.	277	436	713		0.635
Aug. 23	2:30 A.M.	169	195	364		0.867
Sept. 2	2:40 A.M.	146	420	566		0.348
Sept. 8	3:00 A.M.	175	342	517		0.512
Sept. 14	2:30 A.M.	127	160	287		0.794
Sept. 16	2:30 A.M.	105	135	240		0.778
Sept. 18	2:30 A.M.	215	262	477		0.821
Oct. 7	3:00 A.M.	66	176	242		0.375
Totals		1280	2126	3406	Average	0.602
Day runs						
1957						
Sept. 13	8:55 A.M.	233	138	371		1.688
Sept. 13	10:05 A.M.	267	107	374		2.495
Oct. 1	10:55 A.M.	25	15	40		1.667
Oct. 1	11:55 A.M.	54	22	76		2.455
Oct. 1	12:55 P.M.	37	20	57		1.850
Oct. 15	12:55 P.M.	153	88	241		1.739
Oct. 23	11:55 A.M.	298	396	694		0.752
Oct. 23	2:55 P.M.	256	200	456		1.280
Totals		1323	986	2309	Average	1.342

of lightning discharge (the ground-return stroke), it is conceivable that an ELF waveform without an associated VLF oscillation may originate from natural sources other than lightning. However, the results of the present work, as discussed later in this section, imply that these waveforms are indeed generated from lightning. This is in agreement with the results of *Holzer and Deal* [1956], discussed previously, which indicate that at least a very high percentage of the energy in the ELF band originates in the lightning discharge.

b. Relatively greater attenuation in the VLF than in the ELF band. If this should be the case, the VLF oscillation would die out more rapidly than the slow tail. Since attenuation in the VLF band is known to be very low—sometimes l than 2 db per 1000 km at middle latitudes du ing the day [*Wait*, 1958*c*]—it is implied th attenuation in the ELF band may be even low [Note: Experimental evidence to be present later in this section indicates that the VI oscillation dies out more rapidly than do the slow tail for daytime propagation cond tions.]

c. Source effects. If the rate of current fl in the discharge channel is sufficiently slow, or most of the radiated energy may be in t ELF band.

The present data indicate that the absen of VLF energy in some sferics is due primar to a slow rate of current flow in the dischar

annel and, to a lesser extent, to differences VLF and ELF propagation. The absence of LF energy is not at all likely to be associated th the generation of ELF waveforms from urces other than lightning.

3. *The polarity of ELF signals is predominantly negative at night and positive by day.* ecause of this rather unsual result, a polarity unt of additional data was conducted. The sults are given below. A straightforward interetation of the effect will be given later in rms of differences in propagation conditions tween day and night paths.

Polarity count—In order to investigate furer the apparent polarity reversal of ELF aveforms as observed at night and during the y, a polarity count was made of over 5700 erics. The signals were recorded during eight ght runs and eight day runs. The results are esented in Table 2. For the night runs the sitive-to-negative polarity ratio was always s than unity. For the day runs the polarity tio was greater than unity with but one ception (October 23, 11:55 A.M.). Hence, e results are in agreement with the data in ble 1.

Distributions of slow-tail peak amplitudes—nce the antenna is omnidirectional in the rizontal plane, it may receive signals at any ven time from a number of separate storm nters at greatly different distances (for the ta considered here, it is probable that all orms occurred at distances greater than 3000 les). Obviously, the value of the slow-tail ak amplitude will vary, depending on the stance between the storm center and the reiver. In addition, the mean value of the slowl peak amplitude may vary because of eteorological factors which affect the characristics of lightning discharges in the different orm centers. Hence, a broad spread is to expected in the distribution of slow-tail ak amplitudes. Nevertheless, histograms were otted in the hope of obtaining additional inrmation on the properties of slow tails. Figure shows the amplitude distribution for the ELF aveforms that occur in category 1 of Table It is certain that the ELF signals in this tegory were generated by lightning because e preceding VLF oscillation is known to be aracteristic of the lightning discharge. Note the different scales on the horizontal axis for day and night runs. The following results are apparent from Figure 2.

1. *The median values of the amplitude distributions of both positive and negative polarities are greater for the day runs than for the night runs.* This result may be partly due to the occurrence of storms relatively near the receiver during the day. However, it is more likely associated with the measurement process. During the daylight hours attenuation and dispersion are relatively high in the upper portion of the ELF band as compared with the same quantities at night. The attenuation of the higher frequencies results in a relatively smoother waveform. The increased dispersion results in a longer period for each quasi-halfcycle oscillation. Both attenuation and dispersion contribute to a decrease in the peak amplitude. As a consequence, there is a strong tendency for the smaller ELF signals to overlap and lose their separate identity, resulting in a rather smooth noise-background signal. In order to stand out above the background, an ELF waveform will in general have a higher peak amplitude than is necessary for measurement under nighttime conditions. Hence, it is not surprising that the mean value of the peak amplitude acquires a higher value during the day.

Because of the disappearance of the smaller ELF signals, the apparent ELF sferic rate is decreased during the day. For example, the average ELF rate was 5.75 sferics/sec for the day runs analyzed, compared with 46.1 sferics/sec for the night runs.

The greatly reduced sferic rate during the day might be interpreted as being due to a decrease in relatively near thunderstorm activity. On the other hand, the relatively larger median value of the ELF peak amplitude during the day might be interpreted as being due to an increase in relatively near thunderstorm activity. Since the two interpretations are in direct opposition, it is clear that propagation effects, as discussed above, must predominate in determining the ELF amplitudes and rates rather than the meteorological factors which determine the thunderstorm locations. Furthermore, the greatly reduced ELF sferic rate during the daylight hours is characteristic of observations made at UCLA field stations at different locations over

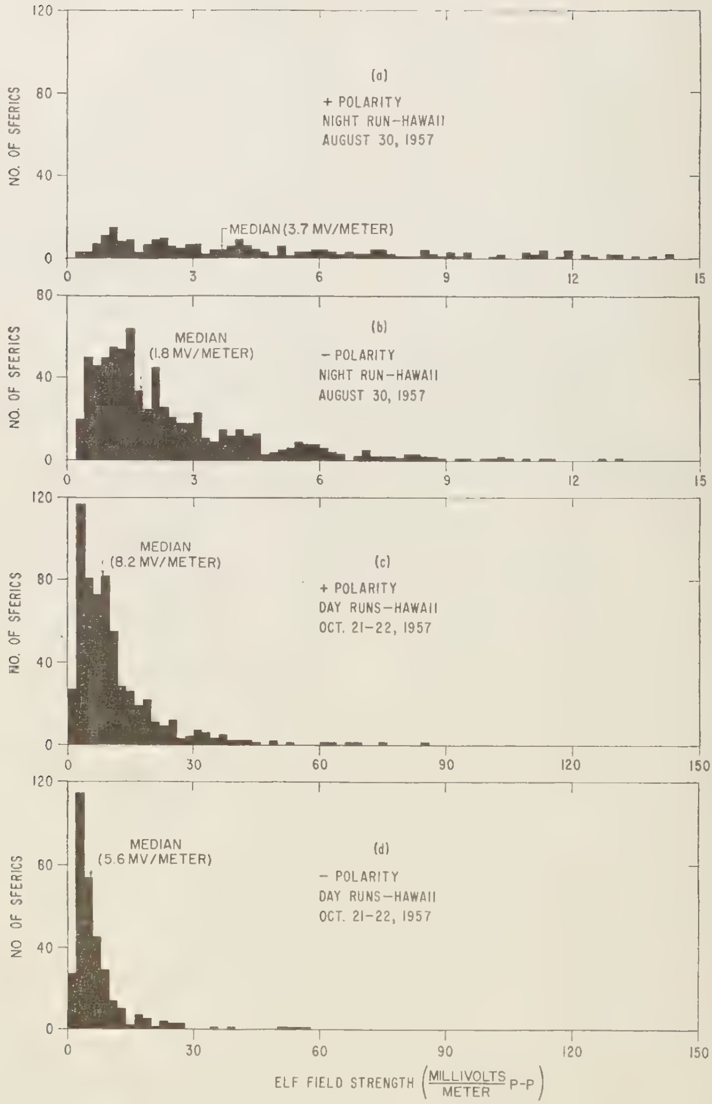

Fig. 2—Distributions for ELF peak amplitudes.

a long period of time. Only when thunderstorm activity is relatively near (say, within 500 km) are the daytime and nighttime sferic rates comparable.

This discussion is not meant to imply that the actual thunderstorm distribution does not affect the character of the signal in the ELF band. In fact, *Holzer and Deal* [1956] were able to relate the diurnal variation of the mean an plitude of the signal in part of the ELF ban (20 to 120 cps) to the diurnal variation in th world-wide thunderstorm distribution. Howeve their observations involved an averaging proc ess that included the contributions of the back ground noise (the small superimposed EL signals), and the argument presented here con

ns only those ELF waveforms that are large ough to be measured individually.

2. *The positive polarity median value exceeds e negative polarity median value for both y and night amplitude distributions.* This re-lt leads to a simple interpretation of the versal of the slow-tail polarity ratio from the ght runs to the day runs. It will be assumed at slow tails are produced in about the same oportion during the day and the night. How-er, since, on the average, the negative slow ils turn out to be of lower amplitude than e positive slow tails, they will disappear into e background noise more rapidly during the ylight hours because of the increase in atten-ation and dispersion. Hence, it is to be ex-ected that the indicated ratio of positive to gative slow tails will be higher for the day ns than for the night runs.

The explanation given above may be suf-cent to account for the reversal of the polarity atio between day and night conditions; how-ver, it is conceivable that meteorological fac-ors may also influence the polarity ratio; that , thunderstorms may develop differently in ifferent geographical locations and during dif-erent times of the day. The result may be an ctual change in the relative number of light-ing discharges in which the direction of cur-ent flow is upward or downward, with a orresponding change in the ratio of the gen-ration of positive and negative slow tails. (For n example of this effect, refer to the discussion f the relative number of intracloud and ground-eturn strokes in heat and frontal storms.)

Histograms were also plotted for the ELF vaveforms for which no VLF oscillations were bserved (category 2 of Table 1). These are ot included but are of the same general ap-earance as the histograms in Figure 2. The imilarity of the distributions strongly suggests hat these waveforms also originate from light-ing discharges despite the absence of the char-cteristic VLF oscillations. If the median values f the amplitude distributions were smaller than he median values of the ELF waveforms of ategory 1, it might be concluded that most of he ELF waveforms in this category came from greater distance than those of category 1 and hat the VLF component disappeared because f the relatively greater attenuation in the VLF band. However, the median values of the am-plitude distribution were found to be similar both for ELF waveforms that possess VLF os-cillations and for those that do not. Hence, it appears that ELF waveforms in both categories are likely to originate in the same thunderstorm area. Furthermore, the polarity ratios for both categories of ELF waveforms are about the same. There appears, then, to be no obvious distinction between the two categories except for the difference in the associated VLF energy.

If the term 'slow tail' is to be taken literally, it cannot be used to describe an ELF waveform not preceded by a measurable VLF oscillation. However, since all ELF waveforms considered here have the same general appearance, and since all appear to have originated from light-ning, it is reasonable to refer to all such wave-forms as slow tails.

It is of interest to compare the results ob-tained here with similar measurements made by *Hepburn* [1957] in England. From 620 ELF waveforms which were studied in detail, he found a positive-to-negative polarity ratio of 7/2. In addition, the waveforms were grouped according to day or night propagation condi-tions, distance from source to receiver, etc. For all categories, the positive-to-negative polarity ratio was greater than 2/1. The results are in approximate agreement with the present work for the daytime records but are in sharp dis-agreement for the night runs.

The discrepancies may partly be attributed to differences in the sensitivity of the record-ing equipment. Because of interference due to power-line harmonics, Hepburn considered only those ELF signals that possessed field strengths greater than 20 mv/m. In the present work, the great majority of ELF signals possessed field strengths of less than the minimum value considered by Hepburn. From Figure 2, it may be observed that the larger ELF signals are predominantly of positive polarity. Hence, if only the larger signals are considered, polarity ratios are obtained that are roughly comparable to those obtained by Hepburn.

Distributions of VLF/ELF amplitude ratios —The peak amplitude of a sferic as observed in either the VLF of ELF band is determined by conditions at the source (the lightning dis-charge) and also by the attenuation and dis-

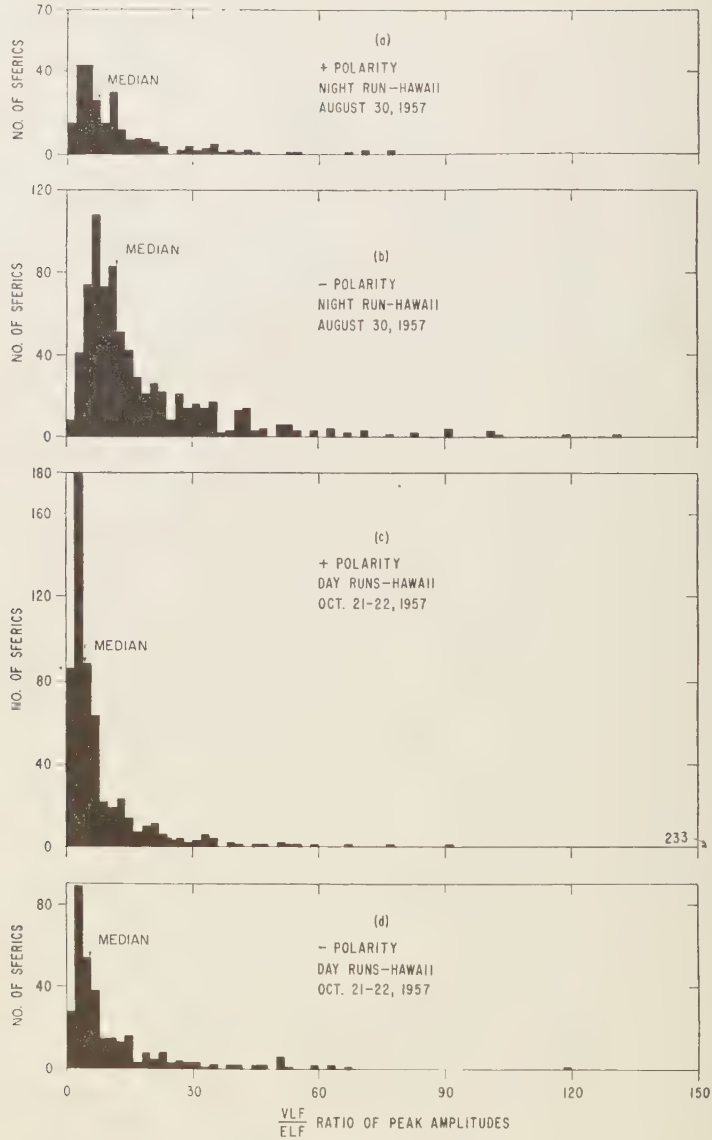

Fig. 3—Distributions for VLF/ELF peak-amplitude ratios.

persion characteristics in the earth-ionosphere waveguide in the band of interest. Because both bands include regions of relatively high transmission, it appears reasonable that the ratio of the VLF to the ELF peak amplitude for any given sferic should be a slowly varying function of the distance between the source and the receiver. Hence, the ratio may be pected to yield information on the relative ergy distribution in the VLF and ELF ba near the discharge channel, irrespective of distance at which the signal is observed. Clea the ratio is only a crude measure of energy tribution. If its variation with distance (wh

ill depend to some extent on the spectral iergy distribution of the individual sferic) greater than anticipated, it will be more difult to apply the ratio to the investigation of urce characteristics.

Nevertheless, ratio distributions were plotted the hope of obtaining information on both urce and propagation effects. Figure 3 shows ie ratio distribution for those sferics for which LF amplitude distributions were plotted in igure 2. The following results are apparent om Figure 3.

1. *The median values of the ratio are higher r signals of like polarity at night than during e day.* The result could be influenced by the ographical location of thunderstorm areas or other meteorological factors, as mentioned eviously. However, the result is in accord ith visual observations made at UCLA over long period of time and appears to be entirely ie to propagation effects. There is a strong iggestion that the relative decrease in peak nplitude for signals in the VLF band is greater ian that for signals in the ELF band for dayme as compared with nighttime propagation onditions. It is known that the VLF attenuaon is greater for a daylight path than for a ark path because of the influence of the *D* yer, which ordinarily exists only during the iy. On the other hand, theoretical consideraons indicate that the *D* layer may be almost ansparent to radiation in the ELF band [*Wait*, 958*a*]. Hence, it seems reasonable to conclude iat propagation in the ELF band will be less ependent on the time of day than will propagaon in the VLF band, and the result presented ere is not surprising.

2. *The negative polarity median value of the tio exceeds the positive polarity median value r both day and night ratio distributions.* The sult implies that, on the average, the peak of ectral energy distribution of the radiation ilse is at a higher frequency when the slow il is of negative polarity. The effect seems be related to differences in mechanism beveen discharges that generated positive and egative slow tails.

Possible Origin of Slow Tails

It is generally agreed that the typical thunderoud is bi-polar in character and of positive polarity; that is, with the concentration of positive charge higher up than the negative charge. However, measurements of the potential gradient near thunderclouds indicate that the charge distribution in some clouds is reversed and that the charge distribution may vary to some extent with the geographical location of the thunderstorm. In addition, a relatively small positive charge often occurs near the base of a cloud below the main negative charge [*Chalmers*, 1957].

Lightning discharges may occur between positive and negative charge centers within a single cloud, between clouds, and between a cloud and the ground. The waveform and relative intensity of the VLF electromagnetic radiation accompanying the discharge varies in a complex manner, according to the nature of the discharge, and has been studied by a number of workers. From the results of *Watt and Maxwell* [1957] and others, it may be concluded that the largest part of the energy radiated in the VLF band is associated with ground-return strokes (although a significant amount of energy was found to be radiated from step and dart leaders, etc.) From measurements made in England, *Horner* [1958] concluded that almost all of the radio noise in the VLF band could be accounted for by ground-return strokes; but from similar measurements made in Australia it appeared that significant VLF energy might originate in other portions of the discharge.

From the results of Watt, Maxwell, and Horner, it may be tentatively concluded that most of the sferics considered in Figures 2 and 3 originated in ground-return strokes, since they possessed measurable VLF components. If this is assumed to be the case, it is of interest to compare the polarity ratios obtained here with the polarity ratios obtained by other workers from close-in observations of ground-return strokes. A close agreement may be anticipated, since the theory of ELF propagation as discussed earlier indicates a one-to-one correspondence between the direction of current flow in the discharge channel and the initial polarity of the slow tail. However, the anticipated agreement does not materialize, as will be made clear in the following discussion.

From measurements in England of electrostatic field changes close to thunderstorms,

Pierce [1955*a*,*b*] found that over 90 per cent of all ground-return strokes are of positive polarity, corresponding to the lowering of a negative charge to the ground. The relatively few ground-return strokes of negative polarity may be explained as being due to discharges between the ground and the large positive charge at the top of the cloud, or to the relatively small positive charge at the cloud base. *Brook* [1957] made similar measurements in New Mexico. He considered only the ground-return strokes as determined by visual observations. Only one stroke out of 700 produced a negative field change. Hence, it appears that the positive-to-negative polarity ratio of the ground-return stroke should always be much greater than unity.

The results presented above indicates that, on the average, slow tails are predominantly negative by a factor of more than 3:1. However, if it is assumed that most slow tails originate from ground-return strokes, the results of Pierce and Brook imply that the polarity ratio should be a large positive number. The discrepancy may be removed by hypothesizing that most of the negative slow tails do not originate from ground-return strokes. In the measurements of the electrostatic field referred to previously, Pierce measured rapid-field changes which were associated with ground-return strokes and were predominantly of positive polarity. He also measured slow-field changes which were associated with intracloud strokes and air discharges and were predominantly of negative polarity. He found that the ratio of slow-negative to slow-positive field changes was about 2:1 for heat storms and about 7:1 for frontal storms. Hence, if it is assumed that slow tails are produced by intracloud as well as by ground-return strokes, a reasonable agreement is attained between the close-in measurements of Pierce and the results reported here.

The above explanation of the observed slow-tail polarity ratio would be entirely plausible if the negative slow tails were not accompanied by large VLF oscillations. However, since the VLF oscillations are present, the explanation implies that a considerable amount of VLF energy is associated with intracloud strokes. In fact, by comparing the histograms of Figures 2 and 3 it may be ascertained that the median VLF peak amplitude is about the same slow tails of both positive and negative polari Hence, if negative slow tails are generated intracloud strokes, and if the VLF peak amp tude is taken as a measure of the VLF ene of the sferic, we are led to the conclusion t intracloud strokes are also responsible fo large part of the total energy in the VLF ba This result is in disagreement with the conc sions of Watt and Maxwell, and of Horner, which most of the VLF energy could be ass ated with ground-return strokes. Hence, above explanation of the observed slow-polarity ratio does not appear to be satisfacto

It should be pointed out that the VLF p amplitude may be taken as a crude meas of VLF energy only if all the received sfe are similar in waveshape and in time durati This appears to be the case in the present periment, as determined from visual obser tions of the triggered VLF waveforms. H ever, such observations may be misleading, it is conceivable that the VLF energy associa with the negative slow tails may be substanti less than that indicated by the VLF p amplitudes. If this should be the case, the agreement indicated above would be resol and the origin of negative slow tails in int cloud strokes would again appear to be plausi It is clear that additional experimental w on the generation of slow tails is needed. particular, it would be desirable to record complete VLF-ELF waveform at a series stations in a direct line as the wave moves o ward from a discharge at a known location.

Acknowledgments—The work presented h is part of an investigation of ELF electromagn propagation conducted at the Institute of G physics, UCLA. The collection, reduction, partial analysis of the data were conducted UCLA under Contract AF 19(604)-1300 with Geophysics Research Directorate, Air Force Ca bridge Research Center. The analysis was co pleted and the present paper was prepared un the sponsorship of Stanford Research Institute

I am particularly indebted to Patricia B who was responsible for the reduction of data UCLA. I am also indebted to Robert Holzer Edward Smith of UCLA and to Raymond Nel of SRI for their comments and assistance in data analysis and in the preparation of this pa I should also like to express my appreciation Henry Blanchard and Edgar Post, who arran for that portion of the work conducted at SR

Appendix

Estimate of VLF field strength from spike amplitude—The VLF peak amplitude may be imated from the amplitude of the spike by nsidering the amount of attenuation introced by the 1000-cps low-pass RC filter. However, any such estimate is subject to error because of the frequency roll-off characteristics db/octave) of the filter. The ratio of the LF amplitude to the amplitude of the spike obviously a function of the spectral energy tribution of the sferic. In order to obtain nethod of calculating field strengths for those rics that did not trigger the VLF sweep, both VLF and the spike amplitude were measd for a large number of triggered waveforms. e ratio noted above was calculated in each e, and an average value was obtained which s used as a correction factor for calculating LF amplitudes for non-triggering signals. For se signals which did trigger the VLF sweep was found that the VLF amplitude, as calated from the spike amplitude and correcn factor, rarely differed from the true VLF plitude by more than a factor of 2. Hence, estimate introduces a maximum uncertainty 2 in the calculated values of each individual LF/ELF peak-amplitude ratio. However, it believed that the errors introduced are likely be averaged out for the large number of rics considered, and that the results would substantially the same if a more accurate thod of calculation were possible.

For the night runs about 90 per cent of all LF amplitudes were determined by the method cussed above. On the other hand, because of ferent propagation conditions encountered ring the day runs and correspondingly different gain settings, the VLF channel was trigred for all but about 10 per cent of those dayne sferics for which a spike was observed. nce, the method was used only rarely to callate peak amplitudes for the day runs.

References

PLETON, A. E., R. A. WATSON-WATT, AND J. F. HERD, On the nature of atmospherics. II, *Proc. Roy. Soc. London A., 111,* 615–653, 1926.

OOK, M., *Thunderstorm Electricity,* New Mexico Inst. Mining and Technol. Research and Develop. Div., Socorro, New Mexico, October 1957.

BRUCE, C. E. R., AND R. H. GOLDE, The lightning discharge, *J. Inst. Elec. Engrs. London, 88,* 487–505, 1941.

CHALMERS, J. A., *Atmospheric Electricity,* Pergamon Press, London, pp. 211–218, 1957.

FLORMAN, E. F., Quarterly report on Project T-506/NBS, *Natl. Bur. Standards, U. S., Rept. 3558,* Boulder, Colo., November 10, 1955.

HEPBURN, F., Atmospheric waveforms with very low frequency components below 1 kc/s known as slow tails, *J. Atmospheric and Terrest. Phys., 10,* 266–287, 1957.

HOLZER, R. E., World thunderstorm activity and extremely low frequency sferics, in *Recent Advances in Atmospheric Electricity,* Pergamon Press, London, p. 559, 1958.

HOLZER, R. E., AND O. E. DEAL, Low audio-frequency electromagnetic signals of natural origin, *Nature, 177,* 536–537, 1956.

HORNER, F., The relationship between atmospheric radio noise and lightning, *J. Atmospheric and Terrest. Phys., 13,* 140–154, 1958.

LIEBERMANN, L., Extremely low-frequency electromagnetic waves, II propagation properties, *J. Appl. Phys., 27,* 1477–1483, 1956.

PIERCE,, E. T., Electrostatic field changes due to lightning discharges, *Quart. J. Roy. Meteorol. Soc., 81,* 211–228, 1955*a*.

PIERCE, E. T., The development of lightning discharges, *Quart. J. Roy. Meteorol. Soc., 81,* 229–240, 1955*b*.

SCHUMANN, W. O., On the propagation of long electric waves around the earth and signals from lightning, *Nuovo cimento, 9,* 1116–1138, 1952.

SCHUMANN, W. O., Uber die zeitliche Form und das Spektrum ausgesendeter Dipolsignale in einer dielektrischen Hohlkugel mit leitenden Wanden, *Verlag Bayerischen Akad. Wiss., Munich,* 1956.

WAIT, J. R., The attenuation vs. frequency characteristics of VLF radio waves, *Proc. IRE, 45,* 768–771, 1957.

WAIT, J. R., An extension to the mode theory of VLF ionospheric propagation, *J. Geophys. Research, 63,* 125–135, 1958a.

WAIT, J. R., Propagation of VLF pulses to great distances, *J. Research Natl. Bur. Standards, 61,* 187–203, 1958b.

WAIT, J. R., A study of VLF field strength data—both old and new, *Geofis. pura e appl., 41,* 73–85, 1958c.

WATT, A. D., AND E. L. MAXWELL, Characteristics of atmospheric noise from 1 to 100 kc, *Proc. IRE 45,* 787–794, 1957.

World Meteorological Organization, Secretariat, World distribution of thunderstorm days, Part 2, *Tables of Marine Data and World Maps,* Geneva, Switzerland, 1956.

(Manuscript received August 10, 1959.)

Upper-Air Density and Temperature: Some Variations and an Abrupt Warming in the Mesosphere

L. M. JONES, J. W. PETERSON, E. J. SCHAEFER, AND H. F. SCHULTE

Department of Aeronautical and Astronautical Engineering
University of Michigan
Ann Arbor, Michigan

Abstract—Measurements of upper-air densities and temperatures from 12 flights of the rocket-borne falling sphere are presented. They show little seasonal variation at 32° and 38°N, but large variations in a few winter days at 59°N. A low arctic density at 60 km results in a linear latitude density gradient of about 2 per cent per degree of latitude. Such a gradient was measured in a latitude survey. An abrupt warming at 45 km was detected at Fort Churchill in January 1958 and related to a warming of larger scope detected by balloons. The average air temperatures above Fort Churchill from January to March are warmer at 75 km and cooler from 50 to 30 km than at 32° to 38°N.

ntroduction—The technique of measuring per-air density to altitudes of about 90 km measuring the drag acceleration of falling eres ejected from rockets has been in use e 1952. Two versions, both developed at the iversity of Michigan, have yielded results 13 flights. The flights were carried out at ite Sands, New Mexico (32°N), Wallops nd, Virginia (38°N), at sea in the North antic and in Davis Strait (49°, 58°, 66°N), at Fort Churchill, Manitoba (59°N), at such es that, in a limited sense, synoptic investigas of significant variations in density and temature are possible.

n the first four flights inflatable nylon spheres et in diameter were carried aloft in Aerobee kets. The spheres carried miniaturized dop- transponders and were tracked by DOVAP n the ground. Data from these flights are ussed below, but the technique and errors, ing been reported previously [*Bartman and ers*, 1956], are not further discussed. In the e recent version, a rigid sphere, 7 inches in meter and equipped with an omnidirectional elerometer, was used (Fig. 1). In this design desired drag acceleration is measured inally and directly so that a ground reference acking) is not required. Thus, the only und facility necessary in addition to a ncher and balloon-sondes is a telemetering und station. The resulting simplicity permits nchings to be carried out away from a major rocket base, and in 1956 five firings were made from the deck of the U.S.S. *Rushmore* (LSD-14). Seven of the small spheres reported here were carried in the Nike-Cajun rocket [*Jones and others*, 1959], one was carried in a Nike Deacon rocket [*Jones and Bartman*, 1956],

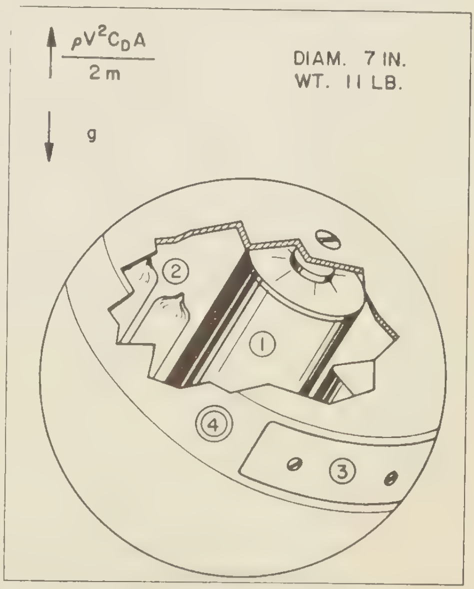

FIG. 1—Sphere and accelerometer: (1) Accelerometer; (2) transmitter and auxiliary circuits; (3) antenna; (4) pressure or electrical port.

and one at Fort Churchill was carried in an Aerobee rocket whose primary function was to transport the grenade experiment for the determination of upper-air temperature and winds [*Stroud and others,* 1958]. An interesting feature of the last eight flights is that the data reduction, originally carried out with desk calculators [*Jones and others,* 1958], was programed for computer. This not only enhances the synoptic capability but also helps to eliminate computational errors. In a continuing effort, automatic data readout is being developed as well.

Technique—In the IGY program the experiment was simplified by the use of an 11-pound rigid sphere, machined from dural to a diameter of 7 inches. The sphere is ejected from the rocket somewhere between 55 and 70 km on the ascent. The sensor is a transit-time accelerometer [*Jones,* 1956] which measures, in any direction, the acceleration of drag on the sphere. In this device a small bobbin is alternately caged and released, at 1-sec intervals, within a cavity which is the same distance (3/16 inch) from the bobbin along all radii. A 10-μ sec RF pulse is transmitted at the instant of bobbin release and another at the instant of contact of bobbin with cavity. The time between the two pulses together with the distance provides a measure ($a = 2s/t^2$) of the relative acceleration of the sphere with respect to the bobbin. Since their relative velocity is negligible, the bobbin is drag-free, and thus the measured acceleration is the drag acceleration of the sphere. The pulses are transmitted by a 400-Mc/s transmitter in the sphere which drives a flush-mounted slot antenna at a peak power of 32 watts. The pulses are received on the ground with two oppositely polarized helical antennas. The mixed demodulated receiver outputs result in an essentially isotropic signal from the sphere. The pulses are recorded on a multichannel magnetic tape which also carries a precision 100-kc/s signal. The 100-kc/s signal is started at rocket take-off. The raw data consist of accelerometer transit times as a function of rocket time.

In the data reduction process [*Peterson and others,* 1959], drag accelerations are computed as a function of rocket time. These values at high altitudes are, to within a negligible error, symmetrical about peak time. The peak time is obtained from the symmetry and an appro[...] mate peak altitude determined from the rad[...] measured performance of previous Nike-Ca[...] rockets. In some cases, the rockets have b[...] tracked, thus providing the peak data wh[...] the absence of up-leg data prevents use of [...] symmetry method. In two flights both meth[...] were used. The trajectory is calculated by d[...]ble integration of the vector sum of grav[...]tional and drag accelerations with respect [...] time, starting at peak. A small correction [...] horizontal velocity, which is estimated f[...] the launching angle (usually 85°), is ma[...] Having obtained the trajectory, the densit[...] calculated from the drag equation

$$ma_D = \rho V^2 C_D A/2$$

where

m = sphere mass
a_D = drag acceleration
ρ = ambient density
V = velocity
C_D = coefficient of drag
A = sphere cross-sectional area

Velocity values are known from the traject[...] analysis. Values of C_D as a function of Reyn[...] number and Mach number are taken from [...] compilation of values measured in balli[...] ranges and wind tunnels over the range of th[...] numbers encountered by the flight sphe[...] After ρ has been calculated as a function [...] altitude down to balloon heights, the resul[...] compared with densities obtained from ballo[...]sondes, and an adjustment, typically less t[...] 1 km, is made in altitude so that the sp[...] data and balloon data coincide. The validit[...] the process is supported by the fact tha[...] the three large-sphere flights (SC-29, 30, [...] and in one small-sphere flight (DAN 2) [...] which ground tracking was used, the den[...] data from the sphere and balloon experim[...] coincided in the overlap interval (Figs. 2 [...] 3). After the altitude adjustment is made, [...] trajectory and density calculations are [...]peated, for small corrections, starting from [...] new initial altitude.

Once the density has been obtained a[...] function of altitude, the ambient tempera[...] is calculated by the integral relation

$$T_h = \frac{\int_h^{h_0} \rho_h g \, dh}{\rho_h R/M} + \frac{\rho_0}{\rho_h} T_0 \qquad (2)$$

ained by combining the equations of state
l of hydrostatic pressure, where

T = absolute temperature
= density
= acceleration of gravity
= altitude
R = gas constant
M = molecular weight (known to be constant from 0 to 90 km)

this process the integration is performed wnward from a high initial altitude h_0. A ue of T_0 for the starting altitude h_0 must be osen. A reasonable choice is that of the ARDC nosphere [*Minzner and Ripley,* 1956]. It can shown that the error in T_h due to a large or in the choice of temperature T_0 at the rting altitude will be eliminated within 15 . Therefore, temperature results are given altitudes about 15 km below the measured nsities.

In a typical good flight (AM 6.03) the sphere s ejected at 70 km on the up-leg and reached eak altitude of 170 km. Drag measurements rted just below 100 km (on both the ascent d descent) at which point the drag accelera- n was 1.25×10^{-8}g. The maximum vertical locity of 1490 meters/sec occurred at 44 km. maximum acceleration of 9.2 g was encount- ed at 24.4 km.

Errors—In the sphere experiment, errors due winds are neglected. The neglect of a verti- wind of 20 meters/sec would cause a maxi- um error of about 5 per cent in density in the nge of the experiment, whereas the neglect of horizontal wind of 100 meters/sec would use a 3 per cent error. Horizontal winds eater than 100 meters/sec are rare in the per atmosphere. The magnitude of vertical nds is generally unknown.

If the bobbin is imperfectly centered, the in of the sphere imparts an initial velocity the bobbin, and the resulting scatter in the easured accelerations increases with altitude. is effect becomes noticeable at 70 to 80 km d has prevented measurement of densities ove 90 km.

In the best range of the experiment (30 to 75 km) the major error is that due to uncertainty in coefficient of drag. *Bartman* [1956] and *Peterson and others* [1959] estimated the probable error in C_D to be about ± 2 per cent for values of C_D near 1. At low Reynolds numbers (above 75 km) the coefficient of drag and its error increase. Density, being inversely proportional to C_D in the drag equation, has the same percentage errors. Temperature is a function of the quotient of the integral of density by the density, and there is a tendency for errors to compensate slightly. Practically, the percentage errors in temperature may be taken to be the same as those in density. Thus, for the small-sphere experiment the estimated probable errors in density and temperature are ± 2 per cent below 75 km and ± 5 per cent above 75 km. Because temperatures are usually plotted with suppressed zero, as in Figure 5, the scatter is apparently magnified and smoothing by averaging over 3- to 5-km intervals was used. In Figure 6 the probable errors of the averages computed from 4 to 7 points are indicated by bars. To avoid the errors due to an error in the choice of T_0 in equation (2), as discussed above, the temperatures are plotted to about 15 km below the highest densities.

The importance of balloon radio-sonde data to 25 or 30 km in the absence of ground tracking should be noted. For example, in the shipboard firings the accelerometer mechanism experienced difficulty in caging the steel bobbins at 25 km where the accelerations approached 10 g. The resulting altitude error accumulated down to the low balloon altitudes amounted to ± 2 km, which is equivalent to a large density error. The difficulty was eventually circumvented by using Weather Bureau balloon data for the same times from nearby weather stations and ships. The Fort Churchill flights in which magnesium bobbins were used gave much better results. In addition, the balloon data to 30 km provided by the hypsometer-equipped sondes (launched by the White Sands Signal Agency at Fort Churchill) contributed greatly to the confirmation of the sphere data in the high-drag region.

Although acceleration data are recorded all the way to impact, a low-altitude limit of about 18 km to which densities may be calculated is set by two aerodynamic phenomena. Here the

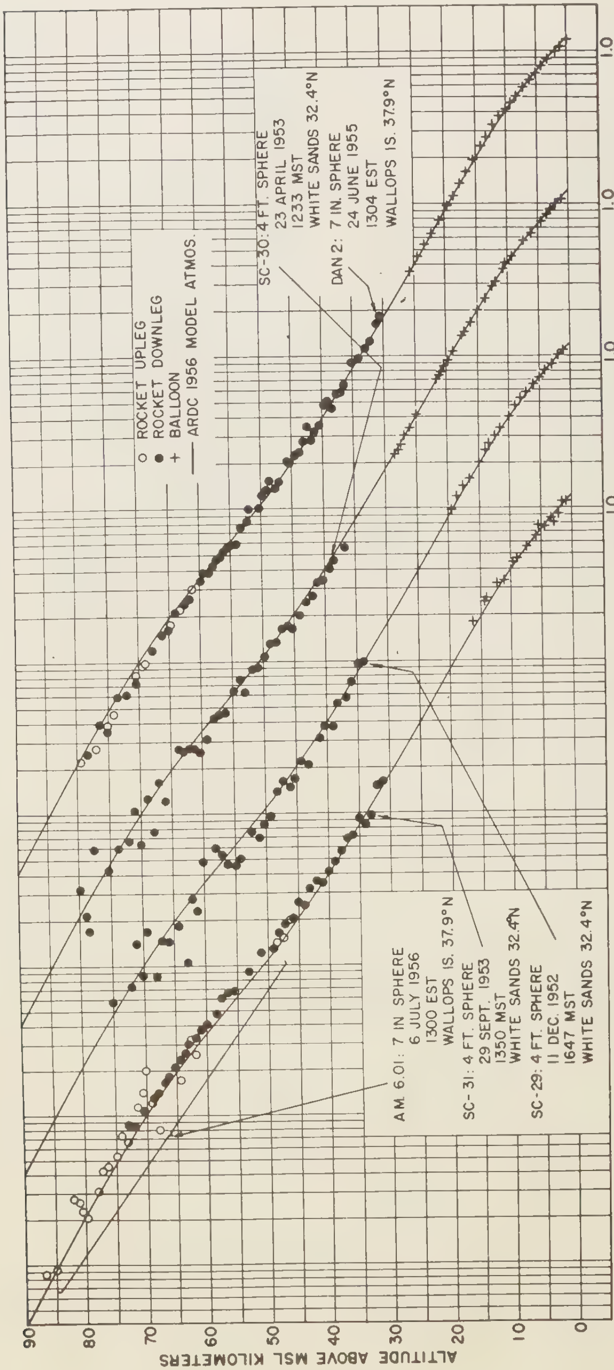

FIG. 2—Upper air density. Five flights at various seasons: White Sands, New Mexico (32.4°N), and Wallops Island, Virginia (37.9°N).

t that the Mach number falls below 1.3 l the drag coefficient curve falls away rather rply from a value of unity suggests that character of the flow about the sphere y be changing. The Reynolds number is ut 5 × 10^5, which is in the right range for ndary-layer transition phenomena [*Gold-n*, 1938]. In this case the drag is very sensi-e to minor differences in surface finish on sphere and turbulence in the air. As a sequence, large variations in the ballistic-nel values for C_D and discrepancies between se and the flight spheres are to be expected. ow 18 km also, scatter in the acceleration a increases. This is believed to be caused by unsteady condition of flow accompanied by eral accelerations which cannot be distin-shed from the vertical by the omnidirectional elerometer. Other aerodynamic experiments h spheres have revealed such a phenomenon *unnon*, 1928; *Liebster*, 1927].

Results—The unsmoothed densities of 12 hts are plotted as a function of altitude in ures 2, 3, and 4. In these plots and in Fig-e 5 the solid lines are taken from the ARDC del Atmosphere [*Minzner and Ripley*, 1956], ich well represents the atmosphere at 32°N d which serves as a convenient reference for nparison. In the density plots, the results m individual flights are displaced by one ade in density, whereas the altitudes are ed up to facilitate comparison.

Figure 2 shows the results of two small-here flights and three large ones at White nds (32.4°N) and Wallops Island (37.9°N). seasons of the year are represented between 52 and 1956. Inasmuch as independent track-g was used in all these flights, the balloon data re not used to determine sphere altitudes, and e generally good agreement between balloons d spheres may be seen. The flights confirm the DC values as good averages for these lati-des. A small variation amounting to ±11 r cent at 50 km can be seen. The variation es not seem to have a seasonal pattern. Just ove 50 km the two summer flights, AM 6.01 d DAN 2, are slightly above and slightly be-w the ARDC reference, respectively.

In Figure 3 the results of the shipboard firings 1956, in which a latitude survey was at-mpted, are shown. Data from a winter rocket (SC-29) at White Sands are also included so that values from 32.4°N to 65.6°N can be com-pared. The largest change is near 60 km, where the negative density gradient with increasing latitude is nearly linear and amounts to 1.9 per cent (of the density at the median latitude) per degree of latitude. Variations in density at a single northern latitude, shown by the next group of flights at Fort Churchill, indicate that a latitude density gradient such as the one de-tected by the shipboard flights might or might not be expected at any given time, depending on the northern densities.

Results of four firings at Fort Churchill in the winter of 1958 are shown in Figure 4. It is apparent that the winter densities at Fort Churchill are generally lower than those at 32°N, as represented by the ARDC curve. At 50 km the average of the four flights is 26 per cent below the ARDC value at the same alti-tude. The relative constancy of the surface pres-sure distribution over the earth inhibits similar depressions in density at lower altitudes. In Figure 4 the densities at 20 km coincide with the ARDC value, and at the surface the average of the four plots is 12 per cent higher than the ARDC value. *Sissenwine and others* [1958] have shown that at a similar latitude (St. Paul's Island, Alaska, 57.1°N) the point of maximum departure of balloon-measured densities from the ARDC values is −8 per cent at 14 km for the January average of several years. The cor-responding January average density from the three rocket flights at 50-km altitude is 29.6 per cent less than the ARDC value. Although larger variations in density are to be expected at higher altitudes than at low, one may wonder whether or not these are typical changes, espe-cially in view of the fact that in the 2-day period from January 27 to 29 the density at 50 km increased 79 per cent over the January 27 low. The presence of an anomaly is indicated by the temperatures. The temperatures, cal-culated from the densities and averaged in Figure 5, illustrate the corresponding large in-crease on January 27 to 29 in the mesosphere. Abrupt warming at balloon altitudes early in the year has been reported in several instances; for example, by *Scherhag* [1952], who discovered the effect, and by *Craig and Hering* [1959]. *Teweles and Finger* [1958] described an abrupt

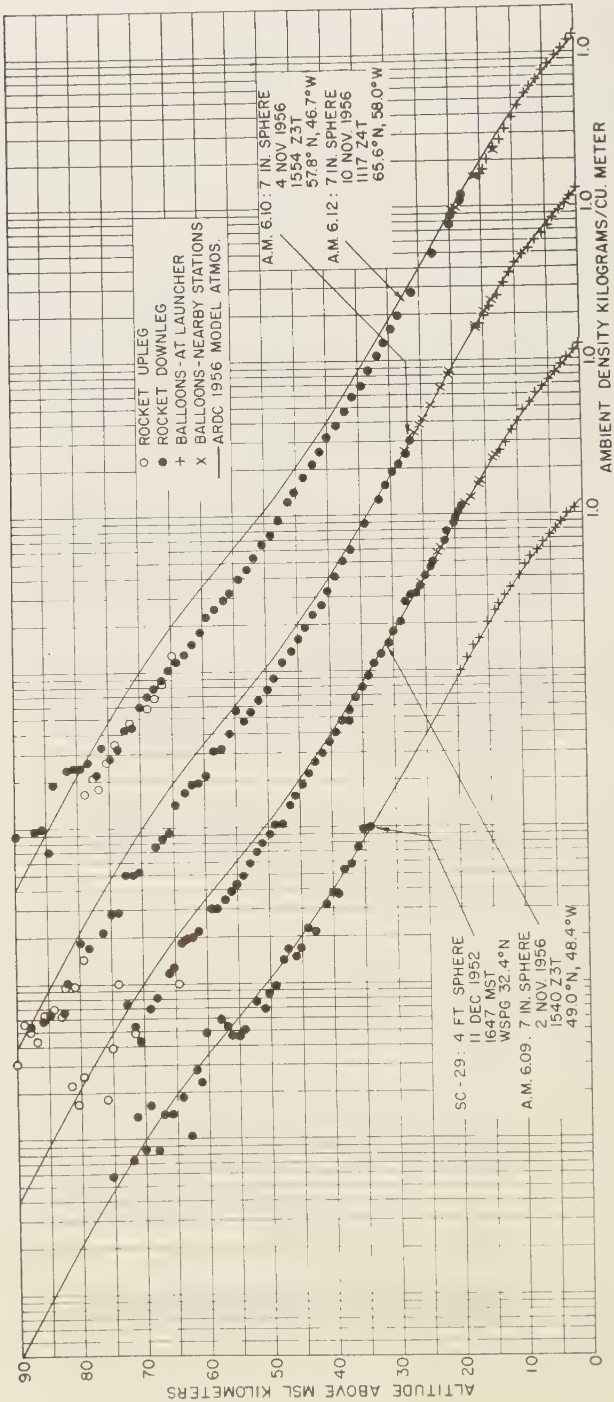

FIG. 3—Upper air density. Four wintertime flights at various latitudes.

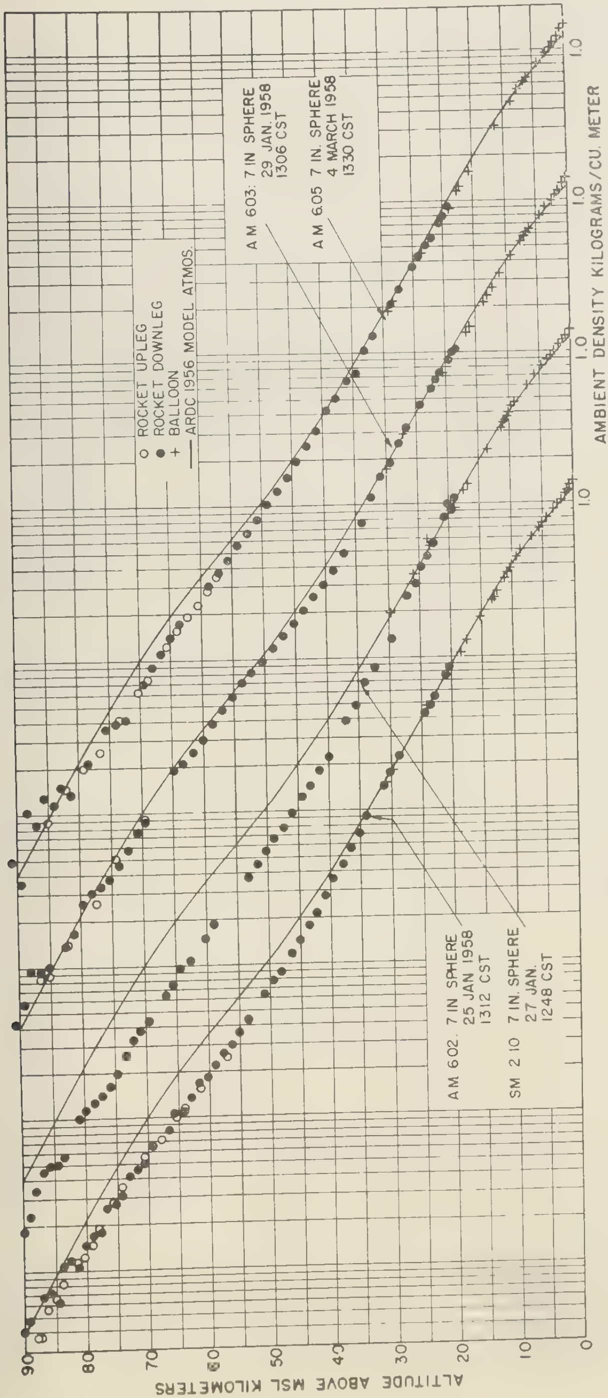

FIG. 4—Upper air density. Four wintertime flights at Fort Churchill, Manitoba (58.7°N).

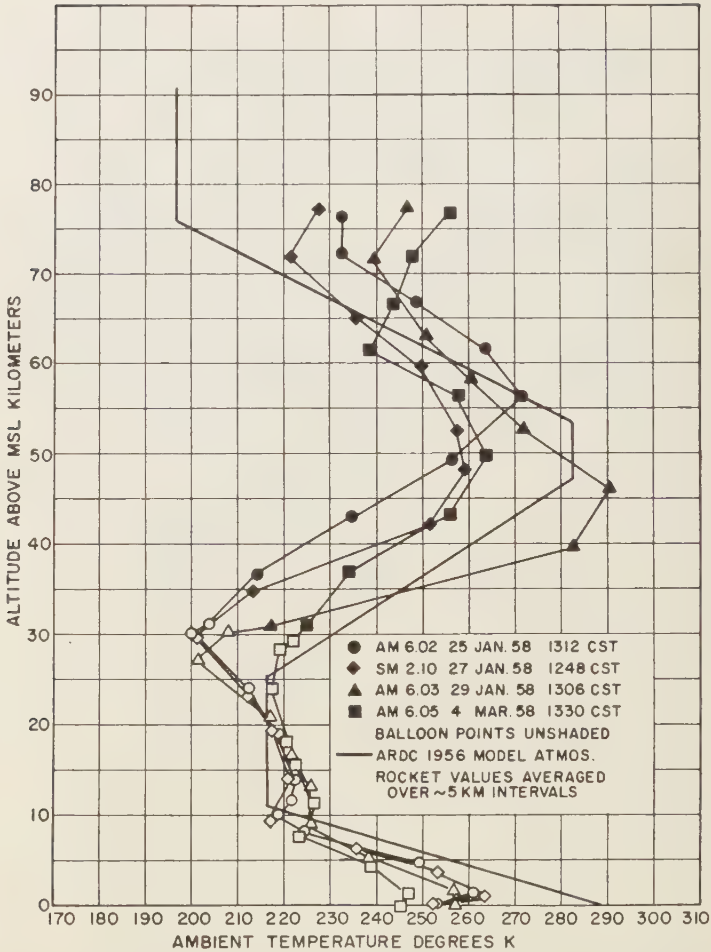

FIG. 5—Upper air temperature. Four wintertime flights at Fort Churchill, Manitoba (58.7°N).

change in stratospheric circulation accompanied by warming at 25 mb (~25 km) in January 1958. They show that at Washington, D. C., the warming started on January 27, and by January 31 an increase of 22°K had occurred, after which the temperature dropped. Temperatures at various constant altitudes for January, February, and March as obtained from balloons and rockets at Fort Churchill are plotted in Figure 6. The warming may be seen at 20 km; it started about January 30 and rose approximately 17°K by February 3, after which it declined to typical winter averages in late Feb-

ruary and early March. At 30 km, again fro balloon data (which are unfortunately not cor plete), the rise in temperature was not le than 30°K and appeared to start about Janua 28 or 29. The date and magnitude of the ter perature peak cannot be ascertained. At 45 k the rocket data show an increase of 47°K star ing about January 26. Although the magnitu and date of the peak are again not know the highest temperature was reached on Ja uary 29, which was early in the rise of t 30-km temperatures and definitely before a change in the 20-km temperatures. The rock

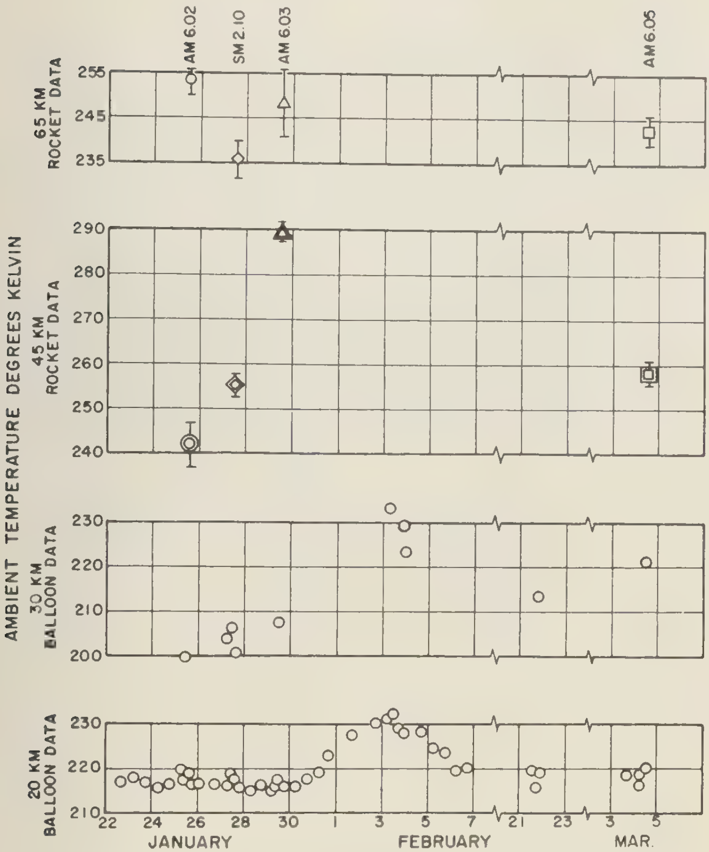

IG. 6—Abrupt warming at balloon and rocket altitudes, Fort Churchill, Manitoba (58.7°N), winter 1958.

ata at 65 km are also shown. The changes are ot as great as at lower altitudes and less significance can be attached to them because of ie larger errors. However, it is interesting to ote that at 65 km the highest temperature ccurred on January 25 and to speculate hether an even earlier rise may have occurred t this altitude. The over-all picture presented y the data is one of a warming at 45 km (and robably higher) which moves downward 25 m in four days and which decreases in magniude during the process. *Palmer* [1959] hypothezes that during an explosive warming the ratopause (base of the region of positive temerature gradient) moves downward with time ıd that in the region immediately above the stratopause a relatively large downward movement of air occurs. He states: "This strongly indicates that the breakdown of the vortex occurs first at very high levels (above 30 km) and proceeds, like the propagation of a disturbance, downward toward the tropopause." The Fort Churchill sphere data indicate that the temperature increase required to accompany an adiabatic downward motion of air does indeed occur at high altitudes and propagates downward. There is, however, a significant difference in the events at Fort Churchill and those at Alert (82.5°N), described by Palmer. He shows at Alert, at the 15-km level, a large increase in density strongly correlated with an increase in the coronal index and the acceleration of the

orbital period of Sputnik 1957β_1. At Fort Churchill, on the other hand, the density at 15 km shows no unusual gradients between January 1 and February 7. The only density change at rocket altitudes is the increase which occurs simultaneously with the temperature increase at these altitudes. This suggests that the Fort Churchill warming at rocket altitudes may result from the lateral motion at moderate velocities of an effect originating elsewhere, a process consistent with Teweles' description of events at lower altitudes. An alternative view of the time of descent of the temperature peak at Fort Churchill is possible; namely, that instead of being due to the adiabatic warming of a descending air mass it is due to the lateral movement of a warm air mass having a slant profile.

The average temperature profile of the northern winter atmosphere obtained from the sphere flights is not unexpected [see, for example, *Pant*, 1956]. Relative to the atmosphere at 32° to 38°N there is a warming at 75 km which averages 40°K. At 50 and at 30 km, on the other hand, the temperature averages are lower by 25°K than at 32° to 38°N. At 40 km wintertime densities are lower at 59°N than at 32°N; this is consistent with the measurements of *LaGow and others* [1958].

Acknowledgments—The data presented here resulted from the efforts of many people over a period of years. Often the work of our colleagues, F. L. Bartman, F. F. Fischbach, W. H. Hansen, and N. J. Wenk, was as intensive as our own. We are indebted to Air Force Cambridge Research Center for cooperation and financial support throughout, to the National Science Foundation for financial help during IGY, and to the Signal Corps for supporting the early inflatable-sphere work. We wish also to thank the people at White Sands, Wallops Island, and Fort Churchill and aboard the U.S.S. *Rushmore* for their invaluable aid in launching the rockets.

References

Bartman, F. L., L. W. Chaney, L. M. Jones, and V. C. Liu, Upper-air density and temperature by the falling sphere method, *J. Appl. Phys., 27,* 706-712, 1956.

Craig, R. A., and W. S. Hering, The stratospheric warming of January-February 1957, *J. Meteo 16,* 91–107, 1959.

Goldstein, S., *Modern Developments in Fl Dynamics,* Oxford Univ. Press, 495 pp., 1938

Jones, L. M., Transit-time accelerometer, *R Sci. Instr., 27,* 374–377, 1956.

Jones, L. M., and F. L. Bartman, A simpli falling sphere method for upper air dens *Univ. of Mich., Eng. Research Inst. Rept. 2 10-T,* 1956.

Jones, L. M., F. F. Fischbach, and J. W. Pet son, Seasonal and latitude variations in up air density, *Natl. Acad. Sci., IGY Rocket R Ser., 1,* 47–57, 1958.

Jones, L. M., W. H. Hansen, and F. F. Fis bach, Nike Cajun and Nike Deacon, in *Sou ing Rockets,* H. E. Newell, Jr., ed., McGr Hill, New York, 190–219, 1959.

LaGow, H. E., R. Horowitz, and J. Ainswor Rocket measurements of the arctic upper atm phere, *Natl. Acad. Sci., IGY Rocket Rept. S 1,* 26–37, 1958.

Liebster, H., Über den Widerstand den Kug *Ann. Physik, 82,* 541–562, 1927.

Lunnon, R. G., Fluid resistance to mov spheres, *Proc. Roy. Soc. London, A, 118,* 6 690, 1928.

Minzner, R. A., and W. S. Ripley, The AR model atmosphere, 1956, *Air Force Surveys Geophysics, 86,* Air Force Cambridge Resea Center, Bedford, Mass., 201 pp., 1956.

Palmer, C. E., The stratospheric polar vorte winter, *J. Geophys. Research, 64,* 749–764, 19

Pant, P. S., Circulation in the upper atmosph *J. Geophys. Research, 61,* 459-474, 1956.

Peterson, J. W., H. F. Schulte, and E. J. Sch fer, A simplified falling-sphere method for up air density, Part II, *Univ. of Mich., Eng. search Inst. Rept. 2215-19-F,* 1959.

Scherhag, R., Die Explosionartigen Stratosph nerwärmungen des Spätwinter 1951/1952, *Deut. Wetterdienst in der US-Zone, 38,* 51 1952.

Sissenwine, N., W. S. Ripley, and A. E. C Behavior of atmospheric density profiles, *Force Surveys in Geophysics, 109,* Air F Cambridge Research Center, Bedford, M 1958.

Stroud, W. G., W. R. Bandeen, W. Nordb F. L. Bartman, J. Otterman, and P. Tı Temperatures and winds in the Arctic as tained by the rocket grenade experiment, *N Acad. Sci., IGY Rocket Rept. Ser., 1,* 5 1958.

Teweles, S., and F. G. Finger, An abrupt cha in stratospheric circulation beginning in January 1958, *Monthly Weather Rev., 86,* 23 1958.

(Manuscript received July 30, 1959.)

Barbados Storm Swell

WILLIAM L. DONN AND WILLIAM T. MCGUINNESS

Lamont Geological Observatory
(Columbia University)
Palisades, New York

Abstract—Severe and damaging surf often strikes Barbados and other islands of the Lesser Antilles. Owing to the broad reef shelf, the nature of this surf has not been well understood. Wave and tide recorders maintained in Barbados during IGY have furnished useful data for the explanation of this phenomenon. The strong swell responsible for the coastal surge has been related to intense extratropical cyclones in the North Atlantic Ocean through use of wave travel times based on the group velocity appropriate to the period of the observed swell. A procedure for future forecasts is suggested.

ntroduction—Unusually high and often dam-ıg sea waves have long beset the coast of bados in the British West Indies. These es have not been associated with any local nown Caribbean storms. Attempts to explain m on the basis of tsunamis or submarine l-slides also proved unsuccessful. A major iculty heretofore has been the lack of any cise observational information on the wave ameters. This problem was overcome with establishment of Barbados as an IGY nd Observatory station by the Lamont ological Observatory (Columbia University) ooperation with the Naval Research Labora-. Although similar coastal conditions have n noted at other islands of the Windward Leeward group, this investigation was ricted to Barbados.

he significant oceanographic data were ained from the Mark IX wave meter *odgrass*, 1956], installed at a depth of about feet in water off Bathsheba on the eastern st and the standard tide gage located on tern coast at St. James. Both locations are wn in Figure 1. Note that the wave meter ust outside the coral reef.

n the basis of data obtained, it can be shown t the severe coastal disturbances are the ect effects of high swell radiating from remote ddle-latitude storm areas in the North Atlantic ean. Two severe cases which occurred during

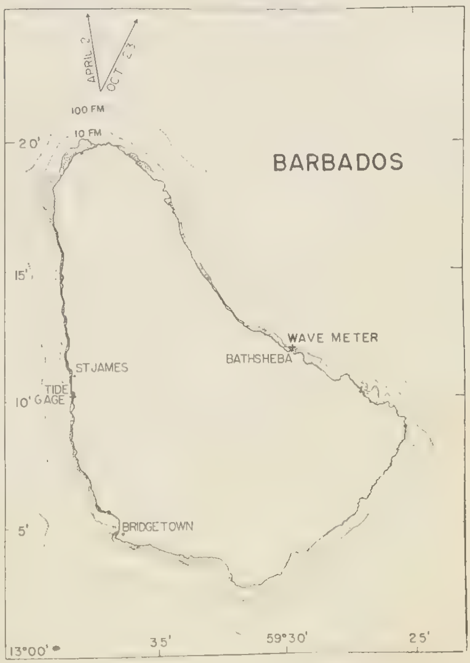

FIG. 1—Chart of Barbados showing 10- and 100-fm depth contours and locations of IGY instruments. The stippled area is a shallow, submerged reef zone.

IGY (1957–1958) will be described in detail in this report and two other confirmatory cases will be described more briefly.

Case I: April 4 to 6, 1958—During this interval

amont Geological Observatory Contribution . 385.

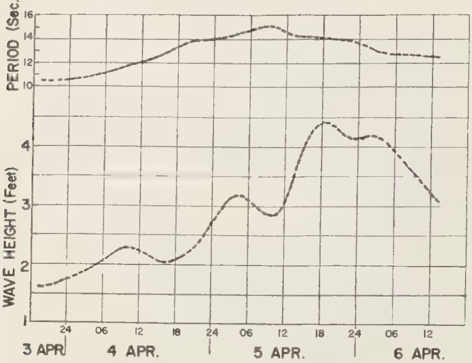

FIG. 2—Bathsheba wave data, April 3 to 6, 1958.

the entire coast of Barbados suffered damage from high swell and surf; strong effects were observed along the lengths of both the eastern and western sides of the island.

Data from the Bathsheba wave meter are summarized in Figure 2. The amplitude curve which represents the significant wave height (the average of the highest one-third of the waves) shows the first increase above background just prior to 2400 on April 3. Maxim wave height occurred at about 1800 on Apr almost two days after the onset. Wave per which increased at about the time of first he increase, reached a maximum of 15 secc shortly before the time of maximum height. period represents the average period of dominant waves measured over a 10-mir interval every two hours.

The St. James marigram for this interva reproduced directly in Figure 3. Although tide well which contains the float is constru to filter out normal swell, the strong surf eff at this time show plainly on the record. interval of high waves on both sides of island can be seen to occur at nearly the s time from a comparison of Figures 2 and 3.

It thus appears that the damaging originated from typical but strong ocean sv and this immediately suggests a probable st origin. Although no directional data are av able for the swell, the absence of any tropica subtropical storms in the area indicates a n remote origin. According to the weather ch of the North Atlantic Ocean, a large, inte

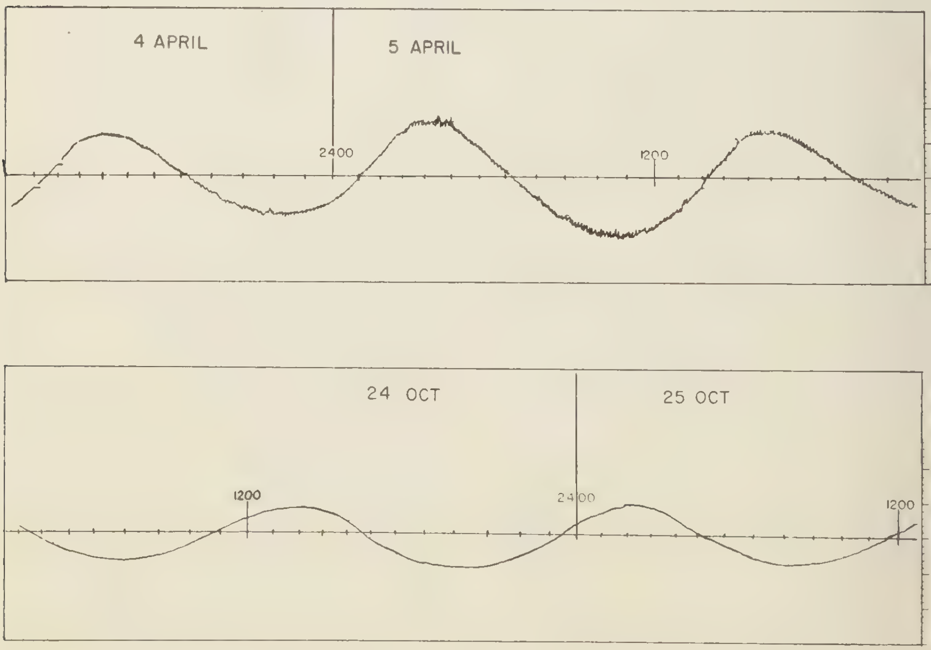

FIG. 3—Photographs of St. James tide records for the cases discussed.

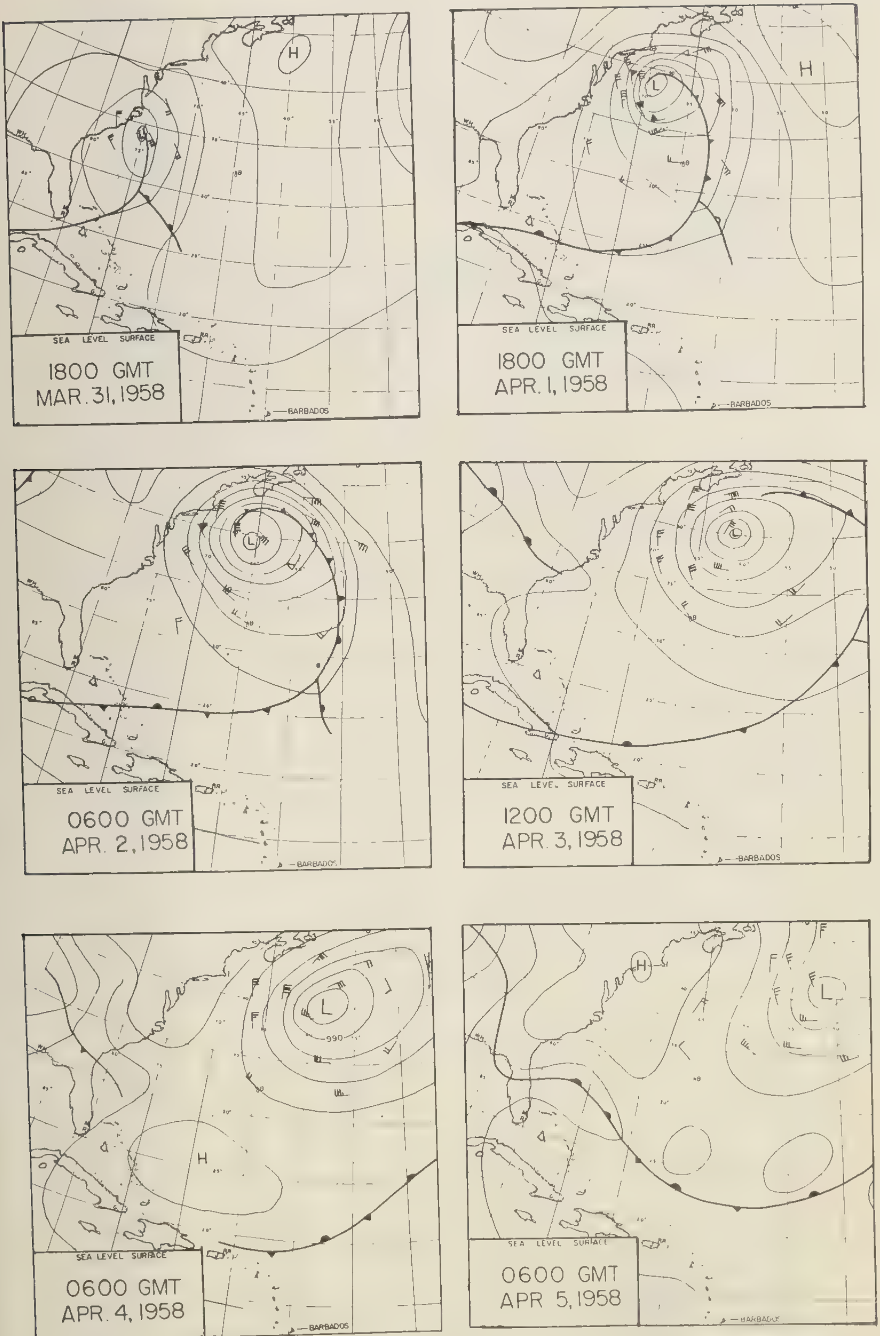

Fig. 4—Weather charts showing the North Atlantic storm associated with case I. (Isobars are drawn for 6-mb intervals. Arrows fly with the wind; each full barb represents 10 knots; each flag, 50 knots.

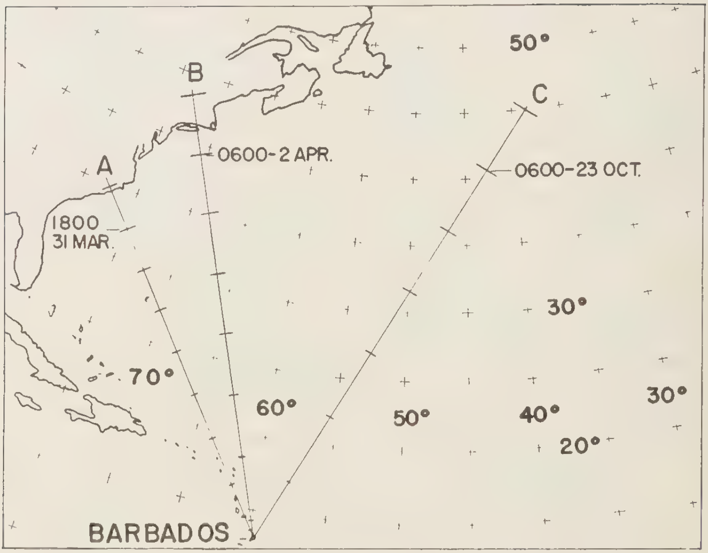

Fig. 5—Chart showing small arcs of probable storm-swell isochrones
Paths *A* and *B* refer to case I; *C*, to case II

extratropical cyclone traveled northeastward in the western part of the ocean after originating off Cape Hatteras on March 31. The progress and development of this storm from March 31 to April 5 is summarized in the six charts of Figure 4. During April 1 and 2, 45- to 50-knot observed winds prevailed over a fairly long southerly fetch in the western half of the storm.

A simple test of the relation of the Barbados swell to this storm is made by using travel times for the waves corresponding to two points on the wave curves, one near the beginning and one at maximum.

The wave period at 0800, April 4, was 11 seconds. Using a group velocity of 16.75 knot we have constructed position arcs, or isochrone as along ray *A*, at prior intervals of 12 hour and for the times of standard weather char (Fig. 5). When compared with the positions possible generating areas shown on the weath charts, the isochrone for 1800, March 31, appea to correspond well with the position of t storm at that time. Similarly, if we use t group velocity of 22.5 knots for the 15-sec wav at 0900 on April 5, it is evident that the isochro of the wave position for 0600, April 2 (as f

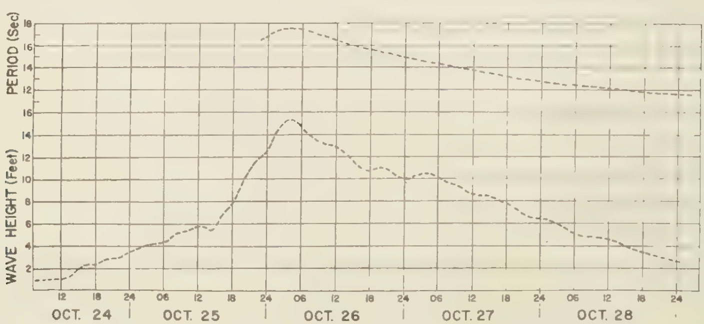

Fig. 6—Bathsheba wave data, October 24 to 28, 1958

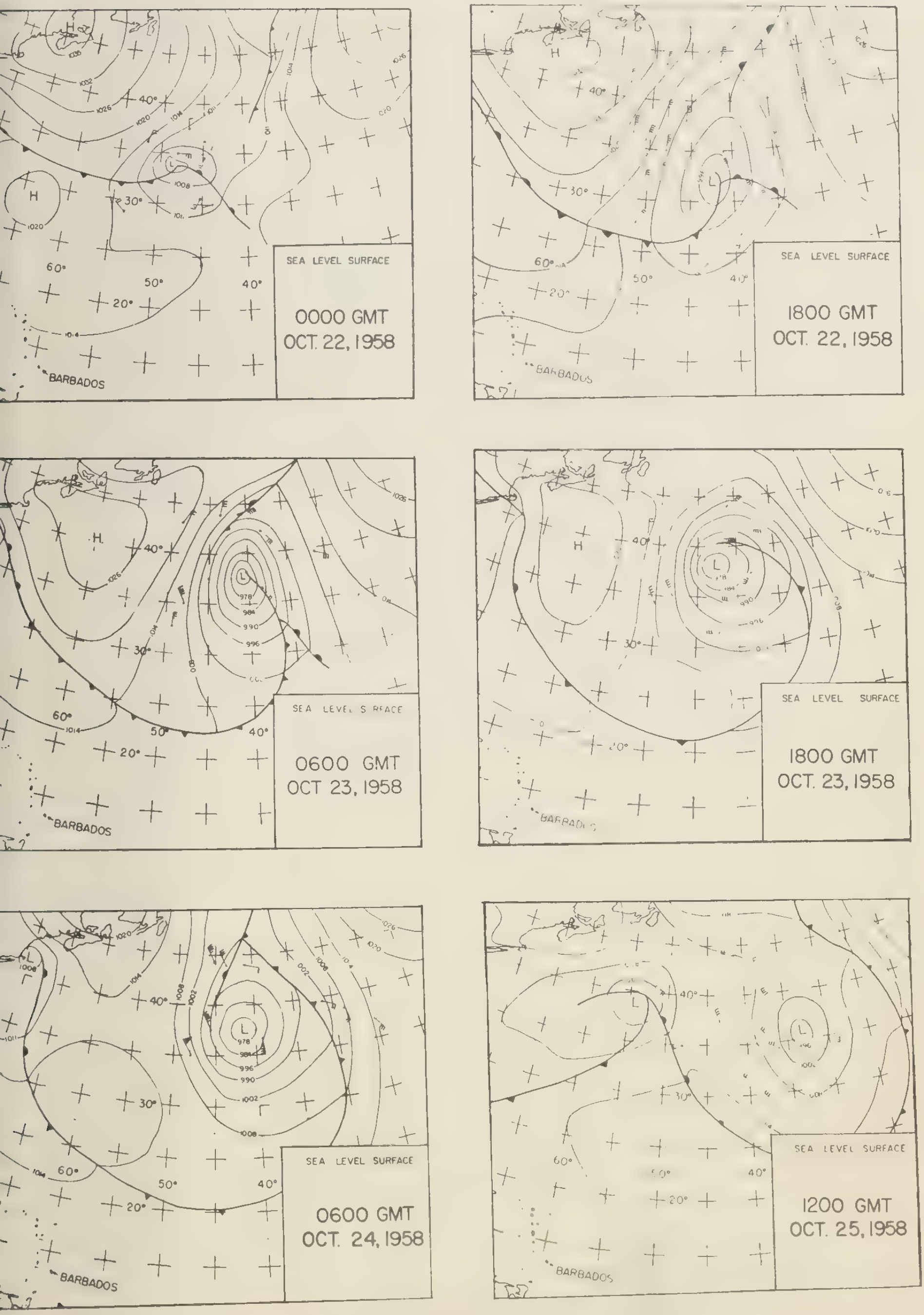

Fig. 7—North Atlantic weather charts showing the storm associated with case II.

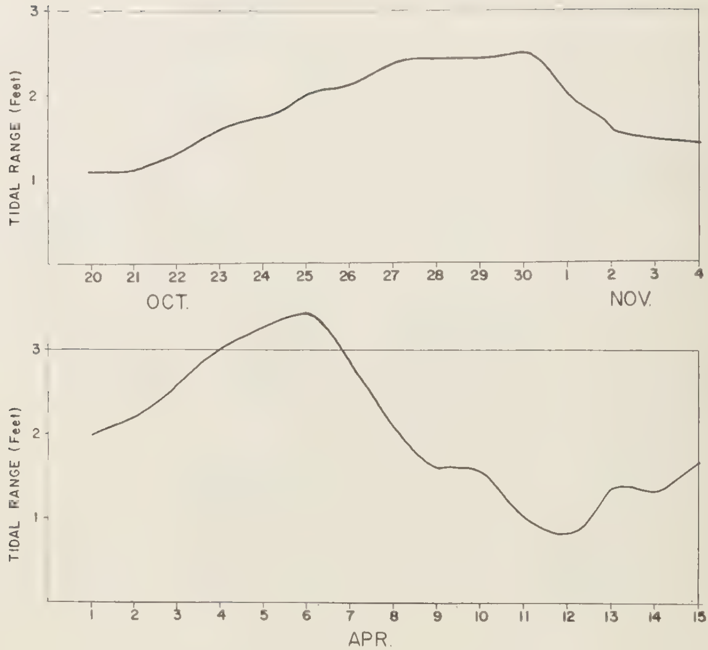

FIG. 8—Curves showing the tidal range associated with the storm swell at cases I and II.

ray *B*), intersects the intense storm area at about the same time. A discrepancy of 2 to 3 hours in precise meeting of the waves and storm is well within the experimental error of the procedures involved, particularly as the weather charts are issued at only 6-hour intervals. Note that as the storm moved northeastward the position of best fit kept pace. It thus seems definite that the Barbados swell originated in this coastal storm and that the longer period and higher waves were generated later and at a somewhat greater distance from the station.

Case II: October 24 to 28, 1958—During October 25 and 26, 1958, the eastern coast of Barbados was battered by extremely high, unusually severe surf. Waves up to 30 feet in height pounded the coast through the night and early morning of the 25th and 26th. Fishing boats of all sizes were hurled onto the beach, and water and sand cascaded into the rooms and cellars of coastal dwellings.

The wave record of this storm from the deep-water recorder at Bathsheba is shown in Figure 6. According to the amplitude curve, the earliest indication of wave increase occurred at abo 1200 on October 24, followed about a day lat by a relatively rapid rise in wave height. should be noted that during the morning October 25 and prior to the rapid rise, the dee water wave height already exceeded that the storm of April 4 to 6, described above, a the surf was even then described by fishermen being of record height.

Although maximum significant wave heig which occurred between 2400 and 0600, Octob 26, was about 15 feet, individual waves reach higher than 18 feet even in the relatively de water above the wave recorder.

Maximum wave period of nearly 18 secon was simultaneous with maximum height. U fortunately, wave period during the initial h of the disturbance could not be read from t records. Both wave height and period decreas slowly during the next three days, with reco heights still occurring through October 26 and 2

The North Atlantic weather charts (Fig. show the growth and decay of a large, inten low-pressure area (extratropical cyclone) betwe

ctober 22 and 25. During the two days of aximum intensity (October 23 and 24) the orm moved very slowly, with the center close 40°N, 40°W.

We followed the method described above and ed a group velocity of 27 knots for the waves maximum period at time of Barbados wave aximum, and we found that a good coincidence swell and storm occurred during the morning October 23 (Fig. 5, ray *C*). The swell isochrone r 0600 intersects the storm area at the same ne and certainly indicates that the maximum urbados swell probably originated in the storm a time when it was large and intense. As the orm was nearly stationary, the resulting wave neration received greater effect from the tch, duration, and speed of the wind than it ould have if the storm had followed the more mmon 20-to-30-knot speed to the northeast.

No reports of unusual surf were made for the estern coast during the interval of record as along the eastern shores. The marigram 'ig. 3) shows no prominent surf activity during is time, such as was evident on the record of pril 4 to 6.

Discussion—The effects of these storms thus ffered in magnitude and distribution of the vell. Although the reported winds did not differ gnificantly for the April and October storms, e pressure gradient for the October storm was stinctly stronger in the western half, at least uring the interval centered around 1800 on ctober 23. Further, the duration of maximum nds, as well as the fetch, was distinctly greater r the October storm.

Although the possibility of somewhat higher nd speeds plus the increased duration and tch can at least qualitatively account for some the difference between the Barbados swell r these storms, there still seems to be a large explained differential.

An attempt was made to arrive at quantitative timates of expected swell by applying the ave and swell forecast procedures given in ydrographic Office Publications 603 and 604. ne error in height, period, and arrival times tween forecast and observed swell was too rge to provide an explanation for the discrepancy between the two storms, and it was so too large for good operational forecasts.

A large part of this error and of the difference between the two storms may be explainable on the basis of refraction. The directions of wave travel are indicated in Figure 1, which shows arrows pointing toward each of the storms. Clearly, the swell from the April storm, in arriving from the north, would spread southward along both the eastern and western coasts of Barbados but would suffer considerable refraction in developing surf along the shore. It is quite evident from air photographs of refracted swell that the resulting extension of the crests may result in considerable decrease in amplitude. Some change in period is also likely.

Swell from the October storm, arriving from the northeast, would strike much more directly on the eastern coast, with relatively little refraction, while the western coast would be mostly sheltered from this swell. Although severe coastal extratropical cyclones with appropriate fetch to produce Barbados rollers may occur a few times a year, mid-ocean storms like that of October 1958 are much more rare, as are cases of the extreme Barbados swell generated by this storm.

Qualitatively, at least, the difference in distribution and magnitude of the swell between the April and October storms thus seems explainable on the basis of refraction and sheltering. Adequate shore data are not available to us at

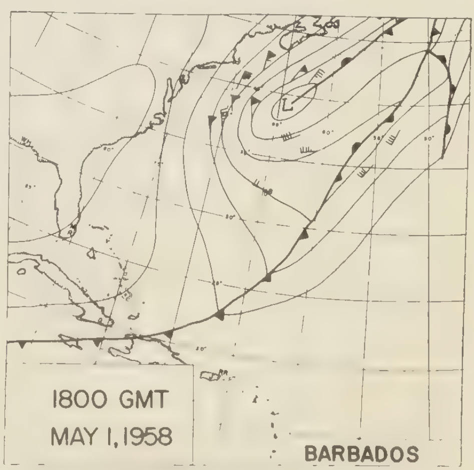

Fig. 9—Chart showing severe extratropical cyclone associated with high Barbados surf on May 3 to 5, 1958.

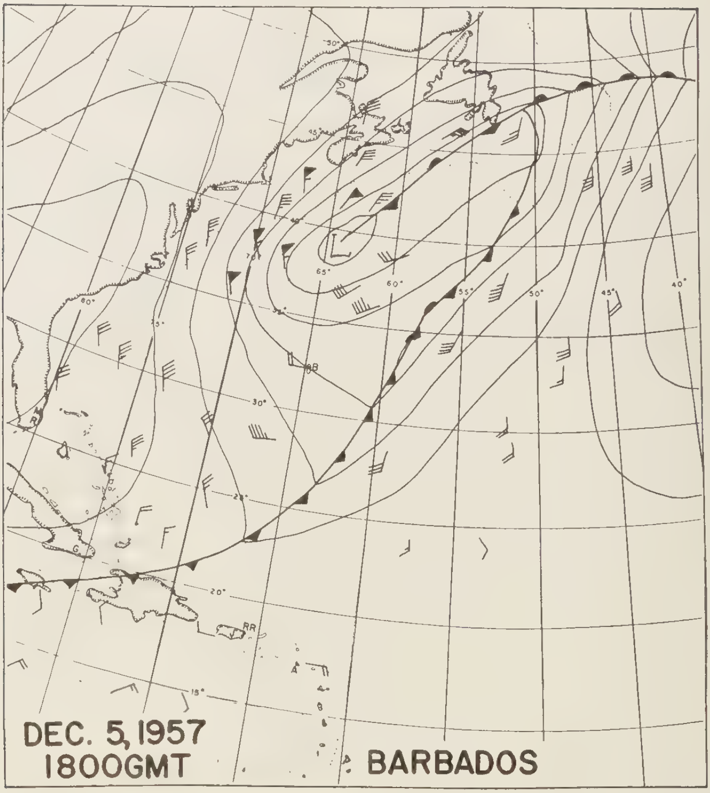

FIG. 10—Chart showing severe storm associated with high Barbados surf on December 7 to 9, 195

present for evaluating these effects quantitatively.

Tidal effects—The relation between the occurrence of storm swell and the phase and range of tide seems also to be of importance in determining shore effects. The difference between the range of the spring and neap tides at Barbados (St. James) is about 2 feet, resulting from a 3-foot spring tide and a 1-foot neap tide range. Tide-range curves for April and October are shown in Figure 8. Clearly, the high surf of April 4 to 6 occurred at exactly the time of spring tide and that of October 25 and 26 occurred about halfway between spring and neap tides. Normal swell, particularly at times of low tide or neap tide range, tends to break on the reef and leave the shore unmolested. Swell at times of spring tide can clear the reef and break on shore during high water. High swell which may arrive during the high phase of spring tides th becomes a threat. Even the effects of the hi swell of October 25 and 26 were modulated the tide phase, as the severest effects we reported for the afternoon and early morni of the 25th and 26th, respectively, or at t times of high tide.

Although part of the failure in the wa forecasting attempts mentioned above was result of subjective elements in estimating fet and duration, this effect could partially removed in the 'hindcasting' process in whi the terminal swell was recorded. However, t recorded swell was certainly modified in amp tude and period by coastal refraction. T effect has not yet been evaluated, but it certai introduces further difficulty in correlating o served and forecast swell. Further, for purpo of verification, the power spectrum of the o

ved swell should be correlated with the fore-
t spectrum. At present, it seems that an
equate warning of a dangerous surf condition
uld be obtained from qualitative estimates
sed on North Atlantic weather data and local
e heights. Considerable refinement can be
de in this method by maintaining case
tories.

Other cases—Another case of high surf for
58 occurred during May 3 to 5, and an earlier
e occurred during December 7 to 9, 1957.
ving either to incomplete installations or
temporary breakdowns of wave-recording
uipment, complete wave records of these
rms were not obtained. However, on the
sis of reports plus available data, the North
lantic weather charts were examined at the
propriate earlier times suggested by the
esent study, and it was found that two intense
stern North Atlantic storms had existed at
ese times. Winds exceeding 50 knots and
nilar in location and behavior to those of the
rm of April 1958 were reported. Figures 9 and
show the appearance and location of these
rms at about the time of maximum develop-
nt.

Conclusions—Storm rollers and surf at
rbados (and in the Lesser Antilles, in general)
t related to local storms seem to be explainable
the basis of generation in large and intense
d-latitude extratropical cyclones in the North
lantic Ocean. By simply monitoring weather
arts of the North Atlantic Ocean it should be
ssible to make qualitative forecasts of the
rival of the storm swell in the Barbados area
least two or three days in advance. Special
ecautions should be taken if this arrival is
pected during the interval of spring tides.

Further detailed study, including wave-spectrum determination and refraction corrections, will be necessary in order to make possible the quantitative forecasting of the precise arrival time, height, and period of the storm swell.

From the study thus far it appears that storms to the north (off the eastern coast of the United States) generate swell which affects both sides of Barbados but which suffers considerable amplitude loss from refraction. It is probable that mid-ocean storms of great intensity will principally strike the eastern coast with an effect that will be a function of size, intensity, and route of travel of the storm.

The explanation of the Barbados surf in terms of high swell from distant storms places this swell in a class with the well-known 'rollers' of the South Atlantic and Indian oceans. These long-period rollers, also of distant-storm origin, can produce breakers and surf reaching 40 feet in height on the coasts of islands in these oceans.

Acknowledgments—This research was part of IGY Project 9.3 (Island Observatories), supported by a grant from the National Science Foundation to Columbia University (Lamont Geological Observatory). The cooperation of the Naval Research Laboratory and, in particular, of J. E. Dinger is gratefully acknowledged. J. B. Lewis of the Bellairs Research Institute (McGill University) on Barbados supervised the maintenance of field instruments and forwarded records. Roger Zaunere and Rudolph Romano aided in the field installations.

References

Snodgrass, F., Mark IX shore wave recorder, *Proc. First Conf. on Coastal Engineering Instruments, Council on Wave Research,* 61–100, 1956.

(Manuscript received August 6, 1959.)

Formulas for Computing the Tidal Accelerations Due to the Moon and the Sun[1]

I. M. LONGMAN

Institute of Geophysics, University of California
Los Angeles, California

Abstract—A summary of formulas with which the tidal accelerations due to the moon and the sun can be computed at any given time for any point on the earth's surface, without reference to tables, is presented in this paper. These formulas are convenient for computer use.

ntroduction—The basic formulas for the nputation of the vertical and horizontal nponents of tidal acceleration, g_0 and h_0, on igid earth have been given by a number of thors. The analysis is given, for example, by *odson* [1921], *Schureman* [1924], *Pettit* [1954], l *Bartels* [1957]. A good account is also given *Doodson and Warburg* [1941]. Schureman's nual was reissued as a revised edition in 11, but in this paper references are given the older edition in cases where a particular mula no longer appears in the new edition, a result is less accurately given there. The ential first step in all these formulations is expression of the effective tidal acceleration terms of the zenith angle and the distance of tide-producing body. From this point there two main lines of development. Doodson, ureman, and Bartels proceeded to develop lunar and solar tides into their harmonic stituents, whereas Pettit gave formulas h which the tidal forces can be computed h the aid of tables from the *American Nautical manac*.

The author was recently engaged in program- g_0 for an electronic computer. The computer s to display g_0 as a function of time for any en place on the earth's surface, starting at y given epoch. For this purpose it seemed irable to use a closed form for the expression g_0, rather than its harmonic development, l to obviate the use of tables in the computa- n. The formulas of Schureman were cast into form convenient for the purpose, and the resulting expressions were used in a g_0 program for an IBM 709 computer. In view of the usefulness of this program it appears to the author that a summary of the formulas used is of interest.

Theory—The symbols used in this discussion are

- a earth's equatorial radius (6.378270×10^8 cm)
- a' defined in equation (31)
- a_1' defined in equation (32)
- A ascending intersection of moon's orbit with the equator
- c mean distance between centers of the earth and the moon
- c_1 mean distance between centers of the earth and the sun (1.495000×10^{13} cm) [*Pettit*, 1954]
- C defined in equation (34)
- d distance between centers of the earth and the moon
- D distance between centers of the earth and the sun
- e eccentricity of the moon's orbit (0.054899720 [*Shureman*, 1924, p. 172]; 0.05490 [*Shureman*, 1941, p. 162])
- e_1 eccentricity of the earth's orbit
- g_0 vertical component of tidal acceleration due to the sun and the moon
- g_m vertical component of tidal acceleration due to the moon
- g_s vertical component of tidal acceleration due to the sun
- h mean longitude of the sun
- h_0 horizontal component of tidal acceleration due to the sun and the moon

[1] Institute of Geophysics Publication No. 147. is research was supported by the Office of val Research under Contract Nonr 233(19).

h_m horizontal component of tidal acceleration due to the moon
h_s horizontal component of tidal acceleration due to the sun
H height of point of observation above sea level
i inclination of the moon's orbit to the ecliptic
I inclination of the moon's orbit to the equator
l longitude of moon in its orbit reckoned from its ascending intersection with the equator
l_1 longitude of sun in the ecliptic reckoned from the vernal equinox
L terrestrial longitude of general point P on earth's surface
m ratio of mean motion of the sun to that of the moon (0.074804 [*Schureman*, 1941, p. 162)
M mass of moon
N longitude of the moon's ascending node in its orbit reckoned from the referred equinox ($N = \Omega\Upsilon'$ in Fig. 1)
p mean longitude of lunar perigee
p_1 mean longitude of solar perigee
P general point on the earth's surface
r distance from P to the center of the earth
s mean longitude of moon in its orbit reckoned from the referred equinox
S mass of sun
t hour angle of mean sun measured westward from the place of observations
t_0 Greenwich civil time measured in hours
T number of Julian centuries (36,525 days) from Greenwich mean noon on December 31, 1899
α defined in equations (15) and (16)
θ zenith angle of moon
λ terrestrial latitude of general point on earth's surface
μ Newton's gravitational constant
ν longitude in the celestial equator of its intersection A with the moon's orbit (side $A\Upsilon$ in Fig. 1)
ξ longitude in the moon's orbit of its ascending intersection with the celestial equator
σ mean longitude of moon in radians in its orbit reckoned from A
Υ vernal equinox
Υ' referred equinox
φ zenith angle of sun
χ right ascension of meridian of place o observations reckoned from A
χ_1 right ascension of meridian of place o observations reckoned from the verna equinox
ω inclination of the earth's equator to th ecliptic = 23.452° [*Schureman* 1941, p. 16
Ω moon's ascending node

Referring to *Schureman* [1941, p. 13], we se that, if the fifth power of the moon's paralla (which could only contribute less than 0.0 per cent of the total tide-producing force) ignored, the vertical component (upwards) o the lunar tidal force per unit mass at a point on the earth's surface is

$$g_m = \frac{\mu M r}{d^3}(3\cos^2\theta - 1) + \frac{3}{2}\frac{\mu M r^2}{d^4}(5\cos^3\theta - 3\cos\theta) \qquad (1$$

To the same order of accuracy the horizont component is

$$h_m = \frac{3}{2}\frac{\mu M r}{d^3}\sin 2\theta + \frac{3}{2}\frac{\mu M r^2}{d^4}(5\cos^2\theta - 1)\sin\theta \qquad (2$$

The expressions for the components of tid acceleration due to the sun are similar, th terms depending on the fourth power of th sun's parallax being negligible. Thus

$$g_s = \frac{\mu S r}{D^3}(3\cos^2\varphi - 1) \qquad (3$$

$$h_s = \frac{3}{2}\frac{\mu S r}{D^3}\sin 2\theta\,\varphi \qquad (4$$

$$g_0 = g_m + g_s \qquad (5$$

and

$$h_0 = h_m + h_s \qquad (6$$

In order to express g_0, h_0 as functions of th time for any given point P (given latitude and longitude L), it is necessary to obtai θ, φ, d, and D as functions of time, and r as function of latitude (and altitude). *Schurema*

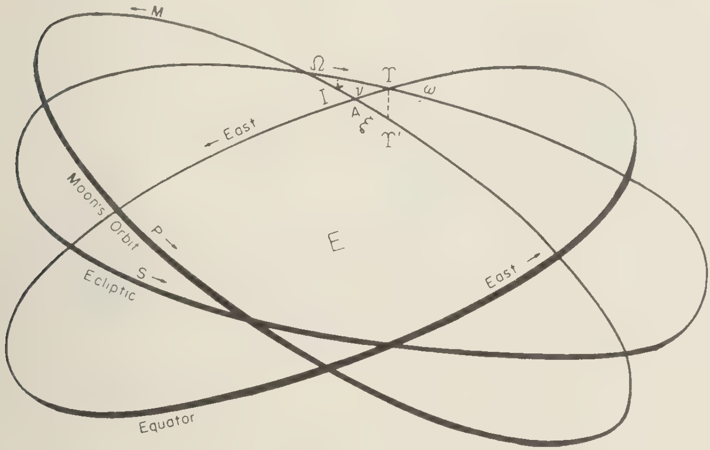

FIG. 1—Orbital parameters.

24, p. 30, equation 81] derives the relation*

$$s\ \theta = \sin \lambda \sin I \sin l + \cos \lambda \left[\cos^2 \tfrac{1}{2}I \cos (l - \chi) + \sin^2 \tfrac{1}{2}I \cos (l + \chi)\right] \quad (7)$$

similar relation holds for the sun's zenith gle φ:

$$s\ \varphi = \sin \lambda \sin \omega \sin l_1 + \cos \lambda \left[\cos^2 \tfrac{1}{2}\omega \cos (l_1 - \chi_1) + \sin^2 \tfrac{1}{2}\omega \cos (l_1 + \chi_1)\right] \quad (8)$$

Schureman [1941, p. 19] gave for the longitude the moon in its orbit

$$= \sigma + 2e \sin (s - p) + \frac{5}{4} e^2 \sin 2(s - p) + \frac{15}{4} me \sin (s - 2h + p) + \frac{11}{8} m^2 \sin 2(s - h) \quad (9)$$

d (p. 162) the following expressions for s, p, h:

$$= 270° \ 26' \ 14.72'' + (1336 \text{ rev.} + 1{,}108{,}411.20'')T + 9.09''T^2 + 0.0068''T^3 \quad (10)$$

$$p = 334° \ 19' \ 40.87'' + (11 \text{ rev.} + 392{,}515.94'')T - 37.24''T^2 - 0.045''T^3 \quad (11)$$

$$h = 279° \ 41' \ 48.04'' + 129{,}602{,}768.13''T + 1.089''T^2 \quad (12)$$

These expressions may be compared with those given by *Bartels* [1957, p. 747]. Bartels' formulas are equivalent to

$$s = 270° \ 26' \ 11.72'' + (1336 \text{ rev.} + 1{,}108{,}406.05'')T + 7.128''T^2 + 0.0072''T^3 \quad (10')$$

$$p = 334° \ 19' \ 46.42'' + (11 \text{ rev.} + 392{,}522.51'')T - 37.15''T^2 - 0.036''T^3 \quad (11')$$

$$h = 279° \ 41' \ 48.05'' + 129{,}602{,}768.11''T + 1.080''T^2 \quad (12')$$

σ is given by the relation

$$\sigma = s - \xi \quad (13)$$

With reference to Figure 1, a little elementary spherical trigonometry shows ξ to be given by

$$\xi = N - \sin^{-1} (\sin \omega \sin N/\sin I) \quad (14)$$

In order to render the inverse sine in this formula

* This relation is not given in *Schureman* [1941], ere the development of the tidal forces has en rearranged.

unique, we also apply a cosine formula to the spherical triangle $\Omega A \Upsilon$. Denoting the side ΩA by α, we then have

$$\cos\alpha = \cos N \cos\nu + \sin N \sin\nu \cos\omega \quad (15)$$

where ν is the side $A\Upsilon$ (Fig. 1) and is the longitude in the celestial equator of its intersection A with the moon's orbit; ν is given by equation (21) below, while $\sin\alpha$ is given, as above, by

$$\sin\alpha = \sin\omega \sin N/\sin I \quad (16)$$

From the values of $\sin\alpha$ and $\cos\alpha$ we compute $\tan(\alpha/2)$ from the formula

$$\tan(\alpha/2) = \sin\alpha/(1 + \cos\alpha) \quad (17)$$

Now since α lies in the interval $(0, 2\pi)$, $\alpha/2$ lies in $(0, \pi)$ and hence when α is computed as

$$\alpha = 2\tan^{-1}[\sin\alpha/(1 + \cos\alpha)] \quad (18)$$

its value is uniquely determined.

The longitude N of the moon's node is given by *Schureman* [1941, p. 162]

$$N = 259° \; 10' \; 57.12'' - (5 \text{ rev.} + 482{,}912.63'')T + 7.58''T^2 + 0.008''T^3 \quad (19)$$

Bartels [1957, p. 747] gives a formula which is equivalent to

$$N = 259° \; 10' \; 59.81'' - (5 \text{ rev.} + 482{,}911.24'')T + 7.48''T^2 + 0.007''T^3 \quad (19')$$

The inclination I of the moon's orbit to the equator is given by

$$\cos I = \cos\omega \cos i - \sin\omega \sin i \cos N \quad (20)$$

I is always positive and varies between about 18° and 28°. Also ν is given in terms of I, N by the relation

$$\nu = \sin^{-1}[\sin i \sin N/\sin I] \quad (21)$$

and here the inverse sine is unique, since we always have $-15° < \nu < 15°$. *Schureman* [1941, p. 162] gives

$$i = 5.145° \quad (22)$$

The angle χ in (7) is given by

$$\chi = t + h - \nu \quad (23)$$

For a point P on the earth's surface with longitude L, the value of t is

$$t = 15(t_0 - 12) - L \quad (24)$$

expressed in degrees.

Equations (9) to (24) enable us to determine the moon's zenith angle from equation (7).

Turning now to equation (8) for the sun's zenith angle, we see that the sun's longitude l_1 is given by

$$l_1 = h + 2e_1 \sin(h - p_1) \quad (25)$$

According to *Schureman* [1941, p. 162] p_1 is given by

$$p_1 = 281° \; 13' \; 15.0'' + 6{,}189.03''T + 1.63''T^2 + 0.012''T^3 \quad (26)$$

and e_1 is given* by *Schureman* [1924, p. 172] as

$$e_1 = 0.01675104 - 0.00004180T - 0.000000126T^2 \quad (27)$$

Bartels [1957, p. 747] gave an almost identical expression for p_1:

$$p_1 = 281° \; 13' \; 14.99'' + 6188.47''T + 1.62''T^2 + 0.011''T^3 \quad (26')$$

The quantity χ_1 is given by

$$\chi_1 = t + h \quad (28)$$

Equations (25) to (28) suffice to determine the sun's zenith angle from equation (8).

Referring to equations (1) to (4) we see that if we use the known values of μ, M, S, that is [*Pettit*, 1954],

$$\mu = 6.670 \times 10^{-8} \text{ cgs units}$$
$$M = 7.3537 \times 10^{25} \text{ grams}$$
$$S = 1.993 \times 10^{33} \text{ grams}$$

the tidal forces are determined if we know d, the distance between the centers of the earth and moon, and D, the distance between the centers of the earth and sun. Both quantities

* *Schureman* [1941, p. 162] merely gives $e_1 = 0.01675$, epoch Jan. 1, 1900.

re variable, being given by the relations Schureman, 1924, pp. 55 and 172]

$$/d = 1/c + a'e \cos(s - p)$$
$$+ a'e^2 \cos 2(s - p)$$
$$+ (15/8)a'me \cos(s - 2h + p)$$
$$+ a'm^2 \cos 2(s - h) \qquad (29)$$

$$1/D = 1/c_1 + a_1'e_1 \cos(h - p_1) \qquad (30)$$

Iere c = mean distance between the centers f the earth and the moon = 3.84402×10^{10} cm. This figure is derived from *Schureman's* [1941, . 162] value c = 238,857 miles. Also

$$a' = 1/[c(1 - e^2)] \qquad (31)$$

' is given by the formula analogous to (31):

$$a_1' = 1/[c_1(1 - e_1^2)]^* \qquad (32)$$

quations (29) to (32) now enable us to determine ne tidal forces at any given point at distance r, y, from the center of the earth. For points on ne earth's surface it is convenient to make se of the known shape of the earth and to xpress r in terms of the height above sea level nd the latitude. Assuming the earth to be an lipsoid with parameters as adopted by *Lecar nd others* [1959], we have

$$r = Ca + H \qquad (33)$$

here C is given by

$$C^2 = 1/(1 + 0.006738 \sin^2 \lambda) \qquad (34)$$

Equations (1) to (34) determine the tidal cceleration at any point on the earth's surface. he (unprimed) equations have been checked by computing a number of cases (using an IBM 709 computer) and comparing the results with computations based on *Pettit's* [1954] paper, and also with computations (unpublished) by Pettit on S.W.A.C. (an electronic computer at the University of California). In every case agreement to within a fraction of a microgal was obtained. To this order of accuracy it is immaterial whether equations (10'), (11'), (12'), (19'), (26') or the unprimed equivalents are used. Furthermore, in the actual program, values of a and C based on the Hayford spheroid model of the earth [*Hayford*, 1910] were used, and here again adoption of the later values given in this paper has no effect on the order of accuracy stated above.

* Equations (29) and (30) are also given by chureman [1941, pp. 20 and 39] but with a' = /c, $a'_1 = 1/c_1$. Essentially, this means that e^2, e_1^2 ave been neglected in comparison with unity.

References

Bartels, J., Gezeitenkräfte, *Handbuch der Physik,* Vol. XLVIII, Geophysik II, Springer-Verlag, Berlin, 1957.

Doodson, A. T., The harmonic development of the tide-generating potential, *Proc. Roy. Soc. London, A, 100,* 305, 1921.

Doodson, A. T., and H. D. Warburg, *Admiralty Manual of Tides,* Her Majesty's Stationery Office, London, 1941.

Hayford, J. F., *Supplementary Investigation in 1909 of the Figure of the Earth and Isostasy,* Govt. Printing Office, Washington, D. C., 1910.

Lecar, M., J. Sorenson, and A. Eckels, A determination of the coefficient J of the second harmonic in the earth's gravitational potential from the orbit of Satellite 1958 β_2, *J. Geophys. Research, 64,* 209–216, 1959.

Pettit, J. T., Tables for the computation of the tidal accelerations of the sun and moon, *Trans. Am. Geophys. Union, 35,* 193, 1954.

Schureman, P., A manual of the harmonic analysis and prediction of tides, *U. S. Coast and Geodetic Survey, Spec. Publ. 98,* 1924.

Schureman, P., A manual of the harmonic analysis and prediction of tides, *U. S. Coast and Geodetic Survey Spec. Publ. 98,* Revised Ed., 1941.

(Manuscript received June 13, 1959; revised October 1, 1959.)

Pack-Ice Studies in the Arctic Ocean[1]

W. Schwarzacher[2]

Department of Meteorology and Climatology
University of Washington
Seattle, Washington

Abstract—The annual stratification of pack ice has been examined. Summer layers are formed either by arrested growth or by thin layers of fresh-water ice. The crystal structure and the salt content of the ice reflect the seasonal cycle. During the growth of ice a pronounced orientation of crystalline structure develops; it is determined by vertical as well as by horizontal temperature gradients.

There is a marked and systematic increase of salinity with depth, ranging from about 0.1 per mil at the surface to 4.0 per mil at a depth of 300 cm. This salinity distribution remains unaltered during the summer melt season.

A tentative attempt has been made to reconstruct the growth history of the ice at Drifting Ice Station A. This shows that the winter growth is strongly related to the thickness of the ice, that the floe on which the station was located was probably eight years old, and that during each of the winters of 1955–1956, 1956–1957, and 1957–1958 the thickness of the ice increased nearly 60 cm.

Introduction—As part of the scientific program Drifting Ice Station A an investigation of heat budget of pack ice was proposed. The in problem appeared to be the study of the wth of floe ice under arctic conditions and, particular, the study of the history of the on which the station was situated. The d work commenced towards the end of y 1958 and lasted until the middle of Septem- 1958. The ice drifted during this period m 84°N, 150°W to 85°N, 140°W.

Nansen [1897] observed that in the Arctic ean the formation of pack ice takes place ry year from December to June, approximate- by freezing on the underside of floes. During summer, part of the old ice is removed by lting from the surface of the floes. Russian entists state that the annual layers of winter can be recognized in section through the floes. *Shumsky* [1955] found evidence on rth Pole III of at least four winter accretions, resenting the years 1950 to 1954. The layers, found on the underside of the floe, had an average thickness of 35 cm. Shumsky believes that some ice is also formed at the surface, leaving layers 10 cm thick every year. Savelev [*Cherepanov*, 1957] tried to estimate the age of the ice on North Pole IV, but, unfortunately, no published data are available. *Cherepanov* [1957] investigated the same floe; by studying thin sections he found evidence of at least nine annual layers, with an average increment of 33 cm.

The previous investigations of the stratification in pack ice were based on only a few sections; in the investigation reported here a SIPRE ice corer was used to obtain complete cores running from the top to the bottom of the ice pack. Each core was inspected and measured; photographs of thin sections and salinity samples were taken from most of the cores.

The macroscopic description of standard ice—The ice examined near Station A was most variable in origin. Each floe was itself a mosaic of older fragments, linked sometimes by pressure ridges and sometimes by stretches of relatively young ice. The boundaries of the floes changed continuously.

For a study of the variation within the ice, cores were taken along predetermined straight lines at intervals of 10 or 20 meters. Even though

[1] This research was supported by the Office of val Research under Project NR 307 244, Con- ct Nonr–477(18).
Contribution No. 46, Department of Meteorol- y and Climatology, University of Washington.
[2] Present address: Department of Geology, een's University, Belfast, Ireland.

areas which showed signs of old pressure ridges were avoided, it was found that only 25 per cent of the cores consisted of old undisturbed ice. Twenty-five such cores were used to compile a standard section, the average thickness of which was 345 cm.

For a study of the details of the stratification the cores were placed on a dark background. This showed quite clearly that the ice increases in age from the lower surface upwards, and the winter ice of 1957–1958 therefore formed the lowest 50 cm. Until July this freshly formed ice was strikingly transparent and in sharp contrast to the older ice, which was milky-grey in color. Later in the summer the recent winter ice became grey and slightly clouded like the older ice, from which it was separated by a thin layer of milky white ice. This layer, which is interpreted as marking the previous summer, had a thickness of 2 to 5 mm, a sharp top, and an irregular, diffuse lower boundary. The interpretation of this layer is well supported by the following: The amount of winter ice formed during 1957–1958 at one locality was determined by direct measurement as being 55 cm (N. Untersteiner, personal communication). The average thickness, determined by the position of the summer layer in the standard section, compared well with this and gave a value of 59.6 cm. Furthermore, a thin layer was repeated at 53.5 cm above the 1957 layer and a third sharp boundary was at 58.9 cm above the 1957 layer. The summer line of 1956 was again only a few millimeters thick, very similar to the summer line of 1957. The summer layer of 1956 was almost always very strongly developed in the form of white opaque ice up to 10 cm in thickness. Usually the upper boundary of this layer was diffuse; the lower boundary was sharp and was frequently underlain by a few centimeters of very clear ice, which, as will be shown, was frozen fresh water. In the 25 cores of the standard section the three summer layers of 1957 to 1955 were well developed and easily correlated; the stratification closer to the surface was, however, less complete and more difficult to interpret. Only seven cores showed a good development of summer layers for 1954 to 1951, and three cores showed layers for 1950. The higher layers followed one another more closely, at intervals of 30 to 25 cm; the ice was very cloudy, and the summer layers showed up white opaque ice. Particularly during the la parts of the summer, liquid inclusions seem be concentrated in the higher parts of the profile and to obscure the older ice stratificati The top 50 cm may contain ice which formed on the surface, the most noticea being layers of very transparent fresh-water i obviously formed in surface pools. This can be recognized by the vertical orientati of the crystal axes which is in contrast with th of the sea-water ice. Snow that has fallen i such pools freezes to form very characteris layers of fine-grained ice. It has been impossib however, to find any annual stratification superimposed ice similar to the one described *Shumsky* [1955], and it seems that most of su surface ice disappears during the summer melti period.

The petrology of the ice—For petrologi examination of the cores, horizontal and verti thin sections were cut with an electric ba saw. In vertical sections the individual cryst of the winter ice appeared as 20- to 30-cm-lo spindle-shaped grains with their vertical a at right angles to the surface of the floe. horizontal sections the grains were more less isometric with cross sections of 2 to 3 c Grain boundaries were often difficult to s as neighboring grains frequently had a ve similar crystallographic orientation, and intimate intergrowth between adjacent grai occurred. The most characteristic feature of salt-water ice is a pronounced horizontal orien tion of all crystal axes. This has been explain by *Weeks* [1957] in the following way: Freezi of salt water leads to a separation of pure and concentrated brine. The pure ice grows thin plates parallel to the basal plane of t crystal, the impurities being concentrated tween the platelets at regular intervals. T brine enclosures have a marked influence on t thermal conductivity of the single crystal, a it is estimated from theoretical consideratio that the thermal conductivity at right angles the crystal c axis is 25 to 50 per cent greater th that parallel to the c axis. Crystals with th axes in the horizontal therefore have the directi of their highest conductivity parallel to the dire tion of maximum heat flow and will, consequence, grow faster.

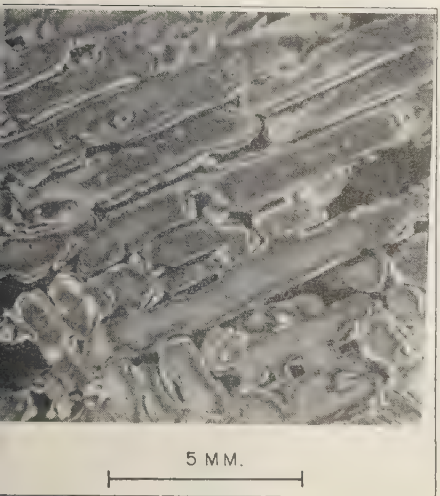

G. 1—Sea-ice section parallel to the crystal axis showing plate structure.

In horizontal sections the lamellar structure salt-water ice can be clearly seen. Along the undaries of the thin ice plates are the brine closures, the shapes of which vary consider-ly with the temperature of the ice. The dis-bution and size of the brine enclosures have significant influence on the physical properties sea ice; they have been studied in detail by *sur* [1958] and *Anderson and Weeks* [1958]. is noteworthy that all measurements of the ickness of ice plates in the present study gave value of 0.902 mm (average from 500 measure-ents). This is just twice the value given by eeks, who found the thickness of ice lamellas be 0.45 mm. In the examined ice, which cludes old ice as well as freshly frozen ice, may be that only alternate 'selected' planes e used for storing brine. Artificial melting n bring out the incipient subdivisions of e observed lamellas (Fig. 1).

A special study was made of the azimuthal ientation of crystal axes. For this purpose ncil rubbings of large horizontal ice sections re prepared and the strike of the plates in each ain measured. The distribution of these rections from a section 25 × 20 cm is plotted Figure 2. It can be seen that the directions the crystal axes in the horizontal were not ndom, and that there was one main maximum

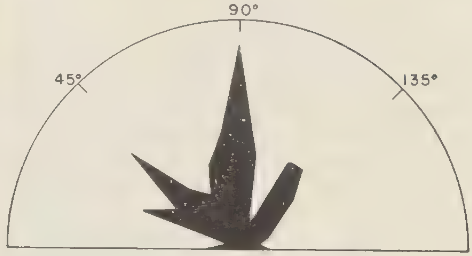

Fig. 2—Strike directions of 280 crystal axes in a horizontal section of 20 × 25 cm.

with two subsidiary maxima roughly 45° on either side. Detailed analysis showed that the neighbor of any grain was likely to have a similar orientation or one in which the grain orientation differed by either 45° or 90°. If we extended the orientation analysis over larger areas, 50 × 50 cm, for instance, then the preferred orientation disappeared, but the relationship between the neighboring grains persisted. This seems to indicate that the azimuthal orientation of a newly formed crystal is determined by the crystals surrounding it. It is suggested that the brine enclosures in a single crystal effect an anisotropic thermal conductivity in the horizontal planes which contain the crystallographic axis. The highest temperature gradients will occur parallel to the strike of the platelets, and new crystals will therefore grow parallel to it. The directions 90° or 45° inclined to the plates are also favored, as they can be the shortest distances between isolated brine enclosures, depending, of course, on their distribution. Unfortunately, this study could not be made in more detail because the temperatures at Station A were too warm during the period of investigation.

The grain-to-grain relationship became very obvious when one studied the intergrowth of crystals. Intergrowth was very common, and it was almost always those crystals with their axes approximately at right angles to each other which showed mutual penertation. The resulting texture had a distinct chessboard appearance, reminiscent of certain twinning patterns in feldspars (Figs. 1 and 3). The slight variability of angles at which intergrowth occurred suggests again a similar mechanism to the one outlined

above rather than any direct crystallographic preference. Chessboard texture has been found to be the normal development of ice which has not been disturbed mechanically during growth. The cross sections of such grains were roughly square in outline, with diameters of 1 to 2 cm.

Active growth of ice occurs from November to June [*Untersteiner*, 1958, and *Untersteiner and Badgley*, 1958]. In the middle of May, when the ice study was started, the underside of the floe showed the development of a so-called skeletal layer [*Weeks and Anderson* 1958]. This layer indicated that freezing was in progress. Disconnected platelets of pure ice protruded from the underside into the water. At this time the uncemented layer had a thickness of 1 to 2 cm; it gradually became thinner and was last observed on June 16. Throughout the remainder of the summer the underside of the ice floe was perfectly smooth; in fact, a small amount of melting took place. At one locality where repeated cores were taken the thickness of the winter ice of 1957–1958 decreased by 2 cm from the beginning of August to the beginning of September.

Thin sections through the summer layer of 1957 showed that the winter-ice growth of 1957–1958 was the direct continuation of that formed during the previous winter. In most instances no new generation of crystals formed, and the crystals of the previous winter which may have been truncated by the summer ablation took up growth again with the same crystallographic orientation. Sometimes the grain boundaries in the vertical sections showed minute offsets, and only occasionally did crystals with slightly different orientations develop. Artificial melting, however, always brought out the summer line and showed that this line was a potential grain boundary, even if the optical orientations of the pre- and post-summer ice was the same. Summer layers, in particular the summer layer of 1955, often showed a different development. In a vertical section one could see that the long spindle-shaped crystals had suddenly decreased in size until they had horizontal diameters of 0.5 to 1 cm and a length of only 2 to 3 cm, forming a layer 1 to 10 cm thick. The preferred orientation of the crystal axes was still horizontal, but deviations up to 30° from this occurred. This ice shows no platy structure in horizontal sections, and its salin was from 1 to 1.5 per mil, which was considera lower than that of the surrounding ice. It therefore believed that this ice formed as fre water ice on the underside of the floes dur summer. *Nansen* [1897] first observed t phenomenon when he measured the growth c one-year-old ice sheet which formed over a le During one winter the lead grew to a thickn of 231 cm, and the growth continued during following summer. Nansen explained that t further growth resulted from the freezing surface melt water which reached the unders of the floe. Due to its low salinity this wa froze when cooled by the sea water. *Unterstei* [1958] and *Untersteiner and Badgley* [1958] m rhe same observation in the camp area of Stat A during the summer of 1957 when melt wa was artificially introduced under the ice holes bored to drain the camp area. Examinat of the distribution of fresh-water ice during summer of 1958 showed clearly that it mainly restricted to the camp area and that occurred under natural conditions only wh the ice was thinner than normal, 200 to 250 c Further, this condition was often observed cl to open leads, which collect a good deal of m water during the summer. The petrographi examination of cores showed that, apart from ceptional years, summer ice did not significan contribute to the ice growth. Partly depend on how much drift took place during the summ fresh water collected only in restricted ar underneath the thinner ice and probably arri there after it had drained into leads. The lo density of the melt water would inhibit it fr percolating through the floe even if the became permeable during the summer.

Both types of annual layering (interrupt growth of large winter-ice crystals and formation of layers of small crystals, interpre as summer ice) have been recorded by *Cherepa* [1957], a fact which seems to indicate t annual layering is generally present in the arc pack ice. For practical purposes it should noted that most stratifications could be se more easily by gross inspection than by mic scopic examination.

The salinity of the ice—To obtain a continu record of the variation of salinity in the i many cores were cut into sections 7 cm l

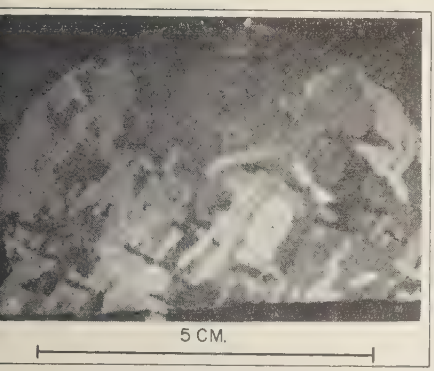

. 3—Horizontal section through sea ice with chessboard-like intergrowth.

l then melted. The salinity of this water s determined by measuring its density at C with a hydrometer. The instrument used s from a standard salinity-measuring kit brated in per mille salinity which, with proper care and temperature corrections, was readable to 1/10 per mil. A few hydrometric measurements were checked by titration on the station, and two cores were analyzed under more favorable conditions at the Oceanography Department of the University of Washington. The hydrometric measurements compared very well with the titrations.

Plots of vertical salinity profiles (Fig. 4) showed a systematic increase of salinity with depth and, superimposed on this, periodic fluctuations which could be correlated with the annual stratification. In order to study systematic variations the mean salinity of 40 profiles has been computed with the surface as the reference level. In order to eliminate short periodic fluctuations the values have been smoothed by using the weighted mean of the graphed value with the salinity from above and below it. The resulting curve (curve *A* in Fig. 5) shows how the salinity from the bottom of the floe to a depth of approximately 170 cm has the

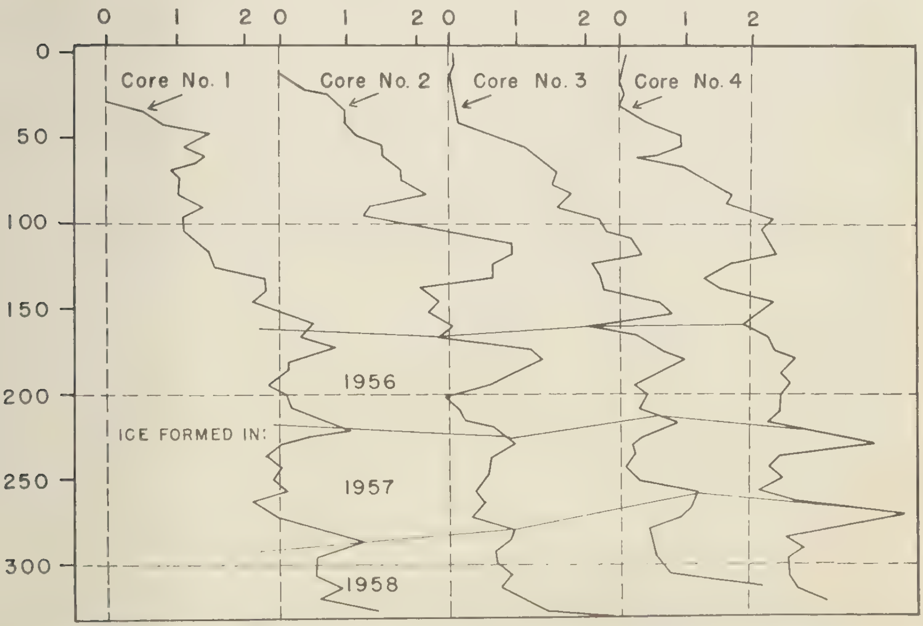

. 4—Salinity profiles of four cores taken at 10-meter intervals. The correlation is based on the ice stratification.

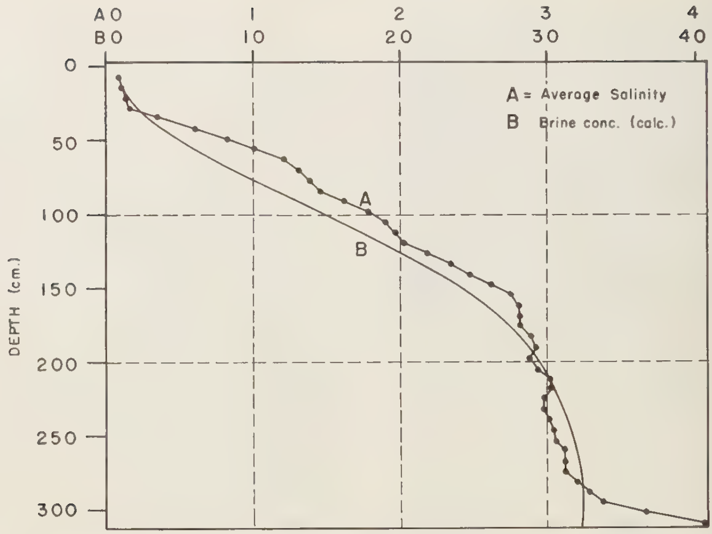

FIG. 5—Curve A: Average salinity of 40 cores based on 2060 salinity determinations, horizontal sca (A) per mille salinity. Curve B: Calculated brine concentration, horizontal scale per mille salinit

nearly constant value of 2.8 per mil, and from there to the surface it falls rapidly to nearly 0.1 per mil. The lowest part of the curve is the least reliable part of the distribution because not all profiles were of equal length. The general shape of the salinity distribution remains unaltered from June to September. When the first salinity profiles were taken in May the ice was still well below freezing, and it is therefore reasonable to assume that the winter salt distribution was unchanged; unfortunately no reliable winter salinity measurements were available. Before interpreting the salinity it is necessary to consider the brine concentration in the ice. This concentration will depend entirely on the temperature within the ice, if we make the reasonable assumption that everywhere within the ice the enclosed brine is at its freezing point. *Assur* [1958] has tabulated this dependence for sea ice. Ice temperatures have been recorded at the station at 50-cm intervals. To supplement these, temperature measurements were taken on several cores directly after they were brought to the surface. The ice temperatures, compiled from all available data, are given in Table 1.

TABLE 1—*Ice temperatures on September 1*

Depth below surface, cm	Temperature, °C	Depth below surface, cm	Temperature, °C
10	−0.05	170	−1.36
20	−0.07	180	−1.41
30	−0.12	190	−1.45
40	−0.19	200	−1.48
50	−0.27	210	−1.51
60	−0.35	220	−1.54
70	−0.44	230	−1.55
80	−0.54	240	−1.57
90	−0.64	250	−1.58
100	−0.75	260	−1.59
110	−0.85	270	−1.60
120	−0.95	280	−1.61
130	−1.05	290	−1.62
140	−1.15	300	−1.62
150	−1.23	310	−1.62
160	−1.30		

From the temperatures the concentration of the brine enclosures was calculated and is shown in Figure 5, curve B. Because the relation between concentration and temperature in t range is practically linear, both temperat and concentration follow the same distributi which is best approximated by a gauss probability function in the cumulative fo The function is part of the solution to the diff ential equation of either heat flow or diffus

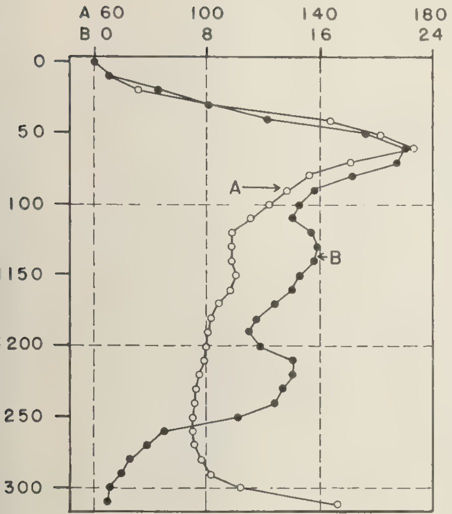

FIG. 6—Curve A (open circles): brine volume ven in per mil. Curve B (full circles): frequency macroscopic brine enclosures in 100 cores. Ver- cal scale depth in centimeters.

rough an infinite plate. As can be seen from gure 5, the observed salinity distribution could most be explained as being due to saturated ine-filled enclosures making up about 10 r cent of the total volume of ice at all levels. here were, however, significant deviations from is; curve A in Figure 6 shows the vertical stribution of the volume of brine enclosures calculated from the salinity of the ice and the eoretical brine concentration. It is seen that e level at which the largest brine enclosures curred is 60 cm below the surface of the ice. his was confirmed by observation; the summer frequently contains large liquid inclusions, metimes holes of up to 2 cm in diameter and metimes irregular pockets of brine, and they e always easily seen in the cores. Curve B in gure 6 shows the frequency with which such closures occurred for each 10-cm level from e hundred cores taken from June to September. here was, as expected, a maximum of liquid closures at a depth of 60 cm below the surface. wo deeper maxima at approximately 130 and 0 cm were probably caused by the periodic linity fluctuations. It was observed that most the recorded lower brine pockets formed shortly after the cores were brought to the surface.

In many cores the lowest 5 to 10 cm had a salt content of 4 to 6 per mil, which is much higher than the salinity of the rest of the core. This increase of salinity developed particularly after the ice stopped growing in thickness (after the middle of June). At this time the temperature of the ice was very close to the ocean temperature and the brine volume was correspondingly high (curve A, Fig. 6). Diffusion of sea water probably took place and increased the salt concentration. It appears that part of this excess salt is retained in the ice when the winter freeze starts again, and the salinity profiles therefore show a periodic fluctuation with high salt contents corresponding to the summer layer. In Figure 4 four selected profiles have been correlated by their annual stratification. It is clearly seen that the summer line for 1957 and 1956 came close to a salinity maximum of 3 to 4 per mil. The summer line of 1955, on the other hand, coincided with a salinity minimum. A study of thirty such correlated profiles showed that the salinity maximum of 1957 was slightly below the summer line, with an avergae displacement of 2.0 cm. The displacement in 1956 was 3.7 cm, which seems to indicate that excessive salt concentrations in the ice migrate downwards at the rate of approximately 2 cm a year. This downward migration explains the observation (already mentioned) that the upper surface of the last two summer layers is developed as a sharp boundary, whereas the lower surface is diffuse. The summer layer of 1955 is more difficult to interpret, because most profiles showed that fresh-water ice was formed during this summer. From the available data it appears that the salinity minimum caused by such fresh-water ice migrates upwards only as indicated by the rather diffuse top boundary and the very sharp bottom boundary of such layers. Salinity distributions can be used for dating the ice but are more difficult to interpret than the ice structure. A summer can be represented either by a salinity minimum or maximum, and both maxima and minima migrate slowly with time.

The salinity distribution of all profiles indicated a progressive loss of salt. This has been explained by purely gravitational drainage or by migration of brine enclosures with the thermal gradient

(*Sverdrup*, 1956]. The exact mechanism of salt loss, however, is still unknown. In general, gravitational drainage of brine would be expected to take place only during the winter months when the base of the ice is warmer than the surface, and the lower brine enclosures would therefore have a lower density. In winter, however, the total brine volume is small and the permeability of the ice is low, a condition which would slow drainage. During the melting period the brine density decreases from the base to the surface of the ice and is therefore gravitationally stable. *Whitman* [1926] showed experimentally that isolated brine enclosures migrate towards warmer surfaces, and involved in the process is melting at the warmer end of the enclosure and freezing at the colder end, together with a continuous mixing, probably by diffusion, of the brine in the enclosure. During summer, brine would be lost at the upper surface, whereas during winter, when the temperature gradients are much steeper, the migration would be downwards. It is very likely that the downward shift of salinity peaks is due to this process, which, however, seems to be very slow. A comparison of curves *A* and *B* in Figure 5 shows that during the summer the brine content was approximately constant at 10 per mil throughout the ice, and excess salt over the temperature equilibrium concentration can be removed only by diffusion towards the upper surface of the ice. This upper surface is kept fresh by precipitation and melt water from ice which has been raised above the level of the floe (pressure ridges). A striking confirmation of salt redistribution by diffusion, which is considered a most important factor, is given by the salinity profiles of two cores in the camp area. One was taken before the melting period started; the second was taken after four weeks during which time fresh water was continuously pumped under the ice surface. Within this time the salinity at a depth of 280 cm had been reduced from 4 per mil to 0.5 per mil, and at 240 cm, from 3.7 per mil to 2.9 per mil. This indicates that diffusion operates to produce a decrease of salinity in the lower ice.

Disturbed ice—In this study the sampling of ice profiles was selective, inasmuch as most cores were taken from areas which superficially showed no signs of ice disturbance. Neverthe-

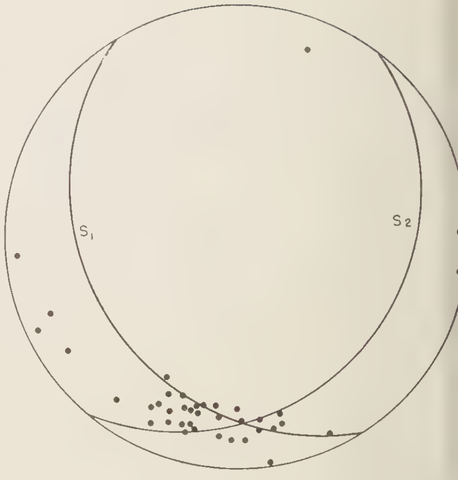

Fig. 7—Orientation of 39 optic axes of ice whi
has been tilted during growth.

less, petrological examination showed that
was very common for ice floes to become slightl
tilted at various stages of their developmen
Under such circumstances a very pronounce
azimuthal orientation of ice crystals develop
In the cores, one can recognize tilting by a
inclination of the stratification and by the fa
that the longest grain axes are perpendicular
the stratification. The crystal growth is influence
by two factors: First, crystals will continue
grow in the same direction as the crystals gre
before tilting occurred, and, second, the maximu
heat flow will still be directed vertically upward
Grains which have their *c* axes parallel to th
axis of tilt are obviously in the most favore
position, and a strong preferential orientatio
of crystals which have their plates parallel
the dip direction will occur. Figure 7 shows th
orientation of crystal *c* axes from a core take
approximately 10 meters from a pressure ridg
The ice must have tilted twice in differe
directions; S_1 is the summer layer of 1956, S_2 th
summer layer of 1957. The ice between the tw
summer layers took the only possible orientatio
in which the plates are perpendicular to bo
boundaries.

Whenever such preferential azimuthal orient
tion occurred the grain shape was also affecte
The horizontal cross section of the grains becam
elongated in the direction of the plates. T

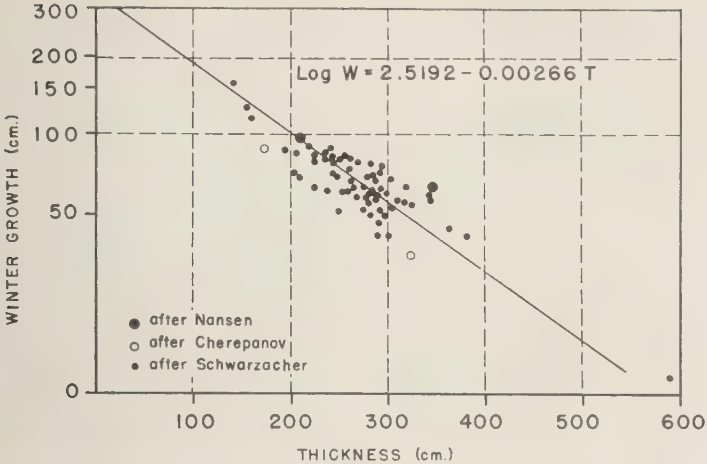

ɢ. 8—Plot of winter growth (vertical scale) against thickness in the previous summer (horizontal scale).

ortest diameter of the grains was at right gles to the plates and varied from 0.5 to 1 cm. ne intermediate diameter in the strike direction the plates was from 3 to 5 cm.

Tilting was observed in almost all profiles ken at the station, but, due to the difficulty taking azimuthally orientated cores, little known of the areal extent of the resulting eferred orientation. One example showed a t of the floe towards a pressure ridge at a stance of about 20 meters from the ridge. is very likely that the strength properties such ice are affected. The ice taken directly om old pressure ridges was not studied in tail; a few examined sections showed an ceptionally small grain size of 1 to 5 mm, a nse milky appearance, and a characteristic w-salinity content.

The growth history of the ice—It is a well-known fact that the pack ice in the Arctic Ocean has everywhere approximately the same thickness; values from 400 cm (Fram) to 218 cm (Sedov) have been reported. At Station A, again neglecting ice locally thickened by pressure ridges, an average thickness of 319.7 cm was determined from 80 measurements. The standard deviation of the measurements was 33 cm, which means that the coefficient of variation was only 10.3 per mil. The yearly ice increase was strongly related to the ice thickness at the time. Figure 8 shows this correlation. The winter ice growth of 1957–1958, determined from 63 cores, has been plotted against the ice thickness of the profiles before the winter growth started. By least squares the following relation is established:

$$\log W = 2.5192 - 0.00266T$$

where T is the thickness of the ice at the end

TABLE 2—*Mean winter growth and standard deviation of pack ice at Station A*

	Winter of 1957–58	1956–57	1955–56	1954–55	1953–54	1952–53	1951–52	1950–51
ean winter owth, cm	59.6	53.5	58.9	36.7	31.1	25.9	26.3	30
andard viation	10.1	8.95	14.4	...	...	...	...	...
umber of easurements	25	25	25	7	7	7	7	3

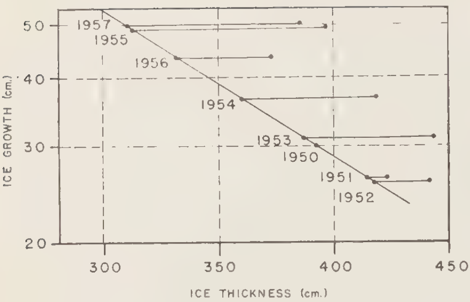

FIG. 9—Thickness of ice from 1951 to 1957. Points at the right side mark the pre-summer thickness, points on the left the post-summer thickness. The vertical scale gives the amount of ice growth in the following winter.

of the summer of 1957 and *W* is the winter growth. Similar results were obtained when the correlation for the winter ice of 1956–1957 was investigated, but allowance had to be made for the ice loss during the summer of 1957. From the data the loss was estimated to be approximately 60 cm.

To get some idea of how the winter growth varied from year to year, measurements were made on selected profiles which showed at least three years' undisturbed growth. The data are the same that were used for the standard ice profile previously discussed. The results are given in Table 2. It is interesting to note that the coefficient of variation for the last three years ranges from 17 to 25 per cent, which is almost twice the variation of the total thickness of the ice. This indicates that there was probably an additional process which regulated the ice thickness, apart from the correlation with the winter increment. A relation between ice thickness and summer loss could be such a mechanism. Completely neglected in establishing the relation of ice growth to ice thickness has been the effect of snow cover, which probably acts as a very effective insulating blanket and may lead to different relations in different winters. Data on growth of ice are rare in the literature; *Nansen* [1897] gives values of winter growth for ice 208 and 336 cm thick, and from *Cherepanov's* [1957] two profiles two further points can be derived. These data are also plotted in Figure 8 for comparison with the data from Station A.

It appears that the thickness-growth relati can be used for determining the ice thickne before and after the melt periods of the la seven years. In Figure 9, the points on the rig side show the ice thickness before the melti started, and the points on the left, the thickne after the melting was completed. The horizont distance between the points gives the summ loss, and on the vertical scale the growth of t following winter is given. The oldest ice 8 to 9 years old. In the years 1950 to 1953 t ice is estimated to have been thick and to ha had an annual increment of 25 to 30 cm similar value of 30 cm was found by Cherepan on North Pole IV for the years 1949 to 195 In 1955 the thickness of the ice decreased greatl The ice loss during this summer was exceptiona great, and the large quantities of melt wat may account for the low salinity and the layers fresh-water ice which were recorded that ye

It is tempting to correlate the changes of i thickness with the circulation in the Arc and to conclude that the ice is again increasi in thickness, but to substantiate such a co clusion would require much more observatio data from different latitudes than is now availab

Acknowledgments—This investigation was spo sored by the Office of Naval Research and w directed by P. E. Church. The staff of the D partment of Meteorology and Climatology of t University of Washington, W. Weeks, and t U. S. Army Snow Ice and Permafrost Resear Establishment have given valuable advice a helped with the preparations for the field wo The author is further indebted to all colleagu at Station A, in particular to A. Assur and Frankenstein who generously shared their equi ment and provided a number of salinity detern nations which have been used for comparis The Department of Oceanography of the U versity of Washington analyzed some ice samp brought back from the field. Quite invaluable h been the cooperation of the Air Force person at Station A.

REFERENCES

ANDERSON, D. L., AND W. F. WEEKS, A theoreti analysis of sea-ice strength, *Trans. Am. Geoph Union, 39,* 632–640, 1958.

ASSUR, A., Composition of sea ice and its tens strength, in *Arctic Sea Ice, Natl. Acad. S Natl. Research Council, Publ. 598,* 106–138, 19

CHEREPANOV, N. W., Opredeleniye vozrasta dre fuyushchikh l'dov metodom Kristallooptich kogo issledovaniya (Age determination of dri

ıg ice by optical study of the crystals), *Prob-emy Arktike, 2,* 179–184, 1957.

NSEN, F., *Farthest North,* 2 vol., A. Constable, ondon, 1897.

UMSKY, P. A., Kirzucheniyu l'dov Severnogo ,edovitoga okeana (Study of the ice of the rctic Ocean), *Vestnik Akad. Nauk SSSR, 2,* 3–38, 1955.

ERDRUP, H. U., *Arctic Sea Ice, the Dynamic North,* vol. 1. United States Chief of Naval Operations, 1956.

EEKS, W. F., Study of the growth of sea ice crystals, *Bull. Geol. Soc. Am., 68,* 1811, 1957.

EEKS, W. F., AND D. L. ANDERSON, An experimental study of strength of young sea ice, *Trans. Am. Geophys. Union, 39,* 641-647, 1958.

WHITMAN, W. G., Elimination of salt from sea-water ice, *Am. J. Sci., 9,* 126–132, 1926.

UNTERSTEINER, N., Arctic sea-ice studies, *IGY Bulletin 12,* 11–15, 1958.

UNTERSTEINER, N., AND F. I. BADGLEY, Preliminary results of thermal budget studies on Arctic pack ice during summer and autumn, in *Arctic Sea Ice, Natl. Acad. Sci. Natl. Research Council, Publ. 598,* 85–95, 1958.

(Manuscript received May 29, 1959; revised September 4, 1959.)

An Automatic Meteorological Data Collecting System[1]

Robert M. Brown

Brookhaven National Laboratory
Upton, Long Island, New York

Abstract—In common with other research and industrial organizations faced with the problems of reducing large volumes of data, the Brookhaven Meteorology Group and Instrumentation Division have developed an automatic data collecting system. This device is capable of accepting meteorological information in the form of either a rotation or a voltage. It then converts these inputs to digital information and records them on a paper punch. The tape punch is extremely fast, and it is possible to scan the required information every 0.6 seconds. This eliminates the need for developing mean data prior to the coding.

Introduction—The Meteorology Group at the 3rookhaven National Laboratory has been ollecting data for the past ten years for the tudy of diffusion of smokes and gases in the ɔwer atmosphere. Most of the data have been ransmitted from a 420-ft tower installation and ecorded on a number of Esterline-Angus and ,eeds and Northrup recorders. The primary ıeteorological variables involved in diffusion tudies (wind direction, wind speed, and temperaure) are the principal parameters discussed in his paper. Many papers have been published elating these measured variables to such henomena as dispersion of gases, turbulence, ustiness, and wind loads in general [*Singer and 'mith*, 1953, 1955; *Singer and Raynor*, 1952]. everal special studies have been made in conunction with other government agencies which eal with the wind and temperature conditions ncountered by such things as projectiles and ıissiles in the lower atmosphere.

In the majority of studies conducted at 3rookhaven, the transmitted information was ecorded, manually read, placed on cards, and nalyzed by computer techniques. The need or an automatic system of digesting the recorded ıformation and putting it on cards had existed or several years. Manual reduction of the ecords was time consuming, tedious, and exensive. An automatic system using paper tape ras installed during the summer of 1958, and everal 'fast runs' were made during the following months. The paper tape is automatically converted to punched cards and they are used in various computations.

The automatic system—The automatic system was built to accept inputs from the types of transmitters in operation on the tower. It was designed to operate in parallel with the existing sensors and recorders. A brief description of the tower equipment and recorders will be given, and the use of their outputs in the new system will be described.

The wind directions were transmitted electrically by small self-synchronous motors. Their design and applications vary somewhat [*Johnson*, 1945], but they have two basic uses: torque transmission or voltage indication. The former was used in obtaining an inked record of both horizontal and vertical wind directions. Three all-weather bi-directional wind vanes [*Mazzarella*, 1952] were used as sensing devices. The wind speeds were transmitted by small direct-current generators and recorded on milliammeter recorders. Temperatures were transmitted by Leeds and Northrup Thermohms (100-ohm copper-wound resistance thermometers) located at eight levels on the tower. A Leeds and Northrup Speedomax recorder was used to record the temperature at the various levels. Figure 1 shows two bivanes and an aerovane on test at one level.

The automatic system used the selsyns as voltage indicators to position the servo units involved in wind-direction measurements. The varying voltages produced by the generators in standard Bendix-Friez Aerovanes are used

[1] Research carried out under the auspices of the Jnited States Atomic Energy Commission.

FIG. 1—Two bivanes and an aerovane mounted at one level on tower.

in the automatic system to determine wind speeds. The various positions of the slide-wire shaft in the Speedomax recorder are used to determine the temperatures in the new system.

Figure 2 is a schematic diagram of a wind vane and the paths that are taken to produce a written and a punched record of wind direction. Two selsyns S are connected electrically to produce an inked record of the wind direction. An extension of this system was developed to give automatic readings on paper tape. Outputs

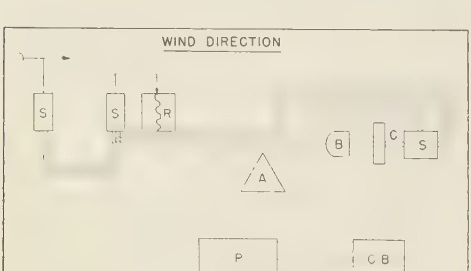

FIG. 2—Schematic diagram of system for recording wind direction.

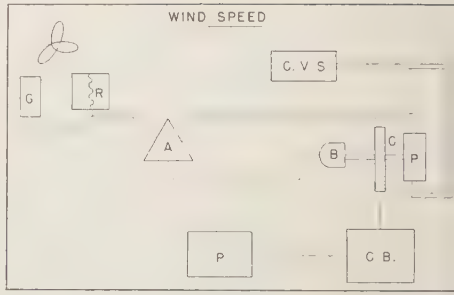

FIG. 3—Schematic diagram of system for recordin
wind speed.

from individual servo units, driven by moto
from a balancing bridge, are fed to a contr
processor which operates a paper punch. Whe
an unbalance occurs in the system, an amplifi
A drives motor B to rebalance it. An encoder
is attached to the driving shaft of the balanci
motor, and the commutator that turns with t
shaft has 1000 possible positions per revoluti
[*Giannini Bull.*]. The commutator readings a
sensed by a control box CB which actuat
certain thyratron tubes, depending on the sign
sent from the commutator. The thyratron tub
in turn actuate solenoids in a paper punch
to perforate the moving paper.

A schematic of the wind-speed system is show
in Figure 3. A propeller turns a generator
which transmits a current to a milliammet
recorder R. The voltage from the generat
is used to produce the punched record of win
speed by comparing it with the voltage from
constant voltage supply CVS through a di
ferential amplifier. The voltages are balance
by turning a potentiometer P by means of
balancing motor B. The encoder is used to se
digital information to the paper punch, as
the wind-direction system.

The temperatures are obtained by placi
an encoder directly on the slide-wire shaft
the Leeds and Northrup temperature recorde
The commutator outputs are sent directly
the control box for analysis and transmissi
to the punch.

The punch, a high-speed perforator (N
BRPE2) made by the Teletype Corporation,
capable of punching 36 digits of information
0.6 sec. Three digits are used for each variab
being sensed; therefore, twelve variables ca

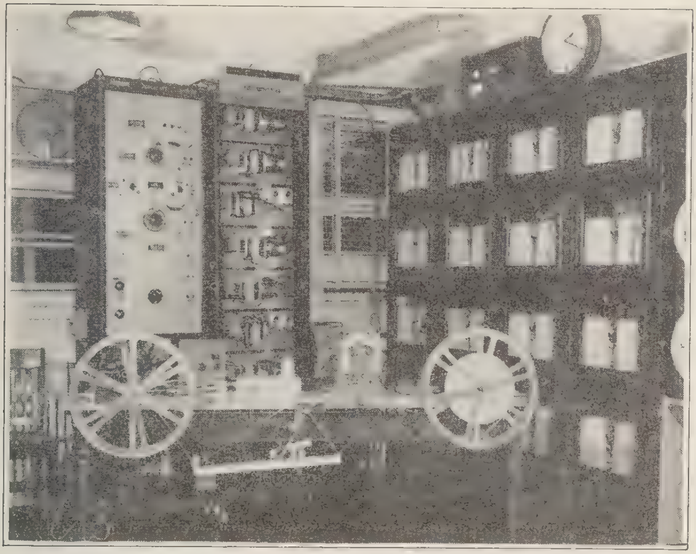

Fig. 4—Photograph of the complete recording system.

punched in 0.6 sec. Actually, nine servo units, e temperature, one temperature-source identiation number, and an end-of-line indicator e punched during the 0.6 sec. At this rate, the elve variables are punched sixteen times in 5 sec.

Calibration—The entire system is shown in gure 4. It includes nine servo units in a rack, control processor with calibrating equipment another rack, and the punch with feed and ke-up reels on a table. The large reels hold ough paper for a continuous 2-hour run.

The transmitters on the tower and the rerders in the panel are first calibrated independtly of the automatic system. The windrection vanes are turned manually to various sitions and the recorded values noted. The nperature elements are calibrated by subrging them in a water bath of known temperare. The automatic system is then calibrated lependently of the paper recorders and transtters. A motor-driven master selsyn is emyed in parallel with the six servo units volved in obtaining wind-direction measurents, and a motor-driven master potentiometer used in parallel with the three servo units volved with wind-speed fluctuations. The ster selsyn is turned to various positions, and the servo units should follow. A light panel, directly behind the punch in Figure 4, is used to indicate the encoder positions during calibration. The master potentiometer is used to calibrate the wind speed in a similar fashion. The punch is calibrated by applying certain encoder positions and noting the punched tape. The final calibration is accomplished when the entire system is ready for a run. The transmitters are turned to various positions, the punch produces a tape, the tape is converted to cards, and the cards are inspected. This last step determines the reliability of the converter.

Results—Comparison tests were made of Esterline-Angus records and punched tape readings. The horizontal and vertical wind direction records were almost identical. The pen drag of the recorders causes little delay in response time of the direction records. However, the wind speed recorders lag behind the punch readings by about two seconds. The milliammeter movements are damped and this, plus some pen drag, could account for this delay in response.

Several 2-hour runs were made during the summer of 1958 in conjunction with a study of the dispersion of oil-fog trails during temperature inversion conditions. The system was almost trouble free, something that was not expected.

There were some difficulties, but they were minor. The major trouble was encountered in converting the tape to cards. Spurious pulses, due to bouncing of the contactors in the punch, would occasionally cause one too many punches in a sampling period of 0.6 sec. The converter was wired so that it stopped when it sensed this condition. A new control processor, being built at the present time, will incorporate fast, slow, and interrupted programs and will be capable of accepting a voltage, a rotation, or a count. It will be described in detail in future publications.

Future developments—It is anticipated that the automatic system, with slow program, will be used in a new climatological study. It will cycle various inputs at predetermined intervals to obtain daily, weekly, and monthly values of some of the variables involved in a study such as this.

A new high-capacity digital computer called 'Merlin' is being built by the Instrumentation Division of Brookhaven. It was designed to handle most of the computer programs used at Brookhaven, and it will accept paper tape directly. This will eliminate the conversion of tape to cards.

Acknowledgments—The planning and construction of the automatic punch system, called 'Punchy I,' was accomplished by the Instrumentation D vision of Brookhaven. W. Higinbotham, R. Chase, and J. Tillinger deserve special credit f their part in the electronic design and constru tion. E. Foster and C. Tomesch provided furth assistance in the construction. M. E. Smith an I. A. Singer of the Meteorology Group gave su gestions concerning the type of information th punch system should provide.

References

Gianninni Bulletin 14300-2B, *Single channel e coder system*, G. M. Giannini & Co., Inc., Pas dena 1, California.

Johnson, T. C., Selsyn design and applicatio *J. Am. Inst. Elec. Engrs.*, Oct. 1945.

Mazzarella, D. A., An all-weather remote-recor ing bivane, *Bull. Am. Meteorol. Soc., 33,* 60–6 1952.

Singer, I. A., and M. E. Smith, Relation gustiness to other meteorological parameters, *Meteorol., 10,* 121–126, 1953.

Singer, I. A., and M. E. Smith, Sampling peri in air pollution evaluation, *Proc. Natl. Air P lution Symposium, 3rd Symposium,* Pasade Calif., 80–85, 1955.

Singer, I. A., and G. S. Raynor, Analysis of m teorological tower data, April 1950–March 19 *Brookhaven Natl. Lab. No. 461 (BNL) T-1* 1952.

(Manuscript received May 27, 1959; revised Se tember 1, 1959; presented at the Fortieth Annu Meeting, Washington, D. C., May 6, 1959.)

The Pole Tide[1]

Richard Haubrich, Jr., and Walter Munk

University of Wisconsin
Madison, Wisconsin
and
Scripps Institution of Oceanography
University of California
La Jolla, California

Abstract—About 10,000 mean monthly values of sea level from 11 tide stations have been analyzed by the method of Tukey to obtain the power spectra in the frequency range of 0.0125 to 6 cycles per year (cpy). The spectral density is on the order of 10^3 mm^2/cpy and is remarkably uniform over this frequency range, with the following exceptions: (i) a sharp rise at the low-frequency tail, from 10^3 mm^2/cpy at 0.1 cpy to 10^5 mm^2/cpy at 0.0125 cpy (presumably associated with variations in recorded sea level arising from continental unrest); (ii) the line spectrum associated with the annual variation and its harmonics; and (iii) a weak peak of 0.84 cpy, barely above noise level, which is identified with the 14-month 'pole tide' corresponding to the earth's free nutation (Chandler wobble). The average pole tide for all stations gives an amplitude twice that predicted by equilibrium theory. The contribution to the peak of the pole tide is largely from three localities: Swinemünde, Marseille, and a combined set of Netherlands stations. Apparently the pole tide is not in accord with equilibrium theory. This raises some questions concerning the interpretation of Love numbers as derived from the period of free nutation.

Introduction

Ever since Euler showed in 1765 that the arth should have a free nutation with a period f 10 months, there have been attempts to de- ect such a motion from precise measurements f latitude. In 1891 a variation in latitude was iscovered by Chandler, but its period was 428 ays instead of the expected 305 days. The xplanation was soon given by *Newcomb* 1892]: Euler's theory applies to a rigid earth; or the actual case, the elastic yield of the olid earth and the fluid yield of the oceans ave to be taken into account, and these in- rease the period of free nutation from 10 to 4 months. For a completely fluid earth a shift n the axis of rotation would result in complete djustment of the figure to the new rotational otential, and no wobble would result; that is, he nutation period would be infinite.

The differential yield of earth and oceans roduces a pole tide. To visualize this we con- ider the case of a rigid earth completely surrounded by an ocean of uniform depth. If the solid earth were turned 90° relative to the axis of rotation so that an equatorial radius coincided with the rotational pole, then the land would be up 20 km relative to the water along the earth's long axis and down 20 km along its short axis. Actually the wobble amounts to about 0.1″ instead of 90°, so that we might expect the pole tide to be on the order of

$$\frac{0.1''}{90°\ 60°\ 60} \times 20 \text{ km} = 6 \text{ mm}$$

The fact that the solid earth also yields when the axis of rotation shifts reduces the measurable tide to about one half of this value. The gravitational attraction of the tide itself (both water and earth) increases it by about one third. We end up with about 5 mm for the expected pole tide. A systematic derivation is given in the section entitled 'Theory.' The pole tide is unique among the tides in not being caused by the sun or the moon.

Tide records are read hourly to an accuracy of perhaps ±1 cm. The detection of a 5-mm

[1] This study was supported by a grant from the National Science Foundation.

Table 1—*Sea-level stations*

Group	Station	Location	Years of record
I	1	Swinemünde, Germany 54°N. 14°E.	1811–1943
	2	Netherlands, 52°N. 5°E. (average of 6 stations)*	1865–1951
	3	Brest, France 48°N. 4°W.	1807–1943
	4	Marseille, France (Marégraphe) 43°N. 5°E.	1885–1946
II	5	Buenos Aires, Argentina 35°S. 58°W.	1905–1946
	6	Baltimore, Maryland 39°N. 77°W.	1902–1955
III	7	Portland, Maine 44°N. 70°W.	1912–1955
	8	Seattle, Washington 48°N. 122°W.	1899–1955
IV	9	Wazima, Japan 37°N. 137°E.	1900–1949
	10	Hososima, Japan 32°N. 132°E.	1900–1949
V	11	Bombay, India 19°N. 73°E. (Apollo Bandar)	1878–1947

*Delzijl, Harlingen, Den Helder, Hoek van Holland, Hellevoetsluis, Vlissingen

pole tide depends then on one's hope that the errors are largely random, so that in the monthly averages of hourly values the errors are reduced by something like a factor $(30 \times 24)^{1/2} \approx 27$ as compared with the error in the hourly values. When we first decided to search tide records for the pole tide, we were not aware that others had been willing to speculate in so marginal an undertaking. The literature turns out to be remarkably large. The first mention of the problem appears to have been made by Lord Kelvin:[2] "The sea would be set into vibration, one ocean up and another down. . . ." The first harmonic analysis was made by *Christie* [1900]. *Bakhuysen* [1913] measured records of sea level at Amsterdam going back to 1700. Further analyses were made by *Przbyllok* [1919], *Baussan* [1951], and *Maksimov* [1954, 1956]. The procedure in all these analyses was to devide the data into as many 7-year series as possible and to derive for each series the amplitude and phase of the sixth harmonic, corresponding exactly to a 14-month period. All these attempts except Przbyllok's were reported as being successful in having established the existence of a pole tide. On the basis of the present study it turns out that the results would not have differed by a large factor if the investigators had searched for a period of 13 months, or 15 months. We have obtained the power spectrum of sea level as a continuous function

[2] Presidential Address, 1876, Section of Mathematics and Physics, British Association for the Advancement of Science.

of frequency. This involves no preconceived a sumption as to the frequency of the pole ti and, furthermore, furnishes an estimate of t 'noise level' at adjoining frequencies. The noi level is very high, and the superimposed spe tral peak of the pole tide is barely detectab

Analysis

The analysis was performed with the aid high-speed digital computers. The procedu follows closely the one adopted by *Munk, Sno grass, and Tucker* (in press) in their study low-frequency ocean waves; and this, in tur is based on the work of *Blackman and Tuk* [1958]. The detection of weak signals in t presence of noise depends rather critically the procedure, and in this section the vital p rameters have been recorded. Subsequent di cussions of the results and their interpretati can be read without reference to this sectio

Observations—Mean monthly values of s level at 11 locations (Table 1) were taken fro the *Publications Scientifiques* of the Associati d'Oceanographie Physique, Union Geodesique Geophysique Internationale. Latitude observ tions consist of unsmoothed values of m_1 and (directional cosines of the pole of rotation, rel tive to its mean position, along Greenwich a 90° east of Greenwich) from the *Internation Latitude Service* for 1900–1954 [*Walker a Young*, 1957, Table 1*a*].

Prefiltering—Three types of numerical filte were applied to the raw data: (1) annual jection (AR); (2) high-pass filtering (HP

TABLE 2—*Computation parameters*

Station	Years	Least count	AR	HP	LP	Δt years	m	Δf (years)$^{-1}$	α	N	ν	95% confidence limits of energy	Figures
;winemünde	1900–1943	1 mm	AR	12	...	1/12	48	1/8	8	502	20	0.6–2.1	1
;winemünde	1900–1943	1 mm	AR	14	5	1/4	160	1/80	80	164	1.6	.2–100	1
Vetherlands	1865–1951	1/6 mm	AR	12	...	1/12	48	1/8	0.22	1015	42	.7–1.7	1, 2
Vetherlands	1865–1951	1/6 mm	AR	14	5	1/4	160	1/80	2.22	336	3.7	.4–9.0	1
Vetherlands	1900–1951	1/6 mm	AR	12	...	1/12	48	1/8	0.22	598	24.	.6–1.9	1
Vetherlands	1900–1951	1/6 mm	AR	14	5	1/4	160	1/80	2.22	196	1.9	.2–50	1
.atitude	1900–1954	0″.01	AR	...	5	1/4	160	1/80	80	218	2.7	.3–20	3

3) low-pass filtering (LP). Annual rejection vas accomplished for each station by subtract-1g from all January values the average Jan-ary value and similarly for other months. This emoves the seasonal variation and its har-1onics; that is, periods of 12, 6, 4, 3, 2.4, and months. The high-pass and low-pass filters re described by *Munk, Snodgrass, and Tucker* in press), Sections 5.4 and 5.3. Half widths f the filters are given in Table 2.

The purpose of these operations is to sup-ress, prior to the analysis, certain parts of he spectrum which are not of primary con-ern in our study. The high-pass filter removes he secular drift in sea level; the low-pass filter mooths the record. If these features at the two xtremes of the spectrum were not suppressed, hey would appreciably contaminate the spec-rum in the central frequencies. The annual term ; particularly troublesome because it is so 1uch larger than the pole tide (typically 20 m as compared with 5 mm) and yet so close 1 frequency. Without prior removal the side ands of the strong annual line would bury the reak spectral line of the pole tide. At the com-letion of the spectral analysis a correction is 1ade for the known response characteristics f the high- and low-pass filters. The plotted pectra are therefore complete as they stand, except for the omission of the seasonal line spectrum.

Power spectra—Figures 1, 2, and 3 show selected spectra. (Graphs of all spectra and a complete list of computation parameters are included in an unpublished dissertation [*Haubrich*, 1958]). Pertinent computation parameters are given in Table 2. Here Δt is the sampling interval; m is the number of spectral estimates in the frequency range of 0 to $m\ \Delta f$, where $\Delta f = (2\ m\ \Delta t)^{-1}$ is the frequency *resolution;* α is the scale factor in going from (least count)^2 to units of power density, mm^2/cpy; and N is the total number of values.

Each spectral estimate of the energy density is subject to random error. It can be shown that the estimates follow a 'chi-squared' probability distribution which depends on a parameter $\nu = 2N/m - 1/2$, 'the number of degrees of freedom.' ν and the associated 95 per cent confidence limits are given in Table 2 for each spectrum. There is thus a 95 per cent probability that the true value of the energy density lies within the stated proportion of the calculated values. For frequency bands composed of several lines the degrees of freedom are larger and the uncertainty limits are correspondingly narrower [*Blackman and Tukey*, 1958, Section 9].

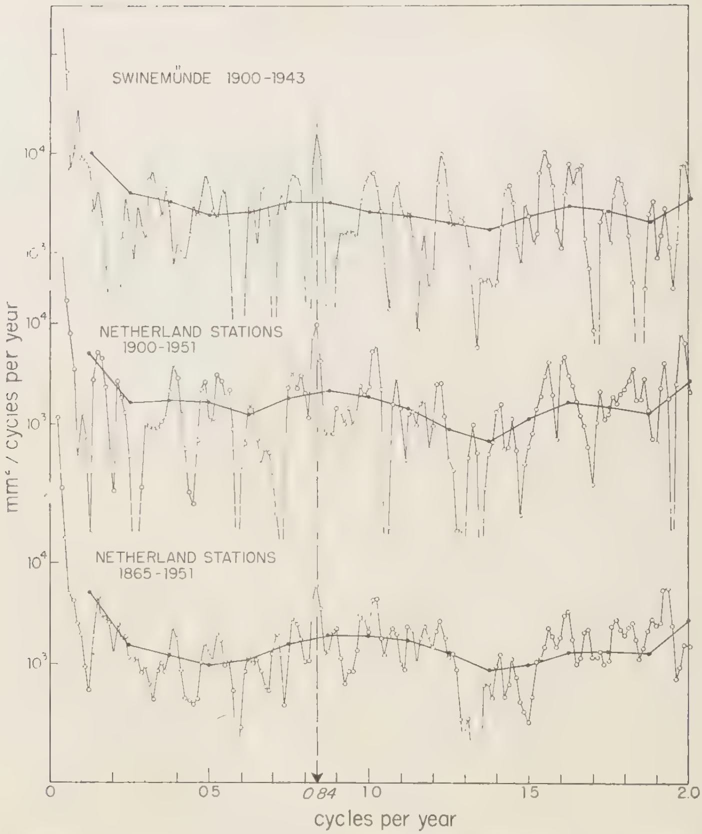

FIG. 1—Power spectra for Swinemünde and the Netherlands stations; solid circles, low-resolutio spectra; open circles, high-resolution spectra.

The spectra are obtained by computing the cosine transforms of the autocorrelations. The result is a smoothed spectrum. As always, there are conflicting desires between high resolution (small Δf) and statistical reliability (large ν). For the low-resolution spectra ($\Delta f = 0.125$ cpy) there is appreciable smoothing; for the high-resolution spectra ($\Delta f = 0.0125$ cpy) there is little smoothing, and the uncertainty limits are very large. In the latter case we might as well have computed the power for each harmonic of the record, without resorting to autocorrelation. The method was used only because it was available in convenient machine-programed form.

Co- and quadrature-spectra—The equilibrium tide for each station was computed for each month from 1900 to 1954 according to (7) using the unsmoothed latitude data [*Walke and Young*, 1957, Table I*a*] and setting 1 + $- h = 0.68$ [Jeffreys, 1952, p. 206]. The value so obtained were analyzed with the recorde sea level to obtain the normalized co- an quadrature-spectra, P and Q (Fig. 4). If th recorded tide is in phase with and proportion to the equilibrium tide, then $P = 1$ and $Q =$ over the frequencies of the pole tide; if th recorded tide lags by 90°, then $P = 0$ an $Q = 1$.

THEORY

For a rigid earth the period of free nutatio would be 10 months. But deformations a caused both in the solid earth and in the ocea

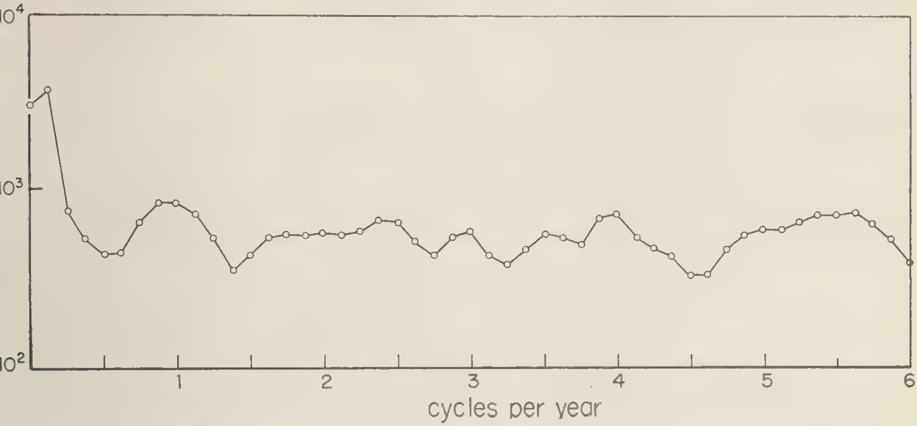

2—Low-resolution spectrum for the Netherlands stations over the entire frequency range of analysis, from 0 to 6 cpy.

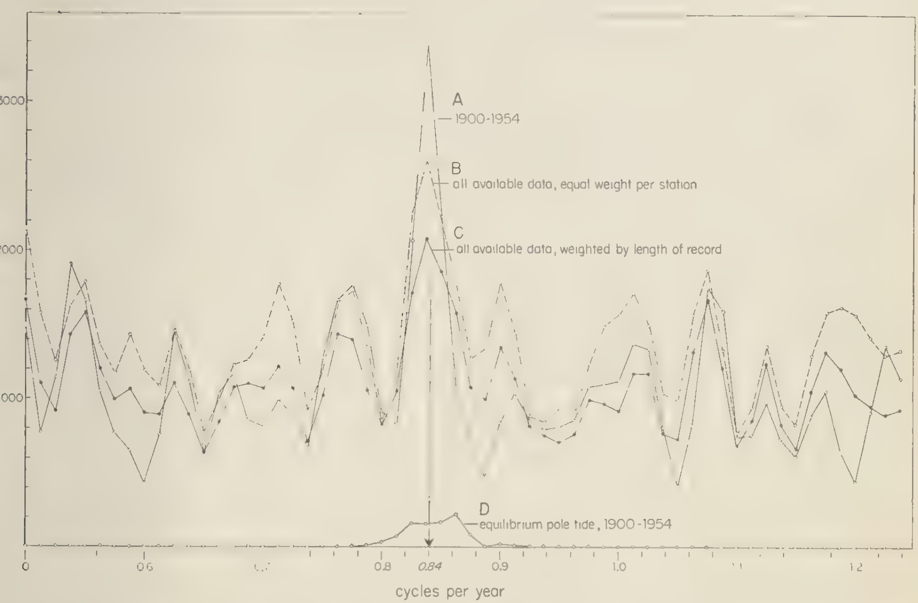

3—Composite high-resolution spectra of the recorded ocean tides (A, B, C) and of the equilibrium pole tide (D).

the potential disturbance associated with nutation. As a consequence of these deformations the period is lengthened to the observed value of 14 months. In this section we inquire about the extent to which lengthening can be associated with deformation in the ocean. Upon subtraction of this oceanic effect, the rigidity of the solid earth can be derived and compared with values obtained from seismic data. We also estimate the ellipticity in the nutation brought about by the uneven distribution of land and sea.

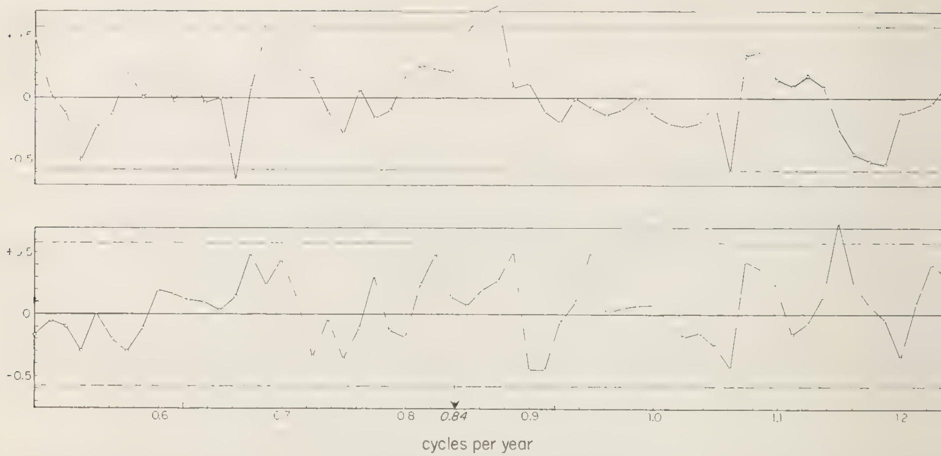

FIG. 4 Composite co-spectrum (top) and quadrature-spectrum (bottom) of the recorded ocean ti versus the equilibrium pole tide.

First, the effect of the water tide alone is considered. Deformation of the ocean bottom due to loading by the tide is then discussed. In this approximate treatment harmonics other than those of degree 2 have been ignored.

Products of inertia of the pole tide—The rotational potential is

$$U_0 = \tfrac{1}{2}\Omega^2 a^2 \sin^2 \theta \qquad (1)$$

where Ω is the earth's rotational velocity, a its mean radius, and θ the colatitude. For small changes in θ the change in potential is given by

$$\delta U_0 = U = \Omega^2 a^2 \sin\theta \cos\theta \, \delta\theta$$

$$= -\Omega^2 a^2 \sin\theta \cos\theta (m_1 \cos\lambda + m_2 \sin\lambda) \qquad (2)$$

where m_1 and m_2 are the direction cosines between the axis of rotation and the x_1-axis (toward Greenwich) and the x_2-axis (toward 90° east of Greenwich), respectively, and λ is east longitude.

As a result of this potential disturbance the sea bottom is raised by hU/g and the sea surface relative to the sea bottom by

$$\xi_0 = \frac{1 + k - h}{g} U \qquad (3)$$

where g is gravity at the surface and k, h, the 'tidal-effective' Love numbers [*Jeffreys*, 1952, p. 204]. Due to the irregular distribution oceans and continents, a correction tide ξ' (introduced by Sir George Darwin) must added so that the total tide,

$$\xi(t, \theta, \lambda) = \xi_0(t, \theta, \lambda) + \xi'(t) \qquad ($$

is consistent with the conservation of mass

$$\int_{\text{oceans}} \xi \, ds = 0 \quad \text{and} \quad ds = \sin\theta \, d\theta \, d\lambda \qquad ($$

It is now convenient to define a functi [*Munk and MacDonald*, 1960, Appendix]:

$f(\theta, \lambda) = 1$ where there are oceans.

$f(\theta, \lambda) = 0$ where there are continents.

Let a_n^m, b_n^m describe the coefficients of degree and order m in an expansion of $f(\theta, \lambda)$ in spherical harmonics. These coefficients have be tabulated by Munk and MacDonald up degree 8. Equation (4), subject to restraint (can now be written

$$\xi = -\frac{1 + k - h}{g} \frac{\Omega^2 a^2}{2} \cdot \left\{ m_1 \left(\sin 2\theta \cos\lambda - \frac{a_2^{\,1}}{5a_0^{\,0}} \right) + m_2 \left(\sin 2\theta \sin\lambda - \frac{b_2^{\,1}}{5a_0^{\,0}} \right) \right\}$$

We shall need the products of inertia associated ith the pole tide. These are

$$_{3} = -a^4 \rho \int_{\text{oceans}} \xi \sin\theta \cos\theta \cos\lambda \, ds = A(T_1 m_1 + R m_2) \quad (8)$$

$$_{3} = -a^4 \rho \int_{\text{oceans}} \xi \sin\theta \cos\theta \sin\lambda \, ds = A(T_2 m_2 + R m_1)$$

here ρ is the density of sea water, A, A, C are e earth's principal moments of inertia, and

$$\frac{R}{+ k - h} = \frac{4\pi\Omega^2 \rho a^6}{Ag}\left[\frac{b_2^2}{35} + \frac{b_4^2}{63} - \frac{a_2^1 b_2^1}{100 a_0^0}\right] = -0.11 \times 10^{-4}$$

$$\frac{T_1}{+ k - h} = \frac{4\pi\Omega^2 \rho a^6}{Ag}\left[\left(\frac{a_0^0}{15} + \frac{a_2^0}{105} - \frac{4a_4^0}{315}\right) + \left(\frac{a_2^2}{35} + \frac{a_4^2}{63}\right) - \frac{(a_2^1)^2}{100 a_0^0}\right] = 3.36 \times 10^{-4} \quad (9)$$

$$\frac{T_2}{+ k - h} = \frac{4\pi\Omega^2 \rho a^6}{Ag}\left[\left(\frac{a_0^0}{15} + \frac{a_2^0}{105} - \frac{4a_4^0}{315}\right) - \left(\frac{a_2^2}{35} + \frac{a_4^2}{63}\right) - \frac{(b_2^1)^2}{100 a_0^0}\right] = 2.16 \times 10^{-4}$$

which we add, for future reference

$$= \frac{8\pi}{15}\left(a_0^0 + \frac{1}{7} a_2^0 - \frac{4}{21} a_4^0\right) - \frac{4\pi}{100 a_0^0}\left[(a_2^1)^2 + (b_2^1)^2\right] = 1.20$$

The equations of motion of the rotation pole re [*Munk and MacDonald*, 1960, 6.1.2]

$$dm_1/dt + \sigma_e m_2 = \sigma_r c_{13}/(C - A)$$
$$dm_2/dt - \sigma_e m_1 = -\sigma_r c_{23}/(C - A) \quad (10)$$

here $\sigma_r = \Omega(C - A)/A$ is the frequency of utation if the earth is rigid, and σ_e is the freuency which allows for the deformation of the lid earth but not of the oceans. The observed equency σ is to be determined for a solution to 0). Making use of (7), (8), and (9), we can now ut the equations of motion in the form

$$\frac{m_1}{dt} + (\sigma_e - T_2\Omega) m_2 - R\Omega m_1 = 0$$
$$\frac{m_2}{dt} - (\sigma_e - T_1\Omega) m_1 + R\Omega m_2 = 0 \quad (11)$$

with the solutions

$$m_1 = M_1 \cos \sigma t$$
and
$$m_2 = M_2 \sin(\sigma t + \beta) \quad (12)$$

provided that

$$\sigma^2 = \sigma_e^2 - (T_1 + T_2)\Omega\sigma_e - (R^2 - T_1 T_2)\Omega^2 \quad (13)$$

$$\tan\beta = -\frac{\Omega R}{\sigma} \quad (14)$$

$$\frac{M_1^2}{M_2^2} = \frac{\sigma_e - T_2\Omega}{\sigma_e - T_1\Omega} \quad (15)$$

We note that $R \ll T_1$, $R \ll T_2$; furthermore $T_1\Omega/\sigma_e$ and $T_2\Omega/\sigma_e$ are small numbers. Accordingly,

$$\sigma = \sigma_e - \tfrac{1}{2}(T_1 + T_2)\Omega + \text{order}\,(T_1\Omega/\sigma_e)^2 \quad (16)$$

The observed frequency of nutation is $\sigma = \Omega/437$. For the usually accepted value, $1 + k - h = 0.68$ [*Jeffreys*, 1952, p. 206], this gives

$$\sigma_e = \Omega/404 \quad (17)$$

so that the oceans increase the period from 404 days to 437 days.

Love numbers for the solid earth—In any geophysical application we are not concerned with the nutation frequency for an earth without oceans but rather with the Love numbers associated with the solid portion of the earth. The relation between the observed frequency of nutation and the Love number k can be put into the form [*Munk and MacDonald*, 1960, 6.2.6 and 5.3.2]

$$\sigma = \sigma_r \frac{k_f - k}{k_f} \quad (18)$$

where

$$k_f = \frac{3G(C - A)}{a^5 \Omega^2} = 0.96 \quad (19)$$

is the 'fluid' Love number, and G is the gravitational constant. Similarly, the frequency σ_e for an earth without oceans can be related to a Love number k_e according to

$$\sigma_e = \sigma_r \frac{k_f - k_e}{k_f} \quad (20)$$

We define

$$k_w = \tfrac{1}{2}k_f(T_1 + T_2)\frac{\Omega}{\sigma_r}$$
$$= \frac{9}{8\pi}(1 + k - h)S\frac{\rho}{\bar{\rho}} \qquad (21)$$

where $\bar{\rho}$ is the mean density of the earth. Equation (16) can be written in either of the forms

$$\sigma = \sigma_e - \frac{k_w}{k_f}\sigma_r \qquad (22)$$

or

$$k = k_e + \frac{9}{8\pi}(1 + k - h)S\frac{\rho}{\bar{\rho}} = k_e + k_w \quad (23)$$

Thus k_w as defined is that part of the Love number k which is due to the oceanic pole tide.

The problem is to evaluate k_e. We may regard $k = 0.29$ as known from the frequency of the Chandler wobble. We have followed two procedures: (a) Consider $(1 + k - h) = 0.68$ as known. Then it follows directly from (22) and (23) that

$$\frac{\Omega}{\sigma_e} = 404, \qquad h = 0.610,$$
$$k_e = 0.235, \quad \text{and} \quad k_w = 0.055 \qquad (24)$$

Procedure (b) is based on a relation

$$h = (h_f/k_f)k_e = 2.05\,k_e \qquad (25)$$

for the 'equivalent Earth' [*Munk and MacDonald*, 1960, 5.6.2], where h_eU/g is the deformation of the solid earth corresponding to the potential k_eU. For the case of no loading, $h = h_e$. According to (25) the ratio h_e/k_e depends only on the density distribution and not on rigidity. Equations (22) and (23) with $h = 2.05\,k_e$ give

$$\frac{\Omega}{\sigma_e} = 396, \qquad h = 0.457,$$
$$k_e = 0.223, \quad \text{and} \quad k_w = 0.069 \qquad (26)$$

Asymptotic cases—It is instructive to compare these results with various asymptotic models of oceans and the earth. For the case $\rho = 0$, we have $k_w = 0$, so that $\sigma = \sigma_e$, which is the appropriate frequency for an earth without oceans. For a rigid earth ($k_e = 0$, $h = 0$) completely surrounded by oceans, $S = 8\pi/15$ and

$$k_w = k = \frac{1}{(5/3)(\bar{\rho}/\rho) - 1} \qquad (2$$

and

$$\sigma = \sigma_r\left(1 - \frac{k}{k_f}\right)$$

If the earth is homogeneous, $k_f = 3/2$. Thus, the ocean density approaches the mean densi of the earth, $\rho \rightarrow \bar{\rho}$, we find $\sigma \rightarrow 0$; the rotation axis becomes unstable. For the actual densi distribution $k_f = 0.96$, so that instability reached when $\rho = 4.5$ g cm^{-3}.

Ellipticity—The pole of rotation describes ellipse

$$m_1^2 - (2\sin\beta\, M_1/M_2)m_1m_2$$
$$+ (M_1/M_2)^2m_2^2 = M_1^2\cos^2\beta \qquad (2$$

The major axis (T_2 being less than T_1) poin toward east longitude λ_0, where

$$\tan 2\lambda_0 = 2R/(T_1 - T_2) = -0.20 \qquad (2$$

and $\lambda_0 = -6^0$

Since β is small, (28) may be written to a go approximation

$$m_1^2/M_1^2 + m_2^2/M_2^2 = 1 \qquad (3$$

The ellipticity is

$$\epsilon = 1 - \frac{M_2}{M_1} = 1 - \frac{\sigma_e - T_1\Omega}{\sigma_e - T_2\Omega} = 0.017 \quad (3$$

For comparison, the ratio of the amplitud of m_1 amd m_2 was taken from the analysis of t unsmoothed latitude data, 1899 to 1954 [*Walk and Young*, 1957, Table Ia]. The result is

$$\epsilon = 1 - M_2/M_1 = 0.01 \pm 0.05 \qquad (3$$

M_1 and M_2 are so nearly equal that the statisti error in the analysis of the latitude data gives large uncertainty in the observed value of But, as far as it goes, there is no inconsisten with the computed value (31). *Fedorov* [19 derived a computed value of ϵ by a meth similar to ours but stated that this value not agree with the observed ellipticity of f nutation.

But the distribution of ocean and contine is not the only source of an ellipticity of t

andler wobble. In the first two decades of s century there was much discussion of the axiality of the earth, a discussion which is ely to be resumed in the light of the satellite servations. A difference in the equatorial ments of inertia will produce an ellipticity the pole path. From geodetic measurements *lmert* [1915] found

$$\frac{B - A}{C - \frac{1}{2}(A + B)} = \frac{1}{46} \qquad (33)$$

ich corresponds to a difference of 230 meters tween the equatorial semi-axes; the major is is along 107°W. *Schweydar* [1916] found at the ratio (33) would produce an ellipticity = 0.016. *Lambert* [1922] attempted to evaluate e ellipticity from different six-year series latitude observations, 1900 to 1917. His lues of ϵ range from 0.02 to 0.20, and the ection of the major axis from 59°W to 116°W. If we can accept Helmert's values, it follows at the ellipticity in the wobble produced by e oceans is of the same order as that produced the ellipticity of the equator, but oriented right angles to it. A comparison of these sults with observations is meaningless because the larger uncertainty in the observed ec- ntricity.

Load deformation—The derivation so far neg- cts the load deformation of the solid earth sociated with the oceanic pole tide. When this taken into account, the ocean effect is reduced about one seventh. In the following approxi- ate treatment we write

$$= k_e + k_w + k_w' \text{ and } h = h_e + h_w' \quad (34)$$

nere $h_w'U/g$ is the deformation of the sea ttom due to loading by the pole tide, and $'U$ is the potential of the load deformation. ith these definitions k_w, k_e, and h_e will have lues somewhat different from those given in e previous sections.

The problem is to derive k_w', h_w' in terms of e other Love numbers. There are two opposing fects. The gravitational attraction by the pole de on the earth lifts the earth by $h_e(k_wU)/g$, d this deformation is associated with a tential $k_e(k_wU)$. The pressure exerted by the le tide on the earth depresses the earth, and is deformation is associated with a potential $-k_e(\rho/\bar{\rho})g\xi$ [*Munk and MacDonald*, 1960, Section 5.8]. The combined effect can be expressed in terms of the 'load Love numbers,'

$$k_w' = -\tfrac{2}{3}k_w h_e \quad \text{and} \quad h_w' = -\tfrac{2}{3}k_w h_e \qquad (35)$$

To include the effect of loading, we write

$$k_w + k_w' = \frac{9S}{8\pi}\frac{\rho}{\bar{\rho}}[(1 + k - h) + (\bar{\rho}/\rho)h_w'] \qquad (36)$$

in analogy with (21). The first part in the bracket is associated with the pole tide, the second part with the displacement of the sea bottom. The factor $(\bar{\rho}/\rho)$ allows for the greater density of the sea bottom.

With k considered to be determined by the observed Chandler frequency, (34), (35), and (36) give five relations between the six unknowns, h, h_e, k_e, h_w', k_w', k_w. Again we have obtained numerical solutions by the following two procedures: (a) Consider the relation $1 + k - h = 0.68$ as given; (b) assume $h_e = 2.05\, k_e$ according to the equivalent earth model (25). The results are

$$\begin{aligned} &\text{(a)} \quad \Omega/\sigma_e = 409, \; h = 0.61, \; h_e = 0.633, \\ &\qquad\qquad k_e = 0.245, \; k_w = 0.054 \\ &\text{(b)} \quad \Omega/\sigma_e = 402, \; h = 0.46, \; h_e = 0.476, \\ &\qquad\qquad k_e = 0.232, \; k_w = 0.061 \end{aligned} \qquad (37)$$

The lengthening of the nutational period which is attributable to the ocean equals (a) 28 days, (b) 35 days for the two models under consideration. Model (b)) gives a value of $1 + k - h = 0.83$, which is larger than the generally accepted value of 0.68. Neglecting load deformation, we previously obtained (a) 33 days, (b) 41 days. The effect of load deformation is then to reduce somewhat the effect of the oceanic pole tide.

Previous investigations—Estimates of the ocean effect on Chandler frequency using static theory have been made by *Larmor* [1915], *Rosenhead* [1929], *Fedorov* [1949], and *Jeffreys and Vicente* [1957b]. Larmor, using a homogenous earth model, found $k_e = 0.231$ after allowing for the distribution of oceans and conti-

nents. He estimated[3] that loading would reduce the ocean effect upon frequency by about 20 or 30 per cent. Rosenhead, using a two-layer earth composed of core and mantle, obtained k_e = 0.346 for the earth without oceans and k = 0.435 with oceans included.[4] The value $k = 0.435$ is far too high to be consistent with the Chandler frequency. Fedorov calculated the effect of oceans, taking into account their distribution but not including loading. Taking $1 + k - h = 0.70$ he obtained $k_e = 0.23$.

Takeuchi [1951] calculated the Love numbers for an earth without oceans and made comparisons with observed values obtained from the Chandler wobble. Using a statical theory of core and mantle he took an earth model based upon the seismic studies of K. E. Bullen and obtained

$$k_e = 0.3067 \quad h_e = 0.6186 \quad l = 0.083$$

for an outermost mantle density of 3.3. Finding the Love numbers, k in particular, to be highly dependent on surface density, Takeuchi also computed the Love numbers for a surface density of 2.7, obtaining

$$k_e = 0.256 \quad h_e = 0.594 \quad l = 0.080$$

Jeffreys and Vicente [1957*b*], using Takeuchi's solution for the mantle and a dynamic theory of the core, obtained a Chandler period of 392 days corresponding to $k_e = 0.208$. Adding the oceans to a homogenous earth with rigidity corresponding to $k_e = 0.208$, they arrived at the observed Chandler period after assuming the effect to be two thirds of that which would be produced by a complete ocean. This model allows for loading but contains the relation $h_e = 5/3\ k_e$, which holds only for a homogenous earth.

[3] Larmor obtained $h/a = \frac{1}{2}\Omega^2 a/g$ for the equilibrium rotational deformation of the oceans at the equator. This neglects the self potential of the water bulge. On the following page an erroneous factor of 2 is introduced which partially compensates for the first effect.

[4] After correction for an error in determining the Love number h (Rosenhead's equations 5.1 and 5.5). Rosenhead's published value, $k = 0.270$, would imply that the oceans *increase* the tidal-effective rigidity.

Discussion

Equation (7) permits us to compute the 'equ librium pole tide' from astronomic observatio of latitude. This has been done for each static for the years 1900 to 1954 using $1 + k - h$ = 0.68. The equilibrium pole tide is proportion to $1 + k - h$ and therefore subject to th same uncertainty as the value of $1 + k -$ An estimate of the uncertainty in $1 + k -$ is by no means straightforward, as will be ap parent from the preceding section. We estima that the factor is known within an accuracy ±20 per cent.

Figures 1 and 2 show some sample spectr of the tide records at individual stations. Th spectra from the 11 tide-gage stations have bee averaged, frequency band by frequency ban using different weight factors (spectra A, B, Table 3, Figure 3). Spectrum D is a simil average of the equilibrium pole tide at th 11 stations. If the sea level obeyed equilibriu theory, then the recorded spectrum A and equ librium spectrum D would be identical. We sha discuss four features of the spectral peak ne 0.84 cpy: frequency, phase, amplitude, an width.

Frequency—The three composite pole-ti spectra all show a peak very near 0.84 cp corresponding to a period of 1.19 years. Th periods given in Table 3 have been calculate by taking the mean frequency of each of th spectral highs (equal energy to both sides of th mean frequency). For spectrum A the value 1.194 years. From latitude observations th period of the Chandler wobble has been est mated at 1.195 ±0.015 years. The results fro the oceanographic and astronomic observatio are compatible.

Phase—Figure 4 shows the values of $P($ and $Q(f)$, the normalized co- and quadratur spectra for the pole tide versus equilibrium tid averaged over 11 stations for frequencies from 0.50 to 1.25 cpy. A result $P(f) = +$ $Q(f) = 0$ means that at frequency f there a zero phase *difference* between the records: th phase itself can be random. For ν degrees freedom, the 95 per cent confidence limits ha been estimated at $\pm 2\nu^{-1/2}$, as shown by t dashed lines. There is a barely significant spectrum at a frequency just above the Chan

Table 3—*Composite spectra*

	Pole tide period, years	Total energy at 14 months peak, mm²	Noise energy, mm²	Pole tide energy, mm²	Amplitude, mm	Total degrees of freedom, ν	80% confidence limits of pole tide energy
A: 1900–1954	1.194	96.13	37.73	58.40	10.8	48	38.2–90.1
B: All years equal weight per station	1.187	90.51	52.40	38.11	8.7	145	25.8–54.4
C: All years stations weighted according to years of record	1.188	110.01	66.05	43.96	9.4	145	29.0–63.8
D: 1900–1954, equilibrium tides	1.182	12.10	0.4	11.70	4.8	12	7.2–24.0

ler frequency, and none at other frequencies. The result may perhaps indicate a tendency toward an in-phase relation between recorded and equilibrium pole tides, but the more important conclusion is that the phase relation is very poor. Swinemünde and the Netherlands stations have a peak in coherence over the Chandler frequencies, and this turns out to be consistent with a zero phase difference [*Haubrich*, 1958].

Amplitude—We have noted that the composite spectra have a peak at the Chandler frequency. Concerning the amplitude of the peak, two features are noteworthy: (i) There are striking differences from one station to the next. Three stations, Swinemünde, Marseille, and the Netherlands show definite peaks at essentially the same frequency, all having energy densities higher than anything on the record except the low-frequency 'drift.' At Bombay there is a peak at 0.84 cpy, but the height is not above the surrounding noise. The remaining seven stations do not show a distinct peak. (ii) The more recent data are characterized by a higher and sharper spectral peak. This is due, in part, to the higher 'noise level' of the older spectra. During the 19th century most of the sea-level stations used the tide pole, which was apparently not suitable for measuring the pole tide, whereas the more recent data are from recording tide meters. But even after allowing for the higher noise level, the composite spectra B and C (which include data from the 19th century) have less energy in the 14-month peak than spectrum A. The difference lies within the uncertainty of the results, but it might indicate a smaller average wobble in the 19th century than in the 20th. There is no way of checking this against latitude observations, inasmuch as these do not go back as far as the tide observations. The difference between older and newer sea-level spectra is apparent also for the Netherlands (Fig. 1), Marseille, and Swinemünde. In fact, in the 1811–1906 spectrum for Swinemünde (not shown) there is no significant peak near 0.84 cpy.

If the pole tide obeyed equilibrium theory with $1 + k - h = 0.68$, then spectra A and D should agree except for experimental noise. In fact, the observed pole tide (spectrum A) has far more energy than spectrum D. After subtracting a general noise level of 1000 mm²/cpy, the pole-tide energy is found to be four times the equilibrium value; accordingly the amplitude ratio is 2:1. From the 80 per cent confidence limits given in Table 3, there is a 10 per cent probability that the pole tide has an energy below 38 mm² and an equal probability that the equilibrium tide has an energy above 24 mm². The probability that the statistical in-

stability of the spectra can account for the discrepancy between A and D is less than 1 per cent.

Maksimov [1954, 1956] has formed 180 seven-year series from 74 stations. From each of these he obtains by Fourier analysis the amplitude and phase of the sixth harmonic corresponding exactly to a 14-month period. No adjoining frequency was investigated, and this removes the possibility of estimating the extent to which noise may affect the results. Maksimov's final averages are 28.4 mm for the observed amplitude and 4.3 mm for equilibrium amplitudes, all referred to $\theta = 35°$. Our averages are 10.8 mm and 4.8 mm without latitude correction, but allowance is made for adjoining noise level. In our analyses the mean noise level in the vicinity of the Chandler frequency ranges from about 400 to 2500 mm²/cpy, depending on the station. For an average station with a mean noise level of 1000 mm²/cpy, the method used by Maksimov would give an amplitude of 12 mm for the noise alone. This is comparable to his mean observed amplitude (before introducing a latitude factor) of 14.4 mm. We conclude that Maksimov's large value is due principally to noise. Analyses by the same method were made on atmospheric pressure [*Maksimov*, 1954]. One might suspect that noise would affect these results in a similar manner.

Width of spectral peak—The sharpness of the spectral peak can be related to the damping of the free nutation. We can see in Figure 3 a remarkable discrepancy between the widths of observed and equilibrium spectra. The observed spectrum appears to involve three adjoining frequencies, and this is just the expected signature of the Tukey method for a spectral line, or at least a peak that is narrow compared with the spectral resolution $\Delta f = 0.0125$ cpy. The spectrum of the equilibrium pole tide extends over many adjoining frequency bands. A convenient dimensionless parameter for portraying the spectral width is the Q. For the equilibrium pole tide, estimates of Q range from 20 to 40, corresponding to damping times of 7.6 to 15.2 years. If our supposition of a sharp spectral peak is correct, the pole tide indicates a Q in excess of 100 and a damping time of more than 38 years.

This is a most surprising result. One can hardly conceive that the ocean has a sharp resonant peak at just this frequency; this would be a most unlikely coincidence and would require a degree of resonance not otherwise found in oceanic oscillations. At one time we suspected that the latitude peak was artificially broadened by nonlinear imperfections in observational technique and data reduction. This would favor oceanographic observations over astronomic observations, an appealing conclusion for geophysicists. But it is odd, to say the least, that the adjoining noise level in the astronomic measurements should be so much lower than that for oceanographic measurements.

At the suggestion of Tukey we undertook an analysis of variance to test the significance of the indicated sharpness of the pole-tide peak. Details are given in the Appendix. We investigated the probability of two alternatives: (i) a sharp (as seen through the Tukey filter) spectral peak at 0.84 cpy; (ii) a spectral width compatible with the latitude observations. For stations in group I (Table 1) the first alternative is more probable, but barely so. For the remaining groups the reverse is true. It would appear that a discussion of spectral width is not profitable with the material at hand.

Other analyses—We have computed the spectrum of mean monthly averages of the water level of Lake Michigan at Milwaukee from 1860 to 1958. There is no indication of a pole-tide peak. The noise level at this frequency is 10 mm²/cpy, which is equal to corresponding values in the open sea.

We have also computed the spectrum of the average tide record (rather than the average of the spectra of individual records, Figs. 3 and 4). This was done as follows: Suppose that $m_1(t)$, $m_2(t)$ are the positions (at times t) of the 'pole-tide pole' to be determined from the recorded tide levels $\xi_i(t)$ at station i. Let

$$a_i = \sin\theta_i \cos\theta_i \cos\lambda_i$$

and

$$b_i = \sin\theta_i \cos\theta_i \sin\lambda_i$$

be coefficients depending only on the positions of the station. By making

$$\sum_{i=1}^{N} [a_i m_1(t) + b_i m_2(t) + z(t) - \xi_i(t)]^2$$

small as possible, $m_1(t)$, $m_2(t)$ and the mura term' $z(t)$ are determined [*Munk and cDonald*, 1960, Section 7.3]. If the pole-tide e obeyed an equilibrium hypothesis, then spectrum of the components of the pole- pole should be associated with a better ıal-to-noise ratio than the average spectrum. fact, the spectra gave no indication of a 14- nth peak.

'he background spectra—The spectra of all ords rise sharply at the low-frequency end, nmencing at about 0.1 cpy. The most obvious erpretation is that we are dealing with a erposition of two separate spectra (apart m the Chandler peak and seasonal line spec- m): (i) a white noise on the order of 10^3 ^{2}/cpy; (ii) a low-frequency peak, diminish- from 10^5 mm^2/cpy at 0.01 cpy to 10^3 mm^2 0.1 cpy and presumably dropping beneath white noise at higher frequencies. The two ctral features are presumably associated with erent geophysical phenomena, but this is by means proven.

The white noise is probably due to meteoro- ically induced fluctuations in sea level. Two sible causes suggest themselves for the low- quency rise: climatically induced changes in rld-wide sea level or the effect of vertical vements of contents. We believe the second ernative to be the more likely. World-wide nges in sea level would be coherent from tion to station and in phase. In fact the ss-spectra between Bombay and Swinemünde *'aubrich*, 1958] are out of phase at the lower quencies. *Munk and Revelle* [1952] plotted ade-to-decade variations in sea level for all ilable tide stations, and it turns out that se decade averages are indeed incoherent.

The total power contained by the low-fre- ency tail is on the order of 50 cm^2. Suppose set $\xi = kt$, corresponding to a linear rise in ter level (or drop in beach level). We set the an elevation equal to zero. The mean-square vation for T years of record is then $k^2T^2/12 =$ cm^2. With $T = 50$ years this gives $k = 0.25$ year^{-1}, which is of the right order.

Conclusions

The composite spectra indicate a pole tide, frequency of which is in good agreement h that obtained from latitude observations. There are a number of puzzling features. The pole tide appears at only four of the eleven stations investigated, and at these stations it is considerably larger than the corresponding equilibrium values. Spectra of the pole-tide pole (which assumes a dependence on latitude and longitude in accordance with equilibrium theory) do not indicate the pole tide at all! Apparently the pole tide does not support an equilibrium hypothesis.

Offhand, this would appear to be an implausible situation. It is known that the fortnightly tide does not deviate radically from equilibrium; accordingly, the 14-month tide, being of longer period, could be expected to agree very closely with equilibrium theory. But this is not a valid extrapolation. The fortnightly tide is a p_2^0 spherical harmonic, the pole tide a p_2^1 harmonic. In the former case the axis of the tidal oscillation remains fixed; in the latter case it does not. The theoretical developments are quite different for the two cases, and we cannot judge whether the dynamic effects on the pole tide are negligible. In the case of the core, *Jeffreys and Vicente* [1957*a*, *b*] have demonstrated that the dynamic effects are important in treating the free nutation.

If the equilibrium argument is not valid and the amplitude of the pole tide varies erratically from place to place, then the analysis of variance as outlined in the Appendix is not pertinent. (We have taken the same B for all stations.) The evidence in favor of the relatively broad spectral peak of the pole tide may not be decisive.

There are difficulties in comparing the tidal-effective Love number k of the planet earth (derived from the period of free nutation) with the corresponding number k_s for the solid earth (derived from seismic observations). These two numbers have often been set equal. The usually quoted value is 0.29. But there should be a difference because of the effects of the oceans and the fluid core. According to Jeffreys and Vicente the effect of the core is to increase k by roughly 20 per cent; the pole tide leads to a reduction by roughly the same amount, equation (37), and the two effects just happen to cancel, provided the pole tide follows the equilibrium law. If this is not the case, then at present there is no way to compare k and k_s.

TABLE 4—*Values of log P_{ij}*

Station, i	α_i	56	57	58	59	60	61	62	63	64	65	66	67	68	69	70	71	72	73	74	75	76	77	78
1	0.2263	0.11	3.36	3.59	3.40	3.70	3.76	3.77	3.65	2.40	0.13	3.87	4.20	3.96	3.12	2.07	0.18	2.92	3.21	3.16	3.22	3.19	3.15	3.50
2	.2356	2.47	2.10	0.56	2.49	3.37	3.53	3.36	3.49	3.31	3.06	3.87	4.00	3.62	2.90	2.90	2.91	3.16	3.12	3.00	3.16	2.98	3.13	3.39
3	.2471	3.56	3.59	3.01	2.56	2.78	3.18	3.65	3.56	3.07	2.84	1.83	1.68	1.44	0.16	2.79	2.74	2.53	3.17	3.00	2.77	3.39	3.36	3.24
4	.2485	1.31	2.71	2.94	2.93	2.83	2.67	2.64	2.82	3.06	2.84	3.39	3.77	3.59	3.00	2.81	0.18	2.31	3.14	3.05	2.64	2.85	2.77	2.68
5	.2210	3.01	2.09	0.11	2.96	3.55	3.68	3.49	3.25	3.29	2.98	2.14	2.95	2.91	2.83	3.15	3.10	2.58	0.19	0.20	0.21	0.21	1.21	1 52
6	.2388	2.53	2.73	2.69	2.31	1.80	1.72	2.24	2.51	2.18	1.36	2.47	2.49	2.93	3.23	2.94	1.14	1.54	2.29	2.86	3.17	3.07	2.57	2.50
7	.2497	1.08	1.08	1.08	0.88	2.37	2.73	2.89	2.84	2.73	2.90	3.21	3.09	2.45	3.04	3.05	2.08	1.15	2.43	2.87	2.76	2.21	2.78	2.76
8	.2471	3.08	3.07	2.52	1.08	1.79	2.72	3.02	2.89	3.23	3.37	3.14	3.14	3.22	3.05	2.32	3.16	3.50	3.30	2.83	2.46	2.54	3.03	3.04
9	.2314	3.01	2.70	2.75	2.41	2.94	2.99	2.53	1.99	3.00	3.29	2.99	2.87	3.30	3.27	2.85	2.75	3.03	2.88	2.80	2.88	2.40	2.91	3.18
10	.2020	3.04	3.06	3.34	3.17	2.22	2.29	2.98	2.94	2.11	2.11	2.46	2.61	3.08	3.31	3.12	2.03	2.35	3.15	3.23	2.85	2.42	2.66	2.63
11	.0951	2.52	2.85	2.58	2.64	2.67	2.06	1.48	1.73	2.00	2.59	2.86	2.77	2.68	2.47	1.14	2.50	3.11	3.02	2.52	2.92	3.03	2.61	2.14
I	.2394	2.98	3.23	3.17	3.01	3.35	3.46	3.52	3.48	3.06	2.80	3.65	3.91	3.64	2.90	2.73	2.53	2.86	3.16	3.06	3.02	3.15	3.15	3.30
II	.2299	2.84	2.51	2.37	2.76	3.27	3.40	3.23	3.03	3.04	2.71	2.33	2.79	2.92	3.07	3.06	2.82	2.33	1.98	2.54	2.85	2.75	2.27	2.30
III	.2484	2.79	2.78	2.24	1.00	2.17	2.73	2.96	2.87	3.05	3.20	3.19	3.12	2.99	3.05	2.82	2.90	3.20	3.06	2.85	2.63	2.41	2.92	2.92
IV	.2167	3.03	2.93	3.16	2.96	2.69	2.75	2.82	2.71	2.73	2.99	2.78	2.75	3.20	3.29	3.01	2.49	2.79	3.05	3.08	2.86	2.41	2.79	2.97
V	.0951	2.52	2.85	2.58	2.64	2.67	2.06	1.48	1.73	2.00	2.59	2.86	2.77	2.68	2.47	1.15	2.50	3.11	3.02	2.52	2.92	3.03	2.61	2.14
S_j'		10	19	18	26	11	22	32	115	427	700	1585	1950	2138	2318	726	2	328	169	42	34	90	57	36
S_j''		0	0	0	0	0	0	0	0	0	0	.25	.50	.25	0	0	0	0	0	0	0	0	0	0

Acknowledgments—We are greatly indebted to ohn Tukey for his frequent advice concerning e analysis of variance.

Appendix

Table 4 contains a double-entry listing of g P_{ij} where P_{ij} is the computed power density f the spectrum for station i (Table 1) at freuency $j\Delta f$, $\Delta f = 0.0125$ cpy. We let σ_i^2 designate e average power density to both sides of the ole-tide peak. We wish to fit the computed ectral densities to some scheme

$$P_{ij} = \sigma_i^2 + B\alpha_i S_j = \sigma_i^2\left(1 + \frac{B\alpha_i S_j}{\sigma_i^2}\right)$$

that

$$\log P_{ij} = A_i + \frac{B_0\alpha_i S_j}{\sigma_i^2}$$

a first order, and

$$\log P_{ij} = A_i + \frac{B\alpha_i S_j}{\sigma_i^2} - \frac{1}{2}\left(\frac{B_0\alpha_i S_j}{\sigma_i^2}\right)^2$$

a second order. Here $\alpha_i = \sin^2\theta_i \cos^2\theta_i$ is the quilibrium scale factor depending on the colatide of the station.

We wish to distinguish between two alternaves: (i) $S_j = S_j'$, the power density of the titude data and (ii) $S_j = S_j''$, the spectrum r a sharp peak at $j = 67$. Values of S_j' and S_j'' re given in Table 4. Included in the former lternative is the presumption that the spectra f the observed tide correspond to the computed titude spectra; in the second alternative, they rrespond to a spectral line at 0.84 cpy.

The following regression schemes are fitted y least squares

$$W_0' = \sum_{ij}\left[\log P_{ij} - A_i - \frac{B_0'\alpha_i S_j'}{\sigma_i^2}\right]^2$$

$$W_0'' = \sum_{ij}\left[\log P_{ij} - A_i - \frac{B_0''\alpha_i S_j''}{\sigma_i^2}\right]^2$$

$$\hat{W}_0 = \sum_{ij}\left[\log P_{ij} - A_i - \frac{\hat{B}_0'\alpha_i S_j'}{\sigma_i^2} - \frac{\hat{B}_0''\alpha_i S_j''}{\sigma_i^2}\right]^2$$

d this determines B_0', B_0'', $\hat{B}_0'$, $\hat{B}_0''$. A ression to a second order is performed, and the llowing residual sums of squares are computed.

$$W' = \sum_{i,j}\left[\log P_{ij} - A_i - \frac{B'\alpha_i S_j'}{\sigma_i^2} + \frac{1}{2}\left(\frac{B_0'\alpha_i S_j'}{\sigma_i^2}\right)^2\right]^2$$

$$W'' = \sum_{ij}\left[\log P_{ij} - A_i - \frac{B''\alpha_i S_j''}{\sigma_i^2} + \frac{1}{2}\left(\frac{B_0''\alpha_i S_j''}{\sigma_i^2}\right)^2\right]^2$$

$$\hat{W} = \sum_{ij}\left[\log P_{ij} - A_i - \frac{\hat{B}'\alpha_i S_j'}{\sigma_i^2} + \frac{1}{2}\left(\frac{\hat{B}_0'\alpha_i S_j'}{\sigma_i^2}\right)^2 - \frac{\hat{B}''\alpha_i S_j''}{\sigma_i^2} + \frac{1}{2}\left(\frac{\hat{B}_0''\alpha_i S_j''}{\sigma_i^2}\right)^2\right]^2$$

To test the validity of (i), we set $B_0'' = 0$ and $B'' = 0$. We note that

$$S' = (W' - \hat{W})/1 \quad \text{and} \quad S = \hat{W}/\nu$$

are independent estimates of the same variance provided that hypothesis (i) is true. The ratio

$$F'' = \frac{S'}{S} = \frac{W' - \hat{W}}{\hat{W}}\nu$$

is distributed according to the 'F-distribution' with 1 and ν degrees of freedom. The degrees of freedom ν of the residual equals the total sample number minus the number of fitted parameters. Similarly, for hypothesis (ii) the ratio

$$F' = \frac{W'' - \hat{W}}{\hat{W}}\nu$$

TABLE 5—*Regression of the pole tide peak near 14 months*

	Station, i					
	1–11	1–4	5–6	7–8	9–10	11
W'	136.88	68.16	39.80	16.37	5.65	5.53
W''	137.91	66.39	41.33	17.92	6.06	5.30
$\hat{W}$	135.72	66.30	39.70	16.16	5.44	6.26
F'	3.87	0.11	1.72	4.57	4.80	0.17
F''	0.28	2.41	1.03	0.53	1.66	1.03
ν	240	86	42	42	42	20
95%	3.92	4.00	4.17	4.17	4.17	4.35
90%	2.75	2.79	2.79	2.84	2.84	2.97

is distributed as $F(1, \nu)$. Values of F' and F'' for various station groups (Table 1) are given in Table 5.

For stations 1 to 4 hypothesis (ii) is favored but not at the 90 per cent level (2.41 does not exceed the 90 per cent upper limit of 2.79). All other groups of stations and the composite average favor (i). A similar analysis (not shown) in the restricted frequency range $j = 60$ to 74 leads to the same conclusions.

References

Bakhuyzen, H. G. Van de Sánde, Über die Änderung der Meereshöhe und ihre Beziehung zur Polhöhenschwankung, *Vierteljahrschr. Astron. Ges., Leipzig, 47,* 218–221, 1913.

Baussan, J., La Composante de Chandler dans la variation des niveaux marins, *Ann. géophys., 7,* 59–62, 1951.

Blackman, R. and Tukey, J., The measurement of power spectra from the point of view of the communications engineer, *Bell System Tech. J., 37,* 185–282, 1958.

Christie, A. S., The latitude variation tide, *Bull. Phil. Soc. Wash., 13,* 103–122, 1900.

Fedorov, E. P., O vliyanii kolebanii urovnya okeana, vizivaemich dvijeniem poliusov zemli, na eto dvijenie, *Doklady Akad. Nauk SSSR, 67,* 647–650, 1949.

Haubrich, R. A., The pole tide, Dissertation for the degree of Doctor of Philosophy (Geology), Univ. of Wisconsin, 1958.

Helmert, F., Neue Formeln für den Verlauf der Schwerkraft im Meeresniveau beim Festlande, *Sitzber. kgl. preuss. Akad. Wiss.,* 676, 1915.

Jeffreys, H., *The Earth,* Cambridge University Press, 1952.

Jeffreys, H., and R. O. Vicente, The theory of nutation and the variation of latitude, *Monthly Notices Roy. Astron. Soc., 117,* 142–161, 1957*a*.

Jeffreys, H., and R. O. Vicente, The theory of nutation and the variation of latitude: The Roche model core, *Monthly Notices Roy. Astron. Soc., 117,* 162–173, 1957*b*.

Kulikov, K. A., The motion of the poles of t earth and variation of latitude, *Ouspekhi A. Nauk, 5,* 111, 1950.

Lambert, W., An investigation of the latitude Ukiah, California, and of the motion of t pole, *U. S. Coast and Geodetic Survey, Sp Publ. 80,* 62–64, 1922.

Larmor, J., The influence of the oceanic wat on the law of variation of latitudes, *Proc. Lo don Math. Soc.* (2), *14,* 440-449, 1915.

Maksimov, I. V., O "poliusnom prilive" v mor atmosfere zemli, *Trudy Inst. Okeanol. Ak Nauk SSSR, 8,* 92-118, 1954.

Maksimov, I. V., Poliusnyi priliv v okeane zen *Doklady Akad. Nauk SSSR, 108,* 799–801, 19

Munk, W. H., and G. MacDonald, *The Rotati of the Earth: A Geophysical Discussion,* Ca bridge University Press, 1960.

Munk, W. H., and R. Revelle, On the geophy cal interpretation of irregularities in the rotati of the earth, *Monthly Notices Roy. Astron. So Geophys. Suppl., 6,* 331–347, 1952.

Munk, W. H., F. E. Snodgrass, and M. J. Tuck Spectra of low-frequency ocean waves, *B Scripps Inst. Oceanog.* (in press).

Newcomb, S., On the dynamics of the earth's ro tion, with respect to the periodic variations latitude, *Monthly Notices Roy. Astron. Soc.,* 336–341, 1892.

Przbyllok, E., Über die sogenannte Polflut in Ost-und Nordsee, *Veröff. des Preus. Geodasisch Inst., no. 80,* Potsdam, 1919.

Rosenhead, L., Tides on a two-layer ear *Monthly Notices Roy. Astron. Soc., Geoph Suppl., 2,* 171–196, 1929.

Takeuchi, H., On the earth tide in the compr sible Earth of varying density and elastici *J. Fac. Sci., Univ. Tokyo, 7,* 1–153, 1951.

Von Schweydar, W., Die Bewegung der Drehac der elastischen Erde im Erdkörper und Raume, *Astron. Nachr., 203,* 103–114, 1916.

Walker, A. M., and A. Young, Further resu on the analysis of the variation of latitu *Monthly Notices Roy. Astron. Soc., 117,* 1 141, 1957.

(Manuscript received July 30, 1959.)

Zonal Harmonics of the Earth's Gravitational Field and the Basic Hypothesis of Geodesy

John A. O'Keefe

Theoretical Division, Goddard Space Flight Center
National Aeronautics and Space Administration
Washington, D. C.

Abstract—The basic hypothesis of geodesy as stated by Vening Meinesz and Heiskanen calls for an extremely smooth gravitational field for the earth as a whole, apart from local irregularities. From satellite measurements of zonal harmonics of orders 2, 3, and 4 it is shown that the actual roughness is about an order of magnitude greater than that demanded by the basic hypothesis of geodesy.

leiskanen and Vening Meinesz [1958] have posed a basic hypothesis of geodesy. They pose that the earth should be considered as ing a form close to that of fluid equilibrium. ey then consider the deviations from equiliım in terms of isostatically reduced gravity malies with respect to the assumed state of d equilibrium. Their hypothesis states that se anomalies show no areas of deviation where mean anomaly multiplied by the area is re than a certain number of milligals gameters)². For this number they propose igure of 30 mgal Mm²; and they further pose that there are no more than ten such iation areas. In their discussion of this othesis they point out that it implies that effect on geoid height of unknown gravity malies in areas remote from a given point P ll not be greater than about ± 2.6 meters. By ote areas they mean areas more than 3000 meters from P. The effect of remote areas on ections is similarly stated as not more than ″.35.

In this paper we propose to test the hypothesis of Heiskanen and Vening Meinesz by comparison with the zonal harmonics of the earth's field as these have recently been determined by measurements from satellites.

The observational data which we shall use are summarized in Table 1, based on the work by *Jacchia* [1959] at Harvard, *Kozai* [1959] at Harvard, *King-Hele and Merson* [1959] in England, and the NASA group [*O'Keefe and others*, 1959]. It will be seen that the agreement on the values of the second, third, and fourth zonal harmonics is excellent, and a firm basis for comparison is provided.

The determination of the value of the second harmonic appropriate to a fluid earth offers some difficulties. *Henriksen* [1959] has pointed out that it is not correct to calculate the hydrostatic value of the earth's flattening by the methods which have been in vogue up to the present, because these methods involve the hypothesis that the real flattening is identical with the hydrostatic flattening. Henriksen begins

TABLE 1—*Summary of recent results on the earth's gravitational field*

	Jacchia	King-Hele	Kozai	NASA	Theoretical	NASA-Theoretical		
						$A_{n,0}$	$g_{n,0}$	$N_{n,0}$
	$-17.557 \pm .010$	$-17.564 \pm .003$	-17.549*	$-17.555 \pm .001$	-17.372	$-.183$	-11.05	-72.1
	...	...	$+.228 \pm .008$	$+.25 \pm .03$	0	$+.25$	$+4.7$	$+15.4$
	$+1.6 \pm .3$	$+0.9 \pm .15$	$+1.4$*	$+1.12 \pm .04$	$+1.95$	$-.83$	$+3.7$	-8.0

These values have been calculated, not from the quantities given in Smithsonian Report #22, but n privately communicated corrections to these values kindly supplied by Dr. Kozai.

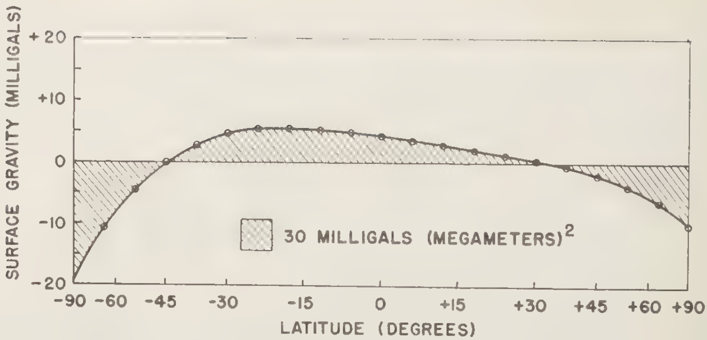

FIG. 1—Combined effect on surface gravity of zonal harmonics 2, 3, 4, referred to a fluid surface witl flattening of 1/299.8.

with the value of $(C - A)/C = H$ and the value of J determined by satellite measurements. Dividing these he obtains the quantity

$$q = J/H \tag{1}$$

where H is the precessional constant or the dynamical flattening and J is the coefficient of the second zonal harmonic in the expression for the earth's potential. From q the hydrostatic value of the earth's flattening can be calculated by the methods of De Sitter, which are presented in a convenient form by *Jones* [1954]. To make the calculation it might appear that two approximations are required; but in fact it turns out that any reasonable value of ϵ can be substituted in the quadratic terms of Jones' equation; and the final value can be obtained in a single approximation. Henriksen finds that the flattening of a fluid earth with the same polar moment of inertia as the actual earth would be 1/300.0; with the NASA values we find 1/299.8.

Since these results may appear surprising, it is useful to emphasize that the older determination of the flattening of the earth from $(C - A)/C$ involved as an essential assumption the proposition that the earth was in hydrostatic equilibrium. The new method is required by the discovery that the earth is not in hydrostatic equilibrium.

The corresponding hydrostatic value of the second zonal harmonic is determined from *Jones'* [1954, p. 9] equation (9); and the fourth harmonic from equation (10) using Bullard's estimates of κ, λ [*Jones*, 1954, p. 13]. We have added these theoretical estimates in column 6 of Table 1. In column 7 we show the coefficient of the d crepancies in potential, and in column 8 t coefficient of the discrepancies in millig between the theoretical values of column 6 a the observed values of column 5. The sum the discrepancies in milligals is graphed Figure 1. The length of a short segment of t abscissa in Figure 1 is proportional to the a of a zone of the earth of the correspondi range in latitude. Hence the area under t curve in Figure 1 is proportional to the c responding deviation in milligals (megameters

In Figure 2 we show the geoid heights abo a fluid earth corresponding to the observ zonal harmonics. For comparison, a height ±2.6 meters is indicated by a shaded zone. Figure 3, the effect of the observed zo harmonics on the deflection of the vertical shown. The shaded zone indicates a range ±0.35.

In comparing the data of Figures 1, 2, and with the basic hypothesis of geodesy, we be in mind the fact that these figures refer to t earth's external gravitational field, whereas t basic hypothesis of geodesy is stated in terms isostatic gravity anomalies. However, th distinction loses most of its significance for t very large areas which are involved here. is believed that the free-air anomalies he obtained can be considered without serio error as isostatic anomalies; thus the comparis of the data of Figure 1 with the basic hypothe of geodesy is believed to be justified.

A question which at once arises is wheth the new values of the zonal harmonics can

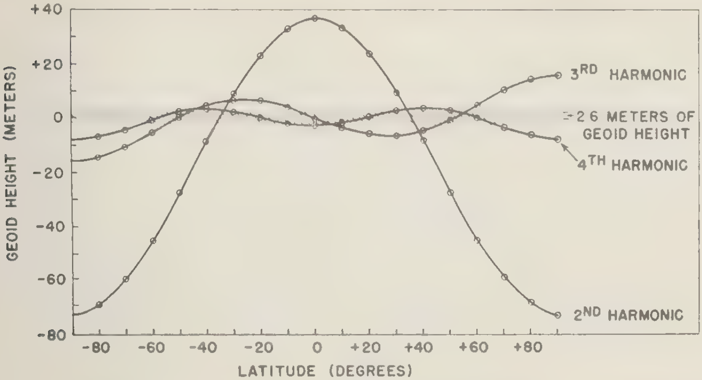

. 2—Effect of 2nd, 3rd, and 4th harmonics on geoid height as referred to a fluid earth with a flattening of 1/299.8.

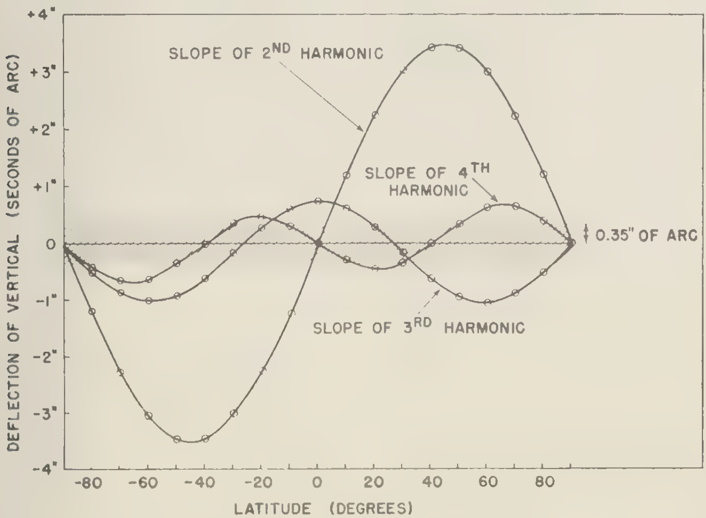

. 3—Effect of harmonics of order 2, 3, 4 on deflection of the vertical in the meridian, referred to a fluid earth with a flattening of 1/299.8.

onciled with measurements of gravity which ve already been made throughout the world. is question has been attacked by *Kaula* 59a, 1959b] who showed that the new values in fact reconcilable.

It is possible to calculate the expected lifenes of these harmonics on the hypothesis at they are maintained by viscous forces in interior of the type discussed by Heiskanen d Vening Meinesz. Their equation (10B-26a), p. 369,

$$t_r L = 6.3 \ Mmy_m \tag{2}$$

where t_r is the time required for the anomaly in the deformed region to fall to $1/e$ of its original value, L is the radius of the deformed region, and the units are megameters (Mm) and thousands of years (y_m), implies a lifetime of the order of a thousand years or less for these

distortions, whose size is comparable to the size of the earth itself.

In order to look more deeply into this question we calculate the loading of the earth's crust which corresponds to these harmonics. As a preliminary, we note the general proposition that every spherical harmonic of the earth's gravitational field corresponds to a linear combination of inertial integrals extended through the earth's interior. For example, the zero harmonic corresponds to the total mass; the first harmonics to first moments; the second harmonics to linear combinations of the moments of inertia such as $C-A$. All these inertial integrals of degree above zero should increase with increasing radius. Hence the minimum mass required to produce a given inertial integral is the mass required to produce it by a surface distribution. Accordingly, if we replace the inertial integrals by surface distribution of mass we shall obtain minimum loading of the interior consistent with our observed harmonics. *Jeffreys* [1952, pp. 182, 183] has pointed out that one milligal of surface gravity corresponds to about 10 meters of rock. It follows that if our observed harmonics were disappearing at the rate called for by equation (2) above we would observe transgressions of the sea corresponding to height changes at rates up to 10 meters per century. Since these are far in excess of the maximum observed rates, we must conclude that the observed harmonics are not maintained by viscous forces of the same type as those called upon by Heiskanen and Vening Meinesz to account for the Fennoscandian uplift. We conclude that the zonal harmonics must be supported either by ordinary mechanical strength in the earth's interior or perhaps by hydrodynamic forces such as those resulting from convection.

In concluding this discussion we wish to point out the bearing of the basic hypothesis of geodesy on the feasibility of measuring geoid heights and deflections of the vertical by gravimetric methods. The difficulty of applying gravimetric methods is simply a difficulty arising from the lack of measurements over wide areas of the earth. The question of whet useful results can now be obtained has b discussed by *Heiskanen and Vening Mei* [1958, p. 74], who say that, at present, employment of Stokes' theory and sim methods 'is warranted only if it is based on above considerations regarding the degree equilibrium obtained by the Earth.' In sh the use of Stokes' theorem and related form can yield useful results only if the conditi of the basic hypothesis of geodesy are fulfil Since they are not fulfilled, we are regretf driven to the conclusion that the employm of these methods requires much more informa than is now available from gravity meas ments alone.

Acknowledgment—The author's thanks are to Mrs. Ann Bailie for her help in the prepara of this paper.

References

Heiskanen, W. A., and F. A. Vening Mein *The Earth and its Gravity Field,* McGraw-I New York, 1958.

Henriksen, S. W., The hydrostatic flattening the earth, *Annals of IGY, 11,* in press, 195

Jacchia, L., The earth's gravitational potentia derived from satellites 1957β_1 and 1958β_2, *Sm sonian Astrophys. Obs. Spec. Rept. 19,* 1–5, 1

Jeffreys, H., *The Earth,* Cambridge Univer Press, 1952.

Jones, H. Spencer, Dimensions and rotation *The Earth as a Planet,* G. P. Kuiper, ed., I versity of Chicago Press, 1954.

Kaula, W. M., Reconciliation of Stokes' func and astro-geodetic geoid determination, *J. G phys. Research, 62,* 61–71, 1959a.

Kaula, W. M., Statistical and harmonic anal of gravity, *Army Map Service Tech. Rept.* p. 101, 1959b.

King-Hele, D. G., and R. H. Merson, A value for the earth's flattening derived f measurements of satellite orbits, *Nature,* 881–882, 1959.

Kozai, Y., The earth's gravitational potential rived from the motion of satellite 1958β_2, *Sm sonian Astrophys. Obs. Spec. Rept. 22,* 1–6, 1

O'Keefe, J. A., A. Eckels, and R. K. Squi The gravitational field of the earth, *Astron J., 64,* in press, 1959.

(Manuscript received August 28, 1959.)

The Three Components of the External Anomalous Gravity Field

H. Orlin

U. S. Coast and Geodetic Survey
Washington 25, D. C.

Abstract—By means of a surface coating determined from the gravity anomalies at sea level and from the geoid heights, the three components of the external anomalous gravity field are computed. This technique is applied to points at and above sea level and comparisons are made with existing methods.

The extrapolation of the earth's gravity field extraterrestrial regions is a significant prob- n in this space age. Mathematically this prob- n may be resolved by applying Gauss and asles' theorem [*Webster*, 1949]. This theorem a special case of Green's formula applied to equipotential surface. The theorem states at outside any equipotential surface of a dis- bution M the same effect as the distribution elf may be produced by distributing over e surface a layer of surface density $\sigma =$ $4\pi k$ times the normal gradient of the po- ntial at the surface. The mass of this entire uipotential layer will be that of the original ernal distribution.

The theorem is applicable to an equipotential rface which encompasses all the attracting atter. The geoid is not quite such a surface cause of the protruding masses. However, e condensation of these masses onto the geoid arcely changes this surface by more than two eters anywhere and the resulting co-geoid is surface to which the theorem can be applied. As is usual in geodetic practice, we consider e two problems of the normal gravity field d the anomalous gravity field separately. We ke the field due to the spheroid of reference the normal field. Formulas applicable to e intensity and direction of this normal field sea level have been in use for some time. eodesists have been concerned only with this ld at or close to the surface, and for relatively all elevations the theoretical gradient has ven them sufficient accuracy for most geodetic rposes. Formulas for the gravity potential at extreme elevations are given by *Helmert* [1884] for the reference spheroid, and from these the components of gravity may be derived. Recently, more tractable formulas have been derived by *Lambert* [1958] which give the components in the direction of the radius vector and perpendicular to the radius vector. Another development by *Cohen* [1957] gives the three (XYZ) components of the gravity vector in a rectangular cordinate system referred to the center of the spheroid of reference. Of course, the X and Y components are equal for an ellipsoid of revolution.

We now consider the effect of the anomalous field which is due to the departure of the earth from a spheroid or an ellipsoid of revolution. For the direction of the gravity vector at sea level, geodesists have leaned heavily upon the modification of Stokes' formula by *Vening Meinesz* [1928]. Vening Meinesz also indicated how this direction might be obtained for a point above sea level, but the method does not seem to have been developed. Seven years ago, *Hirvonen* [1952] considered a function which reduces to Stokes' function for a point at sea level. Theoretically, to determine the direction of the gravity vector anywhere in space one would have to prepare a table of these functions for each elevation. However, Hirvonen found a series of approximating factors which simplify the computations considerably, but this method requires a determination of the direction of the gravity vector at sea level. In addition, he considered Pizzetti's derivation of Stokes' function by means of Pois-

son's integral formula and applied this integral formula to the determination of gravity anomalies at points above sea level. To my knowledge this is the only practical method reported in the literature for the determination of these anomalies.

Let us now return to the surface-density method previously mentioned. The surface density may be considered to be due to a normal field for an ellipsoid of revolution and an anomalous field. If we assume the solution for a normal field as given by Helmert, Lambert, and others, we need to consider only the effect of the anomalous field.

The development by *Stokes* [1849] begins with this surface density or coating, which is the mathematical equivalent of the anomalous masses. The coating reproduces the gravity anomalies, the undulations of the geoid, and the external anomalous field. Stokes assumed that this surface density could be expressed as a series of spherical harmonics and after a number of mathematical transformations eliminated the coating and replaced it with the complicated Stokes' function. To apply this function to points above sea level would require for each altitude extensive tables similar to those prepared by *Sollins* [1947] for sea level. However, if the surface-density distribution were obtained, the determination of the external field would be considerably simplified, as the coating is a mass distribution to which Newton's inverse-square law is directly applicable.

To establish an analytic expression for the coating, we follow Helmert and consider the

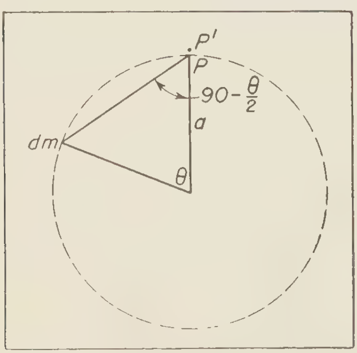

FIG. 1—Attraction of anomalous mass.

potential at a point P on a sphere of radius a of the same volume as the spheroid of referenc or the actual earth, and the normal gradien at a point P' close to and above P (Fig. 1). Th assumption made is that the coating distribute over this sphere and due to the anomalou masses of the actual earth produces the sam field as the coating over the geoid or co-geoi due to the same masses.

The notation follows:

σ = surface density of Stokes' coating
V = total potential at P due to the mas distribution of the actual earth (geoid
U = total potential at P due to the mas distribution of the reference spheroid
N = geoid height or the distance separatin the spheroid and the equipotential sur face of the actual earth of the sam potential, commonly called the geoid
U_0 = V = total potential on the spheroid o reference
T = total disturbance potential at a point due to the anomalous masses
G = normal gradient of V at P or the gravit intensity
γ = normal gradient of U_0 or theoretica gravity on the reference spheroid at point corresponding to P on the geoid
Δg = gravity anomaly = $G - \gamma$
k = gravitation constant = 6.673×10^{-8}
dm = mass element
r = distance of dm from P
θ = angle at the center of the sphere betwee the direction to P and the direction t dm
a = radius of a sphere of equivalent volum to the geoid
n = direction of the normal at P
ρ = mean density of the earth = 5.51 gm/cm³

Assuming the anomalous masses distribute as a coating over the surface of a sphere (Fig 1 we define the potential at P as

$$-T = k \int_s \frac{dm}{r}$$

and the normal derivative

$$\frac{dT}{dn} = k \int_s \frac{dm}{r^2} \frac{dr}{dn}$$

ıt, for a sphere of radius a, $dr/dn = \sin\theta/2$ ıd $r = 2a \sin\theta/2$. Hence

$$dT/dn = -T/2a$$

It can also be shown that the mass at the ɔint P contributes nothing to this normal ɛrivative. However, for a point above the ɪrface, the attraction of a disk of uniform ɛnsity surrounding P upon a particle in conɪct with it at its center is independent of the ɪdius of the disk and is equal to $2\pi k$ times ɛ surface density at P. For such a point P' ɛ normal derivative is given by

$$dT/dn = -T/2a + 2\pi k\sigma$$

ʼhere σ is the surface density at P. ence

$$\sigma = 1/2\pi k\,(dT/dn + T/2a)$$

Returning now to the spheroid and the geoid, ɛ define $T = V - U$, where $U = U_0 + (dU_0/$ ɪ$)N$ + higher order terms $= U_0 + \gamma N$. ence $T = -\gamma N$ as $V = U_0$ by definition. ıking the normal derivative of T, we find

$$\frac{dT}{dn} = \frac{dV}{dn} - \frac{dU}{dn}$$

$$= G - \gamma + \frac{2\gamma N}{a} = \Delta g + \frac{2\gamma N}{a}$$

ıbstituting this expression for dT/dn in the exɛssion for the surface density, we find, after ttting $\gamma = 4/3\ \pi k a\rho$ and $T = -\gamma N$,

$$\sigma = \Delta g/2\pi k + \rho N$$

In discussing the field determined by this ɪrface density, we consider the three comɔnents of the anomalous gravity vector in a ocentric coordinate system (Fig. 2). These mponents are $\triangle g_R$ in the direction of the dius vector, $\triangle g_M$ perpendicular to the radius ɛctor in the plane of the meridian and posiʼe to the south, and $\triangle g_P$ perpendicular to the ɛridan plane and positive to the east.

$$\Delta g_R = \int_s k\sigma \frac{1}{r^2} \cos B\, ds$$

$$\begin{matrix}\Delta g_P \\ \Delta g_M\end{matrix} = \int_s k\sigma \frac{1}{r^2} \sin B \begin{Bmatrix}\sin A \\ \cos A\end{Bmatrix} ds \qquad (1)$$

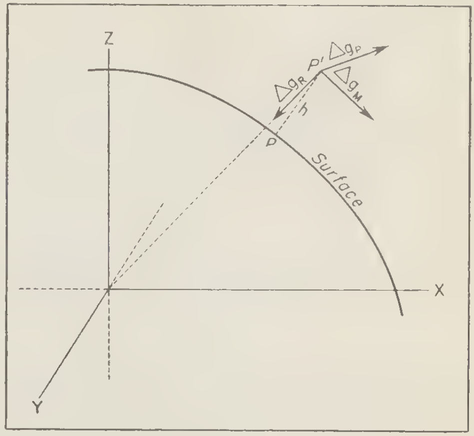

FIG. 2—The three components of the anomalous gravity vector.

where

A is the azimuth from the south,

B is the angle between the radius vector and the direction to the element of surface area ds, and

r is distance of ds from P'.

The sign has been chosen to give the deflection in the sense of astronomic minus geodetic position, in seconds of arc, when multiplied by $1/g \sin 1''$ (g is the acceleration due to gravity at P'. Note: West longitudes are considered positive.)

In practice, the integration is replaced by a summation of small elements of constant surface density. If the elements are small enough we may consider the effects of 'squares' bounded by meridians and parallels, and we may concentrate the entire mass of a square at its center. If the dimension of a side of a square is less than one-tenth of the distance from P', the error is negligible. If this dimension is on the order of one-half of the distance, the error is less than 5 per cent. For squares 10 or more minutes of arc on a side, this error is rarely greater than the assumption that the surface density is constant over the square. Hence, equations (1) are replaced by the following summations:[1]

[1] For computing purposes $k\sigma_i$ is multiplied by 10^8 to give Δg_R, Δg_P, and Δg_N in milligals.

$$\Delta g_R = k \sum_i \frac{\sigma_i \cos B_i \, dS_i}{r_i^2}$$

$$\begin{matrix} -\Delta g_P \\ \Delta g_M \end{matrix} = k \sum_i \frac{\sigma_i \sin B_i \begin{Bmatrix} \sin A_i \\ \cos A_i \end{Bmatrix} dS_i}{r_i^2} \qquad (2)$$

where

B is the angle between the radius vector and the direction to the center of a square, and
dS_i is the area of the square.

Practically, these quantities are expressed in terms of the XYZ coordinates of P' and the center of the square (Fig. 3). The computations are easily adapted to a medium-sized computer.

In the vicinity of the projection of P' onto the surface, a plane area may be assumed, and the effect computed by equations (2) may be compared with the effect of plane rectangular laminae of constant surface density as given by equations (3). Where P' is close to the surface, equations (3) give more accurate results, but the difference is negligible for small squares. Adopting a coordinate system centered at the foot of the perpendicular from P', y in the meridian and positive to the south, and x in the prime vertical and positive to the east (Fig. 4), we obtain the following equations for the attraction of these rectangular laminae.

$$\Delta g_R = k\sigma\left[-\tan^{-1}\frac{x_2 y_1}{h r_2} + \tan^{-1}\frac{x_1 y_1}{h r_1} - \tan^{-1}\frac{x_1 y_2}{h r_4} + \tan^{-1}\frac{x_2 y_2}{h r_3}\right]$$

$$\Delta g_M = k\sigma \log_e \frac{(r_2 + x_2)(r_4 + x_1)}{(r_1 + x_1)(r_3 + x_2)} \qquad (3)$$

$$\Delta g_P = k\sigma \log_e \frac{(r_2 + y_1)(r_4 + y_2)}{(r_1 + y_1)(r_3 + y_2)}$$

Where $x_1 < x_2$, $y_1 < y_2$, and h is the elevation of P'.

In the region surrounding the point P' both the concentration of mass at the center of a square and the gradient of the coating are troublesome. Maintaining a distance-dimension ratio of 2 to 1, the factors for the inner squares

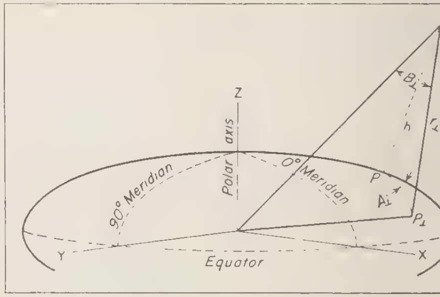

FIG. 3—Coordinate system.

are evaluated by equations (3). Within a rad[...] of 10 minutes of arc the 'circle-ring' method [...] employed. In this region we assume a norm[...] gradient for the coating and set

$$\sigma = \sigma_0 - s \sin A\sigma_x + s \cos A\sigma_y$$

We find for the effect of this inner ring

$$\begin{matrix} -\Delta g_P \\ \Delta g_M \end{matrix} = k \int_s \frac{\sigma s^2 \begin{Bmatrix} \sin A \\ \cos A \end{Bmatrix} dA\,ds}{(s^2 + h^2)^{3/2}}$$

$$= k\pi \begin{matrix} -\sigma_x \\ \sigma_y \end{matrix} [(s^2 + 2h^2)(s^2 + h^2)^{-1/2} - \ldots$$

$$\Delta g_R = k \int_s \frac{\sigma h s \, dA\,ds}{(s^2 + h^2)^{3/2}}$$

$$= 2\pi k\sigma_0[1 - h(s^2 + h^2)^{-1} \ldots$$

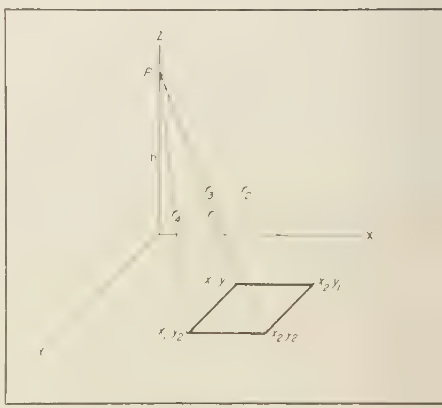

FIG. 4—Plane rectangular system.

TABLE 1—*Components of the gravity vector (C) coating, (SH) Stokes-Hirvonen methods*

Station	Elev., km	Δg_R(C), mgal	Δg(SH), mgal	ξ (C), sec	ξ (SH), sec	η (C), sec	η (SH), sec
Pad	0	+11.6	+17.0	−1.7	−1.1	−0.6	−0.9
	32	+2.8	+8.2	−0.3	+0.1	−1.8	−1.7
	64	−1.1	+3.8	+0.1	+0.4	−1.5	−1.8
Egg	0	+21.7	+30.0	+16.6	+16.1	+0.2	−0.1
	32	−21.4	−13.2	+6.8	+6.5	−4.1	−4.2
	64	−20.8	−12.3	+3.5	+3.5	−4.6	−4.2

ere

is the radius of the inner ring,

$_0$ is the surface density at the foot of the perpendicular from P',

$_x$ is the gradient in the x (as in equations 3) direction,

$_y$ is the gradient in the y (as in equations 3) direction, and

and σ_y are evaluated by Rice's three-gradient thod [*Heiskanen and Vening Meinez*, 1958]. assume a constant density for the 'triangles' ween the circle and the squares. The total ss of a 'triangle' is then assumed to be contrated at the center of gravity of the 'trigle.' A better approximation to Δg_R for nts above sea level is attained if σ_o is reced by the mean value of σ over the inner g.

t is difficult to state what size ring and ares will give the most accurate result with inimum amount of computation. The variain the coating field in the vicinity of the tion may be so irregular as to require exmely small squares and a very small inner cle. However, for a point more than 30 km ve sea level this inner region has a minor ct and 10-min squares are adequate.

Two examples (Table 1) were taken from real gravity field. I chose inner and outer ii of 27.8 km and 516 km, respectively, for Stokes-Hirvonen method. The approximate tribution of squares for the coating method ndicated in Table 2. The field at Pad and at g extended to 5°.5 and 7°.0, respectively.

should be noted that Δg_R represents the ference between observed and theoretical vity at the same point. This differs from the inition of a gravity anomaly in normal geodetic practice. Geodesists define a gravity anomaly as the difference between the gravity value at a point p on an equipotential surface of the potential field of the actual earth and the theoretical gravity value at a corresponding point of an equipotential surface of the potential field of the reference ellipsoid having the same potential as at p. This latter anomaly is given by Hirvonen's method. On the geoid the two anomalies differ by the Bruhn's term, the indirect effect.

The meridian and prime vertical components were computed in milligals and converted to

TABLE 2—*Distribution of 'squares'*

Inner ring	out to 10′
5′ squares	out to 20′
10′ squares	out to 1°.5
20′ squares	out to 4°.0
30′ squares	out to extent of coverage

seconds of arc. One second is approximately equal to 5 milligals. Most of the discrepancy between the two methods can be attributed to the larger field for the coating method. However, not to be overlooked is the fact that the geoid heights in the coating function were determined from a much larger gravity field. Thus with a limited field the coating may define the deflection better than the Stokes' function does.

The large change in the deflection, with elevation, at Egg is of interest. In the vicinity of this station, at the surface, there exists a large gravity gradient. Out to 40 km, the effect in the meridian is +9″.7, and in the prime vertical + 5″.4. The attenuation with elevation, which

FREE-AIR ANOMALIES

-50	-135	-125	-110	-90	-85
110	-120	-110	- 15	-105	-95
-20	+25	-25	-75	-105	-105
+30	+75	+80	0	-60	-100
+50	+75	+85	+85	+50	-75
+50	+65	+75	+90	+95	0

GEOID HEIGHTS

-36	-37	-38	-38	-39	-39
-36	-37	-38	-38	-39	-39
-36	-37	-38	-38	-39	-39
-36	-37	-38	-38	-39	-39
-36	-37	-37	-38	-39	-39
-36	-37	-37	-38	-39	-39

SURFACE DENSITIES times k

-9	-23	-21	-19	-16	-15
-19	-20	-19	-20	-18	-17
-5	+3	-5	-13	-18	-18
+3	+11	+11	-	-11	-17
+7	+11	+12	+12	+7	-13
+7	+9	+11	+13	+14	-1

contoured SURFACE DENSITIES times k

FIG. 5—Coating data.

is rapid in this region, produces the abrupt change from sea level to 32 km.

As additional gravity and geoid-height data become available, the coating method becomes more feasible. The data could be prepared in different forms (Fig. 5). Averages over small squares would be suitable for the large elec-

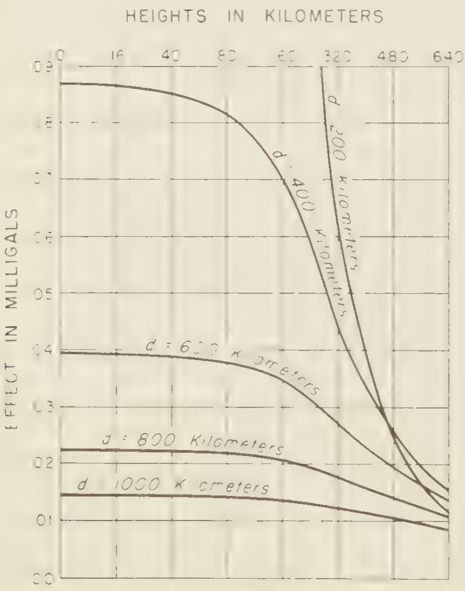

FIG. 6—Horizontal effect.

tronic computers. These averages, the coord nates (XYZ) of the center of each square, an estimates of the accuracy of the anomalies an geoid heights could be recorded on tapes, card etc. The computers could not only determi the components of the gravity vector but al estimates of their accuracy. Where small squares and the gradient over the inner ri are required, a map of $k\sigma \times 10^8 = 0.1592\,\Delta g$ 0.0368 N (Δg in milligals, N in meters) contours of this quantity would be desirable.

The problem which now arises is the exte of the field required for a determination of the components at a particular elevation. The retically, our summation should extend to t antipodes. Practically, we must be satisfi with a limited field and hope that the regi beyond this field balances out.

An indication of the error we commit, in t horizontal and vertical components, may gleaned from Figures 6 and 7, respectively. T effect at various elevations of an avera anomaly of 10 mgal or an average ge height of 43.2 meters in 1° squares (appro mate area 10,500 km²), at various distances from the projection of P' onto the sphero has been computed. The horizontal effects ha not been resolved into their meridian or prin vertical components.

Although the effect of each distant square small, the number of squares is large, and t

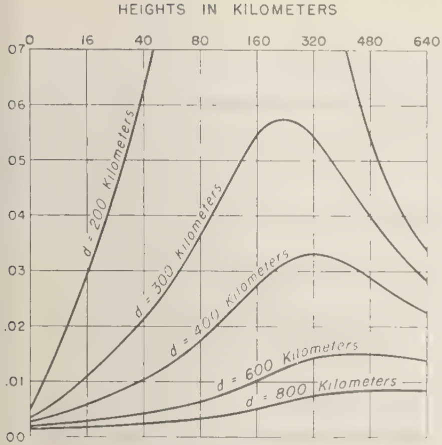

FIG. 7—Vertical effect.

tal effect may be considerable. Isolated large ıomalies are of little consequence at distances eater than 800 km. However, in some regions e average anomaly due to all 1° squares at distance of 800 km is on the order of 25 mgal. ıis produces a vertical component of approxiately 0.7 mgal at all elevations from 160 to 0 km. For the region studied a similar effect ıs found for the squares at distances of 900 d 1000 km. The horizontal components are nerally less adversely affected. As a general le one might adopt for consideration a radius ual to 600 km plus the height of the station. ıtside this region we could hope for some lance, but any systematic effect due to large ıomaly patterns or a persistent geoid gradient ould be considered.

Some remarks concerning the use of the coatg technique where the geoid heights are not ailable may be appropriate. There have been ggestions that the potential be computed om the anomalies alone, and preliminary oid heights determined. These geoid heights could be included in the coating, and the computation for the potential could be repeated. This process could continue until the change in the geoid heights is negligible. How many iterations would be needed is questionable, but the process should converge. However, it might be preferable to determine the geoid heights from Stokes' function and use the coating to refine these quantities as more gravity data become available.

References

COHEN, C. J., A mathematical model of the gravity field surrounding the earth, *Computation and Exterior Ballistics Lab., NPG Rept. 1514, NAVORD Rept. 5135,* February 1957.

HELMERT, F. R., Theorieen der Höheren Geodäsie, v. 2, Leipzig, pp. 141–149, 259–261, 1884.

HEISKANEN, W. A., AND F. A. VENING MEINESZ, *The earth and its gravity field,* McGraw-Hill, New York, 262, 1958.

HIRVONEN, R. A., Gravity anomalies and deflections of the vertical above sea level, *Trans. Am. Geophys. Union, 33,* 801–809, 1952.

LAMBERT, W. D., The gravity field for an ellipsoid of revolution as a level surface (III), *Mapping and Charting Research Lab., Ohio State Research Foundation, Columbus, Ohio, Tech. Paper 716–2,* March 1958.

SOLLINS, A. D., Tables for the computation of deflections of the vertical from gravity anomalies, *Bull. Geod.,* n. s. no. 6, pp. 279–300, 1947.

STOKES, G. G., On the variation of gravity at the surface of the earth, *Trans. Cambridge Phil. Soc., 8,* 672, 1849.

VENING MEINESZ, F. A., A formula expressing the deflection of the plumb-line in the gravity anomalies and some formulae for the gravity field and the gravity potential outside the geoid, *Proc. Koninkl. Akad. Wetenschap. Amsterdam 31,* no. 3, 1928.

WEBSTER, A. G., The dynamics of particles and of rigid, elastic and fluid bodies, Hafner Publishing Co., New York, 367–374, 1949.

(Manuscript received May 18, 1959; presented at the Fortieth Annual Meeting, Washington, D. C., May 4, 1959.)

Statistical and Harmonic Analysis of Gravity

W. M. Kaula

U. S. Army Map Service, Washington 25, D.C.

Abstract—Markov theory is developed in terms of two correlated functions, the free-air gravity anomaly and the elevation of the topography. The Markov methods are applied to the mean anomalies of $1° \times 1°$ blocks to extrapolate from all available observations to obtain estimates of mean anomalies of $10° \times 10°$ blocks world-wide. These estimates are adjusted so that the even-degree zonal harmonics are consistent with the precession of the node of satellite 1958β and so that the inadmissible first- and second-degree harmonics are absent. Spherical harmonic coefficients up to the eighth degree ($P_{8,8}$ terms) for free-air gravity are computed.

An independent autocorrelation analysis is made in order to estimate the variance of mean anomalies of blocks and the variance of each degree of the spherical harmonics. This analysis is utilized as a control on the error variances and covariances of the mean anomaly estimates made by the Markov method.

The results are used in conjunction with the zonal harmonics derived from satellite motions to obtain a best estimate of the exterior potential in spherical harmonics from terrestrial gravimetry up to June 1958 and satellite data up to December 1958. It is planned to revise this estimate periodically as new observational data become available.

Introduction—The importance of the earth's external form and gravity field lies generally in its effect on some system which performs an integration over part of the field. Such systems include survey networks, objects in trajectory or in orbit, and geophysical structures. To make such integrations, information about the gravity field is required in the form either of area means or of an ensemble of harmonic functions. Our purpose in this study is to estimate as closely as possible the actual values and the statistical parameters for both the area means and the harmonic functions from all gravimetric data available (as of June 1958), without resort to geophysical hypotheses.

The estimation of a stochastic phenomenon from nonuniformly distributed observations is a general problem in geophysics. 'Stochastic' denotes a phenomenon which is sectionally continuous in space and time but which is not exactly representable by a finite number of mathematical expressions. The treatment of the acceleration gravity g as a stochastic phenomenon on the earth's surface is the subject of this paper. We treat g rather than some other function of the earth's potential field not because of any advocacy of gravimetric methods in geodesy but because g is the function for which the most widespread observations are available.

The statistical techniques used in this paper are adapted from those for time series as set forth in *Doob* [1953] or *Bartlett* [1956].

There are several questions which must be answered prior to analyzing any stochastic process, including gravity:

1. Is the process stationary; that is, does it have the same statistical properties in all parts of the domain under consideration?

In the case of gravity this a difficult question, since the domain is rather restricted: the surface of a smallish planet. As a practical matter, however, stationariness is imposed with the common-sense assumption that the estimated value of gravity in an area without observations will be equal to the mean value observed in areas with observations under the same conditions. The applied definitions of 'area' and 'same conditions' for continuous functions depend on how detailed and complicated we are willing to make the computations. In *Kaula* [1958], 'area' was defined as a $1° \times 1°$ block, and 'same conditions' as the elevation of the block to the

nearest 1000 feet. In this report 'same conditions' is appreciably more complicated, entailing both elevation and gravity of adjacent blocks.

2. Does physical theory set bounds on the values which the stochastic function can assume?

The limited strength of the earth's crust indicates that the earth cannot depart far from the equilibrium figure of a rotating fluid, certainly not more than 1 part in 10,000 in the potential and in the form of the geoid. Gravity can thus be expressed in the form of a free-air anomaly, a departure from a model established by the hydrostatic theory. The two parameters of the model must be considered to be somewhat arbitrary; but we must refer to some standard, such as the International Gravity Formula, in estimating anomalies for unobserved areas. Use of the International Formula will affect the estimates, as pointed out in equations (4) to (7) of *Kaula* [1958].

The logical reference model suggested is the hydrostatic figure of 1/297.3 [*Bullard*, 1948]. This model was applied; however there is no compelling reason that it is the correct reference, and hence it is fortunate that there is a correction available from a more sensitive means of observation, the artifical satellite.

3. Are any boundary-value or integral conditions imposed?

When we refer gravity observations to the ellipsoidal model, we use heights above the geoid. Hence the geoid must be concentric with the model, and the first-degree spherical harmonics, therefore, must be absent from the gravity field.

For the earth's rotation to be stable, the axis of rotation must coincide with the axis of maximum moment of inertia. The products of inertia must therefore be absent from the earth's gravity field if they are referred to an axis coinciding with the axis of rotation.

These harmonics—P_{10} (sin ϕ), P_{11} (sin ϕ) cos λ, P_{11} (sin ϕ) sin λ, P_{21} (sin ϕ) cos λ, P_{21} (sin ϕ) sin λ—are absent from the real gravity field, and hence they must also be absent from a statistical estimate of the gravity field. The existence of these integral conditions also makes the gravity field in a sense nonstationary, since knowing a part of the total field places constraints on the statistical properties of the unknown reminder.

4. Does the function being observed ha any deterministic relationship to other observe functions?

The gravity field should give zonal harmoni consistent with those obtained from satelli orbits.

The geoid heights derived from the estimate gravity field should be consistent with the geoi height differences estimated from astrogeodet observations. The orientation of astrogeodet datums obtained thereby should be consiste with differences in orientation obtained b interdatum observations, such as HIRAN ar occultation connections, and any modificatio to ellipsoid radius should be consistent wi that obtained by lunar distance measurement.

5. Does the function being observed have ar statistical correlation with other observed fun tions?

The free-air gravity anomalies have a positi correlation with the elevation of the topograph as demonstrated by Table 1 of *Kaula* [1958 Since both gravity and topography (wi negligible exceptions) are uniformly continuou this positive correlation will also apply neighboring values of gravity and topography.

6. Are observations of the function uniform distributed with respect to location?

Not in the case of gravity; there is a gre concentration in areas of advanced technolog and of possible oil resources and an absence other areas of some thousands of miles in exten

7. Are observations of the function uniform distributed with respect to values of the functio to which it is statistically correlated?

Not in the case of gravity; there is an exce of observations on land compared with those sea.

The analysis of a stochastic process may said to have three principal objectives: (*a*) estimate values of a phenomenon where the are no observations; that is, to predict, extr polate, interpolate, etc.; (*b*) to transform t mathematical expression of the phenomenon a form which yields more significant informatio and (*c*) to estimate the accuracy, correlatio etc., of solutions derived from observations the stochastic process.

To accomplish objective (*a*), estimation the gravity anomalies in areas without observ tions, we utilize Markov theory, which dea

th the statistical properties of sequences in iich the probability distribution of the values r any member is a function of the values for ly the immediately adjacent members. For avity the application of the theory seems tuitively justifiable. Consider a sequence of avity anomalies along a geodesic: Δg_1, $_2, \cdots, \Delta g_q$. A gravity anomaly is the integra-on of the attractions of many mass anomalies, ostly in the crust; the effect of each mass omaly is a function solely of position, being versely proportional to the distance squared. ence, the next anomaly along the geodesic, $_{q+1}$, will be affected by these mass anomalies a manner more similar to Δg_q than to any evious members in the sequence, since its sition is nearest to that of Δg_q.

The complication of the correlation with pography necessitates development of the arkov theory in terms of couplets of gravity omaly and elevation $(\Delta g, h)$. The circumstance two dimensions rather than one does not raise eoretical difficulties, but in making numerical timates based on the theory we must make actical modifications in order to keep the ethod manageable. Another theoretical dif-ulty is the arbitrary reference figure on which e estimates are made, a difficulty which is oided by requiring that the even-degree nal harmonics of the final estimates agree th the precession of the node of satellite 1958β.

Objective (*b*) is accomplished by determining e spherical harmonics from the aforementioned avity estimates. Inasmuch as these estimates ry considerably in quality, as measured by eir mean-square error, and are also correlated th each other in many places, the main dif-ulty is to define the most probable spherical rmonic expression corresponding thereto.

Objective (*c*), accuracy evaluation, can theo-tically be accomplished through the use of the same data as were used for making the estimates, but random errors in the sample on which all estimates are based, the groupings used in the frequency counts, and the modifications of strict Markov predictions in making the estimates cause considerable inaccuracy in the estimates of variance, covariance, etc., them-selves. Hence autocorrelation analysis, adapted from the time line to the sphere, is applied as a check, as nearly independent as possible, on these estimates.

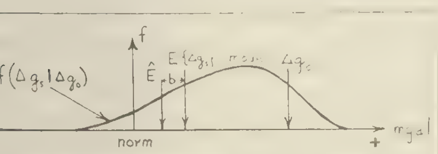

G. 1—Hypothetical frequency distribution of anomalies Δg_s about observed value Δg_0.

Estimation of gravity anomalies—Given an observed anomaly Δg_0 and an arbitrary distance s, the frequency density of anomalies Δg_s at distance s from anomalies $\Delta g = \Delta g_0$ will look like Figure 1.

The conditional frequency density $f(\Delta g_s|\Delta g_0)$ will show the bulk of the values between Δg_0 and the norm of the array. The mean expected value $E\{\Delta g_s\}$ will fall between the mode and the norm, and the mode will be between $E\{\Delta g_s\}$ and Δg_0. $\hat{E}$, an estimate based on a sample, will, in general, differ from $E\{\Delta g_s\}$ by a bias b. Further properties are

$$\int_{-\infty}^{\infty} f(\Delta g_s|\Delta g_0)\, d(\Delta g) = 1 \qquad (1)$$

$$E\{\Delta g_s\} = \int_{-\infty}^{\infty} (\Delta g) f(\Delta g_s|\Delta g_0)\, d(\Delta g) \qquad (2)$$

$\lim_{s\to 0} E\{\Delta g_s\} = \Delta g_0$; that is, at $s = 0$, the curve $f(\Delta g_s|\Delta g_0)$ shrinks to a single vertical line at Δg_0.

$$\lim_{s\to\pi} E\{\Delta g_s\} = 0$$

and

$$\lim_{s\to\pi} f(\Delta g_s|\Delta g_0) = f(\Delta g) \qquad (3)$$

that is, as we move away from the point where $\Delta g = \Delta g_0$, the array regresses to the absolute frequency distribution of all anomalies over the sphere.

Gravity is a continuous function; however, since for any practical application we must deal with a finite set of discrete values, theory is most easily developed in terms of discrete values. In addition, there is the necessity of considering topography as well as gravity.

Let $h = e - 0.62d$, where e is elevation above

sea level and d depth below sea level; or let $h = L - 0.38M$, where L and M are the lithosphere and hydrosphere as defined by *Prey* [1922]. Assume that gravity can have any one of m values with index $i = 1, 2, \cdots, m$, and that topography can have any one of n values, $u = 1, 2, \cdots, n$. Then define the 'couplet' (*not* a vector),

$$x_{iu} = \begin{Bmatrix} \Delta g_i \\ h_u \end{Bmatrix}.$$

P^{iu} = absolute probability of x_{iu}. Summation over all upper indices will always equal one, $\sum_{i,u}^{m,n} P^{iu} = 1$.

$P^{iujv}(s)$ = absolute probability that $x = x_{iu}$ and $x = x_{jv}$ a distance s apart.

$P_{jv}{}^{iu}(s)$ = conditional probability, the probability that $x = x_{iu}$ at distance s from $x = x_{jv}$.

$$P_{jv}{}^{iu}(s) = P^{iujv}(s)/P^{jv} \qquad (4)$$

$$P^{iu} = P_{jv}{}^{iu}(s)P^{jv} \qquad (5)$$

the Chapman-Kolmogorov condition.

Suppression of an index denotes summation with respect to that index,

P^i = absolute probability of Δg_i.

The expected value of Δg, given $h = h_u$, is

$$E\{\Delta g | h_u\} = \frac{x_i P^{iu}}{P^u} \qquad (6)$$

The expected value of Δg, given h_u at the same point and $(\Delta g_j, h_v)$ at distance s away, is

$$E_{s,juv}\{\Delta g\} = \frac{x_i P_{jv}{}^{iu}(s)}{P_{jv}{}^{u}(s)} \qquad (7)$$

So far, all the expressions have been functions of one parameter, s; for application to gravity on a surface, we need expressions that are functions of three parameters. There can be developed expressions for the nine-index quantities $P_{jvkw}{}^{iu}(r, s, t)$, but they are impractical to apply; further, it can be shown that numerical estimates of the five-index quantities $P_{jv}{}^{iu}(r)$ will establish bounds for the eight-index quantities $P_{jvkw}{}^{iu}(r, s, r)$. A further simplification can be made if a unit distance is chosen for which estimates of $P_{jv}{}^{iu}$ can be made from which the $P_{jv}{}^{iu}$ for all other distances can be calculated.

The gravity data used for the counts to esti mate the $P_{jv}{}^{iu}(1°)$ and related functions was th compilation of mean anomalies of 1° × 1 blocks described in *Kaula* [1958].

Three frequency counts were made of the mea anomalies of 1° × 1° blocks: an absolute fre quency count, Δg versus h; a transition coun $\delta\Delta g$ versus δh; and a transition count, $(\Delta g_i, h$ versus $(\Delta g_j, h_v)$. Table 1 gives the results of th $\delta\Delta g$ versus δh count; the mean was +8.51 mga 1000 ft = +0.028 mgal/m. Table 2 is a samp section of the $(\Delta g_i, h_u)$ versus $(\Delta g_j, h_v)$ coun which was made in terms of nine classes Δg: ≦ −70, −69 to −36, −35 to −16, −15 −6, −5 to +5, +6 to +15, +16 to +35, +36 +69, and ≧ +70 mgal; and of six classes h (in thousands of feet): ≦ −10, −9 to −7, − to −3, −2 to 0, +1 to +3, and ≧ +4. Comple results of all three counts are given in *Kau* [1959].

Table 1—*Transition count of 1° x 1° blocks: δ∆ versus δh*

$P_{\delta h}$	Number of cases	δh, ft × 10^3	Mean $\delta\Delta g$, mg
0.497	5214	0	0.0
0.310	3267	1	+8.0
0.091	955	2	+17.9
0.050	521	3	+27.6
0.025	265	4	+38.4
0.011	113	5	+55.8
0.007	72	6	+48.7
0.004	42	7	+56.1
0.003	28	8	+84.8
0.001	12	9	+115.4
0.001	13	10	+107.7

A graph was constructed for each value h_v with the Δg_j as abscissas and the $E\{\Delta g_i\}$ ordinates. Curves were then drawn on th graphs to fit the $E\{\Delta g_i\}$ values belonging each value of h_u. The mean equivalent δh of eac transition h_u versus h_v was computed by utilizi the frequencies $P_{\delta h}$ of the δh as well as th absolute frequencies of the h_u, h_v. From the δh corresponding to each h_u curve based on th actual count, curves corresponding to integr values of δh were then obtained by interpolatio

The graphs in general had the followi properties: The curve for $h_v = h_u$ intersected

TABLE 2—*Transition count of 1° × 1° blocks: (Δg_i, h_u) versus (Δg_j, h_v)*

Part D-5: h_u −2 through 0
h_v +1 through +3

, ft × 10³	Δg_j, mgal	−93.2	−47.2	−23.3	Δg_i, mgal −10	0	+10	+23.8	+47.0	+91.3	n	E_i, mgal
1 to +3	−100.0	12	3	1	1			1			18	−70.5
	−45.3	5	13	26	3	9	4	1			61	−27.1
	−23.6	3	17	77	28	23	10	10		1	169	−16.1
	−10		10	39	37	25	11	5	3	1	131	−9.8
	0	1	7	40	58	75	45	27	3	2	258	−2.0
	+10	3	1	20	37	63	68	39	9	1	241	+4.0
	+24.1	2	3	22	24	54	71	95	24	3	298	+11.0
	+45.5		3	4	4	6	13	43	40	9	122	+29.3
	+94.3		1		2	2	3	8	14	18	48	+51.1

° line at $E\{\Delta g|h\}$; the slopes of the curves ere always less than 45° (between 26° and 30° ound $E\{\Delta g|h\}$), with a flattening out or, in me cases, a reversal of slope at the ends; and e ordinates showed a positive correlation with . The spacings between the curves *averaged* $\{\delta\Delta g|\delta h\}$, that is, +8.5 mgal, but there was wide range of spacings from −5 to +30 mgal.

To extract all information available in the ta it is necessary to construct graphs for lues of h_v in intervals of 1000 ft and to put curves on the graphs with the same interval. he general procedure adopted was that tran- ion rules for $-12 < (h_u, h_v) < +6$ were ose rigorously derived from the transition unts, but that when (h_u or h_v) $\leqq -12$ or $\geqq +6$, e curves were smoothed so as to be reasonably nsistent with the results for more moderate evations. 30 graphs were drawn: one for every

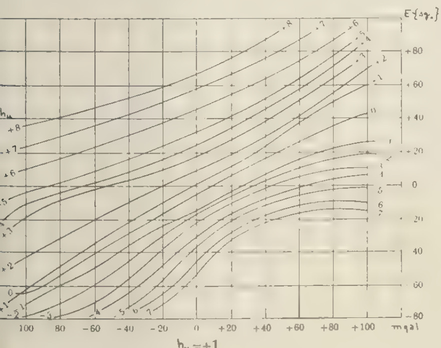

FIG. 2—Transition graph for $h_v = +1$.

values of h from −15 to +8, and for even values from +10 to +20. One of these graphs is given as an example in Figure 2.

The observed values give the mean anomalies for approximately eight thousand 1° × 1° blocks; to fill out the 860 5° × 5° blocks which contain these blocks, we must extrapolate from the 8000 observed blocks to approximately 16,000 more 1° × 1° blocks without observations. Graphs such as Figure 2 give an estimate that is valid for just one case, that of an empty 1° × 1° block immediately adjacent to an observed 1° × 1° value, without any other observed values in the area, and, in fact, without any knowledge of elevations in the area other than within the two 1° × 1° blocks themselves. Three assumptions were therefore made in order to devise a reasonable procedure applicable in all cases:

1. The predictions are strictly Markovian; that is, given Δg_1, h_1, and h_2, $\Delta g_2 = E\{\Delta g_2|\Delta g_1, h_1, h_2\}$ is assumed regardless of what the value of h_3 or other elevations in the area may be.

2. Predictions are based on the nearest observed value(s) only, without any weighted interpolations.

3. The prediction for any 1° × 1° block, n steps distant from an observed value, is based on the prediction(s) for block(s) $n - 1$ steps distant.

For assumptions (1) and (2), an overestimated prediction will be balanced by an underestimate in the immediate vicinity. Assumption (3) was checked by comparison for several cases with the rigorous formula

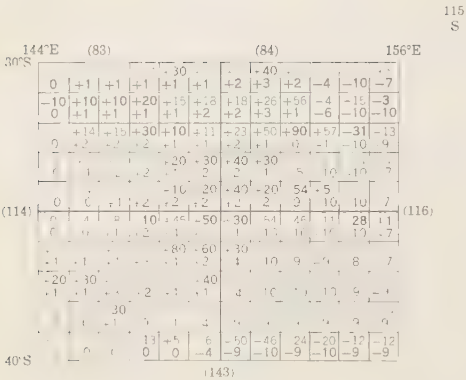

FIG. 3—10°×10° diagram of mean anomalies for 1°×1° blocks. Upper number: free-air gravity anomaly, mgal (heavy print for observed estimates, light print for extrapolated estimates). Lower number: topography ($e - 0.62d$, thousands of feet).

$$E_{2°,juvw} = \frac{x_i P_{k(w)}{}^{iu}(1°) P_{iv}{}^{k(w)}(1°)}{P_{k(w)}{}^{u}(1°) P_{iv}{}^{k(w)}(1°)} \qquad (8)$$

where the parentheses around (w) indicate that summation does not take place with respect to this index.

Based on these three assumptions and on predictions made by rigorous formula for a sample of cases, practical rules were devise for predicting from the graphs anomalies i unobserved 1° × 1° blocks for each of the fiv possible arrangements of an unobserved bloc with respect to observed blocks.

For each 10° × 10° block in the scheme c *Zhongolovich* [1952] a drawing was made, an the mean anomalies and mean elevations c 1° × 1° blocks were recorded thereon. Thes diagrams were used for the extrapolation an interpolation of the mean anomalies of 1° × 1 blocks. In each 1° × 1° block the mean elevatio and the mean anomaly were recorded (observe values in red, first extrapolations in brown second extrapolations in green, third extrapola tions in brown, etc.). Figure 3 demonstrate most of the pertinent features. Note, for exampl the change in anomaly predicted in passin over the coast line. Also shown are some of th instances of overestimates juxtaposed agains underestimates.

Counts of mean anomalies for 5° × 5° block similar to those of 1° × 1° blocks were mad Table 3 gives part of the results of the Δg versu h count; Table 4 gives the results of the $\delta\Delta$ versus δh count; and Table 5 gives a sampl section of the $(\Delta g_i, h_u)$ versus $(\Delta g_j, h_v)$ coun Complete results are given in *Kaula* [1959].

A graph was constructed for each value c

TABLE 3—*Absolute frequency counts of estimated mean free-air anomalies of 5° × 5° blocks (parts A and B combined: 18 to 100 per cent observed)*

Δg, mgal	h, ft × 10^3 −12 −11	−10	−9	−8	−7	−6 −5	−4 −3	−2 −1	0	+1	+2 +3	+4 +5	≧+6	Tota
−51					1									1
−50 to −41				1			1		1					3
−40 to −31		2	3			2	3							10
−30 to −21	8	3	4	10	1	3	2	3		1	3			38
−20 to −11	9	16	10	10	6	7	6	6	4	8	5	1	2	90
−10 to −6	4	9	9	7	4	7	6	4	8	12	5	1	1	77
−5 to 0	1	5	7	8	8	4	1	6	11	10	10	5		76
+1 to +5		1	1	3	5	5	9	2	12	16	9	4		67
+6 to +10		2		4	6	4	7	6	12	19	11	6	1	78
+11 to +20			1	1	2	5	6	14	13	20	14	7	2	85
+21 to +30					1	2	3	5	3	3	4	3	6	30
+31 to +45									1	2	3	3	1	10
+46													3	3
Total	22	38	35	44	34	39	44	46	65	91	65	30	16	569
mean*	−16.1	−11.9	−12.2	−10.2	−2.6	−3.3	−2.0	+3.2	+3.8	+4.0	+4.2	+10.5	+21.7	−0.

* Mean square, 228 mgal²; rms, ±15.1 mgal.

TABLE 4—*Transition count of 5° × 5° blocks: δΔg versus δh*

$P_{\delta h}$	Number of cases	δh, ft × 10^3	Mean* $\delta\Delta g$, mgal
...	348	0	0.00
0.413	464	1	+3.26
0.223	251	2	+4.27
0.140	157	3	+7.56
0.070	79	4	+12.98
0.052	59	5	+12.27
0.039	44	6	+19.25
0.026	26	7	+17.55
0.021	24	8	+25.67
0.007	8	9	+27.4
0.003	3	10	+51.5
0.004	4	11	+29.9
0.003	3	12	+46.0
0.001	1	13	+13.0
0.001	1	15	+131.0

* Weighted mean = +2.86 mgal/1000 ft = +0.0094 mgal/m.

h, for 5° × 5° blocks. The properties of these 5° × 5° graphs were generally similar to those of the 1° × 1° graphs except that the slopes were gentler—between 12° and 26° around $E\{\Delta g|h\}$—and the spacing was smaller, averaging $+2.9\,\delta h$, in agreement with the $\delta\Delta g/\delta h$ mean value.

Graphs were drawn similar to those for the 1° × 1° transitions at a scale of 10 mgal to the inch for every 1000 feet of elevation from −12 to +5.

For the extrapolation and interpolation of the mean anomalies of 5° × 5° blocks, the same simplifying assumptions were made as for 1° × 1° blocks, and similar rules for prediction were devised.

The extrapolation and interpolation of the mean anomalies for the 5° × 5° blocks was made on a series of 48 diagrams, each diagram extending 30° in latitude and covering eight or nine of the 10° × 10° Zhongolovich squares. The reference flattening used for all extrapolations was 1/297.33. In this manner estimates of mean gravity anomalies were made to cover the whole world.

Computation of spherical harmonic coefficients—From equation (15) of *Kaula* [1958] or from celestial mechanics, the precession of the node of satellite 1958β_2 imposes the condition

$$\delta A_2 = A_2 - 0.229 A_4 + 0.028 A_6 \tag{9}$$

The estimated value of δA_2 is +10.14; we may substitute for A_2, A_4, etc., their expression in terms of terrestrial Δg's:

$$+10.14 = \frac{5}{410} \sum \Delta g P_2 - 0.229 \frac{9}{410} \sum \Delta g P_4 + 0.028 \frac{13}{410} \sum \Delta g P_6 \tag{10}$$

or

$$+831.48 = \sum (P_2 - 0.412 P_4 + 0.073 P_6)\,\Delta g$$

There are also the five inadmissible harmonic conditions, such as

$$0 = \sum P_1 (\sin\phi)\,\Delta g \tag{11}$$

These were combined in a matrix equation (the prime indicates a transpose)

$$\underset{6\times1}{H} = \underset{6\times48}{L'}\ \underset{48\times1}{(G + X)} \tag{12}$$

TABLE 5—*Transition count of 5° × 5° blocks:* $(\Delta g_i, h_u)$ *versus* $(\Delta g_j, h_v)$
Part D-5: h_u *−4 through −1*
h_v *0 through +3*

h_v, ft × 10^3	Δg_j, mgal	Δg_i, mgal: −29.9	−13.9	−5.0	+5.8	+13.8	+23.0	n	E_i, mgal
0	−32.5	1		1				2	−17.4
to	−14.5	1	3	2				6	−13.6
+3	−4.4	6	3	9	6	1	1	26	−7.5
	+5.4	7	9	24	10	7		57	−5.4
	+15.5	7	1	11	9	7	1	36	−3.0
	+26.7			2	5	6	2	15	+9.9

where the elements of H are $+831.48$ and five zeros; of L, $(P_2 - 0.412P_4 + 0.073P_6)$ plus the five inadmissible harmonics averaged over each of the forty-eight 30° blocks; of G, the estimates of the mean anomalies; and of X, the corrections thereto. X is to be solved for under the condition that

$$X' V^{-1} X = \text{MIN} \tag{13}$$

V is the variance matrix of the 30° blocks, in which the covariance between 10° blocks within a 30° block was allowed for, but covariance between 30° blocks was assumed to be zero. By customary least squares

$$X = VL(L' VL)^{-1}(H - L'G) \tag{14}$$

The most marked change was due to the satellite P_2, P_4, P_6 condition, which made the equatorial belt more negative and the South Pole area more positive than predicted. The P condition made the Southern Hemisphere more positive, and the $P_{11} \cos \lambda$ condition made the Pacific Ocean more positive.

Corrections to the mean anomalies of 10° × 10

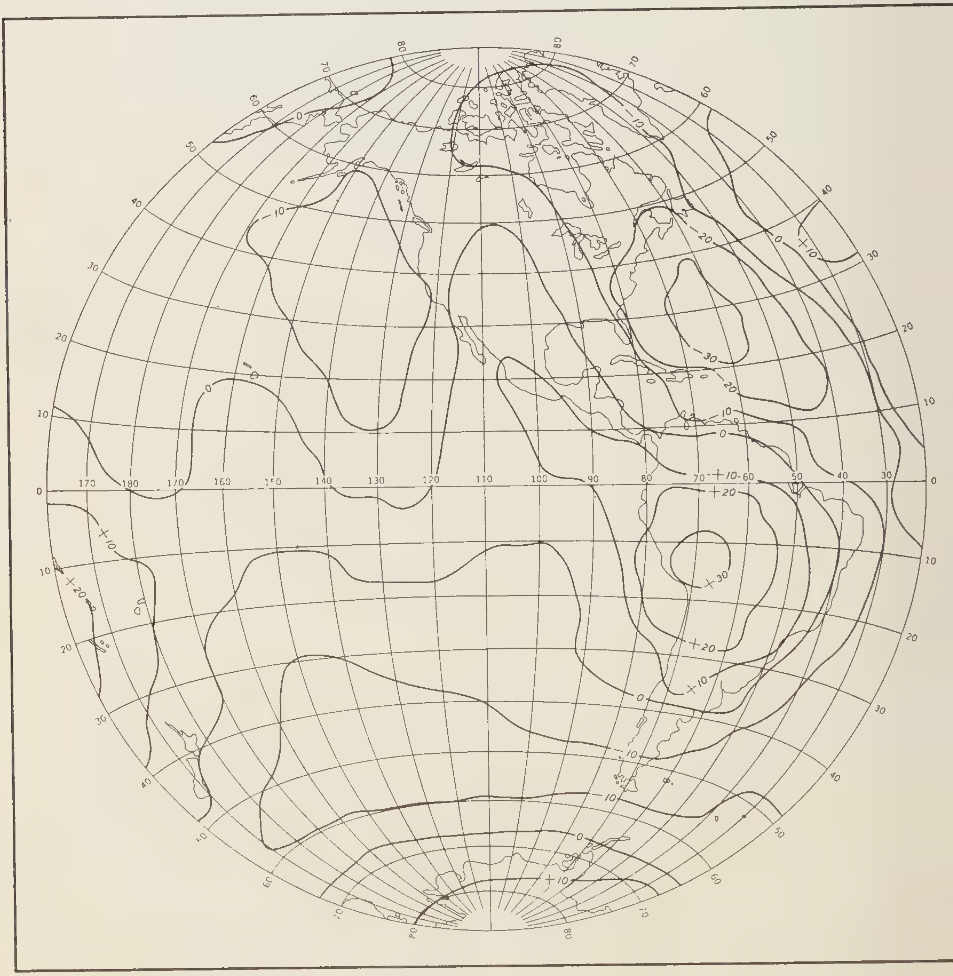

FIG. 4a—Free-air geoid referred to ellipsoid of flattening 1/298.49.

ocks were obtained by weighted apportion-
ent of the corrections to 30° × 30° blocks.

To determine the spherical harmonic coeffi-
nts (up to the eighth degree), the conventional
ethod of summing the products of each
rmonic and the gravity over the sphere was
plied. Harmonic values were obtained from
e tables of *Zhongolovich* [1952]. It had originally
en planned to determine the coefficients by
st squares in order to give greater weight to
the more densely observed area; the justification for not doing so is discussed later.

From the coefficients for the gravity anomalies, the geoid heights were computed by

$$N_{8,i} = \frac{R}{G} \sum_{m,n}^{8} \frac{A_{nm}}{n-1} L_{nm,i} \qquad (15)$$

where the A_{nm} are the coefficients and $L_{nm,i}$ are the values of the spherical harmonics for the block in question. Spherical harmonic coefficients

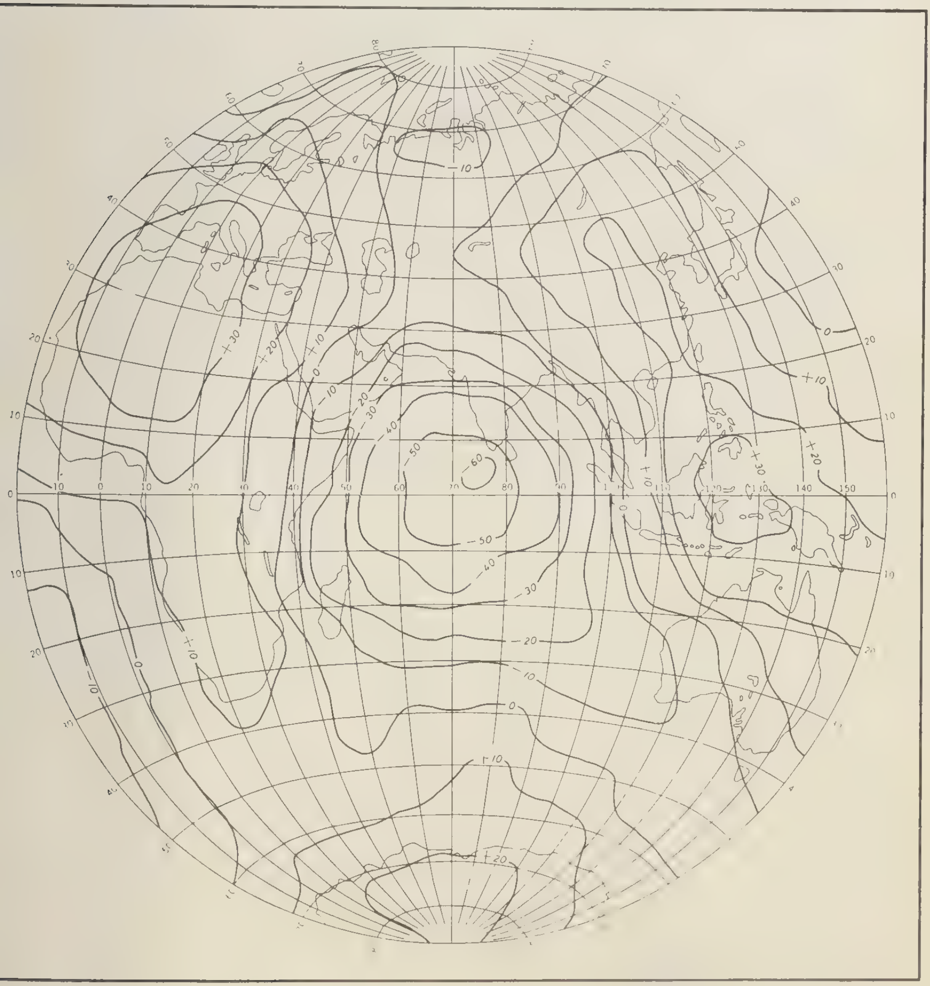

Fig. 4b—Free-air geoid referred to ellipsoid of flattening 1/298.49.

were determined for the conventional spherical harmonics, defined by

$$P_{nm}(\sin\phi)\begin{Bmatrix}\sin\\ \cos\end{Bmatrix}m\lambda = \frac{1}{2^n n!}\cos^m\phi \cdot \frac{d^{n+m}}{d(\sin\phi)^{n+m}}(-\cos^2\phi)^n\begin{Bmatrix}\sin\\ \cos\end{Bmatrix}m\lambda \tag{16}$$

and for the fully normailzed spherical harmonics, defined by

$$H_{nm} = \sqrt{\frac{(n-m)!}{(n+m)!}(2n+1)\kappa} \cdot P_n^m(\sin\phi)\begin{Bmatrix}\sin\\ \cos\end{Bmatrix}m\lambda \tag{17}$$

when $m = 0, \kappa = 1; m \neq 0, \kappa = 2$. The advantage of normalizing is that

$$\frac{1}{4\pi}\int_s [H_{nm}]^2\, d\sigma = 1 \tag{18}$$

for integration over the sphere. Values of k_{nm} needed to convert from Zhongolovich coefficients to conventional coefficients are given by *Zhongolovich* [1952 p. 91]; values of

$$\sqrt{(n-m)!(2n+1)\kappa/(n+m)!}$$

needed to convert from conventional to fully normalized coefficients are given by *Jung* [1956 p. 625].

Also determined were the spherical harmonic coefficients for the topography, $e - 0.62d = L - 0.38M$; they agree very closely with those found by *Prey* [1922].

Table 6 gives fully normalized coefficients for the free-air gravity anomaly from $(n, m) = (0, 0)$ to $(8, 8)$. Figure 4 gives the corresponding geoid heights on a world map. More complete tables for anomalies, geoid heights, and topography as both mean values for $10° \times 10°$ blocks and spherical harmonic coefficients are given in *Kaula* [1959].

Autocorrelation analysis—The methods of analyzing stationary processes in time, such as are described by *Bartlett* [1956, pp. 159–176], are readily adapted to spherical harmonics in order to derive an estimate of amplitudes and frequency distributions independent of any obtained from the coefficients in Table 6.

For convenience, a function such as Δg, expressed in spherical harmonics, is normally

TABLE 6—*Free-air gravity anomalies expressed i fully normalized spherical harmonic coefficients, referred to International Gravity Formula*

n	m	Cosine Coeff. $\bar{A}_{nm}$, mgal	Sine Coeff. $\bar{B}_{nm}$, mgal	n	m	Cosine Coeff. $\bar{A}_{nm}$, mgal	Sine Coeff. $\bar{B}_{nm}$, mgal
0	0	−1.99	...	6	0	+0.84	...
1	0	...	...	6	1	−0.44	−0.30
1	1	...	...	6	2	−0.06	−0.89
2	0	+4.82	...	6	3	−0.50	+0.27
2	1	...	...	6	4	+1.04	−1.21
2	2	+0.70	−0.62	6	5	−1.49	−1.82
3	0	−0.61	...	6	6	−0.15	−0.43
3	1	+1.03	+1.48	7	0	0.00	...
3	2	+0.57	+0.29	7	1	+0.20	+0.14
3	3	+1.91	+1.85	7	2	+1.05	+0.22
4	0	+0.30	...	7	3	+0.93	−0.15
4	1	−0.97	−1.06	7	4	−0.83	+0.45
4	2	−0.09	+1.03	7	5	−0.14	+0.40
4	3	+2.35	−0.53	7	6	−0.95	+0.19
4	4	+0.24	+2.18	7	7	−0.05	−0.24
5	0	−1.65	...	8	0	+0.27	
5	1	−0.96	−0.41	8	1	−0.26	+0.44
5	2	+0.13	−1.07	8	2	+0.70	+0.42
5	3	−0.16	−0.40	8	3	+0.25	+0.73
5	4	+0.93	−0.39	8	4	−0.10	+0.44
5	5	−0.63	−0.14	8	5	−0.69	+0.49
				8	6	−0.21	+0.82
				8	7	+0.81	+0.27
				8	8	−0.87	−0.61

referred to the usual coordinates defined by th rotational axis and the Greenwich meridiar However, Δg can be represented by harmoni development about any axis we want; a trans formation from the development about th earth's axis to any arbitrary axis constitutes rotation of the coordinate system. The propert of interest is that a homogeneous polynomial c a given degree is represented by a sum of poly nomials of the same degree about the new axi after coordinates rotation; that is,

$$x^k y^l z^m = \sum_{u,v,w=0}^{n} a_{u,v,w}'(x')^u(y')^v(z')^w \tag{19}$$

or

$$k + l + m = u + v + w = n$$

$$P_{nm}(\sin\phi)\begin{Bmatrix}\cos\ m\lambda\\ \text{or}\\ \sin\ m\lambda\end{Bmatrix} = \sum_{m=0}^{n} P_{nm}(\cos\psi)\begin{Bmatrix}a_{nm}'\cos\ m\alpha\\ b_{nm}'\sin\ m\alpha\end{Bmatrix} \tag{20}$$

where ψ, α are distance and azimuth on the unit sphere from the new axis.

The next property of interest is that for $\psi = 0°$,

$$P_n(\cos\psi) = 1$$
$$P_{nm}(\cos\psi) = 0, \qquad m \neq 0 \qquad (21)$$

That is, if the coordinates are transformed from the polar axis to any arbitrary point, gravity at that point in the new set of harmonics must be represented entirely by the zonal harmonics P_n.

If we define covariance for a given distance s as the mean product of gravity at an arbitrary point and values on a circle of radius s about the point, only zonal harmonics can contribute to the covariance, since in

$$\frac{1}{2\pi}\int_0^{2\pi} P_{nm}(\cos 0°)\begin{Bmatrix} a_{nm}' \cos m\alpha \\ b_{nm}' \sin m\alpha \end{Bmatrix} \cdot P_{n'm'}(\cos s)\begin{Bmatrix} a_{n'm'}' \cos m'\alpha \\ b_{n'm'}' \sin m'\alpha \end{Bmatrix} d\alpha \qquad (22)$$

$$P_{nm}(\cos 0°) = 0, \quad \text{for} \quad m \neq 0,$$

and in

$$\frac{1}{2\pi}\int_0^{2\pi} a_n P_n(\cos 0°) \cdot P_{n'm'}(\cos s)\begin{Bmatrix} a_{n'm'}' \cos m'\alpha \\ b_{n'm'}' \sin m'\alpha \end{Bmatrix} d\alpha \qquad (23)$$

$$\int_0^{2\pi}\begin{Bmatrix} a_{n'm'}' \cos m'\alpha \\ b_{n'm'}' \sin m'\alpha \end{Bmatrix} d\alpha = 0, \quad \text{for} \quad m = 0.$$

Covariance for distance s can be computed as the mean of all products of values a distance s apart.

Given a full range of covariance values C_s from 0 to π, we should be able to express it either as a set of numerical values C_s or as a sum of zonal harmonics

$$\sum_{n=2}^{\infty} C_n P_n(\cos\psi)$$

The covariance as a sum of products of zonal harmonics has already been discussed;

$$C_s = \sum_{n=2}^{\infty}\frac{1}{2\pi}\int_0^{2\pi} a_n' P_n(\cos 0°) \cdot a_n' P_n(\cos s)\, d\alpha$$
$$= \sum_{n=2}^{\infty} a_n'^2 P_n(\cos s) \qquad (24)$$

where the a_n' are the coefficients of P_n found after rotation of the axes. Now we are interested in the mean case, so we let σ_n^2 be the mean square of a_n'. The total of these mean squares will be the mean square of the gravity field:

$$\sigma^2\{\Delta g\} = \sum_{n=2}^{\infty}\sigma_n^2 \qquad (25)$$

Thus there is on the one hand a numerical C_s derived from the mean of many products of anomalies a distance s apart, and on the other hand there is a theoretical C_s the sum of an infinite set of harmonics $\sigma_n^2 P_n$, with the σ_n^2 as yet undetermined.

$$C_s = \sum_{n=2}^{\infty}\sigma_n^2 P_n(\cos s) \qquad (26)$$

To find σ_N^2 for N, a particular value of n, multiply both sides of (26) by $P_N(\cos s)$.

$$C_s P_N(\cos s) = \sum_{n=2}^{\infty}\sigma_n^2 P_n(\cos s) P_N(\cos s) \qquad (27)$$

Integrate with respect to cos s from 1 to -1.

$$\int_0^{\pi} C_s P_n(\cos s)\sin s\, ds = \int_0^{\pi}\sum_{n=2}^{\infty}\sigma_n^2 P_n(\cos s) P_N(\cos s)\sin s\, ds \qquad (28)$$

On the left, there is a set of numerical values of C_s, each representing a discrete interval Δs, so it must be converted to a sum. On the right, there is a series of integrals for which $n \neq N$.

$$\int_0^{\pi} P_n(\cos s) P_N(\cos s)\, ds = 0 \qquad (29)$$

from the orthogonality property. So

$$\sum_{s=0}^{\pi} C_s P_N(\cos s)\sin s\,\Delta s = \int_0^{\pi}\sigma_N^2[P_N(\cos s)]^2\sin s\, ds \qquad (30)$$

For large Δs and $\Delta s = \pi/k$;

$$\sum_{i=1}^{k} C\{(i - \tfrac{1}{2})\Delta s\} P_N\{\cos(i - \tfrac{1}{2})\Delta s\} \cdot [\cos(i - 1)\Delta s - \cos i\,\Delta s] = \int_0^{\pi}\sigma_N^2[P_N(\cos s)]^2\sin s\, ds \qquad (31)$$

We perform the integration on the right,

$$\sum_{i=1}^{k} C\{(i-\tfrac{1}{2})\,\Delta s\}P_N\,\{\cos\,(i-\tfrac{1}{2})\,\Delta s\}$$

$$\cdot[\cos\,(i-1)\,\Delta s - \cos\,i\,\Delta s]$$

$$= \frac{2\sigma_N^{\ 2}}{2N+1} \qquad (32)$$

And σ_N^2 can be determined.

Estimates of the degree variances σ_N^2 are also obtainable from the harmonic coefficients (Table 6).

$$\sigma_n^{\ 2} = \sum_{m=0}^{n} (\bar{A}_{nm}^{\ 2} + \bar{B}_{nm}^{\ 2}) \qquad (33)$$

for fully normalized coefficients.

The world sample consisted of the mean anomalies for the 569 5° × 5° blocks which are 18 per cent or more observed. Ideally, observed values for points should be used, but the covariances which this sample is intended to obtain are so small that the number of point values small enough to take a reasonable time on the computer yields excessively erratic results.

Eight regional samples were taken, each covering about 10° × 10° in area and with members averaging 100 km apart: South Atlantic, 115 members; western United States, 74 members; East Atlantic, 67 members; U.S.S.R. steppes, 85 members; East Indies, 56 members; Western Europe, 85 members; mid-Atlantic, 78 members; western Atlantic, 95 members. For seven of the regions, second sets were taken rejecting observations differing more than 200 meters in elevation from the mean of the area within 40 km of the station.

Nine local samples were taken, each covering an area of about 2° × 2° and with members averaging 15 km apart: East Texas, 104 members; Lyon, France, 101 members; Ascension Island, 52 members; Tokyo, Japan, westward, 140 members; Johannesburg, South Africa, 126 members; Buenos Aires, Argentina, 84 members; East Venezuela, 79 members; Ohio, 123 members; central Sweden, 99 members. For five of the areas, second sets were taken rejecting observations differing more than 150 meters in elevation from the mean of the area within 20 km of the station.

Regional estimates of covariances were obtained by assigning a weight of 65 per cent to the mean of all oceanic samples and 35 per cent to the mean of all continental samples. $\mathrm{Cov}_{10°}$ was 132 mgal² from the regional samples; it was 82 mgal² from the world sample. A correction of 50 mgal² was subtracted from all the covariances of the regional samples. In similarly fitting the local sample results to the regional, a further correction of 38 mgal² was subtracted from the local covariances to give the final values for Cov_s listed in Table 7.

The covariances of the mean anomalies for the 5° × 5° blocks are so small compared with their variances that the random error of the covariance estimates can be estimated by [*Cramer*, 1946 p. 358]

$$D^2\{m_{11}\} = \frac{\mu_{22} - \mu_{11}^{\ 2}}{n} \approx \frac{[\sigma^2(\Delta g)]^2}{n} \qquad (34)$$

whence $D\{\widehat{\mathrm{Cov}}_s\} = \pm 6$ mgal². Perhaps more serious is the chance of systematic error because the sample of 5° × 5° blocks is 46.9 per cent of $h \geqq 0$ and 53.1 per cent of $h \leqq -1$, whereas ideally it should be 34.6 per cent of $h \geqq 0$ and 65.4 per cent of $h \leqq -1$. The error in $\widehat{\mathrm{Cov}}_s$ caused by the difference in mean anomaly of the actual sample from the ideal is estimated to be on the order of +11 mgal².

Equation (32) was applied to the numerical values in Table 7, and (33) was applied to the numerical values in Table 6. The results are shown in Table 8.

The qualitative explanation of the smaller (33) values is in Figure 1; the quantitative evaluation of the discrepancy is a principal objective of the section on error and bias in this paper.

The relatively small covariances of the mean anomalies of 5° × 5° blocks result in a small covariance of covariance estimates, so $D\{\widehat{\mathrm{Cov}}_s\} = \pm 6$ mgal², and (33) can be used to estimate $D\{\sigma_n^2\}$ as $\pm 0.57\sqrt{2n+1}$. The resulting values from ±1.3 mgal² for $n = 2$ to ±4.6 mgal² for $n = 32$ appear insufficient to explain the fluctuations between successive values in Table 8; something more on the order of $\pm 3\sqrt{2n+1}$ is needed.

The variances and covariances of the mean anomalies of blocks as computed from Table 7 with equation (7) of *Kaula* [1957] are set forth in Table 9.

Table 7—*Estimates of covariance of free-air gravity anomalies*

Arc distance, degrees	Covariance, mgal²	Arc distance, degrees	Covariance, mgal²	Arc distance, degrees	Covariance, mgal²	Arc distance, degrees	Covariance, mgal²
0.0	+1201	21	+35	59	−23	97	+10
0.5	+751	23	+10	61	−38	99	+13
1.0	+468	25	+20	63	−17	101	+15
1.5	+356	27	+18	65	−34	103	+16
2.0	+332	29	+6	67	−17	105	+8
2.5	+306	31	+8	69	−19	107	+13
3.0	+296	33	+5	71	−20	109	−2
4	+272	35	−8	73	−7	111	+19
5	+246	37	−10	75	−6	113	+1
6	+214	39	−13	77	0	115	+10
7	+174	41	−11	79	+3	117	+31
8	+124	43	−7	81	−6	119	+5
9	+104	45	−18	83	+6	122	+26
10	+82	47	−18	85	−6	126	+14
11	+76	49	−18	87	+4	130	+4
13	+54	51	−23	89	−7	134	+2
15	+47	53	−12	91	0	138	−4
17	+45	55	−32	93	−2	145	−23
19°	+34	57°	−23	95°	+4	155	−20
						167°	+5

Error and Bias—The task is to determine the ature and magnitude of the errors which ffect the estimated mean anomalies and har- ıonic coefficients and to explain their dis- repancies from the results of the autocorrelation nalysis. The first step is to define more clearly ıe functions in terms of which this analysis made.

We define an element as one unit of the tochastic phenomenon under study; the elements which are of most concern herein are the mean gravity anomalies of 1° × 1° and 5° × 5° blocks.

Let G = true value of an element.

E = the expectancy, the mean value of all elements in a given set of circumstances, such as elevation, adjacent values, etc. E is a theoretical ideal.

ϵ = $E - G$, the error of the expectancy.

$\hat{E}$ = the estimated value of the element in a given set of circumstances. $\hat{E}$ is a number based on samples, and it is obtained by a procedure such as the Markov estimation of mean anomalies.

$\hat{\epsilon}$ = $\hat{E} - G$, the error of the estimate.

b = $\hat{E} - E$, the bias of the estimate.

Table 8—*Degree variances of free-air gravity anomalies*

$\hat{\sigma}_n^2$, mgal²*	σ_n^2, mgal²†	n	σ_n^2, mgal²†	n	σ_n^2, mgal²†	n	σ_n^2, mgal²†
1.1‡	7.3	9	22	17	12	25	9
11.1	43.6	10	15	18	19	26	11
13.9	29.8	11	18	19	10	27	4
6.6	10.5	12	7	20	7	28	8
10.4	24.2	13	15	21	14	29	5
4.2	2.8	14	23	22	10	30	−2
5.6	22.7	15	22	23	9	31	1
		16	6	24	11	32	2

* By equation (33).
† By equation (32).
‡ $\bar{A}_{22}$, $\bar{B}_{22}$ terms only.

The most important functions to be determined are

$$\mathrm{Var}\,\{\hat{\epsilon}\} = m\{(\hat{E} - G)^2\} \qquad (35)$$

the error variance, a measure of the wrongness of the estimates; and

$$\mathrm{Cov}_s\,\{\hat{\epsilon}\} = m_s\{(\hat{E}_A - G_A)(\hat{E}_B - G_B)\} \quad (36)$$

the error covariance for distance s, a measure

TABLE 9—*Variances and covariances of mean anomalies of blocks of side length s° (mgal²)*

	$s \times s$					
	1° × 1°	2° × 2°	5° × 5°	10° × 10°	20° × 20°	30° × 30°
Var	776	513	350	246	130	85
$\mathrm{Cov}_{s,s}$	494	357	235	101	36	7
$\mathrm{Cov}_{s,2s}$	333	269	94	31	−9	...
$\mathrm{Cov}_{s,3s}$	295	208	48	7	...	...

of how much estimates a distance s apart tend to be wrong in the same direction.

We have

$$\mathrm{Var}\,\{\epsilon\} = m\{\epsilon^2\} = m\{(E - G)^2\}$$

$$= m\{E^2\} - 2m\{EG\} + m\{G^2\} \qquad (37)$$

E is the mean expected value of G, $E = m\{G\}$, so

$$m\{EG\} = m\{Em\{G\}\} = m\{E^2\}$$

and

$$\mathrm{Var}\,\{\epsilon\} = m\{G^2\} - m\{E^2\}. \qquad (38)$$

Similarly

$$\mathrm{Cov}\,\{\epsilon_i, \epsilon_j\} = m\{\epsilon_i\epsilon_j\}$$

$$= m\{E_iE_j\} - m\{E_iG_j\}$$

$$- m\{E_jG_i\} + m\{G_iG_j\}$$

$$= m\{G_iG_j\} - m\{E_iE_j\} \qquad (39)$$

$$\mathrm{Var}\,\{\hat{\epsilon}\} = m\{(E + b - G)^2\}$$

$$= m\{\epsilon^2\} + 2m\{b\epsilon\} + m\{b^2\} \qquad (40)$$

Since $m\{\epsilon\} = 0$, and ϵ is random with respect to b,

$$\mathrm{Var}\,\{\hat{\epsilon}\} = \mathrm{Var}\,\{\epsilon\} + m\{b^2\} \qquad (41)$$

Similarly

$$\mathrm{Cov}\,\{\hat{\epsilon}_i, \hat{\epsilon}_j\} = \mathrm{Cov}\,\{\epsilon_i, \epsilon_j\} + m\{b_ib_j\} \quad (42)$$

From (38),

$$\mathrm{Var}\,\{G\} = \mathrm{Var}\,\{E\} + \mathrm{Var}\,\{\epsilon\} \qquad (43)$$

As a control on the estimation procedure, it is desirable to know Q, defined by

$$\mathrm{Var}\,\{G\} = \mathrm{Var}\,\{\hat{E}\} + \mathrm{Var}\,\{\hat{\epsilon}\} + Q \qquad (44)$$

$$m\{G^2\} = m\{\hat{E}^2\} + m\{(\hat{E} - G)^2\} + Q \quad ($$

$$m\{G^2\} = m\{(E + b)^2\}$$

$$+ m\{(E + b)^2$$

$$- 2(E + b)G + G^2\} + Q$$

Since

$$m\{EG\} = m\{E^2\}, \quad \text{and} \quad m\{E\} = m\{G$$

$$0 = 2m\{b^2\} + 2m\{bG\} + Q \qquad ($$

In the first approximation, b is proportiona to G; if it is assumed that $m\{G\} = 0$, $b =$ so

$$Q = -2m\{(\beta^2 + \beta)G^2\} \qquad ($$

Thus for a negative bias $\beta < 0$, Q will positive. We shall return later to the computa tion of Q in reconciling estimates of Var { and Var $\{\hat{\epsilon}\}$ with independent estimates Var $\{G\}$.

The error variances and covariances of extra olated mean anomalies for the 1° × 1° bloc can be estimated from the transition-frequen counts such as those in Table 2. Use of the counts will result in underestimates becau no allowance can be made for random err in the 'observed' 1° × 1° anomalies in t sample, and because the square of the mean each class of anomalies is less than the me square of the class. The principal value of th variances and covariances from the frequen counts is the variation of Var $\{\epsilon\}$ with h a $|\Delta g|$.

The variances and covariances of $\hat{\epsilon}\{\Delta g|h\}$ a $\hat{E}\{\Delta g_i|\Delta g_j, h_u, h_v\}$ were computed for a varie of cases from the frequency counts of the me anomalies of 1° × 1° blocks to obtain empiri correction factors to be applied to the err variances of mean anomalies of 5° × 5° block

$R(h)$ and $D(|\Delta g|$, pct. obs.). Originally estimates were made of another correction factor, $J(\delta h)$, in order to allow for the variation of topography within a $5° \times 5°$ block, but δh was found to be correlated closely enough with h so that the two could be combined. $R(h)$ varied from 3.0 for $h \leqq -12$ down to 0.5 for $h = -10, -9$, up to 1.7 for $h = -5$, down to 0.5 for $h = 0, +1$, and up to 4.3 for $h \geqq +11$. The extreme values of D were $D(0, 0\%) = 0.93$; $D(110 \text{ mgal}, 0\%) = 1.34$; $D(0, 100\%) = 0.50$; $D(110 \text{ mgal}, 100\%) = 1.0$.

These empirical factors gave numerical expression to the common-sense rules that (1) gravity will vary more erratically near large anomalies than near small, (2) the error variance of extrapolated estimates will approach the Var $\{E\}$ of $E\{\Delta g|h\}$ (Table 3) with an increase in distance from observed values; and (3) gravity will vary more erratically near large changes in elevation than near small. It is also true that gravity will vary more with certain elevations than with others; the best indicators are the Var $\{\epsilon\}$ of the $E\{\Delta g|h\}$.

Because the transition frequency counts of the mean anomalies of $5° \times 5°$ blocks include so many smoothed estimates based on few observations, estimates of variance based thereon are unrealistically low. The most feasible alternative is to assume linear correlation, which is equivalent to assuming the lines to be straight and parallel in Figure 2. Hence $E\{\Delta g_2\}$ can be written algebraically as

$$E\{\Delta g_2|\Delta g_1, h_1, h_2\} = r_1[\Delta g_1 - E\{\Delta g|h_1\}] + E\{\Delta g|h_2\} - E\{\Delta g|h_1\} \qquad (48)$$

where r_1 = correlation coefficient = slope of h_2 line on h_1 graph. For $5° \times 5°$ blocks, the average $r_1 = 0.42$; for $1° \times 1°$ blocks, the average $r_1 = 0.53$. A linear correlation theory was developed, with elevation ignored, using $\text{Var}_{5°}\{G\} = m\{\text{Var}_{5°}\{E_h\}\} \approx 350 \text{ mgal}^2$. The corresponding value for $\text{Cov}_{5°,5°}\{G\} = 0.42 \times 350 = 147 \text{ mgal}^2$.

Now both the $r_{5°} = 0.42$ and the $r_{1°} = 0.53$ are too small because of random errors in the mean anomaly estimates in the samples on which they are based. If it is assumed that the correlation $r_1 = A^2/(A^2 + X^2)$, then Var $\{G\} = A^2 + X^2$ and $\text{Cov}_1\{G\} = A^2$, and X is thus random with zero mean. If it is further assumed that the estimates $\hat{E}$ are affected by a random error of zero mean y, with $m\{y^2\} = Y^2$. Then Var $\{\hat{E}\} = A^2 + X^2 + Y^2$. If y is perfectly random, $\text{Cov}_1\{\hat{E}\} = \text{Cov}_1\{G\} = A^2$, yielding for an estimated correlation coefficient

$$\hat{r}_1 = \frac{A^2}{A^2 + X^2 + Y^2} < r_1 \qquad (49)$$

[*Bartlett*, 1956 p. 265].

The mean anomalies of $5° \times 5°$ blocks have a much smaller proportionate error than the mean anomalies of $1° \times 1°$ blocks, because they are based on more observations. Hence it was assumed the $\text{Var}_{5°}\{G\} = 350$ mgal and $r_{5°} = 0.42$ were correct (actually, 0.67 should have been used). Equation (7) of *Kaula* [1957] was then used to solve for the consistent values $\text{Var}_{1°}\{G\} = 760 \text{ mgal}^2$ and $r_1 = 0.704$.

The linear correlation model was used to compute the error variance, Var $\{\hat{\epsilon}\}$, and the estimate variance, Var $\{E\}$, of the mean anomalies of $5° \times 5°$ blocks for seven cases, varying from 4 per cent to 100 per cent observed. The bias function Q was then obtained from equation (44). $\text{Cov}_{5°,5°}\{\hat{\epsilon}\}$, etc., were computed for the same cases in a similar manner, as were the variances and covariances of extrapolated estimates.

The empirical rules derived from these computations were then tested by applying them to various cases for twenty blocks, of which the true mean anomalies were known.

Since the linear theory was based on a fit to the $\text{Var}_{5°}\{G\}$ and $\text{Cov}_{5°,5°}\{G\}$, it would be imprudent to extend it to covariances for distances greater than 5°. Instead, the results derived from the linear theory were used only as a guide to the magnitude of Cov $\{\epsilon\}$/Cov $\{G\}$, and the Cov $\{G\}$ found from autocorrelation analysis (Table 9) were used as an upper bound to the Cov $\{\epsilon\}$ to determine how they should be extrapolated to greater distances.

The error variances of the estimated mean anomalies of $10° \times 10°$ blocks were computed as

$$\sigma_{10°}^2\{\epsilon\} = \text{Var}_{10°}\{\epsilon\} = \frac{1}{16}\left[\sum \text{Var}_{5°}\{\epsilon\} + 2\sum \text{Cov}_{5°,5°}\{\epsilon\}\right] \qquad (50)$$

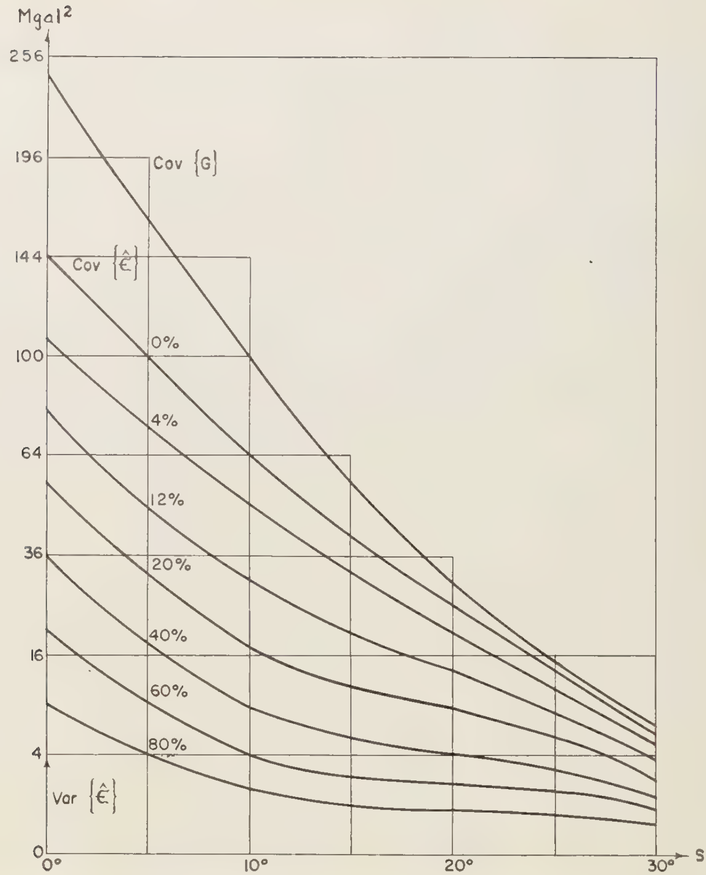

FIG. 5—Error variances and covariances of estimated mean anomalies of $10° \times 10°$ blocks.

The error covariances of estimated mean anomalies of $10° \times 10°$ blocks for $10°$ distance between centers, $\mathrm{Cov}_{10°,10°}\{\epsilon\}$, were computed from the $\mathrm{Cov}_{5°,s}\{\epsilon\}$ for different combinations and observed percentages in the $10° \times 20°$ block. These covariances were found to be almost entirely a function of the observed percentage.

The bias terms Q for $10° \times 10°$ blocks were obtained from the $5° \times 5°$ block Q's in the same manner as the variances.

The mean error variances and covariances of the mean anomaly estimates of the $10° \times 10°$ blocks are summarized in Figure 5.

The mean sum of $\mathrm{Var}\{\hat{E}\} + \mathrm{Var}\{\hat{\epsilon}\} + Q$ for the 410 $10° \times 10°$ blocks was 222 mgal², a discrepancy of -23 mgal² from $\mathrm{Var}\{G\} = 245$, probably due in part to too low Q for squar less than 4 per cent observed and in part to to high $\mathrm{Var}\{G\}$ from inadequate representation ocean anomalies in the autocorrelation analysi

It was originally considered that the spheric harmonics up to the eighth degree should b determined by generalized least-squares fit t the estimated mean anomalies of $10° \times 1($ blocks. However, we estimate from Table that $\sum_{n=2}^{\infty} \sigma_n^2 = 137$ mgal², while $\mathrm{Var}\{\hat{E}\}$ the completely extrapolated $10° \times 10°$ bloc estimates is 60 mgal². Hence the variance these estimates with respect to the harmon expression up to the eighth degree is somewhe between 77 and 197 mgal². But the variance perfect estimates of the mean anomalies

TABLE 10—*Variances of spherical harmonic coefficients (fully normalized)*

n	$\mathrm{Var}_n\{\hat{\epsilon}\}$, mgal²	Q_n, mgal²	$\sum_m(\hat{A}_{nm}^2 + \hat{B}_{nm}^2)$, mgal²	$\hat{\sigma}_n$, mgal²	σ_n^2, mgal²	$\sigma\{\sigma_n^2\}$ mgal²
0	1.16					
2	1.01	0.47	0.87	5.3	7.3	±5.1
3	0.88	0.40	11.11	20.1	43.6	±7.9
4	0.72	0.33	13.86	23.3	29.8	±9.0
5	0.57	0.26	6.60	15.7	10.5	±9.9
6	0.43	0.19	10.38	18.4	24.2	±10.8
7	0.31	0.13	4.18	10.8	2.8	±11.6
8	0.22	0.09	5.60	10.9	22.7	±12.4
Totals	35.9	16.0	52.6	104.5	140.9	±25.9

× 10° blocks is, from Table 9, 245 mgal², 108 mgal² with respect to the harmonics up the eighth degree. Hence the worst possible mates of mean anomalies for 10° × 10° cks do not have appreciably greater differ- es from the eighth degree harmonic expression n do the best estimates, so least-squares ng is pointless. The coefficients were there- found by the simple orthogonal method, ng the fully normalized harmonics H_{nm}.

$$\bar{A}_{nm} = \frac{1}{410} \sum_i H_{nm,i}\,\Delta g_i \qquad (51)$$

ence for the error variance of A_{nm}

$$\bar{A}_{nm}\} = \frac{1}{410^2}\Big[\sum_i H_{nm,i}{}^2\sigma^2\{\hat{\epsilon}_i\}$$

$$+ 2\sum_{i,j} H_{nm,i}H_{nm,j}\,\mathrm{Cov}\,\{\hat{\epsilon}_i, \hat{\epsilon}_j\}\Big] \qquad (52)$$

ince such a small part of the total error iance of $\Delta g_{8,i}$ is expressed by each term $H_{nm,i}$ of the spherical harmonics, for a general mate they can be considered as essentially dom with respect to each other and set *amer*, 1946 p. 173],

$$H_{nm,i}{}^2\sigma^2\{\hat{\epsilon}_i\} = m\{H_{nm}{}^2\}\sum \sigma^2\{\hat{\epsilon}_i\} \qquad (53)$$

$$H_{nm,i}H_{nm,j}\,\mathrm{Cov}\,\{\hat{\epsilon}_i, \hat{\epsilon}_j\}$$

$$= m\{H_{nm,i}H_{nm,j}\}\sum \mathrm{Cov}\,\{\hat{\epsilon}_i, \hat{\epsilon}_j\} \qquad (54)$$

m the same considerations as in (19) to (23),

$$m\{H_{nm}{}^2\} = \bar{P}_n(10°, 0°)$$

and

$$m\{H_{nm,i}H_{nm,j}\} = \bar{P}_n(10°, s_{ij}) \qquad (55)$$

$\bar{P}_n$ is a zonal harmonic averaged over, or between, 10° × 10° blocks, by applying equation (7) of *Kaula* [1957].

The total amount of error variance of the 410 10° × 10° squares was 34,330 mgal²; $\sum \mathrm{Cov}_{10°,10°}\{\hat{\epsilon}\}$ was estimated as 33,600 mgal²; $\sum \mathrm{Cov}_{10°,20°}\{\epsilon\}$, as 38,200 mgal²; and $\sum \mathrm{Cov}_{10°,30°}\{\epsilon\}$ as 8500 mgal². The totals of the bias terms Q were also estimated, and (52) to (54) were applied to derive $\mathrm{Var}_n\{\hat{\epsilon}\}$ and Q_n.

Table 10 sets forth the results for error and bias for each degree of the harmonics, as well as the sum of the estimate variance (from Table 6) plus error variance plus bias terms for each degree (other than 0)

$$\hat{\sigma}_n{}^2 = \sum_m \hat{A}_{mm}{}^2\,\hat{\sigma}^2 + \sum_m \hat{B}_{nm}{}^2$$

$$+ (2n+1)\,\mathrm{Var}_n\,\{\hat{\epsilon}\} + (2n+1)Q_n \qquad (56)$$

compared with the degree variance σ_n^2 from autocorrelation analysis (Table 8). The uncertainty given for σ_n^2 is $\pm 3\sqrt{2n+1}$.

It may also be questioned whether a direct least-squares fit to the available observations, such as was applied by *Jeffreys* [1943] and *Zhongolovich* [1952] to determine the second- and third-degree harmonics, may give unbiased estimates without excessive increase in uncertainty. However, a simple least-squares fit to observations nonuniformly distributed over the earth's surface will give a solution for which

coefficients are too large in absolute magnitude; that is, the harmonic functions will be distorted to fit in the areas where the least-squares fit is being made.

Related functions—From the statistical properties of the free-air anomalies it is relatively easy to derive the statistical properties of geoid heights and deflections from the vertical. The covariance of geoid heights is given by

$$\text{Cov}_s\ \{N\} = \sum_{n=2}^{\infty} \left[\frac{R}{G(n-1)}\right]^2 \cdot \sigma_n^{\ 2}\{\Delta g\} P_n\,(\cos s) \qquad (57)$$

There are two covariances of deflections: a 'co-linear' covariance for the components along the line between the two points in question and a 'transverse' covariance for the components at right angles to this line.

The co-linear covariance:

$$\text{Cov}_s\ \{\rho''\} = \sum_{n=2}^{\infty} \left[\frac{\csc 1''}{G}\right]^2 \frac{(n+1)n}{2(n-1)^2} \cdot \sigma_n^{\ 2}\{\Delta g\}\left[P_n\,(\cos s) - \frac{P_{n2}\,(\cos s)}{n(n+1)}\right] \qquad (58)$$

The transverse covariance:

$$\text{Cov}_s\ \{\tau''\} = \sum_{n=2}^{\infty} \left[\frac{\csc 1''}{G}\right]^2 \frac{(n+1)n}{2(n-1)^2} \cdot \sigma_n^{\ 2}\{\Delta g\}\left[P_{n-1}(\cos s) + \frac{P_{(n-1)2}(\cos s)}{n(n+1)}\right] \qquad (59)$$

As derived from the anomaly statistics, the variance of the geoid height is 1075 m², or $\sigma\{N\} = \pm 32.7$ meters; the variance of the deflection in a random direction is 32.5 sec², or $\sigma\{\delta\} = \pm 5.7''$.

Coefficients for the zonal harmonics up to degree five have been estimated from satellite motions by *O'Keefe and others* [1959] much more accurately than is possible from terrestrial gravimetry. The values of these coefficients in terms of fully normalized free-air anomalies, referred to the International Formula, are

$$\bar{A}_{20} = +4.1 \text{ mgal}$$

$$\bar{A}_{30} = +1.8 \text{ mgal}$$

$$\bar{A}_{40} = -2.1 \text{ mgal}$$

$$\bar{A}_{50} = +0.1 \text{ mgal}$$

The $\bar{A}_{20}$ corresponds to $J = 0.00162375$ a[illegible] flattening of 1/298.24. This flattening toge[illegible] with the value from Table 6, $\bar{A}_{00} = -2.0$ m[illegible] gives as a standard gravity formula in milli[illegible] on the Potsdam system,

$$\gamma = 978042.4(1 + 0.0053023 \sin^2 \phi - 0.0000058 \sin^2 2\phi) \qquad ($$

And if the absolute correction to Potsdan[illegible] -11 mgal [*Morelli*, 1957] is added,

$$\gamma = 978031.4(1 + 0.0053023 \sin^2 \phi - 0.0000058 \sin^2 2\phi) \qquad ($$

Combining Table 6, the zonal harmonics deri[illegible] from satellite motions, and the equatorial ra[illegible] of 6,378,265 meters derived by O'Keefe from [illegible] dynamical parallax and the lunar dist[illegible] measurement of *Yaplee and others* [1958] g[illegible] the best estimate for the total potential [illegible] m²/sec² up to the fourth degree in Table 11.

Conclusions—Like most statistical analy[illegible] the main result of this study is that it g[illegible] some numerical measure of what was kn[illegible] beforehand through common sense—in this c[illegible] that the present distribution of gravity obse[illegible] tions is inadequate to give more than a sket[illegible] indication of the harmonics in the earth's gra[illegible] field. As shown in Table 10, the magnitude[illegible] the estimates averaged but slightly larger t[illegible] their uncertainties.

The difficulty is that the important l[illegible] degree harmonics constitute such a small por[illegible] of the total gravity anomaly affecting a gra[illegible] meter at the earth's surface. The 75 terms [illegible] to the eighth degree comprise only 11 per c[illegible] of the variance (Table 8).

However, aside from methods of poss[illegible] future use, the study does yield some g[illegible] numerical estimates, both statistical and de[illegible] minate. Reasonably firm statistical parame[illegible] include the mean $\delta\Delta g/\delta h$ of $+8.5$ mgal/100[illegible] for 1° × 1° block means, the covariances [illegible] distances less than 10° in Table 7, the varia[illegible] and covariances of area mean anomalies [illegible] Table 9, and the variances of geoid heig[illegible] 1075 m², and of deflections, 32.5 sec². For c[illegible] servative estimates of the effects of gra[illegible] anomalies, the following maximum plaus[illegible] degree variances, $\sigma_n^{\ 2}\{\Delta g\}$, are suggest[illegible]

TABLE 11—*Coefficients for gravitational potential for conventional spherical harmonics* (Eq. 16)

General term: $1/r^{n+1} P_{nm}(\sin \phi)(A_{nm} \cos m\lambda + B_{nm} \sin m\lambda)$ m^{n+3}/sec^2				
n	0	2	3	4
A_{n0}	$+3.98616 \times 10^{14}$	-1.75546×10^{25}	$+2.5 \times 10^{29}$	$+1.12 \times 10^{36}$
A_{n1}		0	+5.83(28)	−2.07(35)
B_{n1}		0	+8.40(28)	−2.25(35)
A_{n2}		+7.41(21)	+1.05(28)	−4.46(33)
B_{n2}		−6.59(21)	+5.25(27)	+5.13(34)
A_{n3}			+1.42(28)	+3.12(34)
B_{n3}			+1.36(28)	−6.69(33)
A_{n4}				+1.11(33)
B_{n4}				+1.11(34)

$^2 < 15$ mgal^2; $\sigma_3^2 < 43$ mgal^2; $\sigma_4^2 < 30$ mgal^2; ^{2} through $\sigma_8^2 < 25$ mgal^2 each.

With the given topographic and gravity data, e procedures applied have several features iich cause the resulting statistical and deterinate estimates to be not quite as good as ey might be. Of these features, only three are t to be causes of concern:

1. Simple free-air anomalies were used, for e practical reason of avoiding the labor of timating the topographic elevations around ery station. If and when this labor is accomished, then the same statistical procedures ould be applied to some type of anomaly for iich the visible terrain effect has been smoothed t, such as the isostatic. In this case, the isostatic duction should be treated as an arbitrary rrection, so that conclusions can be drawn om the results without making them conditional the geophysical assumption made at the ginning. Probably a preferable reduction is e smoothed 'model earth' of *De Graaf-Hunter* 957] both from the idealistic consideration of aking the least assumption about the earth's terior and from the practical consideration of inimizing the chance of mistakes in the produre.

2. The results of the autocorrelation analysis ere unexpectedly erratic, so that they cannot applied as a control as confidently as was ped. The fault is due partly to the imbalance th respect to topography and partly to the lection of the regional and local samples as ocks rather than as long lines. The use of ocks causes considerable correlation between the estimates of covariance within each block. The dependence on an assumed flattening makes the second-degree variance estimate uncertain.

3. The adjustments necessary to meet the satellite-imposed conditions on the zonal harmonics are larger than expected from the estimated uncertainties for these harmonics derived from terrestrial gravity.

The numerical results of the study do not agree closely with previous statistical and harmonic analyses for several reasons:

1. The magnitudes of the estimated mean anomalies of $10° \times 10°$ blocks is appreciably less than those found by *Jeffreys* [1943] and *Zhongolovich* [1952] because they were made by the Markov procedure, which results in smaller magnitudes than the direct averages of observed anomalies. Qualitatively, the explanation is in Figure 1; for the estimated mean anomaly of an area about a single observation Δg_0, the Jeffreys and Zhongolovich procedure gives $E\{\Delta g_m\} = \Delta g_0$, whereas ours gives $E\{\Delta g_m\} = \hat{E}$.

2. The magnitude of the equatorial ellipticity, or P_{22} terms, was much less than that of *Heiskanen and Uotila* [1958]; the magnitude of the second and third degree terms was less than those of Jeffreys and Zhongolovich; and the magnitude of the second through sixth degree terms was less than those of Dubovskiy [*Molodenskiy*, 1945 p. 50] because of (a) smaller estimated anomalies of $10° \times 10°$ blocks, as in (1) above and (b) use of estimated anomalies world-wide instead of fitting by least squares to the observed values.

3. Accuracy estimates of computation of geoid

heights and deflections of the vertical based on the results of the autocorrelation analysis would give smaller uncertainties than do the studies of *Cook* [1950, 1951] and *Molodenskiy* [1945] because these studies were based on the spherical harmonics of Jeffreys and Dubovskiy, respectively. This difference is largely due to the second-degree variance; that is, the inferred equatorial ellipticity.

4. Accuracy estimates of geoid computation based on the autocorrelation analysis would give larger uncertainties than do the studies of *Hirvonen* [1956] and *Kaula* [1957] because these studies were based on limited samples in areas of smooth variation. They also assumed zero correlation between mean anomalies for $30° \times 30°$ blocks, which is almost corroborated: the estimate in Table 9 is 7 mgal² for $\mathrm{Cov}_{30°,30°}\ \{G\}$ or $r = 0.08$.

5. Accuracy estimates of geoid computation based on the autocorrelation analysis would give much larger uncertainties than those stated by *Heiskanen and Vening-Meinesz* [1958 p. 73] because the size of the third- and fourth-degree variances found (Table 8) do not corroborate the hypothesis that isostatic equilibrium prevails over large areas to the extent assumed by Heiskanen and Vening-Meinesz. Taking the area of a $30° \times 30°$ block as $9 \times 4\pi/(410 \times 6.37^2 \times 10^{12}) = 11.16 \times 10^{12}$ m², the value of area $\times\ \sigma\{G\}$ from Table 9 is $11.16 \times 10^{12}\sqrt{85} = \pm 10.3$ mgal Mm² in Vening-Meinesz' terminology. This value applies to free-air anomalies; correcting for isostatic compensation at 37-km depth reduces it to ± 88 mgal Mm², which is still much larger than Vening-Meinesz' 30 mgal Mm² as a maximum to be exceeded not more than 10 times. The 30 mgal Mm² estimate was presumably based on areas appreciably smaller than a $30° \times 30°$ block; this large an area of isostatically reduced anomalies cannot be found without including many interpolated values. For example, if we assume that the mean isostatic correction has the same ratio to the mean anomaly for a $10° \times 10°$ block, there is obtained for the $10° \times 10°$ block area $\times\ \sigma\{G_i\}$

$$= 1.24 \times 10^{12}\sqrt{(62 \times 245)/85}$$
$$= \pm 16.8 \text{ mgal-Mm}^2.$$

The third- and fourth-degree variances indicate that ± 88 mgal Mn² will be considerably exceed for areas larger than a $30° \times 30°$ block.

The statement '. . . isostatic equilibrium . prevails to about 85 or 90 percent' [*Heiskan and Vening Meinesz*, 1958 p. 282] is undoubtec true, but incomplete, since it does not speci depth of compensation nor areas or wavelengt of applicability. Wide deviations exist from a standard depth of compensation; further, demonstrated by the degree variances in Tabl and by the zonal harmonics derived from satell motion, such deviations extend over large are

Hence any gravity-anomaly estimates whi are functions of the topography, whether th be isostatic or statistical, will have large er variances and covariances. In utilizing estima with inherently large uncertainties, the cu tomary recourse is to obtain as many independe estimates as possible. But the errors in estima of gravity anomalies form an essentially co tinuous function, as do the anomalies themselv Hence, in applying gravity data to a geode system, the nearest approach to the customa recourse is to apply the data over the wid possible extent of the system. It is for t reason, as well as to get a clearer grasp of t essentials of the problem, that, rather th estimate accuracy of geoid determination single points, we have emphasized in this stu area means and harmonic functions.

The statistical and harmonic analysis gravity is currently being applied to obtain improved world geodetic system in conjuncti with astrogeodetic and satellite data. In t application both the estimate of the grav field in the form of harmonic coefficients a the statistical parameters are used for the purp of weighting the gravimetric and astrogeode estimates in a generalized least-squares adju ment. Other applications being made of t gravity analysis include estimation of effects orbits and trajectories, planning of gravime surveys, and derivation of the most proba depth of isostatic compensation.

Acknowledgments—I am grateful to J. O'Keefe for granting the opportunity to carry this research; to M. Q. Marchant, Mrs. R. Phillips, J. A. Wilgus, Miss M. A. Marks, a W. I. Zangwill for performing various parts the counting, computing, and checking of formul and to J. L. Williams for programing the UNIV computations.

References

ʀᴛʟᴇᴛᴛ, M. S., *An Introduction to Stochastic Processes,* Cambridge Univ. Press, 312 pp, 1956.

ᴊʟʟᴀʀᴅ, E. C., The figure of the earth, *Monthly Notices Roy. Astron. Soc., Geophys. Suppl., 5,* 186–192, 1948.

ᴏᴏᴋ, A. H., The calculation of deflection of the vertical from gravity anomalies, *Proc. Roy. Soc., A, 204,* 374–395, 1950.

ᴏᴏᴋ, A. H., A note on the errors involved in the calculation of elevations of the geoid, *Proc. Roy. Soc., A, 208,* 133–141, 1951.

ʀᴀᴍᴇʀ, H., *Mathematical Methods of Statistics,* Princeton Univ. Press, 575 pp, 1946.

ᴇ Gʀᴀᴀғғ-Hᴜɴᴛᴇʀ, J., Reduction of gravity observations for Stokes' formula, *Adv. Rept., Spec. Study Group 8, Sect. V, I. A. G.* XI General Assembly IUGG, Toronto, 1957.

ᴏᴏʙ, J. L., *Stochastic Processes,* John Wiley & Sons, New York, 654 pp, 1953.

ᴇɪsᴋᴀɴᴇɴ, W. A., ᴀɴᴅ U. A. Uᴏᴛɪʟᴀ, Some recent studies on gravity formulas, in *Contribs. in Geophys. In Honor of Beno Gutenberg,* Pergamon Press, London, 200–208, 1958.

ᴇɪsᴋᴀɴᴇɴ, W. A., ᴀɴᴅ F. A. Vᴇɴɪɴɢ-Mᴇɪɴᴇsᴢ, *The Earth and Its Gravity Field,* McGraw-Hill Book Co., New York, 470 pp., 1958.

ɪʀᴠᴏɴᴇɴ, R. A., On the precision of the gravimetric determination of the geoid, *Trans. Am. Geophys. Union, 37,* 1–8, 1956.

ғғʀᴇʏs, H., The determination of the earth's gravitational field, (second paper), *Monthly Notices Roy. Astron. Soc., 5,* 55-66, 1943.

ɴɢ, K., Figur der Erde, in *Handbuch der Physik, Geophysik I,* Springer-Verlag, Berlin, 534–639, 1956.

Kᴀᴜʟᴀ, W. M., Accuracy of gravimetrically computed deflections of the vertical, *Trans. Am. Geophys. Union, 38,* 297–305, 1957.

Kᴀᴜʟᴀ, W. M., Gravity formulas utilizing correlation with elevation, *Trans. Am. Geophys. Union, 39,* 1027–1033, 1958.

Kᴀᴜʟᴀ, W. M., Statistical and harmonic analysis of gravity, *Army Map Service Tech. Rept. 24,* 141 pp., 1959.

Mᴏʟᴏᴅᴇɴsᴋɪʏ, M. S., The basic problems of geodetic gravimetry (in Russian), *Proc. Cent. Inst. Geod., Photogr. and Cart., 42,* Moscow, 107 pp. 1945; Translation 59-11-257, Office of Tech. Svcs., Dept. Commerce, Washington, 1959.

O'Kᴇᴇғᴇ, J. A., A. Eᴄᴋᴇʟs, ᴀɴᴅ R. K. Sǫᴜɪʀᴇs, The gravitational field of the earth, *Astrophys. J.,* in press, 1959.

Mᴏʀᴇʟʟɪ, C., Gravimetry, *Rept. Spec. Study Group 5 Sect. IV, I. A. G.* XI General Assembly, Toronto, 1957.

Pʀᴇʏ, A., Darstellung der Höhen-und Tiefenverhältnisse der Erde durch eine Entwicklung nach Kugelfunktionen bis zur 16. Ordnung, *Abhandl, Ges. Wiss. Gottingen, Math.-physik. Kl., N. F., 11,* 1–29, 1922.

Yᴀᴘʟᴇᴇ, B. S., R. H. Bᴜʀᴛᴏɴ, K. J. Cʀᴀɪɢ, ᴀɴᴅ N. G. Rᴏᴍᴀɴ, Radar echoes from the moon at a wavelength of 10 cm, *Proc. I.R.E., 46,* 293–297, 1958.

Zʜᴏɴɢᴏʟᴏᴠɪᴄʜ, I. D., *The External Gravity Field of the Earth and the Fundamental Constants Connected With It* (in Russian), Acad. Sci., Pub. Inst. Th Astr., Moscow, 129 pp., 1952.

(Manuscript received July 25, 1959.)

URNAL OF GEOPHYSICAL RESEARCH VOLUME 64, NO. 12 DECEMBER, 1959

Storage Analysis and Flood Routing in Long River Reaches

E. M. LAURENSON

School of Civil Engineering
The University of New South Wales
Sydney, Australia

Abstract—Numerous flood-routing studies have indicated that the maximum length of reach through which a flood can be routed in a single step is such that time of travel through the reach does not exceed about half of the period of rise of the inflow flood. This paper presents a method of analyzing the storage characteristics of reaches considerably longer than this by arbitrarily inserting a number of hydrographs between the inflow and outflow hydrographs in such a way as to produce single-valued storage-discharge relations for the shorter reaches so formed. These storage-discharge relations are then used in conjunction with a graphical flood-routing procedure to route the inflow successively through the several short reaches and so reproduce the outflow hydrograph.

Introduction—Storage methods of flood routing e based upon the equation of continuity as plied to river reaches, and, if the routing riod t is short in relation to the rate of change discharge, this equation can be represented as

$$\frac{(\ _{1} + I_2)}{2}\, t - \frac{(O_1 + O_2)}{2}\, t = S_2 - S_1 \qquad (1)$$

ere I and O are, respectively, the instantaneous tes of inflow to and outflow from a reach, the bscripts 1 and 2 refer to the beginning and end, spectively, of the routing period t, and S is e volume of storage in the reach above some bitrary datum. In the solution of this equation O_2, S is expressed as either an algebraic or aphical function of outflow or of a weighted erage of inflow and outflow expressed in the m $[xI(1 - x)O]$, x being a weighting factor.

The necessity of expressing the volume of orage in a reach at a given moment as a funcn of the rates of inflow to and outflow from e reach at that moment represents a limitation the length of reach to which storage-routing ethods can be applied in their simple form. is will become clear from consideration of gure 1, which shows diagrammatically two ssible water surface profiles having the same low and outflow stages over a river reach AC. ese are only two of the infinite number of posle profiles, and, as the storage in the reach is ferent for different water surface profiles, it is clear that the volume of storage in the reach is not a single-valued function of the discharges at A and C (inflow and outflow). Over the shorter reach AB, however, rates of inflow and outflow are a satisfactory index of volume of storage. (This presupposes a single-valued relation between gage height and discharge. In a number of very flat rivers, this assumption is not sufficiently valid for normal storage-routing methods to be used, but this complication is not dealt with in this paper.)

The length of reach through which a flood can be routed by ordinary storage-routing methods must be such that storage can be expressed as a single-valued function of weighted average discharge $[xI + (1 - x)O]$; that is, for any given value of $[xI + (1 - x)O]$, the storage in the reach should have a specific value, regardless of whether stages are rising, falling, or steady. Flood-routing research carried out by the author indicates that this requirement is usually met to a satisfactory degree of accuracy when the time of travel of the flood wave through the reach does not exceed about one third to one half of the period of rise of the inflow hydrograph. Investigations described herein offer a solution of the problem of routing floods by rational procedures through long reaches which have times of travel considerably longer than half of the period of rise of the inflow hydrograph.

Method of solution—The solution of the prob-

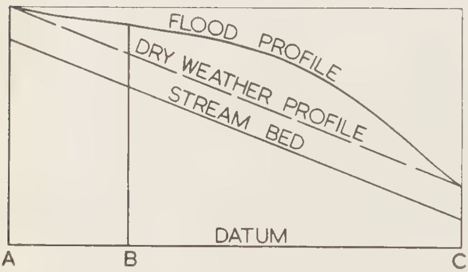

Fig. 1—Diagrammatic representation of water surface profiles.

lem will be illustrated with reference to the flood of September to November, 1944, in the Darling River, the reach considered being from Bourke to Menindee, a distance of 566 river miles of flat meandering stream. Figure 2 shows the hydrographs at the two ends of the reach together with the assumed hydrograph of intermediate losses, and the Menindee hydrograph corrected for these losses. Intermediate losses amount to some 20,000 acre ft from a total flood discharge at Bourke of about 180,000 acre ft, and are presumably accounted for by seepage losses into the river banks and overbank flow that does not return to the river. Distribution of the intermediate losses over the period of the flood must be carried out arbitrarily, and in this case the rate of loss was assumed to vary roughly in the same manner as the Menindee discharge varied. The objective of the procedure to be described is to reproduce the hydrograph

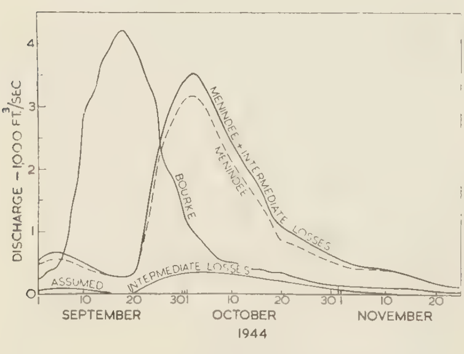

Fig. 2—Hydrographs of the Darling River at Bourke and Menindee, New South Wales, September to November, 1944.

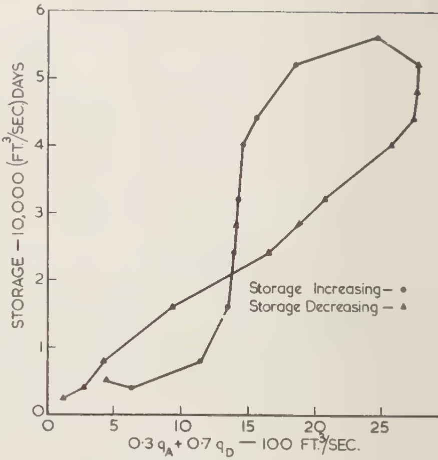

Fig. 3—Storage-discharge relation for reach A D (Bourke to Menindee).

of Menindee flow plus intermediate losses fr the Bourke hydrograph.

It is clear from inspection of the hydrogra that storage (accumulated inflow minus accun lated outflow) cannot be expressed as a sing valued function of discharge $[xI + (1 - x)$ This is further demonstrated by Figure 3, wh shows the storage-discharge relation for reach with $x = 0.3$. Any other value of x wo give an equally bad, or worse, relation. It follo that the flood cannot be routed through t reach in one step by ordinary storage-rout methods.

After unsuccessful trials of a number published methods, which will be mentio later, the procedure adopted to effect the rep duction of the downstream hydrograph (1) arbitrary division of the long reach i three shorter ones by sketching two hypothet hydrographs between the two actual o (2) derivation of storage-discharge relations the three short reaches, and (3) routing of Bourke hydrograph successively through three short reaches by a graphical procedure.

In general, the intermediate hydrogra sketched in must be adjusted by trial and e until single-valued storage-discharge relati are obtained, but the first trial will often sufficiently accurate. If it appears from the f trial that adjustment of the intermediate hyd

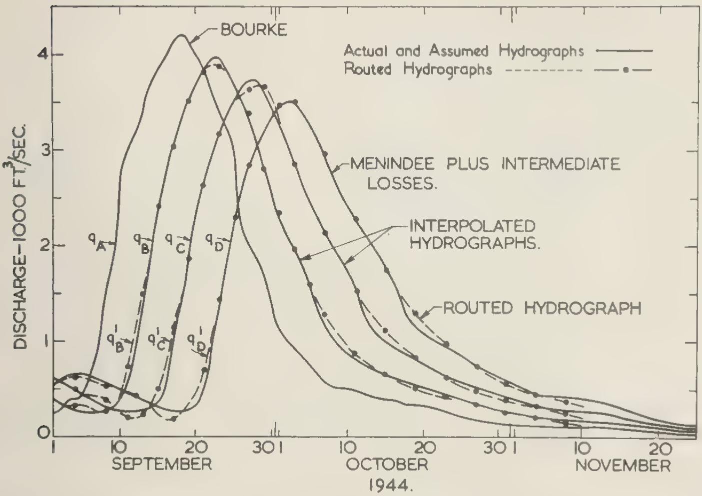

FIG. 4—Interpolation of hypothetical hydrographs and comparison of routed hydrograph with actual hydrograph.

aphs will not yield better storage-discharge lations, a greater number of intermediate ydrographs should be sketched in. The long ach is thus subdivided into a greater number shorter reaches, and acceptable storage-scharge relations will probably be obtained.

Storage analysis—In the case being described, terpolation of the intermediate hydrographs as a simple matter. It was carried out largely y dividing distances between the two end ydrographs into three equal parts (Fig. 4), and e first trial hydrographs so drawn gave very tisfactory storage-discharge relations. As an aid fixing the peaks of the intermediate hydro-raphs it might be noted that when a hydro-raph is routed through a number of consecutive aches the successive peaks fall on a curve that concave upwards. (In this case, the curvature as made very slight and might well have been eater.) It will be noted that minor irregularities the Bourke hydrograph have not been intro-uced in the interpolated graphs, as minor regularities are very quickly damped out by orage in river flow and in flood routing. Also, hen minor irregularities occur on the outflow ydrograph it is usually impossible to reproduce em by routing procedures, and they can ormally be ignored. For convenience in the llowing work, the Bourke hydrograph is referred to as q_A, the first and second intermediate hydrographs as q_B and q_C, respectively, and the Menindee plus intermediate outflow hydrograph as q_D, as labeled in Figure 4.

Preparation of the storage-discharge curves will be illustrated with reference to the reach A to B, for which the appropriate hydrographs are redrawn in Figure 5*a*. The difference in discharge at the two ends of the reach, q_A minus q_B, is plotted against time in Figure 5*b*. The volume of storage in the reach above some arbitrary datum at any time during the flood is equal to accumulated inflow minus accumulated outflow to that time, and the curve of storage against time (Fig. 5*c*) is therefore obtained by graphical integration of the q_A minus q_B curve. As the absolute volume of storage in the reach is not required, the routing process being carried out in terms of *change* in storage ($S_2 - S_1$ in equation 1), the actual position of the zero of the storage scale in Figure 5*c* is unimportant and is fixed merely so as to avoid the inconvenience of negative values of storage.

The appropriate value of x in the function $[xq_A + (1 - x)q_B]$ is that which gives the closest correspondence of the storage-discharge relations for rising and falling stages. Trial calculation of three or four pairs of corresponding points on

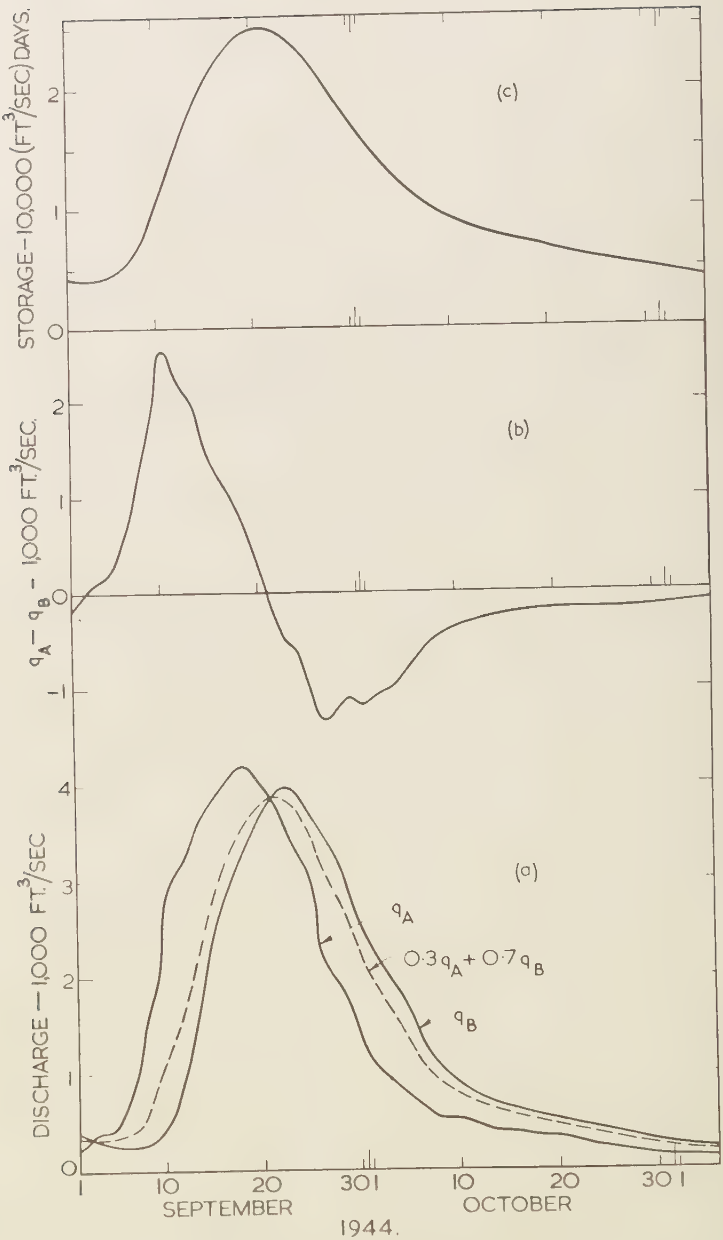

FIG. 5—Storage analysis for reach A to B.

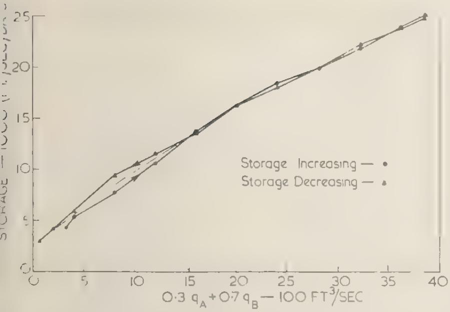

ɪɢ. 6—Storage-discharge relation for reach A to B.

ıe rising and falling limbs of the hydrographs ıdicated that a value of $x = 0.3$ would give storage-discharge relation close to a single-alued function, and, accordingly, the function).$3q_A + 0.7q_B$) was plotted against time in igure 5a by dividing the vertical distance etween the curves in the proportion of 3:7. 'his curve does not represent the hydrograph or any point in the reach but simply indicates weighted average of the inflow and outflow at ny given instant. For successive times throughut the flood, the value of storage from Figure : was then plotted against the corresponding alue of ($0.3q_A + 0.7q_B$) from Figure 5a, and ıe resulting storage-discharge relation is shown ı Figure 6.

Similar analyses were carried out for reaches ' to C and C to D, with $x = 0.3$ in both cases, nd the resulting storage-discharge relations are ıown in Figures 7a and 8a, respectively. In oth of these cases, inspection showed that different values of x would give relations closer to a single-valued function, and new storage-discharge curves were therefore prepared, with $x = 0.33$ for reach B to C and $x = 0.37$ for reach C to D. The resulting curves are shown in Figures 7b and 8b, respectively. For all three reaches, mean storage-discharge curves for use in the routing process were drawn, as shown by the dashed curves in Figures 6, 7b, and 8b.

It might be noted in passing that, once the intermediate hydrographs are drawn, the storage analysis described above can be carried out numerically, but the author finds the graphical method more expeditious.

The routing process—Routing was carried out with a graphical procedure which is similar in some respects to a number of published methods, notably those due to Puls and to *Linsley and others* [1949, pp. 505–507]. Figure 9 shows the routing curves prepared for reach A to B. An intercept chart relating q_B to ($0.3q_A + 0.7q_B$) with q_A as a parameter is first constructed, as shown on the left-hand side of Figure 9. For a given value of q_A this relation is linear, and the slope is independent of q_A, so that the lines are parallel and the construction of this chart is therefore a simple matter.

On the right-hand side of Figure 9 a curve of S/t against ($0.3q_A + 0.7q_B$) is plotted, where S is storage as before and t is the routing period. S/t is thus the rate of discharge which, in time t, the routing period, would provide a volume of storage S. The curve is obtained directly from the storage-discharge relation of Figure 6 by dividing the ordinates by the arbitrarily chosen, constant routing period t—in this case, two

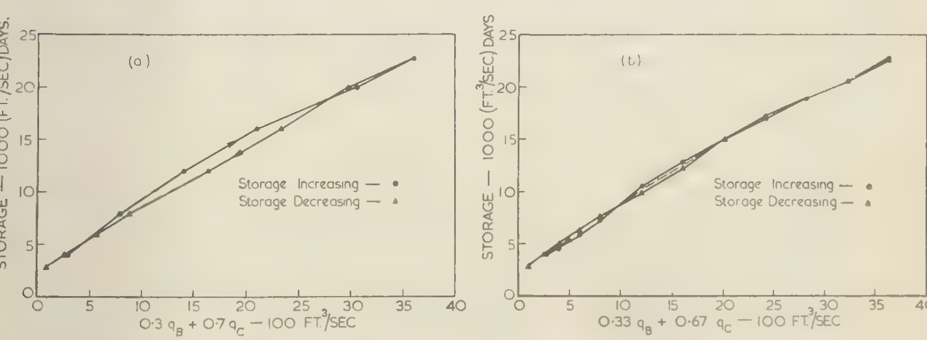

Fɪɢ. 7—Storage-discharge relation for reach B to C, (a) with $x = 0.3$, and (b) with $x = 0.33$

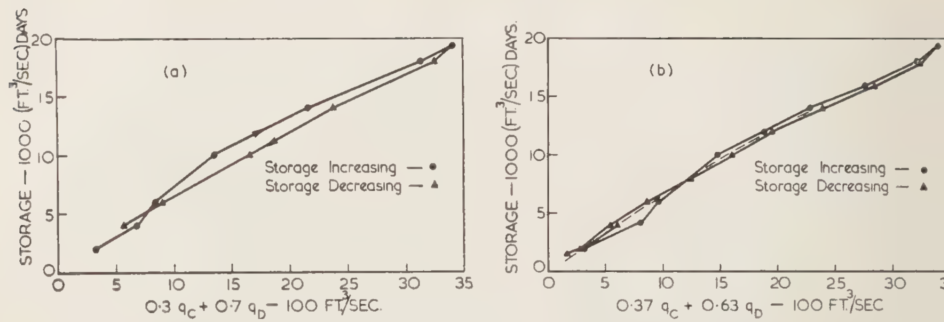

FIG. 8—Storage-discharge relation for reach C to D, (a) with $x = 0.3$, and (b) with $x = 0.37$.

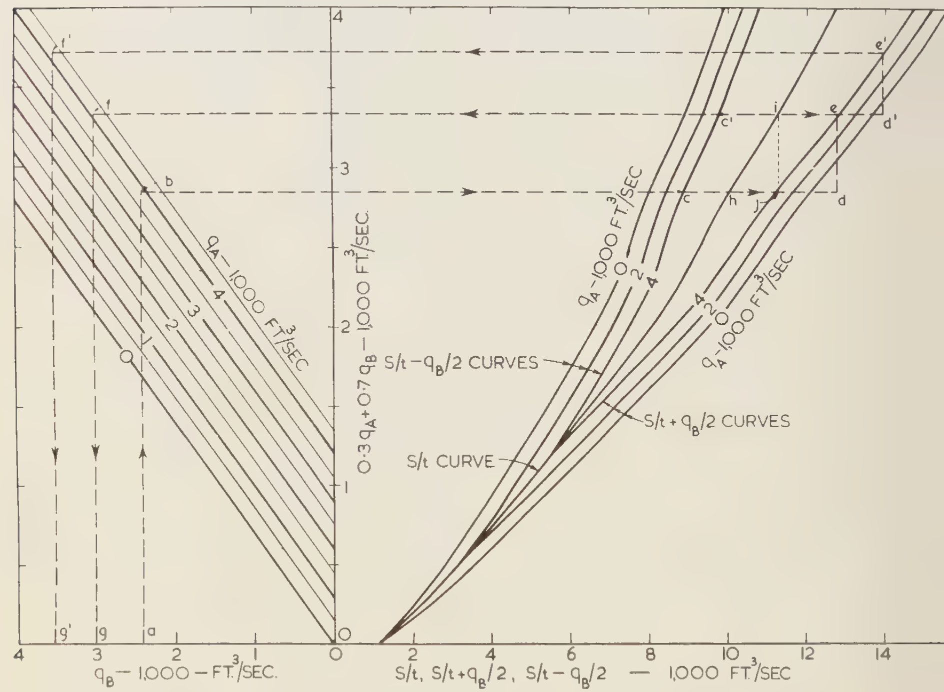

FIG. 9—Routing curves for reach A to B.

days. The S/t curve is not used in the actual routing process but is plotted as a construction line for the $S/t + q_B/2$ and $S/t - q_B/2$ curves. For any given value of $(0.3q_A + 0.7q_B)$, the values of q_B for various values of q_A can be determined from the left-hand side of Figure 9, and families of curves of $S/t + q_B/2$ and $S/t - q_B/2$ for various values of q_A can then be plotted against $(0.3q_A + 0.7q_B)$, as on the rig hand side of Figure 9. It might be noted t the curves of each family are 'equidistant' a 'parallel' in that the horizontal distances betwe them are equal and constant.

As an example of the actual routing procedu the routing period commencing on September will be considered. Commencement of

TABLE 1—*Extract from routing computations for reach A to B*

Date	q_A, ft³/sec	$\bar{q}_A$, ft³/sec	q_B', ft³/sec
Sept. 15	3860		2420
		4000	
17	4130		3010
		4160	
19	4130		3540
		4000	
21	3860		3820
		3610	
23	3390		3870
		3195	
25	2990		3700
		. . .	

ımple at this point of the hydrograph makes possible to avoid confusion in the lower part the diagram, where inflows are small, but is emphasized that the procedure to be scribed can be started at any point of the drograph as long as the initial outflow is own. The outflow q_B on September 15 is 20 ft³/sec. This figure is entered in Table 1, ich also shows the inflow hydrograph q_A and mean rate of inflow in each routing period $\bar{q}_A$ was obtained from the hydrograph and not necessarily exactly equal to the mean of values at the beginning and end of the routing iod. Routing is carried out as follows:

. Entering the left-hand side of Figure 9 h $q_B = 2420$ ft³/sec (point *a*) and $q_A = 3860$ /sec (point *b*) gives the value of $(0.3q_A + 0.7q_B)$ September 15.

2. Entering the right-hand side of Figure 9 h this value of $(0.3q_A + 0.7q_B)$ and with $= 3860$ ft³/sec gives the starting value of $t - q_B/2$ (point *c*).

3. A distance *cd*, representing 4000 ft³/sec, average rate of inflow during the routing iod of September 15 to 17, is marked off rizontally to the right of *c*.

4. Point *d* is projected vertically to the $t + q_B/2$ curve applicable to a q_A value of 30 ft³/sec, the inflow rate at the end of the ıting period. This gives point *e*, the ordinate which is the value of $(0.3q_A + 0.7q_B)$ applying September 17.

5. The rate of outflow q_B on September 17 is found by entering the left-hand side of Figure 9 with this value of $(0.3q_A + 0.7q_B)$ and the appropriate value of q_A, 4130 ft³/sec (point *f*). The indicated value of q_B is 3010 ft³/sec (point *g*), which is entered in Table 1 as q_B' to distinguish the computed values from actual values of q_B.

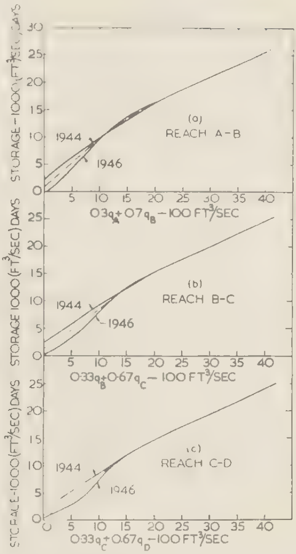

FIG. 10—Comparison of storage-discharge relations derived from the 1944 and 1946 floods, for (*a*) reach *A* to *B*, (*b*) reach *B* to *C*, and (*c*) reach *C* to *D*.

6. For the next routing period, September 17 to 19, the initial value of $(0.3q_A + 0.7q_B)$ is known, (ordinate of point *e*), the initial value of q_A is 4130 ft³/sec, so that $S/t - q_B/2$ curves can be entered directly at point *c'*.

7. Steps 3, 4, and 5 are repeated for this period, as indicated by points *c'*, *d'*, *e'*, *f'*, and *g'*.

The above procedure is carried out, period by period, until the whole flood has been routed.

In the case being described, routing curves similar to those in Figure 9 were prepared for all three reaches; the outflow from the first reach became the inflow for the second and was routed through it, and the outflow from the second reach was routed through the third reach. Results of the three routings have been plotted in Figure 4, in which the actual and assumed hydrographs q_A, q_B, q_C, and q_D are compared with the corresponding routed hydrographs q_A', q_B', q_C', and q_D'. The objective of the

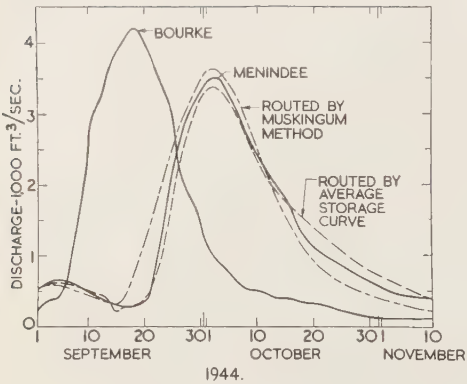

Fig. 11—Results of routing Bourke hydrograph by graphical method with average storage-discharge curves, and by Muskingum method through three reaches each with $K = 5$ days and $x = 0.33$.

procedure, as stated above—to reproduce the Menindee plus intermediate outflow hydrograph from the Bourke hydrograph—has been satisfactorily achieved.

The results demonstrate that satisfactory, singled-valued relations between storage and discharge can be obtained for reaches that are very long in relation to the time base of the flood wave. An interesting extension of the study was to compare the relations obtained from the 1944 flood with those obtained by similar analysis of the flood of May to June, 1946, on the same river. This comparison is shown in Figure 10. For all three reaches, the storage-discharge relations obtained from the two floods are virtually identical for discharges greater than 2000 ft³/sec and are similar for lower discharges. Average curves are shown dashed in Figure 10, and the result of routing the 1944 flood with these average curves is shown in Figure 11. The result is a satisfactory reproduction of the outflow hydrograph, though naturally it is not as good as that obtained with the storage-discharge curves derived from the 1944 flood.

Other possible procedures—Before concluding, it may be of interest to note briefly the unsuccessful attempts to solve this problem. These comprise successive routing through a number of reaches by the Muskingum method, the unmodified lag-and-route method with $x = 0$, and the lag-and-route procedure with lag varying as a function of inflow.

In successive routing by the Muskingu method, the value of K in the linear storag discharge relation

$$S = K[xI + (1 - x)O] \qquad ($$

was taken as the time of travel from Bour to Menindee (15 days) divided by the numb of reaches used. The proper value of x must determined by trial and error, comparing t results of different trials with the actual outfl hydrograph.

Initially, five trial routings by this meth with different numbers of reaches and differe values of x were carried out, and the clos reproduction of the outflow hydrograph achiev was quite unsatisfactory. Subsequent to t determination of the appropriate values of for the three reaches in the storage analy described above, a further routing by Muskingu method was carried out through three reach each with $K = 5$ days and $x = 0.33$. Tl resulted in a much closer reproduction of t outflow hydrograph (Fig. 11), though there a still significant departures from the true hydr graph even with the relatively small degree nonlinearity of the storage-discharge relations Figures 6, 7, and 8. Attempts to reproduce oth floods by this method, with as many as fourte different trial combinations of number of reach and value of x have been even less success because of greater curvature in the storag discharge relations. Routing computations this method have been carried out on UTECO the University of New South Wales' high-spe digital computer, which reduces actual computi time for routing through a large number reaches to about a minute.

Failure of successive routing by the Muskingu method led to consideration of the lag-and-ro method, which seems to have been propo originally by *Clark* [1945]. The storage-discha relation obtained with the lagged inflow shown in Figure 12, and it is clear from t that no storage-routing procedure could succe fully reproduce the outflow hydrograph, as relation is far from a single-valued cur Equally bad or worse relations have b obtained for a number of other floods with t procedure. It is no doubt more applicable ordinary routing problems in which the re is relatively short.

Finally, the lag-and-route method with v

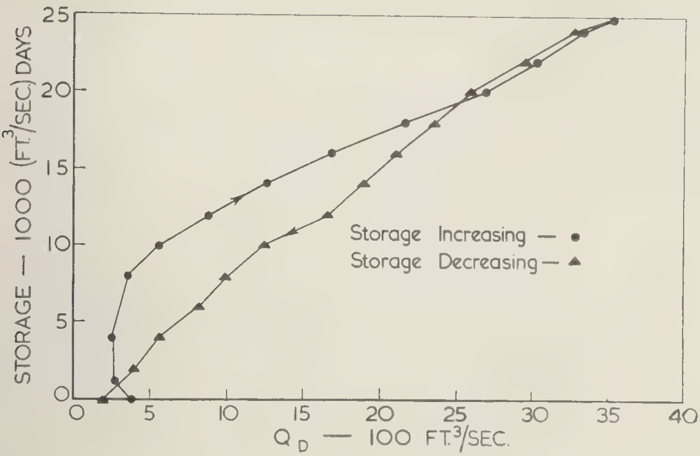

FIG. 12—Storage-discharge relation for lagged inflow hydrograph.

le lag and variable K, as proposed by *Kohler* 958], was investigated. This involves lagging fferent points on the inflow hydrograph by fferent amounts, the amount of lag being a nction of the rate of inflow, and routing the gged inflow with $x = 0$ through storage reprented by a nonlinear storage-discharge relation. was found impossible, however, to lag the flow in the manner described and produce a ngle-valued storage-discharge relation. Conleration of the steep rising limb of the inflow drograph will give an idea of the small scope r lagging the higher discharges less than the w discharges.

Conclusion—Failure of the two variations of e lag-and-route method to produce acceptable orage-discharge relations in this and other ses investigated by the author is no indictment them, as they were not specifically put forward solutions to the problem of routing through ng reaches. Repeated routing through a numr of reaches by the Muskingum method would so give a satisfactory result in cases where near storage-discharge relations are applicable, it these cases appear to be uncommon in New uth Wales rivers.

The close coincidence of the routed hydrograph d the hydrograph of Menindee flow plus termediate losses in Figure 4 indicates the ccess of the method proposed herein for taining storage-discharge relations and routing oods through long reaches. Comparable results have been achieved in other cases not described in this paper. Use of the procedure in flood forecasting would be dependent upon the storage-discharge relations remaining practically constant from flood to flood, and the relation between gage height and discharge at any point being a single-valued curve at stages far higher than those attained in the flood used in the example given above. An indication of the degree of constancy of the storage-discharge relations is shown in Figure 11, but, as the requirements given above apply to any storage routing procedure, and, as this paper does not constitute a flood-forecasting study for the Darling River, they are not further considered here. However, in any case where the two requirements are met, this procedure provides a satisfactory method of routing floods through reaches far longer than those which can be handled by conventional methods.

References

CLARK, C. O., Storage and the unit hydrograph, *Trans. Am. Soc. Civil Engrs., 100,* 1419–1446, 1945.

KOHLER, M. A., Mechanical analogs aid graphical flood routing, *Proc. Am. Soc. Civil Engrs., J. Hydraul., 84, Paper no. 1585,* 14 pp. 1958.

LINSLEY, R. K., M. A. KOHLER, AND J. L. H. PAULHUS, *Applied Hydrology,* McGraw-Hill, New York, 1949.

(Manuscript received June 30, 1959; revised September 11, 1959.)

Helium as a Ground-Water Tracer

RALF C. CARTER, W. J. KAUFMAN,
G. T. ORLOB, AND DAVID K. TODD

Department of Civil Engineering
University of California, Berkeley, California

Abstract—Laboratory and field experiments were conducted with helium as a ground-water tracer. Techniques were developed for the addition and extraction of helium from water. A mass spectrometer and a pressure-volume apparatus were used for helium measurements at concentrations in water ranging from 1.5 to 5.5 $\times$ 10^{-4} milligrams per liter. In the field investigation, flow was traced through a confined aquifer for a distance of 188 feet. Both laboratory and field experiments showed that helium traveled at a slightly lower velocity than chloride. The advantages of helium as a ground-water tracer are its safety, low cost, relative ease of analysis, low concentrations required, and chemical inertness. The disadvantages include the relatively large errors in analysis, difficulties of maintaining a constant recharge rate, time required to develop equilibrium conditions in unconfined aquifers, and possible loss to the atmosphere in unconfined aquifers.

Introduction—Many substances, including dyes, salts, and radioisotopes, have been employed to trace the movement of ground water. Few, if any, can be said to be excellent tracers. One possibility which deserved further study was helium. This element occurs in monatomic form, is slightly soluble in water, is chemically inert, is inexpensive, presents no health or safety hazards, and can be detected in minute concentrations.

This paper is a report of a study of the feasibility of using helium as a ground-water tracer. Attention was focused on dissolving helium in water, extracting it, measuring its concentration in water samples, and studying its flow through porous media in the laboratory and in the field.

Helium is a natural component of the atmosphere; dry air contains 5.24 ppm by volume [*Glückauf*, 1944]. Water in equilibrium with the atmosphere at sea level and at 25°C contains about 8.1 $\times$ 10^{-6} mg/l of helium. Limited data suggest that helium occurs naturally in all ground waters. A survey by *Anderson and Hinson* [1951] of gases released from twenty-four water wells in the Western United States showed helium concentrations ranging from a trace to 0.05 per cent by volume (7.7 $\times$ 10^{-4} mg/l at 1 atmosphere). Under the pressures which exist at great depths, helium contents would be correspondingly greater. Although meager data preclude an evaluation of the effect of naturally occurring helium on its use as a tracer, it was assumed that, with a background determination, added helium could be clearly detected.

The solubility of helium in water depends upon the partial pressure of helium in solution. According to Henry's law,

$$\log G = \log [P/K - P] + \log (2.22 \times 10^5)$$

where G is the concentration of dissolved helium in water (mg/l), P is the partial pressure of helium (mm Hg), and K is Henry's gas constant (10.9×10^7 mm Hg at 20°C). At one atmosphere the maximum helium solubility is approximately 1.5 mg/l. The rate of transfer of helium to or from water is a function of the concentration gradient across a liquid film separating the two phases and the area of contact per unit volume of water.

Measurement of helium—The normal method of measuring helium concentrations is by use of a mass spectrometer. This instrument was employed for part of the analytic work of this study and was calibrated with a standard solution of helium. Degassed distilled water was shaken in an atmosphere of helium gas, and this solution was diluted by adding distilled water. For extraction, 100-ml water samples were placed in test tubes with 12 ml of air. By sharply rotating a tube through a 90° arc the

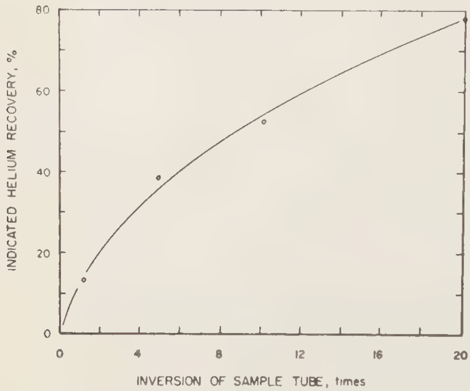

FIG. 1—Effect of number of inversions of sample tube on transfer of helium from water to air.

air was forced through the water as finely divided bubbles.

The resulting air-helium mixture was then transferred to the mass spectrometer and analyzed. The amount of helium transferred to the air was found to depend on the number of inversions of the sample tube (Fig. 1). The minimum detectable concentration was about 0.004 ppm. From analyses of ten identical samples of 0.75 ppm helium, a coefficient of variation of 17.5 per cent was found. The precision of the analysis depends upon the ability of the operator to maintain a uniform extraction technique.

The second method of measuring helium was based on pressure-volume measurements following adsorption of other gases on charcoal cooled to 77°K by liquid nitrogen. The first use of this procedure was reported by *Cady and McFarland* [1907]; subsequently, an improved apparatus was developed by *Frost* [1946b] in connection with helium-tracing of natural gas [*Frost*, 1946a]. A detailed review of this approach to helium measurement was published by *Anderson and Hinson* [1951].

An inexpensive adaptation of the Frost pressure-volume apparatus was constructed by the senior author. Figure 2 shows a schematic diagram of the apparatus. Before starting an analysis, air in the apparatus is evacuated by the pumps at right, and the charcoal is baked by placing a heating coil around the charcoal tube. The safety trap serves as an emergency pressure release during baking. The heating coil is then replaced by a liquid nitrogen flask, and the tube for the water-air sample is attached at left. The clamp above the sample is opened to allow the helium-air mixture to reach the charcoal tube. Adsorption of all but inert gases (mostly helium) is completed within ten minutes. Helium is then admitted into the McLeod gage where two sets of measurements of pressure and volume are obtained by manipulation of the 3-way stopcock. Details of the construction, cost, and operation of the apparatus, as well as pressure-volume computations, can be found in *Carter*

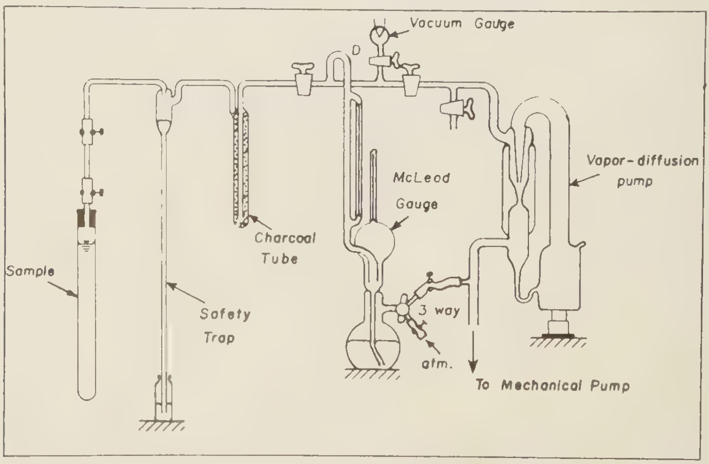

FIG. 2—Schematic diagram of pressure-volume apparatus for helium analysis.

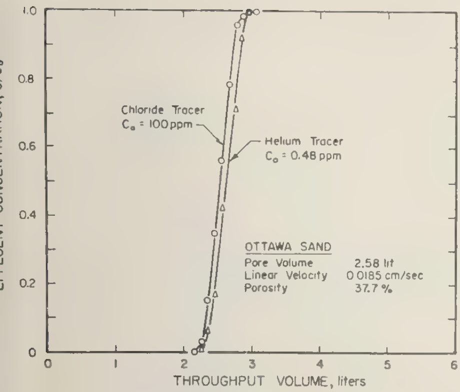

Fig. 3—Helium and chloride breakthrough curves in Ottawa sand column.

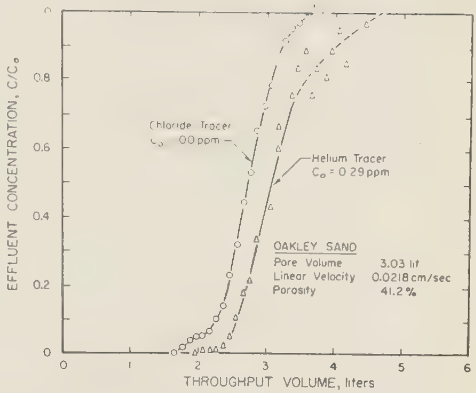

Fig. 4—Helium and chloride breakthrough curves in Oakley sand column.

nd others [1959]. Analyses of ten samples con-aining 1.5 ppm helium showed a 72 per cent ecovery with a coefficient of variation of 6.3 er cent.

Movement of helium through porous media—To study the feasibility of using helium as a ground water tracer, experiments were conducted or flow through sand columns, for movement hrough a confined aquifer from a recharge well, nd for flow through an unconfined sand channel.

In the column studies helium was traced hrough Ottawa and Oakley sands and chloride ons were introduced as a comparative tracer. Lucite columns 4 inches in diameter and 4 feet ong were packed with sand to a depth of 36 nches. Each column was equipped with an nderdrain, a constant head source of water, nd piezometric tubes.

The Ottawa sand consisted of nearly spherical quartz grains having an effective size of 0.41 mm nd a uniformity coefficient of 1.30. After the olumn was filled with Ottawa sand it was aturated with carbon dioxide gas, and degassed vater was passed through the column until a onstant permeability, indicating saturation, vas observed. The resulting column had a orosity of 37.8 per cent and a permeability of 132 darcys. Experiments were conducted by owering the liquid level to the upper sand surface and then filling the reservoir above the medium with a solution of 0.48 ppm helium nd 100 ppm chloride. The tracer solution passed hrough the column with an average linear velocity of 0.0185 cm/sec. Samples were collected in 100-ml aliquots and were analyzed for helium with a mass spectrometer and for chloride by the mercurimetric method [*American Public Health Assoc. and others*, 1955]. The results of one experiment plotted as breakthrough curves appear in Figure 3. It can be seen that the two tracers gave nearly identical results, except that the helium lagged slightly behind the chloride curve.

Identical experiments were carried out with an Oakley sand. This material has a small but appreciable clay content and has an exchange capacity of 3.0 meq/100 g. The effective size was 0.02 mm with a uniformity coefficient of 11.2. The porosity was 41.2 per cent, and a permeability of 82 darcys was measured. The results of one experiment are shown in Figure 4, indicating an appreciable lag of the helium behind the chloride.

The field investigation was conducted at the well field of the Engineering Field Station, University of California. The facility consists of a 12-inch well penetrating a 4-foot confined aquifer at a depth of 90 feet and a group of small observation wells in the vicinity. Details of the field installation are described in *McGauhey and Krone* [1954]. The large well was equipped as a recharge well by pumping water from another aquifer 700 feet away and piping it to a 13-foot sump where a positive displacement pump recharged it underground at a rate of 35.5 gpm. Helium was metered into the recharge water

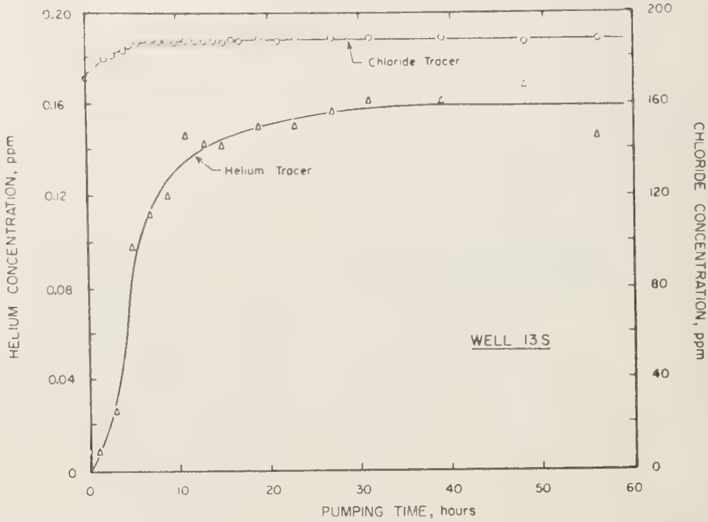

FIG. 5—Helium and chloride breakthrough curves at 13-foot observation well.

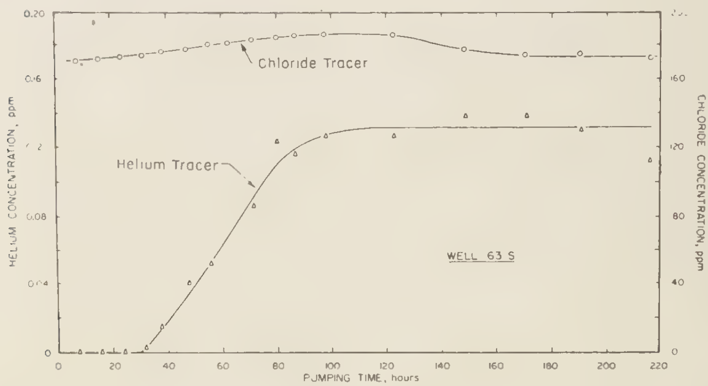

FIG. 6—Helium and chloride breakthrough curves at 63-foot observation well.

at the sump with a standard oxygen pressure-reduction-valve and gages and a calibrated orifice. A helium concentration of 0.185 ppm was created in the water, as determined from the volume of the helium tank, the absolute temperature, and the decrease in pressure during the tracing experiment. The addition was continuous for 11.3 days. At the same time the chloride tracer was introduced as a concentrated solution by a Sigma pump into the intake line of the recharge pump. The natural chloride content of the ground water was 172 ppm; this was increased to 188 ppm after addition of the tracer. Chloride w added during the first four days of the rechar period.

Various operational difficulties were encou tered in working with helium in the field. Ch among these was the variation of input ra of helium from that preset for delivery. T control orifice was calibrated at 68°F, but t ambient temperature differed considerably fro this in the field. Because the density of gas a the cross-sectional area of the orifice (abo 2.2×10^{-5} cm²) varied with temperature, t

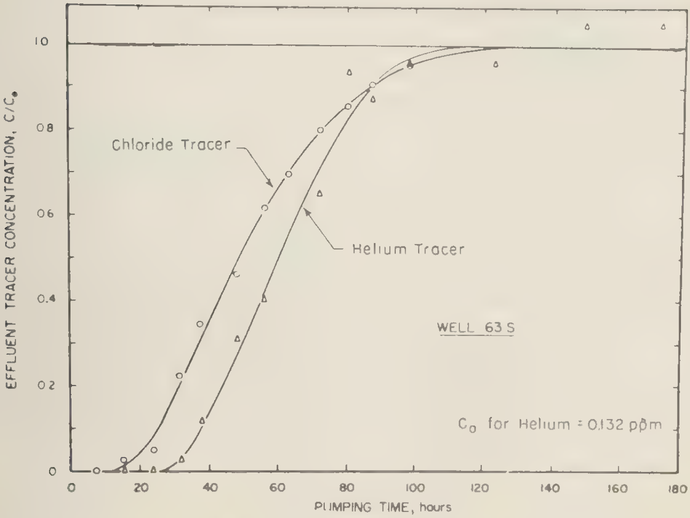

FIG. 7—Normalized helium and chloride breakthrough curves at 63-foot observation well.

te of gas flow fluctuated daily. A constant-mperature control for the orifice would have iminated this problem.

Analysis of samples of water at the recharge ell indicated that only 27 per cent of the added elium was in solution. That not in solution llected along the upper side of the suction pe, and some was undoubtedly lost to the mosphere from the pump. At the first observaon well, 13 feet from the recharge well, the covery concentration showed a 14 per cent ss of helium. At the 63-foot well another 16 r cent was lost, whereas no loss between the 0-foot well and the 63-foot well could be tected. Although the exact nature of the losses unknown, it is believed that inaccuracies in e input rate, losses at wells, and inaccuracies analyses may be important factors. Introicing helium on the pressure side of the pump ould have reduced some of these errors.

Breakthrough curves for the two tracers at e 13-foot well are shown in Figure 5. Correonding data from the 63-foot well appear in gure 6, and in normalized form for easy comrison in Figure 7. Values of the concentration tio greater than 1 in Figure 7 result from the lection of a mean maximum observed helium ncentration. Helium was traced a maximum stance of 188 feet from the recharge well.

The third set of experiments was conducted in a horizontal channel filled with a coarse (No. 8) Monterey sand. The channel was 1 foot wide and filled with sand to a depth of 16 inches and to a length of 11 feet. Two perforated observation wells completely penetrated the sand at 1 foot from each end of the sand section. Water containing helium entered at one end of the channel, and a steady-flow condition was maintained. One experiment was conducted with an average wetted depth of 7.5 inches and an average travel time of 6 hours between wells; in a second one the wetted depth was 14 inches and the travel time was 9.5 hours. Results showing helium concentrations at different times after adding the tracer appear in Table 1. Helium input rates were not uniform; nevertheless a considerable time lag is apparent before equilibrium conditions were reached at the two wells. A similar lag was observed when helium was stopped and flow through the channel was maintained.

Discussion of results—The column studies indicated that helium could serve as a satisfactory tracer of ground water and, from the shape of its breakthrough curve, could indicate the dispersion characteristics of a medium [*Rifai and others*, 1956]. The interesting item in these results was the time lag of the helium in

TABLE 1—*Loss of helium tracer from an unconfined aquifer*

Water depth, in.	Sampling time, hr.	Helium concentration, ppm Upstream well	Downstream well
	22	0.086	0
	24	0.102	0.00055
7.5	26	0.088	0.0015
	49	0.077	0.026
	75	0.073	0.062
	95	0.067	0.075
	32	0.278	0.0065
	62	0.295	0.053
	82	0.250	0.102
14	129	0.313	0.184
	152	0.377	0.254
	200	0.360	0.364
	324	0.324	0.347

relation to the chloride ion. A similar lag between chloride and tritium was reported by *Kaufman and Orlob* [1956] and was attributed to diffusion of tritium into adsorbed water in the medium.

If two water tracers pass through a given porous medium under identical conditions, it would be anticipated that identical breakthrough curves would be observed, provided that the tracers passed through the media without modification or loss. Should one tracer move through at a slower rate than the other, the difference would be apparent by a displacement in the breakthrough curves. Such a lag could be the result either of a sorption of the tracer by the medium or of a different effective pore volume. The area to the left of a breakthrough curve is a measure of the pore volume. In Figure 3 the volume for helium is 3.7 per cent larger than for chloride; in Figure 4 it is 15.8 per cent larger. One hypothesis which might explain this phenomenon, but which cannot be tested with the available data, is that the very small neutral helium atoms diffuse into minute crevices in grain surfaces or between small particles. In contrast, the larger charged chloride ions cannot enter or collect in these smallest openings in the medium. One fact supporting this hypothesis is that the relative loss of helium in the Oakley sand (containing grains down into the clay range and a large specific surface area) greatly exceeded that in the Ottawa sand (consisting almost entirely quartz sand grains).

The results of the field investigation al show that helium can serve as a ground-wat tracer through confined aquifers. The heliu curve in Figure 7 lags behind the chloride cur by 17.0 per cent; this difference, like the colum results, may be attributed to the adsorptic of helium on the fine-grained materials of t aquifer. The different slopes of the breakthrou curves in Figure 7, if they may be consider significant, suggest different dispersion rate however, if dispersion is treated as a propert of a given porous medium, then the deviatic of the helium curve from the chloride curve c be attributed to a variation in the rate of heliu addition or to a rate-limiting sorption phenon enon.

Results of the laboratory channel experimen imply that helium would not be practical as tracer through unconfined aquifers. For the tw depths tested the time required to devel inequilibrium at the downstream well amount to about 16 times that required for the avera flow velocity. It is believed that the helium cam out of solution in contact with entrapped air the capillary zone. When the capillaries becam saturated with helium, the effluent helium co centration approached a constancy nearly equ to that of the influent. It is probable that lo to the atmosphere continued to occur upwa through the capillary zone.

Conclusions—The experimental data indica that helium is a feasible ground-water trace It has advantages of being inexpensive, safe handle, relatively easy to measure, necessa in only minute concentrations, and chemicall inert. On the other hand, relatively large erro are common in measurements, operationally is difficult to maintain uniform input concentr tions, and the times required for equilibriu conditions to develop in unconfined aquife are excessively long. Further study is neede to explain the observed lag of helium behi chloride in flow through porous media.

Acknowledgments—This study was support by the Water Resources Center of the Universit of California.

REFERENCES

AMERICAN PUBLIC HEALTH ASSOCIATION AN OTHERS, *Standard methods for the examinati*

of water, sewage, and industrial wastes, 10th Ed., American Public Health Assoc., New York, 522 pp., 1955.

Anderson, C. C., and H. H. Hinson, Helium-bearing natural gases of the United States, analyses and analytical methods, *U. S. Bur. Mines Bull. 486,* 141 pp., 1951.

Cady, H. P., and D. F. McFarland, The occurrence of helium in natural gas and the composition of natural gas, *J. Am. Chem. Soc., 28,* 1525–1526, 1907.

Carter, R. C., D. K. Todd, G. T. Orlob, and W. J. Kaufman, Measurement of helium in ground water tracing, *Water Resources Center Contrib. 21,* Univ. of Calif., Berkeley, 56 pp., 1959.

Frost, E. M., Jr., Helium tracer studies in the Elk Hills, Calif., field, *U. S. Bur. Mines Rept. Invest. 3897,* 6 pp., 1946*a*.

Frost, E. M., Jr., Improved apparatus and procedure for the determination of helium in natural gas, *U. S. Bur. Mines Rept. Invest. 3899,* 16 pp., 1946*b*.

Glückauf, R., Simple analysis of the helium content of air, *Trans. Faraday Soc., 40,* 436–439, 1944.

Kaufman, W. J., and G. T. Orlob, Measuring ground water movement with radio-active and chemical tracers, *J. Am. Water Works Assoc., 48,* 559–572, 1956.

McGauhey, P. H., and R. B. Krone, Investigation of travel of pollution, *Calif. State Water Pollution Control Board Publ. 11,* 218 pp., 1954.

Rifai, M. N. E., W. J. Kaufman, and D. K. Todd, Dispersion phenomena in laminar flow through porous media, *Inst. Engr. Research Rept. 93–2,* Univ. of Calif., Berkeley, 157 pp., 1956.

(Manuscript received August 3, 1959; presented at the Fortieth Annual Meeting, Washington, D. C., May 5, 1959.)

The Origin of Thermoremanent Magnetization

JOHN VERHOOGEN

University of California
Berkeley, California

Abstract—Thermoremanent magnetization (trm) generally has several components characterized by a range of coercive force. The component of trm which has the highest stability with respect to ac-demagnetization is believed to reside in stressed regions surrounding dislocations. Because of their size and shape, these regions behave much as single-domain particles.

Notation

b is a Burgers displacement vector

F_σ is magnetic strain energy

H_c and H_{c0} are, respectively, the coercive force of temperature T and at room temperature T_0

H_{cr} is the demagnetizing field that must be applied to cancel the remanent magnetization after the specimen has been withdrawn from the demagnetizing field

H_{ex} is the external field

H_s is the critical field, or intrinsic coercivity, required to reverse the direction of magnetization in a single-domain grain, or in a small region of volume v within a multidomain grain

H_f and H_p are, respectively, the fluctuation field and the dispersion field in Néel's theory

J_s and J_{s0} are, respectively, the saturation magnetization per unit volume at temperature T and at room temperature T_0

J_t is the induced magnetization at temperature T

J_{tr} and J_{tr0} are, respectively, the thermoremanent magnetization produced by cooling from the Curie temperature to T and T_0

J_{ir} and J_{ir0} are, respectively, the isothermal magnetization produced at temperature T and T_0

K is the magnetocrystalline energy per unit volume

k is Boltzmann's constant

$\bar{m}$ is an average magnetic moment

N is a shape-demagnetization factor

n is the number of strained regions or dislocations per unit volume

Q is the ratio of the trm acquired in a weak field H_{ex} to the induced magnetization χH_{ex} acquired at room temperature in the same field

T is temperature, T_0 is room temperature, T_β a 'blocking' temperature

v is a small volume

α is a fractional volume

θ is the Curie temperature

λ is a magnetostriction coefficient

μ is rigidity

ν is Poisson's coefficient

σ is a stress; σ_i is internal stress

χ_0 is the initial susceptibility per unit volume at room temperature

χ_m is the maximum initial susceptibility observed below the Curie point

Introduction—In spite of the great geological interest in the natural thermoremanent magnetization (trm) of lava, particularly basalts, very little is known of the mechanism by which it is acquired. A beautiful theory of the trm of very small particles, which accounts for many properties of thermally magnetized materials, was developed by *Néel* [1949]. This theory would be quite satisfactory for our present purpose if it were applicable to particles with mean radii greater than 10^{-6}cm or so, as most ferromagnetic grains in basalts usually have dimensions of the order of 10 to 50 microns or more. Although grains of smaller sizes may be present in some lavas and could account for a part of their natural trm, they could not account for all of it because of their low concentration. Besides, trm is not confined to single-domain particles; it can also be produced in massive specimens of nickel, magnetite, pyrrho-

tite, etc. [*Grabovskii and others*, 1956; *Uyeda*, 1958].

Néel, [1955] extended his theory of trm to include large multidomain grains. This new theory is based on the expansion of the hysteresis cycle that must take place during cooling; it is predicated on a law of variation of the coercive force of the type

$$H_c/H_{c0} = (J_s/J_{s0})^2 \qquad (1)$$

and leads to the expression for trm

$$J_{tr0} = \frac{2}{N}(H_{ex}H_{c0})^{1/2} \qquad (2)$$

The theory may be objected to on the grounds that (*a*) there is considerable doubt as to the applicability of (1) to all lavas, as the coercive force commonly decreases nearly linearly with increasing temperature in a manner which varies from sample to sample, and which depends on the previous history of the sample; (*b*) *Nagata* [1953, p. 158] has shown that J_{tr0} usually varies H_{c0}, not as $(H_{c0})^{1/2}$; (*c*) J_{tr0} varies generally as H_{ex}, not as $(H_{ex})^{1/2}$, when H_{ex} is small; (*d*) as the trm, on this model, is picked up only in the temperature range where $H_{ex} \geq H_c$, a rock with $H_{c0} = 100$ oersted, placed in an external field of 0.5 oe, would acquire its trm only in the range where $J_s/J_{s0} \leq 0.07$, that is, within a few degrees of the Curie point; experiments show, on the contrary, that trm is usually acquired over a temperature range extending a good 100° or 150° below θ. Finally, Néel predicts that the ratio Q of the trm acquired in a small field H_{ex} to the magnetization induced by the same field at room temperature would be

$$Q = 2(H_{c0}/H_{ex})^{\frac{1}{2}} \qquad (3)$$

which does not fit experimental results very well. For instance, *Nagata's* [1953] specimen No. 17 has $H_{c0} = 60$, $Q = 5.4$, whereas equation (3) gives $Q = 22$ for $H_{ex} = 0.5$.

Having noticed discrepancies of this kind *Néel* [1955] modified his theory to include the effect of the field H_f arising from thermal fluctuations and obtained the result

$$J_{tr0} = \frac{H_{ex}}{N}\left(\frac{H_{c0}}{H_f}\right)^{\frac{1}{2}} \qquad (4)$$

which still makes J_{tr0} proportional to $(H_{c0}$ and presents the additional difficulty of evalu ing H_f (see below). This relation does not count any better than does (2) for the satu tion of J_{tr0} described below.

Stacey [1958] has recently put forward greatly simplified theory according to wh trm is acquired at temperatures such that b the magnetocrystalline and magnetostrict energies may be neglected. Only the magne static energy (self-demagnetization) prevent grain from attaining saturation. Thus the duced magnetization at high temperature is lieved to be simply

$$J_t = H_{ex}/N$$

and, apart from a small correction arising fr the dispersion of ferromagnetic grains in an ert matrix,

$$J_{tr0} = \frac{H_{ex}}{N}\frac{J_s}{J_{s0}} \qquad ($$

Stacey's basic assumptions are questionab particularly with regard to the vanishing magnetostrictive energy. When compared wi measured values of trm, formula (5) leads approximate agreement only if it is assum that the rock contains a much larger amou of ferromagnetic material than it actually doe in some instances, Stacey was forced to the co clusion that the total amount of Fe indicat by the chemical analysis of the whole rock magnetically 'active,' although a substant part of it is known to be present in parama netic silicates. The 'normative' content of ma netite Fe_3O_4 that Stacey used as a measure the amount of magnetite actually present is al likely to be too large, as it is calculated on t assumption that all the Fe_2O_3 revealed chemical analysis is present in magnetite; act ally, much of it may be present in pyroxenes ilmenite, and the 'normative' magnetite conte of basalts, which averages about 4 to 5 per ce by weight, is generally found to exceed t amount of this mineral (2 to 3 per cent) th is recovered after crushing and careful sep ration.

A further objection to Stacey's treatme must be noted. If both magnetocrystalline a magnetostrictive energies vanish at temper

ures well below the Curie point, so does the wall energy; the thickness of the Bloch walls would become very large (theoretically infinite) and the domain structure would disappear. The magnetostatic energy could then be reduced only by allowing neighboring spins to set themselves at a small angle to each other in such a way that the gains in magnetostatic energy would balance the increase in exchange energy. The magnetization induced by an external field would then depend on the ratio of the field energy to the exchange energy, which Stacey disregarded.

Hopkinson effect—The initial susceptibility commonly rises with increasing temperature and reaches a maximum value χ_m 100° or 200° below the Curie point (Hopkinson effect). *Uyeda* [1958] pointed out that trm is acquired in the temperature range where χ is large and suggested that the Hopkinson effect is closely related to the acquisition of trm. However, many exceptions may be found to Uyeda's statement. *Nagata* [1953] described rocks (for instance, his No. 17 with a Curie temperature of 590°C) for which the susceptibility is maximum at 300°C, well below the temperature range in which trm is acquired.

Alberts and Shepstone [1958] accounted for the Hopkinson effect in iron by the marked decrease in magnetocrystalline energy, which tends to zero above 600°C. (The Curie temperature of iron is 770°.) Magnetization by rotation, which is difficult at room temperature, thus becomes easy above 600°C and contributes to the initial susceptibility. The susceptibility, however, does not become infinite, as it would if the coercivity vanished entirely; the ratio of χ_m/χ_0 is, in fact, rarely larger than 2. This seems to exclude the Hopkinson effect as the main source of trm, as the maximum value of trm would then be

$$J_{tr0} = \frac{J_{s0}}{J_s} \chi_{\max} H_{ex}$$

and the corresponding Q value would be less than 2 (J_{s0}/J_s). *Uyeda* [1958] measured a Q ration of 10 on a massive sample of nickel for which J_{s0}/J_s is about 3 and χ_m/χ_0 about 2; he also measured a Q ratio of 12 on nickel powder which shows hardly any Hopkinson effect, and he concluded from heat-treatment experiments that the trm of nickel is more probably related to internal stresses. Furthermore, if trm arose essentially from high-temperature rotation, its coercivity at room temperature would be at most $K/2J_{s0} \sim 200$ oe for magnetite; ac-demagnetization commonly indicates a coercivity that is larger than this value.

Effect of grain size—For reasons that are not clearly understood, the initial susceptibility of multi-domain grains in the size range of 0.1 to 100 microns decreases with decreasing grain size, whereas the coercivity increases. *Roquet* [1954] observed that in fields less than 235 oe, large grains of magnetite have a larger irm than smaller ones, in agreement with their larger susceptibility; larger grains, however, also have a smaller trm, which suggests that trm is not controlled essentially by the initial susceptibility, that is, by displacement of domain walls. Roquet also observed that the irm acquired in strong fields by large grains is less than that of smaller grains of the same material, in agreement with the general observation that the trm acquired in weak fields has many properties in common with the irm acquired in strong fields. This tends to confirm Néel's view that a fluctuating field of thermal origin and of high intensity is necessary for the acquisition of trm.

Interpretation of trm in terms of the fluctuation field—As noted above, Néel's formula (4) is based on the idea that obstacles to wall displacements or to rotation of the spontaneous magnetization may be overcome, at sufficiently high temperatures, by the fluctuation field H_f due to thermal agitation. The origin of this field may be explained as follows. In any small volume v, thermal lattice vibrations produce local, instantaneous strains, which, by magnetostriction, cause the direction of spontaneous magnetization to depart locally from its mean direction. These departures also produce locally the appearance of 'free' poles and of a corresponding internal 'dispersion' field, the root mean square H_p of which Néel evaluates to be $(4\pi kT/3v)^{1/2}$. The fluctuating field H_f is directly proportional to H_p, from which it differs by the inclusion of a characteristic time, and depends critically on the volume v, which Néel takes to be such that vJ_s corresponds to a Barkhausen discontinuity. For H_f to be effective, that is, to be of the same order as the

coercive field, v must be of the order of 10^{-18}cm^3, that is, of the same order as the volume of a grain in Néel's theory of single-particle domains, which owe their properties, and notably their ability to come to equilibrium with the external field at high temperature, to thermal fluctuations.

Properties of trm—In spite of abundant data, it remains difficult to characterize trm, which varies from one specimen to the next in a manner reminiscent of a structure-sensitive property. Even its magnitude, for a given external field, is imperfectly known; results obtained in different laboratories are difficult to compare because of differences in experimental conditions and materials. *Nagata* [1953] gave values for rocks, mostly basalts and andesites. *Uyeda* [1958] studied mostly fine powders of solid solutions of Fe_3O_4-Fe_2TiO_4. *Roquet* [1954] used a variety of materials in the form of powders dispersed in an inert matrix; some of her samples are synthetic and very pure, and others are 'natural' magnetites containing a very large amount of impurities in unstated form (14.5 per cent SiO_2 and 10.5 per cent CaO in the chemical analysis). *Grabovskii and others* [1956] used massive specimens. Only exceptionally are *all* relevant properties of the samples fully described.

The following generalizations seem to emerge:

1. In solid solutions of Fe_3O_4 and Fe_2TiO_4, or in other impure magnetites, trm does not depend critically on composition, although J_{s0} *and* θ do.

2. J_{tr0} depends on field strength. In weak fields it rises nearly proportionally to H_{ex}, but in strong fields the relation is not linear and J_{tr0} becomes proportional to tanh aH_{ex}, where a is a constant. The saturation implied by this formula is reached at about 100 to 200 oe or less; the saturated value of J_{tr0} is notably less than the saturation magnetization J_{s0} and depends on grain size and other factors.

3. J_{ir0} is systematically less than J_{tr0} produced in the same field; a much stronger field is required to reach a saturated value, which is, however, about the same as the saturated value of J_{tr0}. As an example, Roquet found that for a sample of pure magnetite a field of 70 oe is necessary to produce an irm equal to the trm produced by a field of 0.5 oe; J_{ir0} reaches saturation near 3000 oe, as against 200 oe for J_{tr} Numerical values, which may be typical, ar given in Table 1.

TABLE 1—*Typical magnetic properties of members o the magnetite [Fe_3O_4]—ulvospinel [Fe_2TiO_4] series [After Roquet, 1954 and Uyeda 1958]*

	Fe_3O_4	0.11 Fe_2TiO_4 ·0.89 Fe_3O_4	0.67Fe_2TiO ·0.33 Fe_3O_4
Grain size microns	0.1	100	10
θ, °C	582	550	123
J_{s0}	450	78	23
J_{tr0} for $H_{ex}=2$ oe	9.1	0.77	0.69
J_{ir0} for $H_{ex}=2$ oe	3.3×10^{-3}	...	...
H_{c0}	...	20	7
Q	17	2.2	4.8

The trm of lavas depends, of course, on th amount of magnetite[1] and other magnetic min erals present; for basalts exposed to a field o about 0.5 oe, trm is usually 1 to 5 $\times$ 10^{-3} time the saturation magnetization of the same speci men. Q is usually in the range of 0.5 to 10, al though much larger values are occasionally en countered.

4. In general, J_{tr0} and Q vary proportionall to the coercive force H_{c0}, although the latte needs to be more carefully defined (see below)

5. Trm generally follows Thellier's additivit law, according to which J_{tr0} is the sum of th partial thermoremanent magnetizations acquire in successive temperature intervals between and room temperature. Most of the trm is ac quired within 100° or 150° of the Curie point very little is acquired between 400° and 20 for magnetite.

6. When a sample carrying trm is heated, it remanent magnetization decreases in a wa that is characteristic of the field in which it trm was originally acquired. When acquired i weak fields, trm decreases appreciably only i the immediate neighborhood of the Curie point

[1] The term magnetite is used here to designat the most abundant ferromagnetic phase in basalts which is usually a cubic mineral with the spine structure and a composition approaching Fe_3O but which usually also contains variable amount of Ti, Mg, Al, etc.

when acquired in strong fields (for example, 500 oe), it first decreases linearly, then more rapidly. By contrast, J_{iro} decreases rapidly with increasing temperature when acquired in weak fields, but if acquired in strong fields it varies very much as J_{tro} does.

7. J_{tro} decreases much more slowly with time than J_{iro}, and also has greater stability with respect to ac-demagnetization (see below).

Coercive force—As noted above, the term is used in different senses and requires careful definition. It is usually understood to mean the field required to reduce to zero the apparent magnetization of a specimen either while the specimen is still in that field (Uyeda's H_c) or after removal of the field (Uyeda's H_{cr}). The coercive force so defined is not a characteristic property of the material, as it depends on the intensity of the original field in which the specimen acquired its remanent magnetization and on its mode of acquisition. Roquet noted that, in general, the coercive force for a trm acquired in a weak field is just that field which would produce in a previously demagnetized specimen an irm equal and opposed to the trm, which it does not necessarily destroy. This is well shown, for instance, by Roquet's experiment on specimen M'_2 of pure magnetite, for which the coercive force H_{cr} necessary to cancel, after removal of the field, the trm produced by a field of 0.42 oe is precisely equal to the field (70 oe) necessary to induce an irm of the same intensity as the trm. It is thus not surprising that the coercive force so measured should increase in proportion to the trm when the latter is small; more generally, one would expect a relation of the type $J_{tro} = aH_{co} + bH^2_{co}$, where a and b are constants. Nor is it surprising that H_c and H_{cr} for isothermal magnetization tend to a constant value when the original magnetizing field exceeds that required for saturation of J_{iro} [see, for instance, *Uyeda*, 1958, Fig. II-3].

A more suitable measure of the stability of trm is obtained by placing the specimen in an ac-field, special precautions being taken to ensure that the ac-field acts for equal times in *all* directions. The ac-field necessary to destroy trm, that is, to redistribute randomly the direction of magnetization in all grains and domains, cannot be defined by a single number; in general there is a curve, or 'spectrum,' showing what fraction of the original magnetization is left after application of an ac-field of stated intensity. This spectrum is commonly found to extend to fields greatly in excess of the coercive force as ordinarily measured; whereas an ac-field of a few oersteds may be sufficient to destroy a large fraction (up to 0.8 or 0.9) of the original trm of some specimens, a small fraction of it may vanish only in ac-fields of 500 oe or more. The spectrum for irm is characteristically much narrower and is usually restricted to fields no larger than the original magnetizing field. The spectrum occasionally shows a low-field portion separated from a high-field one by an interval in which the remanent magnetization varies but little as a function of the intensity of the demagnetizing field.

Such experiments leave little doubt that trm arises from a number of causes or mechanisms characterized by widely different values of their coercivity. That part of it which has a low coercivity probably arises from blocking of walls and is similar in principle to irm. The portion that corresponds to the high-field end of the spectrum must reside in carriers characterized by very high and variable coercivity.

Temperature dependence of the coercive force—Probably the most common interpretation of trm in large grains is, roughly, that the coercive force decreases with increasing temperature more rapidly than the saturation magnetization decreases [compare *Stacey*, 1958], thus allowing a weak external field to induce a relatively large magnetization which remains frozen in when, upon cooling, the coercive force rises and the domain walls become blocked on obstacles of increasing height or steepness. There is abundant evidence, however, that in most cases the coercive force does not vanish or even become smaller than the earth's field, except within a very few degrees of the Curie point. This is illustrated, for instance, by Uyeda's plots of H_c and H_{cr} versus temperature, or by the experiments of *Grabovskii and others* [1956]. These authors measured both J_t, the magnetization induced by cooling from θ to T in a weak field (0.5 oe), measured with the field on, and the remanent magnetization J_{rt} measured under exactly the same conditions and at the same temperature, after removal of H_{e}.

The ratio of J_{rt} to J_t is very close to 1 at room temperature, about 0.85 at 400°C and 0.7 at 500°C, and is still nearly 0.5 very close to the Curie point. If the coercive force actually vanished above a certain temperature, J_{rt} would be zero from that temperature to θ.

There is, indeed, no reason to expect the coercivity of magnetite to vanish, except at the Curie point itself. Magnetite stands, with respect to its anisotropy and magnetostriction, between nickel (low anistropy, high magnetostriction) and iron (high anisotropy, low magnetostriction). The thermoremanent properties of magnetite are similar in many respects to those of nickel. The magnetocrystalline anisotropy of both Fe and Ni is known to decrease rapidly and to effectively vanish 150° or so below their respective Curie points, but magnetostriction does not. This explains the finite susceptibility at high temperature of Fe [*Alberts and Shepstone*, 1958] and the nonvanishing coercivity of Ni [*Kneller*, 1956], the latter being so strongly dependent on mechanical deformation and heat treatment as to leave no doubt that it is directly related to the magnitude of internal stresses.

Néel's theory of the coercive force—The dispersion field mentioned above also plays an important role in *Néels* [1946] theory of the coercive force. Briefly, Néel considers the effects of local, permanent stresses σ_i to be randomly distributed. These stresses produce local variations in the direction of spontaneous magnetization, the appearance of magnetic poles, and a corresponding dispersion field. Consider a small region, roughly spherical in shape, subject to a stress σ_i such that the critical field H_s required to reverse the magnetization against the magnetostrictive energy (3/2) $\lambda\sigma_i$ is $H_s =$ (3/2) $(\lambda\sigma_i/J_s)$. If this is less than the demagnetizing Lorentz field $\approx$ (4/3) πJ_s, exerted by the surrounding domain in which the region is imbedded, the local direction of magnetization will make an angle of less than 90° with that of the magnetization in the surrounding domain, and it will spontaneously reverse whenever a 180° wall sweeps over it. This reversal also changes the sign of the magnetostatic energy of the free poles. The wall then stops in the position for which the distribution of magnetic poles and corresponding magnetostatic energy is most favorable. This leads to an evaluatio[n] of the coercive force, here defined as the fiel[d] necessary to drive a wall over roughly one ha[lf] of the width of a domain, which is, for mag[-]netite, ($\lambda = 4 \times 10^{-5}$) and for $\sigma_i = 3 \times 1$[0...] dynes/cm²

$$H_c = 250\alpha + 100\alpha' \qquad (6$$

where α is the fraction of the total volume i[n] which the local stress reaches the arbitraril[y] chosen value 3×10^9, and α' is the volum[e] fraction of nonmagnetic impurities. Note tha[t] the numerical coefficient 250 is only appropri[-]ate to the particular value $\sigma_i = 3 \times 10^9$; a[s] local stresses may be expected to show consid[-]erable scatter with regard to intensity, ther[e] will be a distribution of value of the numerica[l] coefficients with a corresponding distributio[n] of volume fractions. The 'spectrum' of the co[-]ercive force mentioned above may arise in th[is] way.

Stressed regions as carriers of trm—Conside[r] a stressed region of small size characterized b[y] an internal stress σ_i such that the critical fiel[d] (intrinsic coercivity) H_s required to reverse th[e] direction of magnetization in this region is H[...] $= 3\lambda\sigma_i/2J_s$, where λ is the average magneto[-]striction coefficient, $\lambda = 2/5\lambda_{100} + 3/5_{111}$. Fo[r] regions of nearly spherical shape, the demag[-]netizing field ($\approx 4/3\ \pi J_s$) of the surroundin[g] domain will be larger than H_s if $\sigma < 10^{10}$ dynes[/]cm²; magnetization within the region will there[-]fore always have a component along the direc[-]tion of magnetization of the surrounding do[-]main. If, on the other hand, the demagnetizin[g] factor of the stressed region is very small, th[e] magnetization within the region will be inde[-]pendent of that of the surrounding domain.

The very high value of the ac-demagnetizin[g] field of some lavas ($H_\sim > 500$ oe) suggests tha[t] a fraction of their trm is carried in regions hav[-]ing an intrinsic coercivity H_s of 500 oe or mor[e] at room temperature, corresponding to $\sigma_i = 3 \times$ 10^9 for $J_s = 400$ ($\lambda = 4 \times 10^{-5}$ for magnetite)[;] at higher temperature, H_s would be smalle[r] as λ probably decreases faster than J_s. Con[-]sider the properties of an assembly of region[s] of cylindrical shape with a length l many time[s] greater than their radius r, and assume tha[t] their axes are distributed isotropically, so tha[t] 1/3 will, on the average, be parallel to the ex[...]

ternal field H_{ex}. Their demagnetizing factor N will be much smaller than 1. At the high temperature at which trm is acquired, the average magnetization of the sample will be of the order of $\chi_{max}H_{ex}$, so that the effective field acting along the axis of a stressed region is $H_{ex} + N\chi_{max}H_{ex} \approx H_{ex}$. The stressed regions will come to equilibrium with the external field in a reasonably short time, provided that

$$\frac{vH_s}{T} \approx 3 \times 10^{-18}$$

as calculated for magnetite from *Néel's* [1949] theory of the relaxation time of small grains. For $H_s = 225$ oe, $v = 1 \times 10^{-17}$ for $T = 750°$K. This volume is consistent with, say, $r = 3 \times 10^{-7}$ cm, $l = 3 \times 10^{-5}$ cm. At lower temperatures, the relaxation time, which is proportional to $\exp(vH_s/T)$, rises rapidly as T decreases and H_s increases, and reaches at temperature T_β a value which is sufficiently great to cause the magnetization in the regions remains essentially frozen in. The corresponding average moment $\bar{m}$ of the assembly at room temperature is accordingly

$$\bar{m} = vJ_{s0} \tanh vJ_sH_{ex}/kT_\beta \qquad (7)$$

and if n is the number of regions per unit volume, the corresponding trm is

$$J_{tr0} = \tfrac{1}{3}n\bar{m} = \tfrac{1}{3}nvJ_{s0} \tanh vJ_sH_{ex}/kT_\beta \qquad (8)$$

which reduces in low fields to

$$J_{tr0} = \tfrac{1}{3}\alpha vJ_sJ_{s0}H_{ex}/kT_\beta \qquad (8')$$

where $\alpha = nv$ in the volume fraction occupied by the cylindrical stressed regions. Saturation of trm is explained by the hyperbolic tangent form of (8); it will be reached when $vJ_sH_{ex}/kT_\beta \approx 2$, which, combined with $vH_s/T = 3 \times 10^{-18}$, yields

$$(H_{ex})_{sat} \approx 10^2(T_\beta/T)(H_s/J_s) \approx 10^2$$

as observed by Roquet. If the whole of trm resides in stressed regions, their fractional volume α is easily obtained from the saturated value of trm: $\alpha = 3(J_{tr0})_{sat}/J_{s0}$. This fraction for Roquet's sample of magnetite, described above, would be about 0.43.

Stresses around dislocations—The size, shape, internal stress, and number of cylindrical regions per unit volume are best interpreted in terms of dislocations. The stress field of a screw dislocation with axis parallel to z is [*Cottrell*, 1953, p. 36]

$$\sigma_{xz} = \sigma_{zx} = -\frac{\mu b}{2\pi}\frac{y}{x^2 + y^2}$$

$$\sigma_{yz} = \sigma_{zy} = \frac{\mu b}{2\pi}\frac{x}{x^2 + y^2}$$

all other stress components being zero. In these relations μ is the rigidity (0.4×10^{12} dynes/cm² for magnetite) and b is the Burgers displacement vector, which is usually of the order of a few atomic spacings. The field is radially symmetrical; written in cylindrical coordinates it is

$$\sigma_{\theta z} = \sigma_{z\theta} = \mu b/2\pi r$$

Expressing the magnetic strain energy F_σ under the usual form

$$F_\sigma = -\tfrac{3}{2}\lambda_{100}[\alpha_1^2\sigma_{xx} + \alpha_2^2\sigma_{yy} + \alpha_3^2\sigma_{zz}]$$
$$- 3\lambda_{111}[\alpha_1\alpha_2\sigma_{xy} + \alpha_2\alpha_3\sigma_{yz} + \alpha_3\alpha_1\sigma_{zx}]$$

where $\alpha_1 \cdots \alpha_3$ are the direction cosines of the magnetization, it is easily seen that F_σ is minimum when spins are distributed on a 45° cone around the z axis; the component of magnetization along the dislocation axis is thus $J_s\sqrt{2}/2$. For $b \simeq 2 \times 10^{-8}$ cm, the average stress within a cylinder with outer radius $r = 2 \times 10^{-7}$ cm would be about 5×10^9 dynes/cm².

Similarly, consider an edge dislocation with displacement vector b along the x axis, zx being the slip plane and z the dislocation line. The stress field, expressed in cylindrical coordinates, is

$$\sigma_{rr} = \sigma_{\theta\theta} = \sim D \sin\theta/r$$

and

$$\sigma_{r\theta} = \sigma_{\theta r} = D \cos\theta/r$$

where $D = \mu b/2\pi(1\text{-}\nu)$, ν being Poisson's coefficient. This corresponds to compression above the slip plane and tension below it, with a shear stress that is maximum in the slip plane. For a substance with positive magnetostriction, this stress field would align spins along the dislocation line. Stresses are of the same order as for screw dislocations with similar displacement vectors.

Note that σ_i varies roughly as $1/r$ while v is proportional to r for a dislocation of given length, so that the relaxation time for a dislocation of given length is independent of the radius assigned to it.

Number of dislocations—The number n of dislocations may be evaluated from the measured trm, by means of equation (8), if one knows what fraction of the total trm resides in the stressed regions. This fraction is best evaluated from the ac-demagnetization spectrum. As no other sources are likely to contribute a coercive force in excess of a few hundred oersteds (see equation 6), whatever part of the original trm remains after exposure to an ac-field greater than, say, 350 oe must reside in dislocations. This fraction is occasionally found to be as high as ½, although it is commonly no more than 0.1. An upper limit for n may thus be found by using a factor of ½. Now consider a rock with total trm $= 5 \times 10^{-3}$ containing p per cent (by volume) of magnetite. The remanent magnetization per unit volume of magnetite is thus roughly $5 \times 10^{-3}/p$, and that part of it which resides in dislocations is $2.5 \times 10^{-3}/p$. Then $n = 3J_{tr0}/\bar{m} = 6J_{tr0}kT_\beta/pv^2J_{s0}J_s$ if $H_{ex} = 0.5$ oe. For $T_\beta = 750°$K, $J_s = 0.5J_{s0} = 2 \times 10^2$, one finds

$$n = 2 \times 10^{14}/p$$

or $n = 10^{16}$ for $p = 0.02$. This number should be multiplied by a factor of 2 or so, to take account of the fact that a region of the type considered has no stability when placed in a domain magnetized at 90° to the dislocation axis; for the demagnetizing field $2\pi J_s$ acting normally to the axis will generally be greater than H_s. The total number n is then equivalent to about 7×10^{10} dislocation per cm² as an upper limit, which is not unreasonable. The volume fraction $\alpha = nv$ will in general be less than 0.2.

Demagnetization curves—Although equation (8) does not explicitly contain σ_i, the strength of the dislocations and corresponding stresses will affect J_{tr0} through v, as, for given relaxation time, v is inversely proportional to H_s, which is proportional to σ_i. As J_{tr0} in weak fields is proportional to v^2, the fractional contribution to the total trm of dislocations of various strengths will decrease as their strength increases, and the ac-demagnetization curve should fall off rapidly with increasing field. The ac-demagnetization will affect, however, only those regions for which the relaxation time is of the order of the period of the alternating field; regions with longer relaxation times which may have acquired a net moment by sufficiently slow cooling will be demagnetized only in ac-fields larger than their intrinsic coercivity, and this will tend to spread the demagnetization curve towards higher fields. In addition, the low-field region extending to a value of H_s given approximately by equation (6) will show the effects of demagnetization of the components of trm that are related to blocking of walls, hindered rotations, etc. The shape of demagnetizing curve will thus be difficult to predict and will vary from sample to sample.

Summary—The ac-demagnetization spectrum and, notably, the differences between the demagnetization spectra for irm and trm indicate that several factors normally contribute to trm. That part of it which has stability characteristics comparable to those of irm is probably caused by a mechanism of blocking of domain walls, such as that which produces irm at ordinary temperatures. Part of trm is probably due to the rapid decrease in magnetocrystalline anisotropy energy near the Curie point and is related to the increase in susceptibility in that temperature range. Finally, that part of trm which has the highest stability and ac-coercivity probably resides in strained regions surrounding dislocations.

Strained regions contribute to the coercive force in the manner described by Néel; because of variations in shape, stress, etc., they actually contribute a spectrum of coercive forces. Among these strained regions there may be some, as mentioned above, that will be roughly cylindrical in shape, with a length many times greater than their radius. These have the interesting property that, because of their shape, the field along their axis is nearly equal to the external field and is independent of the direction of magnetization in the surrounding space.

Consider now a population of such regions, one-third of which will, on the average, have their axes parallel to an external field H_{ex}. These regions will essentially behave as single-domain particles and acquire at high temperature a net magnetization parallel to the field,

e intensity of this magnetization being proportional to tanh vJ_sH_{ex}/kT or, in weak fields, H_{ex}. As the temperature falls, the relaxation nes rises, and the magnetization acquired at gh temperature remains frozen in; trm then s all the properties described by Néel for small rticles. At the same time, the magnetocrystale energy increases, and the domain structure comes fixed. Finally, when the external field removed, one ends up with about equal propies of domains parallel and antiparallel to $_x$, both of which still contain strained regions gnetized parallel to H_{ex}. The strained regions antiparallel domains must be energetically favorable because of exchange energy across eir boundaries; their stability depends on the gnitude of their strain anisotropy.

Trm and irm acquired in strong fields will be ntical with respect to stability (ac-demagization, and temperature variation), proled that the field be greater than the critical d H_s required for reversing the direction of gnetization around a dislocation. Roquet's periments on the thermal stability of trm d irm suggest a critical field of the order of) oe; the same order of magnitude is obned from the ac-demagnetization curve.

The most stable part of trm, which is of eater importance in paleomagnetism, is thus ectly proportional to n, the number of disations per unit volume. This number should pend on the history of the rock and should nerally be smaller in well-annealed materials in rocks that have cooled very slowly. This y be the reason why the stable component of e trm of basic plutonic rocks is generally ınd to be an order of magnitude less than t of their rapidly chilled extrusive equivats, or why trm is commonly greater in the lled margins of a lava flow than in its inter. Metamorphic rocks, which commonly restallize after deformation and likewise cool wly, should similarly have a relatively small n of low stability, in spite of a large magite content and normal value of their susptibility.

Acknowledgments—This research was supported in part by a grant from the Petroleum Research Fund, administered by the American Chemical Society, and in part by the American Petroleum Institute. Grateful acknowledgment is hereby made to the donors of said funds. The author is indebted to Allan Cox and John Kern for helpful discussions. Dr. Cox's experiments on ac-demagnetization suggested to the author the present interpretation of trm.

References

Alberts, L., and B. J. Shepstone. On the initial magnetization of α-iron at high temperatures, *Phil. Mag., 3,* 700 706, 1958.

Cottrell, A. H., *Dislocations and Plastic Flow in Crystals,* Clarendon Press, Oxford, 1953.

Grabovskii, M. A., and G. N. Petrova, The stability of remanent magnetization of rocks. *Izvest. Akad. Nauk SSSR, Ser. Geofiz.,* 290–296, 1956 (Assoc. Tech. Services Translation RJ-744).

Grabovskii, M. A., G. N. Petrova, and L. I. Isakova, The origin of the thermoremanent magnetization of rocks, *Izvest. Akad. Nauk SSSR, Ser. Geofiz.,* 56-66, 1956 (Assoc. Tech. Services Translation RJ-743).

Kneller, E., Ueber die Temperaturabhängigkeit der Bestimmungsgrössen der technischen Magnetisierungskurve von Nickel, in *Beiträge zur Theorie des Ferromagnetismus und der Magnetisierungskurve,* W. Köster, ed., Springer, Berlin, 82–139, 1956.

Nagata, T., *Rock Magnetism,* Maruzen Co., Tokyo, 1953.

Néel, L., Bases d'une nouvelle théorie générale du champs coercitif, *Ann. univ. Grenoble, 22,* 299–343, 1946.

Néel, L., Théorie du trainage magnétique des ferromagnétiques en grains fins, *Ann. géophys., 5,* 99–136, 1949.

Néel, L., Some theoretical aspects of rock-magnetism, *Adv. Phys., 4,* 191–213, 1955.

Roquet, J., Sur la rémanence des oxydes de fer et leur intérêt en géomagnétisme, *Ann. géophys., 10,* 226 247 and 282 325, 1954.

Stacey, F. D., Thermo-remanent magnetization of multi-domain grains in igneous rocks, *Phil. Mag., 3,* 1391–1401, 1958.

Uyeda, S., Thermo-remanent magnetism as a medium of palaeomagnetism. *Japan. J. Geophys., 2,* 1–123, 1958.

(Manuscript received July 31, 1959.)

The Concentration of Vanadium, Chromium, Iron, Cobalt, Nickel, Copper, Zinc, and Arsenic in the Meteoritic Iron Sulfide Nodules[1]

Walter Nichiporuk and Arthur A. Chodos

California Institute of Technology
Pasadena, California

Abstract—The concentrations (based on graphite-free nodules) of vanadium, chromium, cobalt, nickel, copper, zinc, and iron have been determined by X-ray fluorescence analysis in twenty-two troilite nodules from twelve iron and two silicate meteorites. These elements were determined, in addition, in the del Norte County, California, terrestrial troilite.

It was found that the concentration ranges of the elements are extremely broad and do not differ greatly for the three types of troilites studied.

The elements chromium and nickel, which are present in the largest concentrations, are distributed over the ranges which also appear to be the broadest. The copper range is the narrowest, and the cobalt range is comparable to that of nickel. Since in most cases concentrations of vanadium, zinc, and arsenic lie below the respective detection limits, the effective concentration ranges for these elements may be as broad as, if not broader than, the ranges for the other elements. The content of iron varies within wider limits than those defined by all iron values previously reported.

An abundant free-iron phase which occurs in troilite nodules indicates that a complete segregation of the iron sulfide and iron phases was not attained.

Introduction

The iron sulfide (troilite) nodules are found in all meteorites as distinct segregates from the silicate and metal phases. A precise knowledge of concentrations of elements in these nodules is of importance in determining the composition of meteoritic matter and in estimating the physical and chemical conditions under which they were formed.

Vanadium, chromium, cobalt, nickel, copper, zinc, arsenic, and iron have been studied by *I. and W. Noddack* [1930], *Goldschmidt and Peters* [1933], and more recently by *Lovering* [1957]. In all cases these investigators analyzed a small number of troilite nodules. Their results, which are collected in Table 1, show that the concentrations of the individual elements, particularly the concentrations of nickel, cobalt, and chromium, differ by factors as large as 15 to 30.

For this reason a new investigation of the distribution in troilite nodules of the elements shown was undertaken in order to find out whether a larger assemblage of nodules and independent analytical methods would give

Table 1—*Concentration in per cent (numbers involving decimals) and in parts per million (integral numbers) of eight elements in troilite nodules as reported by previous investigators*

Investigators	V	Cr	Co	Ni	Cu	Zn	As	Fe
I. and W. Noddack [1930]	45	0.12	0.21	2.88	0.42	0.15	0.10	61.10
Goldschmidt and Peters [1933]			2.0	100	0.10			
Goldschmidt [1938]						0.2-0.6		
Goldschmidt [1954]	~0.15	0.1-16.0						
Lovering [1957]	8-320	900->1.0	12-0.28	600-~1.0	500-0.15			

[1] This work was done under the U. S. Atomic Energy Commission Contract AT (11-1) 208. Publications of the Division of the Geological Sciences, California Institute of Technology, Pasadena, Calif. Contribution No. 932.

results that are more consistent than the sets of results previously reported.

Experimental Procedure

Basis of the method—The X-ray flourescence analysis as developed [*Chodos and Nichiporuk*, 1958] for this study is based on the assumption [*Coulliette*, 1943] that the sum of the elements being determined is 100 per cent. Inasmuch as the troilite nodules are mainly iron sulfide, we have on a sulfur-free basis

$$\mathrm{Fe} + \mathrm{V} + \mathrm{Cr} + \mathrm{Co} + \mathrm{Ni} + \mathrm{Cu} + \mathrm{Zn} + \mathrm{As} = 100 \text{ per cent} \quad (1)$$

Hence

$$\mathrm{Fe} = \frac{100 \text{ per cent}}{1 + \frac{\mathrm{V}}{\mathrm{Fe}} + \frac{\mathrm{Cr}}{\mathrm{Fe}} + \frac{\mathrm{Co}}{\mathrm{Fe}} + \frac{\mathrm{Ni}}{\mathrm{Fe}} + \frac{\mathrm{Cu}}{\mathrm{Fe}} + \frac{\mathrm{Zn}}{\mathrm{Fe}} + \frac{\mathrm{As}}{\mathrm{Fe}}} \quad (2)$$

The working curves are plotted with the elements-to-iron intensity ratios as the ordinates versus the elements-to-iron concentration ratios as the abscissas.

Sampling—Information on the troilite samples studied is given in Table 2. Each analysis sample represents a single troilite inclusion with a surface diameter of at least 4 mm. The troilite inclusions in the Brenham pallasite specimen were considerably smaller ($\sim$2 mm) and in order to obtain the minimum of 120 mg sample weight used in this work, the troilite sample of this meteorite was made up of several of these smaller inclusions.

In sampling, extensive precautions were taken to minimize the metallic and silicate contaminations and to exclude the discernable (reddish-brown) oxidized material.

The samples were ground to about 100 mesh and the resulting (120 to 280 mg) powders were tested with a cylindrical (12.5 $\times$ 0.9 cm) magnet. Small (2 to 3 mg) powder portions were taken for the X-ray diffraction patterns. The remaining bulk was converted to a gravimetric oxide form in order to avoid the use of an impure ferrous sulfide reagent as a matrix for standards and to analyze troilite nodules for carbon.

Preparation of samples and standards—All reagents used were of a high degree of purity. The nitric acid sample solutions were evaporated to near-dryness and the residues taken up in distilled water. Small globules of free sulfur and insignificant, hard, gray-black residues were left in solution. The enstatite residue (3.2 per cent) from the Cullison (chondrite) troilite and the chromite residue (2.2 per cent) from the del Norte County, California, terrestrial troilite were discarded.

Graphite was filtered off, dried at 110°C, weighed, converted to carbon dioxide according to *Craig's* [1953] procedure, and analyzed in a Nier, 60°, sector-type mass spectrometer which incorporates modifications by *McKinney and others* [1950].

The mixtures of iron sulfate and nitrate obtained by evaporating the sample solutions were ignited to constant weight at 600°C. Of the resulting oxide ('infinitely thick' sample) 100 mg was placed for counting in a shallow portion of a Zytel holder. No effort was made to fill any definite area or to obtain a reproducible sample surface.

The standards were prepared by mixing nitric acid solutions of spectrographic iron with the solutions of known concentrations of the analysis elements, all computed on the basis of 250 mg weight of free metals. The standard solutions were treated with 2 to 3 ml of 6 normal sulfuric acid and processed in the same manner as the solutions of the analysis samples.

Apparatus and X-ray lines—A tungsten target tube in a Norelco X-ray spectrograph was operated at 50 kv and 35 ma. A lithium fluoride analyzer crystal was used in combination with 0.020 $\times$ 4 inch parallel plate collimator. The detector was an argon-methane-filled proportional counter and all determinations were conducted in a helium atmosphere. A pulse-height analyzer was used for the determination of vanadium in order to eliminate higher-order tungsten radiation.

The analytical lines used are shown in Table 3. The figure of 80 ppm which appears for the sensitivity of chromium and nickel denotes the concentration of these elements in the lowest standard. The sensitivities and intensities to be

TABLE 2—*Samples used in determination of elements*

Name	Class	Sample description	Sources
Coahuila	H	300 mg of chips and powder, slightly tarnished.	Clifford Frondel, Harvard University
Indian Valley	H	Inclusion 12 × 5 × 4 mm in a 10.5-gram slice; steel-gray color; hardness greater than normal; great resistance to grinding; inclusion adjoins directly Fe-Ni phase.	H. H. Nininger, Am. Meteor. Museum
Sikhote-Alin	Ogg-H	Inclusion 12 × 10 × 2 mm in a 37-gram bar, surrounded by a disconnected sequence of schreibersite (Fe_3P) inclusions (up to 1 cm long) which in places appear to be in a direct contact with iron sulfide.	A. A. Yavnel', Committee on Meteor., Moscow, U.S.S.R.
Canyon Diablo	Og	1 gram of chips from a large sample used in lead determinations. Larger chips contain firmly imbedded metallic specks.	C. C. Patterson, Calif. Inst. of Technology
Canyon Diablo (1)	Og	Loosely bound inclusion, 10 × 10 × 2 mm in a large exhibition slice; it adjoins a jagged rim of schreibersite, on the average 1 mm wide.	Geochem. Lab. Collection, Calif. Inst. of Technology
Odessa	Og	The same slice, 3.7 × 2.7 cm: large nodule 17 × 11 × 4 mm	H. H. Nininger, Am. Meteor. Museum
Odessa (1)		small nodule 6.5 × 5 × 6 mm; 1.5 cm apart. The small nodule abuts the Fe-Ni phase; the large one is rimmed by a discontinuous skin (~0.3 mm) of schreibersite.	
Henbury	Om	500-mg chip from a larger troilite sample used in lead determinations.	C. C. Patterson, Calif. Inst. of Technology
Henbury (1)		150 mg of small chips.	J. F. Lovering, Austral. National Univ., Canberra
Toluca	Om	Five small chips.	Geochem. Lab. Collection, Calif. Inst. of Technology
Toluca (1)		28 × 18 mm inclusion in a section.	Geochem. Lab. Collection, Calif. Inst. of Technology
Toluca (2)		4 × 4.5 × 8 mm edge-exposed inclusion in an 8-gram jagged fragment.	H. H. Nininger, Am. Meteor. Museum
Toluca (3)		19 × 9 × 10 mm edge-exposed inclusion in a 217-gram section.	Geochem. Lab. Collection, Calif. Inst. of Technology
Ballinoo	Of	Two chips of about 1 gram, steel-gray color; hardness greater than normal; great resistance to grinding.	J. F. Lovering, Austral. National Univ., Canberra

TABLE 2—*Continued*

Name	Class	Sample description	Sources
Bear Creek	Of	300 mg of chips.	H. H. Nininger, Am. Meteor. Museum
Cambria	Of	Two fragments of 250 mg.	H. H. Nininger , Am. Meteor. Museum
Duchesne Duchesne (1) Duchesne (2)	Of	All three samples came from nodules in a 23 × 13 cm slice. According to a photograph of the slice, the nodules seem to adjoin directly the Fe-Ni phase.	H. H. Nininger, Am. Meteor. Museum
Moonbi	Of	Edge-exposed half (10 × 10 × 10 mm) of an inclusion in 30-gram cutting. The interior half of the inclusion borders directly on the Fe-Ni phase.	J. F. Lovering, Austral. National Univ., Canberra
Brenham	P	Small (∼2 mm) inclusions attached to loose metal and silicate chips.	H. H. Nininger, Am. Meteor. Museum
Cullison	C	4.5 × 6 × 16 mm inclusion in a silicate bar.	H. H. Nininger, Am. Meteor. Museum
del Norte Co., California, terrestrial troilite		Fragments.	L. T. Silver, Calif. Inst. of Technology

expected from a 100-mg sample are also included in the table. The numbers in parentheses for cobalt, copper, and zinc represent the concentration limits in which the reliability of the working curves increases. The intensities in counts per second are given for these concentrations.

TABLE 3—*Sensitivity and intensity of the Kα lines from sulfur-free standards*

Element	Line	Sensitivity, ppm	Net intensity, counts/sec
Fe	Kβ		
V	Kα	20	20
Cr	Kα	80	100
Co	Kα2°	40 (100)	20
Ni	Kα	80	100
Cu	Kα2°	40 (100)	15
Zn	Kα	20 (80)	15
As	Kα	80	5

The counting rates were determined for pea and background with a minimum of 25,0(counts for each peak. When the peak intensit was low, the same number of counts was al taken for background; otherwise 6400 coun were sufficient.

The intensity ratio of the element peak the iron peak was used to obtain the element-t iron concentration ratio from the working cur for each element. The ratios were then summe (equation 2) and the concentration of iron w calculated. The iron concentration and t element-to-iron concentration ratio yield t element concentration. All resulting concentr tions are computed to a carbon-free troili basis.

Accuracy—We tried to estimate reasonab limits of the error in our method by checki chemically the X-ray fluorescence results f iron and nickel, and by studying the followi

TABLE 4—*Comparative determinations of iron and nickel*

Troilite nodule	Iron, per cent X-ray fluorescence	Iron, per cent Photometry	Nickel, per cent X-ray fluorescence	Nickel, per cent Gravimetric analysis
ılinoo	$78.5_0 \pm 0.0_8$ (5)*	$78.9_6 \pm 0.6_3$ (6)		
uchesne			6.61 ± 0.06 (3)	7.25 (1)
uchesne (2)			3.46 ± 0.01 (2)	4.12 (1)
dian Valley	$78.0_3 \pm 0.0_8$ (2)	$79.6_3 \pm 0.4_4$ (6)		
›luca (1)	$62.3_4 \pm 0.0_1$ (2)	$62.3_8 \pm 0.3_7$ (8)		
on sulfide reagent		$63.6_3 \pm 0.1_7$ (5)		
on sulfide reagent		63.5_3 (stoich.)		

* The number of determinations, averaged in each case, is given in parentheses.

ror-contributing sources: the interelement fects due to the absorption and enhancement ıenomena, the effects from the matrix comısition, and the possible volatilization of arnic. Following is a brief summary of this udy.

Iron and Nickel—Iron was determined by easuring light transmission at 510 μ of aliquots, ntaining 2 to 5 γ Fe/ml in the form of the ange ferrous orthophenanthroline complex *3andemer and Schaible*, 1944]. The troilite mples and a comparison sample of the ferrous sulfide reagent (Braun Corp., August 20, 1947), each weighing about 30 mg, were decomposed by a combined action of the solution of bromine in carbon tetrachloride and concentrated nitric acid.

Nickel was determined gravimetrically. The iron and nickel results obtained by chemical and X-ray fluorescence techniques are compared in Table 4.

Interelement effects—In a system as complex as the one we are studying, there is the possibility of a wide variety of interelement

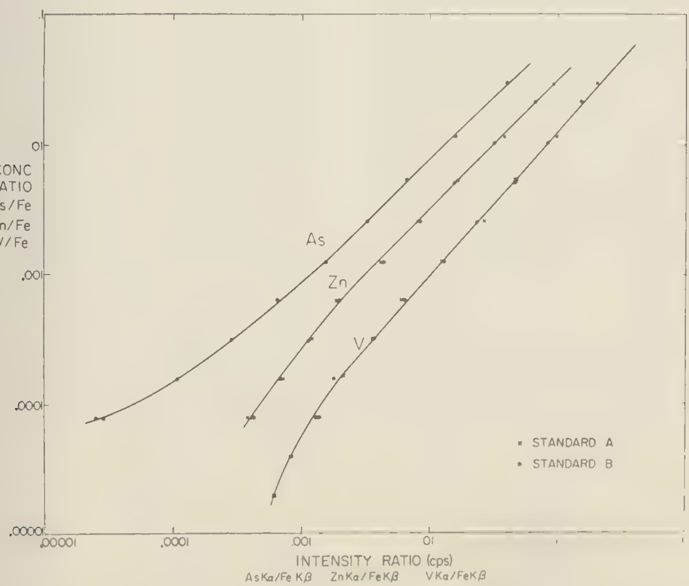

FIG. 1—Working curves for vanadium, zinc, and arsenic.

TABLE 5—*Mineral composition and magnetic properties of troilite nodules*

Nodules	Class	Magnetic properties	Minerals observed
Coahuila	H	Magnetic	Troilite, pyrrhotite, daubreelite, chrompicotite
Indian Valley	H	Strongly magnetic	Alpha iron, troilite, daubreelite
Sikhote-Alin	Ogg-H	Magnetic	Troilite, daubreelite, chrompicoti
Canyon Diablo	Og	Strongly magnetic	Troilite, iron phosphide (FeP), alpha iron, pyrrhotite
Canyon Diablo (1)		Magnetic	Troilite, graphite, pyrrhotite
Odessa	Og	Magnetic	Troilite
Odessa (1)		Magnetic	Troilite, graphite
Toluca		Nonmagnetic	Troilite, graphite
Toluca (1)		Magnetic	Troilite
Toluca (2)	Om	Magnetic	Troilite
Toluca (3)		Magnetic	Troilite
Ballinoo	Of	Strongly magnetic	Alpha iron, troilite, pyrrhotite
Bear Creek	Of	Nonmagnetic	Troilite
Cambria	Of	Magnetic	Troilite, pyrrhotite
Duchesne	Of	Magnetic	Troilite, pyrrhotite
Duchesne (2)		Magnetic	Pyrrhotite
Moonbi	Of	Strongly magnetic	Pyrrhotite, troilite, chrompicotit
Brenham	P	Nonmagnetic	Troilite, pyrrhotite
Cullison	C	Strongly magnetic	Troilite, alpha iron
del Norte County, California, terrestrial troilite		Nonmagnetic	Troilite, chrompicotite

effects. In order to study these effects and to evaluate the technique, we have prepared and analyzed, using the original reference curves such as illustrated in Figure 1, a large number of standards in which the concentration and the combination of the elements were varied. Accuracies of 5 to 10 per cent of the amount added are indicated above the concentration level of 0.1 per cent. The readings for copper are 20 per cent low at a 1 per cent concentration level. At lower levels the second-order copper line is very weak, and erratic results are often obtained.

Matrix composition effects—The element-to-iron intensity ratios for nickel, chromium, copper, and cobalt have been found to vary with the degree of the conversion of the iron sulfate matrix to iron oxide. The variation is particularly large in the temperature range of 300° to 450°C. In the range of 600° to 850°C the weight of the matrix remains constant within 1 per cent, and any temperature in this range represents optimum conditions for the intensity-ratio measurements.

Volatile versus involatile elements—The typical curves in Figure 1 show that arsenic and zi are subject to a deviation from theoretic linearity similar to that of refractory vanadiu This and the stability of the arsenic counts the Odessa (1) nodule, after its repeated igniti in the temperature range of 600° to 750°C, le to the conclusion that our experimental pr cedures have not caused a measurable volati zation of arsenic.

Precision—The reported concentrations (Tab 8) represent averages of two to five determin tions, made over periods of two days to s months. The mean deviations from the avera are 3 per cent for nickel, a few parts per thousa for iron, 5 per cent for cobalt, chromium, a vanadium (above 13 ppm), and 10 per cent f copper, zinc, and arsenic. For the latter tw the concentration levels were higher than 50 pp

MINERAL PHASES AND MAGNETIC PROPERTIE OF TROILITES

The mineral phases as identified in the X-r diffraction patterns of the investigated troliti are shown in Table 5, column 4. The order the listing of the phases is approximately th

TABLE 6—*Standard X-ray patterns used in this study*

Mineral	Description	Reference
Troilite	Synthetic FeS with 50 to 51.2 atom per cent sulfur	*Hägg and Sucksdorff* [1943]
	del Norte County, California, troilite	*Harcourt* [1942]
Pyrrhotite	Noranda, Quebec, pyrrhotite, $Fe_{1-x}S$, where $x = 0$ to 0.2	*Harcourt* [1942]
Alpha iron	Artificial iron	*U.S. National Bureau of Standards*
Iron phosphide	Artificial FeP	*Imperial Chemical Industries of Northwich, England*
Graphite	Spectrographically pure reagent	*African Exploration Chemical Industries Ltd., Transvaal, Africa*
Daubreelite	Synthetic $FeCr_2S_4$	*Lundquist* [1943]
Chrompicotite	Rhodesian mineral $(Fe, Mg)O \cdot (Cr, Al)_2O_3$	*Clark and Ally* [1932]

of the decreasing intensity of three or less strongest peaks of each phase. The patterns were prepared with filtered Fe$K\alpha$ and Cu$K\alpha$ radiations, and the detection sensitivity of the X-ray diffractometer (Norelco) used was about 4 to 5 per cent.

The patterns obtained were compared with the standard X-ray patterns listed in Table 6.

The stoichiometric iron sulfide pattern of *Hägg and Sucksdorff* [1933] persists over the range of 50 to 51.2 atom per cent sulfur. On this basis the troilites recorded in Table 5 very probably have this composition range. Therefore, they may represent either a pure troilite, a pure pyrrhotite, or a mixture of both.

The nodules expressly shown to contain pyrrhotite along with troilite have in their patterns the spacing $d = 2.06$ A which matches the principal spacing in the pattern for Noranda pyrrhotite [*Harcourt*, 1942].

The chromite phase was identified by a comparison of hardness and color of insoluble residues from nodules with the same properties in chrompicotite which was isolated from the del Norte, California, troilite. Intensities of magnesium and aluminum lines in the emission spectra of the residue-producing nodules were also used. In addition, we relied upon the mineralogical work of *Kvasha* [1958], who showed that chromite is a constant microscopic constituent of the troilite phase of the Sikhote-Alin meteorite.

A check examination of the Ballinoo nodule in a polished section (x600) confirmed its ternary composition as given in Table 5. It also showed that the components involved—free iron, troilite, and pyrrhotite—form a fine-grained, closely knit mixture.

Other mineral mixtures include the free iron-troilite-daubreelite, troilite-daubreelite-chromite, and troilite-pyrrhotite-graphite. Absent are troilite-iron-chromite and troilite-iron-graphite mixtures.

Graphite phase—Graphite was obtained (see Experimental Procedure) in isolated form and was studied in more detail. The results are given in Table 7. Column 3 shows the isotopic composition in per mil deviation δ from the C^{13}/C^{12} ratio of the carbon dioxide extracted from the standard Chicago belemnite (PDB-1). The isotopic data incorporate the correction factor of 1.07 [*Craig*, 1953] for the abundance of O^{17}. The loss of graphite due to possible oxidation by nitric acid was not more than 2.5 per cent.

A reference to *Craig's* [1953] carbon diagram shows that the graphites in Table 7 are lighter than carbonates, diamonds, and the carbon dioxide gases from Yellowstone Park, but heavier than most graphites, as well as plant, igneous, and sedimentary forms of carbon.

TABLE 7—*Graphite content and isotopic composition of four troilite nodules*

Sulfide nodules	Graphite, weight per cent	δ-value (c^{13}/c^{12}) per mil
Canyon Diablo (1)	11.6	−6.0
Odessa (1)	30.0	−5.2
Henbury	5.0	n.d.
Toluca	9.9	−5.2

TABLE 8—*Concentrations in per cent (numbers involving decimals) and parts per million (integral numbers) of eight elements in troilite nodules*

Meteorites	Class	V	Cr	Co	Ni	Cu	Zn	As	Fe
Coahuila	H	414	5.57	134	0.55	0.10	99	<50	55.7_1
Indian Valley	H	99	2.59	0.26	2.90	676	<50	<50	78.0_3
Sikhote-Alin	H-Ogg	70	1.58	115	0.91	821	<50	<50	62.5_5
Canyon Diablo*	Og	39	0.71	45	165	152	<50	<50	62.7_8
Canyon Diablo (1)†	Og	47	0.66	150	0.17	680	211	<50	59.6_4
Odessa	Og	29	0.56	185	0.26	185	<50	<50	62.6_7
Odessa (1)	Og	27	0.51	350	0.49	0.34	0.33	140	61.8_1
Henbury	Om	60	0.61	373	0.13	0.15	353	<50	62.5_6
Henbury (1)	Om	68	0.60	18	0.14	534	122	273	62.6_9
Toluca	Om	32	0.41	0.21	1.98	758	521	<50	60.8_0
Toluca (1)	Om	38	0.41	0.12	0.65	143	<50	<50	62.3_4
Toluca (2)	Om	63	0.68	268	0.55	66	83	<50	62.2_5
Toluca (3)	Om	35	0.41	0.20	1.76	557	<50	<50	64.3_3
Ballinoo	Of	<13	0.12	0.30	4.82	771	<50	<50	78.5_0
Bear Creek	Of	<13	0.22	0.12	0.33	127	263	<50	62.5_5
Cambria	Of	23	0.23	80	0.70	284	<50	<50	63.2_0
Duchesne	Of	<13	181	0.60	6.61	276	101	<50	54.3_6
Duchesne (1)	Of	<13	281	713	0.49	133	77	<50	63.0_4
Duchesne (2)	Of	<13	191	0.51	3.46	504	<50	<50	56.0_2
Moonbi	Of	103	0.91	583	1.12	0.11	242	<50	59.8_0
Brenham	P	24	0.16	0.20	0.54	206	63	<50	62.6_0
Cullison	C	<13	79	547	1.22	0.15	61	<50	67.0_2
del Norte County, California, terrestrial troilite		<13	327	0.25	0.39	0.26	559	0.27	62.2_4

* The results are based on the portion of the sample free of metallic inclusions (Tables 2 and 5).
† Numbers denote different nodules from individual meteorites, as in Tables 2 and 5.

Magnetic properties of nodules—The results of magnetic tests are given in column 3 of Table 5. The terms are defined as follows: nonmagnetic, the powdered sample (120 to 560 mg) is totally unattracted by the magnet; magnetic, attraction ranges from a small fraction to over one half of the total sample; strongly magnetic, the entire sample is attracted by the magnet.

RESULTS AND CORRELATIONS

Table 8 gives concentrations of the elements studied in graphite-free nodules from twelve iron and two silicate meteorites, and in a terrestrial troilite from del Norte County, California. The structures in column 2 are arranged in the order of decreasing width of the alpha-iron bands or the increasing concentration of nickel.

The high zinc result reported for the smaller Odessa nodule is uncertain because of the possible contamination of the samples. The suspected source is the molding clay used as a mount for the metal section in which the Odessa nodules were enclosed. An analysis of the clay showed about 2 per cent zinc. In addition, chromium, nickel, and copper were found in quantities of 100 ppm.

The iron, cobalt, and copper concentrations in the Canyon Diablo (1) nodule include corrections for the amounts of these elements found in graphite after its isolation and washing. For the other graphite-containing nodules these corrections were negligible.

Uniformity of troilites from individual iron meteorites—It is generally supposed that monomineralic troilite nodules of a single meteorite possess trace-element compositions which are quite uniform. If this is true, then one would obtain, in view of the uniform composition of individual iron meteorites [*Goldberg and others*, 1951; *Yavnel'*, 1954; *Lovering and others*, 1957]

TABLE 9—*Concentrations of chromium, manganese, nickel, and copper in troilites from different parts of the Sikhote-Alin meteorite*

	Cr in per cent		Mn in ppm		Ni in ppm		Cu in ppm	
	One troilite	Nine troilites	One troilite	Nine troilites	One troilite	Nine troilites	One troilite	Nine troilites
Average	1.32	1.10	290	230	580	560	540	1400
Error (one troilite)	±0.13		±30		±60		±270	
Error (nine troilites)		±0.23		±50		±250		±1000

sulfide-metal partition ratios of elements which would be constant for different parts of a given meteorite. Our studies, however, make it appear that troilites from individual meteorites possess compositions which vary considerably from one troilite to another.

The first investigation of the uniformity of troilites from a single meteorite was performed by *Yavnel'* [1956]. He made quantitative spectrographic determinations of chromium, manganese, nickel, and copper in twenty samples from a single iron-and schreibersite-free troilite of the Sikhote-Alin meteorite. He further determined the same elements in duplicate in nine troilites from different parts of this meteorite. His results are shown in Table 9, from which it can be seen that, although the averages in both cases—with the exception of copper—are very much the same, the standard errors of the determinations involving nine troilites exceed by a factor of 2 to 4 the error in the analysis of a single troilite. Yavnel' concluded that the elements studied are nonuniformly distributed among the individual troilites of the Sikhote-Alin meteorite.

It should be pointed out that in a more recent study of troilites from this meteorite *Dyakonova* [1958] obtained results which confirmed Yavnel's conclusion in regard to chromium. However she stated at the same time that the chromium variations observed were most probably due to chromite. Its constant occurrence in the troilite phase of Sikhote-Alin was reported by *Kvasha* [1958]. It is possible, then, that small fluctuations in the chromium results, as shown in Table 9, may also be due to the chromite.

In this study two to four troilites were available from each of the five different iron meteorites. Except for the Odessa and Duchesne, the other meteorites were represented by different specimens. The troilite samples ranged from 120 to 560 mg and were composed of a reasonably pure iron sulfide (troilite-pyrrhotite) phase. The two Odessa inclusions (Table 2) were markedly different in size and were situated within 1.5 cm of each other. The results of the study are given in Table 8.

When we consider the fact that errors were contributed by the sampling, the chemical, and the X-ray procedures, we are led to the conclusion that, whereas chromium and vanadium are fairly uniformly distributed among troilites from individual meteorites, the remaining elements vary significantly from one troilite to another.

Comparison of troilites from iron and silicate meteorites and from terrestrial occurrence—Our limited studies show that, irrespective of their mineral compositions, the troilite nodules from iron and silicate meteorites possess trace-element compositions which do not differ from each other in any major respect.

Thus, the nodules from two silicate meteorites were found to contain the amounts of the elements studied which consistently fell into the ranges of the meteoritic iron troilite types. Within these ranges, for example, the nodules from the Cullison chondrite and the Moonbi iron are seen to be nearly identical with respect to their contents of cobalt, nickel, and copper. Similarly, the nodules from the Brenham pallasite and the Toluca (1) iron resemble each other very closely with respect to these same elements.

In the case of the terrestrial troilite which occurs in large serpentine and magnetite masses [*Eakle*, 1922], a similar comparison shows that, with the exception of a high (0.27 per cent) arsenic concentration, this troilite contains amounts of the other elements which place it within the composition range of the meteoritic troilites.

Any conclusion, however, as to whether the

troilites from meteoritic and terrestrial sources represent in reality a continuum of troilite types must await a more detailed study.

Chromium and vanadium—The principal trend in the distribution of chromium and vanadium in troilite nodules is the apparent increase of the chromium and vanadium concentrations with increasing width of the alpha-iron bands of the corresponding iron meteorites.

In general, chromium and vanadium decrease or increase simultaneously, but not congruently, when different nodules are compared. Considering the nodules from all meteorites, the variation in the chromium-vanadium ratio is from about 10 to 260. When, however, only the monomineralic nodules from the individual meteorites (Canyon Diablo, Odessa, Henbury, and Toluca) are compared, it is found that the ratio remains constant within 2 to 23 per cent. This shows the coherence of chromium and vanadium in the iron sulfide phases, formed in equilibrium with the chemically uniform iron-nickel phases [*Goldberg and others*, 1951; *Yavnel'*, 1954; *Lovering and others*, 1957].

The proportion of the troilite phase in iron meteorites [*Chirvinskii*, 1948: 1.4 per cent by weight; *Henderson and Perry*, 1958: 2.7 to 6.0 per cent] together with their chromium [*Lovering and others*, 1957] and vanadium [*I. and W. Noddack*, 1930] abundances indicates that troilite inclusions should be taken into consideration when calculations of the chromium and vanadium composition of these meteorites are made. The contribution of troilite [5.0 to 6.0 per cent by weight: *Prior*, 1916; *I. and W. Noddack*, 1930; *Goldschmidt*, 1938; *Daly*, 1943; *Urey*, 1952] to the corresponding composition of the silicate meteorites appears to be negligible.

The present vanadium range is in good agreement with the vanadium spread of 8 to 320 ppm observed in *Lovering's* [1957] data, but it does not agree with the averages of 45 ppm and 0.15 per cent vanadium reported by *I. and W. Noddack* [1930] and *Goldschmidt* [1954], respectively.

The chromium range includes, with the exception of the upper chromium limit in *Goldschmidt's* data [1954], all previously determined concentrations of the element. The dependence of this range on the daubreelite and chromite phases is evident.

Nickel and cobalt—The nickel and cobalt concentrations depend only to a very limited extent upon the free-iron phase (Table 5). Out of the eight highest (1.12 to 6.61 per cent) nickel concentrations observed, only three (Indian Valley, Ballinoo, Cullison) can be correlated with the presence of an abundant iron phase. The remaining five concentrations, including the highest in the Duchesne nodule, are characteristic of the nodules that are composed of a nearly pure troilite-pyrrhotite phase. The fact that no detectable nickel-sulfide phase apparently exists at these high nickel levels is in striking contrast to the existence of the daubreelite and chromite phases at comparably high chromium levels.

When compared with chromium, concentrations of nickel and cobalt vary over narrower ranges: 172 ppm to 6.61 per cent for the former and 18 ppm to 0.60 per cent for the latter. In general, the concentration of cobalt increases with increasing nickel concentration. However, the trend is irregular, with the nickel-cobalt coherence being less pronounced than the corresponding chromium-vanadium coherence.

In this connection it is significant that the troilites from individual iron meteorites (Canyon Diablo, Odessa, Henbury, Toluca, Duchesne) possess the nickel-cobalt ratio which, unlike the nearly constant chromium-vanadium ratio, varies by factors ranging from 1 to 5. When all troilite nodules are taken into account, it is found that their nickel-cobalt ratios fluctuates from 3 to 88, whereas for the metal phases which enclose these nodules it fluctuates only from 12 to 24.

It is further observed that nickel concentrations are usually higher than chromium concentrations in troilite nodules of those meteorites whose nickel content progressively increases above the 8 per cent level.

The nickel and cobalt concentrations here reported are comparable to the average concentrations given by *I. and W. Noddack* [1930], but they are definitely higher than the nickel and cobalt concentrations obtained by *Goldschmidt and Peters* [1933] and more recently by *Lovering* [1957].

Arsenic and zinc—The arsenic concentrations are generally lower than the zinc concentrations, and perhaps they are also lower than the concentrations of all other lesser elements studied. When compared with the average arsenic concentration (0.1 per cent) given by *I. and W.*

oddack [1930] the concentrations indicated y the present detection limits of this element re lower by a factor of at least 20. The neutron ctivation results of 0.03 to 0.07 ppm arsenic ported by *Smales and others* [1958] for a anyon Diablo troilite nodule strongly suggest hat this factor may actually be much too small.

The zinc concentration, except for its very gh but uncertain value (0.33 per cent) in the dessa (1) troilite, varies by a factor of at least), and like the arsenic concentrations it is wer than the average zinc concentration (0.15 er cent) given by *I. and W. Noddack* [1930] and e zinc concentration range (0.2 to 0.6 per cent) ported by *Goldschmidt* [1938].

Copper—The concentrations obtained for opper are lower than the average copper .42 ppm) results reported by *I. and W. Noddack* 930]. At the same time, the intermediate alues of these concentrations show a satis- ctory agreement with the range of the copper alues given by *Lovering* [1957].

Copper is distributed over the range (66 ppm 0.34 per cent) which resembles most closely hat of the vanadium variations. However, nlike vanadium and also cobalt, copper is not oherent with either chromium or nickel. Also, here seems to be very little relation between e copper concentrations and the presence in oilites of mineral phases other than the iron lfide phase.

From the copper-abundance data [*Lovering d others*, 1957] for iron meteorites (100 to 250 om) it appears that the troilite phase, within s estimated abundance limits [*Chirvinskii*, 1948; *Henderson and Perry*, 1958], makes a small variable contribution to the copper composition of these meteorites.

Iron (total)—The total iron contents of the troilite nodules studied are shown in the last column of Table 8. The majority of the iron values are clustered around the 62 per cent level. However, it can be seen that significant departures occur from this level, with the result that the present (54.4 to 78.5 percentage by weight) iron range is vastly broader than the iron spread defined by all previous iron determinations.

Within this range the iron concentrations lower than 60 per cent are associated primarily with the chromium-rich phases (Table 5), whereas the iron concentrations higher than 67 per cent are due to the presence in the troilite nodules of a free-iron phase (Table 5).

Iron–Iron Sulfide Composition of Troilite Nodules

Because of its special significance in connection with the problem of the separation of phases in meteorites, some elaboration will be made on the iron–iron sulfide composition of troilite nodules.

The preliminary data on the four iron-bearing troilite nodules have been given in Table 5. The calculated iron–iron sulfide compositions of three of these nodules are given in Table 10. Omitted from the table because of an irregular and spotlike occurrence (Table 2) of its iron inclusions is the Canyon Diablo nodule. Columns 6 and 7 show the contents of the iron sulfide and

Table 10—*Metallic iron and iron sulfide content of three troilite nodules (all data in per cent by weight)*

Troilites and control standards		Total iron content	Sum of all other elements	Sulfur (by difference)	Sulfur (determined)	Iron sulfide (calculated)	Free iron (calculated)
1		2	3	4	5	6	7
dian Valley	H	78.0	5.84	16.1	13.8	44.1	55.9
allinoo	Of	78.5	5.33	16.2	13.7	44.4	55.6
ullison	C	67.0	1.45	31.5		86.3	13.7
eS reagent		63.6 (63.53) (stoich.)			32.0 (36.47) (stoich.)		
$_2SO_4$ reagent					18.3 (18.40) (stoich.)		

the iron phases, respectively. The former includes the iron sulfide equivalent of the daubreelite phase in the Indian Valley nodule, and the latter the free-iron equivalent of the lesser elements in all three nodules.

The calculations are based on the data from Table 8. For a ready reference, these data are reproduced in an appropriate form in columns 2 and 3. The sulfur content in column 4, used in determining the proportion of the iron sulfide phase, was determined by difference, and that in column 5 represents a gravimetric check determination of this content in two (the Indian Valley and Ballinoo) troilites with two sulfur-containing shelf reagents employed as control standards.

The errors in the barium sulfate precipitation from the sample solution and the presence of inert impurities in the samples may have caused the observed difference between the gravimetric and the calculated sulfur results.

Furthermore, the assignment of the lesser elements entirely to the free-iron phase of the troilites considered increases somewhat the proportion of that phase relative to the iron sulfide phase. However, the elements nickel and cobalt most certainly favor the former over the latter.

It is seen that within these errors the calculated results (14 to 56 per cent) fully confirm the free-iron abundance trends as shown in Table 5. In addition, it appears that 0 to 5 per cent free-iron range, based on both the 4 to 5 per cent sensitivity of the X-ray diffractometer used and the observed magnetic properties of troilites, is quite probable. It should, however, be kept in mind that pyrrhotite, in all cases where it is present, could also account for the moderate degree of magnetism observed in troilites (Table 5) which lie below the indicated free-iron detection limit. On the other hand, *Perry* [1944] stated that the actual analyses showed troilite to contain 3 to 4 per cent iron in solid solution. This proportion, considerably greater than the solid solubility of 1.5 per cent iron in iron sulfide reported by *Treitschke and Tammann* [1906], was attributed by him to the presence of iron in the form of particles occluded along the grain boundaries in the troilite and not actually in solid solution.

This broad range of the free-iron contents of troilites, particularly the existence of troilites

TABLE 11—*Variations in composition of troilites as shown by previous and present results*

Elements	Variation ratios: Present results	Variation ratios: All previous results
Vanadium	>30	200
Chromium	700	180
Iron	1.4	
Cobalt	330	230
Nickel	340	50
Copper	50	8
Zinc	>60 (?)	3
Arsenic	>5	

with a preponderant free-iron phase, indicates that complete separation of troilite and metal did not occur.

SUMMARY

The element compositions of troilites are summarized in Table 11. The summary is given in terms of the variation ratios (the ratios of the highest to lowest concentration observed) for each of the elements studied. For comparison the corresponding ratios from the results of the previous investigators (Table 1) are also included.

Acknowledgments—We are greatly indebted to the following individuals who donated samples used in this investigation: C. Frondel, Harvard University; C. C. Patterson, California Institute of Technology; A. A. Yavnel', Committee on Meteorites, Academy of Sciences, U.S.S.R.; J. F. Lovering, Australian National University; and L. T. Silver, California Institute of Technology. The isotopic carbon analyses by Irene Vidziunas and supplementary spectrographic analyses by Elizabeth Godijn are greatly appreciated. We gratefully acknowledge the help and many suggestions given us by S. Epstein, L. T. Silver, G. Kullerud, and E. P. Henderson. We thank Harrison Brown for a critical review of the manuscript.

REFERENCES

BANDEMER, S. L., AND P. J. SCHAIBLE, Determination of iron, *Ind. Eng. Chem., Anal. Ed., 16*, 317–319, 1944.

CHIRVINSKII, P. N., Klark sery v zheleznykh meteoritakh (Clarke of sulfur in iron meteorites), *Akad. Nauk, S.S.S.R., Meteoritika, 4,* 71–74, 1948.

CHODOS, A. A., AND W. NICHIPORUK, An application of the mutual standards concept to X-ray fluoresence spectroscopy. The analysis of meteoritic sulphide nodules for eight elements

Proc., Seventh Annual Conf. Ind. Appl. of X-ray Analysis, Univ. of Denver, 247–255, 1958.

[C]lark, G. L., and A. Ally, X-ray examination of chrome ores: (I) Lattice dimensions; (II) Theoretical densities, *Am. Mineralogist, 17*, 66–74, 1932.

[C]oulliette, J. H., Spectrographic determination of nickel and chromium in stainless steel, *Ind. Eng. Chem., Anal. Ed., 15*, 732–734, 1943.

[C]raig, H., The geochemistry of the stable carbon isotopes, *Geochim. et Cosmochim. Acta, 3*, 53–91, 1953.

[D]aly, R. A., Meteorites and an earth-model, *Bull. Geol. Soc. Am., 54*, 401–456, 1943.

[D]yakonova, M. I., Khimicheskii sostav Sikhote-Alinskogo meteorita (Chemical composition of the Sikhote-Alin meteorite), *Akad. Nauk S.S.S.R., Meteoritika, 16*, 42–48, 1958.

[E]akle, A. S., Massive troilite from del Norte County, California, *Am. Mineralogist, 7*, 77–80, 1922.

[G]oldberg, E., A. Uchiyama, and H. Brown, The distribution of nickel, cobalt, gallium, palladium and gold in iron meteorites, *Geochim. Cosmochim Acta, 2*, 1–25, 1951.

[G]oldschmidt, V. M., Geochemische Verteilungsgesetze der Elemente, *Skrifter Norske Videnskaps-Akad. Oslo, I., Mat.-Naturv. Kl.*, 148 pp., 1938.

[G]oldschmidt, V. M., *Geochemistry*, edited by A. Muir, Clarendon Press, Oxford, 730 pp., 1954.

[G]oldschmidt, V. M., and C. L. Peters, Zur Kenntnis der Troilit-Knollen der Meteoriten, *Nachr. Ges. Wiss., Göttingen, Math.-physik. Kl.*, 278–287, 1933.

[H]ägg, G., and I. Sucksdorff, Die Kristallstruktur von Troilit und Magnetkies, *Z. physik. Chem., Leipzig, B, 22*, 444–452, 1933.

[H]arcourt, G. A., Tables for the identification of ore minerals by X-ray powder patterns, *Am. Mineralogist, 27*, 63–113, 1942.

[H]enderson, E. P., and S. H. Perry, Studies of seven siderites, *Proc. U. S. Natl. Museum, 107*, 339–403, 1958.

[K]vasha, L. G., Mineral'nyi sostav i struktura Sikhote-Alinskogo meteorita (Mineral composition and structure of the Sikhote-Alin meteorite), *Akad. Nauk S.S.S.R., Meteoritika, 16*, 49–58, 1958.

[L]overing, J. F., Temperatures and pressures within a typical parent meteorite body, *Geochim. et Cosmochim. Acta, 12*, 253–261, 1957.

Lovering, J. F., W. Nichiporuk, A. A. Chodos, and H. Brown, The distribution of gallium, germanium, cobalt, chromium and copper in iron and stony-iron meteorites in relation to nickel content and structure, *Geochim. et Cosmochim. Acta, 11*, 263–278, 1957.

Lundquist, F., The crystal structure of daubreelite, *Arkiv Kemi, Mineral., Geol., 17*, paper 12, 4 pp., 1943.

McKinney, C. R., J. M. McCrea, S. Epstein, H. A. Allen, and H. C. Urey, Improvements in mass spectrometers for measurement of small differences in isotope abundance ratios, *Rev. Sci. Instr., 21*, 724–730, 1950.

Noddack, I., and W. Noddack, Die Häufigkeit der chemischen Elemente, *Naturwiss., 18*, 757–764, 1930.

Perry, S. H., *Metallography of Meteoritic Iron*, U. S. Government Printing Office, 206 pp., 1944.

Prior, G. T., On the remarkable similarity in chemical and mineral composition of chondritic meteoric stones, *Mineral. Mag., 17*, 33–38, 1913–1916, publ. 1916.

Smales, A. A., D. Mapper, J. W. Morgan, R. K. Webster, and A. J. Wood, Some geochemical determinations using radioactive and stable isotopes, *Proc. Second U. N. Intern. Conf. on the Peaceful Uses of Atomic Energy, 2*, 242–248, 1958.

Treitschke, W., and G. Tammann, Über das Zustandsdiagramm von Eisen und Schwefel, *Z. anorg. Chem., 49*, 320–335, 1906.

Urey, H. C., The abundances of the elements, *Phys. Rev., 88*, 242–252, 1952.

Yavnel', A. A., Otmositel'mo admorodnosti Khimicheskogo Sostava Sikhote-Alinskogo zheleznogo meteorita (concerning the uniformity of the chemical composition of the Sikhote-Alin iron meteorite), *Akad.* Hauk *S.S.S.R., Meteoritika, 11*, 107–116, 1954.

Yavnel', A. A., O primesiakh v nekotorykh mineralakh Sikhote-Alinskogo zheleznogo meteorita (On impurities in some minerals of the Sikhote-Alin iron meteorite), *Akad. Nauk S.S.S.R., Meteoritika, 14*, 87–91, 1956.

(Manuscript received June 22, 1959; revised September 29, 1959; presented at the Thirty-Ninth Annual Meeting, Washington, D. C., May 6, 1958.)

Letters to the Editor

AROUND-THE-WORLD ECHOES OBSERVED ON A TRANSPOLAR TRANSMISSION PATH

Johannes Ortner

Kiruna Geophysical Observatory
Kiruna, Sweden

Three backscatter-sounder transmitters with frequencies 11.805, 17.900, and 24.025 Mc/s operated by the Geophysical Institute in College, Alaska (64.8°N, 147.8°W), have been monitored at Kiruna Geophysical Observatory (67.8°N, 20.4°E) since May 1958 for investigations of transpolar communication with special reference to the effects of aurora.

The College–Kiruna path length is 5200 km; the position of both stations can be seen in Figure 1.

The transmitters are pulsed with a peak pulse output power of 4 kw; the pulse length is 2 msec; and the pulse repetition frequency 18.75 c/s. The transmitter antennas are three-element Yagis. As receiver antennas a rhombic aerial is used for 12 and 18 Mc/s, and a three-element Yagi for 24 Mc/s, both pointed north. The receivers are Standard Radio model SR 25, Hallicrafter SX-100, and Hammarlund SP-600. The outputs of the receivers modulate the intensity of oscilloscopes, the sweeps of which are synchronized with the pulse repetition frequency of the transmitters. As the synchronization is only approximate the incoming pulse is moving slowly over the screen of the oscilloscope. The intensity of the light spots is recorded on continuously moving film. The advantage of this method of recording signal strength (an example is shown in Fig. 2) is that it is possible to identify the reception even in the presence of fairly strong interference.

The transmitting antennas have been rotating, except during the period December 23 to February 24, when the Yagis were pointed to the north. During this period the pulse reception records in Kiruna were very useful for multipath transmission studies. Up to five different transmission paths at the same time could be found on the 18 Mc/s recordings. The propagatio[n] modes for these different paths can be explaine[d] by a different number of hops via the F_2 laye[r] or combinations of E_s and F_2 layer hops.

In the two periods December 24 to January [.] and February 18 to 24, during which the recep[-] tion records of 18 Mc/s were most nearly perfect there was found a pulse with a time delay tha[t] was much longer than can exist for any of th[e]

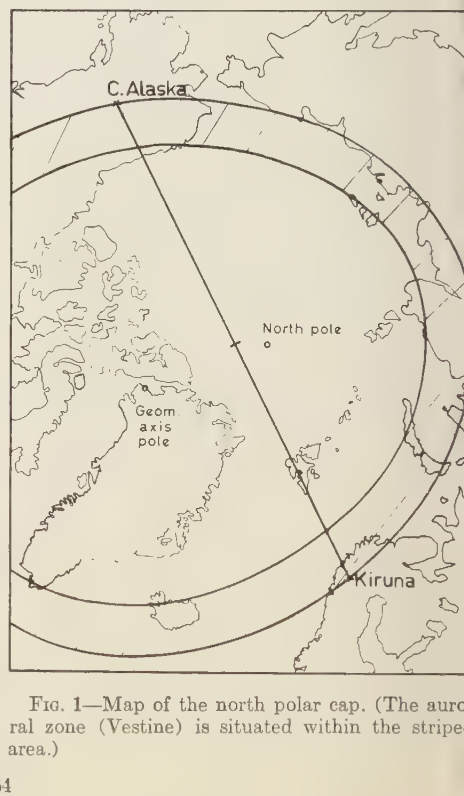

Fig. 1—Map of the north polar cap. (The auro[-] ral zone (Vestine) is situated within the stripe[d] area.)

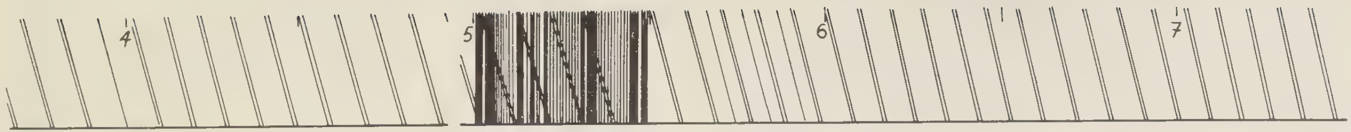

FIG. 2—Tracing of the pulse reception record of December 30, 1958, 0400–0700 MET. (Observe the different propagation paths, and note that the signal is visible even in the presence of interference.)

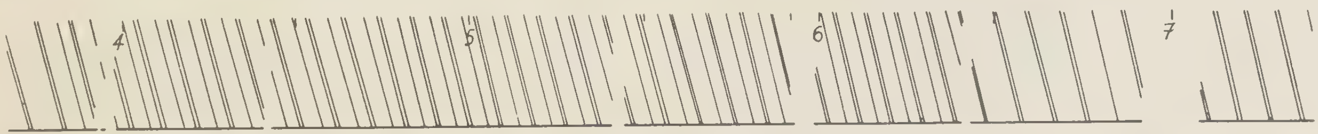

FIG. 3a—Tracing of the pulse reception record of January 5, 1959, 0400–0700 MET. (Observe the high signal strength of the around-the-world echo. The fadeouts before the hours and half hours are assumed to originate from some failure of the keying mechanism of the call letters, which are transmitted each half hour.)

TABLE 1—*Times for the around-the-world echoes observed in Kiruna*

Date	Magnetic activity index Ap*	Sunspots†	Forenoon, MET	Magnetic activity Kp* (00-03 UT)	Afternoon, MET	Magnetic activity Kp* 15-18 UT
12/24	7	185		2	1750–1810	1+
25	4	222		0		1+
26	13	239		2+		3+
27	12	206		3	1650–1700	3−
28	14	170	0530–0545	3−	1750–1800	3
29	10	162	0530–0550 0700	2	1750–1810	2−
30	12	172	0535–0600	2−	1720–1925	3
31	7	156		1+	1800–1830	2−
1/1	1	201		0		0+
2	3	201		0		1+
3	6	207		2+	1730–1830	1
4	7	217	0550–0620	1−		3−
5	25	243	0345–0625	1+		4
2/18	4	159		1−		2−
19	12	175		4−		2+
20	4	150	0440–0500 0605–0615 0705–0800	1	1850–1855	1−
21	6	163	0425–0550	0+	1730–1735 1800–1815	1+
22	17	158		4+		3
23	15	186		4−	1425–1600 1730–1915	1−
24	4	190	0455–0555 0630–0700	0+		1

* J. Bartels, IAGA, Committee on characterization of magnetic activity.
† Zürich provisional relative sunspot numbers.

possible direct modes of transmission from College to Kiruna (which are less than 6 msec). This special pulse shown in Figure 3*a* could be seen around 0600 in the morning and 1800 MET in the evening. The exact times are listed in Table 1, which gives a survey for all 20 days analyzed.

Figure 3*b* is an enlarged picture of the original reception record. One sweep of the oscilloscope takes 53.3 msec (pulse repetition frequency 18.75 c/s). The time difference between the unusual pulse and the nearest usual one is 22 msec. The most probable explanation for such a long time interval is to assume an around-the-world echo. If the long-delayed pulse is attributed to the third sweep (160 msec) before the nearest one, a time for around-the-world propagation of $160 - 22 = 138$ msec is obtained, which is in good accordance with what can be found in the literature [*Lassen*, 1956]. Some of the ol served time differences are somewhat le (down to 20.5 msec), so the upper limit of tl around-the-world path obtained in this way 139.5 msec. The direct transmission time f the College–Kiruna path is unimportant f this calculation, since both the two signa giving the described time delay have to pa the distance College–Kiruna, before the delay one is propagated another cycle around t world.

The possibility that the signal is propagat backward over the great-circle path was inves gated, although it is not very probable since t backlobs of both the transmitter and receiver a tenna should be responsible for a communicati on this route. If we assume 138 msec as the pro gation time around the world we find 18 ms for the forward propagation College to Kiru

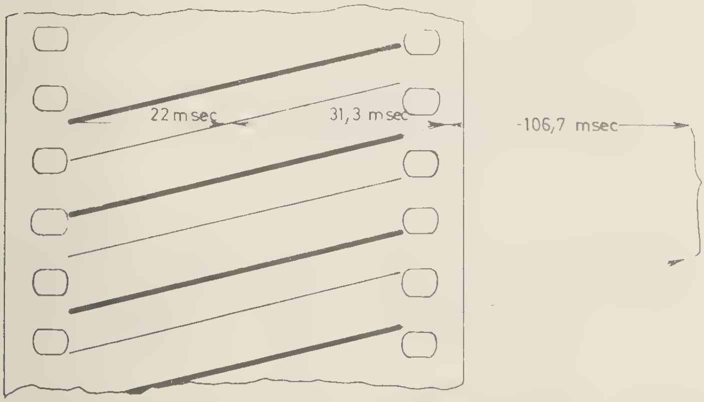

FIG. 3b—Enlarged sketch of Figure 3a with time delay description between the different pulses.

d 120 msec for the backward. Such a pulse ould be visible on the recordings 5 msec before e nearest direct propagated one, since the ne for 2 sweeps is 107 msec and the time fference between the forward- and backward-opagated signal would be 102 msec. Such a ne delay has never been observed.

The magnetic and solar activity of the 20 ected days was very low, as can be seen in ble 1. The long-path echo occurred 18 times 40 observed mornings and evenings, but correlation has been found for the cases en the signal was not propagated around the rth and the magnetic activity.

A detailed investigation of relations between e boundary of the sun's shadow on the earth d the propagation path shows that both llege and Kiruna have exactly the same tance from this boundary at just the times en the special echoes occurred (0600 and 00 local time), or in other words the rays of e sun are at these times exactly touching the eat-circle path through the transmitter and eiver station at the earth equator.

The field strength of the around-the-world eived signal is sometimes not more attenuated an a direct-propagated pulse (see Fig. 3a). erefore, the best explanation for the propaga-n mode is to assume tilted reflections, as ey have been described in the literature *ted*, 1958; *Chvojková*, 1954; *Stein*, 1958] ring recent years. Signals propagated in this y can pass long distances without the necessity of re-entering the absorbing *D* region, except on the last leg. This can explain best the high signal strength after such a long propagation path.

No similar echoes have been monitored on 12 or 24 Mc/s.

Studies will be continued, analyzing all the material on pulse receptions. Furthermore, it is planned that the rotating transmitter antennas will be stopped directed toward Kiruna for some more periods to get a better picture of the whole propagation mechanism.

Acknowledgments—The author is greatly indebted to Dr. Bengt Hultqvist for several valuable discussions and to Mr. Sven Olsen, the engineer, for help with the receiver equipment. For the operation of the transmitters by the Geophysical Institute, College, Alaska, the author is greatly obligated to Dr. Leif Owren. The work on which this communication is based has been supported by the European Office of Air Research and Development Command (Contract 61(514)–1314).

REFERENCES

CHVOJKOVÁ, E., Über den Weltumlauf der Radiostrahlen, *Bull. Astron. Inst. Czech.*, *5*, 104–111, 1954.

ISTED, G. A., Round-the-world echoes, *Marconi Rev.*, *21*, 173–183, 1958.

LASSEN, H., *Rund-um-die-Erde-Signale, Antennen und Ausbreitung*, Springer-Verlag, pp. 117–119, 1956.

STEIN, S., The role of ionospheric-layer tilts in longrange high-frequency radio propagation, *J. Geophys. Research*, *63*, 217–241, 1958.

(Received September 25, 1959.)

ATMOSPHERIC DIFFUSION AND NATURAL RADON

J. R. PHILIP

Division of Plant Industry, C.S.I.R.O., Canberra, Australia

Wilkening [1959] reports valuable and interesting observations on the diurnal and annual cycles of natural radon concentration near the ground. He interprets the cycles as due to known periodicities in the intensity of turbulent exchange processes in the atmosphere. Provided that the rate of exhalation of radon from the ground is 'essentially independent of the time of day,' is also independent of the season, and is spatially constant, his interpretation must be the correct one.

Unfortunately, his attempt to deduce the daily variation of eddy diffusivity from his observations is not entirely satisfactory.

The most important objection to his analysis is that he applies a steady-state form of the diffusion equation to what is demonstrably a transient phenomenon. The correct equation is

$$\partial N/\partial t = \partial/\partial Z[K(\partial N/\partial Z)] - \lambda N$$

Here we follow Wilkening's symbolism. N(curie cm^{-3}) is the radon content, t (sec) is time, Z (cm) is elevation above the ground, K (cm^2 sec^{-1}) is the diffusivity, and λ (= 2.1×10^{-6} sec^{-1}) is the decay constant of radon.

If $\partial N/\partial t$, the time rate of change of radon content, were negligibly small compared with the other terms of this equation, use of the steady-state equation would be justified. However, check of Wilkening's data reveals that $\partial N/$ varies from about -35×10^{-21} to $+30 \times 10^{-}$ curie cm^{-3} sec^{-1}, whereas λN lies within tl range of 0.17×10^{21} to 1.26×10^{-21} curie cm sec^{-1}. That is, the neglected term is of a muc greater order of magnitude than one of the tw terms retained in Wilkening's equation. Und such circumstances, a steady-state analysis the diurnal cycle has no validity.

The problem is further confounded by tl known fact (which Wilkening recognizes) th K is altitude-dependent.

It would appear that little reliance can l placed on the quantitative estimates of tl diurnal cycle of eddy diffusivity given in Wilke ing's paper. Unfortunately, it is easier to l critical than to supply the analysis which is r quired to put the connection between rado concentration and eddy diffusivity on a sound quantitative basis.

REFERENCE

WILKENING, M. H., Daily and annual cours of natural atmospheric radioactivity, *J. Geophy Research, 64,* 521–526, 1959.

(Received June 29, 1959; revised August 26, 195

DISCUSSION OF PAPER BY F. D. STACEY, 'THE POSSIBLE OCCURRENCE OF NEGATIVE NITROGEN IONS IN THE ATMOSPHERE'

D. R. Bates[1]

Boulder, Colorado

The suggestion has recently been made *acey,* 1959] that molecular nitrogen has an stable negative ion which may be formed and stroyed by the radiationless processes

$$N_2 + e \rightleftharpoons N_2^- \tag{1}$$

at, in consequence, the disappearance of ctrons at low gas densities (corresponding the F_2 layer) follows an attachment law; d that, in consequence also, the ionic re- mbination process

$$N_2^+ + N_2^- \rightarrow 2N_2 \tag{2}$$

uses the effective recombination coefficient be strongly pressure-dependent as observed the laboratory by *Bialecke and Dougal* [1958]— ough not by *Faire and Champion* [1959]. e purpose of the present note is to point out at the supposed negative ions are necessarily too rare to have the effects suggested.

Noting that the concentration of electronic tes in phase space is $2\omega_0/h^3$, where ω_0 is the tistical weight of the neutral molecule and s Planck's constant, it is readily seen that, if e free electrons have a Maxwellian distribution temperature T, then in equilibrium

$$n(N_2^-)/n(e) = \mu n(N_2) \tag{3}$$

with

$$\mu = \frac{\omega_1}{2\omega_0}\left\{\frac{h^2}{2\pi k m T}\right\}^{3/2} \exp(-\epsilon/kT) \tag{4}$$

in which n denotes the number densities of the species indicated, ω_1 is the statistical weight of the negative ion and ϵ is its excess energy with respect to the neutral molecule, k is Boltzmann's constant, and m is the mass of the electron. Take the statistical weight factor, $\omega_1/2\omega_0$, to be unity (which cannot introduce significant error); and, in order to favor the suggestions under consideration, take ϵ to be zero. Numerical substitution in (4) then yields

$$\mu = 4 \times 10^{-16}/T^{3/2} \text{ cm}^3 \tag{5}$$

where T is in degrees Kelvin. It is immediately apparent from this that the negative ion to electron ratio (3) is so minute that the possible formation of N_2^- can be completely ignored both in the ionosphere and in the laboratory work on recombination mentioned.

[1] On leave from Queen's University, Belfast, rthern Ireland.

References

Bialecke, E. P., and A. A. Dougal, Pressure and temperature variation of the electron ion recombination coefficient in nitrogen, *J. Geophys. Research, 63,* 539–546, 1958.

Faire, A. C., and K. S. W. Champion, Measurements of disassociative recombination and diffusion in nitrogen at low pressures, *Phys. Rev., 113,* 1–6, 1959.

Stacey, F. D., The possible occurrence of negative nitrogen ions in the atmosphere, *J. Geophys. Research, 64,* 979–981, 1959.

(Received September 9, 1959.)

AUTHOR'S REPLY TO THE PRECEDING DISCUSSION

F. D. STACEY

Geophysics Department, Australian National University
Canberra, Australia

Professor Bates' theoretical argument (preceding note) depends very critically on the assumed value of ϵ in his equation 4. Taking ϵ to be zero does not favor my suggestions; indeed, it is equivalent to stating that nitrogen has no electron affinity, which it was the purpose of my paper [*Stacey*, 1959*a*] to question. *Davidson and Larsh*'s [1950] data indicated that nitrogen has an appreciable positive electron affinity and therefore that ϵ is negative and several times kT. This would give the exponential factor in Bates' equation 4 a large value and completely alter his conclusion.

Until more certain experimental evidence is available the existence of N_2^- ions is an open question, but to discount them on the basis of a theoretical value of ϵ is unsound. For many years the existence of He^- was 'disproved' in t same way, but this ion is now accepted.

It is necessarily very difficult to make cisive experiments on account of the expect very short life of N_2^-. The possibility of usi electron mobility measurements as in liqu argon [*Stacey*, 1959*b*] might be considered.

REFERENCES

DAVIDSON, N., AND A. E. LARSH, Conductiv pulses induced in insulating liquids by ioniz radiations, *Phys. Rev.*, *77*, 706–711, 1950.

STACEY, F. D., The possible occurrence of negat nitrogen ions in the atmosphere, *J. Geoph Research*, *64*, 979–981, 1959*a*.

STACEY, F. D., Electron mobility in liquid arg *Australian J. Phys.*, *12*, 105–108, 1959*b*.

(Received September 29, 1959.)

Corrigendum

Dr. A. J. Dessler called attention to the omission of the following paragraph from the beginning of the Letter to the Editor, "Hydromagnetic propagation of sudden commencements of magnetic storms" by W. E. Francis, M. I. Green, and A. J. Dessler, which appeared on page 1643, October 1959 issue of this JOURNAL:

"It has been suggested that the world-wide sudden commencement of magnetic storms are propagated around the earth by means of hydromagnetic waves [*Dessler*, 1958]. These hydromagnetic waves are generated by the impact of the solar wind on the earth's magnetic field over the sunlit hemisphere a distance of about six earth radii. The diff ence in transit time for a wave traveling the equatorial plane to reach the noon me dian and the midnight meridian at the eart surface is calculated to be approximat eleven seconds. This is approximately the lay time observed for the sudden commen ment's appearance on the dark hemisph relative to its appearance on the sunlit he isphere [*Gerard*, 1959]. Our present estim supersedes the previous estimate of two m utes for the time required for the wave propagate around the earth [*Dessler*, 1958]

Journal of

GEOPHYSICAL RESEARCH

Tables of Contents

VOLUME 64, NO. 1, JANUARY 1959 PAGE

VOLUME 64, NO. 2, FEBRUARY 1959

VOLUME 64, NO. 3, MARCH 1959

VOLUME 64, NO. 4, APRIL 1959

VOLUME 64, NO. 5, MAY 1959

VOLUME 64, NO. 6, JUNE 1959

VOLUME 64, NO. 7, JULY 1959

VOLUME 64, NO. 8, AUGUST 1959

VOLUME 64, NO. 9, SEPTEMBER 1959

VOLUME 64, NO. 10, OCTOBER 1959

VOLUME 64, NO. 11, NOVEMBER 1959

VOLUME 64, NO. 12, DECEMBER 1959

Index of Names

Journal of Geophysical Research, Volume 64

January–December 1959

Note. (*a*) indicates abstract; (*l*) indicates letter to the editor.

J. Geophys. Research, 64 (1), 1-132; (2), 133-270; (3), 271-388; (4), 389-488; (5), 489-586; (6), 587-695; (7), 697-864; (8), 865-1132; (9), 1133-1362; (10), 1363-1615; (11), 1617-2036; (12), 2037-2187.

Information for Contributors
to the *Journal of Geophysical Research*

Manuscripts—Send manuscripts to J. A. Peoples, Jr., Department of Geology, University of Kansas, Lawrence, Kansas. Manuscripts, including proof copies of figures, should be submitted in triplicate to expedite review and publication. Manuscripts should be in English, typewritten on heavy paper on one side of page only, double spaced (including abstracts and references), with generous margins.

Ample space should be allowed for mathematical expressions, which should be typed or very plainly written by hand. Particular attention should be given to legibility of subscripts and superscripts and to differentiation between capital and lower case letters. Unusual symbols and cumbersome notations should be avoided. Fractional exponents should be used in preference to root signs, and the solidus (/) should be used for fractions wherever its use will save vertical space.

Authors are urged to have their papers critically reviewed by their associates for scientific validity, manner of presentation and use of English before submitting them for publication.

Abstracts—An abstract must accompany each manuscript. It should be a concise but comprehensive condensation of the essential parts of the paper, suitable for separate publication, and adequate for the preparation of general indexes to geophysical literature.

References and footnotes—References should be indicated in the text by the insertion in brackets of the author's name and the year of publication, thus: [*Trelease*, 1951]. If the author's name is part of the text, only the year is bracketed. If there are two or more references citing different papers published in the same year by the same author, distinguish them by the letters a, b, c after the year. At the end of the paper, list all references alphabetically by the authors' names. Include in each entry the following: name of senior author, followed by his initials; names of junior authors, each preceded by his initials; title of paper (or book); title of publication or journal; volume number; inclusive page numbers; year of publication. Abbreviations of journals follow the style used in *Chemical Abstracts*. If in doubt, give the full title of the publication or journal. When a book is cited, add the publisher's name, the city of publication, and the total number of pages. Reference to specific pages may be made in the text if appropriate. Acknowledge unpublished reports and private communications in the text, not as references. Avoid footnotes to the text; use parenthetic sentences instead of footnotes if possible.

Tables and figures—Material suitable to tabular form should be arranged as a table and may be typewritten on a separate page, Tables must be numbered according to their sequence in the text, and each table should have a title. Column headings should be short and self-explanatory; more complete explanation may be given in footnotes to the table. Authors should avoid repeating in the text material which is given in tables or figures.

Figures should be prepared with the column width of this Journal in mind (a scale of two to four times that of the published figure is usually adequate). Lettering and symbols should be large enough to stand reduction and remain legible. Captions should be typed on a separate page, not lettered in the figures. Necessary legends or lettering in the figures should be executed to meet competent drafting standards, not typewritten. If the author cannot arrange for suitable lettering, he may send the drawings with the lettering lightly penciled in or shown on a proof copy, and the lettering will be done at the editorial office.

Line drawings should be in India ink on white paper or tracing cloth. Coordinate paper should be avoided, but, if used, it must be blue-lined and the coordinate lines which are to show must be inked.

Photographs are acceptable only if they have good intensity and contrast. They should be unmounted, glossy prints.

Figures should be identified by numbering lightly in pencil, and 'top' of each figure should be indicated.

Acknowledgments—Acknowledgments should be made only for significant contributions by the author's professional associates. A brief closing statement will usually suffice.

References

American Chemical Society, *List of periodicals abstracted by Chemical Abstracts*, Chemical Abstracts Service, Ohio State Univ., Columbus, 314 pp., 1956.

American Institute of Physics, *Style Manual*, American Institute of Physics, New York, 28 pp., 1951.

American Mathematical Society, A manual for authors of mathematical papers, *Bull. Am. Math. Soc.*, 49, no. 3, pt. 2, 1–16, 1943.

Emberger, M. R., and M. R. Hall, *Scientific writing*, Harcourt, Brace and Co., New York, 469 pp., 1955.

Taft K. B., J. F. McDermott, and D. O. Jensen, *The technique of composition*, 3rd ed., Farrar and Rinehart, New York, 628 pp. 1941.

Trelease, S. F., *The Scientific paper—how to prepare it, how to write it*, Williams and Wilkins Co., Baltimore, 175 pp., 1951.

U. S. Geological Survey, *Suggestions to authors of the reports of the United States Geological Survey*, 5th ed., U. S. Govt. Printing Office, Washington, 255 pp., 1958.

William Byrd Press, *Mathematics in type*, Richmond, 58 pp., 1954.

AMERICAN GEOPHYSICAL UNION

UNSELFISH COOPERATION IN RESEARCH

INFORMATION CONCERNING CORPORATION MEMBERSHIP

The American Geophysical Union is a non-profit scientific organization established by the National Research Council. It is the American National Committee of the International Union of Geodesy and Geophysics, and its Executive Committee is the Committee on Geophysics of the National Research Council.

Extracts from the Statutes:

Article 3. Membership—The membership of the American Geophysical Union shall be as follows:

(e) *Corporation Members*—Corporations and other organizations interested in geophysics elected by the Executive Committee of the Union. The designated representative of each such organization shall enjoy the privileges of a Member.

(Continued on next page)

Cut along this line

American Geophysical Union

PROPOSAL FOR CORPORATION MEMBERSHIP

To the Executive Committee, American Geophysical Union
1515 Massachusetts Ave., N.W., Washington 5, D. C.

Gentlemen:

As an indication of our interest in the aims and activities of the American Geophysical Union, and to assist in maintaining and extending its program of publication and other work in the development of the geophysical sciences, the undersigned applies for Corporation Membership in the AGU and, until further notice, agrees to pay annual dues, currently at the rate of $100 per unit of corporation membership, in accordance with the information set forth above.

Company or Organization ______________________________

By ______________________________ Title ______________________________

(Signature)

(over)

(*Continued from previous page*)

Extracts from the By-Laws:

(2) . . . Members of class (e) shall pay dues of not less than $100 for each calendar year; . . .

(21) One copy of each issue of (a) the *Transactions*, (b) *Journal of Geophysical Research*, (c) any published *List of Members and Officers*, and (d) any other publication which may be approved for *free distribution* to the membership by the Executive Committee of the Union, shall be sent to each . . . Corporation Member. . . . Each . . . organization in good standing may purchase any available publication of the Union at a discount from printed price list to non-members. The General Secretary is authorized to establish discounts for sales of publications.

Action of the Executive Committee, November 29, 1946:

(1) A list of corporation members shall be published on one or more pages immediately after the final page of text in each issue of the *Transactions*.

(2) A list of corporation members shall be included in the Membership Directory as a distinct unit.

AMERICAN GEOPHYSICAL UNION

1515 Massachusetts Ave., N.W.
Washington 5, D. C.

Cut along this line

Address ______________________________

City ________________ State ________________

General fields of activity ______________________________

The following person is designated as our representative in this membership ________________ Title ________________

Number of units of membership desired (this will be taken as one unless otherwise indicated) ________________

Place ________________

Date ________________

AMERICAN GEOPHYSICAL UNION — UNSELFISH COOPERATION IN RESEARCH

AMERICAN GEOPHYSICAL UNION

1515 Massachusetts Avenue, N.W., Washington 5, D. C.

Established by the National Research Council in 1919 for the development of the science of geophysics through scientific publication and the advancement of professional ideals.

QUALIFICATIONS FOR MEMBERSHIP

he membership of the AGU shall consist of Members, Associate Members, Student Members, and orporation Members.

Those eligible as candidates for election to the grade of MEMBER shall be:

MEMBER (a) Persons who have made an active contribution to geophysical research through observation, publication, teaching, or administration. Definite evidence should be presented to the Membership Committee. "Publication" may include books, articles, unpublished manuscripts, inventions, or development of geophysical instruments.

(b) Persons who have made active practical application of geophysical research. It should be shown that the nominee's work has not been purely routine, but that it has tended to create new knowledge of, or to broaden or strengthen the application of, geophysical research. In general, the minimum qualifications for membership will be not less than three years of professional experience in some phase of geophysics.

(Continued on next page)

Cut along this line

APPLICATION FOR MEMBERSHIP

Please refer to qualifications on reverse side and designate below type of membership desired:

Member ($10) ☐ Associate ($10) ☐ Student ($4.50) ☐ (1960)

Application forms for Corporation Membership are available upon request.

1. ______________________________
Surname *First Name* *Middle Name*

2. ______________________________
Preferred mailing address for publications

____
Permanent address

3. ______________________________ 4. ______________________________
Place *Month* *Day* *Year of Birth* *Country of citizenship/naturalization*

5. ______________________________
Nature of work and title and/or military rank; name and address of organization with which you are associated.

6. Check section or sections with which affiliation is desired.
- ☐ Geodesy
- ☐ Seismology
- ☐ Meteorology
- ☐ Geomagnetism and Aeronomy
- ☐ Oceanography
- ☐ Volcanology, Geochemistry, and Petrology
- ☐ Hydrology
- ☐ Tectonophysics

7. **EXPERIENCE (List below, use added sheets as necessary)**

Dates: From To Name and address of organization Title, duties, nature of work

8. **EDUCATION (List below, use added sheets as necessary)**

Dates: From To School Address Major Subject Degree, if any; year

(over)

(Continued from previous page)

Those eligible as candidates for election to the grade of ASSOCIATE MEMBER shall be:

ASSOCIATE MEMBER — Persons who have an active interest in physical processes of the Earth or technical assistance in the application of geophysics. In general, the minimum qualification for associate membership will be acceptable training or experience in some field of geophysics or allied science.

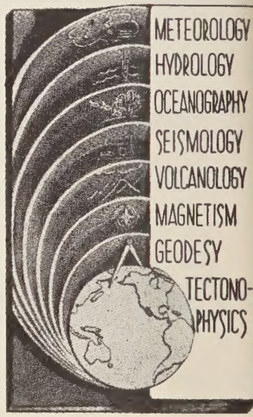

CORPORATION MEMBER — Corporations and other interested organizations shall be eligible as candidates for election to CORPORATION MEMBERSHIP. They shall have the privilege of designating a representative who has the rights and privileges of Members (use special form).

STUDENT MEMBER — Those eligible as candidates for election to the grade of STUDENT MEMBER shall be persons who are graduate or undergraduate students in residence at least half-time and who are specializing in the geophysical sciences. Teaching or research assistants enrolled in more than half of a full-time academic program may also be eligible for Student Membership. Student Members shall have all the privileges of Members except that they shall not vote or hold office.

Cut along this line

---

*9. References: Please list below names and addresses of two or three references; include members of the AGU or others who know you well.

*10. Titles of technical contributions or publications, particularly those in the geophysical sciences, and where published.

*11. Brief statement of any special interests or qualifications in the geophysical sciences.

Date________________ ________________________________

Written Signature

12. (STUDENT MEMBERS ONLY) The person whose signature appears above is known to me and is

a student majoring in______________________(subject) at______________________

(Name of college or university) expected to graduate in__________(year) with the degree of__________

☐ He is a full-time student, or ☐ a teaching or research assistant enrolled in more than half of a full-time academic program.

____
(Signature of faculty sponsor)

☐ Check here if faculty sponsor is a member of AGU and willing to act as a regular sponsor for associate membership as well.

________________________________ ________________________________
(Typed or printed name of sponsor) *(Title)*

* Applicants for student membership may omit Questions 9, 10, and 11, but must fill in Question 12. Please return form with check or money order payable to American Geophysical Union, 1515 Massachusetts Ave., N.W., Washington 5, D. C.

Contents

(Continued from back cover)

(Journal of Geophysical Research, Vol. 64, No. 12, December 1959)

Contents

INTERNATIONAL SYMPOSIUM ON FLUID MECHANICS IN THE IONOSPHERE

(Edited by R. Bolgiano, Jr.)

(*End of the Symposium; other contents continued inside back cover*)